

FINAL REPORT

DIESEL ENGINE IGNITION AND COMBUSTION

JAY A. BOLT
N. A. HENEIN

PERIOD JULY 1, 1964 TO DECEMBER 1, 1968

FEBRUARY 1969

This project is under the technical supervision of the:

Propulsion Systems Laboratory
U. S. Tank-Automotive Center
Warren, Michigan

and is work performed by the:

Department of Mechanical Engineering
The University of Michigan
Ann Arbor, Michigan

under Contract No. DA-20-018-AMC-1669(T)

enon

UMR 0425

no. 11

DISTRIBUTION LIST

Contract Distribution

<u>Name and Address</u>	<u>No. of Copies</u>
U. S. Tank-Automotive Center Propulsion Systems Laboratory Warren, Michigan 48090 Attn: SMOTA-RCP	4

Internal Distribution

Professor J. A. Bolt	4
Professor E. T. Vincent	1
Professor N. A. Henein	2

TABLE OF CONTENTS

	Page
LIST OF FIGURES NOT INCLUDED IN PREVIOUS PROGRESS REPORTS	vi
I. INTRODUCTION	1
II. SUMMARY OF WORK DONE	2
III. CONCLUSIONS	4
IV. SIGNIFICANT ACCOMPLISHMENTS	12
V. SUMMARY OF WORK INCLUDED IN THE SECTIONS OF THE REPORT	13
Section 1 (Progress Report No. 06720-1-P). Review of Previous Work Done	17
Section 2 (Progress Report No. 06720-2-P). Preliminary Work On: (a) Combustion Instrumentation; (b) Accumulator Fuel Injection System	79
Section 3 (Progress Report No. 06720-3-P). Combustion Instrumentation on Lister-Blackstone Engine	109
Section 4 (Progress Report No. 06720-4-P). Experimental Results on Lister-Blackstone Engine	129
Section 5 (Progress Report No. 06720-5-P). Development of Instrumentation on ATAC-1 Engine	185
Section 6 (Progress Report No. 06720-6-P). a. Analysis of Experimental Results on the Lister-Blackstone Engine. b. Publishing an SAE Paper on "Ignition Delay in Diesel Engines"	199
Section 7 (Progress Report No. 06720-7-P). a. Development of Instrumentation to Measure Smoke Intensity. b. Author's Reply to the Discussions on the SAE Paper "Ignition Delay in Diesel Engines"	267
Section 8 (Progress Report No. 06720-8-P). Effect of Air Charge Temperature on I.D. and Other Combustion Phenomena of Three Fuels	309

TABLE OF CONTENTS (Concluded)

	Page
Section 9 (Progress Report No. 06720-9-P). Effect of the Following Variables on I.D. and Other Combustion Phenomena: (1) Air Charge Temperature; (2) Type of Fuel; (3) Engine Speed; (4) Coolant Temperature	405
Section 10. Effect of Fuel-Air Ratio on Ignition Delay and Other Combustion Phenomena	538
Section 11. Effect of Anti-Smoke Additive on Smoke Intensity and Other Combustion Phenomena	552
Section 12. Effect of Air Charge Pressure on Ignition Delay and Other Combustion Phenomena	564
Section 13. Effect of Density on the Ignition Delay	570

LIST OF FIGURES NOT INCLUDED IN PREVIOUS PROGRESS REPORTS

Figure		Page
Part III—Conclusions		
1.	Different definitions used for ignition delay.	1
Section 10		
1.	Effect of fuel-air ratio of thermal loading on cooling and lubricating systems.	541
2.	Effect of fuel-air ratio on percentage heat losses to the cooling and lubricating systems.	542
3.	Effect of fuel-air ratio on cylinder head wall temperature.	543
4.	Effect of fuel-air ratio on minimum wall surface temperature.	544
5.	Effect of fuel-air ratio on the smoke intensity.	545
6.	Effect of fuel-air ratio on exhaust gas temperature.	546
7.	Effect of fuel-air ratio on ignition delays.	547
8.	Ignition delay: Observed and corrected to 1600°R.	548
9.	Effect of fuel-air ratio on peak gas pressure.	549
10.	Effect of fuel consumption per cycle on peak gas pressure.	550
11.	Effect of fuel-air ratio on BMEP and BSFC.	551
Section 11		
1.	Smoke intensity for diesel fuel with and without anti-smoke additive.	554
2.	Maximum pressure gradient for diesel fuel with and without anti-smoke additive.	555

LIST OF FIGURES NOT INCLUDED IN PREVIOUS PROGRESS REPORTS (Concluded)

Figure	Page
3. Rate of change of pressure gradient for diesel fuel with and without anti-smoke additive.	556
4. Effect of anti-smoke additive on the ignition delay.	557
5a. Pressure rise delay versus the reciprocal of the absolute mean temperature for diesel fuel with additive.	558
5b. Pressure rise delay versus the reciprocal of the absolute mean temperature for diesel fuel without additive.	559
6. Effect of anti-smoke additive on exhaust gas temperature.	560
7. Effect of anti-smoke additive on the peak gas pressure.	561
8. The specific fuel consumption for diesel fuel with and without additive.	562
9. Effect of the intake air temperature on the wall surface temperature for diesel fuel with and without additive.	563

Section 12

1. Effect of pressure at the start of injection on ignition delay.	566
2. Log I.D. vs. log mean pressure during delay.	567
3. Effect of inlet surge tank pressure on ignition delay.	568
4. Effect of surge tank pressure on the peak gas pressure and maximum pressure gradient.	569

Section 13

1. Effect of density on ignition delay at a constant mean pressure during I.D.	574
2. Effect of density on ignition delay at a constant mean temperature during I.D.	575

I. INTRODUCTION

This project was undertaken for the U.S. Tank-Automotive Command with the principal objective of studying the combustion problems and limitations of diesel engines under cylinder conditions corresponding to very high output turbo-charging. Reports of Russian work at very high supercharging pressures gave some of the incentive to begin this study in 1964.

A principal point of investigation centered on the effect of high cylinder air pressures and temperature on the ignition delay for the fuels of principal interest for land vehicles for military use. During the progress of the work there has been a great interest in combustion studies under severe operating conditions such as with high coolant temperatures, very high supercharging pressures, and temperatures. Combustion phenomena, other than the ignition delay, were also studied. These included rates of heat release, rates of pressure rise, maximum gas pressures, combustion chamber wall temperatures, thermal loads, and exhaust smoke.

A survey of the literature relating to diesel engine combustion was undertaken at the beginning of the project. This study constitutes Section 1 of this report. This survey showed that there is a great need for a correlation between the ignition delay and the air charge temperature and pressure. Such correlations are essential for design and future research work. In the early part of the contract period, attention was also given to improved injection systems to better provide a high ratio of maximum to minimum fuel quantity per injection. An accumulator type of fuel injection system was operated on a test bench in an effort to evaluate the high flow ratio possibilities of this type system. This study is included in Section 2 of this report.

During the first two years of the project, the experimental work was done by utilizing a Lister-Blackstone single cylinder diesel engine, modified to permit prechamber pressure, temperature, start of injection, and flame observations to be made. The main purpose of this work was to develop the instrumentation while waiting for the ATAC-1 engine. The data obtained on the Lister-Blackstone engine has proved to be valuable, and was published as an SAE paper. This work is included in Sections 3, 4, and 6 of this report.

Later in the project the ATAC single-cylinder research engine became available, as manufactured by the international Harvester Company, and it was used for all the experimental combustion work. This engine has two types of combustion chambers, a direct injection and a prechamber type. All the tests on this project were run with the open chamber cylinder head. The development of instrumentation for this engine is included in Section 5 of this report. The instrumentation included a Hartridge Unit Smokemeter, which is given in Section 7.

A correlation was obtained between the ignition delay and the air charge temperature. The experimental work covered many fuels ranging from diesel to gasoline. A wide range of temperatures was covered. This correlation is given in Section 8 of this report.

The effect of other variables on the ignition delay and other combustion phenomena has also been studied. These variables include: engine speed, coolant temperature, fuel-air ratio, anti-smoke additive, air charge pressure. This work is given in Sections 9 to 13 of this report.

The work is continuing as this report is being prepared, with tests being run with engine inlet manifold pressures of four atmospheres, together with measurements of the undesirable exhaust emissions.

II. SUMMARY OF WORK DONE

The outline of work done on this project is arranged in this section to correspond to work statements in the original contract, and with work statements of a series of supplements to the contract during the life of the contract.

1. ENGINE INSTRUMENTATION

The instrumentations were made to provide simultaneous measurement of the following engine data.

- a. Power output and engine speed
- b. Gas pressure during the cycle
- c. Illumination due to combustion
- d. Wall surface temperature during the cycle
- e. Wall temperature in the fire deck near the inlet and exhaust valves
- f. Fuel pressure before the injector
- g. Injector needle lift
- h. Air flow rate into the engine and its temperature and pressure before the inlet valve
- i. Fuel flow rate
- j. Intensity of smoke in the exhaust gases, their temperature and pressure

The studies included in this report were primarily conducted with CITE referee grade fuel (Mil-F-45121). The trends of ignition delay and combustion characteristics for diesel No. 2 and Mil-G-3056 referee grade gasoline were also investigated.

2. EFFECT OF GAS PRESSURE

The effect of gas pressure at the time of injection on ignition delay and combustion characteristics was studied for pressures ranging from 270 psia to 1200 psia. The tests on the "Lister Blackstone engine" covered a range from 270 psia to 600 psia. The tests on the "ATAC-1" engine covered a range from 370 psia to 1200 psia.

3. EFFECT OF GAS TEMPERATURE

The study of the effect of gas temperature at the time of injection on ignition delay and other combustion phenomena was made on the ATAC-1 engine over a range of temperatures from 935°F to 1980°F.

4. EFFECT OF GAS DENSITY

This study was made at different combinations of pressures and temperatures to determine if density was an independent variable affecting ignition delay.

5. COMPARISON BETWEEN THE RESULTS

Comparison between the results obtained on the Lister-Blackstone engine (prechamber combustion) and the ATAC engine (open chamber) relative to ignition delay parameters.

6. EFFECT OF ANTI-SMOKE ADDITIVE

This study was made to determine the effectiveness of fuel additives in reducing smoke in the exhaust gases emitted from the engine.

7. EFFECT OF ENGINE SPEED

This study was made to determine the effect of engine speed on ignition delay, smoke, and other combustion characteristics in the ATAC-1 open chamber engine. The fuel used was CITE referee grade fuel (Mil-F-45121).

8. EFFECT OF COOLANT TEMPERATURE

This study was made to determine the effect of coolant temperature on ignition delay and other combustion phenomena. The coolant temperature ranged from 150°F to 305°F. The fuel used for these tests was CITE referee grade fuel (Mil-F-45121), in the ATAC-1 open combustion chamber engine.

9. MEASUREMENT AND ANALYSIS

Measurement and analysis of the effect of higher coolant temperature on the fuel injection process.

10. EFFECT OF FUEL-AIR RATIO

Study the effect of fuel-air ratio on the ignition delay and other combustion phenomena. The fuel used was CITE referee grade fuel (Mil-F-45121), in the ATAC-1 open combustion chamber engine.

III. CONCLUSIONS

The following conclusions were reached from the present study and the review of the previous work done on the process of ignition and combustion in bombs and engines.

A. IGNITION DELAY DEFINITIONS

Different definitions appeared in the literature for the ignition delay. All these definitions agreed that the start of the ignition delay is at the start of injection. The difference between these definitions is in the criteria used to define the end of ignition delay. These criteria can be summarized as shown in Fig. 1.

A study of the above criteria indicates that these phenomena do not occur simultaneously during the early stages of the auto ignition process. Therefore it is to be expected that the corresponding delay periods will not be equal. The experimental results on the Lister-Blackstone (prechamber), and ATAC-1 (open chamber) engines showed that in general illumination due to combustion occurs after the pressure rise due to combustion is detected. In other words, the illumination delay period is longer than the pressure rise delay.

It can be concluded that the measurement of ignition delay in terms of the pressure rise is the most practical, and was found to be more reproducible. It also has the greater engineering significance.

All the correlations for the present project are made for the pressure rise delay.

B. PROCESSES TAKING PLACE DURING THE IGNITION DELAY

The processes that take place during the ignition delay can be divided into two types; physical and chemical. The physical processes include fuel jet disintegration, heating of the fuel, and diffusion of the fuel vapor to form a combustible mixture. The chemical processes include the preignition reactions. These processes occur simultaneously after the start of injection. However, the ignition delay period can be considered as composed of two periods. During the first period most of the physical changes take place, and during the second period most of the chemical changes take place. Or

$$I.D._p = I.D._{ph} + I.D._{ch}$$

DEFINITIONS

- End of I.D.
- 1. I.D.P Start of Pressure Rise
- 2. I.D.T Start of Temperature Rise
- 3. I.D_{IL} Start Light Emission
- 4. I.D.H.M.T. (Engines)
- 5. I.D. $\Delta P=0$ Pressure Rise to Original Pressure (Bombs)
- 6. I.D. $\Delta P=0$ Pressure Rise to 10 PSI Above Original Press.(Bombs)
- 7. I.D. ΔM Combustion of a Certain Mass of Fuel

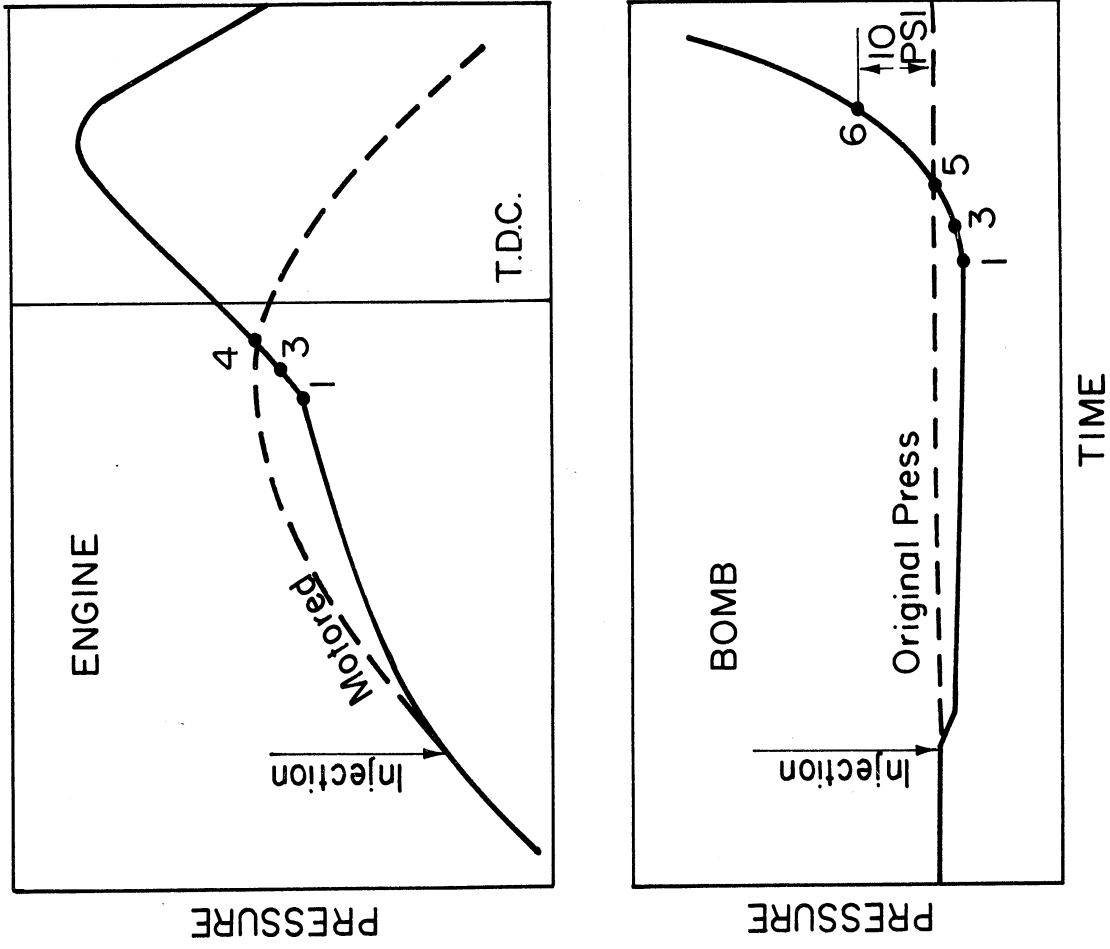


Fig. 1. Different definitions used for ignition delay.

The physical processes that take place to form a combustible mixture under the engine conditions, were found to take a very short period of time compared to the total ignition delay. This indicates that most of the delay period is occupied with chemical changes.

C. EFFECT OF AIR CHARGE TEMPERATURE ON IGNITION DELAY AND OTHER COMBUSTION PHENOMENA

1. Effect on Ignition Delay

The ignition delay continuously decreased with the increase in the air charge temperature for diesel No. 2 and Mil-G-3056 referee grade gasoline fuels. A very slight increase in the ignition delay for CITE referee grade (Mil-F-45121) fuel was noticed between 700°F and 745°F.

The rate of decrease of the I.D._p with the increase in temperature is greatest for gasoline. At a temperature of 106°F the ignition delay of gasoline is 2.142 times that of CITE fuel. But, at 700°F the ignition delay of gasoline is almost equal to that of the CITE fuel.

2. Correlation Between the Air Charge Temperature and the Ignition Delay

The best correlation was found to be of the form

$$I.D._p = \frac{Ae^{E/RT}}{p^n}$$

where A = constant

E = activation energy, Btu/lb mole, which can be considered equal to the minimum energy that should be achieved by the reactants before the start of combustion

R = Universal gas constant, Btu/lb mole·°R

T = absolute temperature, °R

p = absolute pressure

n = index of pressure

3. Apparent Activation Energy for Different Fuels

The experimental results show that the apparent activation energy for the different fuels is as follows:

<u>Fuel</u>	<u>E_a Btu/lb mole</u>
Diesel No. 2	5,230
CITE fuel	10,430
Gasoline fuel	14,780

A straight line relationship seems to exist between the apparent activation energy and the cetane number of the fuel. For fuels of cetane numbers between 17 and 58 the following relationship is obtained

$$E_a = 15500 - 230(\text{CET. No.} - 15)$$

4. Effect of Air Charge Temperature on Noise

Two methods have been used to find the noise level: (1) Direct observation. (2) Analysis of the pressure crank angle traces to determine the maximum pressure gradient and its rate of change. At atmospheric temperature the highest noise level is produced with the engine running on gasoline. However, at high inlet temperatures, above 600°F, the noise level with gasoline is the same as CITE and diesel fuels.

5. Effect of Air Charge Temperature on Smoke in Exhaust

The smoke was measured with a Hartridge smokemeter. The lowest smoke concentration was obtained with gasoline, followed by diesel No. 2 fuel. CITE fuel produced the highest smoke intensity. The high smoke level of CITE fuel is partly due to the after-injection which has been observed with this fuel. The increase in air charge temperature affected the smoke intensity of the different fuels in different ways. For diesel fuel, an increase in air charge temperature reduced the smoke intensity. For the more volatile fuels (CITE and gasoline) the smoke increased with the charge temperature. This is believed to be due to changes in the degree of atomization and penetration of these fuels at the higher temperatures.

D. EFFECT OF SPEED ON IGNITION DELAY AND OTHER COMBUSTION PHENOMENA

1. Effect of Engine Speed on Ignition Delay

The apparent effect of the increase in engine speed is to decrease the ignition delay. However, if a correction is made for the effect of increase in the charge temperature with speed, the ignition delay was found to increase with speed. The conditions of the tests carried out to study the effect of speed on ignition delay were carefully adjusted to eliminate the change in any parameter other than the engine speed.

2. Effect of Speed on Smoke Intensity

An increase in speed from 1500 rpm and 3000 rpm caused an increase in the smoke intensity from 40 to 60 Hartridge units.

3. Effect of Speed on Wall Temperatures

The increase in speed produced the following effects in the wall temperature at the different locations in the cylinder head.

- a. The wall surface temperature in the valve bridge of the fire deck increased at a high rate with the increase in speed from 1000 rpm to 2000 rpm, after which the temperature leveled off. At 1000 rpm the surface temperature was 435°F and reached 509°F at 2900 rpm.
- b. The swing in the surface temperature decreased from 37°F at 1000 rpm to 13°F at 2900 rpm.
- c. The wall temperature at the midpoint between the gas side and coolant side in the fire deck showed a different trend.
 - (1) Near the exhaust valve the temperature increased from 326°F at 1000 rpm to 360°F at 2900 rpm.
 - (2) Near the inlet valve the temperature remained constant at about 267°F.

4. Effect of Speed on Thermal Loading

The thermal loading which is equal to the sum of the heat lost to the water jackets and lubricating oil increased with speed. However, the thermal loading as a percentage of the heat input in the fuel decreased from 20% at 1000 rpm to 14% at 2900 rpm.

E. EFFECT OF COOLANT TEMPERATURE ON COMBUSTION PHENOMENA

1. Effect of Coolant Temperature on Ignition Delay

The increase in the coolant temperature from 156°F to 305°F did not affect the ignition delay. The value of I.D._p over the whole temperature range at a mean pressure of 700 psia was 0.680 msec.

2. Effect of Coolant Temperature on Thermal Loading

The increase in coolant temperature reduced the percentage heat loss to the coolant and lubricating oil from 17.7% at 156°F to 13.8% at 305°F. The total heat loss decreased from 1660 Btu/hp hr at 156°F to 1230 Btu/hp hr at 305°F.

3. Effect of Coolant Temperature on After Injection

The increase in coolant temperature caused the after injection to decrease till a temperature of about 230°F, after which it increased again.

F. EFFECT OF TYPE OF FUEL ON I.D. AND HEAT RELEASE RATE

The results of the heat release computations, for the diesel No. 2 and CITE fuels, showed that the following processes occur during the ignition delay before the pressure rise due to combustion is detected:

1. A negative heat release at the beginning of the ignition delay, due to fuel evaporation and the endothermic reactions that take place shortly after fuel injection. The negative heat release is observed for the two fuels during a major part of the ignition delay.

2. The negative heat release is followed by very slow reactions causing a slight increase in the rate of heat release. The end of the pressure rise delay measured from the pressure trace, coincides with the end of these slow reactions, before the start of the very high speed reactions.

The negative heat release period as well as the total ignition delay period are shorter for diesel No. 2 fuel than for CITE fuel. These results support the previous conclusions reached, that the activation energy for diesel No. 2 fuel is smaller than that for CITE fuel, causing the preignition reactions for the diesel fuel to be faster and the delay period shorter than for the CITE fuel.

The ignition delay is followed by a period of very rapid or explosive type reactions during which the energy of reaction of the fuel is released. These reactions occupied a relatively short period compared with the total ignition delay.

The maximum rate of heat release for the diesel fuel was found to be about 75% of that for CITE fuel.

G. EFFECT OF FUEL-AIR RATIO ON IGNITION DELAY AND OTHER COMBUSTION PHENOMENA

1. Effect of Fuel-Air Ratio on Ignition Delay

The apparent effect of the increase in the fuel-air ratio is to decrease the ignition delay. But when the ignition delay was corrected for the change in the gas temperature, the ignition delay was found to remain constant over the entire range of the fuel-air ratio.

2. Effect of Fuel-Air Ratio on Smoke Intensity

The smoke intensity increased with the fuel-air ratio.

3. Effect of Fuel-Air Ratio on Wall Temperature

The surface wall temperature increased with the fuel-air ratio from 383°F at 0.014 fuel-air ratio to 665°F at 0.056 fuel-air ratio. The coolant temperature was held constant at 170°F.

H. EFFECT OF ANTI-SMOKE ADDITIVE ON IGNITION DELAY AND OTHER COMBUSTION PHENOMENA OF DIESEL NO. 2 FUEL

1. Effect on Ignition Delay

The anti-smoke additive has little effect on ignition delay.

2. Effect on Smoke Intensity

The anti-smoke additive reduced the smoke intensity for air charge temperatures between 100°F and about 300°F. At higher temperatures its effect is not pronounced.

3. Effect on the Apparent Activation Energy

The anti-smoke additive has no effect on the apparent activation energy of the fuel.

I. EFFECT OF AIR CHARGE PRESSURE ON IGNITION DELAY

The increase in air charge pressure reduces the ignition delay. The

present tests covered pressures at start of injection from 350 psia to about 1200 psia. Future tests are planned to extend these pressures to higher values, in order to reach a general conclusion on the effect of pressure on the ignition delay.

J. EFFECT OF FUEL ON TROUBLES IN ENGINE OPERATION

1. The fuel leakage past the injector needle and the fuel plunger has been noticed to be excessive with CITE and gasoline fuels. This required frequent change of the lubricating oil in the fuel-pump sump, and cleaning of the injector.

2. Gasoline fuel produced a deposit over the injection system parts and required frequent cleaning.

IV. SIGNIFICANT ACCOMPLISHMENTS

1. The work on this project resulted in publishing the following papers:

- A. "Ignition Delay in Diesel Engines" by N. A. Henein and Jay A. Bolt, paper no. 670007, presented to the Annual Meeting of the Society of Automotive Engineers, Detroit, Mich., Jan. 9-13, 1967. This paper and discussion are published in the 1968 SAE Trans., Vol. 76, Sec. 1, pages 27-39.
- B. "Correlation of Air Charge Temperature and Ignition Delay for Several Fuels in a Diesel Engine" by N. A. Henein and Jay A. Bolt, paper no. 690252, presented to the International Automotive Engineering Congress of the Society of Automotive Engineers, Detroit, Mich., Jan. 13-17, 1969. The discussions prepared and presented concerning this paper showed great interest from both universities and industry in the results reached, and future papers to be presented.
- C. "Diesel Exhaust Smoke: Effect of Some Fuel and Engine Factors on Its Formation" by N. A. Henein and Jay A. Bolt. This paper was presented at the West Coast SAE Meeting, August 1969 in Seattle, SAE paper No. 690557.

2. The experimental results of this work showed the important effect of after injection on the smoke intensity in the exhaust. A proposal was prepared and submitted to the U. S. Public Health Service for future work. The title of this project is "Fuel Injection System Analysis—Diesel Smoke Reduction." A grant has been awarded to The University of Michigan to study this topic.

3. A paper dealing with the unpublished results of this work done on this project will be presented at the "Diesel Combustion Symposium" to be held in England by the Institution of Mechanical Engineers in April 1970.

This paper is being prepared and permission for publication will be requested from ATAC.

4. Another contract for further work in this area has been sponsored by ATAC at The University of Michigan. This contract is for one year starting January 28, 1969.

The work on this new contract is in progress. Operation and study of combustion phenomena at supercharging pressures higher than those reached in the present contract will be a principal objective.

V. SUMMARY OF WORK INCLUDED IN THE SECTIONS OF THE REPORT

The description and the results of the work done, as indicated above in items 1 to 10, are included in the following sections of this report.

Section 1

This section covers a review of the published literature concerning the auto ignition of liquid fuels injected into hot air. Special emphasis was given to the ignition and combustion processes in diesel engines. This review is given in Progress Report No. 1.

Section 2

This section covers the preliminary work done on combustion instrumentation and the accumulator fuel injection system:

- a. Development of combustion instrumentation on "Nordberg Model 4FS1 diesel engine"
- b. Studies on the accumulator fuel injection system

This work is reported in Progress Report No. 2.

Section 3

This section covers the development of combustion instrumentation for a Lister-Blackstone precombustion chamber engine. This work is reported in Progress Report No. 3.

Section 4

This section covers the experimental results on the Lister-Blackstone engine. This work is reported in Progress Report No. 4.

Section 5

This section covers the development of the combustion instrumentation on the ATAC open combustion chamber engine. This work is reported in Progress Report No. 5.

Section 6

This section covers the analysis of the experimental results obtained on the Lister-Blackstone engine to determine the following:

- a. To find numerical correlation between the ignition delay and the air charge pressure
- b. To compare the results of the tests on the Lister-Blackstone engine with previous studies made in engines and in bombs
- c. To present a paper to the SAE annual meeting held in Detroit, Jan. 1967. The title of this paper is "Ignition Delay in Diesel Engines."

This work is covered in Progress Report No. 6.

Section 7

This section covers the following:

- a. Development of instrumentation to measure the smoke intensity in exhaust of the ATAC-1 engine
- b. Author's reply to the discussions brought out by the SAE members on the paper "Ignition Delay in Diesel Engines" as mentioned in Section 6.

This work is covered in Progress Report No. 7.

Section 8

An analysis of the experimental results from the ATAC-1 engine to determine the effect of the air charge temperature on the following:

- a. Pressure rise and illumination ignition delays
- b. Air pressure at start of injection
- c. Mean gas pressure during the ignition delay
- d. Wall surface temperature in the valve bridge of the engine cylinder head fire deck
- e. Volumetric efficiency
- f. Air flow rate
- g. Peak gas pressure during the cycle
- h. Maximum pressure gradient after start of combustion
- i. Rate of change of pressure gradient after the start of combustion
- j. Smoke intensity
- k. Brake specific fuel consumption

This work is covered in Progress Report No. 8.

Section 9

This section covers the following:

- a. The results of the experimental studies made on the ATAC-1 engine to find the effect of the air charge temperature on the combustion phenomena of the following fuels.
 1. CITE referee grade (Mil-F-45121) fuel;
 2. Diesel No. 2 fuel; and
 3. Mil-G-3056 referee grade gasoline fuel.

- b. Comparison between the above three fuels concerning:
 1. Delay period
 2. Global activation energy of the preignition reactions of the three fuels
 3. Smoke intensity
 4. Specific fuel consumption

- c. Comparison between the rates of heat release of the above three fuels, under naturally aspirated condition.

- c. Effect of engine speed on the ignition delay and other combustion phenomena over a speed range from 1000 rpm to 3000 rpm. The phenomena of interest in this study included:
 1. Ignition delay
 2. Smoke intensity
 3. Surface wall temperature
 4. Thermal loading on the cooling and lubricating systems

- e. Effect of coolant temperature on the combustion process of CITE fuel. The coolant used for these tests was ethylene glycol at temperatures up to 305°F. The phenomena studied included the ignition delay, wall temperature, thermal loading, and after injection.

This work is covered in Progress Report No. 9.

Section 10

This section gives the results of the experimental work done on the ATAC-1 engine to find the effect of the fuel-air ratio on the ignition delay and other combustion phenomena. The experiments were done at two levels of coolant

temperatures 170°F and 250°F. The coolant used at the higher temperature was ethylene glycol.

Section 11

This section gives the results of the work done to study the effect of anti-smoke additive on the ignition delay and other combustion phenomena. The smoke additive used was a barium compound, trade mark "SMOGO," as supplied by Lubrizol Corporation, their No. 565. One of the combustion phenomena of interest was the global activation energy for the preignition reactions of the fuel with and without the fuel additive.

Section 12

This section covers the results of the work done to find the effect of the air charge pressure on the ignition delay and other combustion phenomena.

A correlation was obtained between the I.D._p and the mean pressure during the ignition delay.

Section 13

This section includes the analysis made to determine if the density is an independent variable affecting the ignition delay. The average air density during the ignition delay changed from 0.84 lbm/cu ft to 2.38 lbm/cu ft for CITE fuel. In other tests made on different fuels, the average density changed from 0.755 lbm/cu ft to 1.225 lbm/cu ft.

SECTION 1

PROGRESS REPORT NO. 1

REVIEW OF PREVIOUS WORK DONE

THE UNIVERSITY OF MICHIGAN
COLLEGE OF ENGINEERING
Department of Mechanical Engineering

Progress Report

DIESEL ENGINE IGNITION AND COMBUSTION—A BIBLIOGRAPHY

Jay A. Bolt
Capt. Robert K. Nicholson

ORA Project 06720

under contract with:

U.S. ARMY
DETROIT PROCUREMENT DISTRICT
CONTRACT NO. DA-20-018-AMC-1669T
DETROIT, MICHIGAN

administered through:

OFFICE OF RESEARCH ADMINISTRATION ANN ARBOR

September 1965

TABLE OF CONTENTS

	Page
OBJECT	22
INTRODUCTION	23
COMMENTS AND SUMMARY	24
CHRONOLOGICAL LIST OF REFERENCE PAPERS	25
LIST OF REFERENCES BY AUTHORS	25
DIESEL ENGINE COMBUSTION--GENERAL	26
BOMB EXPERIMENTS	44
NACA COMBUSTION APPARATUS TESTS	50
SPRAY FORMATION AND FUEL VAPORIZATION	54
DROPLET BEHAVIOR	60
HEAT RELEASE DURING COMBUSTION	65
"M-SYSTEM" OF COMBUSTION	69
ACCUMULATOR NOZZLE SYSTEM	72
ENGINE WALL HEAT TRANSFER	74
TURBOCHARGER EFFECTS	75

OBJECT

The object of this investigation is to experimentally determine in an engine the influence of cylinder air temperature and pressure on diesel ignition lag and combustion phenomena, especially under the conditions corresponding to very high supercharge. It is a further object to determine the influence of other engine variables on the combustion phenomena, for example, hot surfaces in the chamber.

INTRODUCTION

There is military interest in diesel engines which can operate with very high supercharge pressures. This results in an increased range of cylinder air pressure and temperature conditions at the time of fuel injection and ignition.

This project was initiated to investigate ignition and combustion phenomena attending operation through this increased range of pressure and temperature, including those corresponding to supercharge pressure ratios up to 5:1.

The activity during the first year of this project has been threefold, as follows:

1. To conduct a literature survey to more clearly establish the present state of the art of diesel engine ignition and combustion, particularly with respect to wide ranges of cylinder air pressure and temperature.
2. To begin the assembly of engine equipment and instrumentation for the observation and measurement of combustion phenomena in a single cylinder research engine, and to make initial measurements of such items as ignition lag, in preparation for later experimental programs with a new single cylinder research diesel engine to be supplied by the Army.
3. To make tests of a bench rig of an accumulator type fuel injection system which would be adaptable to use with either a one-shot (single firing cycle) or continuous operation of the test engine. Such a system also has the possible merit of being capable of a wider range of maximum to minimum injection quantity and thus have advantages for a highly supercharged engine.

This report covers the bibliography and literature survey of item 1 above.

A second report, O6720-2-P, covers the development and assembly of the engine instrumentation (item 2 above), and the work done on the accumulator injection system (item 3 above).

Both of these reports cover the period from July 1, 1964 to June 30, 1965.

COMMENTS AND SUMMARY

The literature concerning diesel engine combustion is very large. However, most of the published information has resulted from experimental observation concerning the performance of engines; little is known or published about the fundamental combustion phenomena. For example, we are not certain why diesel combustion is so prone to produce soot and smoke.

Since the emphasis of this project will be on the basic effects of cylinder air temperatures and pressures, references selected are mainly concerned with these parameters, although, unavoidably, all aspects affecting the combustion process have been included to some extent. The references cited reveal that the cylinder air temperature and pressure, in addition to their direct influence on combustion, also have many indirect effects, including effects on spray formation and droplet evaporation. In fact the air pressure and temperature affect all the variables that control the ignition and combustion process.

An effort was made to condense and present the information contained in the various references in the most useable manner. In some cases, conclusions reached by the individual authors are presented, in some cases the papers are paraphrased in detail, and in other cases, the references are summarized. No attempt was made to write a paper on the subject of diesel combustion—only to present the information contained in the selected references in as few words as possible. Comments as to the value of various papers have been made when deemed appropriate.

The most comprehensive studies of variables affecting ignition delay have been done with bombs. With the exception of the work of Wolfer (Ref. 52) these have involved a stagnant air charge, and usually result in longer ignition lag periods than reported with engines. No comprehensive study of engine variables which affect the ignition delay have been conducted with engines. It seems appropriate that this should be done, especially in view of the interest in the very wide ranges of cylinder air pressure and temperature used by highly supercharged diesels.

CHRONOLOGICAL LIST OF REFERENCE PAPERS

<u>Year</u>	<u>Paper No.</u>	<u>Year</u>	<u>Paper No.</u>	<u>Year</u>	<u>Paper No.</u>
1964	3	1961	1	1952	7
	15		11		8
	50		44		21
1963	2		47	1950	17
	18		49	1949	6
				1948	54
	26	1957	10	1942	4
	35		33	1938	12
	38		41		13
	39		48		22
	42	1956	9		52
	53		24	1936	14
1962	5		31		25
	16		32		34
	20		45		36
	37	1955	19	1935	23
	43	1954	40		28
	46				29
				1932	27
					30
				1924	51

LIST OF REFERENCES BY AUTHORS

<u>Author (first)</u>	<u>Paper No.</u>	<u>Author (first)</u>	<u>Paper No.</u>
Alcock, J. F.	15	Meckel, N. T.	35
ASME Publ.	54	Meurer, J. S.	45,46
Austen, A. E. W.	43,44	Michailova, M. N.	25
Barman, G. L.	38	Mullins, B. P.	33
Bassi	53	Nagoo, F.	37
Battelle Institute	41	Olson, D. R.	20
Boerlage, G. D.	12	Overbye, V. D.	49
Clarke, J. S.	5	Prieda, T.	44
Cohn, M.	23	Rosen, C. G. A.	2
Elliott, M. A.	6	Rothrock, A. M.	13,27-29
El-Wakil, M. M.	31,39,40	Selden, R. F.	22
Garner, F. H.	7-11	Stinson, K. W.	18
Gaydon, A. G.	4	Taylor, C. F.	17
Gerrish, H. C.	30,36	Tausz	51
Holfelder, O.	34	Tsao, K. C.	16
Hooker, R. J.	48	Voinov, A. N.	26
Hull, W. L.	50	Wentzel, W.	14
Hurn, R. W.	21,24	Wilson, G. C.	19
Hussmann, A. W.	47	Wittek, H. L.	3
Knight, B. E.	44	Wolfer, H. H.	52
Lewis, B.	1	Yu, T. C.	32
Lyn, W. T.	42,44		

DIESEL ENGINE COMBUSTION—GENERAL

1. Lewis, B. and von Elbe, G., Combustion, Flames, and Explosions of Gases, N.Y.: Academic Press, Inc., 1961 (textbook, 700 pages).

A comprehensive review of combustion; includes a section on combustion of hydrocarbons, and a few paragraphs about the combustion problem in diesel engines. One of the best general references on the subject of combustion.

"Fundamental research should ultimately contribute toward improved understanding and control of technical combustion processes, particularly in engines. To accomplish this it is necessary to analyze the engine process in terms of the fundamental physical and chemical processes that occur in the various phases of starting and operation. At present this has been pursued only to a very small extent. Too often engine studies are confined to observations of the effect of fuel and engineering variables on overall performance in a manner that excludes the possibility of recognizing the controlling physical and chemical processes. While development of modern engines has been eminently successful, this success has only been made possible by the accumulation of a very large volume of empirical information and by the continual maintenance of large and costly testing facilities. The question may be asked whether timely fundamental research could not have eliminated a large portion of this testing that has been carried on and is still continuing on a world-wide scale, and whether practical developments could not have been materially facilitated by scientific knowledge?"

(Taken from the Preface of the book of Lewis and Von Elbe.)

2. Rosen, C.G.A., "Matching Fuels to Diesel Combustion Systems," SAE Trans., Vol. 71, 1963, pp. 259-271.

Much still remains to be done in broad scale research to correlate all the factors which yield superior performance, to include the following factors:

1. Combustion chamber configuration
2. Stroke-bore ratio
3. Combustion air density or compression ratio
4. Fuel constituents
5. Spray characteristics
6. Turbulence factors
7. Mixture formation
8. Combustion chamber temperature gradient
9. Ignition delay, both physical and chemical
10. Heat release rates

Diesel fuels are highly complex mixtures of hydrocarbons of several different classes. Thus, the ignition and combustion behavior of a diesel fuel is the resultant of the behavior of all the various types of hydrocarbons present. The aromatics and olefins have been pointed out as retarding the ignition process; and certain peroxides and amyl nitrates have accelerated or shortened ignition delay. One can speculate on what the combining factors may be to influence the rather significant chemical delay and pre-flame chemistry.

The subject of spray characteristics has been given considerable attention by many. Anyone who has cut his eye teeth in the diesel game in air injection spray formation recognizes the advantage of minimum droplet size to reduce ignition lag and of having available a high energy vehicle such as injection air to provide the needed dispersion and penetration of the fuel spray. The precombustion chamber engine is a partial attempt to achieve the same results by utilizing an energized combustion gas to propel the unburned or partially burned fuel particles into the space where fuel finds its equivalent of air. The logical objective is to increase the surface of the fuel in small, well-dispersed droplets which find their equivalent of air to achieve vaporization and to complete combustion. Ignition lag is a function of the square of the radius of the fuel droplet. When fuel is supplied in droplet form, it is impossible to obtain the same heat release and flame characteristics as from a completely vaporized mixture of the same air/fuel ratio. In the diesel engine there is only a small period allotted for mixture formation since most of the fuel burns as a diffusion flame when it leaves the injector, although the initiation of the burning process occurs when an element of premixed carburant reaches its self-ignition temperature.

It is commonly accepted that the process of mixture formation and combustion is different when fuel is injected prior to the swirl creation or after it. The following effects of a combustion swirl is created in the main chamber by early auxiliary or pilot injection; the major part of the main injection takes place flaming in the high temperature gases. In such an environment the cracking of fuel molecules is liable to occur resulting in slow and smoky combustion with rapid initial pressure rise. The improvement on the combustion achieved by the swirl, therefore, is not so large. In contrast to this, when the swirl is set up after ignition, the acceleration of mixture formation and combustion is limited to the later stage but is effective enough to make the after-burning period shorter. The swirl effect in this case realizes a smokeless combustion with fairly low peak pressure.

In particular the theoretical and practical approaches have been combined to draw attention to certain areas in which further design and experimental work is required. Heat losses and mixing processes are parameters which come under this heading and which require further quantitative definition and study. It is also evident that many combustion processes can be completed much faster than the rates currently being used, and this points the way in

which combustion theory indicates that progress will be made. The first of the processes that must be considered when dealing with combustion in diesel engines is the delay period that exists between injection and ignition. This delay period is affected by both physical and chemical factors. The length of the chemical delay period is dependent upon the rate of the chemical reactions occurring during the delay period and it is of interest, therefore, to consider the physical variables which affect reaction rates and consequently chemical delay. The effects of initial air temperature and fuel temperature are quite distinct and are bound up with the whole question of the cold starting of engines. From elementary reaction kinetics, it is known that the logarithm of the rate of a chemical reaction varies linearly with the reciprocal of the absolute temperature. Since ignition delay is an inverse measure of the reaction rate, a linear relation is to be expected between the logarithm of ignition delay and the reciprocal of the absolute temperature. In a simplified form which is of value in analyzing delay factors and which further points to the problem of delineating the portion of time allocated to physical delay to the time required for chemical delay, the following formula may prove of interest.

$$t = 1200 \frac{r^2 \sigma_f C_p}{k} \log_e \frac{\theta_c - \theta}{\theta_c - \theta_1}$$

where:

t = ignition lag, sec

r = radius of fuel droplet, ft

σ_f = specific wt. of fuel, lb/ft.³

C_p = specific heat

k = heat conductivity for air

θ = temperature of fuel

θ_c = compression temperature

θ_1 = self-ignition temperature of fuel

(A more accurate equation for ignition lag was presented by Tsao, Myers, and Uyehara in the 1962 Transactions of the SAE, Reference 16).

The high-speed photographs of combustion show that the highest rate of burning, in general, occurs immediately after ignition and the flame is essentially premixed in nature with low luminosity. This period of high rate of heat release is, however, very short and is followed by the main period

which is essentially one of diffusion with high luminosity and a comparatively lower rate of heat release.

There is an optimum peak pressure for which efficiency is a maximum. For 40 degree crank angle duration of combustion, this peak pressure is approximately 1000 psi at 15:1 compression ratio; and increases by about 100 psi per ratio to 25:1 ratio. The efficiency increases by about 0.7% per ratio from 15:1 to 20:1 and by about 0.3% per ratio from 20:1 and by about 0.3% per ratio from 20:1 to 25:1 compression ratio. The rate of pressure rise depends critically on the shape of heat release diagram. The shorter the heat release period the higher the optimum peak pressure. Forty degrees crank angle appears to be a reasonable duration for combustion. A reduction from 40 to 25 degree crank angle results in only 2% increase in efficiency but with greatly increased peak pressure and rate of pressure rise. It is considered that for a given peak cylinder pressure, the optimum compression ratio to use from the standpoint of maximum efficiency and minimum rate of pressure rise is that which gives a compression pressure some 200-300 psi lower than the limiting pressure. It may be said that the evidence so far obtained supports the view currently held in many quarters; that mixing is the major controlling process in combustion in a diesel engine. A linear relation appears to exist between burning rate and speed so that in terms of crank angle the burning time is nearly constant within the speed ranges investigated.

The work of Tsao, Myers, and Uyehara indicated the relation of rpm and compression ratios on heat transfer and gas temperature. By obtaining the pressure and temperature at the beginning of injection, ignition delay data was obtained and correlated. The data shows that engine speed per second decreased ignition delay and that a combustion bomb is a reasonable approximation to a zero rpm engine. The work of Dr. Meurer further substantiates the influence of combustion chamber envelope temperatures on ignition delay and combustion procedure.

3. Wittek, H. L., Rosen, G.G.A. and List, Hans, "Diesel Engine Design- Past, Present, and Future," SAE Preprint, presented at San Francisco, August 1964.

In this paper, the authors outline diesel engine development from 27 January 1897 to the present time, concentrating on automotive and special application type engines. They state that today's challenge is in fields of specific output and size, to make the diesel competitive with the gasoline engine, and in noise control and exhaust emissions.

They state that friction is the factor that limits diesel engine operation to speeds below 4400 rpm. Direct injection results in lower pumping losses, less heat rejection, and less complicated heat configurations, and

requires lower compression ratios, hence would logically be the type of engine resulting in lower friction losses. The goal is 1 mm³ of injected fuel per in.³ of displacement with perfectly clean exhaust over the full speed range.

The paper goes on to describe the needs in the field, and special types of engine components that have been developed to limit peak cylinder pressures and hence, limit friction losses and reduce weight and size (and increase performance) of diesel engines.

4. Gaydon, A. G., Spectroscopy and Combustion Theory, London: Chapman and Hall, LTD., 1942.

This book contains discussion of the several ways in which spectroscopy has been applied to combustion problems, to include visible, near ultra-violet, infrared region emissions and the use of absorption spectra for following combustion processes. Also included are the applications of spectroscopy to combustion to determine the lifetimes of activated molecules, the lag in the equipartition of the energy liberated by the combustion processes, and the calculations of the heats of dissociation and thermodynamic quantities.

5. Clarke, J. S., "Initiation and Some Controlling Parameters of Combustion in the Automobile Engine," Trans. SAE, Vol. 70, 1962, pp. 240-261.

The author explains that from elementary reaction kinetics, it is known that the log of the rate of a chemical reaction varies linearly with $1/\text{Temp. Abs.}$. He quotes from the work of Elliot to show that the log of the reaction period (delay) in an engine does not vary linearly with $1/T_{\text{abs}}$. In the low temperature range, the curve for cetane is asymptotic to a slope of 33.7 kcal/mole, which is of the same order as the activation energy generally assumed for hydrocarbon combustion. In the high-temperature region of the same curve, the slope suggests an activation energy of 1.03 kcal/mole, which is far below any activation energy recorded for hydrocarbon combustion reactions. It is of the order of apparent activation energies where evaporation and diffusion are the controlling factors.

It has been demonstrated that heating of fuel and then injecting it onto a baffle in an air stream showed that spontaneous ignition could be achieved at an air stream temperature as low as 17°C with an air/fuel ratio of 10.7. Curves showing the influence of temperature, pressure, and air velocity are included in the paper.

6. Elliott, Martin A., "Combustion of Diesel Fuel," SAE Trans., Vol. 3, July 1949, pp. 491-512.

The author states that the higher speeds and outputs of modern diesel engines requires a fundamental knowledge of the physical and chemical factors of diesel combustion. He asserts that it is not possible to separate the physical and chemical aspects of the process.

The diesel combustion process is sectioned as follows by the author:

1. The delay period (physical and chemical)
2. The period of rapid combustion (wherein the accumulated fuel from the delay period burns)
3. The period of combustion controlled by injection rate
4. The period of afterburning

The combustion process is discussed as follows:

1. Physical Delay

- a. Air movement (turbulence)
- b. Droplet size (for a diameter of 10 microns or less, the time of vaporization is equal to or less than 0.6 milliseconds)
- c. Amount of available air (required for complete combustion)

2. Chemical Delay

Reaction Kinetics are discussed to include a discussion on the energy of activation. The integrated Arrhenius equation is discussed, and it is brought out that the natural log of the rate of reaction varies linearly with $1/T$. This would mean that an increase in the temperature results in an increase of the rate of reaction, e.g., increasing the temperature from 1000 F to 1300 F would result in a 100-fold increase in the reaction, according to his calculations. He further discusses the kinetic theory of gases and the steps that oxidation takes in the diesel engine—a chain reaction, with CO, aldehydes, peroxides, and hydrocarbon-free radicals as intermediate products.

3. Physical and Chemical Factors Affecting Ignition Delay

- a. Temperature: Ignition delay decreases with temperature increase, but the log of delay is not linear with $1/T$, due to the interplay of physical and chemical delays.
(Empirical formulas for the delay period of various fuels are presented).
- b. Pressure: Ignition delay is reduced by increasing pressure; the dependence on pressure being much greater at lower pressures. The effect is basically due to the partial pressure of oxygen. An empirical expression is given for chemical delay, involving both absolute temperature and pressure.

- c. Concentration of Fuel: The overall fuel/air ratio is not a satisfactory criterion, as conflicting results for minimum delay ratios have been determined. There is not data available on the minimum concentration of fuel or minimum fuel/air ratio below which ignition will not occur under conditions existing in an engine.
- d. Fuel Properties: The system of cetane numbers is explained and it is emphasized that environment is important in attaching quantitative significance to the cetane number system with reference to ignition delay periods. We need information on the effect of chemical structure on reaction rates. Low thermal stability of a fuel is associated with high oxidation rates. Some chemical additives act as ignition accelerators (such as amyl nitrate or acetone peroxide.)

4. Inflammation

This period of rapid combustion starts when a small local region has ignited and is on the verge of spreading throughout the fuel/air mixture. The mixture at this instant is very heterogeneous, and would probably contain, in any small volume, droplets of fuel, fuel vapor unmixed with air, mixtures of vapor and air, and air with no fuel. The pictures of Landen show regions of intense combustion, dark regions, etc., and also indicate the presence of extreme temperature gradients in the total combustion space (as do all of the pictures and films taken). Inflammation occurs in regions in which the local average fuel/air ratio is greater than 0.015 lb/lb. The author then continues with a rather complete discussion of the process of combustion using the results of many tests to support the text.

5. Other Factors

The author discusses the reaction velocity in relation to diesel engine knock, the effects of turbulence on inflammation, and the products of incomplete combustion. He suggests that more information is needed on the performance of fuels during the inflammation period, with particular attention to the fundamental factors affecting reaction rate. He states (postulates) that "uncontrolled" burning during the inflammation stage is controlled by: amount of fuel injected, the time of the cycle, rate of injection, duration of ignition lag, air temperature, air pressure, type fuel, turbulence, atomization of fuel, cooling of charge during cycle, load, compression ratio, blow-by, cetane number (volatility).

7. Garner, F. H., Morton, F., Nissan, A. H., and Wright, E. P., "Pre-Flame Reactions in Diesel Engines-Part I," Journal of the Institute of Petroleum, Vol. 38, 1952, pp. 301-312.

The authors used a CFR F5 diesel fuel test engine and a Crossley BVD-1 precombustion chamber engine to test the effects of various additives of diesel engine fuel. They determined that the effect of additives upon the cetane number appears to be primarily of a chemical nature, although there is the possibility that physical effects are also evidenced, say, altered surface tension of the fuel might influence break-up of the fuel spray by controlling the final droplet size. They postulate that the additive improves combustion by contributing to the establishment of conditions favoring the initiation of pre-flame reactions.

8. Garner, F. H., Malpas, W. E., Morton, F., Reid, W. D., and Wright, E. P., "Pre-Flame Reactions in Diesel Engines-Part II," Journal of the Institute of Petroleum, Vol. 38, 1952, pp. 312-343.

The results of Part I prompted the authors to investigate the pre-flame reactions of the two engines used in Part I. A gas sampling valve was developed that allowed the sampling of cylinder gases at any point in the cycle (the valve opened for 2° crank angle at any predetermined point in the cycle). The extracted gases were then sampled for chemical content. Four fuels were used in the test; a paraffinic, an aromatic, a naphtheic, and a combination paraffinic aromatic with olefins.

For all four fuels tested, peroxides and aldehydes were detected during the pre-flame period. There was a tendency for peak concentrations of aldehydes and peroxides to be associated with the point of ignition, and low concentrations (relatively) to be associated with the point of peak pressure.

The authors state that their work has established that peroxides and aldehydes are formed by the reaction of the injected fuel with the hot, compressed cylinder air--misfiring of the cylinder confirmed this. They further state that there is evidence of at least two separate reaction mechanisms in the engine; a low temperature reaction occurring during the delay period (defined as the time of injection until the point of beginning of rapid cylinder pressure rise), and a high temperature reaction occurring after ignition. The delay period reactions occur around 662°F and result in the formation of peroxides and aldehydes which reach peak concentrations at the point of ignition. Then follows a period of considerably higher temperature which results in a second peak concentration of peroxides and aldehydes. At this time, they suspect that cracking (pyrolysis) of the fuel molecules takes place.

Different fuels gave different lengths of delay period, leading the authors to speculate that the delay period in a diesel engine may be dependent

upon the extent to which peroxides may be formed. Under cold starting conditions, the formation of large amounts of aldehydes may prevent the peroxide concentration from reaching the limit necessary for auto-ignition.

9. Garner, F. H., Grigg, G. H., Morton, F., and Reid, W. D., "Pre-Flame Reactions in Diesel Engines-Part III," Journal of the Institute of Petroleum, Vol. 42, 1956, pp. 69-94.

Using improved equipment, the authors extended the investigations discussed in Part II. Their discussion contains the following information.

It is well established that in the vapor phase combustion of hydrocarbons, that oxidation reactions occur at temperatures below those required for spontaneous ignition. Ignition in the low temperature region involves the formation of peroxides and a "cool flame", while in the high temperature region peroxides play little part, and "cool flames" are absent.

With early injection, ignition is delayed because the air temperature is not hot enough at the time of injection for auto-ignition. With late injection incomplete combustion of the fuel also results in poor engine performance. The relation of pre-flame reactions is then discussed in conjunction with a discussion of early and late injection.

High concentrations of aldehydes encountered suggest that the oxidation of the fuel at low temperatures leads to a reaction in which aldehydes are formed (due to a chain reaction in which oxidation of the fuel is caused by the peroxy radical). As the reaction temperature further increases (due to compression) the aldehydes are further oxidized, ultimately resulting in essentially CO_2 and H_2O . When fuel is injected early, the effect of the reduction in temperature is to increase the delay period, permitting a marked increase in aldehyde concentration, and "using-up" some of the aldehydes by the "cool-flame" reaction, thereby lessening the efficiency of the "hot" combustion.

10. Garner, F. H., Morton, F., Saunby, J. B., and Grigg, G. H., "Pre-Flame Reactions in Diesel Engines," Journal of the Institute of Petroleum, Vol. 43, 1957, pp. 124-130.

The authors state that the combustion process in diesel engines may be investigated by two different methods:

1. Analysis of the reactants and products at varying stages during the reaction, as has been the case in their previous work.
2. A thermodynamic approach based on pressure and temperature measurements.

This paper is a study of the effects of temperature and pressure on the ignition lag controlled by varying the compression ratio and observing the effect on the point of flame arrival.

The engine, a CFR-ASTM diesel fuel test engine, incorporated a pre-combustion chamber head with a silica window that could be replaced by a metallic disc. The point of ignition then was determined either by observation with a photomultiplier unit or by the "bouncing pin" method.

Conclusions reached are essentially as follows:

1. Evaporation rate of the fuel droplets seems to be the most important factor affecting physical delay lag. The rate of evaporation is influenced by:
 - a. properties of the fuel
 - b. compression air temperatures and pressures
 - c. droplet velocity (relative to cylinder air velocity)
 - d. air swirl
 2. It was concluded that physical delay is not the controlling factor in the total delay time.
 3. The reaction between the fuel vapor and the oxygen in the cylinder may take place via several different processes:
 - a. "cool flame" ignition
 - b. hot (carbon) ignition
11. Garner, F. H., Morton, F., and Saunby, J. B., "Pre-Flame Reactions in Diesel Engines-Part V. A study of Temperature, Pressure, and Ignition Delay," Journal of the Institute of Petroleum, Vol. 47, 1961, pp. 175-193.

The effect of compression ratio on pre-flame reactions in a diesel engine have been used to give some insight into the pre-combustion reaction, and were investigated in previous work. The nature of the delay period and the effect of pressure and temperature on ignition lag were examined and compared with results obtained on rapid compression machines. However, the exact ignition temperatures could not be determined at that time due to lack of sufficient instrumentation. In this test, a two-color optical pyrometer capable of recording rapidly fluctuating temperatures was employed, and enabled accurate temperature determination. Pressure was recorded simultaneously using a capacitance type pressure pick-up. The data obtained is presented in the form of numerous curves, photographs, and tables.

The authors determined the following:

1. After injection of fuel (droplets) into the cylinder, the physical state of fuel vapor and air may consist of four zones:
 - a. the inner zone of unvaporized fuel
 - b. the second zone of vaporized fuel unmixed with air
 - c. a third zone of fuel-air mixture of variable fuel concentrations
 - d. a final zone of fuel-free air.

(Conclusions reached and presented by Elliott in 1949.)

2. A postulated theory of combustion, and the relation of cylinder temperature to the conduct of this combustion.

NOTE: The series of five papers summarized above constitutes a complete and scholarly investigation into the nature of the pre-flame reactions, and diesel combustion as a whole. The various authors were a group of chemists, engineers, and students studying at Cambridge; their work appears to be some of the best available in the literature.

12. Boerlage, G. D., and Broeze, J. J., "The Combustion Process in the Diesel Engine," Chemical Reviews, Vol. 22, No. 1, Feb. 1938, pp. 61-87.

The authors present an analysis of the diesel process essentially as follows:

1. Mixture Formation

In order to obtain small drops upon injection, the injection pressure and cylinder air density should be high, the orifice of the nozzle small, and the fuel viscosity low. The temperature of the cylinder then causes rapid evaporation of the injected droplets. However, fine atomization leads to poor overall distribution in the volume of the cylinder, and here turbulence comes into effect. In general, high wall temperatures are extremely useful to vaporize liquid droplets of fuel.

2. Self-Ignition

The vaporization of fuel causes a momentary decrease in the cylinder pressure due to abstraction of heat. However, this effect is soon overshadowed by the heat generated by chemical reaction. The delay period is defined as the time lapse from the beginning of fuel injection to either flame conditions or the beginning of rapid pressure rise. Pressure rise due to "flameless combustion" was observed in a motored CFR engine, which the authors cite in their analysis of flame nuclei propagation. They state that although turbulence promotes mixing and heat transfer to the droplets,

hastening physical delay, it also transfers heat from the nuclei of combustion and disperses the areas of mixture favorable to combustion. A graph shows that for high cetene numbers, high turbulence results in shorter delays, while for low cetene numbers, low turbulence results in shorter ignition lag. The next section is a discussion of fuels along with the then three theories of combustion.

3. Combustion Stages

- a. Delay (physical and chemical)
- b. Inflammation of fuel present at that moment
- c. Injection controlled combustion
- d. Afterburning of fuel not yet burned

4. Physical and Chemical Aspects of Combustion

- a. Inefficient mixing
- b. Deposits of liquid fuel on the combustion chamber walls
- c. Long delays resulting in lean mixture and low flame temperatures
- d. Dissociation of the flame gases, especially at high loads, reducing the maximum flame temperature
- e. Chilling of the flame near the cool (relatively) cylinder walls.

The article closes with a further general discussion of diesel engine combustion. It was apparently a classic for its time.

13. Rothrock, A. M., and Selden, R. F., "Factors Controlling Diesel Engine Performance," *Chemical Reviews*, Vol. 22, No. 1, Feb. 1938, pp. 89-106.

The paper begins with an illustrated discussion of the fuel jet as it is injected and typical nozzle configurations are covered, to include a study of droplet size distribution under various pressures. Then combustion and combustion chamber design are discussed, with emphasis on the physical distribution of fuel in the cylinder volume, illustrated with photographs. The photographs show, among other things, that the spray core disintegrates only after the spray is cut-off.

This is a much cited reference for more modern articles, but it is not too applicable to the current combustion problem.

14. Wentzel, W., "Ignition Process in Diesel Engines," NACA TM 797, June 1936.

The heating and vaporization process of fuel droplets in the CI engine is analyzed on the basis of the theory of similitude—according to which, the period for heating and complete vaporization of the average sized droplet is only a fraction of the actually observed ignition lag. The result is that

ignition takes place in the fuel vapor--air mixture rather than on the surface of the drop. The theoretical result is in accord with experimental observations of Rothrock and Waldron. The combustion shock occurring at lower thermal compression temperatures, especially in the combustion of coal tar oil, is attributable to a simultaneous igniting of a large fuel vapor volume formed prior to ignition.

A ponderous expression relating factors affecting the heating and vaporization process of a fuel droplet is developed in the text, followed by a section where the various parameters used in the expression are calculated (c_p , c_y , etc.). Vaporization of droplets due to injection is discussed, including that the initial ignition does not show up on the indicator card because of the heat of vaporization of the spray core. The ignition lag, however, is defined as the period that exists from the start of injection until there is a visible pressure rise on the indicator card. The author further points out that there might be a chemical delay as a part of the overall ignition delay.

The remainder of the paper discusses the various referenced test results in an attempt to compare the author's analysis with them. He further explains the reason for rapid combustion (detonation) when ignition lag is long.

15. Alcock, J. F. and Scott, W. M., "Some More Light on Diesel Combustion," SAE Paper 872A, presented at the Summer Meeting, Chicago, June 1964.

This paper discusses the process of combustion, as revealed by high speed photography, in a small, high speed diesel engine. Two direct injection type engines and one pre-chamber type engine were investigated, and selected combustion sequences are both reproduced and discussed in the paper.

General conclusions reached as a result of this study are as follows:

1. In small engines, much of the fuel strikes the chamber wall and moves along it.
2. Swirl is greater than has hitherto been supposed, and squish is much less.
3. Most of the flame is of the carbon-rich diffusion type
4. Soot from very rich mixtures is always formed at high loads, but it can burn later in the cycle, leaving a clean exhaust.
5. Combustion knock does not seem related to the total fuel in the combustion chamber on ignition, but is rather related to the amount of fast burning mixture present.

General Comments:

1. Direct measurement of air/fuel mixture velocities was not accomplished by the "tracers" employed in an attempt to do so were thrown out of the mixture by centrifugal forces.

2. Most flame velocities are under 400 ft/sec., and this is much less than detonation or shock waves, which leads them to believe that normal diesel knock is not detonation.

3. Spray velocities change little with an increase of engine speed.

4. Flame velocities normal to the swirl (radial velocities in the direct injection chambers) are also roughly independent of engine speed, but the circumferential velocities are roughly proportional to engine speed.

5. With normal delay, little of the heat release seems due to pre-mixed combustion, as evidenced by comparison of the pressure rise and the luminous flame curves.

6. Near TDC, the rate of change of pressure is roughly proportional to the rate of heat release.

7. Flames observed in the early stages of combustion are believed due to complete combustion, not partial oxidation of the fuel particles.

8. Ignition usually occurs in fine spray blown off the fuel jets or splashed off the wall. It seems that the multiple flame nuclei are connected by "hot" flames from fuel not completely vaporized.

9. The peak temperatures of the carbon flame appear to be approximately 4532°F, hence the effects of radiation in engine heat transfer would be significant.

10. There is a visible carbon flame at high loads to about half stroke, then the color fades to red as the cylinder contents are cooled.

11. Diesel knock does not seem related to detonation as the flame velocities are too low. Knock, which appears dependent on the amount of fuel in the chamber, might be controlled by rationing the amount of fuel injected before ignition.

16. Tsao, K. C., Myers, P. S., and Uyehara, O. A., "Gas Temperatures During Compression in Motored and Fired Diesel Engines," Trans. SAE, Vol. 70, 1962, pp. 136-145 and 154.

The authors used a modified CFR engine with a slot cut across the top of the piston to provide an unobstructed optical path through the combustion chamber during the entire engine cycle. Access to the interior of the engine was obtained through use of sapphire windows installed in the cylinder wall to transmit radiation from the source and gases. The "null method" of infrared temperature measurement was used, employing an optical pyrometer.

The data reported was based on the rapid increase in temperature as the criteria for the end of the delay period. Operating variables were engine speed and compression ratio for motored cycles; intake air pressure and temperature, fuel quantity per cycle, engine speed, and fuel cetane number for the firing cycles.

Motored Engine Data Conclusions

1. Effect of speed on compression temperature: The temperature increases as speed increases, due to the induction work done on the gas during the intake process. The rate of change levels off at higher engine speeds (above 2000 rpm). Temperatures ranged between 1480-1700°R for a 15.8 CR, 600-1800 rpm, and 1320-1530°R for 12.5 CR, 300-1800 rpm.

2. Effect of engine compression ratio: Compression temperatures are higher at the higher compression ratios. The conclusion is drawn that heat transfer is greater at the higher CR due to increasing surface/volume ratio (and greater temperature differential) as observed by contrasting computed vs. observed curves (computed polytropic compression with $n = 1.394$).

Fired Engine Data and Correlation with Ignition Delay

1. Compression temperature is higher due to higher inlet air temperature.
2. The compression temperature increases with engine speed, but the curves begin to level off around 15-1800 rpm. Higher inlet temperatures result in a greater rate of temperature rise than lower inlet temperatures due to less time for heat transfer.
3. Ignition delay is shorter for higher compression temperatures and, for points where compression temperatures are the same, ignition delay is less for the higher engine speed. Bomb data for the same fuel and compression temperatures has about double the lag time, and curves for the bomb data are much steeper (the effect of temperature rise decreases delay time more rapidly until the curves meet at about 1550°R).

4. Generally, more fuel injected per cycle decreased the delay until at a point approaching full load, the delay began to increase.

5. Higher intake pressures reduced the delay somewhat; more on a percentage basis in the engine than in the bomb, which is perhaps caused by the increased turbulence within the engine. The temperatures were little affected as the p_i/p_e ratio was increased, but rose slightly.

6. When compression temperatures and pressures at the point of injection held constant, an increase in engine speed reduced the absolute delay time but the delay in terms of crank angle degrees increased.

17. Taylor, C. F., Taylor, E. S., Livengood, J. C., Russell, W. A., and Leary, W. A., "Ignition of Fuels by Rapid Compression," Quarterly Transactions of the SAE, April 1950, pp. 232-274.

A rapid compression machine was built by the authors in the Sloan Laboratory. It used a charge of nitrogen at 500 psi to rapidly compress a homogeneous charge of fuel and air in the cylinder of the device, causing the charge of fuel and air to self-ignite. A window was provided for pictures. Fuels were generally of the type used in SI engines (benzene, heptane, and n-butane for a special study). However, compression ignition caused combustion of the fuel, hence test results should be applicable to diesel combustion study.

The following were some of the conclusions reached:

1. Autoignition occurs at a higher temperature (and pressure) if the rate of compression is increased.
2. Delay period decreases with increases in temperature and pressure.
3. The mixture affects duration of delay period and the intensity of the resultant "explosion".
4. The reaction starts from many points (usually) and is progressive. A correlation exists between the rate of inflammation and the rate of pressure rise in the corresponding pressure-time record.
5. Most of the flame photographs show that the reaction is not very homogeneous—great numbers of small luminous spots are formed, and these spots persist for long intervals with surprising stability in size and shape. It has been established that these spots are not due to the presence of fuel droplets.
6. Autoignition of n-heptane is relatively rapid, benzene is relatively slow, and iso-octane is intermediate.

18. Stinson, Karl W., ed. Diesel Engineering Handbook, 11th ed., N.Y.: Diesel Publications, Inc., 1963.

Chapter 5, pp. 41-49.

This section is a general discussion of combustion in the I.C. engine; however, the bulk of material is concerned with diesel combustion. The combustion process is divided into four phases; the delay period, the period of rapid combustion, the combustion of the remainder of the charge as it is injected, and the afterburning period.

The delay is composed of the period of physical mixing of the fuel droplets with cylinder air (physical delay) and the chemical delay period, which includes preflame oxidation in localized regions (temperatures from 1000 to 2000°F), the catalytic effects of the wall surfaces, the high temperature of the mix, and miscellaneous particles from the last cylinder charge, plus cracking of the fuel vapors to produce materials with a high percentage of carbon.

The various factors that affect the delay period are discussed, to include engine design, type of fuel, etc. Factors that reduce delay include reduction of droplet size injected, increased air temperature of inducted air charge, increased pressure of air charge in the cylinder, greater turbulence of the air in the cylinder, and a higher cetane number of fuel used. Curves supporting the above factors are included in the discussion.

19. Wilson, Grover C., "Development and Application of Automotive Fuels, Gasoline and Diesel," SAE pamphlet SP-137, Engineering Know-How in Engine Design, Part 3, 1955, pp. 21-24.

Section I of the above reference is a discussion of diesel engine combustion, included in the article so that a thorough discussion of diesel fuels might be based on this information. The topics discussed include cetane rating, the ignition delay period (including curves), and the various factors influencing the delay period. These factors include the physical delay due to formation of fuel-air mixture in the cylinder, the "pre-flame" and "cool-flame" reactions, effects of pressure and temperature on the chemical delay, and a discussion of camera and bomb studies current at the time.

20. Olson, D. R., Meckel, N. T., and Quillian, R. D., Jr., "The Operation of CI Engines on Wide Boiling Range Fuels," Trans. SAE, Vol. 70, 1962, pp. 551-569.

Some of the conclusions reached by the authors are as follows:

1. Ignition delay and average rates of pressure rise are highly correlated to fuel properties and can be satisfactorily predicted from linear multiple regression equations.
2. Maximum combustion pressure is poorly correlated with fuel properties and depends primarily upon engine design and conditions of operation.
3. Except for the Hercules pre-combustion chamber engine where ignition delay was relatively insensitive, the delay period and rates of pressure rise increased with a decrease in cetane number.
4. Under maximum load conditions (greatest amount of fuel injected), the maximum combustion pressures and average rates of pressure rise increase as the delay period increases.
5. Under minimum load conditions (1000 rpm) the maximum combustion pressure decreases with an increase in the delay period as a result of combustion occurring late in the expansion stroke.

BOMB EXPERIMENTS

21. Hurn, R. W. and Hughes, K. J., "Combustion Characteristics of Diesel Fuels as Measured in a Constant-Volume Bomb," Quarterly Trans. SAE, Jan. 1952, pp. 24-35.

The technique employed in this investigation utilized single-shot injection of a metered quantity of fuel into an externally heated reactor containing air under pressure. With the arrangement, including instrumentation, ignition delay, rate of pressure rise, and other effects were observed or calculated for the combustion of the injected fuel under any given circumstances.

Since few fuels exhibit a well-defined point at which rapid combustion may be said to begin, ignition lag was defined as that interval of time between the start of rapid fuel injection and the time at which the original pressure in the bomb is restored by heat released by the burning fuel. Temperature limits and pressure limits in the area of study were 850-1050°F and approximately 275-675 psig, respectively.

It was noted that ignition lag increased with a decrease in pressure, due most probably to (1) less conductivity between heated air charge and injected fuel and (2) cooling effect of the injected fuel is greater at lower pressures hence lowering the bomb initial pressure and temperature. At a certain point, $T = 1000^{\circ}\text{F}$, ignition delay increased with an increase in pressure, attributed to (1) less favorable spray development at the higher pressures, and (2) quenching action of N_2 as the N_2/O_2 ratio was increased due to increase of total pressure, the partial pressure of O_2 being maintained constant by the use of artificial atmospheres. The results show, however, that the ignition lag is greatly influenced by the available O_2 , and greater pressures must increase the availability of O_2 .

Curves are presented for pressure-temperature-ignition lag relationships (see Taylor and Taylor). Volatility and the type of fuel (base stocks) were also studied in their effects on ignition lag, as well as the relation of cetane numbers. It was found that for cetane numbers above 44 there were no appreciable decreases in ignition lag (there was discernable difference however).

22. Selden, R. F., "Auto-Ignition and Combustion of Diesel Fuel in a Constant-Volume Bomb," NACA Report 617, 1938.

The variations in ignition lag and combustion associated with changes in air temperature and density were studied for a diesel fuel in a constant-volume bomb. The highest temperature approximated that obtained in the CI engine operated in the usual range of advance angles. The test air densities ranged from something less than compression density in an engine with normal aspiration to a value corresponding to a considerable boost. Density varied between 0.59-1.48 lbm/ft.³ and temperature ranged from 870 to 1255°F. Ignition lag in this study was defined as the period from the start of injection to the first evidence of a pressure increase over that exhibited by the motored engine.

Conclusions reached by the author are as follows:

1. For fuel injection into a constant-volume bomb containing stagnant air at a temperature and pressure equivalent to those existing in the CI engine, the ignition lag was essentially independent of the injected fuel quantity and was of the same magnitude as in the engine.
2. For the fuel used, the possible decrease in the ignition lag for a given increase in air temperature or density became quite small at temperatures and densities in excess of those generally occurring in CI engines.
3. The combustion efficiency improved as the ignition lag was lengthened, hence it should be worthwhile to use those fuels in an engine whose ignition lag corresponds to the higher permissible rates of pressure rise. The "useless afterburning" decreased as the ignition lag was lengthened.
4. The ignition lag tended to increase and the maximum rate of pressure rise definitely decreased upon the addition of inert gases to an air charge of fixed concentration.

NOTE: Although the conclusions reached by the author do not seem to be applicable to the current problems of diesel combustion, the basic information and curves contained in the article are deemed among the best presented by the various authors.

23. Cohn, M. and Spencer, R. C., "Combustion in a Bomb with a Fuel-Injection System," NACA Report 544, 1935.

Fuel injected into a spherical bomb filled with air at a desired density and temperature could be ignited with a spark a few-thousandths of a second after injection, an interval that is comparable with the ignition lag experienced by the CI engine. The effect of several variables on the

extent and the rate of combustion was investigated. Time intervals between injection and ignition of $3-6 \times 10^{-3}$ seconds (and one of 5 minutes), initial air temperatures of 212-482°F, initial air densities of 5, 10, and 15 atmospheres, and air/fuel ratios of 5-25 were investigated.

The 5-minute interval between injection and spark permitted the fuel to vaporize completely, which served as a control to those parts of the experiment where ignition followed injection after a short time. An increase in temperature decreased the reaction time for both short and long periods, but increased the extent of combustion for only the short-period mixtures. For the long period mixture, increasing the air density lengthened the reaction time, but decreased it for the short period mixtures at pressures of 5 and 10 atmospheres. However, at 15 atmospheres pressure, the reaction time for the short period charge increased.

Conclusions

From the results obtained it must be concluded that the extent and rate of combustion of a fuel injected in the liquid state, particularly at low air temperatures and densities, are dependent upon the distribution and the condition of the fuel at the moment of ignition. At high air temperatures and densities, a marked similarity exists in the course of combustion of liquid fuel injected into the bomb and ignited immediately and that of a fuel allowed to vaporize completely before ignition.

24. Hurn, R. W., Chase, J. O., Ellis, C. F., and Huges, K. J., "Fuel Heat Gain and Release in Bomb Autoignition," Trans. SAE, Vol. 64, 1956, pp. 703-711.

All data reported were obtained through testing with a constant volume combustion bomb, as temperature and pressure control considerations were more easily handled with this type of test "set-up". Heat transfer between the injected fuel and the gas medium in the bomb were calculated from pressure data by common thermodynamic relationships. Heat release data were calculated by comparing pressure-time curves that resulted from the injection of fuel into an oxidizing atmosphere to that obtained by injection into an inert atmosphere.

A primary objective was to determine how fuel volatility affects vaporization and heating of the fuel.

Conclusions reached as a result of bomb testing include the following:

1. The heat absorbed within a given time interval increases in the same order as the thermal conductivities of the gases, and decreases with increase of gas densities (the rate of heat absorption increases with increased diffusivity of the gas).

2. The rate of heat absorption is not materially influenced by the quantity of fuel injected except during the terminal period of heat transfer.

3. Higher gas temperatures result in higher rates of heat transfer.

The data show that chemical heat release occurs only after an appreciable interval of time during which the fuel is heated and may be partly or wholly vaporized. The rapidity of this heating and associated ignition delay are influenced markedly by the physical properties of the surrounding gas. Fuel volatility and chemical structure have relatively little influence on the rate of heat transfer to the fuel in the pre-reaction period. It is also shown that the delay period before release of chemical energy and the rate of chemical energy release are influenced both by the chemical composition of the fuels and by gas-to fuel heat transfer rates during the pre-reaction period.

25. Michailova, M. N. and Neumann, M. B., "The Cetene Scale and the Induction Period Preceding the Spontaneous Ignition of Diesel Fuels in Bombs," NACA TM 813, Dec. 1936.

The authors attempted to define a process of determining cetene numbers of diesel fuels using a combustion bomb because of the high cost of the Waukesha engine at that time in the USSR. They calibrated the bomb with mixtures of cetene and 1-methyl naphthalene (mesitylene). In so doing, they observed that the cetene numbers obtained in such a manner were some 5 to 10 units lower than they should have been.

It was established that the effect on the induction period (delay) changes little at pressures and temperatures above 1022°F and 294 psia. The authors further determined that for cetene numbers above 50, changes in length of delay period are insignificant with further changes of cetene number.

The tests were conducted in a metal bomb heated by a nichrome spiral; fuel was injected from a Bosch jet using a special plunger pump. The delay criteria are not included in the report. The amount of fuel injected corresponded to a coefficient of excess air of 1.7 at 308.5 psia and temperature of 1076°F. The bomb wall temperatures ranged between 1067-1184°F.

26. Voinov, A. N., "Combustion and Carburation in Diesel Engines," FTD-TT63-31, Foreign Technology Division, Air Force Systems Command, 1963.

Experiments were conducted using a single cylinder, double acting engine (bomb), fed a homogeneous mixture of air and fuel, the engine assembly heat stabilized by means of water jackets filled with an organic silicon coolant. Special attention was paid to a precise estimate of the compression temperatures

and pressures as the author believes that they are the basic parameters of determining ignition conditions. Mixtures of fuel and nitrogen were used for the determination of pressures and temperatures in conjunction with a "resistance thermometer," piezo-quartz pressure sensor, and a multi-slit photo recorder. The pressures and temperatures that produced ignition were determined at 5° ATDC.

Results from the experimentation with a variety of fuels showed that there is a definite "low-temperature region" characteristic of each fuel where ignition is in greater measure determined by the temperature than by the pressure, but at a certain point, the picture reverses. When the temperature is further raised, the pressure-temperature relation is again changed (plot of $\log p$ as a function of $1/T$), but the instrumentation could not yield accurate results.

Various mixtures of fuel and excess air demonstrated that at low temperature and high pressure, the greatest inclination to autoignition is exhibited by mixtures near stoichiometric with pronounced pressure minimums. When the temperature is raised, the minimums smooth out and are displaced in the direction of rich mixtures. The tendency to ignite is with high temperatures and rich mixtures for given pressures.

The author separates ignition of homogeneous fuel-air mixtures as follows:

1. Point pre-ignition occurring at extremely small (point) foci, which results in the propagation of fronts of turbulent flame (as in spark ignition).
2. Space autoignition in certain volumes of finite size propagating with considerably higher velocities (100-300 m/s) than in 1.), with weak primary shock waves. The flame front is not well defined.
3. Explosive or "quasi-detonational" ignition, with shock waves, accompanied by propagation of flame front at supersonic speeds.

The experimental results indicated that the type of autoignition experienced was dependent on the pre-ignition process temperature. As delay time became shorter due to higher pressures and temperatures, ignition progressed from type 1) to type 3) as described above.

At first inspection, the indicator diagrams gave the impression that with a rise in the temperature of combustion, the ignition delay increased and that the intensity of the cold flame reaction dropped. However, replots of the data in the form of relative increase of absolute pressure over current compression pressure with delay plotted on the dependent variable axis shows that there is a hot flame at some unchanged value of relative

pressure rise. "Critical values" of relative increase in pressure in the pre-ignition stages remain constant for various mixtures of the same fuel and appear independent of pressure and temperature.

"Practical conclusion": The most favorable conditions for the origin of volume autoignition (detonation) are realized by no means in the hotter portions of the charge. The ignition in the hotter portions occur first, but is of a point nature. In the colder parts of the charge, the pre-flame processes are delayed in development, but then proceed most rapidly with the higher pressures created by the pressure rise within the cylinder.

Conclusions

1. The tendency towards autoignition is not closely associated with the composition of the mixture.
2. At low temperatures of compression, the stoichiometric mixture ignites most easily (at lowest pressure), while at high temperature, the rich mixture exhibits the maximum tendency towards autoignition. In the range of low temperatures, ignition is dependent mostly on the pressure.
3. When there is no "cold flame", or only a slight one, ignition is of a point nature.
4. Volume autoignition is aided by a mixture uniform in temperature, high in pressure, and with a fuel of relatively low combustion temperature, and with weak heat transfer from the reacting mixture. At high temperature, and with greater heat transfer from expansion, ignition of even fuels prone to detonation acquires a point nature.
5. Volume autoignition never starts near a hot surface (where ignition is of a point nature), just as it does not start near a flame front propagating from a spark.

NACA COMBUSTION APPARATUS TESTS

27. Rothrock, A. M., "The NACA Apparatus for Studying the Formation and Combustion of Fuel Sprays and the Results from Preliminary Tests," NACA Report 429, 1932.

This paper describes in detail the NACA apparatus built at the Langley Memorial Aeronautical Laboratory for the study of the formation and combustion of fuel sprays under conditions closely simulating those occurring in the then high speed diesel engine. The results of many of the NACA tests published were a direct result of experimentation with this apparatus.

Preliminary conclusions presented by the author are as follows:

Although the tests, the results of which are presented in this report, were conducted primarily to determine the range of usefulness of the apparatus, there are a few conclusions that can be drawn from the photographs.

1. The reproducibility of the fuel sprays under the same test conditions was satisfactory.
2. High air temperatures slightly decrease the penetration and increase the dispersion of the fuel sprays.
3. Air velocities of approximately 300 ft/sec in the combustion chamber have a decided effect on the penetration and dispersion of the fuel sprays from single hole orifices.
4. The effect of the air velocity on the fuel spray is dependent on the number, arrangement, and size of the discharge orifices.
5. The physical properties of the fuel have an important effect on the dispersion and penetration of the fuel sprays.
6. The rate of combustion of the fuel spray can be decreased by forcing ignition to take place before injection is completed.
7. Ignition can be forced to take place before injection is completed by increasing the temperature of the cylinder and the combustion chamber water jackets.

28. Rothrock, A. M. and Waldron, C. D., "Effects of Air-Fuel Ratio on Fuel Spray and Flame Formation in a Compression-Ignition Engine," NACA Report 545, 1935.

In this test, high-speed motion pictures were taken at the rate of 2,500 frames per second of the fuel spray and flame formation in the combustion chamber of the NACA combustion apparatus (5.0 in. bore x 7.0 in. stroke, 13.2:1 CR, 1500 rpm). The engine was motored to the test speed, and then a single charge of fuel was injected (with jacket and fuel temperatures held relatively constant). An optical indicator was used to obtain the pressure-time relationship in the combustion chamber. The air/fuel ratio was varied from 10.4-365:1. Definite stratification of the charge was observed in the combustion chamber at the higher ratios, even though moderate air flow was present. The start of burning relative to the fuel sprays was not affected by the air/fuel ratio, nor was the flame spread greatly affected by the ratio. Flame spread, after the point of maximum cylinder pressure was reached was relatively slow.

The paper contains excellent pictures of the injection and inflammation process, clearly showing the multiple points of flame propagation observed by so many investigators.

29. Rothrock, A. M. and Waldron, C. D., "Some Effects of Injection Advance Angle, Engine-Jacket Temperature, and Speed on Combustion in a Compression-Ignition Engine," NACA Report 525, 1935.

An optical indicator and a high speed motion picture camera capable of operating at the rate of 2,000 frames per second were used to record simultaneously the pressure development and the flame formation in the combustion chamber of the NACA combustion apparatus. Tests were made at engine speeds of 570 and 1,500 rpm. The engine jacket temperature was varied from 100-300°F and the ignition advance angle from 13° after TDC to 120° BTDC. An accumulator type injection system is used to inject fuel through the nozzle into the cylinder. Ignition lag was defined as the time interval between the start of injection and the start of pressure rise caused by combustion as shown on the indicator card. Excellent reproductions of picture frames are included in the paper as well as numerous data curves.

Conclusions reached by the authors are as follows:

1. The ignition lag in an engine with a quiescent combustion chamber should be decreased to that value required to prevent objectionable rates of pressure rise. The ignition lag should not be decreased to less than this value because by so doing the effectiveness of the combustion is decreased.

2. With a short ignition lag in a quiescent combustion chamber the burning starts in the spray envelope and from there spreads throughout the combustion chamber. With a long ignition lag the burning may start at any point in the chamber. In either case the burning may start at one point or simultaneously at several points.
 3. The course of the combustion (aside from the original chemical properties of the fuel) is affected by:
 - a. the time interval between the start of injection and the start of combustion
 - b. the temperatures and pressures existing in the combustion chamber during this time interval.
 - c. the temperature and pressure of the air and the distribution of the fuel at the start of combustion.
 4. In case the ignition lag is too long, it may be decreased considerably by increasing the temperature of the engine coolant.
 5. If the ignition lag is short, increasing the temperature of the engine coolant decreases the ignition lag sufficiently to decrease the rate of pressure rise but may in some cases decrease the effective combustion of the engine.
30. Gerrish, H. C. and Voss, F., "Influence of Several Factors on Ignition Lag in a Compression-Ignition Engine," NACA TN 434, Nov. 1932.

An investigation was made to study the influence of fuel quantity, injection advance angle, injection valve opening pressure, inlet-air pressure, compression ratio, and engine speed on the time lag of CI single-cylinder engine, as determined by an analysis of indicator card diagrams. Injection lag was considered to be the interval between the start of injection, as determined with a Stroborama and visually observing fuel spray, and the start of effective combustion, as determined from the indicator card, this being the point where 4.0×10^{-6} lbm of fuel had been effectively burned. The NACA universal test engine was used in the studies.

The conclusions (or observations) made in reference to the above stated test objectives are as follows:

1. Fuel quantity: at constant speed for some advance angle and rate of injection, from 1.2×10^{-4} to 4.1×10^{-4} lbm of fuel injected had no appreciable effect on delay (ignition lag).
2. Injection advance angle: increases or decreases of lag time are observed according to whether density, temperature, or turbulence are the controlling influence.

3. Valve opening pressure (pressure on fuel being injected): ignition lag time increased with increase of injection pressure.
4. Inlet air pressure: the lag decreased linearly (almost) with an increase in inlet air pressure. However, temperature was not held constant, as the compressor had no after cooler.
5. Compression ratio: the lag was decreased by increasing the compression ratio.
6. Engine speed: the ignition lag decreased with increasing engine speed.

The report presents the above trends in the form of curves, but gives only a superficial explanation as to why the various results were obtained.

SPRAY FORMATION AND FUEL VAPORIZATION

31. El Wakil, M. M., Myers, P. S., and Uyehara, O. A., "Fuel Vaporization and Ignition Lag in Diesel Combustion," Trans. SAE, Vol. 64, 1956, pp. 712-729.

In this paper, correlation of theoretical analysis with experimental data from both combustion bomb and diesel engine tests is presented. Previous known experimental facts concerning ignition lag are presented as follows:

1. An increase in inlet air pressure and temperature, in fuel temperature, and in jacket water temperature all decrease ignition lag to varying degrees.
2. Ignition lag decreases with engine speed. This is generally attributed to an increase in turbulence with speed. However, it has been found that in bomb experiments, that increased turbulence does not give a decrease in ignition lag. Probably actual compression temperatures increase with speed.
3. There is a reasonably good inverse relationship between the cetane and octane scales. Since ignition delay in a SI engine is predominately chemical, octane number would presumably be related to chemical delay. This would indicate that the chemical delay was rate-determining.
4. While fuel volatility seems to affect ignition lag, the accompanying change in fuel structure seems more important. For example, iso-octane and n-heptane have markedly different ignition lags, but about the same volatility, while cetane and iso-octane are markedly different in both volatility and ignition lag.
5. Small concentrations of additives affect ignition lag. Although they possibly affect spray formation and physical delay, it seems more likely that they act in a chemical manner.
6. In a constant-volume bomb with everything else held constant, an increase in quantity of fuel injected increases ignition lag if combustion begins near the end of injection. This would indicate a fuel cooling or a concentration effect.

Paper conclusions are as follows:

1. It seems almost certain that adiabatic saturation is approached closely in the spray core. As distance from the spray center increases, the air-fuel mix becomes progressively leaner with consequently higher air-vapor temperatures. Under these conditions adiabatic saturation is approached less rapidly. At the extreme edge of the spray a few single droplets will almost certainly be found.
 2. The closeness and rate of approach to adiabatic saturation conditions varies with distance from the spray core in a different manner for fuels of different viscosities and volatilities.
 3. A volatile fuel does not receive heat that much more rapidly than a non-volatile fuel, as would be expected from differences in their volatility.
 4. Under adiabatic saturation conditions, a non-volatile fuel has as good a chance, or better, to achieve the combination of temperature and vapor/air ratio required for self-ignition and rapid combustion.
 5. Physical delay is not a negligible portion of total ignition delay. It may, in fact, be larger than the chemical delay.
 6. Injection delay may not be of negligible magnitude in an operating engine.
 7. While there are some differences in the way in which different fuels receive heat during spray break-up, major difference between fuels of varying cetane number lies in the manner in which they release chemical energy during the very early reactions.
 8. For the same fuel, total physical and chemical delays are smaller in an operating engine than in a combustion bomb operated at the highest temperature estimated to exist in the engine.
32. Yu, T. C., Uyehara, O. A., Myers, P. S., Collins, R. N., and Mahadenan, K. M., "Physical and Chemical Ignition Delay in an Operating Diesel Engine Using the Hot-Motored Technique," Trans. SAE, Vol. 64, 1956, pp. 690-702.

Studies of combustion flame temperatures in diesel engines at the University of Wisconsin had not shown much difference between fuels. Thus, it was decided to make a detailed study of the pressure change occurring during ignition delay.

Ignition delay parameters are as follows:

1. Pressure
2. Temperature
3. Composition of compressed gases
4. Rate of injection
5. Vaporization of injected fuel
6. Rates of reaction of vaporized fuel

Because of the small magnitude of the pressure changes being studied (a maximum of 13 psi with the peak firing pressure about 1000 psi), the reproducibility of the engine, instrumentation, and techniques was of special interest.

Conclusions generated as a result of the testing are as follows:

1. There are small differences between fuels either in injection lag or in spray break-up time.
 2. Once spray break-up is accomplished there are small differences in the rate at which fuel sprays receive heat from the compressed air. A volatile fuel does not seem to receive heat more rapidly than a non-volatile fuel.
 3. The larger the cetane number, the smaller the peak value of the change in pressures between the fired and the unfired cycles.
 4. Once spray break-up has occurred there is appreciably more variation in the rate of early chemical reactions than there is in rate of fuel vaporization.
 5. Vaporization of fuel on a weight basis does not seem to be much more than half completed by the time rate of heat evolution due to chemical reaction exceeds the absorption of heat due to vaporization.
33. Mullins, B. P., "Bubble-Points, Flammability Limits, and Flash Points of Petroleum Products," Combustion Researches and Reviews, eds. B. P. Mullins and J. Fabri, London: Butterworths Scientific Publ., 1957.

Relationships between the bubble-points,* flammability limits, and flash-points of a fuel have been demonstrated numerically for four hydrocarbon fuels

*The "bubble-point" of a hydrocarbon fuel is the temperature at which equilibrium exists between the wholly condensed fuel and an infinitesimal quantity of its vapor mixed with air in the ratio 1/R. When R is zero, the condition is known as the normal bubble point, or, in the case of a single pure hydrocarbon, the boiling point.

ranging from aviation spirit to gas oil. The mean molecular weights of the fuels vapors at the bubble-points have been computed and several nomographic methods of presenting corrected bubble-point data are outlined with examples.

Weak and rich flammability limits in air of the four fuels were calculated over a range of static pressures. The weak limit curve represents the conditions of the closed flash-point test and so by differentiation of the curve, a flash-point pressure correction factor was obtained for each fuel. Excellent agreement between theoretical and measured values was found in all cases and a simple general rule for estimating flash points is given. Work includes data for pressures up to 10 atm. (Paper is primarily concerned with prediction of conditions relative to safe storage of the fuels tested).

34. Holfelder, O., "Ignition and Flame Development in the Case of Diesel Fuel Injection," NACA TM 790, March 1936.

The process of ignition and combustion in the case of spray injection into heated air was investigated. Pictures were taken of the spray (500/sec) while temperatures and pressures were recorded simultaneously on oscillograms. The delay period was ascertained by a comparison of the pictures taken and the pressure trace on the oscillograph. Different nozzles and fuels were used in a cylinder with no turbulence. Precombustion chambers were investigated.

Conclusions are essentially as follows: The variation of the pressure (rise) in the cylinder depends on the ignition timing and the manner of combustion, which depends on fuel, mixture ratio in cylinder, and physical and chemical changes before combustion. The author contends that only a portion of the charge is vaporized, and that this vaporization process is equivalent to a cracking process, which is not desirable. Also, he contends that in addition to partial vaporization, oxidation of the hydrocarbons yields unstable peroxides, the oxidation of which favors ignition.

The report includes an extensive description of the test equipment. Other test "set-ups" are criticised. The basic parts used were a MAN diesel cylinder with window, an electric air pre-heater, special camera, and dynamometer-motor combination. The procedure used was to heat the air to 750-840°F, then compress it to 367-440 psia, and then inject the fuel. The pictures, taken with the aid of a strobe lamp, are quite clear.

Conclusions. The combustion of fuel sets in at some intermediate condition between liquid and gaseous phases, starts mostly at the spray edge, and where atomization is unusually fine. The author refutes the idea that complete or extensive atomization takes place before ignition. After combustion has started, injected fuel burns immediately upon injection into the combustion chamber. Higher temperatures shorten the ignition lag more effectively than great air density.

Tests with a precombustion chamber showed that the preheated chamber produced combustion that had the energy (almost) of a detonation, and was very effective in the main chamber. It was estimated that the flame front entered the main chamber at a velocity of about 82 ft/sec.

35. Meckel, N. T. and Quillian, R. D., Jr., "CIE Fuel—Low Temperature Influence on Injection and Combustion," SAE paper No. 656A, Jan. 1963.

The paper describes a study to define the influence of low temperatures (to -65°F) on CI engine fuel injection characteristics and resulting effects on engine combustion phenomena.

At high engine operating speeds, viscous fuel formed a normal spray pattern. As viscosity was increased, the fully developed spray penetration increased, and the cone angle decreased. Higher viscosity did not change injection timing with unit injectors, but did with the plunger pump system.

The data show that effects of low fuel temperatures on engine combustion were minor. Spray characteristics at cranking and low speed operation may contribute to marginal combustion at low temperatures. The study indicates that standard analytical techniques may not adequately predict low temperature fuel performance.

36. Gerrish, H. C. and Ayer, B. E., "Influence of Fuel Oil Temperature on the Combustion in a Prechamber CI Engine," NACA TN 565, April 1936.

Results of experimentation showed that heating the fuel oil to 750°F increased the injection period, changed the rate of injection, and eliminated the spray core. Engine tests showed that the ignition lag, rate of pressure rise, and maximum cylinder pressure were reduced. The IMEP, fuel economy, and thermal efficiency were slightly increased. Operation of the engine was smoother, the exhaust cleaner, and carbon formation less than when the fuel was heated to only 124°F .

Because the theoretical constant pressure cycle is more efficient than the constant volume cycle, the experiment attempted to reduce the ignition lag through fuel heating so that ignition could be controlled by the injection rate. All changes observed were slight.

The ignition lag was defined as the period between the start of injection and the time when 4.0×10^{-6} lbm of fuel was effectively burned as determined by analysis of the indicator card.

37. Nagoo, F. and Kakimoto, H., "Swirl and Combustion in Divided Combustion Chamber Type Diesel Engines," Trans. SAE, Vol. 70, 1962, pp. 680-696.

This paper is a study, using photos taken by the authors, of the swirl and combustion characteristics of the divided combustion chamber type diesel engine. The authors were most interested in the physical mixing of the injected fuel in relation to air swirl, and the various effects of piston cavity configuration, wall temperatures, and the various types of "pre-combustion" chamber configurations on combustion in the divided type chamber engines.

DROPLET BEHAVIOR

38. Barman, G. L. and Johnson, J. H., "Single Drop Theory Used to Appraise Injection Against Swirl in Diesels," SAE Journal, Vol. 71, April 1963, pp. 57-60.

Conclusions

1. Air motion induced by the spray must be included in calculations. This induced air motion increases spray penetration.
2. If the spray axis is directed into the squish area, the motion of the fuel droplets is but little affected by squish. Fuel vapor motion may, however, be much affected by squish.
3. Injection of fuel droplets against the swirl is less likely to cause impingement of the drops on the cylinder wall than would radial injection, but "piling-up" of the drops may occur, causing locally rich mixtures, with possibilities of smoke and slow burning.

Discussion

The above conclusions are based on computations, made with various simplifying assumptions with respect to the interaction and behavior of fuel droplets and the air motion in the cylinder. Curves (polar plots) illustrating the paths calculated are included, for swirl ratios of 10:1 an engine speed of 1800 rpm, and a mean droplet size of 0.001 to 0.004 in diameter.

39. El-Wakil, M. M., and Abdan, M. I., "Ignition Delay Analyzed from Self-Ignition of Fuel Drops," SAE Journal, Vol. 71, April 1963, pp. 42-45.

Conclusions

An experimental and theoretical study of the self-ignition of individual drops of pure hydrocarbons subjected to air streams at high temperatures and atmospheric pressure shows that:

1. The lengths of the physical and chemical ignition delay periods are generally comparable, although the physical delay becomes relatively less than the chemical delay at higher airstream temperatures for the more volatile fuels.

2. Physical, chemical, and total ignition delays are shorter, the more volatile the fuel, the smaller the initial diameter of the drop, and the higher the initial drop liquid and airstream temperatures. The difference between fuels of different volatilities becomes less important however, at the higher airstream temperatures.
3. The flame persisted for a short period of extra time after the liquid had completely evaporated, in almost all cases.
4. Two distinct types of flame were observed. One, occurring at low airstream velocities, was a diffusion-type flame, which usually started at the lower end of the drop and then surrounded the drop completely. The other, called a detached flame, and occurring in the case of high airstream velocities, started and stabilized itself in a narrow plane above the drop. The height of this plane was a function of airstream velocity. It varied between one and three inches. The airstream velocity at which transition from diffusion to detached flame occurred was determined for volatile and non-volatile fuels over a wide range of air temperatures. It is believed that the transition velocity is a function of the flame velocity. It increased with air temperature, but was rather insensitive to fuel volatility, especially at low air temperatures.

Because ignition in the case of the detached type of flame occurs at higher values of Reynolds number than is expected in the much smaller droplets in actual combustors, and because it does not lend itself to the boundary layer analysis that was used in this study, the analysis was restricted to diffusion type flames.

Discussion

In general, total ignition delay increases with increasing number of carbon atoms in the molecule, that is, as the fuel volatility decreases. Cooling of the core of the injected spray affects the ignition delay in actual engines. Empirical correlations for diffusion-type flames based on data of the physical investigation were obtained for physical and total ignition delay in seconds.

40. El-Wakil, M. M., Uyehara, O. A., and Myers, P. S., "A Theoretical Investigation of the Heating-Up Period of Injected Fuel Droplets Vaporizing in Air," NACA TN 3179, 1954.

This report presents a detailed study of the unsteady-state portion of the total vaporization time of single fuel droplets injected into air. Calculations were performed for numerous combinations of fuels, initial droplet radii, temperatures and velocities, air pressures and temperatures.

When fuel is injected into a stream of moving air, it leaves the injector nozzle first as a ligament or sheet after which this ligament or sheet breaks down into different size droplets originally moving at the same speed. If the velocity of these droplets is higher than the air velocity, then they start slowing down relative to the air, with the smaller droplets slowing down faster, and penetrating a lesser distance while losing their mass faster and earlier along their travel path. The mass of vapor given away by each droplet is carried along with the air through the combustion chamber. To this vapor is continuously added the vapor given away by the larger droplets that have been formed later in time but that reached that point because of their more rapid and greater penetration. The total amount of fuel vapor present at a certain cross section of the combustion chamber therefore consists of the total vapor given away by all the drops before reaching that cross section.

Much more discussion is presented relative to droplet motion and mass transfer. The work is primarily oriented towards conditions existing in the combustor of a gas turbine engine, but is applicable to conditions in the diesel engine cylinder.

Some conclusions (deductions) reached by the authors are essentially as follows:

1. For the same fuel, the unsteady state becomes relatively larger in magnitude with respect to the total vaporization time the higher the air temperature.
2. For the same temperatures, the unsteady state is relatively larger in magnitude with respect to the total vaporization time the higher the volatility of the fuel.
3. High volatility fuels have lower wet bulb temperatures for the same air conditions.
4. At relatively low air temperatures extremely low volatility fuels have wet bulb temperatures close to the air temperatures and spend only a very small portion of their vaporization time in the unsteady state. At high air temperatures however, the difference between the air and wet bulb temperatures increases.
5. For any one fuel the wet bulb temperature is higher the higher the air pressure or temperature.

Numerous curves were generated as a result of the theoretical analysis. In order to confirm the conclusions reached, experimentation was conducted, and the results are contained in the paper.

41. Wright Air Development Center Technical Report 56-344, ASTIA Document No. AD 118142, "Injection and Combustion of Liquid Fuels," Battelle Memorial Institute, March 1957.

Chapter 18 - Droplet Combustion, by A. Levy

The combustion process in a liquid fuel-vaporized fuel-air mixture is far more complex than that in a homogeneous fuel-air mixture. Part of the combustion may take place between the vaporized fuel and extremely small droplets, and the air, and fuel in large droplet form may burn as individual diffusion-type flamelets. The discussion of the burning of droplets is therefore introduced by a short review of the information in Chapters 4 and 10 on some of the effects of the size distribution of the droplets. The various theories of droplet combustion, which are closely related to theories of evaporation, are then considered. The chapter is concluded with a review of the experimental results on flammability limits and propagation rates in fuel mists, and the effect of the physical properties of fuel sprays in flame stability limits in high velocity streams.

Studies of droplet combustion disclose the two parts of combustion delay, the physical delay of evaporation and the chemical delay associated with pre-flame reactions. Three combustion zones occur in such a process:

1. There is the preflame zone where intermediate oxidation products are formed. Cool-flame radiation from the activated formaldehyde occurs here also.
2. There is the flame front where the fast reaction occurs. The delay here is a function of the temperature, pressure, and reaction mechanism.
3. There is the main flame where the unevaporated fuel eventually vaporizes and ignites. This flame region depends upon the drop-size distribution for its total flame length. To date, there has not been sufficient effort placed on the burning in this last region.

A mathematical analysis of the burning rate yields the conclusions that to increase the burning rate it is necessary to:

- a. increase the flame temperature
- b. decrease reaction zone thickness, that is, increase diffusion rate of the fuel, or increase reaction rate, or decrease the radius of the drop.
- c. increase the thermal conductivity
- d. decrease the latent heat of evaporation of the fuel.

The effect of turbulence on droplet combustion would probably be to increase the rate of combustion due to additional heating by convection. However, in the case of small droplets, turbulence would not be likely to have a large effect, since the relative velocity of the air would not be very much greater than that of the drop, and would tend to move the drop with it. Burning times for kerosene droplets with diameters of 10 to 50 microns is estimated to be in the range of 10^{-5} to 10^{-4} seconds, and 50 to 100 microns roughly in the range of 10^{-4} to 10^{-3} seconds.

Chapter 19 - Diffusion Flames, by A. Levy and A. A. Putnam.

Combustion in an atmosphere containing products of combustion, to some extent, either through the combustion process proceeding, or through incomplete scavenging, has a large effect on the efficiency of the over-all combustion process:

1. A sharp lowering of the flame temperature, especially in rich mixtures where more oxygen is needed for complete combustion. A corollary to this is the reduced efficiency in the evaporation of the fuel spray.
2. Cracking and polymerization is increased. Ordinarily, a certain amount of cracking occurs in the primary zone. This is actually beneficial, since the cracking produces volatile hydrocarbons. But the lack of oxygen reduces the benefit of the cracking and permits more polymerization.
3. The limits of flammability are reduced.

Note: Although this publication is primarily directed towards gas turbine combustion, since the combustion in the combustor is of the fuel-injection, heterogeneous mixture process, much of the basic research, findings, and theory are applicable to diesel combustion.

HEAT RELEASE DURING COMBUSTION

42. Lyn, W. T., "Study of Burning Rate and Nature of Combustion in Diesel Engines," Ninth Symposium (International) on Combustion, New York: Academic Press, 1963, pp. 1069-1082.

The burning rates in diesel engines are studied in detail and the rate-controlling factors are examined in this paper. Chemical kinetics based on activated collision could not play a part because otherwise the whole process would be very temperature sensitive, and this is not consistent with results obtained from experimental investigation, according to the author. The temperature drop during the expansion stroke would demand a drop in burning rate far greater than is shown by experiment, while the proportional increase in burning rate with engine speed cannot be accounted for by the small increase in cycle temperature. The major factors affecting the burning rate are injection rate, engine speed, and combustion chamber design, all of which directly affect mixing. The burning processes in a direct injection diesel engine generally may be divided into three phases as follows:

1. 1st Phase: The premixed part of the fuel jet burns with a non-luminous flame, and this phase exhibits the highest burning rate. It lasts for only 5-7° of crank angle rotation.
2. 2nd Phase: In this phase about 80% of the heat is released in a period of some 40° crank angle rotation, and the burning rate exhibits a general decay—this phase is characterized by a diffusion flame.
3. 3rd Phase: This low rate burning may last throughout the remainder of the expansion stroke and contributes only some 10% of the total heat released. The nature of the combustion is not clear, at present.

In order to obtain data for this investigation, a single cylinder, direct injection engine (4.5 in. bore x 5.5 in. stroke) is instrumented so that the rate of injection may be calculated from needle lift (orifice area) and pressure drop across the orifice, while burning rate is calculated from measured cylinder pressure and engine geometry. A second engine, equipped for Schlieren photography, was used to study air movement and combustion control through variation of compression temperatures and pressures.

The paper discussed in detail the affects of combustion chamber design, and postulates on the source of the heat released in the "tail" of the heat release (burning) diagram as well as the effects of load, speed, and timing on the burning rate within the cylinder.

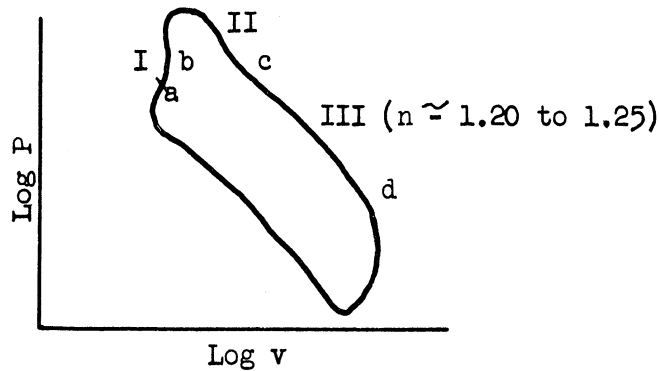
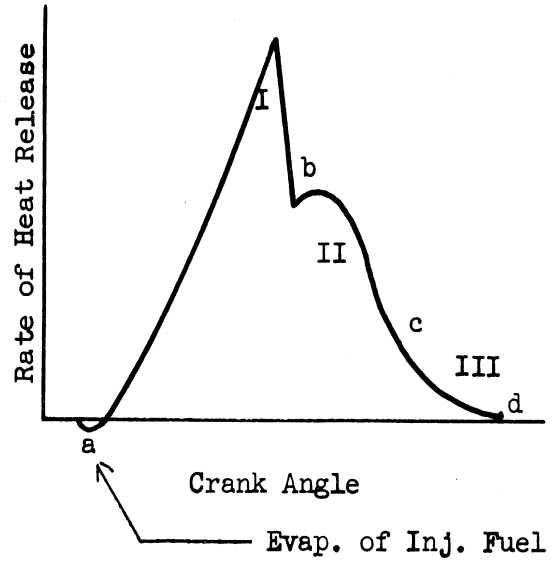
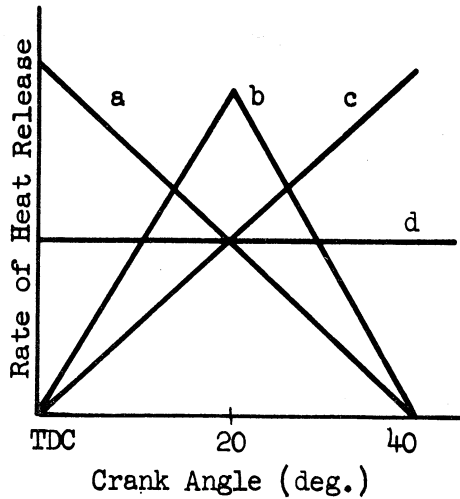
43. Austen, A. E. W., and Lyn, W. T., "Some Steps Toward Calculating Diesel Engine Behavior," Trans. SAE, Vol. 70, 1962, pp. 526-550.

The authors desire to perfect ways of predicting the behavior of diesel engines from given engine geometry to obtain optimum performance of the engine and to determine the injection equipment that will give the desired performance. They developed a means of calculating the injection characteristic (fuel flow vs. crank angle diagram) from the injection equipment geometry, completely described in other papers. A (Leo) computer program has been developed, and the correlation between the predicted and observed performance is quite close.

In this study, the authors investigated the relationship between the rate of heat release and the shape of the cylinder pressure diagram and cycle efficiency. Since little is known about the form of heat release diagrams of actual engines, or the amount of heat transferred during the combustion period, it was decided to assume some simple geometrical forms of rate-of-heat-release and then calculate the resultant cylinder pressure, cycle efficiency, rate of pressure rise, and peak pressure. Various simplifying assumptions are made to facilitate the calculations. Calculated curves presented relate cylinder pressures as function of crank angle and timing of injection for the various heat release diagrams chosen. In addition, curves are presented for cycle efficiency, maximum pressure, and rate of pressure rise for various compression ratios.

Conclusions reached are as follows:

1. Late timing generally results in a reduction of both maximum pressures and rate of pressure rise, most pronounced with a sloping rate of heat release (b. or c.).
2. Cycle efficiency increases with advanced timing.
3. Peak pressure and maximum rate of pressure rise increase with an increase in compression ratio.
4. For a given heat release diagram, there is an optimum peak cylinder pressure above which no gain in efficiency can be expected.
5. In general, optimum peak pressures for 15:1, 20:1, and 25:1 CR's are 1000, 1500, and 2000 psi respectively.
6. There is little advantage to be gained by burning fuel in a period shorter than 40 degrees of crank angle.



Other conclusions and/or observations are presented. Comparison with actual engine test shows good correlation with the theoretical calculations. If the heat release diagram were known specifically for a given engine, much could be predicted. Optimum heat release would be within 40 degrees crank angle rotation, with the peak pressure maintained to the end of the heat release period (which is not a physical possibility, as described).

The authors then attempted to determine the relation between injection characteristics and the heat release diagram desired. An engine and photography were used in this phase of the project, in conjunction with the previous calculations. Their results show three phases of combustion:

1. The initial phase, with a high rate of heat release (5 deg.)
2. A gradually decreasing rate of heat release (40 deg.) with some 80% of the heat released in this phase.
3. The "tail", with small, but distinguishable rate of heat release.

Although the rate of pressure rise should theoretically increase with the amount of fuel evaporated and mixed during the delay period, the experimentally determined points do not accurately portray this as they are quite scattered. An ultimate objective of this work was to predict the cylinder-pressure diagram. Because the test results were almost unbelievably close, in order to support their work, the authors have formulated an "interim" hypothesis of the combustion process, which is essentially as follows:

1. The first period is burning of homogeneous mixtures found locally within the cylinder (non-luminous).
2. The second period consists of jets of fuel burning as turbulent diffusion flames (predominantly displaying radiation from carbon particles).
3. The "tail" of the combustion process is the burning of small carbon particles, the unburned part of which join (condense or coagulate) when cooled during exhaust to form smoke.

The above paper was essentially a formulation of information contained in the following papers, plus other information current at that time.

44. The Institution of Mechanical Engineers, Proceedings of the Automobile Division, 1960-61.

1. Knight, B. E., "Fuel-Injection System Calculations."
2. Lyn, W. T., "Calculations of the Effect of Rate of Heat Release on the Shape of Cylinder-Pressure Diagram and Cycle Efficiency."
3. Austen, A. E. and Lyn, W. T., "Relation Between Fuel Injection and Heat Release in a Direct-Injection Engine and the Nature of the Combustion Process."
4. Priede, T., "Relation Between Form of Cylinder-Pressure Diagram and Noise in Diesel Engines."

"M-SYSTEM" OF COMBUSTION

45. Meurer, J. S., "Evaluation of Reaction Kinetics Eliminates Diesel Knock-the-M-Combustion System of MAN," Trans. SAE, Vol. 64, 1956, pp. 250-272.

According to the author, there are two phenomena in diesel combustion that cause the most trouble and which we desire to eliminate:

1. Combustion noise, a more or less intense knocking depending on the fuel properties.
2. Exhaust smoke which develops before excess air is fully used up.

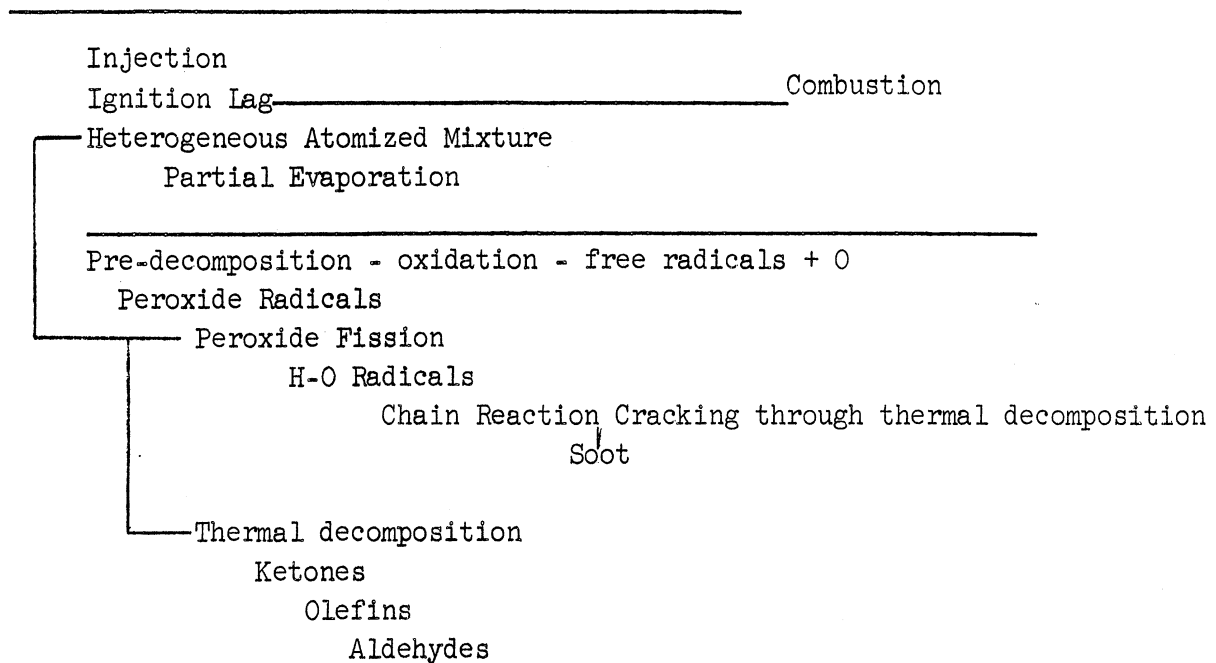
Reaction kinetics provide the basis for deriving a few rules to observe in order to eliminate the above characteristics of diesel combustion:

1. Minimize the portion of fuel involved in autoignition
2. Allow fuel to oxidize gradually and try to heat fuel and air together
3. Mix fuel and hot air fast enough to effect a stoichiometric air/fuel ratio before ignition starts, and make sure no more fuel is mixed at any time than can burn with a permissible pressure rise.

The author then analyzes his engine design to show how it accomplishes the above objectives by injection of a film of fuel onto the wall of the combustion chamber (dome of the piston) with consequent vaporization of the fuel due to the combined effects of heat transfer to the fluid film from the hot wall surface and air velocity due to swirl of the inducted air, imparted by a masked valve.

46. Meurer, J. S., "Multifuel Engine Practice," Trans. SAE, Vol. 70, 1962, pp. 712-728.

The combustion process in a diesel engine is represented as follows by the author:



High compression temperatures and ratios are needed to produce a sufficiently rapid molecular decomposition of the fuel which tends to slow down excessive reaction rates because the surface of injected droplets has a tendency to be enriched with oxygen. This leads to a surprisingly high initial rate of combustion which is even higher than for homogeneous gas mixtures. The oxygen enrichment on the droplet surface leads either directly to peroxide formation at the interface around the droplet, or certain free radicals which are formed during the oxidation process which adsorb another oxygen molecule forming peroxides. Since peroxides are unstable and tend to form free radicals (particularly under the prevailing pressure and temperature conditions), the development of rapid chain reactions cannot be avoided. The heat from the initial spontaneous reactions overheats those parts of the fuel droplets which did not participate in the initial oxidation which leads to cracking of the original fuel molecules into molecules with smaller numbers of carbon atoms, exhibiting small reaction rates and leading to soot formation. The initially rapid reaction is sustained by fuel molecules whose reaction rates are continuously decreasing due to decomposition. Thus, the diesel engine "molds" its fuel in such a way that the initially explosive reactions are subsequently converted into slow combustion, at the expense of smoke in the exhaust.

47. Hussmann, A. W. and Maybach, G. W., "The Film Vaporization Combustor," Trans. SAE, Vol. 69, 1961, pp. 563-574.

The author first compares the two present methods of preparing the air/fuel mixture for use in an internal combustion engine; the carburetion

process which renders a premixed flame comparable to a bunsen burner flame, and the injection of atomized fuel droplets resulting in a diffusion flame. He then notes that premixed flames are essentially free from formation of solid carbon particles as intermediate combustion products, while diffusion flames produce a considerable amount of carbon in the intermediate stages of the combustion process. If the combustion zone of the idffusion flame is sufficiently large and hot, and if sufficient oxygen is available, then the carbon will burn. If the diffusion flame is quenched, or if not enough oxygen is present, then smoke and carbon deposits will result, the amount dependent on the fuel used.

He states that the ideal mixture formation is the intimate molecular mixing of hydrocarbon molecules with the oxygen molecules in the combustion air. With the finest fuel atomization possible, a droplet of only 50 microns in diameter still contains about 2×10^{14} molecules of fuel ($M = 196$).

The "M-System" of combustion is then reviewed, and the application of this system to turbine combustor combustion is discussed, along with the advantages and disadvantages of this application. The specific problems of fuel vaporization are discussed, and are essentially as follows:

1. The attachment of liquid films onto the inside wall surfaces - in the presence of high velocity gas streams...
2. The spread of such films
3. The stability behavior of such films
4. The problem of simultaneous heat transfer and mass transfer between a high temperature, high velocity gas stream and the liquid film (there is an optimum temperature for wall surface, slightly above the vaporization temperature of the main fuel fraction; higher temperatures not only slow down the rate of evaporation due to the Leiden frost phenomenon but may lead to partial cracking of overheated fuel vapors and consequently slower rates for later combustion).
5. Flame stability.

"Blue flame" combustion could be maintained for air/fuel ratios of 42-67:1 for air pressures in of 30 psia and 50-75:1 for air pressures of 40 psia. The air temperature in the 345°F. If the combustion products were recirculated beyond a critical time in the combustor, the flame would become strongly luminescent, showing that the fuel vapors were being cracked, hence slowing down the combustion reaction.

ACCUMULATOR NOZZLE SYSTEM

48. Hooker, R. J., "Orion, A Gas-Generator Turbocompound Engine," Trans. SAE, Vol. 65, 1957, pp. 293-330.

The objectives of designing the accumulator nozzle system are as follows:

1. To reduce the duration of fuel injection into the cylinder for a given quantity of fuel.
2. To isolate from the injection process the influence of the volume of tube between pump and nozzle.
3. To increase the fuel pressure, on which control of injection is dependent, without overloading the pump-drive mechanism.
4. To increase initial fuel-flow rate so that a greater percent of fuel might be burned at a constant combustion-chamber volume.
5. To eliminate pump delivery valves.
6. To enable use of an eccentric cam.
7. To extend the pumping over a larger camshaft angle.
8. To eliminate the need for a leak-off line.
9. To use somewhat smaller injection tubes since the charging rate is much reduced.

The principle of operation of the accumulator system is that the stored energy in the compressed fuel provides the potential energy for injection of the fuel into the combustion chamber. As the pump plunger reciprocates through the total stroke as indicated, the helix at the top of the plunger will cover the filling-line hole, trapping a volume of fuel. The trapped volume of fuel is a function of the angular position of the helix. As the plunger continues to lift, the fuel is pumped through the injection line into the nozzle body. Pumping continues until the spill edge at the bottom of the plunger matches the spill hole, at which time the pressure is relieved in the plunger-barrel volume and the injection line.

Initially, the spring holds the needle on its seat at the nozzle tip, and the cuff on its seat at the nozzle top. When pumping starts, the cuff

is lifted from its seat, and fuel flows into the nozzle body; in accordance with the compressibility, the pressure of the fuel within the nozzle is increased. When fuel delivery is interrupted by spilling of the injection lined, the cuff returns to its seat retaining the pressure within the nozzle. Since the fuel pressure times the area is greater than the spring force, the needle is thereby forced upward opening the spray orifice for the injection of the fuel.

Flow continues until the pressure within the nozzle body is less than that required to overcome the spring force, at which time the needle closes. The cycle is then complete and ready to be repeated.

While the quantity per injection is a function of the plunger angular position, the beginning of injection is controlled by the position of the "spill edge" on the plunger.

The objectives above were all obtained with this nozzle. There is only one critical dimension that has to be closely controlled—the lift of the needle. The peak injection pressure used was about 14,000 psi, but pressures well over 20,000 psi have been tested. It can be stated that this nozzle does not require the preciseness of quality control that other nozzles need. They were operated on all 14 cylinders of the Orion project for several hundreds of nozzle hours.

NOTE: A schematic of the system, a photograph of the actual nozzle parts, and a graph of the pressure-time relations in the operating system are shown on page 317 of this reference.

ENGINE WALL HEAT TRANSFER

49. Overbye, V. D., Bennethum, J. E., Uyehara, O. A., and Myers, P. S., "Unsteady Heat Transfer in Engines," Trans. SAE, Vol. 1961, pp. 461-494.

The authors have performed an extensive engineering analysis of unsteady heat transfer through the cylinder wall of a spark-ignition engine. However, the work is just as applicable to the diesel engine. In addition to the theoretical analysis there is extensive test work presented in an attempt to correlate theory with actuality.

The most pertinent conclusions are presented as follows:

1. The maximum heat transfer rates in unsteady heat transfer may differ by as much as a factor of 20 when they are compared with the steady-state values, i.e., the amount of heat actually reaching the coolant per unit time. This clearly indicates that considerable heat is transferred from the gases to the wall during combustion and expansion and then is transferred back to the gases during intake and compression.
2. It appears that greater harm due to deposits, that is, decreased volumetric efficiency and high gas temperatures during compression would occur primarily in connection with nonhomogeneous deposits, but this requires further investigation. Also, the chemical structure and boiling points, plus additives of fuels significantly influences the thermal characteristics of engine deposits.
3. Deposits greatly affect the rates of heat transfer to the cylinder walls.

TURBOCHARGER EFFECTS

50. Hull, W. L., "High-Output Diesel Engines," Trans. SAE, Vol. 72, 1964, pp. 68-78.

The author attempted to simulate the effects of a turbocharger on a direct injection diesel engine by controlling intake manifold pressure and exhaust back pressure by means of electrically operated valves and building air pressure. The engine used was a Caterpillar single cylinder test engine, converted to direct injection (4.5 in. bore x 5.5 in. stroke, 15.45:1 CR).

The author stated that the energy in the exhaust gas which drives the turbocharger depends on the exhaust gas temperature, assuming that the gas enthalpy is only a function of temperature. Then, by computation, he was able to construct a plot of turbine pressure ratios vs. compressor pressure ratios for lines of various constant temperatures. It was shown that at low exhaust temperatures that the turbine must operate at higher pressure ratio than the compressor, hence the engine operates under a back pressure that is greater than the intake manifold pressure, with efficiencies assumed as follows:

Turbine.....	75%
Compressor.....	70%
Mechanical Losses.....	5%

It was determined that as intake manifold pressure was increased from 30 to approximately 90 in. Hg. abs., Fmep was little affected, but both Bmep and Imep increased linearly almost 200% (Bmep from 120—302 at 2400 rpm with aftercooling simulated to 200°F, for example).

Curves are presented that illustrate the results of the tests; exhaust temperature, maximum cylinder pressure, and time rate of pressure rise are plotted with Bmep as the independent variable for both 1800 and 2400 rpm. It is interesting to note that although the higher pressure boosts produce the higher maximum pressures, as is to be expected, the lower pressure boosts yield the greater rates of pressure rise and higher exhaust temperatures for the same values of Bmep.

51. Tausz, J., and Schulte, F., "Determination of Ignition Points of Liquid Fuels Under Pressure," NACA TM 299, Jan. 1925. (A translation from German reference).

This is one of the earliest references found showing the relation of pressure to ignitability of gasoline, gas oil, and benzene. The plots show

that increase in absolute pressure reduces the ignition temperature of these fuels.

52. Wolfer, H. H., "Ignition Lag in the Diesel Engine," (Der Zundverzug im Dieselmotor," VDI Forschungsheft No. 392, 1938, pp. 15-24.

In this classic publication experimental work was conducted in a special bomb so arranged that an inner liner comprising most of the bomb inner wall could rotate. This made it possible to have injection occur into a rapidly rotating charge in the bomb, thus simulating the charge motion of a diesel engine chamber. The work appears to have been done very carefully, and good results were obtained.

The influence of various factors was investigated in two bombs. The experiments were partly verified in an engine. The ignition lag is strongly influenced by air pressure and temperature, the ignition lag being reduced as either is increased. An equation is presented below, which relates the ignition lag, temperature and pressure.

The ignition lag was also influenced by the following:

1. Excess air quantity
2. Shape of chamber
3. Fuel injection pressure
4. The geometry of the fuel orifice
5. Turbulence
6. Fuel temperature if less than 100°C

Wolfer presented the following equation from his studies, for fuels having a cetane number greater than 50:

$$Z = \frac{.44}{p^{1.19}} (e)^{\frac{4650}{T}}$$

where

Z = ignition lag

p = absolute pressure at end of compression, in atmospheres

T = absolute temperature at end of compression, centigrade

e = base of natural logarithms.

A three-dimensional plot of these variables is shown in the paper.

53. Bassi, A., "Experimental Investigations into Diesel-Engine Injection Systems," Sulzer Technical Review. Research Number, 1963.

One portion of this paper presents the results of a study of ignition delay and combustion phenomena in large Sulzer engines, (900 mm bore), for heavy fuel oil, and gas oil.

The equation of Wolfer (Ref. 52) was generally verified but the constant of .44 was modified for the fuels used. Based on the Sulzer engine tests, the constant was found to be 0.38 for gas oil and 0.482 for heavy oil.

This engine work, however, shows a relatively good correlation with the bomb work of Wolfer, since Wolfer's general constant for fuels in his bomb having a cetane number greater than 50 lies between the values for heavy oil and gas oil determined in a large engine cylinder.

54. ASME Publication, "Diesel Fuel Oils, Production Characteristics and Combustion," 1948. 128 page Booklet; Lectures of 19th ASME Oil and Gas Power Conference, 1947.

A series of three lectures and discussions. Chapter four on combustion of diesel fuel oils was given by Martin Elliott. This is a good review of the subject.

SECTION 2

PROGRESS REPORT NO. 2

PRELIMINARY WORK ON:

- a. Combustion Instrumentation
- b. Accumulator Fuel Injection System

THE UNIVERSITY OF MICHIGAN
COLLEGE OF ENGINEERING
Department of Mechanical Engineering

Progress Report

DIESEL ENGINE IGNITION AND COMBUSTION

Jay A. Bolt
Kenton C. Ensor

ORA Project 06720

under contract with:

U. S. ARMY
DETROIT PROCUREMENT DISTRICT
CONTRACT NO. DA-20-018-AMC-1669T
DETROIT, MICHIGAN

administered through:

OFFICE OF RESEARCH ADMINISTRATION ANN ARBOR

September 1965

TABLE OF CONTENTS

	Page
LIST OF FIGURES	84
OBJECT	85
INTRODUCTION	86
PART I. DEVELOPMENT OF ENGINE INSTRUMENTATION FOR COMBUSTION STUDIES	87
Introduction	89
Description	89
Air Flow Control	89
Combustion Measurements	94
PART II. THE ACCUMULATOR FUEL INJECTION SYSTEM	97
Introduction	99
Description of the Injection System	99
Test of an Accumulator System	102
Testing of Accumulator System	102

LIST OF FIGURES

Figure	Page
1. Photograph of Nordberg engine.	91
2. Photograph of test cell and instrumentation.	92
3. Oscilloscope traces to determine engine ignition delay.	96
4. Schematic of accumulator injection system.	100
5. Diagram of accumulator system as built for bench testing.	103
6. Photograph of bench rig—accumulator injection system.	104
7. Performance characteristics of accumulator injection system.	106
8. Transient pressures at nozzle of accumulator injection system.	107

OBJECT

The object of this investigation is to learn more about the influence of engine variables on ignition delay and combustion phenomena in an engine cylinder, especially under the conditions corresponding to very high supercharge.

INTRODUCTION

There is military interest in diesel engines which can operate with very high supercharge pressures; an engine intake air pipe pressure of 5 atmospheres can be considered as an objective. A supercharge pressure of 5 atmospheres for an engine of 10:1 compression ratio will result in a cylinder air pressure at the time of fuel injection of approximately 1800 psi, with a corresponding air temperature of approximately 1700°R.

This project was initiated to investigate ignition and combustion phenomena attending these high pressures and temperatures in an engine cylinder.

The approach during the first year, covered by this progress report, has been threefold, as follows:

1. To conduct a literature survey to more clearly establish the present state of the art of diesel ignition and combustion as it relates to wide ranges of air pressure and temperature.
2. To begin the assembly of engine equipment and instrumentation for the observation and measurement of combustion phenomena in a single cylinder engine, and to make initial measurements of such items as ignition, in preparation for later work.
3. To make tests of a bench rig of an accumulator-type fuel injection system which would be adaptable to use with a one-shot (one firing cycle) operation of the test engine. Such a system also has the possible merit of being capable of a wider range of maximum to minimum injection quantity, and thus have advantages for a highly supercharged engine.

The bibliography listed under item 1 above is presented in ORA Report No. 06720-1-P.

The progress in preparing the engine and test equipment together with preliminary combustion observations is contained in Part I of this report.

The work done with the accumulator fuel injection system is presented in Part II of this report.

PART I

DEVELOPMENT OF ENGINE INSTRUMENTATION FOR COMBUSTION STUDIES

INTRODUCTION

During the first year of the project the object has been to assemble engine equipment and instrumentation, and to develop techniques and personnel capability for studying the combustion process in a diesel cylinder. This has been done with a single-cylinder Nordberg engine. Within the next year this engine will be replaced with a new high output single-cylinder research engine to be supplied by the U. S. Army for the research program.

DESCRIPTION

The equipment has been assembled around a one-cylinder Nordberg engine, Model 4FS1, of 4-1/2 in. bore by 5-1/4 in. stroke with a displacement of 83.5 in.³ This engine has a Lanova-type combustion chamber. The engine is shown on Fig. 1, with some of the auxiliary equipment. The engine equipment falls into two categories—control and measurement of air flow to the engine, and measurements related to the combustion process.

AIR FLOW CONTROL

Provision has been made to supply the engine with air at any pressure from 0 to 3 atmospheres and any temperature from 75 to 450°F with a mass flow rate from 0 to 485 lb/hr. By later modification of the air measuring system at least 5 atmospheres of engine air supply pressure can be provided.

The laboratory compressed air is used to supply the engine through a critical flow air meter as shown in Fig. 2, item 7. The critical flow design was selected as it permits accurate air flow measurements regardless of downstream pressure fluctuations caused by the one-cylinder engine and also provides an easy means of supplying and controlling the air supercharge pressure. The air meter consists of four critical flow orifices piped and valved together in such a manner that any or all of the orifices can be used to supply the engine. The upstream air pressure can be regulated to give any engine inlet air pressure or air flow desired within the range of the air meter. The air meter was built and calibrated to +1.0% accuracy in The University of Michigan laboratories. Calibration curves for the orifices have been plotted and copies are available for use.

1. Nordberg model 4FS1 engine
2. Instrumentated injector
3. Provisions for solar cell and pressure pickup in head (hidden)
4. Exhaust surge tank
5. Intake surge tank
6. Intake air heater
7. Back side of critical flow air meter
8. Back of dynamometer console

Fig. 1. Photograph of Nordberg engine.

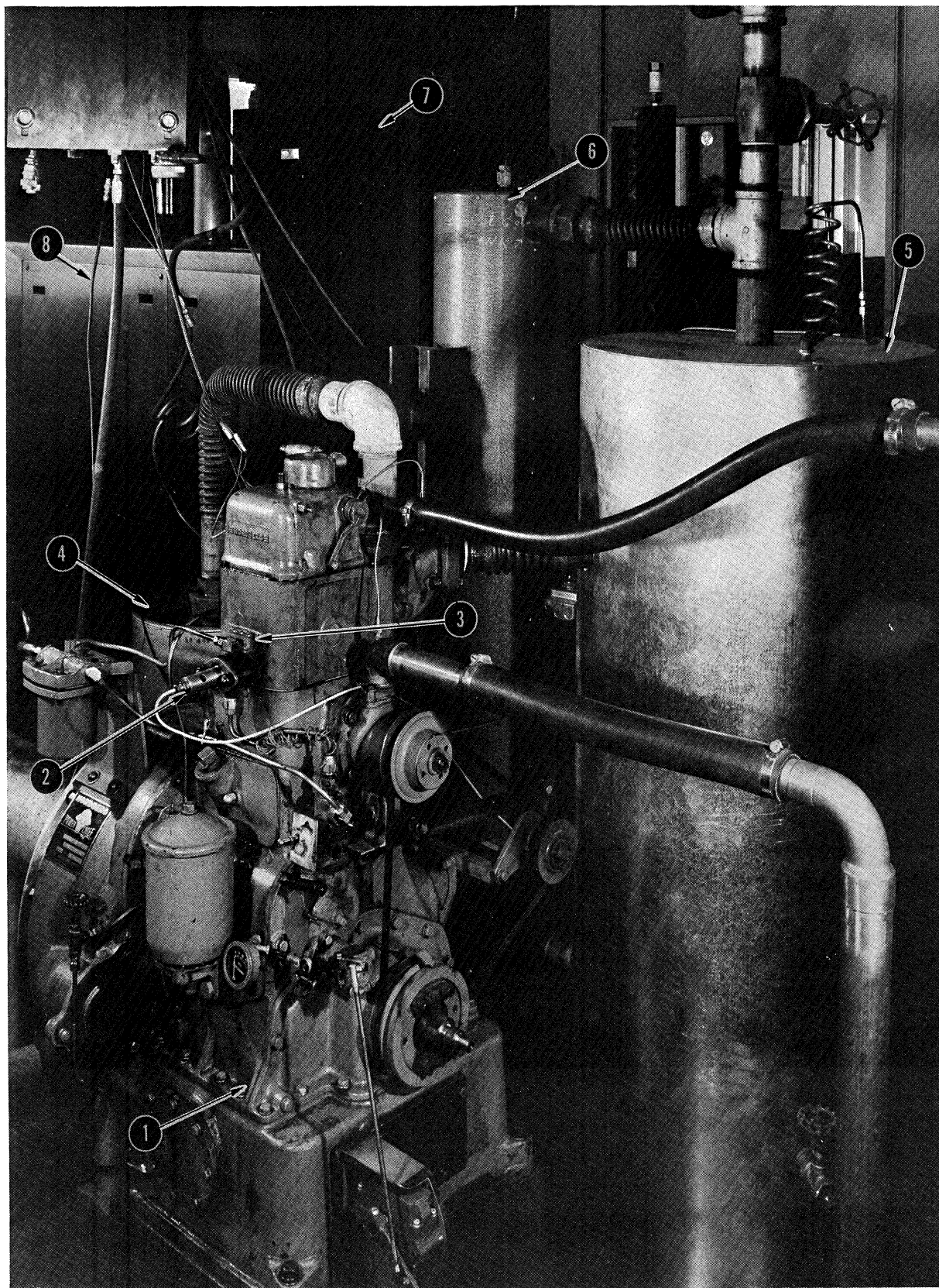


Fig. 1

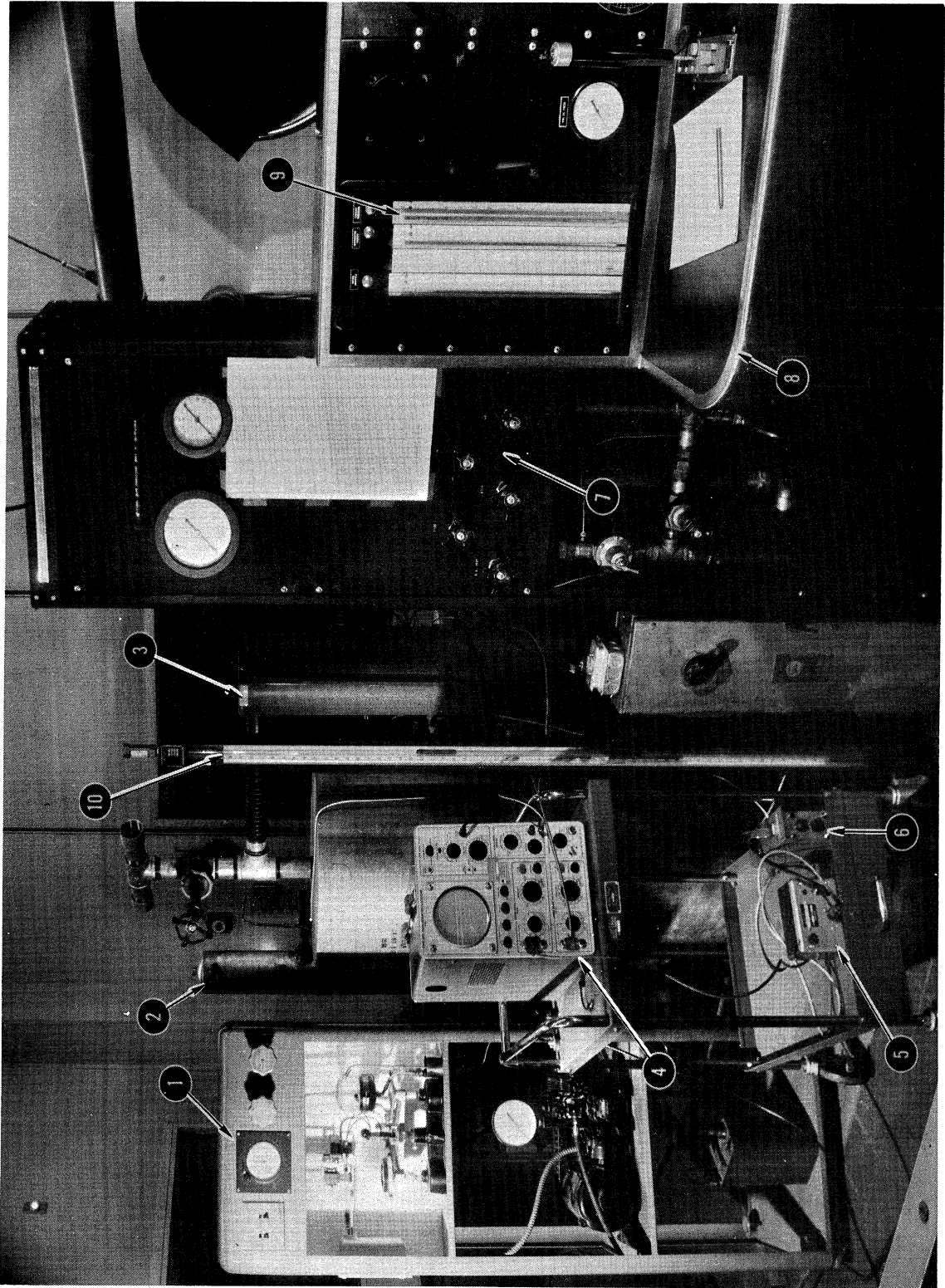


Fig. 2

1. Fuel weighing stand
2. Cooling tower
3. Intake air heater
4. Oscilloscope
5. Distance detector power supply
6. Kistler charge amplifier
7. Critical flow air meter
8. Dynamometer console
9. Exhaust pressure manometer
10. Intake air manometer

Fig. 2. Photograph of test cell and instrumentation.

After the air leaves the air meter it is passed through a Chromalox electric air heater of 20 kilowatt capacity, as shown in Fig. 1, item 6. The heater is thermostatically controlled and has the capacity to heat the maximum air flow from room temperature to 450°F. Smaller air flows can be heated to temperatures up to a maximum temperature of approximately 800°F.

From the air heater the air is directed to an inlet air surge tank of 5.6 ft³ capacity, as shown in Fig. 1, item 5. The purpose of this tank is to exclude the possibility of inlet air pressure fluctuations due to a resonant condition in engine air supply system. The tank is connected to the engine by a 10-in. section of flexible metal tubing and is insulated to reduce heat losses from the air.

A surge tank of 2.4 ft³ capacity, shown in Fig. 1, item 4, is connected to the exhaust manifold of the engine by a 4-ft length of tubing. Immediately after the tank is a gate valve to regulate engine exhaust back pressure.

The remainder of the equipment connected to the engine is typical for a test cell installation and includes a dynamometer for motoring or absorbing power, fuel and cooling water supply, fuel weighting stand, and an electronic counter for determining engine speed. Also included is a Honeywell-Brown Electronik self-balancing potentiometer for measuring temperatures.

The above equipment makes it possible to measure or control at least the following variables:

1. Inlet air pressure, temperature, and mass flow;
2. Exhaust temperature and pressure;
3. Fuel consumption and power output; and
4. Engine speed and pertinent temperature.

COMBUSTION MEASUREMENTS

Ignition delay is defined as the time delay from the injection of the first fuel into the combustion chamber until combustion begins. To measure the ignition delay it is necessary to measure both the point in time when fuel injection begins and the point in time when combustion begins, the difference being the ignition delay.

The Nordberg engine uses a Bosch injection pump and a Bosch nozzle holder with a single hole nozzle and pintle-type pop-off valve for injection. The nozzle holder has been modified so that a Bently D-152 distance detector system can be used to sense the motion of the nozzle pintle. Injection is judged to begin at the instant the pintle lift begins. Most, if not all, investigations use the pintle lift method to determine the beginning of injection but most use

either a capacitance-type pick-up or a linear differential transformer (L.D.T.) to sense the pintle motion. We selected the Bently system to detect pintle motion because it is as easy to adapt to the injector as either the capacitance pick-up or the L.D.T., and the general instrumentation is self-contained, and easier to operate than the other two systems. Experience to date indicates the pintle lift is a very stable measurement of the beginning of injection and should yield an error of less than 1/20 millisecon in determining the beginning of injection. This can be seen by reference to the oscilloscope photographs, Fig. 3, each of which is at least six pintle lift cycles superimposed on one photograph. Note that the six pintle lift traces appear to be but one trace due to the excellent repeatability of the pintle lift motion.

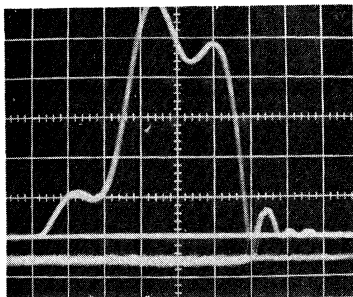
At the present time we have two means of determining when combustion begins. The first is a pressure time trace of cylinder pressure. In this method combustion is judged to begin when the compression pressure deviates from an ideal compression due to the addition of combustion heat. Kistler pressure measurement equipment is available in the laboratory for this type of study but to date we have not made extensive use of it.

The second method of determining the beginning of combustion, and the method toward which we have directed most of our effort, is to detect the light in the combustion chamber. The light will be at a very low level before combustion begins and will rise as the combustion process proceeds. Combustion is judged to begin at the first change of intensity of light in the combustion chamber. To detect combustion light we are using a silicon solar cell behind a 3/8-in. diameter quartz window in the combustion chamber. This cell has a response time of 20 microseconds and is sensitive to light in the range of 4000 to 110,000 angstroms wavelength. The main advantage of using the solar cell to detect the beginning of combustion is its low cost and very simple circuitry. Repeatability of the solar cell appears to be excellent as reference to Fig. 3 shows. The solar cell traces have a maximum variability of 0.4 millisecond which could, in part at least, be due to a variation in the combustion process. The solar cell pick-up was designed and built in the Instrument Shop of The University of Michigan.

The delay period has been noted below the trace photographs of Fig. 3. These times are the interval between the start of the lift of the injector pintle and the trace which indicates that the solar cell is receiving light from the combustion.

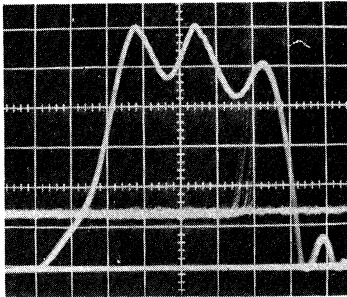
Sweep .5 msec/cm Sweep Magn x 1 Solar cell inside chamber Solar cell ampl 200 μ v/cm
 Bentley ampl 2 v/cm inj. Flin-atmos pressure 1/8 and 3/16 orifice P_{upstream} - 95 PSIG

INJECTION SET 18



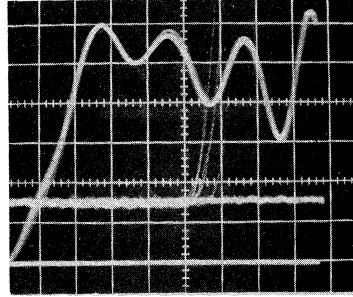
2.90 msec Delay

INJECTION SET 10

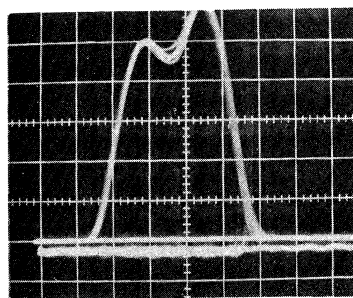


2.70 msec Delay
800 RPM

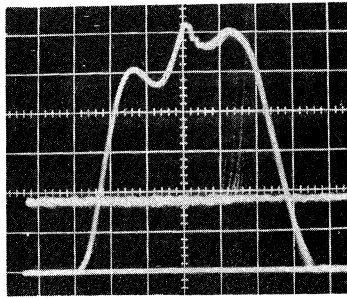
INJECTION SET 2



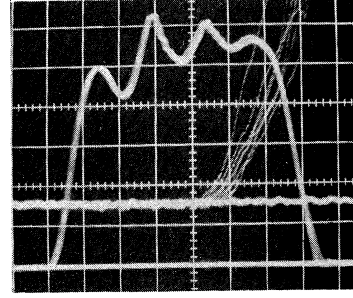
2.60 msec Delay



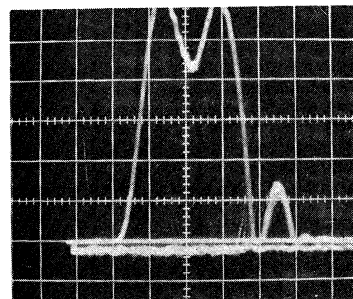
2.0 msec Delay



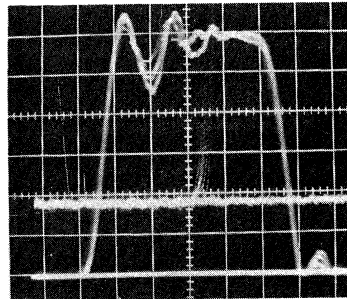
2.1 msec Delay
1200 RPM



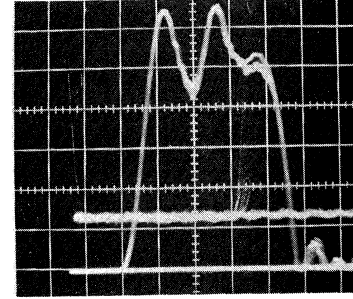
2.25 msec Delay



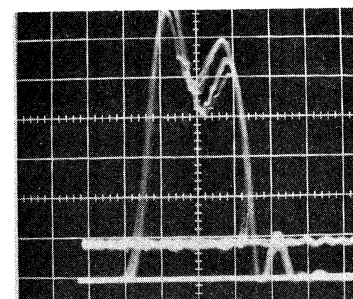
1.70 msec Delay



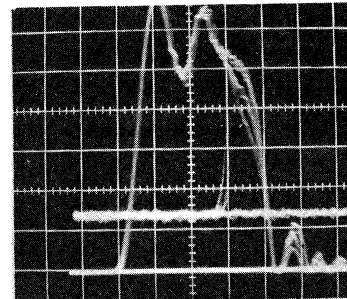
1.60 msec Delay
1600 RPM



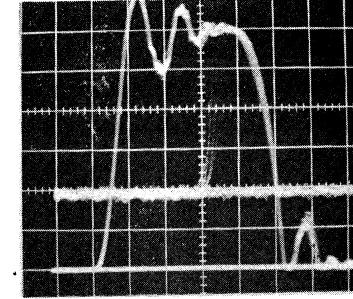
1.55 msec Delay



1.55 msec Delay



1.40 msec Delay
2000 RPM



1.40 msec Delay

Fig. 3. Oscilloscope traces to determine engine ignition delay.

PART II

THE ACCUMULATOR FUEL INJECTION SYSTEM

INTRODUCTION

Investigation of the diesel engine combustion characteristics at very high pressures may make it desirable to operate the engine with only single firing cycles (one-shot operation) to avoid mechanical and thermal difficulties with the engine. Mainly for this reason it was decided to make some preliminary tests of an accumulator-type system, which would be adaptable to the single injection requirement.

The accumulator system also offers theoretical advantage concerning two pressing requirements of high output ordnance diesel engines.

The first requirement is an injection system that can accurately deliver the small amount of fuel required at idle, which is essentially the same for a low and a high BMEP engine, and that can accurately deliver the large amount of fuel required at full load, which is proportionally higher as the BMEP increases. The ratio of maximum fuel delivered to minimum fuel delivered is termed the turndown ratio and can be seen to increase directly as the engine BMEP is increased. The ability of current injection systems to produce a satisfactory turndown ratio at present outputs is being pressed and it is reasonable to expect acute problems in this area when outputs are significantly raised.

The second requirement is a standard injection system which can be fitted to a large range of engine sizes with only minor changes to the injection system itself. It is felt that the accumulator system has the potential of satisfying both of the above requirements.

DESCRIPTION OF THE INJECTION SYSTEM

Figure 4 is a schematic of the elements of an accumulator system. The principle of operation of this system is that of storing the energy required to inject the fuel in an accumulator. Since the fuel has compressibility, as measured by the bulk modulus of the fuel, this mode of energy storage is analogous to storing energy in a spring. The amount of fuel injected will depend on the amount of energy stored which in turn depends only on the volume of the accumulator, the bulk modulus of the fuel and the pressure under which it is stored.

Figure 4 shows the basic elements which comprise an accumulator injection system, as follows:

1. High pressure pump;
2. Master accumulator and high-pressure relief valve;
3. Timed distributor;
4. Slave accumulator; and
5. Nozzle holder.

The function of the high-pressure pump is to supply fuel at a pressure somewhat above the pressure to which the accumulator is being charged. A range of pressures from 2000 to 10,000 psi would be quite practical. The quantity of fuel pumped by the high-pressure supply pump need not be metered but it must be approximately twice the amount actually required for injection.

The purpose of the master accumulator is to reduce the pulses from the high-pressure supply pump and to provide a reservoir so that small volume changes in the system do not cause large pressure changes. The high pressure relief valve could be a throttle or governor controlled valve, in either event this is the point in the system where external control over the amount of fuel injected is maintained.

The timer-distributor has two functions. First, it must provide communication of the fuel pressure from the master accumulator to the nozzle. Second, at the proper time in the engine cycle it must stop flow from the master accumulator to the nozzle and vent the pressure above the nozzle plunger to atmospheric, which permits injection to take place as described below.

The nozzle assembly is the same in construction, and operation as a standard pintle-type nozzle except that it has provisions for subjecting the top side of the pintle to the pressure from the timed distributor. Thus the fuel pressure as well as the usual spring hold the nozzle closed. One side of the slave accumulator is connected to the injection fuel passage in the nozzle holder, the other side is connected to the timed distributor.

The events which take place in the nozzle holder slave accumulator assembly over an injection cycle is as follows: The timer distributor allows communication of the pressure in the master accumulator to the nozzle assembly and slave accumulator. Injection does not take place as the fuel pressure is aiding the spring to hold the pintle closed in the nozzle holder. Fuel flows to the slave accumulator until a zero pressure difference exists across the check valve in the slave accumulator and at this point the system is ready for an injection. The nozzle assembly top line is then vented to atmospheric pressure by the timer distributor. The pressure in the accumulator does not decrease since the check valve is closed but the pressure on the top side of the pintle in the nozzle holder is reduced so that only the spring is holding the pintle down. The pressure in the slave accumulator is high enough, say 4000 psi, so that the spring force on the pintle is overcome and injection occurs. The amount of fuel injected is determined by the initial pressure in the slave accumulator, the accumulator volume and the bulk modulus of the fuel. The cycle is repeated when

the timer distributor allows communication of pressure from the master accumulator to the nozzle holder-slave accumulator line.

TESTS OF AN ACCUMULATOR SYSTEM

A bench rig of an injection system using the accumulator principle has been built from parts available in our Automotive Laboratory. Figure 5 is a diagram showing the arrangement of the system as used for the bench tests. Figure 6 is a photograph of the bench rig, showing the components and much of the plumbing. The timers, or interrupters, of Figs. 5 and 6 were made by producing a steel block to hold a conventional diesel injection pump plunger and sleeve. The valving action was obtained by rotating the standard pump plungers in the sleeves. The cog belt drives and vari-speed motor which provide the variable speed of rotation can be noted on Fig. 6.

TESTING OF ACCUMULATOR SYSTEM

Preliminary tests were run with the system described to learn about its merits and problems. These tests were run with frequency of injection from 200 to 1250 injections per minute, and with the accumulator pressure varied from 4000 to 7000 psi. These tests were run with an accumulator volume of 0.29 in.³ The results of these tests are shown on Fig. 7. It will be noted that the injection nozzle delivery of the experimental equipment is greater than that predicted by hydraulic theory, especially at the higher pressures.

In an effort to better understand the hydraulic phenomena that were occurring, a Kistler pick-up was installed in the injector, to sense the pressure in the line joining the injector to the accumulator. Four typical photographs of oscilloscope pressure traces are shown on Fig. 8.

Photograph Fig. 8(b) shows substantial fluctuation of the nozzle supply pressure during successive cycles. Figure 8(c) indicates that at 1000 cycles/minute the pressure hardly had fully built up before the discharge occurred. Figure 8(d) shows that at 1250 cycles/minute the maximum nozzle pressure was falling off, probably due to insufficient charging time.

From this preliminary bench work we have learned that the volume of liquid in the parts of the system subject to fluctuation must be kept at a very minimum, consistent with adequate size of flow passage. Also, the quality of the parts must be of a high order to minimize leakages and obtain consistent operation.

Note: The pressure interrupter and relief interrupter are timed together so that when one is open the other is closed.

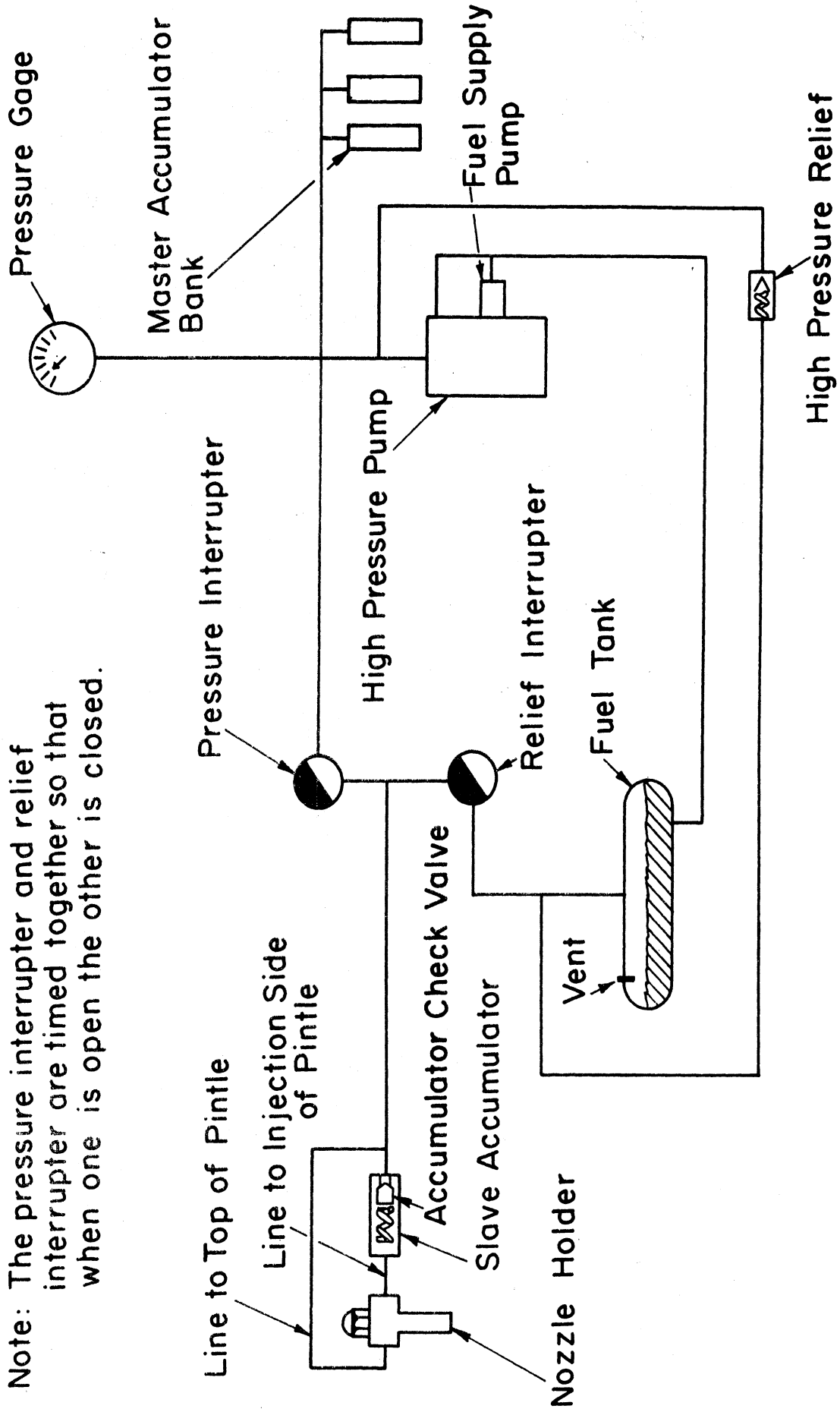


Fig. 5. Diagram of accumulator system as built for bench testing.

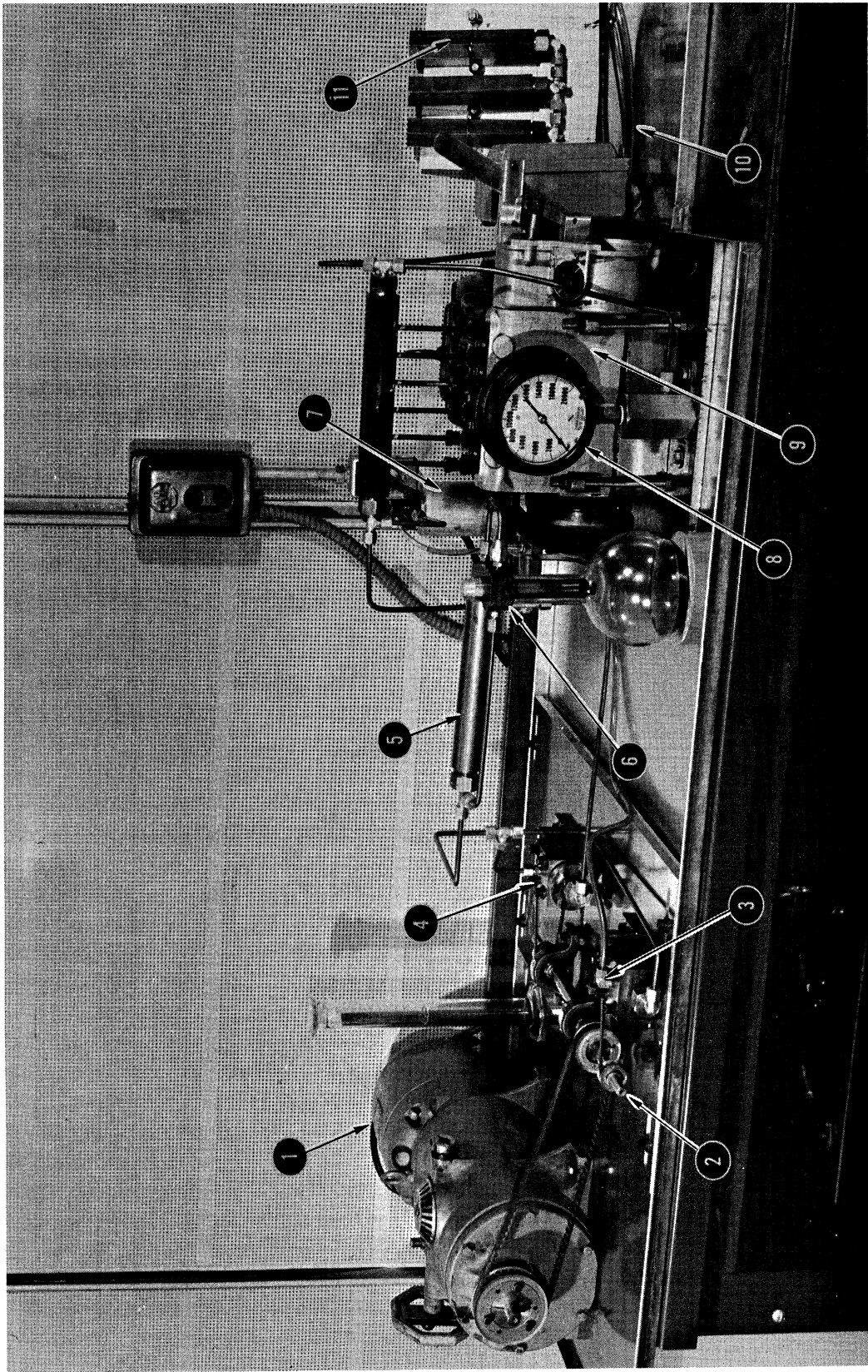


Fig. 6

1. Variable speed drive
2. Jack shift to time interrupter
3. Relief interrupter
4. Pressure interrupter
5. Slave accumulator
6. Nozzle accumulator
7. High pressure relief valve
8. 20,000 psi pressure gage
9. High pressure pump
10. Lines to fuel tank and low pressure pump
11. Master accumulator bank

Fig. 6. Photograph of bench rig—accumulator injection system.

— ACTUAL DELIVERY
 - - - THEORETICAL DELIVERY

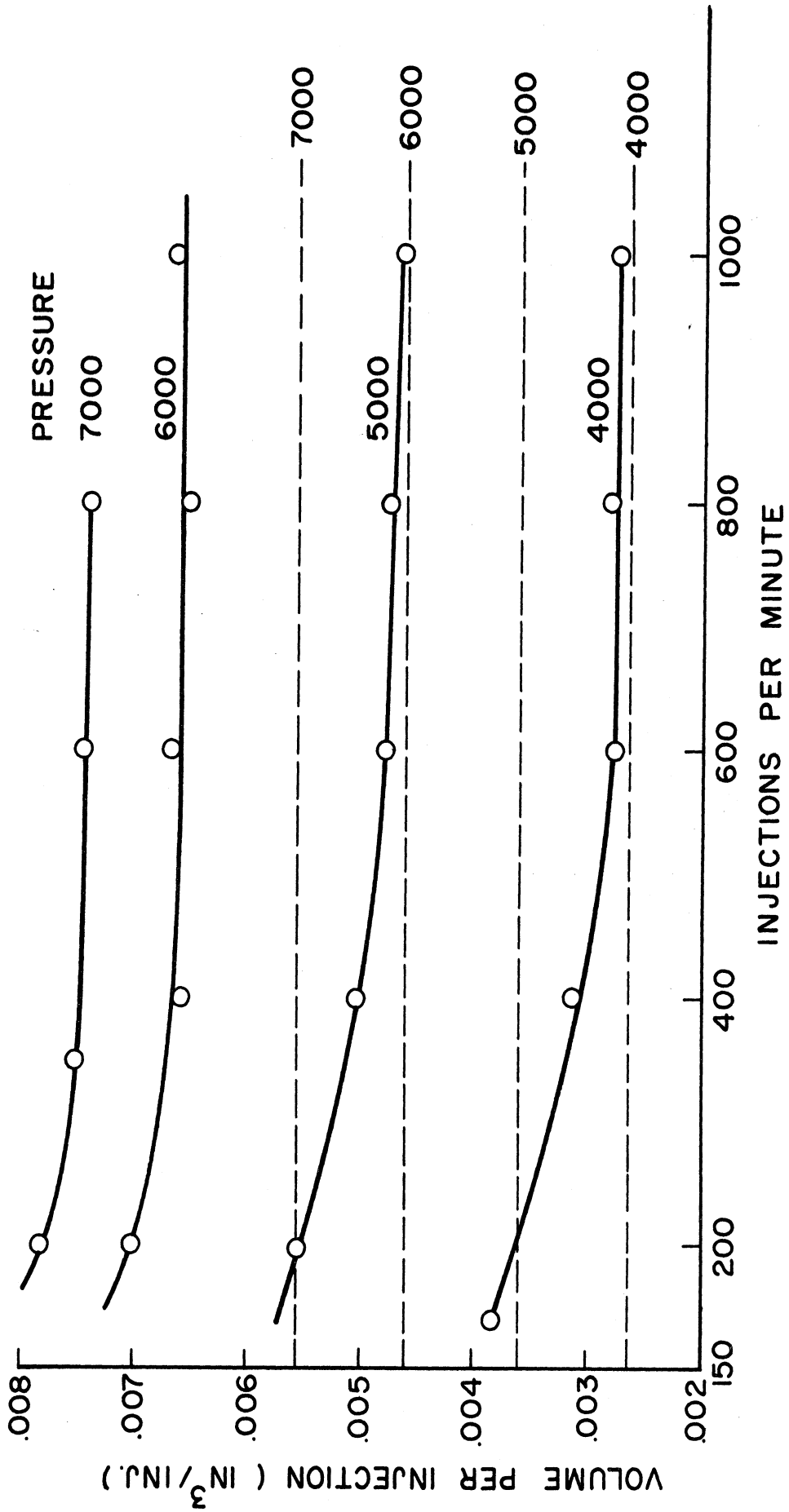
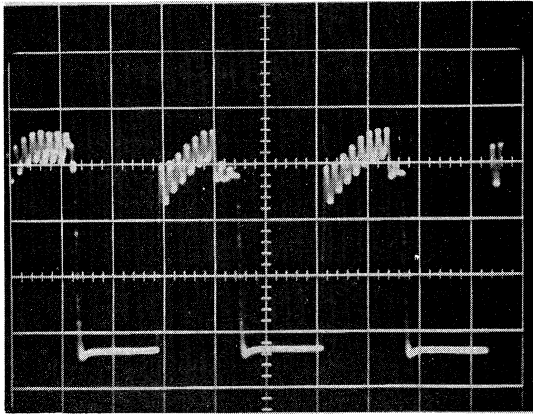
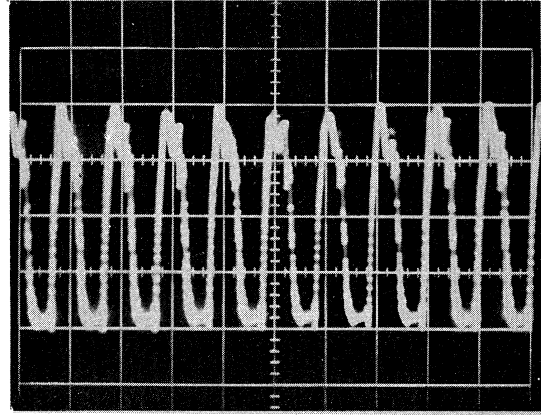


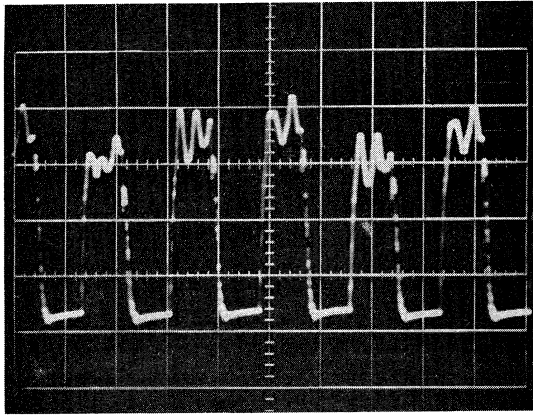
Fig. 7. Performance characteristics of accumulator injection system (accumulator vol. = 0.29 in.³).



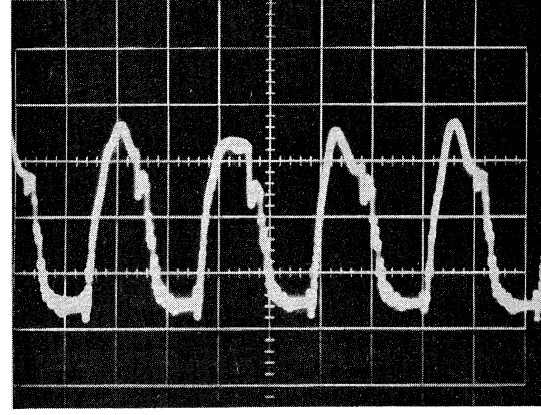
(a)
 Time sweep .1 sec/cm
 Calibration 1000 psi/cm
 Speed 200 RPM



(c)
 Time sweep 50 msec/cm
 Calibration 1000 psi/cm
 Speed 1000 RPM



(b)
 Time sweep 50 msec/cm
 Calibration 1000 psi/cm
 Speed 600 RPM



(d)
 Time sweep 20 msec/cm
 Calibration 1000 psi/cm
 Speed 1250 RPM

Fig. 8. Transient pressures at nozzle of accumulator injection system. (valve closing pressure = 1600 psi; accumulator vol. = 0.29 in.³).

To obtain a quality of performance suitable for operating the test engine, the bench system would have to be quite completely re-engineered and many new precision parts built. It has been decided that instead we will, at least for our initial test work, use the regular engine injection system. If single shot operation is desired, it will be done by rapidly positioning the pump rack from no load to the desired load position.

SECTION 3

PROGRESS REPORT NO. 3

COMBUSTION INSTRUMENTATION ON LISTER-BLACKSTONE ENGINE

THE UNIVERSITY OF MICHIGAN
COLLEGE OF ENGINEERING
Department of Mechanical Engineering

Progress Report

For the period 1 September 1965 to 31 December 1965

DIESEL ENGINE IGNITION AND COMBUSTION

Jay A. Bolt
N. A. Henein

ORA Project 06720

under contract with:

U. S. ARMY
DETROIT PROCUREMENT DISTRICT
CONTRACT NO. DA-20-018-AMC-1669T
DETROIT, MICHIGAN

administered through:

OFFICE OF RESEARCH ADMINISTRATION ANN ARBOR

December 1965

TABLE OF CONTENTS

	Page
LIST OF FIGURES	114
INTRODUCTION	115
THE LISTER-BLACKSTONE ENGINE SETUP	116
PHOTOGRAPHS	118
PLANNED TESTS TO BE RUN ON LISTER ENGINE	118

LIST OF FIGURES

Figure	Page
1. Picture of Lister-Blackstone Setup.	119
2. Original Combustion Chamber of Lister-Blackstone Engine.	120
3. Modified Combustion Chamber of Lister-Blackstone Engine.	121
4. Modified Chamber Plug Showing Positions of Solar Cell and Pressure Transducer and Thermocouple.	122
5. Chamber Plug With Instruments Fitted to Cylinder Head.	123
6. The Degree Marking Unit.	124
7. Oscilloscope Traces for Gas Pressure, Fuel Pressure, Needle Lift, Solar Cell Output and Crank Angles.	125
8. Fuel Injector Fitted With a Needle Lift Detector and a Pressure Transducer.	126
9. Fuel Pump With its Rack Controlled by a Micrometer.	127

INTRODUCTION

This report covers the work carried out during the period from September 1, 1965 to the end of December, 1965. In the course of planning the program for this period we took into consideration the time available before receipt of the new high output Army Research engine, which is expected to be received during January or February, 1966. The work carried out includes five major items:

1. A study of the work previously done by other investigators, as covered by a previous Bibliography Report,* on the combustion process in diesel engines. This is done with a special concern to the instruments used for such work, and the possible ways for developing them and improving their accuracy.
2. Setting up a second engine (Lister-Blackstone) in a separate room, which will be available for testing while the Army supplied engine is being put into operation, and thereafter. A picture of this set-up is shown in Figure 1.
3. Testing and calibrating the instruments after being fitted on the Lister-Blackstone engine.
4. Running tests on the Lister-Blackstone engine to investigate the several factors that affect ignition delay and combustion in the diesel engine, and to gain experience in the techniques needed for such a research.
5. Planning the procedure of tests to be run on the Army Research engine, and the method of processing the data.

One of the instruments we are using to detect the start of combustion in the engine is the silicon solar cell, described in a previous report.** The first time this cell was used in our laboratory was with the Nordberg Diesel engine, referred to in the same previous report. A study of the combustion process in the Nordberg engine (with a Lanova single lobe combustion chamber) indicated that the combustion is not confined to the main chamber but occurs also in the minor and major cells. Due to the complexity of the combustion

*Diesel Engine Ignition and Combustion—A Bibliography, by Jay A. Bolt and R. K. Nicholson, 06720-1-P Report, The University of Michigan, Sept. 1965.

**Diesel Engine Ignition and Combustion by Jay A. Bolt and Kenton C. Ensor 06720-2-P Report, The University of Michigan, Sept. 1965.

process in the Lanova combustion chamber it was decided that the use of the solar cell for indicating the start of combustion in this type of chamber is not of great significance for diesel ignition lag investigations. The most suitable type of chamber, for evaluating the solar cell for combustion research, is that in which the fuel injection and the start of combustion is confined to one chamber. In search for such an engine a visit was made to the General Motors Corporation, Diesel Engine Division, in Detroit to investigate a single cylinder, open chamber, research engine. The General Motors engines have 2 or 4 valves in the cylinder head with limited space for mounting instruments. Also, the installation of the injection valve lift measuring equipment would be very difficult for the unit injector of General Motors.

After considering all aspects of the problem, it was decided to use the "Lister-Blackstone" British engine available in our laboratory. This engine has a Ricardo swirl type combustion chamber. This chamber has been modified to allow the mounting and testing of the solar cell, together with a Kistler pressure pickup to be used for this investigation.

Considering the period of time available before receiving the Army engine, it was thought to be useful to begin the experimental program on the Lister engine, after testing and calibrating the instruments. This is being done without affecting the set up prepared and described in the previous report for testing the Army engine.

THE LISTER-BLACKSTONE ENGINE SETUP

This engine is a single cylinder, four-stroke cycle, liquid cooled, 4-1/2 inch bore, 4-3/8 inch stroke, and has a rated power of 8 bhp at 1200 rpm. This engine is especially attractive for combustion research because there is easy access to the swirl chamber, or pre-combustion chamber. The design, therefore, makes it practical to modify the swirl chamber, and to place pressure pickups and other instruments into the wall of the swirl chamber. It was also found to be practical to modify the combustion chamber of the engine to run tests at variable compression ratios. Figure 2 shows a section in the cylinder head with its original auxiliary chamber and the compression ratio change-over valve. Figure 3 shows the cylinder head after modification and shows the variable compression ratio sleeve and the chamber plug. The construction of this plug allows the compression ratio to be varied in the range from 15:1 to 22:1.

Figures 4 and 5 show the chamber plug and the method of mounting the pressure transducer, solar cell and a surface thermocouple.

Shop air is used to supercharge the engine after being passed through a surge tank fitted just before the engine. The pressure in the tank is measured

and considered equal to the supercharging pressure. The temperature is measured in the tank and in the cylinder head before the inlet valve. The air consumption is measured by a critical pressure type flowmeter.

The gas pressure inside the cylinder is obtained by the use of an oscilloscope, together with a Kistler pressure transducer and a degree marking unit. The Kistler transducer is mounted on the combustion chamber plug as nearly flush as possible with the inside surface of the combustion chamber. The output of the transducer is fed to a charge amplifier and then to a dual beam oscilloscope. The trace obtained on the screen is photographed by a polaroid camera attached to the oscilloscope.

The degree marks are produced by a steel disc, 20 inches diameter, 1/8 inch thick, mounted on the engine flywheel. The rim of the disc was slotted at 3° intervals, with deeper slots at 45° intervals, Figure 6. A magnetic pick-up was mounted on the engine bedplate, with its pole close to the rim. The alternating voltage generated by the rotation of the disc was applied to channel B of the dual beam oscilloscope mentioned before. The corresponding trace obtained on the screen consisted of a serrated line across the horizontal diameter of the screen as shown in Figure 7. Every 3 and 45° were thereby marked, and one of the deep 45° slots in the disc was aligned at the T.D.C. The crank angle position on the oscilloscope traces can therefore be determined.

The temperature of the inside surface of the combustion chamber is measured by a special Nickel-Steel thermocouple. The location of this thermocouple can be adjusted to coincide with the point where the fuel spray from the injector hits the surface.

The fuel injection system is instrumented, Figure 8, so that the start and rate of injection can be calculated from measurements of the needle lift and fuel pressure before the nozzle. The needle lift is measured by a Bentley D-152 distance detector system. The injection is considered to begin at the instant the needle lift begins. The fuel pressure before the nozzle is obtained by a Kistler transducer fitted on the injector body. The rate of injection (especially during the delay period) will be calculated from the pressure difference before and after the nozzle and the area of flow as computed from needle lift measurements. To ensure reproducibility of the plunger setting in the fuel pump the position of rack is controlled by a micrometer as shown in Figure 9.

A sample of the traces obtained for the gas pressure, fuel pressure, needle lift, solar cell output and crank degrees is shown in Figure 7.

PHOTOGRAPHS

One of the methods which was studied and found to be very useful for the detection of the start of combustion in the engine is high speed photography. To apply high speed photography to this engine, a fused quartz window was obtained to replace the combustion chamber modified plug. As shown in Figure 3 the diameter of this plug is very near to the diameter of the swirl chamber, which makes it feasible to take pictures of the whole combustion chamber. It is hoped that photographs will help in detecting the start of combustion and in analyzing the many processes which occur within the short time from the beginning of injection to the end of combustion. High speed photography equipment and skills are available to us on campus if such work seems desirable.

PLANNED TESTS TO BE RUN ON LISTER ENGINE

The aim of running these tests is to gain experience in the different techniques that will be used on the Army Research engine, as well as to collect data on a swirl type chamber to be compared with the other types of combustion chambers.

Tests are presently planned for the following conditions:

1. Variable inlet pressures to study the effect of gas pressure at the time of injection on ignition delay and combustion characteristics.
2. Variable compression ratios to study the effect of combined pressure and temperature on ignition delay and combustion characteristics.
3. Variable loads.
4. Variable speeds.
5. The above tests are to be carried out by using the following fuels:
 - a. CITE referee grade (MIL--45121 B) fuel.
 - b. Diesel fuel VV-F-800 Grade II.
 - c. MIL-G-3056B referee grade gasoline fuel.

These fuels have been ordered from Ashland Oil and Refining Co., Ashland, Kentucky, and are now stored in the Automotive Laboratory.

The data processing will be done on a digital computer and the necessary programming is now under preparation.

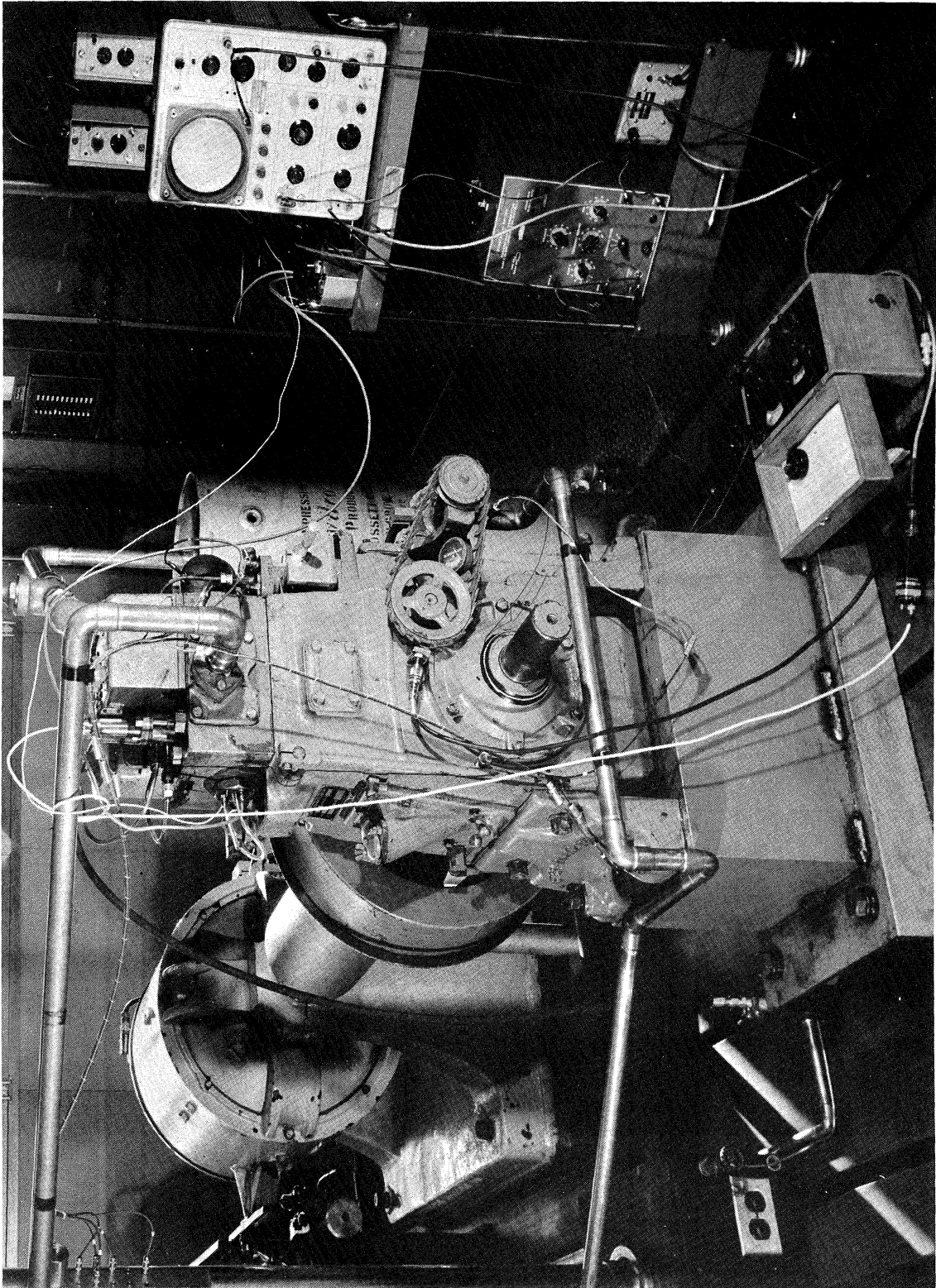


Figure 1. Picture of Lister-Blackstone Setup.

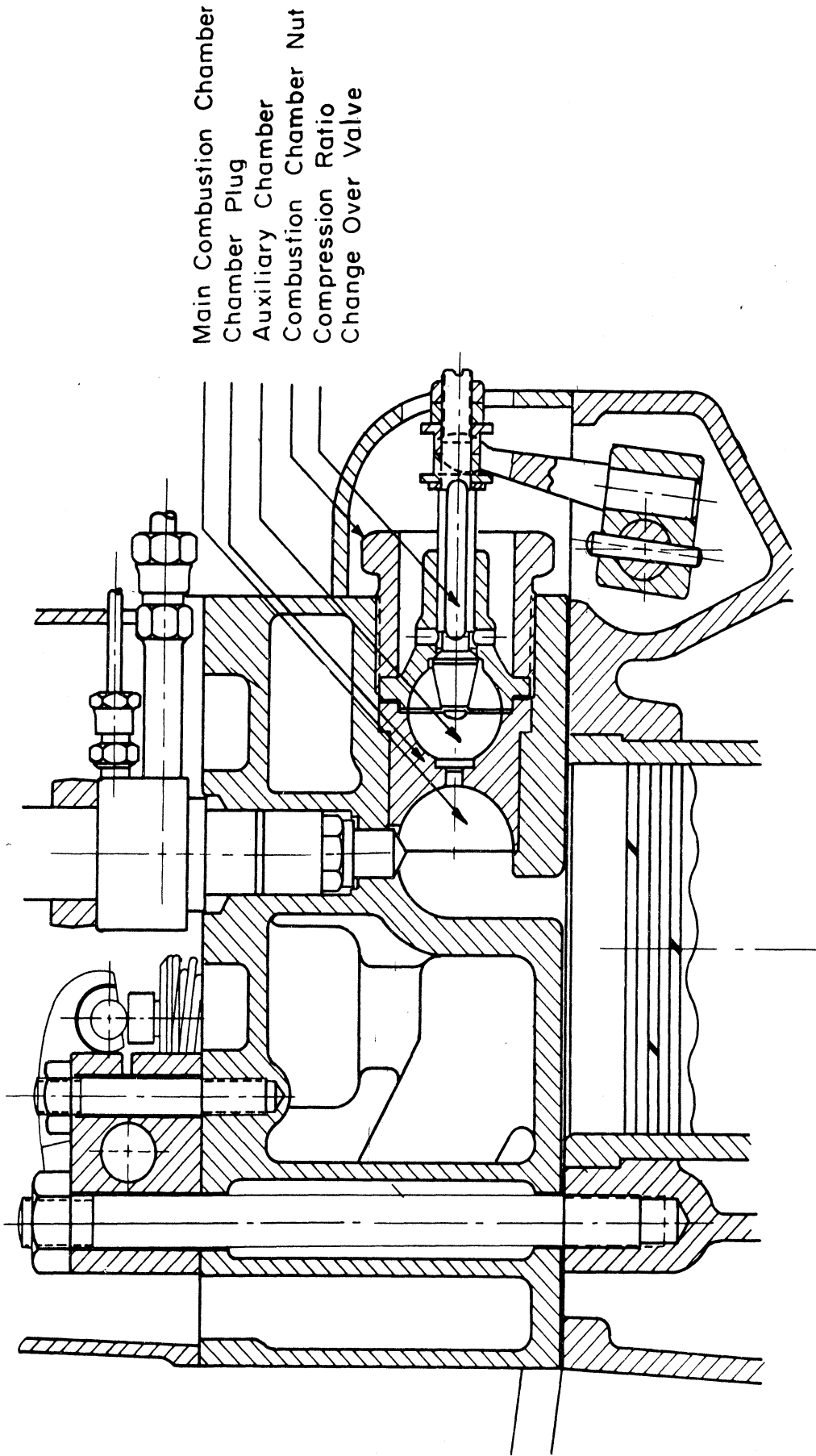


Figure 2. Original Combustion Chamber of Lister-Blackstone Engine.

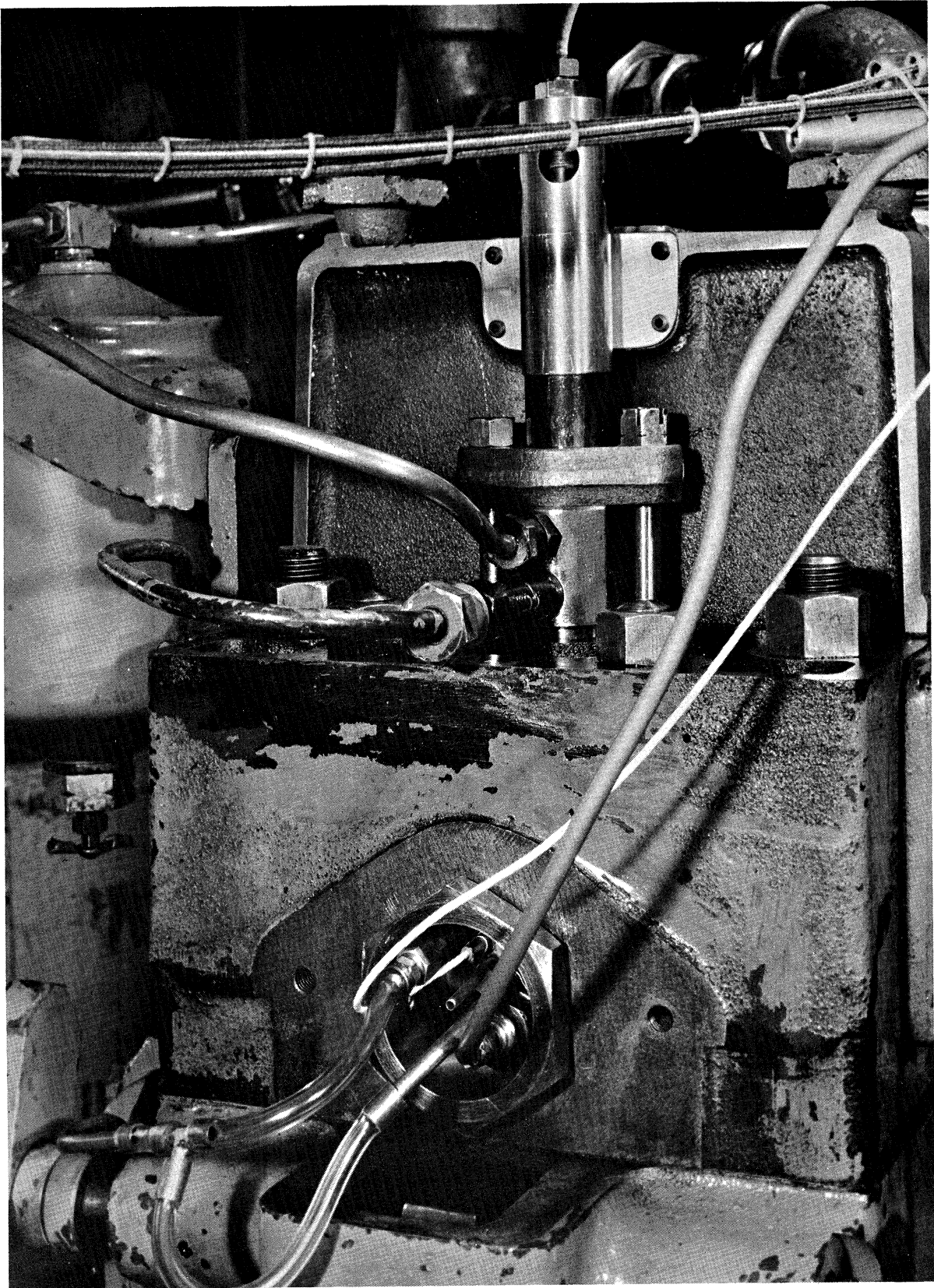


Figure 5. Chamber Plug With Instruments Fitted to Cylinder Head.

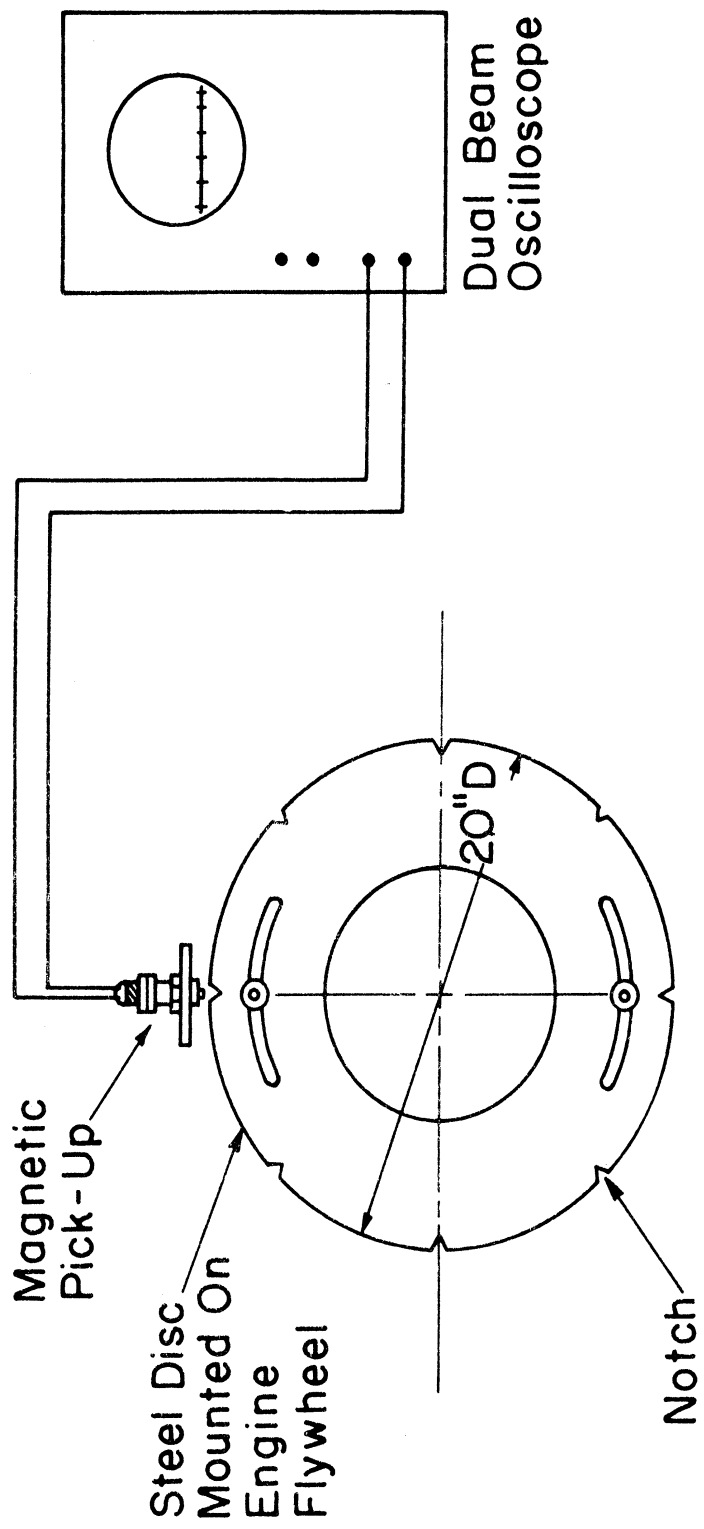
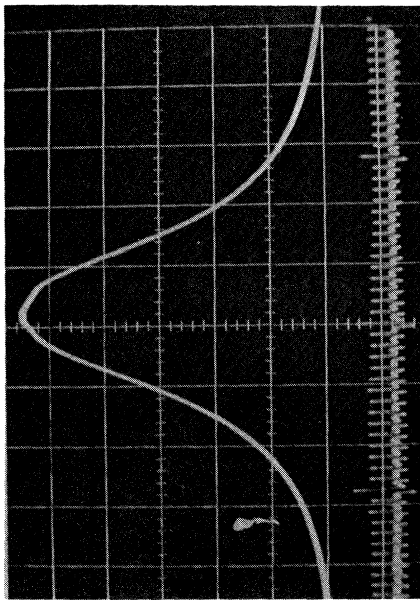
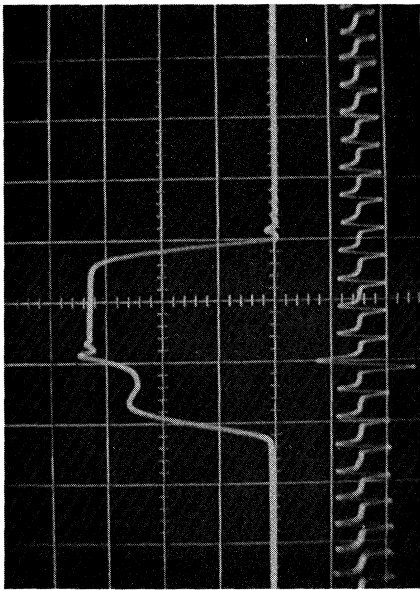


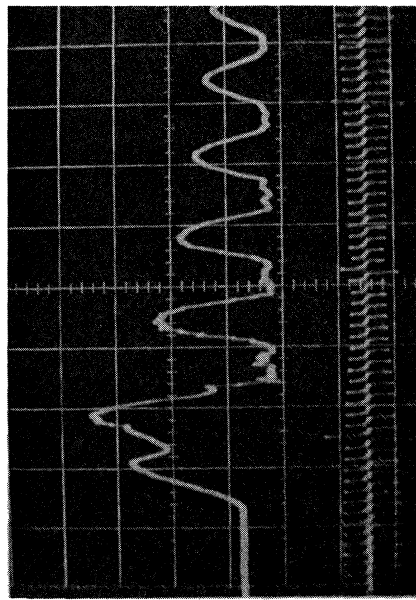
Figure 6. The Degree Marking Unit.



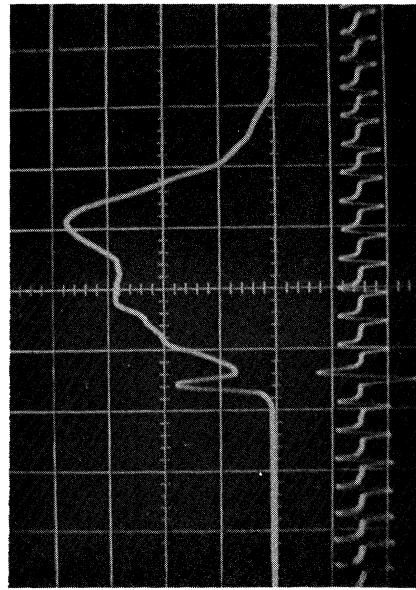
Gas Pressure vs Crank Degrees



Needle Lift vs Crank Angles



Fuel Pressure vs Crank Angles



Solar Cell Output vs Crank Angles

Figure 7. Oscilloscope Traces for Gas Pressure, Needle Lift, Solar Cell Output and Crank Angles.

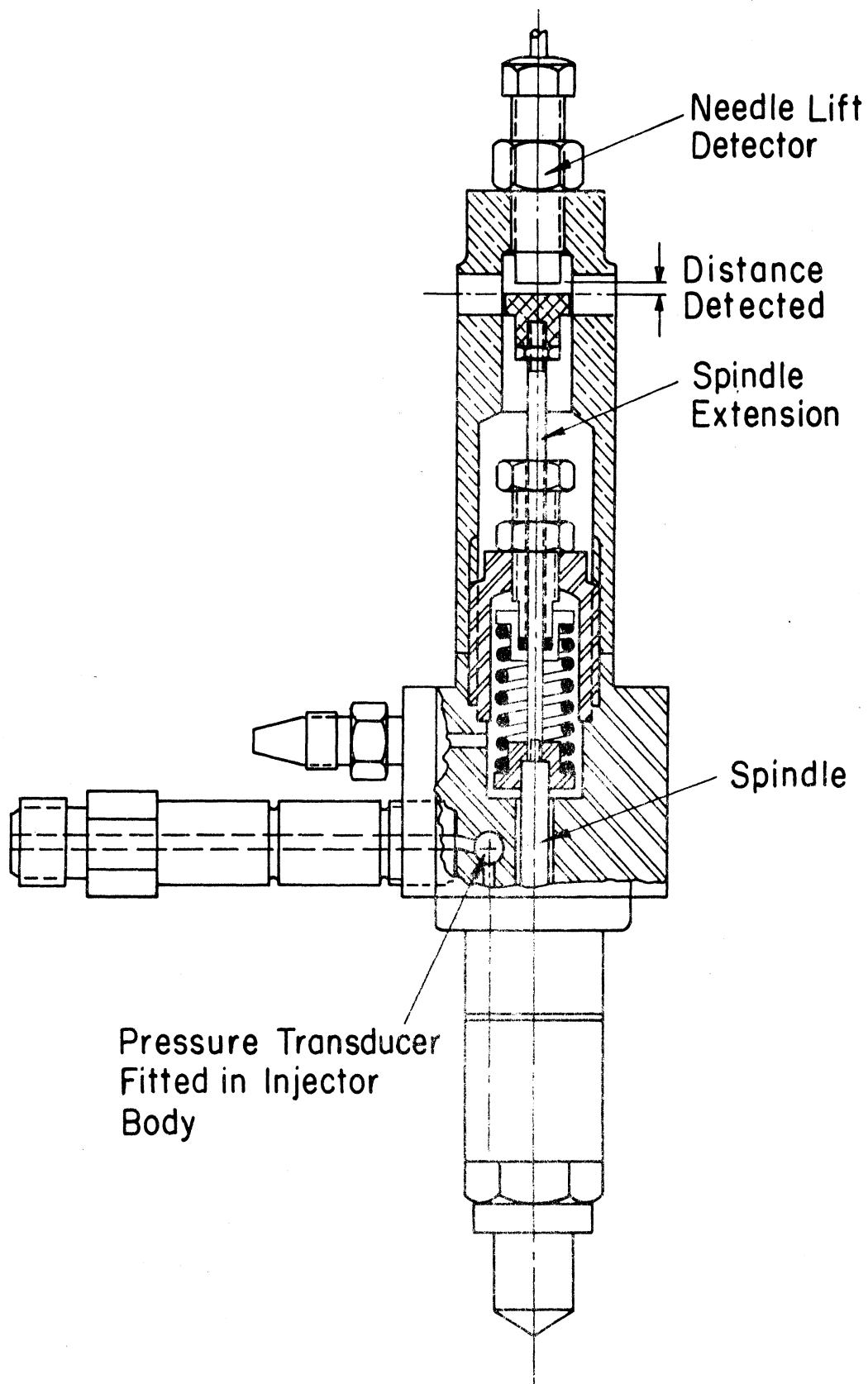


Figure 8. Fuel Injector Fitted With a Needle Lift Detector and a Pressure Transducer.

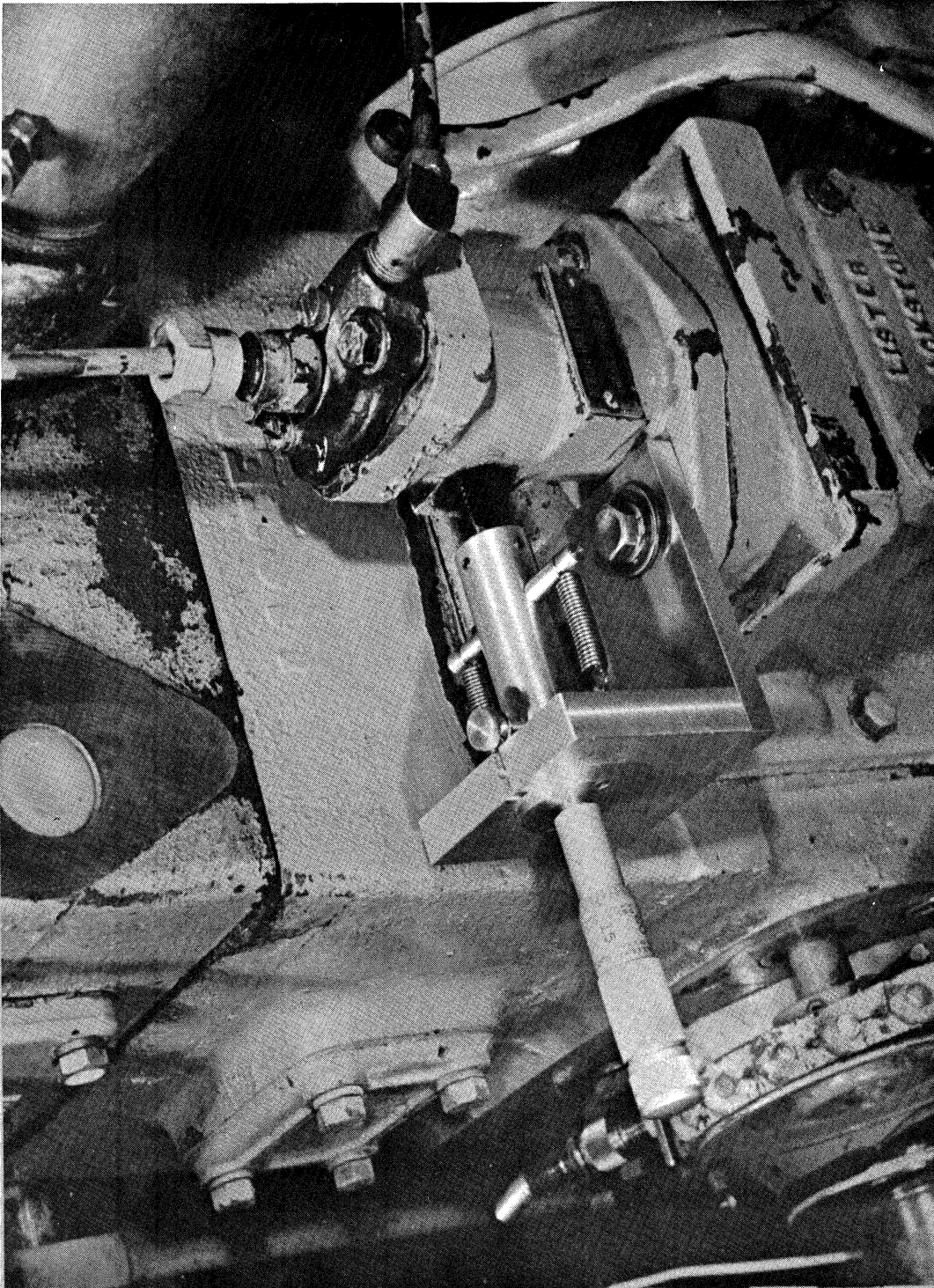


Figure 9. Fuel Pump With its Rack Controlled by a Micrometer.

SECTION 4

PROGRESS REPORT NO. 4

EXPERIMENTAL RESULTS ON LISTER-BLACKSTONE ENGINE

THE UNIVERSITY OF MICHIGAN
COLLEGE OF ENGINEERING
Department of Mechanical Engineering

Progress Report
For the period January 1, 1966 to March 31, 1966

DIESEL ENGINE IGNITION AND COMBUSTION

Jay A. Bolt
N. A. Henein

ORA Project 06720

under contract with:

U. S. ARMY
DETROIT PROCUREMENT DISTRICT
CONTRACT NO. DA-20-018-AMC-1669T
DETROIT, MICHIGAN

administered through:

OFFICE OF RESEARCH ADMINISTRATION ANN ARBOR

May 1966

TABLE OF CONTENTS

	Page
LIST OF FIGURES	135
NOMENCLATURE AND SYMBOLS	137
INTRODUCTION	139
IGNITION DELAY—DEFINITIONS	141
REVIEW OF PREVIOUS WORK	142
Wolfer's Formula	142
Bauer's Formula	142
West's Formula	143
Rosen's Formula	143
Tsao, Myers, and Uyehara Formula	143
EXPERIMENTAL WORK	146
A. Crank Position for Maximum Pressure in a Motored Engine	146
B. Effect of Fuel-Air Ratio on Ignition Lag	148
C. Effect of Injection Pressure on Ignition Delay	150
D. Effect of Surface Temperature on Ignition Delay	153
E. Effect of Turbulence on Ignition Delay	153
COMPUTATIONS	164
A. Gas Temperature	164
B. Rate of Heat Release	164
C. Index of Compression and Expansion	167
D. Rate of Fuel Injection	169
E. Combustion Computations	169
CONCLUSIONS	173
RECOMMENDATIONS	174
APPENDIX I: INSTRUMENTATION IMPROVEMENT	175
A. Pressure-Rise Delay	175
B. Illumination Delay	179
APPENDIX II: TEST CONDITIONS AND RESULTS	181
A. Test Conditions	181
B. Results	181

TABLE OF CONTENTS (Continued)

	Page
APPENDIX III: HEAT RELEASE	182
BIBLICGRAPHY	183

LIST OF FIGURES

Figure		Page
1	Ignition lag vs. $T_c \log P_c$ by West.	144
2	Maximum pressure advance in motored Lister Blackstone engine ($N = 980$ rpm, coolant temperature = 104.5°F).	147
3	Effect of fuel-air ratio on ignition delay, and injection advance.	149
4	Effect of fuel-air ratio on B.S.F.C. and I.S.F.C.	151
5	Effect of injector opening pressure on ignition delay.	152
6	Effect of injector opening pressure on I.S.F.C.	154
7	Effect of cooling water temperature on ignition delay.	155
8	Effect of cooling water temperature on injection start.	156
9	Turbulence in modified combustion chamber of Lister engine.	157
10	Air speed in the tangential passage to the swirl chamber of Lister engine at 1000 rpm.	158
11	Effect of engine speed on illumination delay.	160
12	Effect of engine speed on pressure-rise delay.	161
13	Effect of engine speed on I.S.F.C.	162
14	Effect of engine speed on injection advance.	163
15	Gas pressure and temperature during the cycle.	165
16	Rate of heat release and accumulated heat release diagrams.	166
17	P-V relationship on a Log-Log sheet.	168
18A	Nozzle needle assembly.	170
18B	Area for fuel flow vs. needle lift.	170

LIST OF FIGURES (Continued)

Figure		Page
19	Rate of fuel injection and accumulated fuel diagrams.	171
20	Pressure and pressure differentiating circuits.	176
21A	Pressure trace.	177
21B	Pressure differential trace.	177
22	Lag between the pressure and the pressure differentiating circuits.	178
23	Visicorder traces.	180

NOMENCLATURE AND SYMBOLS

- a = constant
 A = area of cylinder bore, in.²
 A_f = area of flow for fuel, in.²
 b = constant for each fuel
 C = constant for each fuel
 c_d = coefficient of discharge
 c_p = specific heat at constant pressure, $\frac{\text{BTu}}{\text{lbm } ^\circ\text{F}}$
 c_v = specific heat at constant volume, $\frac{\text{BTu}}{\text{lbm } ^\circ\text{F}}$
 D = diameter, in.
 g = gravitational acceleration, ft/sec²
I.D. = ignition delay in milliseconds if not otherwise stated
 J = mechanical equivalent of heat, $\frac{\text{ft lbf}}{\text{BTu}}$
 K = ratio of specific heats
 k_a = thermal conductivity for air, $\frac{\text{BTu}}{\text{ft}^2 \text{ } ^\circ\text{F}/\text{ft.}}$
 m = mass, lb
 n = constant, or index of a polytropic process
 N = revolutions per minute
 P = gas pressure, psia
 P_a = air gauge pressure before flow meter
 P_b = barometric pressure, in. Hg
 P_c = compression pressure at start of injection, psia, or atm
 P_f = fuel pressure, psia

- Q = quantity of heat, Btu
 r_f = radius of fuel droplet, ft
 R = universal gas constant, $\frac{\text{lb} \cdot \text{ft}}{\text{lbm} \cdot ^\circ\text{R}}$
 t_c = chemical ignition delay, sec
 T_a = air temperature before air flow meter, $^\circ\text{F}$
 T_c = compression temperature at start of injection, $^\circ\text{F}$, $^\circ\text{R}$, or $^\circ\text{K}$
 T_{ci} = cooling water temperature at inlet to engine, $^\circ\text{F}$
 T_{ce} = cooling water temperature at exit from engine, $^\circ\text{F}$
 $T_{exh.}$ = exhaust gas temperature, $^\circ\text{F}$
 T_f = temperature of fuel, $^\circ\text{F}$
 T_i = self ignition temperature of fuel, $^\circ\text{F}$
 U = internal energy
 V = volume
 W = work
 W_B = brake load on dynamometer, lb
 θ = crank angles, degree
 ζ_f = specific weight of fuel, lb/ft^3
 X = exponent

INTRODUCTION

The work which had been done in the period from January 1, 1966, to March 31, 1966, included both theoretical and experimental investigations of the combustion process in diesel engines. Some work has been done to study the possibility of improving the sensitivity of the instruments assembled on the Lister-Blackstone engine, as described in a previous report(2).*

The theoretical part deals with an analytical study of the process of combustion of hydrocarbons in general, with special emphasis on the environment that occurs in the diesel engine. This theoretical study verified that there are factors which can significantly affect the combustion process, other than the pressure and temperature of the air, and the type of fuel. Unfortunately these factors have not been emphasized or evaluated in most previous publications. These factors are:

1. the fuel-air ratio
2. the injection pressure
3. turbulence
4. wall temperatures

It was decided to study these factors and to run experiments to find out how much they affect the combustion process. This was done to establish a test procedure for future runs in which these factors will be held constant or nearly so.

Prior to the above investigation on the factors that affect the combustion process, an additional experimental study was carried out concerning the air pressure and temperature at the end of the compression stroke. This investigation started after comparing the pressure and crankangle traces and observing that, with the engine motored, the point of maximum pressure is in advance of the point of T.D.C. A thermodynamic analysis was then made for the air during the compression stroke, the results of which supported our conclusion that the heat loss from the air to the cylinder wall is the main reason for the pressure reaching a maximum before top dead center.

The study made for the possible improvement of the accuracy of the instrumentation was in the following areas:

1. the detection of the point of pressure rise due to combustion. This had been done by applying a differential circuit to the output signal of the cylinder pressure transducer.

* Numbers in parantheses refer to the Bibliography.

2. The simultaneous recording of all signals for the same cycle, by using a Minneapolis-Honeywell visicorder. This simultaneous method of recording eliminates the errors caused by cycle to cycle variations.
3. The detection of the start of illumination more accurately by using a photo multiplier instead of the solar cell.

A complete cycle analysis was made for a sample run and a computer program was written for the same run.

This report covers a review of the previous work done and the results of the experimental work and cycle analysis.

IGNITION DELAY--DEFINITIONS

Previous investigators used various definitions for the ignition delay, based on the criteria used to define the end of this delay period. Most of the investigators used the start of pressure rise resulting from combustion as the end of this period. Others used the start of temperature rise due to combustion, or illumination.

In this investigation, it was noted that the start of pressure rise and the start of illumination did not occur simultaneously, and it seemed logical to differentiate between the different delay periods. The start of the illumination can be considered to be the end of the preflame chemical reactions of the first fuel particles to ignite. The start of illumination probably does not coincide with measurable pressure increase due to combustion. At this stage of the work it was found useful to define the different delay periods as follows:

1. Physical delay: is defined as the period of time required for the physical changes to occur to the fuel from the liquid phase to the vapor phase. It can be considered equal to the period of time between the beginning of injection and the beginning of preflame reaction.
2. Chemical delay: is defined as the period from the end of the physical delay to the beginning of ignition. During this period preflame reactions are considered to occur.
3. Illumination delay: is the time that elapses between the beginning of injection and the start of illumination.
4. Pressure rise delay: is the time that elapses between the beginning of injection and a measurable pressure rise due to combustion.
5. Temperature rise delay: is the time that elapses between the beginning of injection and a measurable temperature rise due to combustion. Evidently the illumination, pressure rise, and temperature rise delays are different from the physical and chemical delays.

Most of the literature concerning diesel combustion utilizes the pressure rise delay, probably because it is the easiest to measure, and because it is the most important from an engineering viewpoint. The pressure rise delay is often referred to as being the sum of the physical and chemical delays. In view of the above definitions, it is believed that this is inaccurate. In this report the ignition delay will be given in terms of illumination and pressure rise delays.

REVIEW OF PREVIOUS WORK

Most of the reported work on ignition delay was in the form of experimental investigations in a constant volume bomb. Little work was done on an engine. Few formulae are available for the ignition delay, and most of them relate the delay with the air pressure and temperature only. The following is a brief review of the formulae available.

WOLFER'S FORMULA (9)

The relation between the chemical delay and pressure and temperature can be derived from chain reaction theory and is given by the following equation:

$$t_c = \frac{C e^{\frac{b}{T_c}}}{P_c^n} \quad (1)$$

This formula applies to a homogeneous gas-phase reaction.

Wolfer used this equation for diesel fuels in a spherical constant volume vessel, and evaluated the constants and obtained the following formula.

$$\text{I.D.} = \frac{0.44}{P_c^{1.19}} e^{\frac{(4650)}{T_c}} \quad (2)$$

where: I.D. is in milliseconds, T in degree Kelvin, and P in atmospheres. The vessel was so arranged that turbulence could be created by a rotating inner liner. However, no reference for turbulence was given in this formula.

BAUER'S FORMULA (3)

Bauer put forward a theory that ignition delay, to a first approximation, is a function of $T_c \log P_c$, where P_c is in atmospheres, and T_c is degrees Kelvin or

$$\text{I.D.} = f(T_c \log P_c) \quad (3)$$

The exact nature of this function was not stated, but it was noticed that the experimental results showed similar characteristics to Wolfer's experiments in the constant-volume vessel.

WEST'S FORMULA (8)

West measured the pressure rise delay by running tests on a single-cylinder, open chamber diesel engine, 4.5" x 5.75", C.R. = 15.8:1, at a speed of 1000 rpm, at intake pressures ranging from 30" Hg. to 56" Hg. The results of ignition delay were correlated in terms of $T_c \log P_c$ as suggested by Bauer and are shown in Figure 1.

ROSEN'S FORMULA

Rosen in the paper of Ref. 6 gave a formula to relate the ignition delay with fuel properties, droplet size and compression temperature as follows:

$$\text{I.D.} = \frac{1200 r_f^2 \zeta_f c_p}{k_a} \log_e \frac{T_c - T_f}{T_c - T_i} \quad (4)$$

TSAO, MYERS, AND UYEHARA

The experimental results of these workers, Ref. 7, for the delay period were obtained from tests carried out with a C.F.R. engine incorporating a modified piston. The end of the delay period was considered to be at the point at which rapid increase in temperature occurred. The "null method" of infrared temperature measurement was used, employing an optical pyrometer.

The formula given by the author's is an empirical relationship for ignition delay as a function of the temperature, pressure, and engine speed. The formula for temperature rise ignition delay is as follows:

$$\text{I.D.} = 1000 e^x - 1000 \quad (5)$$

where

$$x = \frac{1}{1000} \left(\frac{123}{P_c} + 0.415 \right) \left\{ \left(\frac{-36.3}{T_c} + 0.0222 \right) N + \left(\frac{47.45 \times 10^3}{T_c} - 26.66 \right) + \left(\frac{T_c}{1000} - 1.45 \right) \left(\frac{1000 - N}{60} \right) \right\} \quad (6)$$

where the pressures are in psia and temperatures in °R. This equation in the simplified form is as follows:

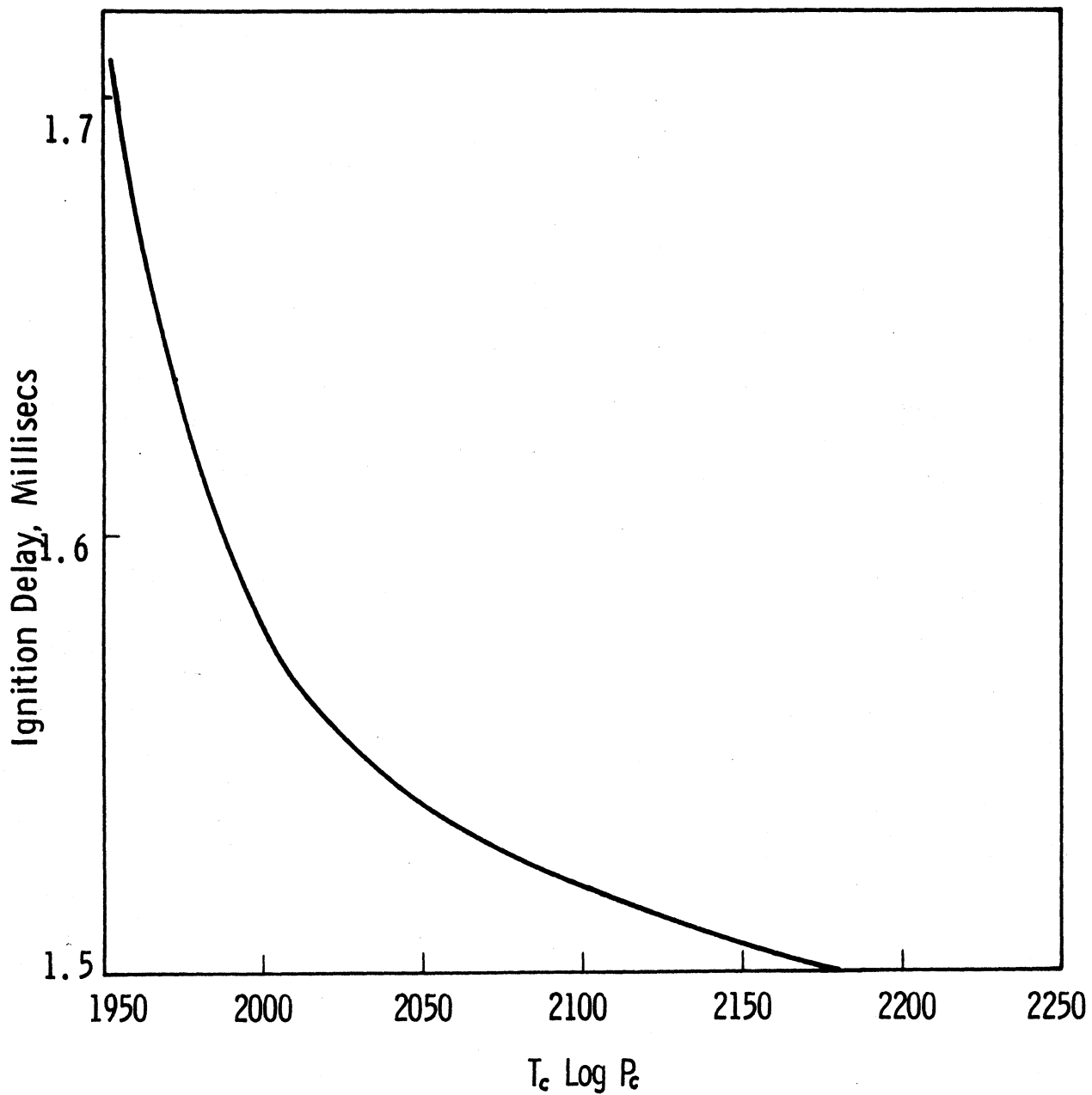


Figure 1. Ignition lag vs. $T_c \log P_c$ by West. (T_c in degrees Kelvin, P_c in psia).

$$\text{I.D.} = \left(\frac{123}{P_c} + 0.415 \right) \left\{ \left(\frac{-36.3}{T_c} + 0.0222 \right) N + \left(\frac{47.45 \times 103}{T_c} - 26.66 \right) + \right. \\
 \left. \left(\frac{T_c}{1000} - 1.45 \right) \left(\frac{1000 - N}{60} \right) \right\} \quad (7)$$

EXPERIMENTAL WORK

A. CRANK POSITION FOR MAXIMUM PRESSURE IN A MOTORED ENGINE

It has commonly been assumed that the maximum pressure occurs at T.D.C. in a motored engine and often the maximum pressure point has been used to determine the phase relationship. In our experimental data on the Lister engine it was noticed that the point of maximum pressure occurs in advance of the T.D.C. as shown in Figure 2. In this report the difference between the crank angle at which maximum pressure occurs, and the T.D.C., will be called the maximum pressure advance in a motored engine. After re-examining the accuracy of the marking unit, which is set to determine the crank degrees on the scope screen, the engine was motored in the reverse direction. The pressure traces obtained indicated that maximum pressure also occurs, at almost the same point, before T.D.C. The difference between the maximum pressure advances in the two opposite directions is 0.2° of a crank angle. This is considered to be due to the change in heat losses caused by the change in valve timing when the engine was cranked in the opposite direction. This test indicated that the settings of the degree marking disc and pickup probe are correct.

A thermodynamic analysis was then made on the air during the compression stroke and the following formula was obtained for the pressure gradient at T.D.C.

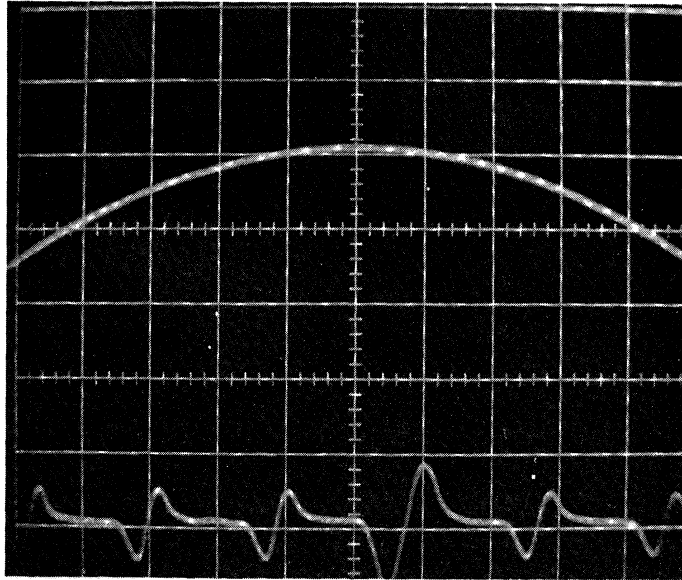
$$\frac{dP}{d\theta} = \frac{R}{c_v} \cdot \frac{1}{V} \cdot \frac{dQ}{d\theta} \quad (8)$$

where

$$\frac{dQ}{d\theta} = \text{rate of heat transfer to the air with respect to crank angle degrees.}$$

At the end of the compression stroke the heat transfer $dQ/d\theta$ has a negative sign because heat is lost from the air to cylinder walls. Therefore $dQ/d\theta$ should have a negative sign indicating that the maximum pressure for a motored engine should occur before T.D.C.

This conclusion is also supported by published data of Tsao et al., (Ref. 7), for the compression temperature in a diesel engine. The compression temperature was measured by applying the infrared null method. Figures 3, 5, and 9 of this reference indicate that the maximum temperature occurs before T.D.C. during the compression stroke. Accordingly the maximum pressure should also occur before T.D.C.



Point of
Max. Press.
T.D.C.
Advance

Figure 2. Maximum pressure advance in motored Lister Blackstone engine ($N = 980$ rpm, coolant temperature = 104.5°F).

This analysis indicated that the maximum pressure advance at the end of the compression stroke of a motored engine is mainly caused by the cooling losses. And, since the gas pressure and temperature at the end of compression in the engine affect the delay period, therefore the cooling losses should have an effect on delay period. This effect has been investigated and the results are given in Section D of this experimental work.

B. EFFECT OF FUEL-AIR RATIO ON IGNITION LAG

In a chemical process concentration of the reactants is an important factor that affects the rate of reaction. In the diesel engine, at the time of ignition there occur in the combustion chamber local fuel-air ratios ranging from zero to infinity. Ignition takes place in some region where the fuel-air ratio is optimum. This is generally in the envelope of the spray and is affected by many parameters such as type of fuel, its atomization, penetration and air turbulence. However, it is believed that if these factors are kept constant there exists some limits on the lean and rich sides beyond which the ignition will not occur or, at least, will be irregular. Starting with the lean limit, it is believed that an increase in fuel-air ratio would increase the probability of ignition start and the reaction speed and consequently reduce the ignition delay.

To find the effect of fuel-air ratio an ignition delay experiments were run at variable fuel-air ratios with the other parameters kept constant. On the lean side the engine was motored with fuel injection and combustion. The amount of fuel injected was reduced, and fuel-air ratios as low as 0.00216, (0.0325 stoichiometric), were reached. With the engine producing power the fuel-air ratio was increased up to 85% the stoichiometric ratio. With higher fuel-air ratios erratic operation of the engine occurred due to a very late after injection. By examining the cylinder pressure under these conditions it was noticed that ignition of the left-over fuel from the previous cycle occurred before the start of injection.

The results of this series of runs are plotted in Figures 3 and 4. Figure 3 indicates that the limit of irregular combustion on the lean side is at a fuel-air ratio of 0.0059 (0.089 - the stoichiometric ratio). The general trend of this figure indicates that the ignition delay decreases with the increase in fuel-air ratio. An increase in fuel-air ratio from .011 to 0.043 caused the illumination ignition delay to decrease by 32%. It should be noted that at higher fuel-air ratios, the solar cell did not operate properly. The decrease in pressure rise delay amounted to 34% by an increase in fuel-air ratio from 0.011 to 0.0568.

The effect of fuel-air ratio on decreasing the ignition lag is actually more than indicated in Figure 3, because at higher fuel-air ratios fuel injection starts at an earlier angle before T.D.C. i.e , at lower air pressures, temperatures, and densities. The advance in the start of fuel injection at different fuel-air ratios is shown also in Figure 3.

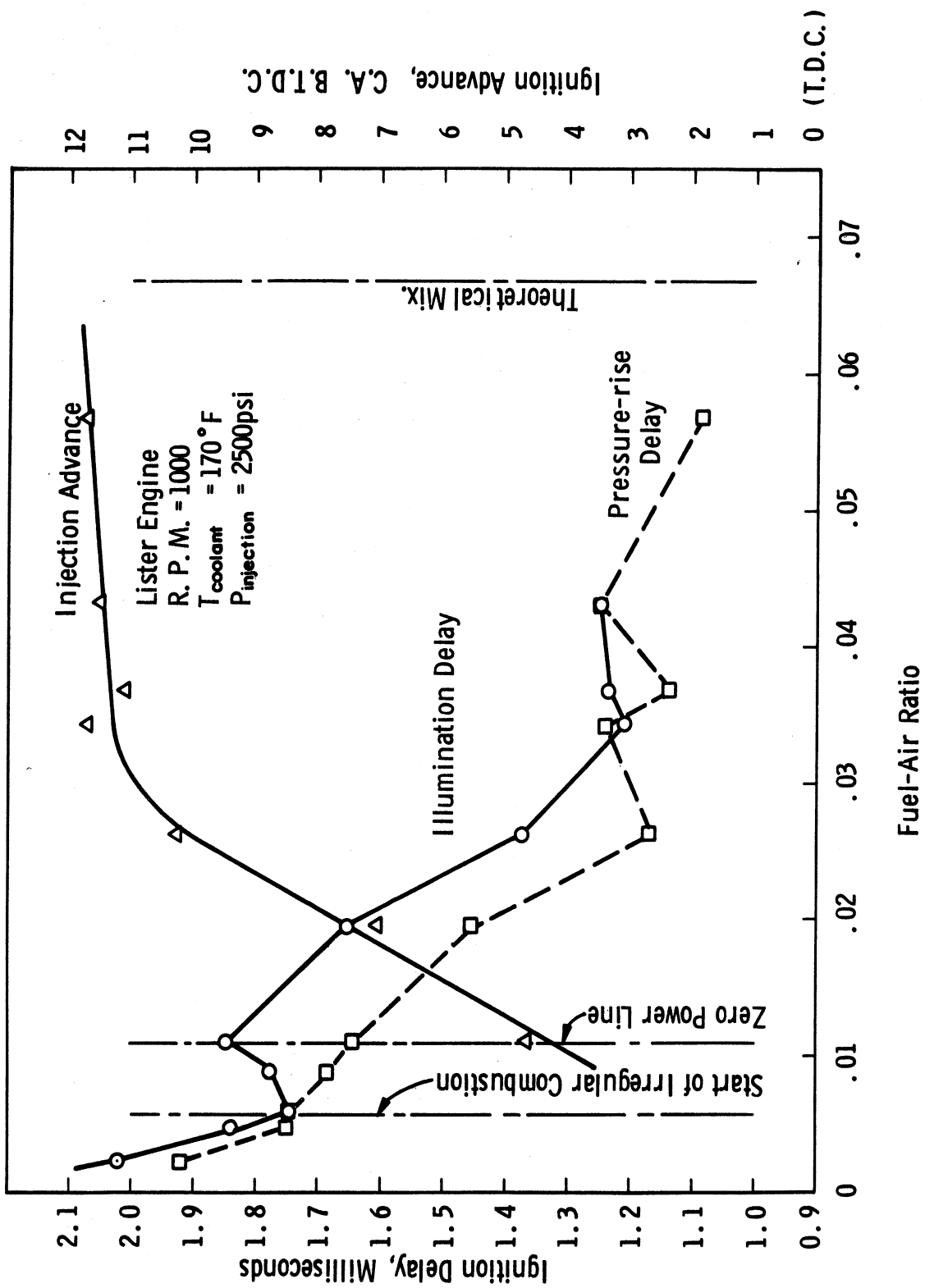


Figure 3. Effect of fuel-air ratio on ignition delay, and injection advance.

The earlier injection at higher fuel-air ratios is believed to be due to the leaking characteristics of the plunger-barrel assembly in the fuel pump. Although the clearance between the plunger and barrel is very small yet the path of the fuel from the high pressure region to the ports changes with the relative position of the plunger-helix with respect to the barrel ports. At high loads, the path of the fuel is long and the leakage is less. Another factor that may anticipate in the fuel injection advance is the throttling effect at the opening and closing of the ports.

The injection advance at high fuel-air ratios can be eliminated by retarding the injection timing. This is not feasible in the Lister engine, but will be possible with the new ATAC engine.

The effect of fuel-air ratio on B.S.F.C. and I.S.F.C. is shown in Figure 4. An increase of fuel-air ratio from 0.11 to 0.0568 caused an increase of 52% in I.S.F.C. The increase in I.S.F.C. with fuel-air ratio, in spite of the earlier injection and shorter delay indicates that ignition delay has no significance to the overall combustion efficiency.

C. EFFECT OF INJECTION PRESSURE ON IGNITION DELAY

In Section B of this experimental work the effect of the fuel concentration on ignition delay was investigated quantitatively. In this part the quality of the fuel-air mixture will be studied as far as its effect on ignition delay.

It is known that many factors influence mixture formation in the diesel engine, including the mean spray velocity at the nozzle, atomization, penetration, evaporation, and mixing with air. Among the factors that substantially affect the mixture formation especially at beginning of the injection process, is the differential pressure across the nozzle orifice. The fuel pressure before the nozzle is primarily a function of the setting of the needle opening pressure. In order to investigate the effect of changing the fuel-air mixture state or quality in the cylinder the opening pressure was changed from 1000 psi to 4000 psi. The effect on ignition lag and S.F.C. are shown in Figures 5 and 6, respectively. Figure 5 indicates that as the injector opening pressure is increased starting from 1000 psi both the illumination and pressure-rise delays are reduced reaching a minimum at a pressure of 2300 and 2500 psi, respectively. At higher injection pressures the ignition lag is again increased.

This is expected, because in a heterogeneous mixture, such as that of the diesel engine, the fuel-vapor concentration depends upon the rate of evaporation of the spray droplets and their orientation in the combustion chamber. A study of the process of injection and spray formation indicates that, for an injector similar to that used in the Lister engine, the spray atomization and penetration depend greatly on the injection pressure. The higher the injection pressure, the more the degree of atomization and the less the penetration. At pressures near 4000 psi, the fuel takes the shape of a finely atomized spray,

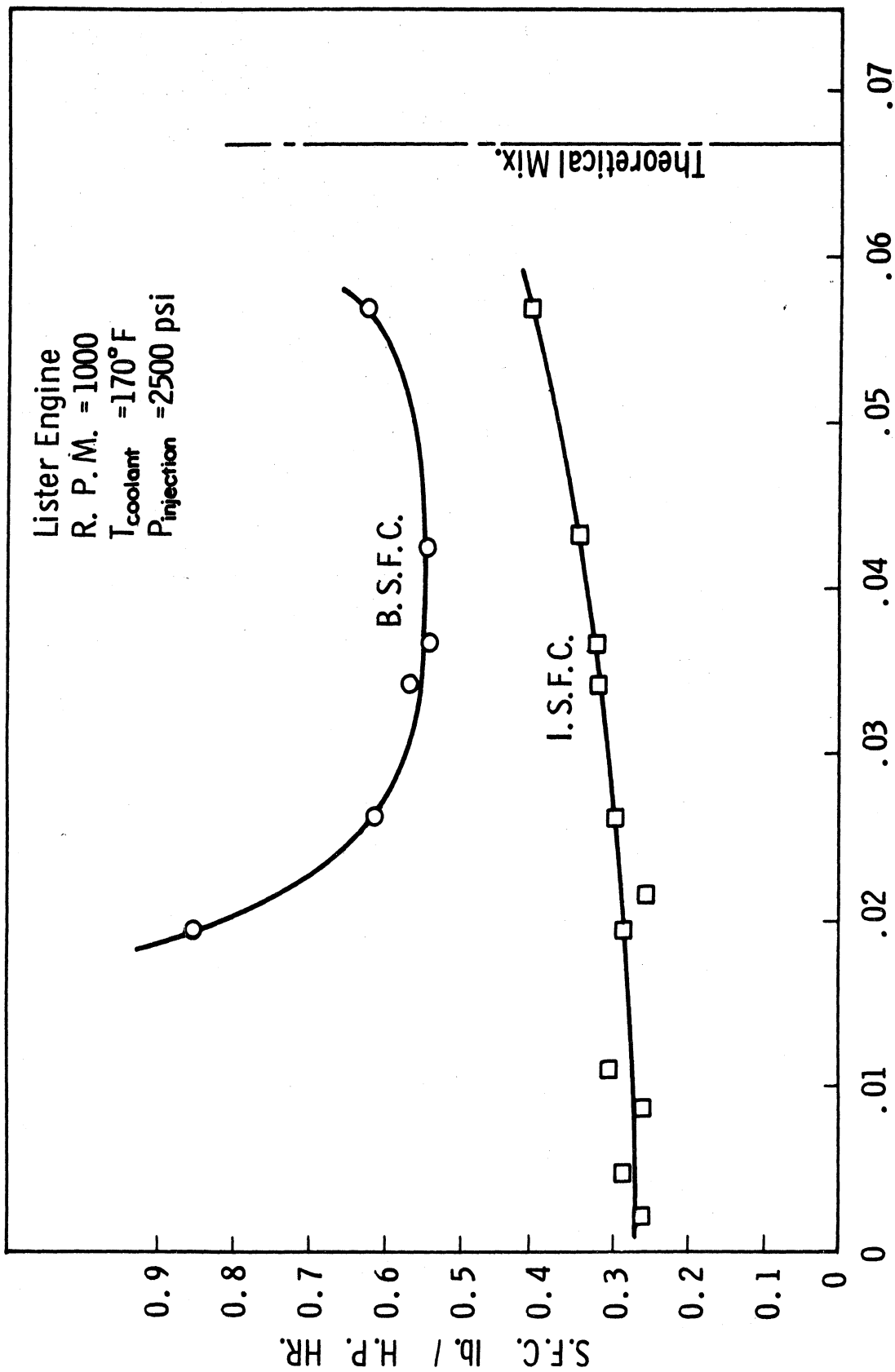


Figure 4. Effect of fuel-air ratio on B.S.F.C. and I.S.F.C.

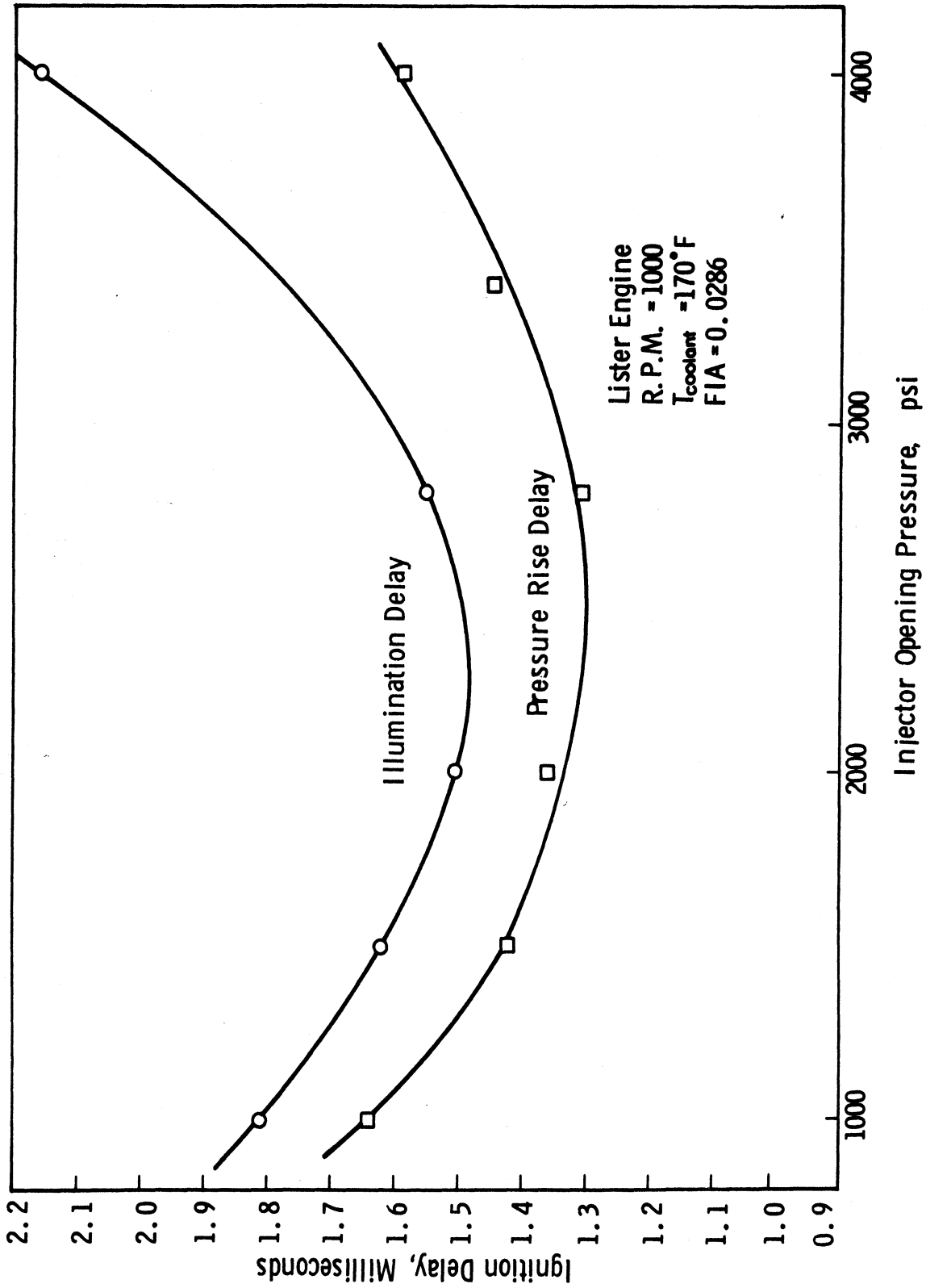


Figure 5. Effect of injector opening pressure on ignition delay.

concentrated near the injection nozzle forming a rich mixture in this area. The far parts of the chamber are left without fuel. This type of fuel distribution caused by changes in injection pressure caused the increase in ignition delay at the higher injection pressures.

The effect of the injection pressure on combustion efficiency is indicated in the I.S.F.C. curve, Figure 6. It shows that best efficiency is obtained at injection pressure giving minimum delay.

D. EFFECT OF SURFACE TEMPERATURE ON IGNITION DELAY

Since the air temperature and pressure at the point of injection are functions of the rate of heat loss to the walls as indicated in Section A of this experimental work, it is to be expected that cooling water temperature would affect ignition delay. To investigate this point a series of tests were carried out on the engine at various cooling water temperatures ranging from 70°F up to 200°F. The results are plotted in Figure 7 and indicated that at higher temperatures the ignition delay is reduced. The reduction in pressure rise delay was consistent and amounted to 20% by increasing the cooling temperature from 70 to 200°F.

The cooling water temperature did not only affect the ignition delay, but also it affected the start of injection. Figure 8 shows this effect and an advance of two crank angle degrees was caused by decreasing the water temperature from 200°F to 70°F. This is of special interest in studies of cold starting problems.

E. EFFECT OF TURBULENCE ON IGNITION DELAY

Very little work has been done, in previous investigations to find the effect of turbulence on ignition delay. This is believed to be due to the complicated effect of turbulence on heat exchange between the gas and the walls, injection and vaporization, distribution of the vapor in the chamber. In the Lister engine the turbulence at the end of the compression stroke is caused by forcing the air through the tangential passage between the main chamber and the spherical chamber, as shown in Figure 9.

At the compression ratio used for the present series of runs (13.92:1), the volume of the chamber is equivalent to 6.55% of the total swept volume, and the area ratio of the connecting passage to the piston area is 3.22%. With this configuration, the air in the passage is estimated to obtain velocities as high as 164 fps during the compression stroke, at an engine speed of 1000 rpm (Reference 1). The air speed in the passage at different crank angles is shown in Figure 10.

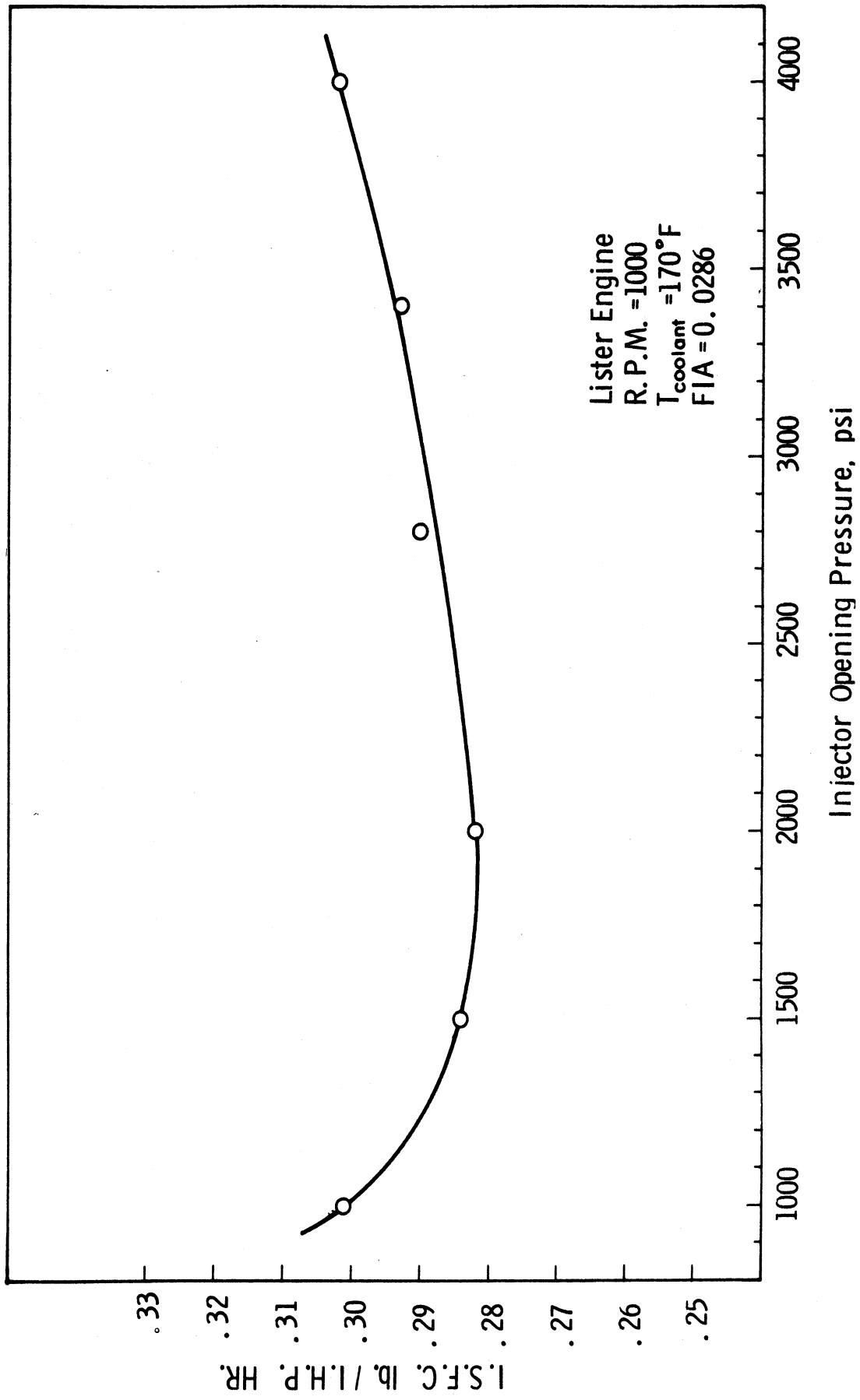
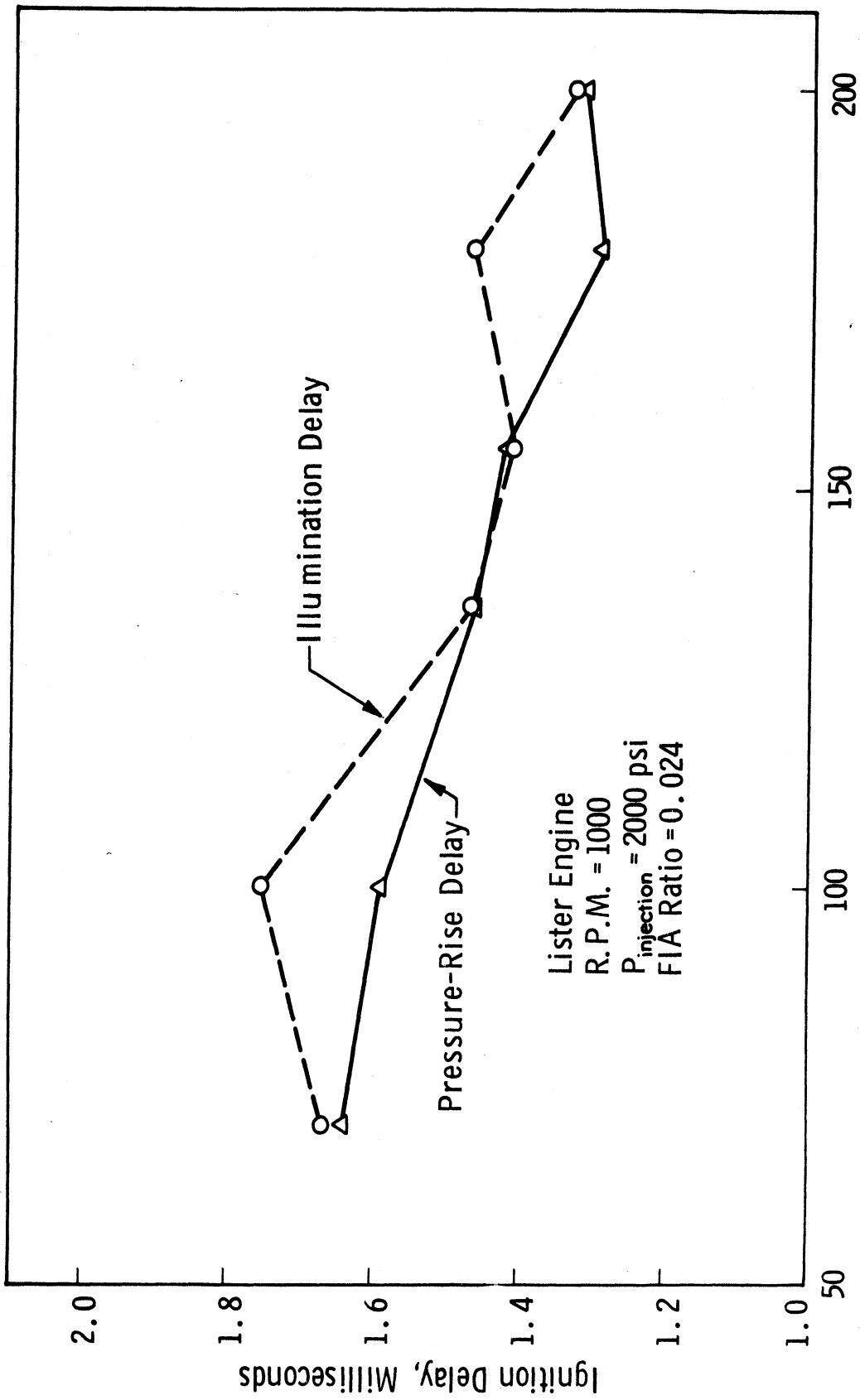


Figure 6. Effect of injector opening pressure on I.S.F.C.



Cooling Water Temperature °F at Outlet

Figure 7. Effect of cooling water temperature on ignition delay.

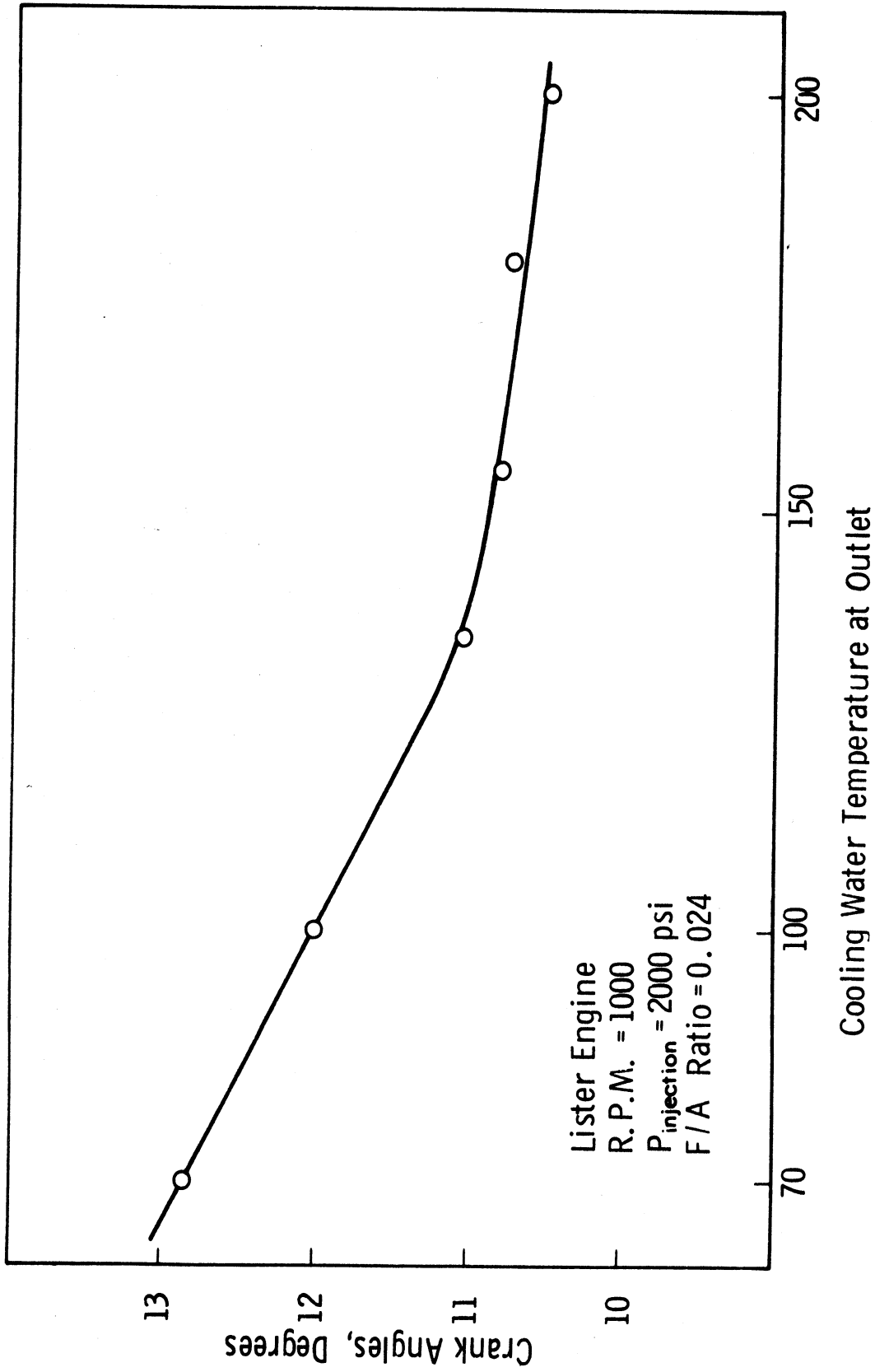


Figure 8. Effect of cooling water temperature on injection start.

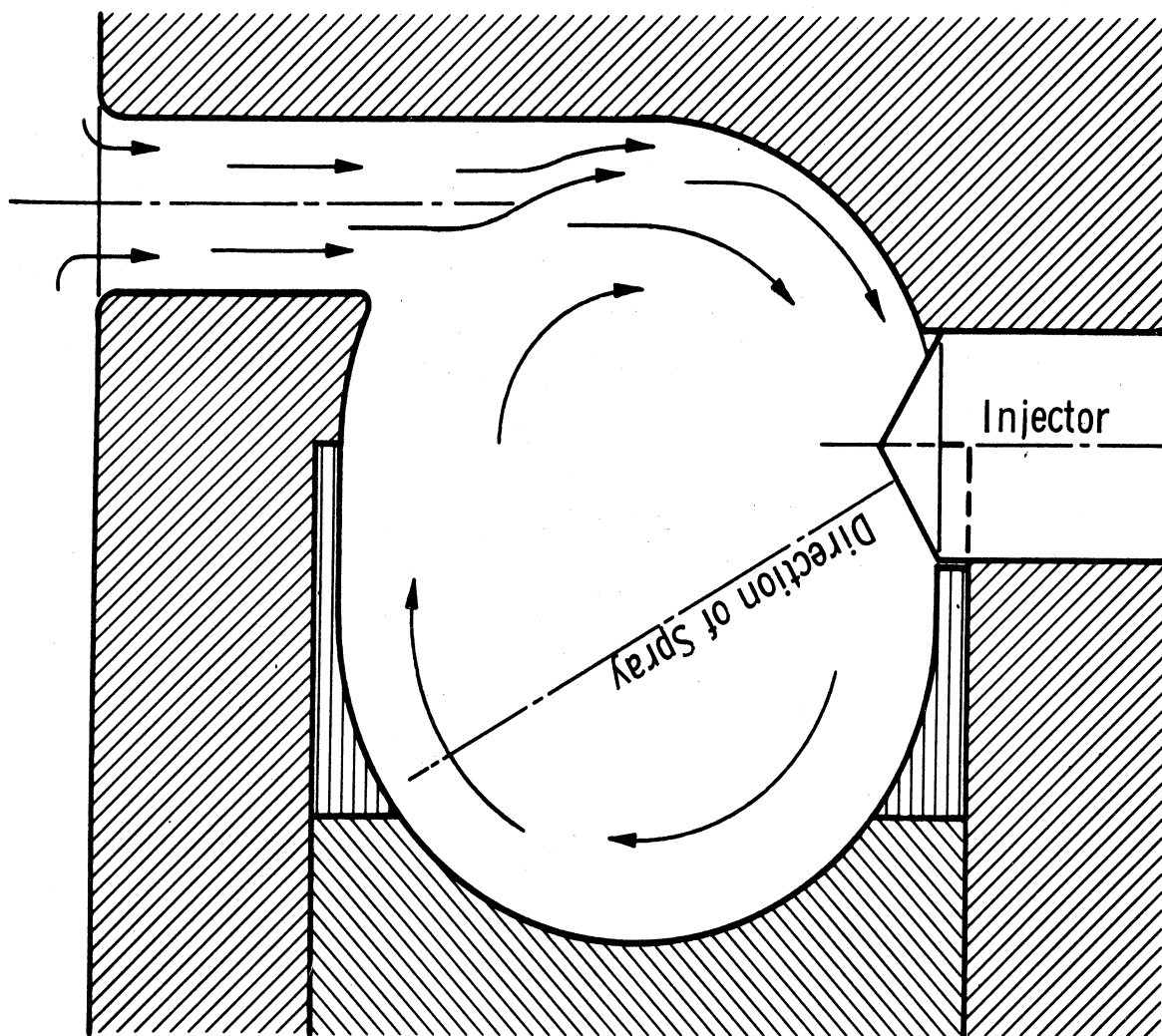


Figure 9. Turbulence in modified combustion chamber of Lister engine.

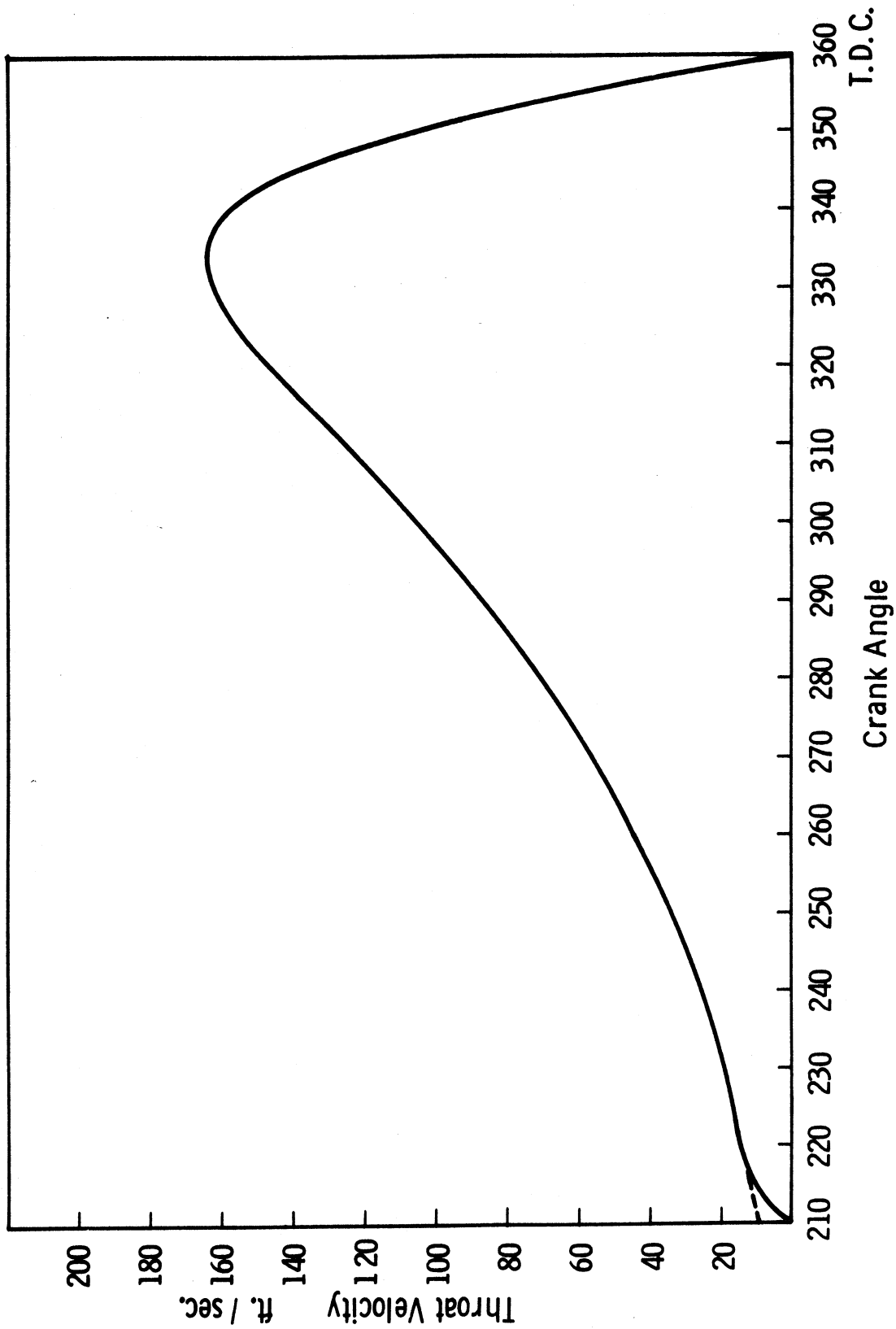


Figure 10. Air speed in the tangential passage to the swirl chamber of Lister engine at 1000 rpm.

The effect of increased speed on decreasing the illumination and pressure-rise delays is shown in Figures 11 and 12.

It is noticed that both ignition delays increase in terms of crank degrees and decrease in terms of milliseconds. An increase of engine speed from 500 rpm to 1200 rpm caused a drop of 28% in illumination delay and 40% in pressure rise delay. The effect of increased turbulence on the specific fuel consumption is shown in Figure 13.

It is to be noted that the increase in turbulence, caused by increasing engine speed, is not the only factor that is responsible for the decrease in delay period. Other factors are the increase in air pressure and temperature at higher speeds. However, this is partially counteracted by the effect of injecting the fuel earlier in the compression stroke, i.e., at temperatures and pressures lower than those that might occur nearer to T.D.C. The injection advance at the different speeds is measured from the traces and plotted in Figure 14.

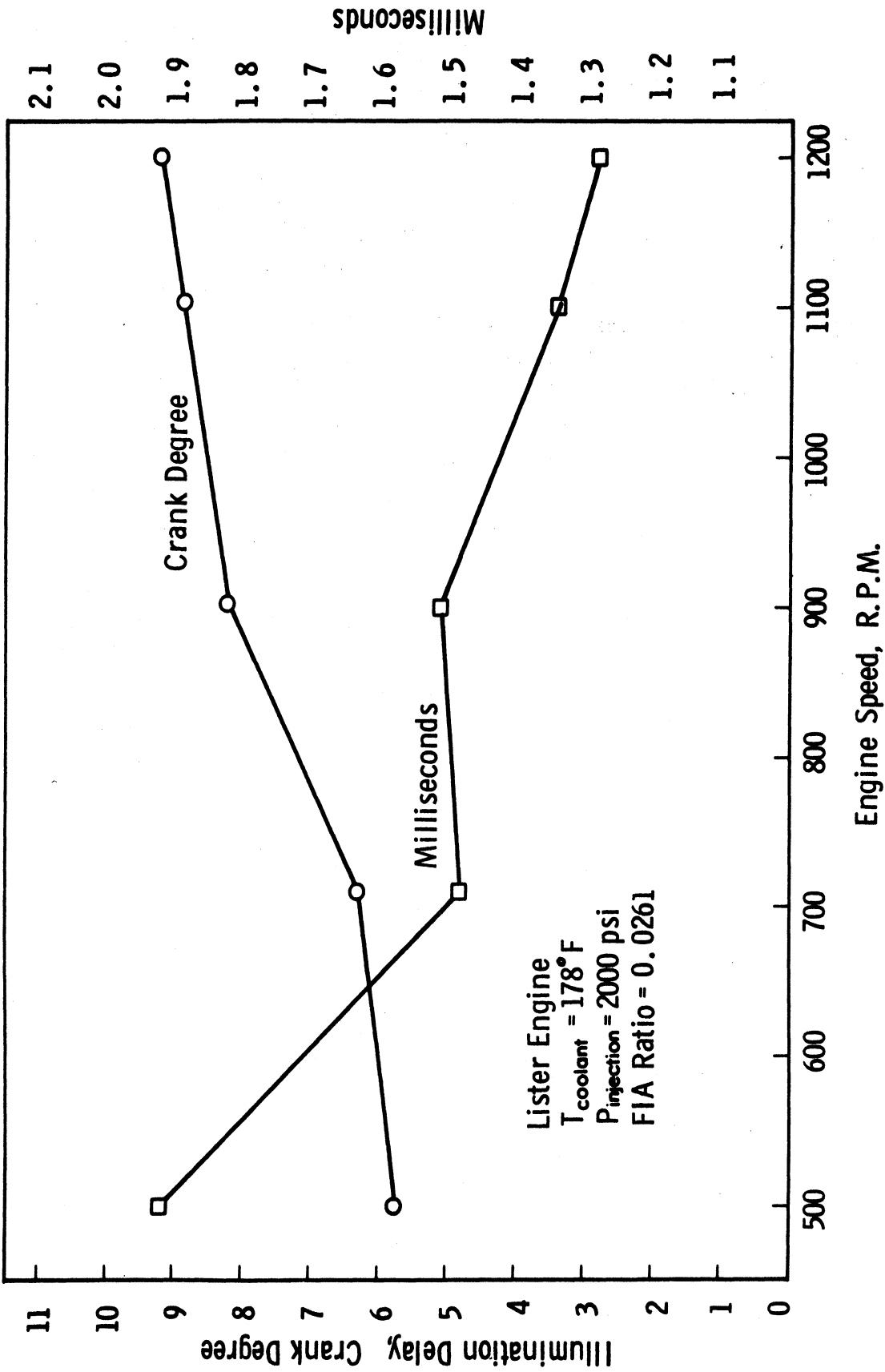


Figure 11. Effect of engine speed on illumination delay.

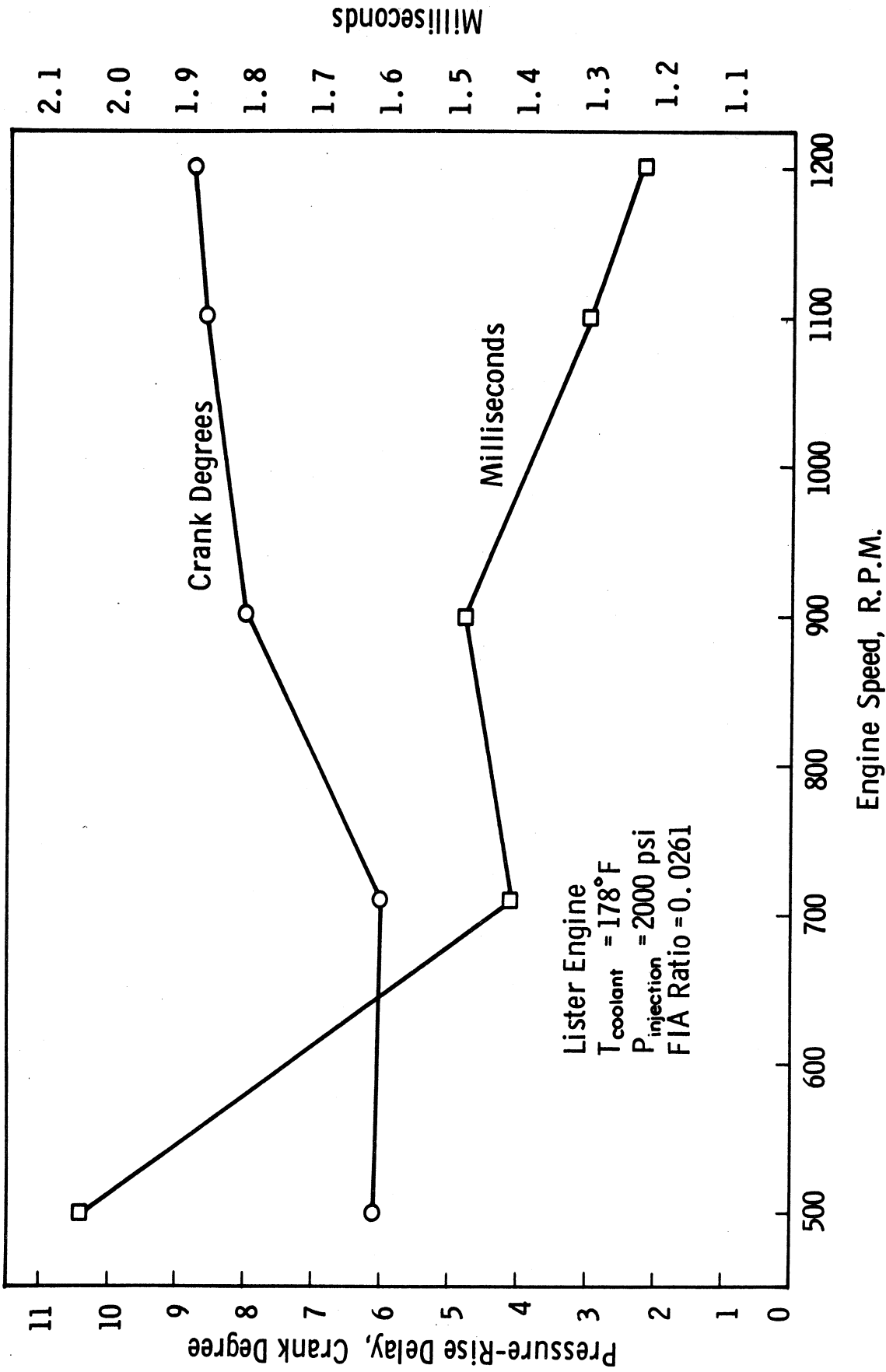


Figure 12. Effect of engine speed on pressure-rise delay.

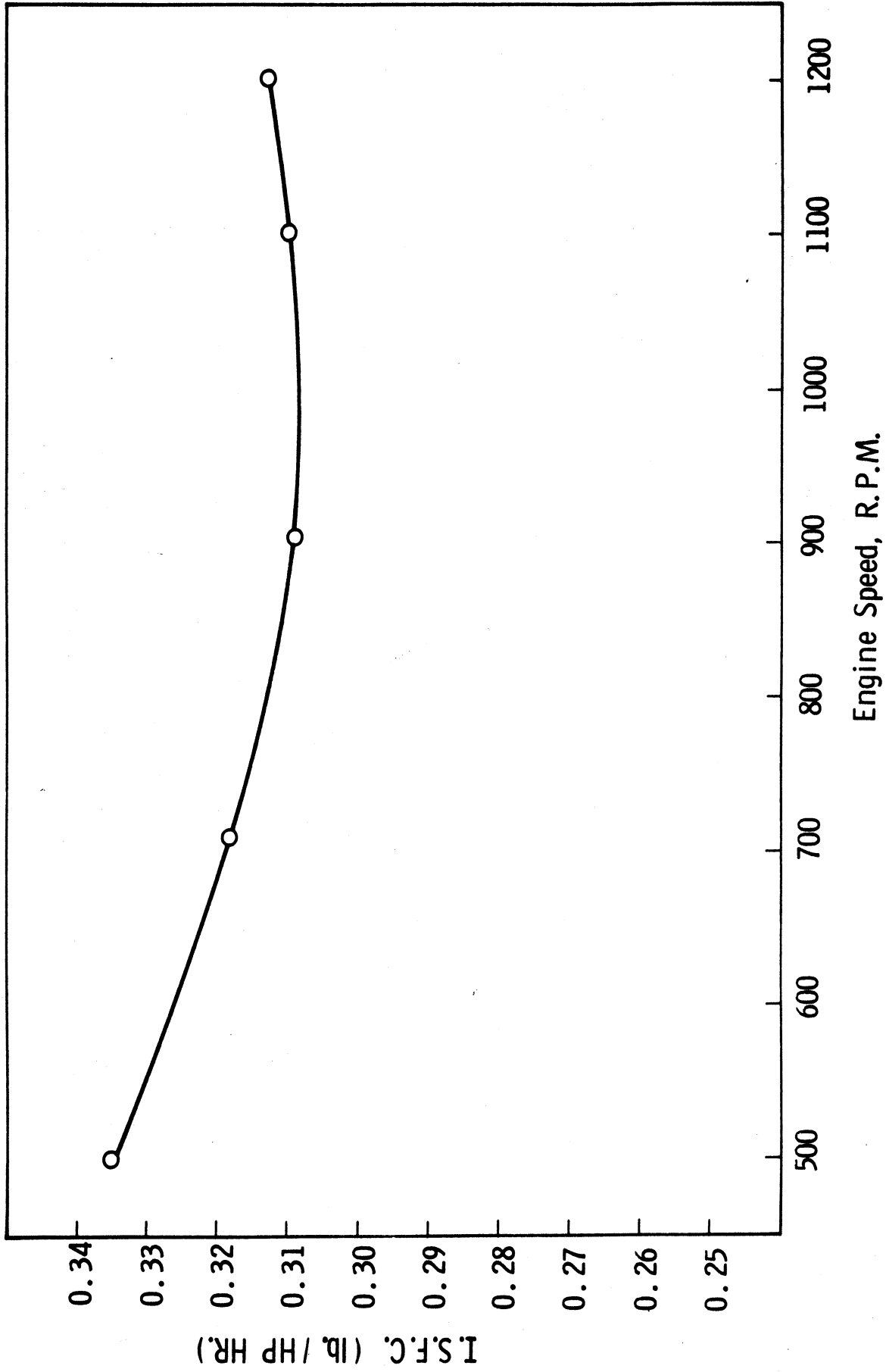


Figure 13. Effect of engine speed on I.S.F.C.

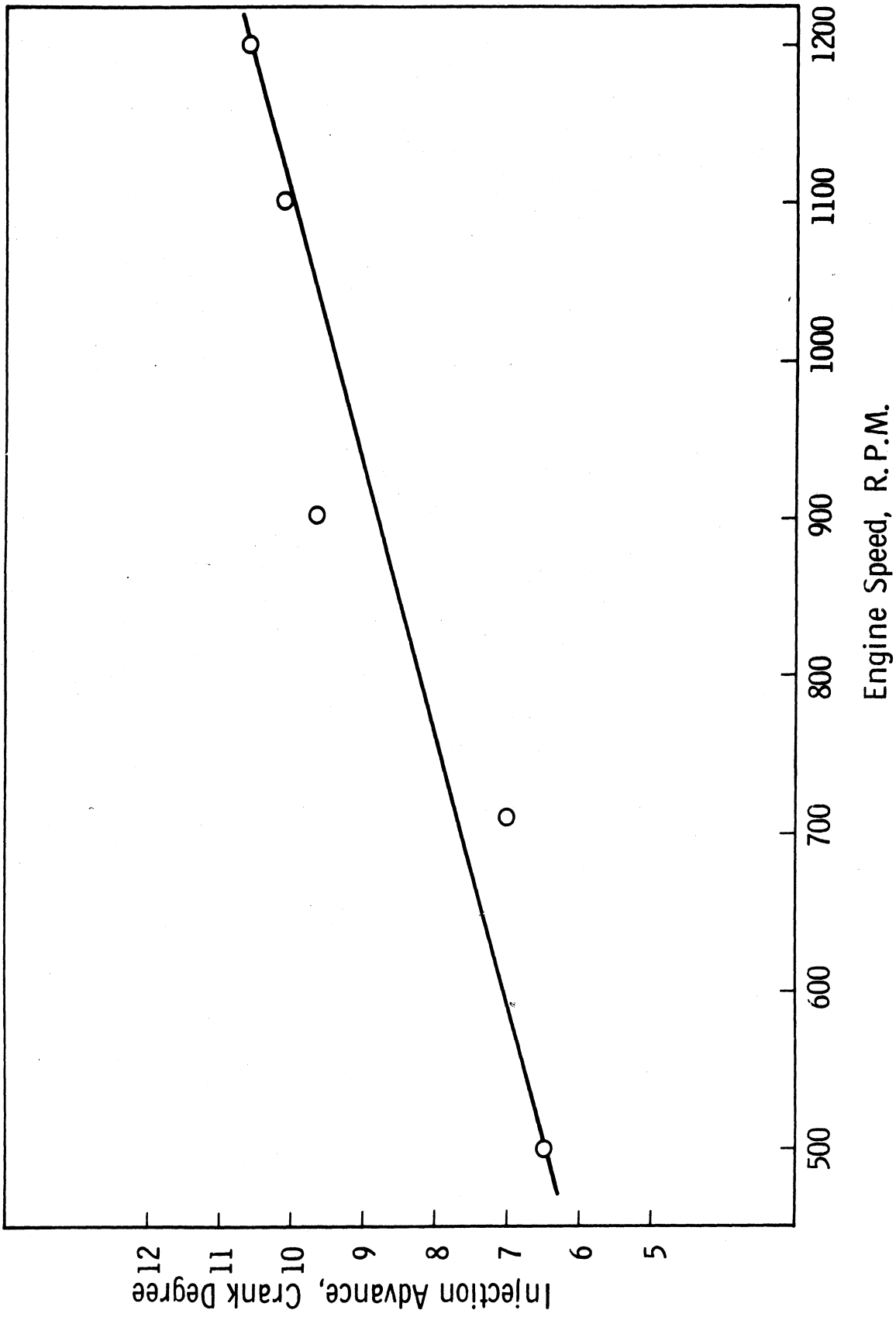


Figure 14. Effect of engine speed on injection advance.

COMPUTATIONS

These computations are based on the experimental measurements taken while testing the engine under the conditions given in Appendix II.

A. GAS TEMPERATURE

The average gas temperature at any point in the cycle was calculated from the measured air flow, fuel flow, and the cylinder pressure, by using the equation of state. The gas temperature is shown in Figure 15, together with the gas pressure.

B. RATE OF HEAT RELEASE

The rate of heat release was derived from the first law of thermodynamics, Appendix III, and is given by:

$$\frac{dQ}{d\theta} = \left(\frac{c_v}{R} + \frac{1}{J} \right) P \frac{dV}{d\theta} + \left(\frac{c_v}{R} \right) V \cdot \frac{dP}{d\theta} \quad (9)$$

The values computed for the rate of heat release and accumulated heat release are plotted in Figure 16. This figure indicates that there is a negative heat release when injection first starts at 356 crank degrees, or 4° before T.D.C. This is probably due to heat losses to cylinder walls and in heating up and evaporating the fuel. The rate of heat release reaches zero at 2.5° before T.D.C. indicating that the amount of energy produced from the reaction is just enough to balance the heat losses from the gas to the walls. The maximum value of heat release is 0.0395 BTu/crank degree at a crank angle of 373, after which it drops continuously till the start of after-injection. The increase in the heat release rate between 390 and 420 seems to be due to the energy released from the combustion of the after-injected fuel.

This diagram shows also that the heat release continues till near the end of the expansion stroke. This is believed to be due to the very late addition of fuel in the after-injection which continued to an angle of 396. To check the phenomena of heat release near the end of the expansion stroke the P-V relationship was plotted on a log-log sheet, from which the index of each process can be obtained, and the condition of heat transfer to or from the gas is indicated.

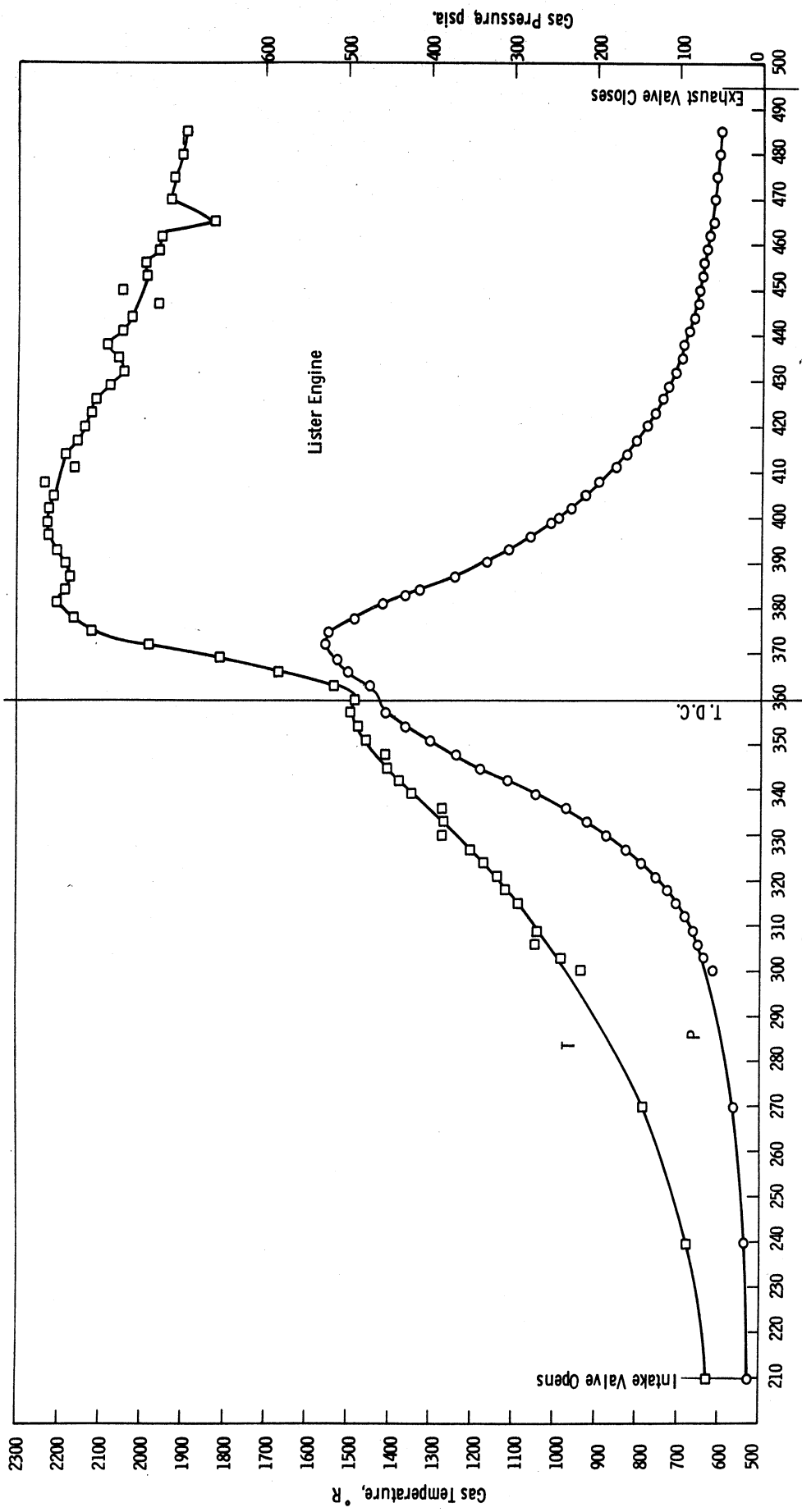


Figure 15. Gas pressure and temperature during the cycle.

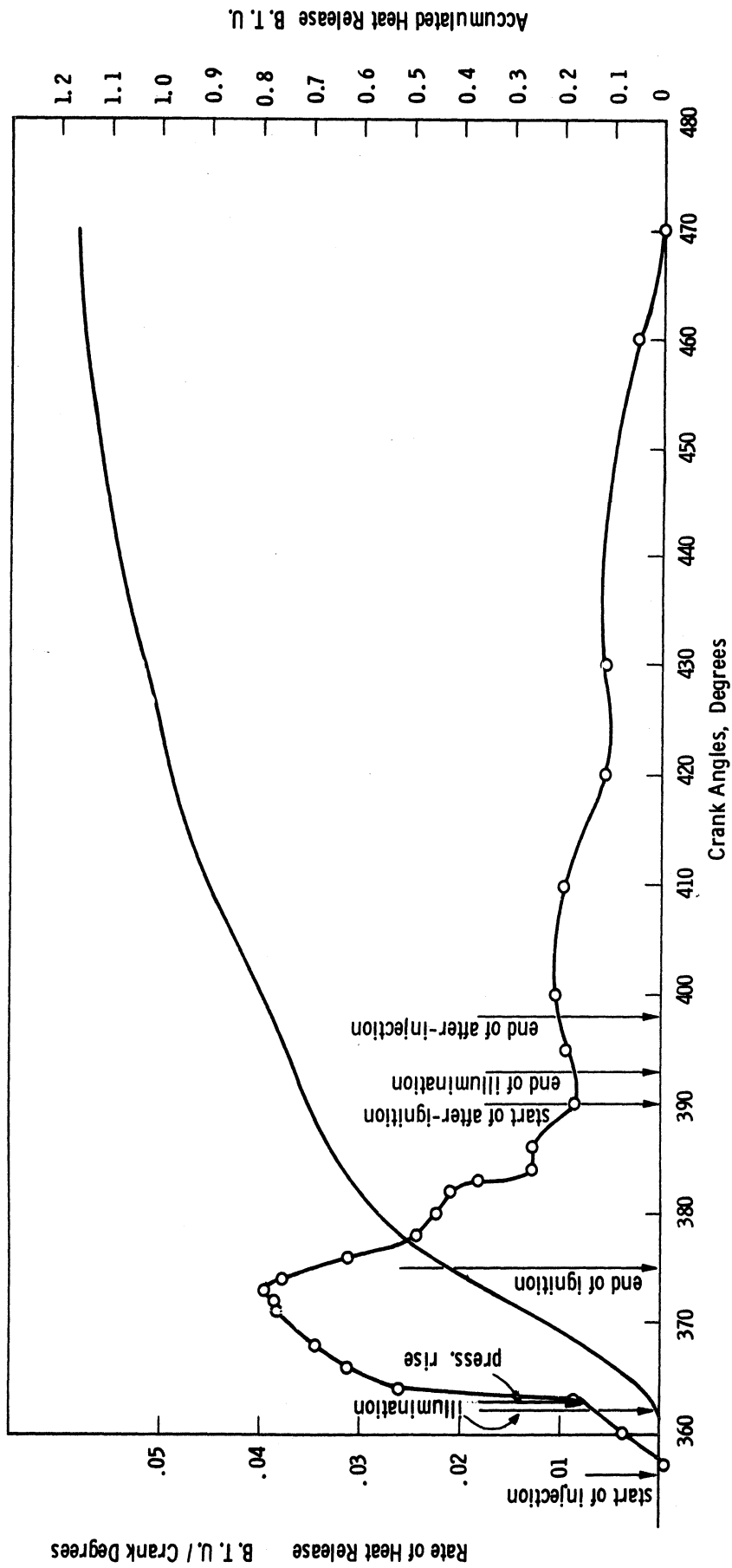


Figure 16. Rate of heat release and accumulated heat release diagrams.

C. INDEX OF COMPRESSION AND EXPANSION

In order to calculate the index of compression and expansion the gas pressure and volume are plotted on a log-log sheet as shown in Figure 17. For the compression stroke the index of compression (the value of n) changed from 1.392 at the early part of the stroke to 1.11 at the end of compression. For the early part of the expansion stroke the index started with a negative value of -1.026, increased to zero shortly after T.D.C., reached 0.99 during the early part of the expansion, and increased to 1.15 at the end of the expansion stroke.

The factors that affect the index of compression and expansion are:

1. the rate of heat release due to combustion
2. the rate of heat exchange between the gas and walls
3. the physical properties of the gas as regards composition and specific heats
4. the blowby rate. In general the blowby rate is small if the cylinder and piston are in good conditions.

At the beginning of compression work is done on the gas, which is still at a temperature lower than wall temperature. The combined effect of compression work and heat gain from the walls result in a value of 1.392 for n . This value is the highest in the whole cycle. The conditions are not the same near the end of compression. Heat is lost to the walls, the specific heats are higher due to increase in temperature and the gas blowby rate is also high. All these factors cause a drop in the value of n to 1.11.

At the beginning of expansion stroke the rate of heat release due to combustion is the dominating factor and $n = -1.026$. The pressure reaches its maximum shortly after T.D.C.

As the piston goes on the expansion stroke, work is done by the gases, but heat is still being released causing index to be 0.99 which is very near to isothermal expansion in which case the net heat added to the gas is equal to work done by the gases. The value of n continues to increase, as the piston proceeds near end of expansion, where it reaches 1.15.

For a polytropic process the heat added to the gases can be given by:

$$dQ = mC_n (T_2 - T_1) \quad (10)$$

where

$$c_n = -c_v \frac{K - n}{n - 1} \quad (11)$$

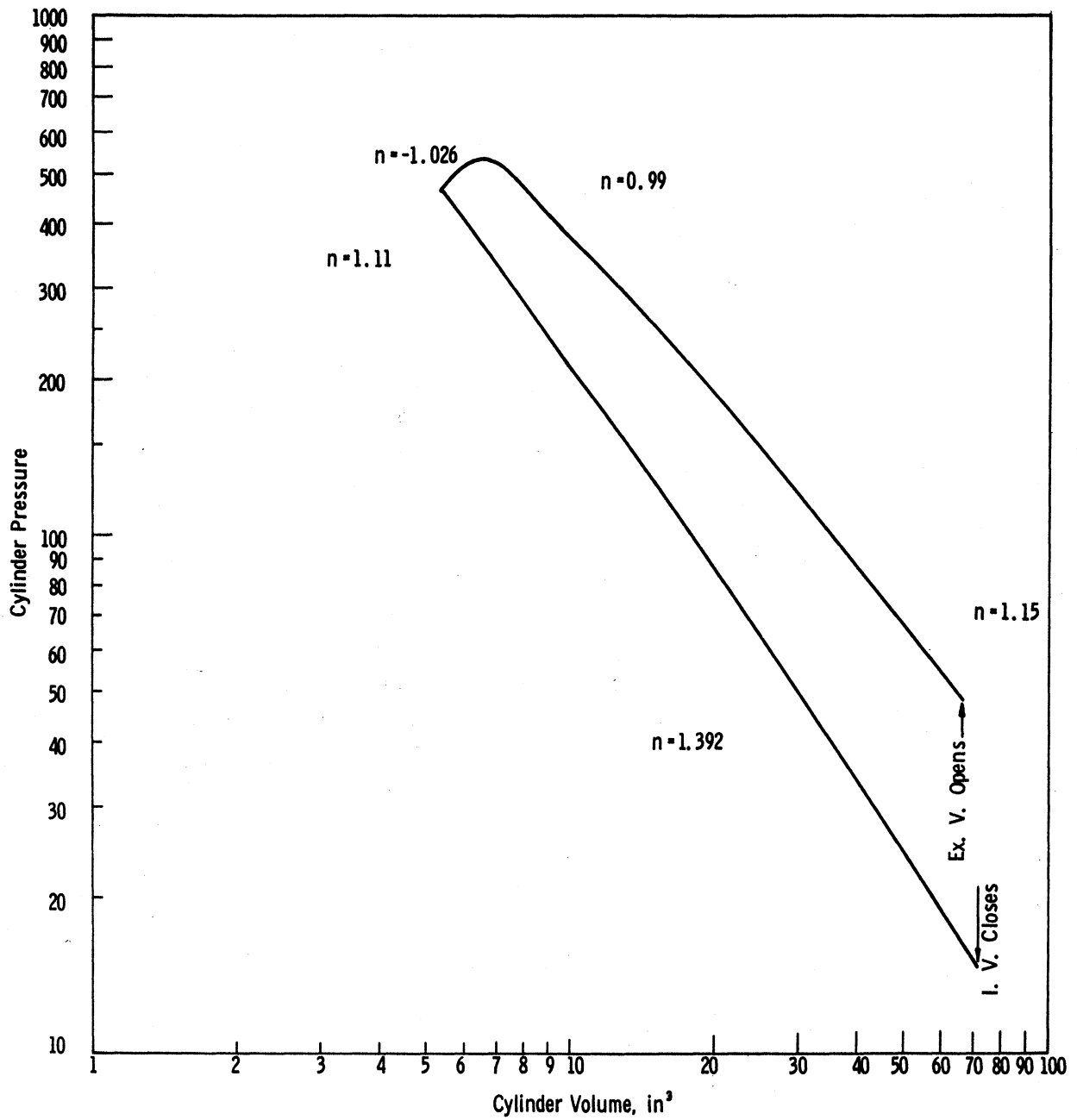


Figure 17. P-V relationship on a Log-Log sheet.

T_2 and T_1 are the gas temperatures at the end and beginning of the process consecutively.

Near the end of the expansion stroke $K = 1.315$, and $n = 1.15$ (obtained from the log-log sheet). Therefore according to equation (10) some heat should be released. This conclusion supports the results of the heat release computations.

D. RATE OF FUEL INJECTION

The rate of fuel injection into the cylinder was computed from the pressure difference across the nozzle, the area of flow, and a coefficient of discharge c_d .

$$m_f = c_d A_f \sqrt{2g \zeta_f (P_f - P_g)} \quad (12)$$

The value for c_d was computed from the measured fuel consumption and the accumulated fuel injection, as calculated from Equation (12) with $c_d = 1$. The value obtained for c_d is 0.891. It is to be noted that the coefficient of discharge depends on the general form of the orifice, the ratio of its length and diameter and the injection pressure. In our case the ratio of length to orifice diameter is equal to 6.4. By referring to values for c_d , obtained by previous investigators for similar orifices, under the same injection pressures, it was found to be 0.88 (4).

Figure 18a is a cross section in the nozzle-needle assembly. Figure 18b indicates that the area of flow between the needle and seat is smaller than the orifice area for lifts less than 0.0008 in. For higher lifts the area of flow is limited by the orifice area which equals 0.0000865 in².

The rate of fuel injection and the accumulated injected fuel at different crank angles are calculated and plotted in Figure 19. From this figure it is noticed that after injection started at an angle of 389°, or 14 crank angle degrees after the end of the first injection.

E. COMBUSTION COMPUTATIONS

The experimental results for this sample run are as follows:

Start of injection	=	4.2 B.T.D.C.
Illumination (solar cell)	=	2 A.T.D.C.
Pressure rise	=	2.5 A.T.D.C.
Illumination delay	=	6.2°C.A.
	=	<u>1.03 millisec.</u>
Pressure rise delay	=	<u>1.117 millisec.</u>

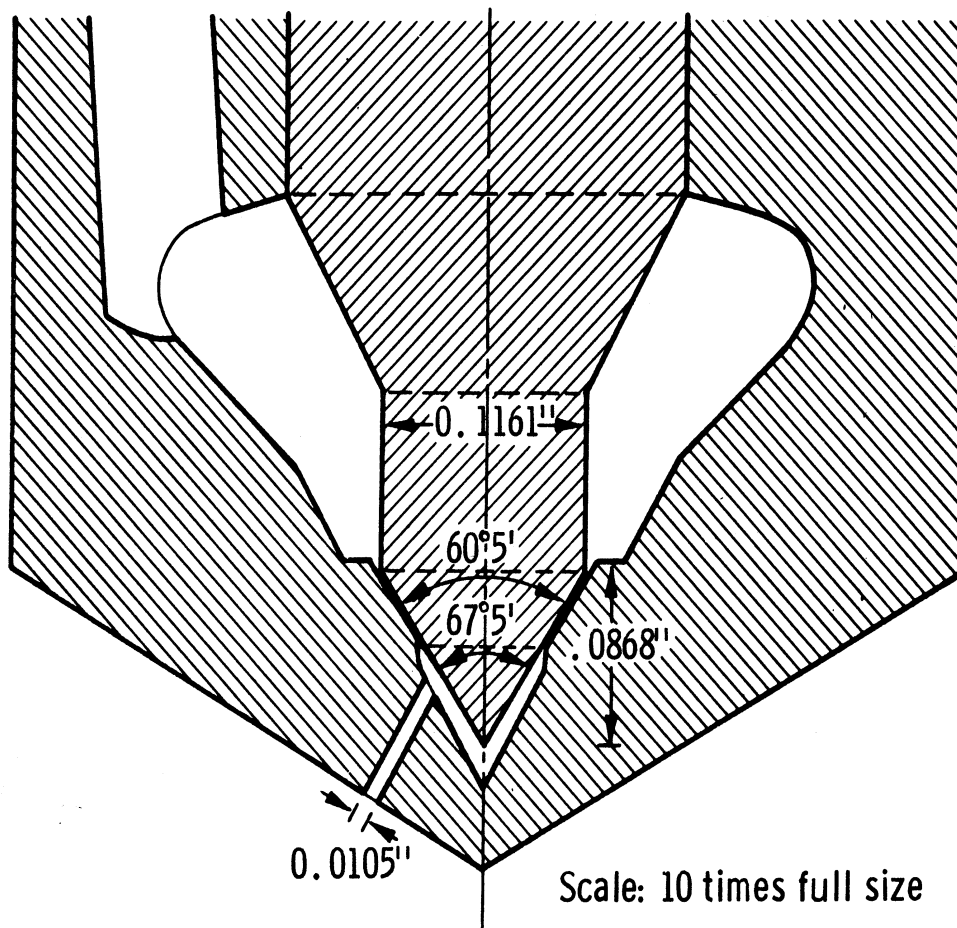


Figure 18A. Nozzle needle assembly.

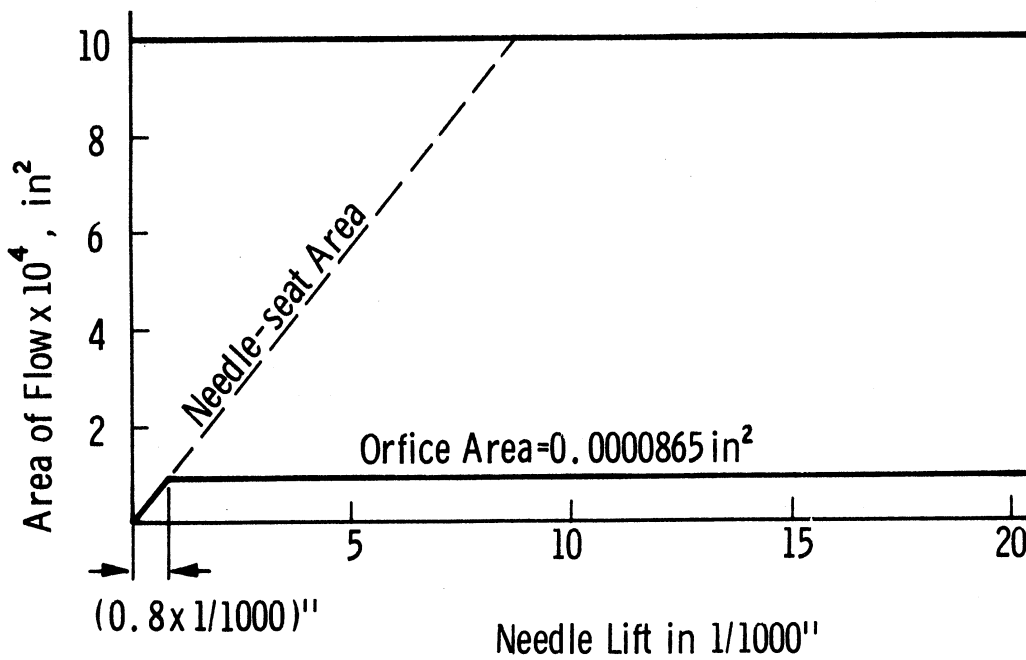


Figure 18B. Area for fuel flow vs. needle lift.

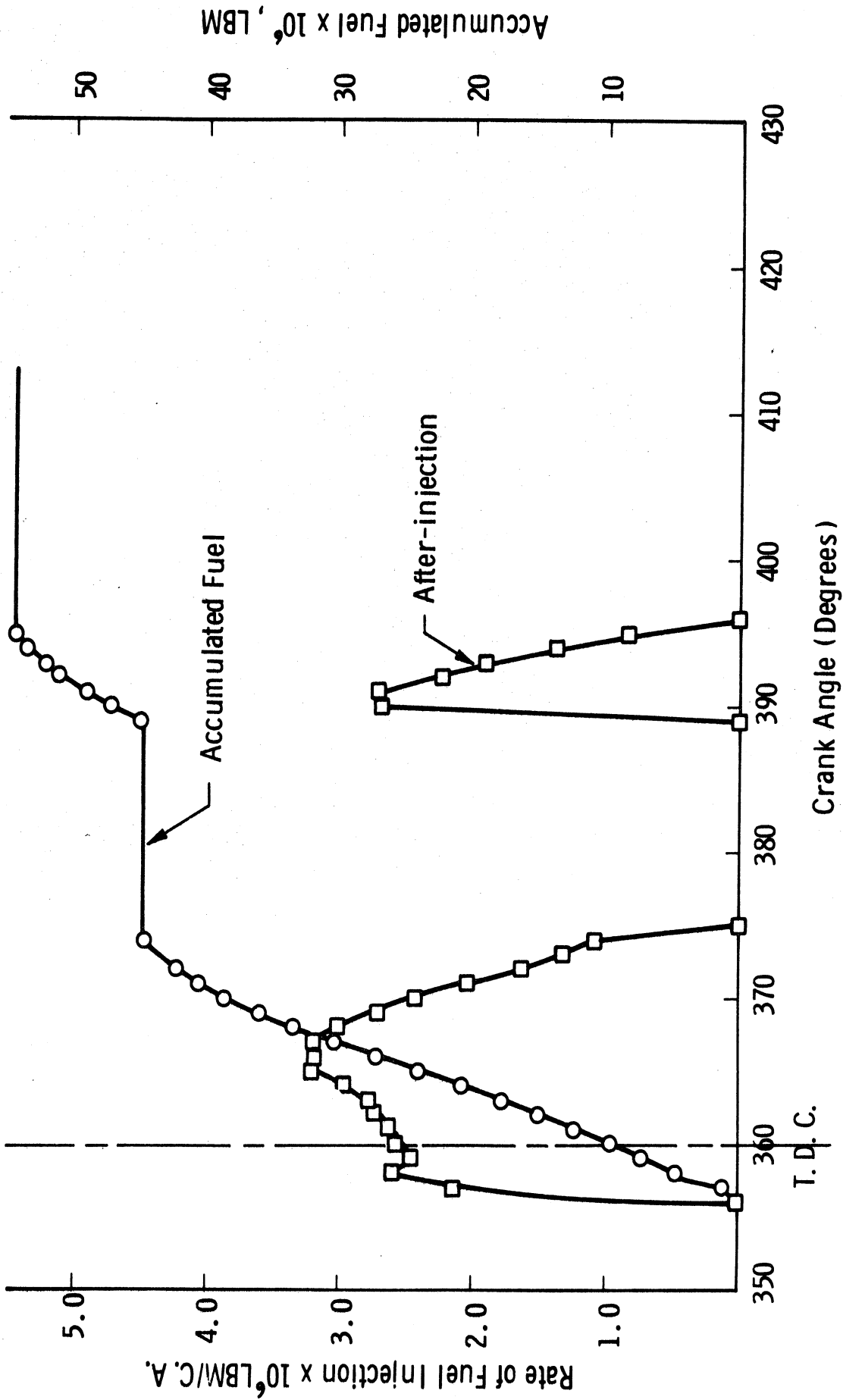


Figure 19. Rate of fuel injection and accumulated fuel diagrams.

By applying the different formulae for the delay period the following results are obtained:

Wolfer's Formula

Pressure rise delay = 2.98 millisec.

Bauer's and West Formula

(from Figure 1) at T log P = 2180,
Pressure rise delay = 1.5 millisec.

Tsao, Myer's, and Uyehara Formula

Temperature rise delay = 2.11 millisec.

CONCLUSIONS

The ignition delay period has most commonly been taken to be the elapsed time from the beginning of injection to the point where measurable pressure rise due to combustion occurs. Some research workers have also measured the time until illumination due to burning began, and others have noted the start of temperature rise due to burning. However, a review of this work shows that little discussion and comparison has been made between the different delay periods. Measurements have been made for this project of the period from the beginning of injection until measurable pressure rise due to combustion occurs, and until illumination due to burning occurs. These measured time intervals are usually different. Therefore, for a thorough study of the diesel ignition delay and combustion process, it seems desirable to observe and report each of them. Consequently, the ignition delay has been identified as 'pressure rise,' 'temperature rise,' or 'illumination delay.' Because the 'temperature rise' is very difficult to measure, our future studies will only include 'pressure rise' and 'illumination delay.'

The formulae available for the ignition delay are based on test data relating to a specific set of engine conditions. However, it has been established that a large group of variables other than air pressure and temperature have a significant effect on the ignition delay. These include the fuel concentration in the air, the conditions of the spray as regards its atomization and orientation in the chamber, the air turbulence, and the cylinder wall temperature.

The results of the experimental part of this work indicated that the increase in fuel-air from 0.011 to 0.043 caused a drop of 32% in the illumination delay. An increase in fuel-air ratio from 0.011 to 0.0568 caused a drop of 34% in the pressure rise delay. The results of the experiments carried out to investigate the effect of the degree of atomization and penetration indicated that both the pressure rise and illumination delays reach a minimum value at a nozzle opening pressure of about 2400 psi. The results of experiments at different cooling water temperatures indicated that a reduction in water temperature from 200°F to 70°F caused an increase of 20% in pressure rise delay. The effect of turbulence was studied by varying the engine speed. An increase in engine speed from 500 rpm to 1200 rpm caused a drop of 28% in illumination delay and 40% in pressure rise delay.

In future runs for the determination of the effect of pressure, temperature on ignition delay the conditions of the test as regards fuel-air-ratio, injection pressure, coolant temperature and engine speed will be kept constant and recorded.

RECOMMENDATIONS

Since the Lister engine and associated equipment which had been used in this investigation have proved to be very useful for this project, it is recommended that we continue to operate this set-up while installing and operating the army A.T.A.C. engine. This will help us to obtain information on a divided combustion chamber system. Comparison of the test results of this engine with the open chamber A.T.A.C. engine will be of great value in studying the combustion phenomena in diesel engines.

Another important advantage of the Lister engine is the large access hole into the combustion chamber, having a diameter equal to that of the swirl chamber. This has permitted us to have three extra access holes to the combustion chamber, and to use a large quartz window to photograph the combustion phenomena.

The Lister set-up is instrumented to obtain information on the effect of pressure, temperature, and density on ignition lag of different fuels. It also allows measurement of the ignition lag at four compression ratios in the range 14:1 to 22:1. In the present tests a C.R. of 14:1 has been used to avoid interruption of work due to engine failure that might occur at the high compression ratios. It is believed that the tests of different fuels at higher C.R. will be of great value for this research, especially to determine if density is an independent variable affecting ignition delay.

APPENDIX I

INSTRUMENTATION IMPROVEMENT

During the course of running the tests to investigate the effect of the different parameters on ignition delay, it was noticed that some improvements on instrumentation can be made. However, it was decided to continue these tests with the same instruments as mentioned in a previous report, Ref. 2, in order to make a comparative study on the effect of the different parameters on the ignition delay. These improvements are still on the way and have been made as an attempt to determine more precisely pressure rise and illumination delays, and to eliminate the error caused by cycle to cycle variations. A definite conclusion about the superiority of some of them over the instruments now in use is not reached yet as the work is still on the way.

A. PRESSURE-RISE DELAY

The point at which pressure rise due to combustion could be found from a pressure differential trace displayed on the oscilloscope screen. The differential circuit used is shown in Figure 20, together with the pressure circuit. The differential trace obtained is shown in Figure 21, together with the pressure trace. It was noticed that there is a phase shift between the two traces.

To study the magnitude of the phase shift between the two traces a series of runs were carried out with the engine motored. The lag of the zero differential pressure behind the maximum pressure at different crank angles was measured and plotted in Figure 22. From this figure the lag is 0.438 millisecon. at 700 rpm and 0.405 millisecon at 120 rpm. It was also noticed that the lag depends to a great deal on the capacitance of the circuit.

Another difficulty encountered with this method was the determination of the point at which the slope change occurs due to combustion.

Due to the above difficulty and phase lag dependence of the system capacity the results of this method seemed not as accurate as that using the pressure trace. The results included in this report are for the pressure rise delay as measured from the pressure trace only.

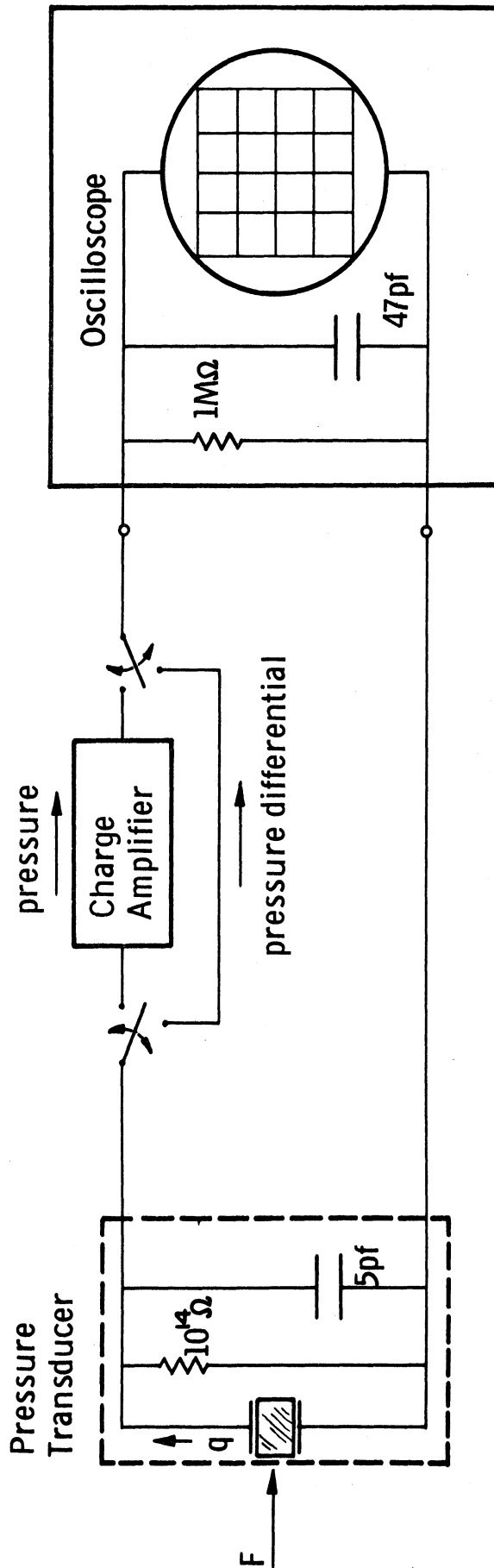


Figure 20. Pressure and pressure differentiating circuit.

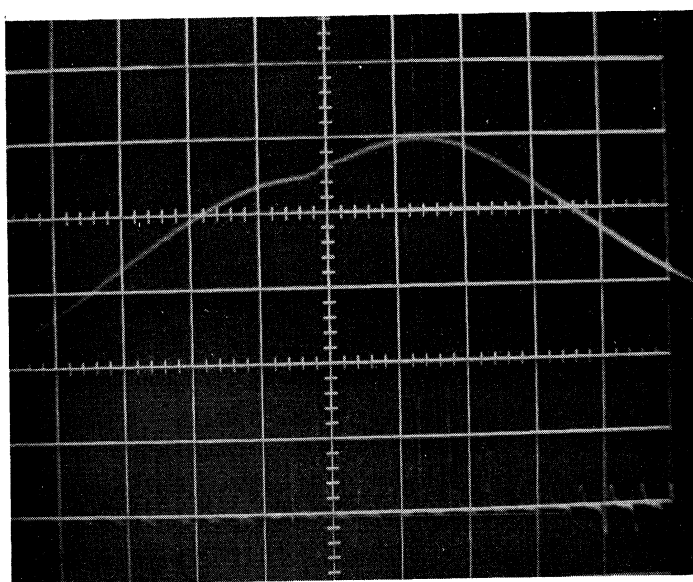


Figure 21A. Pressure trace.

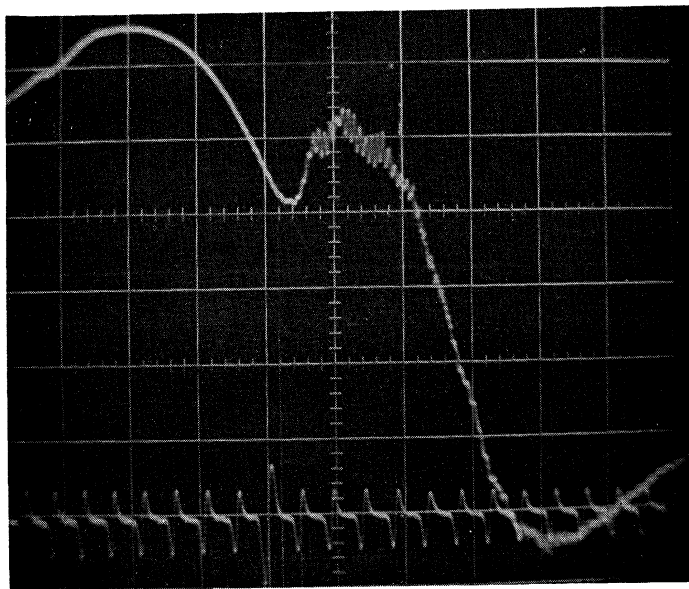


Figure 21B. Pressure differential trace.

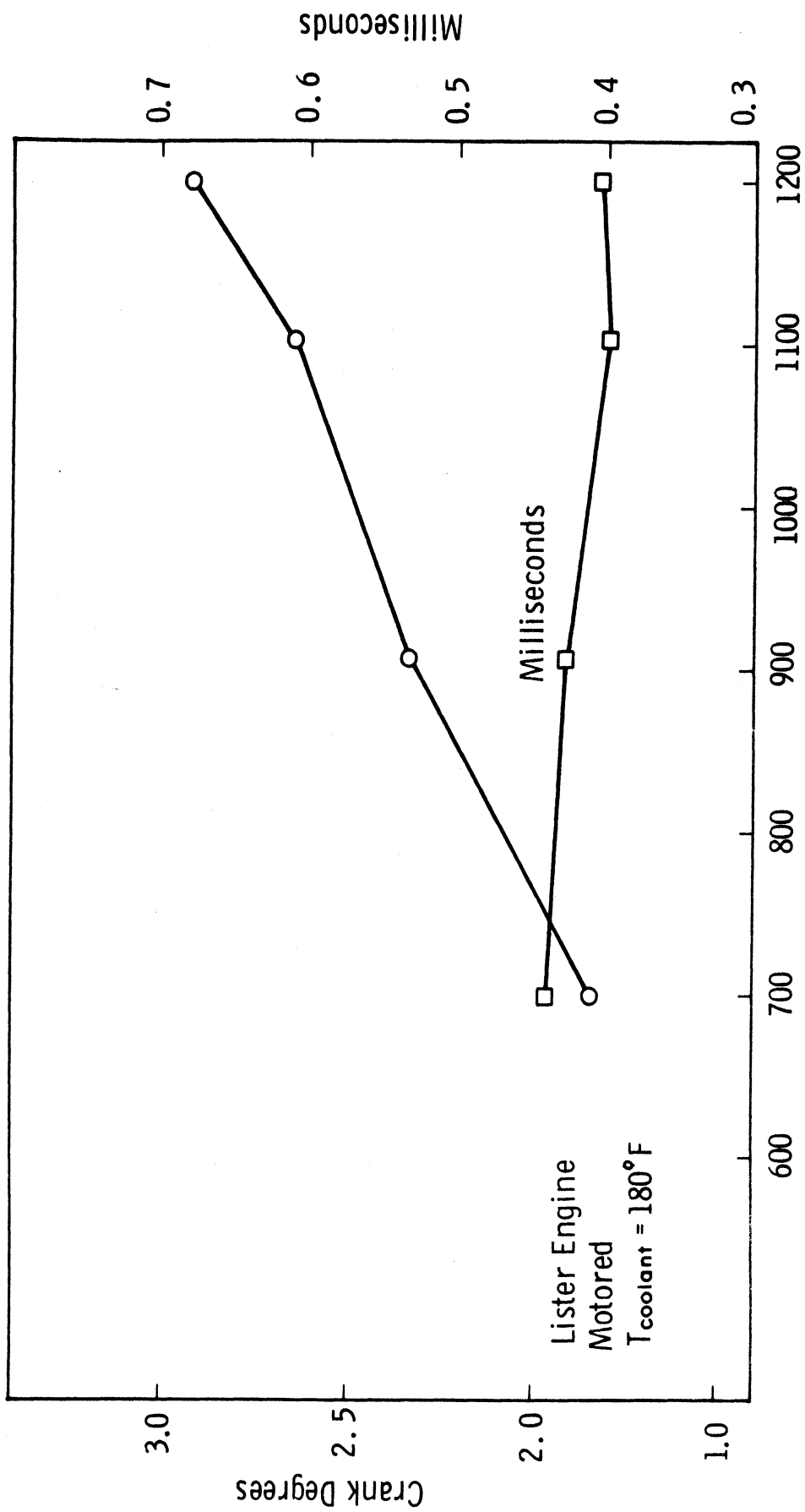


Figure 22. Lag between the pressure and the pressure differentiating circuits.

B. ILLUMINATION DELAY

A study on the possibility of using an instrument more sensitive than the solar cell is now under way. This study was initiated to study in greater detail the reasons for the difference between the measured illumination delay period and the pressure rise period. In some runs we noticed that illumination delay is shorter than the pressure rise delay, while in other runs the opposite was observed.

The instrument we are trying to use is a photomultiplier, which is now being fitted on the combustion chamber of the Lister engine. The results obtained from this instrument will be included in the next report.

Visicorder

Most of the records of combustion phenomena for this project were made with a dual beam oscilloscope and a polaroid camera. In order to eliminate the error caused by cycle-to-cycle variation with these instruments a Honeywell direct recording visicorder, with 12 channels was also used. The signals for gas pressure, crank angles, fuel pressure, needle lift, and solar cell are fed simultaneously to the galvo-amplifiers of the visicorder. The traces obtained are shown in Figure 23. The speed of recording was set at maximum value, 80 in./sec, and the engine speed was as low as 500 rpm. However, such a recording speed was not high enough to obtain traces large enough to give the degree of accuracy required. Consideration is now being given to the purchase of a visicorder with a recording speed of 160 in./sec.

Solar Cell

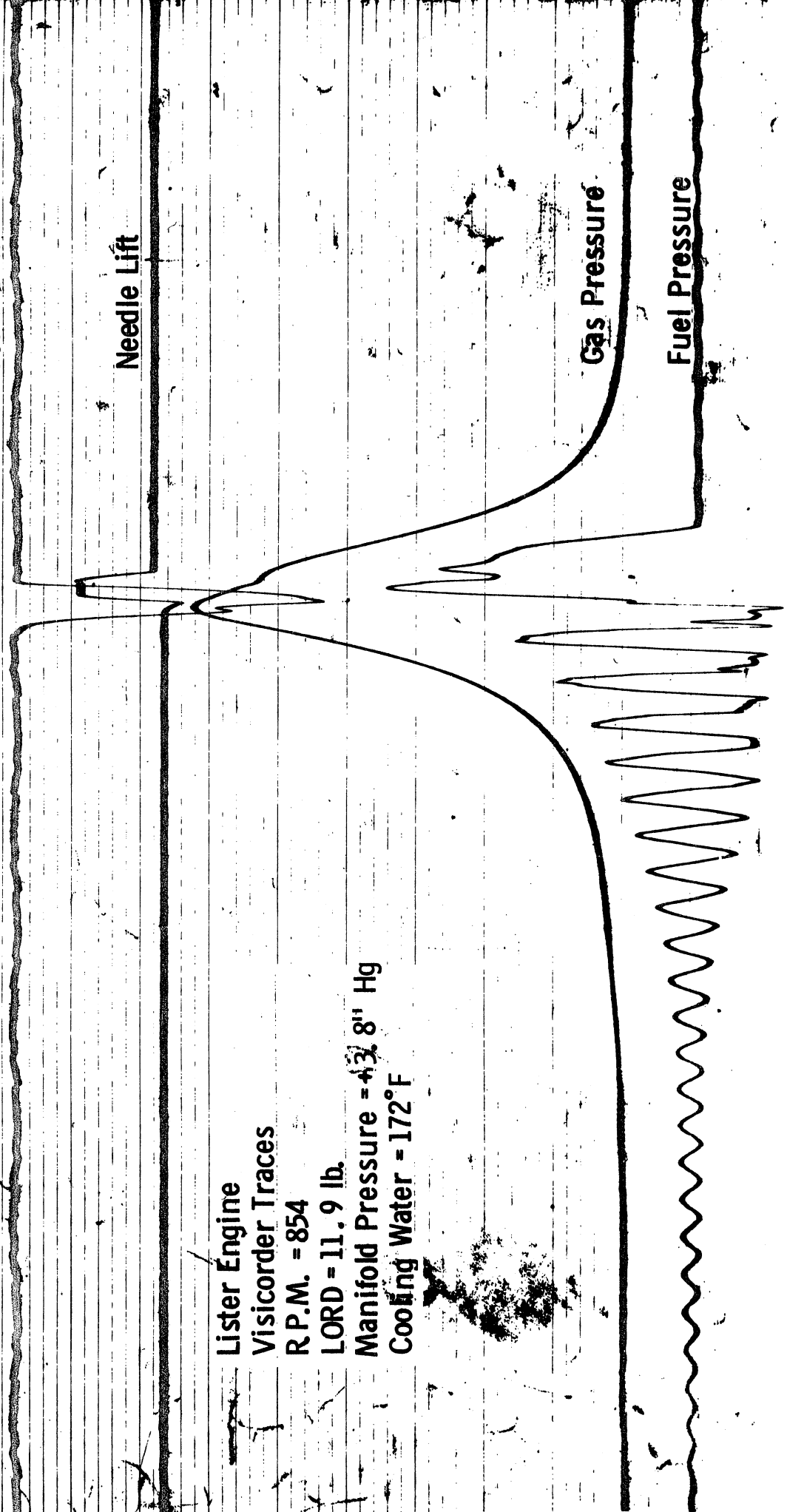
Needle Lift

Gas Pressure

Fuel Pressure

Crank Angles

Lister Engine
Visicorder Traces
R.P.M. = 854
LORD = 11.9 lb.
Manifold Pressure = 43.8" Hg
Cooling Water = 172°F



APPENDIX II

TEST CONDITIONS AND RESULTS

TEST CONDITIONS

Barometric pressure = 30" Hg
Gauge pressure in inlet surge tank = 0
Gauge pressure before flowmeter = 85.5 psi
Air temperature before flowmeter = 71°F
Air temperature in inlet manifold = 102°F
Cooling water temperature at inlet = 162°F
Cooling water temperature at exit = 174°F
Exhaust gas temperature = 495°F
Average time for consumption of 0.12655 lb of fuel = 4.32 min
(fuel leakage from injector = 23.5 cm³/hr)
Brake load = 16
Revolutions per minute = 1000 rpm

RESULTS

Air flow rate = 74.2 lb/hr
Fuel flow rate = 1.714 lb/hr
Fuel-air ratio = 0.0231
Brake horsepower = 2.67
B.M.E.P. = 30.4 psi
B.S.F.C. = 0.645 lb/B.H.P., hr

APPENDIX III

HEAT RELEASE

According to the first law of thermodynamics

$$\begin{aligned}dQ &= dU + dW \\ &= m c_v dT + p \frac{dV}{J} \\ \frac{dQ}{d\theta} &= m c_v \frac{dT}{d\theta} + \frac{p}{J} \frac{dV}{d\theta}\end{aligned}\tag{13}$$

From the equation of state

$$\frac{dT}{d\theta} = \frac{1}{mR} \left(p \frac{dV}{d\theta} + v \frac{dP}{d\theta} \right)$$

Substituting in equation (13) we get

$$\begin{aligned}\frac{dQ}{d\theta} &= \frac{c_v}{R} \left(p \frac{dV}{d\theta} + v \frac{dP}{d\theta} \right) + \frac{p}{J} \frac{dV}{d\theta} \\ &= \left[\left(\frac{c_v}{R} + \frac{1}{J} \right) p \frac{dV}{d\theta} + \left(\frac{c_v}{R} \right) v \frac{dP}{d\theta} \right]\end{aligned}\tag{14}$$

BIBLIOGRAPHY

1. Alcock, J. F., "Air Swirl in Oil Engines," Proc. I.M.E. (London), Vol. 128, 1934, pp. 123-193.
2. Bolt, Jay A., and Henein, N. A., "Diesel Engine Ignition and Combustion," 06720-3-P report. The University of Michigan, Dec. 1965.
3. Bauer, S. G., "Ignition Lag in Compression Ignition Engines," Engineering, Vol. 148, p. 368, 9 (1939).
4. Heldt, P. M., "High-Speed Diesel Engines," 7th ed., Nyack, N. Y., 1953, p. 117.
5. Keenan, J. H. and Kaye, J., "Gas Tables," New York: John Wiley and Sons Inc., 1950.
6. Rosen, C. G. A., "Matching Fuels to Diesel Combustion Systems," SAE Trans. Vol. 71, 1963, pp. 259-271.
7. Tsao, K. C., Myers, P. S. and Uyehara, O. A., "Gas Temperature During Compression in Motored and Fired Diesel Engines," SAE Trans., Vol. 70, 1962, pp. 136-145.
8. West, A. C. and Taylor, Denis, "Ignition Lag in a Supercharged Compression-Ignition Engine," Engineering, April 11, 1941, p. 281 and 282.
9. Wolfer, H. H., "Ignition Lag in the Diesel Engine (Der Zundverzug im Dieselmotor), V.D.I. Forschungsheft No. 392, 1938, pp. 15-24, English translation-RAE report No 358.

SECTION 5

PROGRESS REPORT NO. 5

DEVELOPMENT OF INSTRUMENTATION ON ATAC-1 ENGINE

PROGRESS REPORT NO. 5

DIESEL IGNITION AND COMBUSTION

J. A. BOLT
N. A. HENEIN

PERIOD APRIL 1, TO JULY 31, 1966

AUGUST 1966

This project is under the technical supervision of the:

Propulsion Systems Laboratory
U. S. Army Tank-Automotive Center
Warren, Michigan

and is work performed by the:

Department of Mechanical Engineering
The University of Michigan
Ann Arbor, Michigan

under Contract No. DA-20-018-AMC-1669(T)

I. BACKGROUND

A program to study the combustion process in supercharged diesel engines has been developed at The University of Michigan. This program is primarily concerned with the ignition delay and the effect of the different parameters on it. A special concern is given to the effect of pressure, temperature, and density on the ignition delay.

The different types of delay have been studied and an emphasis is made on the pressure rise delay and illumination delay. The instruments needed for the measurement of these two delay periods have been developed and a continuous effort is being made to improve their accuracy.

This research is being done on two experimental engines. One is the ATAC high output open combustion chamber engine, and the other is a Lister Blackstone swirl combustion chamber engine.

II. OBJECTIVES

A. To study how gas pressure at the time of injection affects ignition delay and combustion. The effects will be studied at pressures ranging from approximately 300 to 1000 psia.

B. To study how gas temperature at the time of injection affects ignition delay. The temperatures will range from approximately 900°F to 1500°F.

C. To study various combinations of pressures and temperature to determine whether density is an independent variable affecting ignition delay.

D. To conduct all these studies with three fuels: CITE refree grade (Mil-F-45121) fuel, diesel no. 2 fuel, and Mil-G-3056 refree grade gasoline.

III. CUMULATIVE PROGRESS

A. Lister Engine

This engine has been set on a test stand, connected to a dynamometer, and completely instrumented to measure power, rates of flow of air, fuel, and coolant, and temperatures at different points in the engine. Traces can be obtained for cylinder pressure, fuel pressure, needle lift, illumination, surface temperature, and crank angles. Shop air is used to supercharge the

engine, and a surge tank is placed between the airflow meter and the engine.

The original combustion chamber of this engine has been modified so that compression ratios can be adjusted from 14:1 to 22:1. A quartz window with a diameter equal to that of the swirl chamber has been manufactured to fit into the modified combustion chamber, for more accurate observation of illumination delay.

Four series of tests have been made to investigate the effect of factors other than pressure, temperature, and density on ignition delay. The purpose is to eliminate their effects on measurements of delay periods, or at least to have them under control. These factors are fuel-air ratio, fuel injection pressure, engine speed, and cooling-water temperature. The results of these series having shown that these factors affect the delay period significantly, it has been decided to keep them constant during the runs made to investigate the effect of pressure and temperature.

B. ATAC Engine

Since this engine was received just before the beginning of this reporting period, all the progress is reported under the next section.

IV. PROGRESS DURING THIS PERIOD

A. Lister Engine

The effect of pressure on the ignition delay has been investigated for gas pressure (at point of injection) ranging from 264 to 604 psia. The results obtained for the delay period differ from those obtained by previous investigators, which were made on a constant-volume bomb or a different type of combustion chamber. In studying the reasons for this discrepancy, it was found necessary to make series of runs at speeds of 600, 800, and 1000 rpm, to investigate the effect of speed on ignition delay. The results of the runs at 600 rpm are shown in Figure 1.

B. ATAC Engine

The instrumentation of this engine has been completed. The engine has been connected to an electric dynamometer. It is supercharged with shop air that has been passed through a surge tank fitted just before the engine. Another surge tank is fitted on the exhaust side. The pressures in the two tanks can be regulated to the required values.

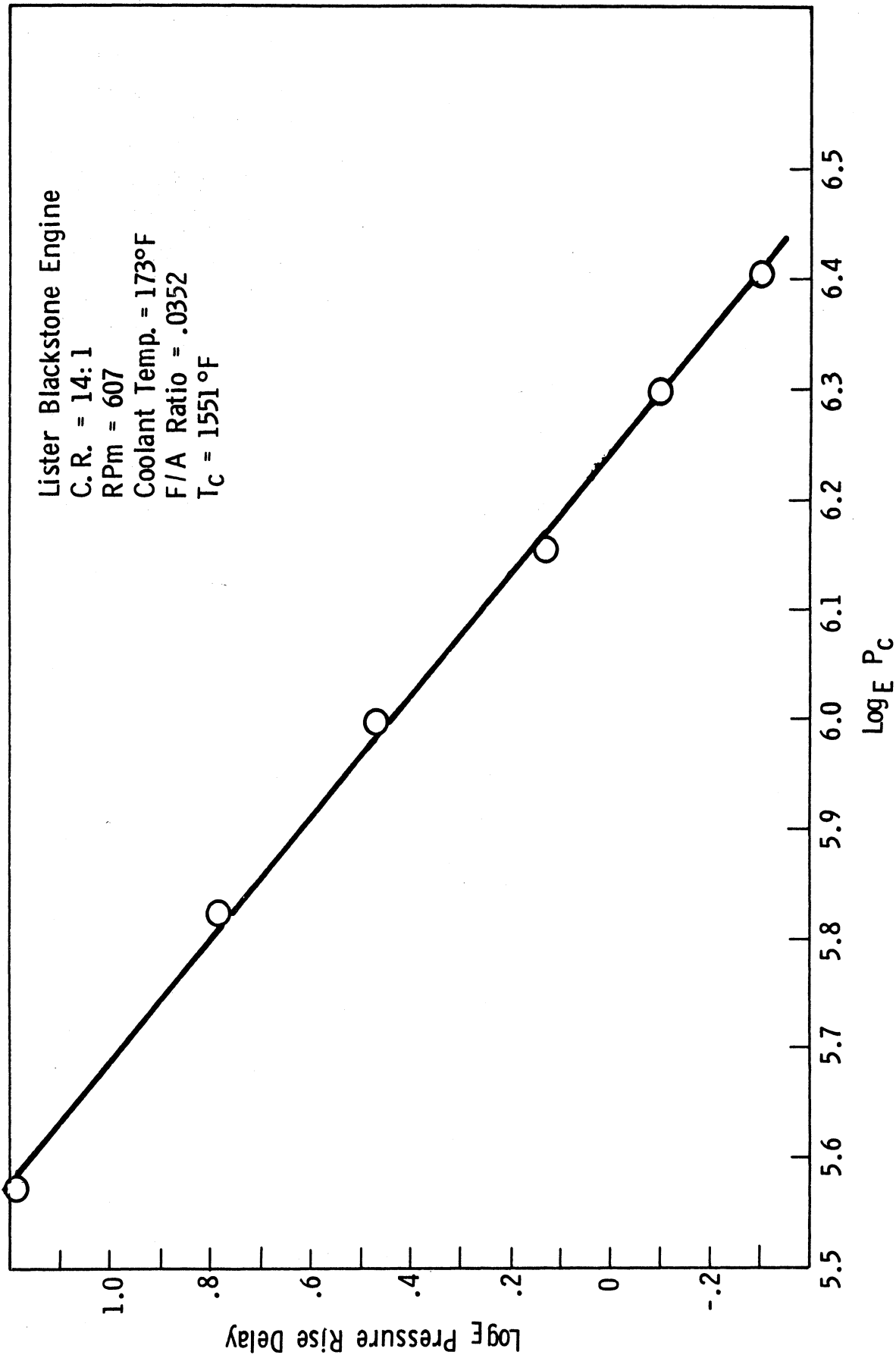


Figure 1. Effect of pressure on ignition delay.

A Kistler pressure transducer is fitted in the hole furnished by the International Harvester Company. Two more holes were drilled in the cylinder head above the piston cavity. One hole is fitted with a quartz window, and the other is to be fitted with a surface thermocouple, as shown in Figures 2, 3, and 4.

The top dead center of the engine determined by the dial gage method, was found to be $1/2$ crank degree past the top dead center mark engraved on the flywheel.

The degree marks are produced by a steel disc 18 inches in diameter and $1/8$ inch thick, mounted on the coupling between the crankshaft and the dynamometer. Holes $1/16$ inch in diameter are drilled around the periphery at 3° intervals, and larger holes, $1/8$ inch in diameter, at 45° intervals. A magnetic pickup has been used to produce corresponding pips on the oscilloscope screen every 3° , with bigger pips every 45° . One of the bigger holes is aligned at top dead center.

The temperature of the inside surface of the combustion chamber is to be measured by a surface thermocouple placed between the inlet and exhaust valves.

The fuel-injection system is instrumented so that the start and rate of injection can be calculated from measurements of the needle lift and fuel pressure before the nozzle. The position of the pressure transducer in the injector is shown in Figure 5. The position of the plunger w.r.t., the barrel, and the injection timing are both controlled by micrometers.

V. PROBLEM AREAS AND CORRECTIVE ACTION

1. Failure of Kistler pressure transducers after a relatively short period of operating time.
2. Delay of delivery of newly ordered Kistler pressure units. The delay reaches about three months.
3. Difficulty of seeing the oil level in the lower sump due to deposits accumulated on the sight glass.

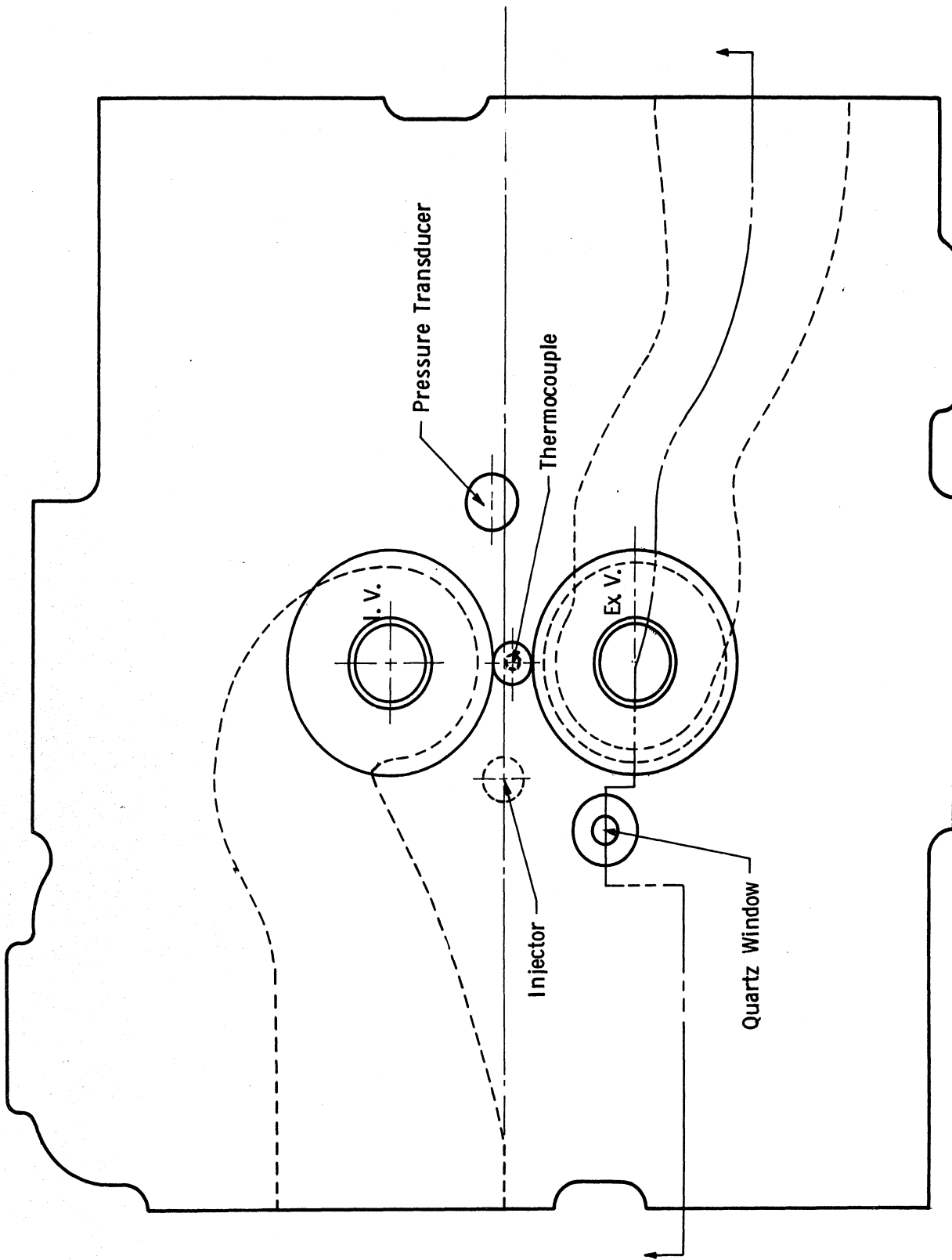


Figure 2. Position of pressure transducer, thermocouple, and quartz window in cylinder head (ATAC engine).

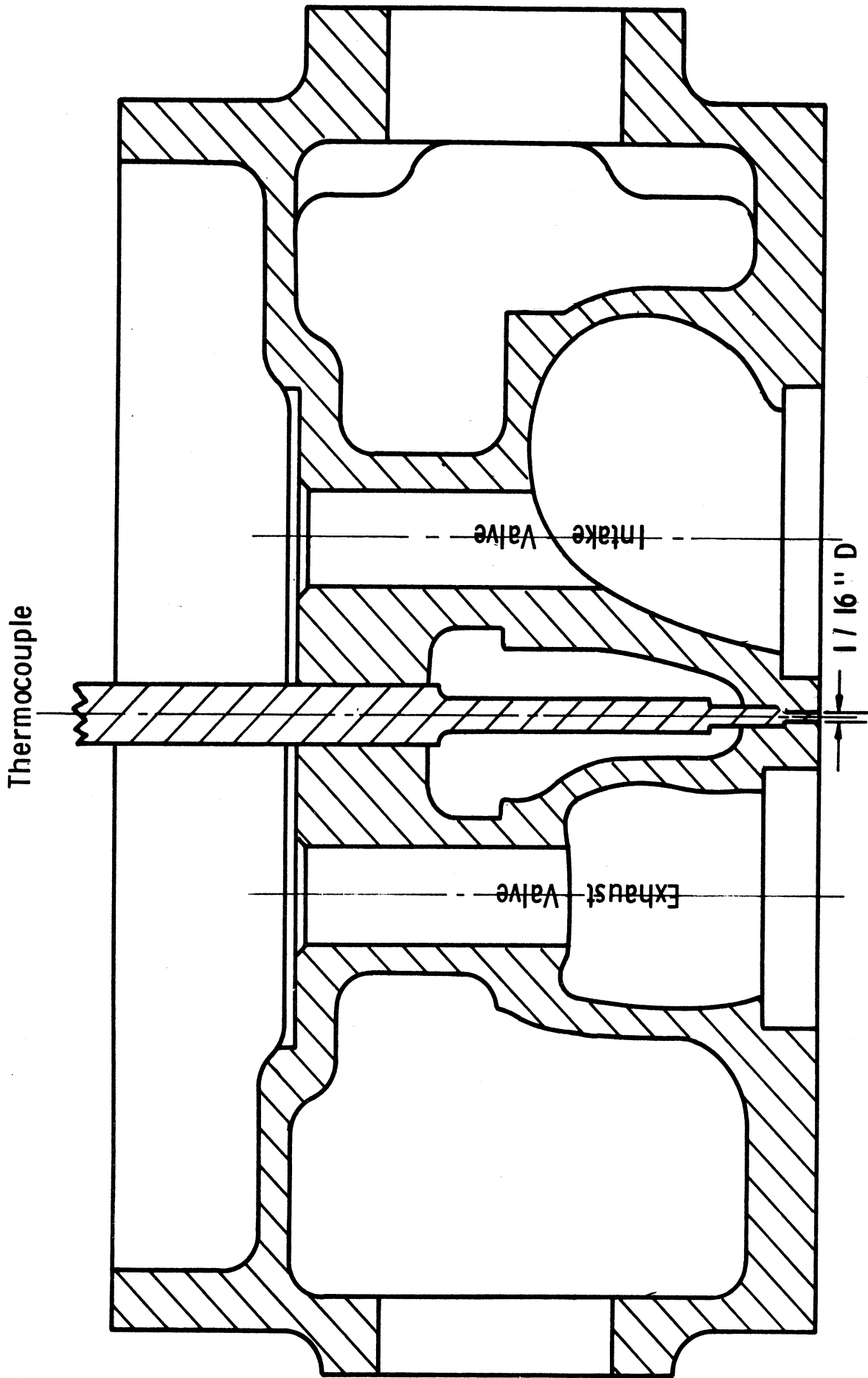


Figure 3. Surface thermocouple in cylinder head (ATAC engine).

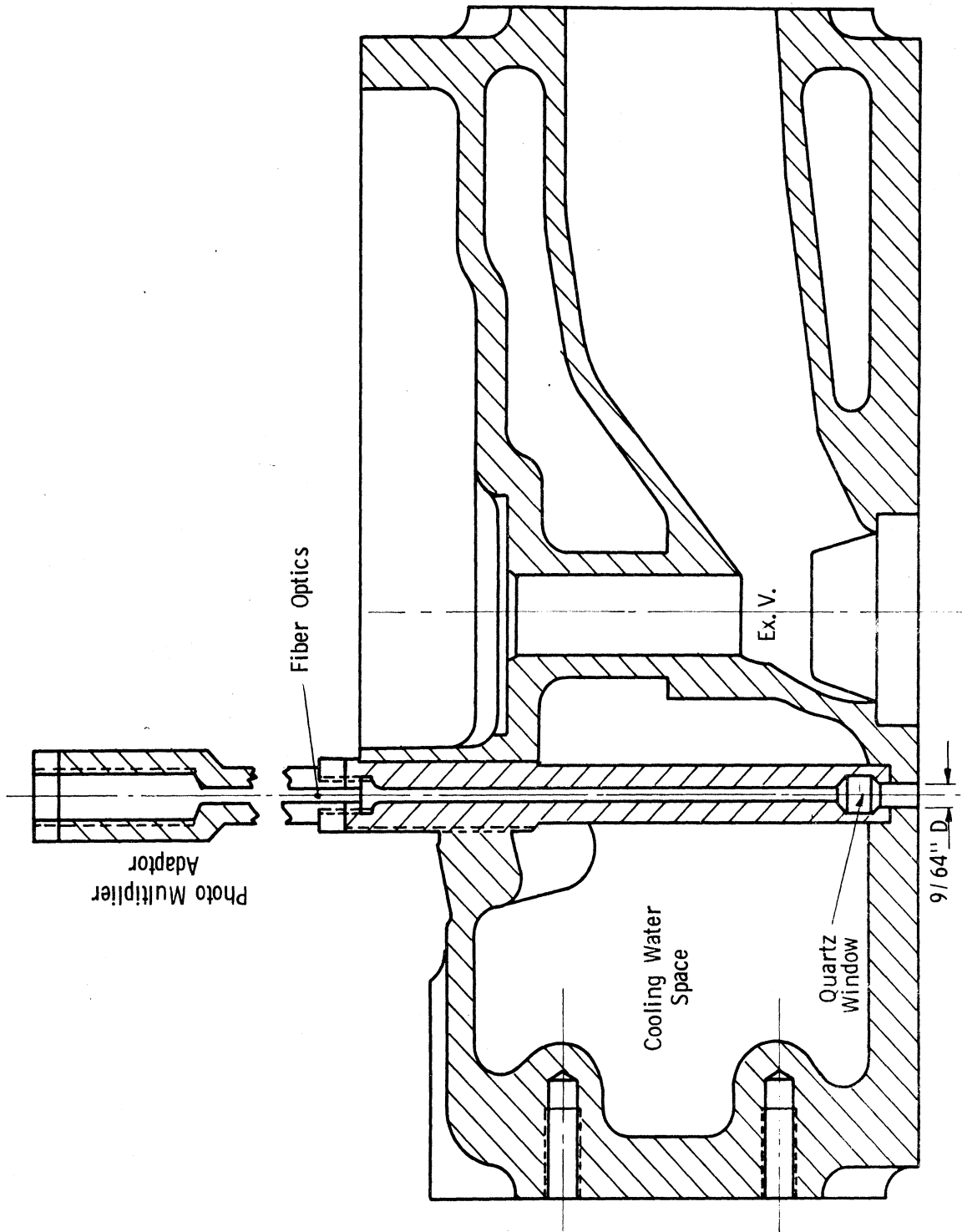


Figure 4. Quartz window in cylinder head (ATAC engine).

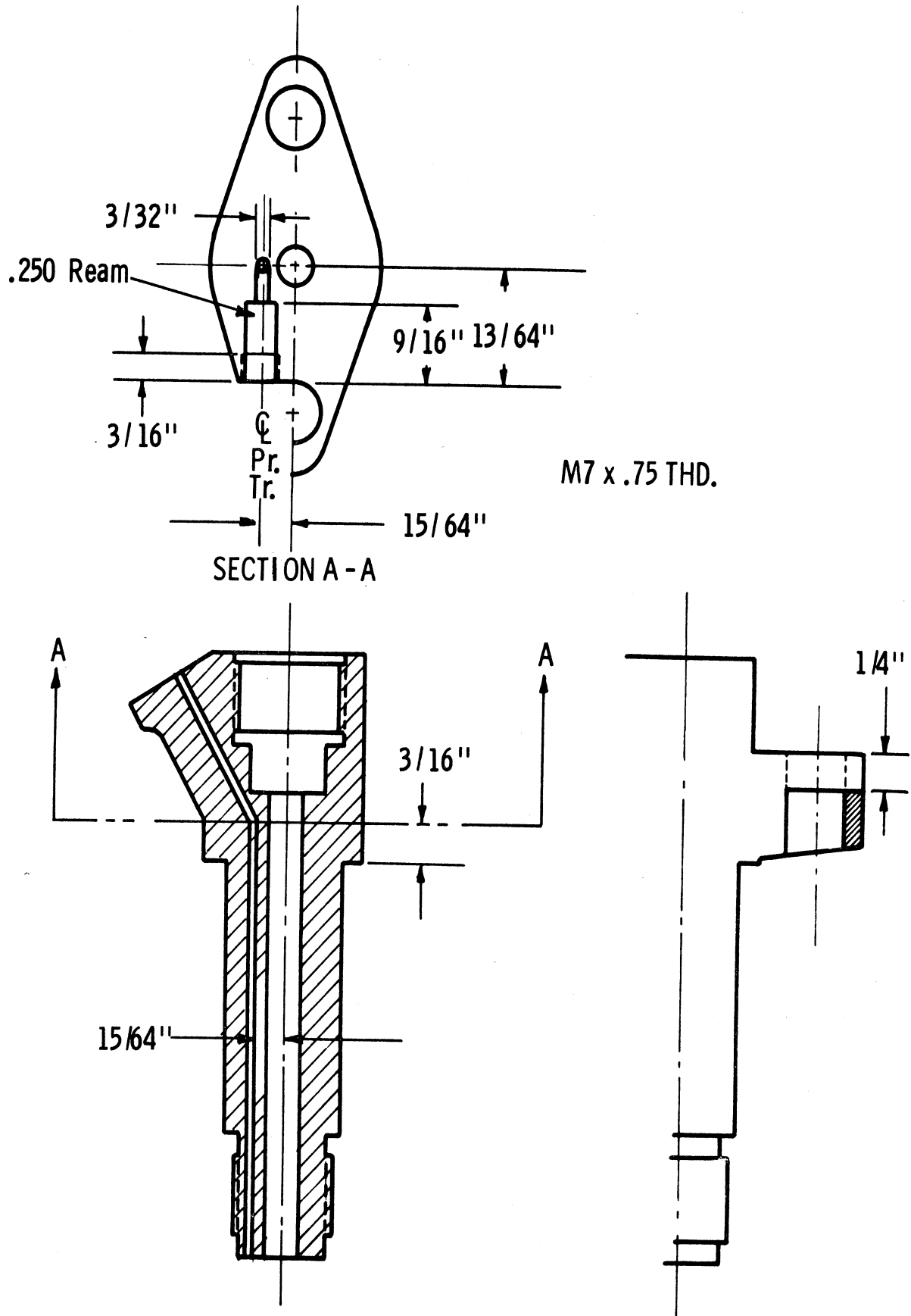


Figure 5. Injector showing position of pressure transducer (ATAC engine).

VI. FUTURE PLANS

A. Next Period

1. To continue experimental investigations to determine the effect of pressure on ignition delay of the three different fuels in the Lister engine.
2. To investigate the effect of pressure, temperature, and density on ignition delay in the ATAC engine.
3. To study the cause of discrepancy between our results and results of previous work.

B. Overall

1. To investigate the effect of pressure, temperature, and density on ignition delay with the different fuels.
2. To process the experimental data on a digital computer.

C. Changes From Original

Since turbulence has been found to affect ignition delay significantly, it will be studied along with temperature, pressure, and density.

VII. SIGNIFICANT ACCOMPLISHMENTS

(April, May, June, and July)

1. The ATAC engine has been installed on a test stand, connected to a dynamometer, and completely instrumented, with gas-pressure transducers, fuel-pressure transducers, a needle-lift detector, a surface thermocouple, an illumination detector, and a degree-marking unit.
2. The top dead center of the ATAC engine has been precisely determined, and the clearance volume measured.
3. Tests to find the effect of pressure on delay in the Lister engine have been completed.
4. Comparison of the results of ignition delay in the Lister engine indicated that speed (or turbulence) is a major factor.

5. In June, Professor J. A. Bolt agreed to present to the SAE some of the results of the work accomplished under this contract. Mr. Floyd Lux has given his general approval for this presentation to be at the annual meeting of the SAE in January 1967, subject to final clearance of the complete paper by ATAC. The paper will be prepared by N. A. Henein and J. A. Bolt.

VIII. PROJECT STATUS

A. Funds and Expiration Date of Contract

Original contract
July 1, 1964, to January 1, 1965 \$23,020

Modification No. 1
Extension of contract to March 1, 1965;
no increase in funds.

Modification No. 4
Extension of contract to June 1, 1965;
no increase in funds.

Modification No. 7
Extension of contract to February 28, 1966;
addition of \$18,000 to contract funds for a total of. \$41,020

Modification No. 8
Extension of contract to February 27, 1967;
addition of \$37,000 to contract funds for a total of. \$78,020

B. Meetings and Trips

On May 3, Professor J. Bolt, at the invitation of the Cummins Engine Company, attended a one-day meeting at Cummins in Columbus, Indiana, to hear a presentation by Dr. S. Meurer of the MAN Company of Germany, concerning their spark-ignited combustion system, called the FM system. Professor Bolt's thoughts concerning this system were sent to Mr. F. Lux in a memorandum dated May 10, 1966.

SECTION 6

PROGRESS REPORT NO. 6

- a. Analysis of Experimental Results on the Lister-Blackstone Engine
- b. Publishing an SAE Paper on "Ignition Delay in Diesel Engines"

PROGRESS REPORT NO. 6

DIESEL ENGINE IGNITION AND COMBUSTION

JAY A. BOLT
N. A. HENEIN

PERIOD AUGUST 1, TO NOVEMBER 30, 1966

DECEMBER 1966

This project is under the technical supervision of the:

Propulsion Systems Laboratory
U. S. Army Tank-Automotive Center
Warren, Michigan

and is work performed by the:

Department of Mechanical Engineering
The University of Michigan
Ann Arbor, Michigan

under Contract No. DA-20-018-AMC-1669(T)

TABLE OF CONTENTS

	Page
I. BACKGROUND	204
II. OBJECTIVES	204
III. CUMULATIVE PROGRESS	204
A. Lister Engine	204
B. ATAC Engine	205
IV. PROGRESS DURING THIS PERIOD	206
V. PROBLEM AREAS AND CORRECTIVE ACTION	206
VI. FUTURE PLANS	207
A. Next Period	207
B. Overall	207
C. Changes from Original	207
VII. SIGNIFICANT ACCOMPLISHMENTS	207
VIII. PROJECT STATUS	208
Funds and Expiration Date of Contract	208
ADDENDUM	209

I. BACKGROUND

A program to study the combustion process in supercharged diesel engines has been developed at The University of Michigan. This program is primarily concerned with the ignition delay and the effect of the different parameters on it. A special concern is given to the effect of pressure, temperature, and density on the ignition delay.

The different types of delay have been studied and an emphasis is made on the pressure rise delay and illumination delay. The instruments needed for the measurement of these two delay periods have been developed and a continuous effort is being made to improve their accuracy.

This research is being made on two experimental engines. One is the ATAC high output open combustion chamber engine, and the other is a Lister Blackstone swirl combustion chamber engine.

II. OBJECTIVES

A. To study how gas pressure at the time of injection affects ignition delay and combustion. The effects will be studied at pressures ranging from approximately 300 to 1000 psia.

B. To study how gas temperature at the time of injection affects ignition delay. The temperatures will range from approximately 900°F to 1500°F.

C. To study various combinations of pressures and temperature to determine whether density is an independent variable affecting ignition delay.

D. To conduct all these studies with three fuels: CITE refree grade (Mil-F-45121) fuel, diesel no. 2 fuel, and Mil-G-3056 refree grade gasoline.

III. CUMULATIVE PROGRESS

A. Lister Engine

This engine has been set on a test stand, connected to a dynamometer, and completely instrumented to measure power, rates of flow of air, fuel, and coolant, and temperatures at different points in the engine. Traces can

be obtained for cylinder pressure, fuel pressure, needle lift, illumination, surface temperature, and crank angles. Shop air is used to supercharge the engine, and a surge tank is placed between the airflow meter and the engine.

The original combustion chamber of this engine has been modified so that compression ratios can be adjusted from 14:1 to 22:1. A quartz window with a diameter equal to that of the swirl chamber has been manufactured to fit into the modified combustion chamber, for more accurate observation of illumination delay.

Four series of tests have been made to investigate the effect of factors other than pressure, temperature, and density on ignition delay. The purpose is to eliminate their effects on measurements of delay periods, or at least to have them under control. These factors are fuel-air ratio, fuel injection pressure, engine speed, and cooling-water temperature. The results of these series having shown that these factors affect the delay period significantly, it has been decided to keep them constant during the runs made to investigate the effect of pressure and temperature.

B. ATAC Engine

The instrumentation of this engine has been completed. The engine has been connected to an electric dynamometer. It is supercharged with shop air that has been passed through a surge tank fitted just before the engine. Another surge tank is fitted on the exhaust side. The pressures in the two tanks can be regulated to the required values.

A Kistler pressure transducer is fitted in the hole furnished by the International Harvester Company. Two more holes were drilled in the cylinder head above the piston cavity. One hole is fitted with a quartz window, and the other is to be fitted with a surface thermocouple.

The top dead center of the engine determined by the dial gage method, was found to be $1/2$ crank degree past the top dead center mark engraved on the flywheel.

The degree marks are produced by a steel disc 18 inches in diameter and $1/8$ inch thick, mounted on the coupling between the crankshaft and the dynamometer. Holes $1/16$ inch in diameter are drilled around the periphery at 3° intervals, and larger holes, $1/8$ inch in diameter, at 45° intervals. A magnetic pickup has been used to produce corresponding pips on the oscilloscope screen every 3° , with bigger pips every 45° . One of the bigger holes is aligned at top dead center.

The temperature of the inside surface of the combustion chamber is to be measured by a surface thermocouple placed between the inlet and exhaust valves.

The fuel-injection system is instrumented so that the start and rate of injection can be calculated from measurements of the needle lift and fuel pressure before the nozzle. The position of the plunger w.r.t., the barrel, and the injection timing are both controlled by micrometers.

IV. PROGRESS DURING THIS PERIOD

The results obtained from the tests on the Lister engine were analyzed to find a correlation between the cylinder pressure and the pressure rise delay. A computer program was made for this purpose. The best correlation was found to be of the form

$$\text{I.D.}_p = \frac{C}{p^n} \quad (\text{a})$$

This form was found to be in agreement with the forms given by previous investigators as shown in the Addendum.

To examine the validity of Eq. (a), the previously published experimental results on bombs and engines were analyzed using the same computer program. It was found that all previous experimental results on ignition delay could be correlated with an equation similar to Eq. (a). However, the values of C and n were found to be different for each set of data. The details of this analysis is given in the Addendum.

A thermodynamic analysis was also made by taking into consideration the different types of energy that affect the pressure rise delay. This analysis indicated that the measured pressure rise delay is partially dependent on several thermodynamic characteristics of the chamber including its volume, rates of heat addition and loss, and any work done during the delay period. A portion of the differences in the ignition delays reported for bombs and engines are due to these factors. The details of this thermodynamic analysis is also given in the Addendum.

V. PROBLEM AREAS AND CORRECTIVE ACTION

One of the Kistler pressure transducers, recently received, has a leakage problem. It was sent back to the Kistler Company for repair or replacement.

VI. FUTURE PLANS

A. Next Period

To investigate the effect of pressure and injection timing on ignition delay in the ATAC engine, for the three test fuels listed in the contract.

B. Overall

1. To investigate the effect of pressure, temperature, and density on ignition delay with the different fuels.
2. To process the experimental data on a digital computer.
3. Report results.

C. Changes from Original

Since turbulence has been found to affect ignition delay significantly, it will be studied along with temperature, pressure, and density.

VII. SIGNIFICANT ACCOMPLISHMENTS

A paper has been prepared and scheduled for presentation at the Annual Meeting of S.A.E. on January 9, 1967. The title of the paper is "Ignition Delay in Diesel Engines" by N. A. Henein and Jay A. Bolt. A complete copy of the paper was sent to ATAC for clearance.

VIII. PROJECT STATUS

Funds and Expiration Date of Contract

Original contract
July 1, 1964, to January 1, 1965..... \$23,020

Modification No. 1
Extension of contract to March 1, 1965;
no increase in funds.....

Modification No. 4
Extension of contract to June 1, 1965;
no increase in funds.....

Modification No. 7
Extension of contract to February 28, 1966;
addition of \$18,000 to contract funds for a total of. \$41,020

Modification No. 8
Extension of contract to February 27, 1967;
addition of \$37,000 to contract funds for a total of. \$78,020
(funds will be exhausted about January 1, 1967)

A continuation contract is being negotiated which will become effective December 1, 1966.

Addendum

IGNITION DELAY IN DIESEL ENGINES

(S.A.E. Paper No. 670007)

by

N. A. Henein
Jay A. Bolt

To be presented at S.A.E. Annual Meeting, January 9, 1967

ABSTRACT

The ignition delay in diesel combustion has been studied in a turbulent chamber engine. The criteria used to define the end of this period are the pressure rise and illumination due to combustion. The pressure rise delay is generally shorter and more reproducible than the illumination delay. The effect of the following factors on the ignition delay were studied: cylinder pressure, fuel/air ratio, fuel injection pressure, cooling water temperature, and engine speed. The data concerning the effect of cylinder pressure on the pressure rise delay period, at constant air temperature, were correlated and compared with previous experimental results.

The analysis indicated that the pressure rise delay is affected by physical and chemical factors as well as thermodynamic parameters that control the several forms of energy during the delay period.

INTRODUCTION

Previous investigators have shown that it is practical to divide the diesel combustion process into stages. The first stage that follows the start of injection, and precedes burning, is called the delay period. The duration of this period greatly affects the intensity of the subsequent burning and the resulting noise and roughness.

During the past fifty years many observations have been made with constant volume bombs, and in engines, to determine the factors which influence this delay period. A survey and correlation of the available past published work was carried out to provide background for our own experimental work.

Many definitions have been used to denote the duration of the delay period, mainly because different phenomena were used to indicate the end of this period. The pressure rise due to combustion, or the illumination from combustion, have most commonly been used to define the end of this period. In some cases the temperature rise due to combustion was considered the end of this period.

The work reported here is the first part of a research project to study the effect of high pressures and temperatures corresponding to very high supercharge conditions on the ignition delay and combustion phenomena in diesel engines. In the course of assembling the instrumentation and developing the necessary test techniques it became more apparent that the influence of other factors should be determined, because they could not be kept entirely constant. These included the fuel/air ratio, the fuel injection pressure, air turbulence, and the cooling water temperature. The effects of these variables, and the effect of air pressure are included in this paper. The work concerning the influence of cylinder air temperature on combustion has not been completed, and will be reported separately in a later paper.

IGNITION DELAY--DEFINITIONS

Numerous definitions for the ignition delay have been used. All are agreed on the definition of ignition delay as the period extending from the beginning of injection to measurable combustion. The problem arises from measuring the point where combustion begins. In the majority of the investigations combustion is considered to begin at the point of a measurable pressure rise due to the release of the energy of combustion. In other work, the point of temperature rise or the point of light emission is used. Definitions that will differentiate between the different delay periods will help to clarify and understand the phenomena. The following definitions are proposed:

1. Physical delay is defined as the period of time required for the physical changes to occur to the fuel from its liquid phase at the injection temperature to the vapor phase at the self-ignition temperature. It can be considered equal to the period of time between the beginning of injection and the beginning of preflame reactions. This period will be referred to as I.D.Ph.
2. Chemical delay is defined as the period of time elapsed from the end of the physical delay to the beginning of ignition. During this period preflame reactions are considered to occur, and will be referred to as I.D.Ch.
3. Illumination delay is the time that elapses between the beginning of injection and the start of illumination. This period will be referred to as I.D.II.
4. Temperature rise delay is the time that elapses between the beginning of injection and a measurable temperature rise due to combustion. This period will be referred to as I.D.T.
5. Pressure rise delay is the time that elapses between the beginning of injection and a measurable pressure rise due to combustion. This period will be referred to as I.D.p.

Other definitions which were not used frequently will be referred to in the literature review. The methods used in previous studies for measuring these delay periods will be briefly reviewed.

LITERATURE REVIEW

A great variety of equipment and procedures have been used to measure the ignition delay associated with the self-ignition of hydrocarbon fuels. The different combustion chamber configurations used included constant volume bombs, rapid compression machines, as well as motored and fired engines. In this review some description of the combustion chambers used and the means for measuring the ignition delay is included, to help the reader understand the reasons for some of the variations in the reported results.

Studies of the autoignition of fuel and air mixtures, and measurement of the delay periods were started as early as 1922 by Tizard and Pye.^{1,2*} They did their experimental work on a high compression machine with a cylinder 3 inches in diameter and with an 8-inch stroke. The compression ratio was varied from 6:1 to 9:1. Their experiments were made on gaseous fuels under static and turbulent conditions. They produced turbulence in the gaseous mixture by means of a fan fitted at the top of the cylinder. They observed that a delay period existed before the occurrence of pressure rise due to combustion, which they found to decrease with increase in turbulence.

Otto Alt³ in 1923, followed by Kurt Neumann⁴ in 1926, and F. Sass⁵ in 1927, made investigations on combustion of liquid fuels in diesel engines and proposed the idea that preliminary evaporation of the fuel was not necessary for producing ignition. In other words, they considered that there was no physical delay before ignition of the liquid fuel.

Tausz and Schulte⁶⁻⁷ between 1925 and 1928 established the idea of physical delay period in liquid fuel combustion. They indicated that no incipient ignition can take place in the liquid fuel and that, it should be evaporated before being ignited. They observed also that increase in pressure reduces the self-ignition point, and that the self-ignition temperature of a fuel is lower in pure oxygen than in air.

The presence of the physical delay was further established by photographs taken by Rothrock and Waldron⁹ in 1932. They photographed the fuel spray in the NACA combustion apparatus¹⁰ and observed that vaporization precedes ignition, and that its rate affects the process of combustion.

The variation in the pressure rise delay with increase in pressure was measured by Boerlage and Broeze¹¹ in 1931. They made tests utilizing a single cylinder, direct injection, 4-stroke cycle, slow speed diesel engine, for

*Numbers refer to Bibliography.

compression pressures ranging from 375 psi to 600 psi. They proposed a hyperbolic relationship between the pressure rise delay and compression pressure.

$$\text{I.D.}_p = \frac{K}{P} \quad (1)*$$

They also concluded¹² that the pressure rise delay depends on the thermal stability and structure of the fuel molecule. This conclusion was reached after they compared cetene ($C_{16}H_{32}$) and Tetraisobutylene ($C_{16}H_{32}$) and found that the latter has a poor ignition quality due to its molecular structure.

Gerrish and Voss¹³ in 1932 used a different definition of the delay period from the above five definitions. They considered the end of ignition delay to be the point on the indicator card, where 4.0×10^{-6} pound of fuel had been effectively burned. The engine used for their test was the single-cylinder NACA universal test engine.¹⁴ They found that an increase in inlet temperature, air pressure, compression ratio and engine speed reduce the delay period. They also found that a variation in the amount of fuel injected (or F/A ratio) has no appreciable effect on the delay, thus defined.

Wentzel¹⁵ in 1936 computed the physical delay period by making a theoretical analysis of the process of heating and vaporization of fuel droplets in the diesel engine. He compared the computed values for the physical delay with measured values of pressure rise delay in constant volume vessel.¹⁶ He found great deviation between the two values. In his discussion he attributed this great deviation to improper assumptions in his calculations or to the existence of a chemical delay period.

Otto Holfelder¹⁷ in 1936 measured the illumination delay at different air temperatures and densities in a constant volume bomb, under conditions of no turbulence. He took pictures (500 pictures/second), of the process of combustion of different fuels.

Wolfer¹⁸ in 1938 measured the pressure rise delay in two different constant volume bombs, and provided an expression for this delay period as a function of the air pressure and temperature.

$$\text{I.D.}_p = \frac{0.44 e^{4650/T}}{P^{1.19}} \quad (2)$$

where P is in atmospheres and T in degrees Kelvin.

As this formula is of great interest in diesel combustion the experimental

*A list of symbols is given in Appendix I of the Addendum.

equipment and procedure used will be described in some detail. His first bomb was a cylinder, 3.13 inches in diameter and 19 inches long. The second bomb was spherical, 7.88 inches in diameter. Turbulence was produced in the second bomb by means of two shaft-driven rotating hemispherical shells adjacent to the interior bomb walls. The effective bomb volume between the heater shells had a height of 2 inches. The air pressure before injection ranged from 118 psia to 393 psia in the first vessel and 172 psia to 705 psia in the second vessel. The tests covered temperatures ranging from 600°F to 947°F. Wolfer did not reach a definite conclusion concerning the effect of the air turbulence and no values were given concerning the speed of rotation of the two spherical shells. He concluded that his equation gave fairly accurate results for all fuels having cetane number greater than 50. He also concluded that ignition delay was "more or less" independent of fuel/air ratio, shape of the combustion chamber, the fuel nozzle, the injection pressure, air turbulence, and the fuel temperature if it is not initially higher than 100°C.

Small¹⁹ continued the work started by Wolfer on the spherical bomb and investigated the effect of turbulence on the ignition delay. He made two tests, one with the air static and the other with the heater shells spinning at 1000 rpm. He reported that no marked difference in the pressure rise delay was observed between the static and swirling conditions.

Robert Selden^{20,21} in 1938 and 1939 studied the effect of air temperature and density on the pressure rise delay. He carried out his tests in a cylindrical bomb, 3 inches in diameter and 3-7/8 inches long. The range of temperatures covered was 870°F to 1255°F and the densities from 0.69 lb/cu ft to 1.18 lb/cu ft. Fuel/air ratios covered were from 13.3:1 to 60:1. He also concluded that the fuel/air ratio had no effect on the ignition delay. He indicated that the possible decrease in ignition delay for a given increase in air temperature or density became quite small at temperatures and densities in excess of those generally occurring in C.I. engines.

Schmidt²² in 1939 provided a formula for the chemical ignition delay for the simple case of bimolecular reaction between two gases without a chain reaction.

$$\text{I.D.}_{\text{Ch}} = \frac{e^{-(E/RT)} \sqrt{T}}{P} a'B \quad (3)$$

where:

P and T are the initial pressure and temperature, respectively.

B = factor that allows for the reduction of ignition delay resulting from the increased rate of burning during the delay period, which is due to the temperature rise within this interval.

a' = factor dependent on the fuel/air ratio.

He considered that the chemical portion of ignition delay for normal engine fuels could be reproduced by a formula similar to Eq. (3). Because of the intermediate chain reactions the pressure would appear as a power with an exponent n. Equation (3) took the form:

$$\text{I.D.} = \frac{e^{+(b'/T)} \sqrt{T}}{P^n} a'B \quad (4)$$

where:

b' represents E/R.

Schmidt reduced Eq. (4) to the Wolfer equation because he noticed that the effect of the exponential function was so predominant that the lesser changes in T, a', and B were not important. Equation (4) then took the form:

$$\text{I.D.} = \frac{c e^{b/T}}{P^n} \quad (5)$$

Bauer²³ in 1939 put forward a formula in which the ignition delay, to a first approximation, is a function of T log P, where P is in atmospheres, and T in degrees Kelvin, or

$$\text{I.D.} = F_n (T \log P)$$

or

$$\text{I.D.} = F_n (P e^T) \quad (6)$$

He measured the illumination delay in an engine of 3-3/8-inch bore by 5-inch stroke. Compression temperatures and pressures at the end of the illumination delay period were calculated by assuming a polytropic index of 1.3. He found the above expression by trial and error, which he believed to cover the experimental data with reasonable accuracy.

It is to be noted that Eq. (6) indicates that ignition delay is a function of e^T while Wolfer's, Schmidt's, and Semenov's²⁴ equations indicate that the ignition delay is a function of $e^{b/T}$.

West and Denis Taylor²⁵ in 1941 measured the pressure rise delay by running tests on a single-cylinder open chamber diesel engine, 4.5-inch bore,

5.75-inch stroke, C.R. = 15.8:1 at a speed of 1000 rpm, at intake pressures ranging from 30 inches Hg to 56 inches Hg. The results of ignition delay tests were correlated in terms of $T \log P$ suggested by Bauer and are shown in Figure 1.

Starkman²⁶ in 1946 studied the effect of pressure, temperature, and fuel/air ratio on the pressure rise delay in a C.F.R. diesel engine and in a bomb. The volume of the bomb was equal to the clearance volume of the engine. He found that the pressure rise delay is reduced by the increase in any of the above factors, and that it is shorter in the engine than in the bomb.

Elliott²⁷ in 1949 made a detailed analysis to find the effect of temperature on the pressure rise delay. He used the results of Muller²⁸ and Wolfer as reproduced by Jost.²⁹ Elliott gave a formulae for the ignition delay as being the sum of the physical and chemical delays, and which he found to be in agreement with the results of Starkman.²⁶ For methylnaphthalene the formula is:

$$\text{I.D.} = 0.977 e^{1070/T} + 2.18 \times 10^{-8} e^{14510/T} \quad (7)$$

For cetane the formula is:

$$\text{I.D.} = 0.710 e^{1070/T} + 3.47 \times 10^{-14} e^{17620/T} \quad (8)$$

Hurn and Hughes³⁰ in 1952 investigated the effect of pressure, temperature, and fuel composition on the pressure rise delay in a constant volume bomb. The bomb, 2.5 inches in diameter, and 3.5 inches long, was externally heated, and contained air or artificial atmospheres with different partial pressures of oxygen. The temperatures ranged from 850°F to 1050°F, the pressures varied from 275 psi to 675 psi, the oxygen percentage varied from 15% to 40% and the cetane number of fuels varied from 37.2% to 53.7%.

They found that there is a certain percentage of oxygen that results in a minimum delay. They found also that the difference in ignition delay shown by the fuels became less as the air pressures and temperatures were elevated.

Hurn, et al.,³¹ in 1956 studied the factors that govern the heating of injected fuels and the release of chemical energy in the autoignition process. They injected fuels of different volatility in a constant volume bomb, 2-1/2 inches in diameter and 4 inches long, containing different gases. Their data showed that chemical heat released occurred only after an appreciable interval of time during which the fuel was heated and partly or wholly vaporized. The rapidity of this heating, and associated ignition delay, were influenced markedly by the physical properties of the surrounding gas. Fuel volatility

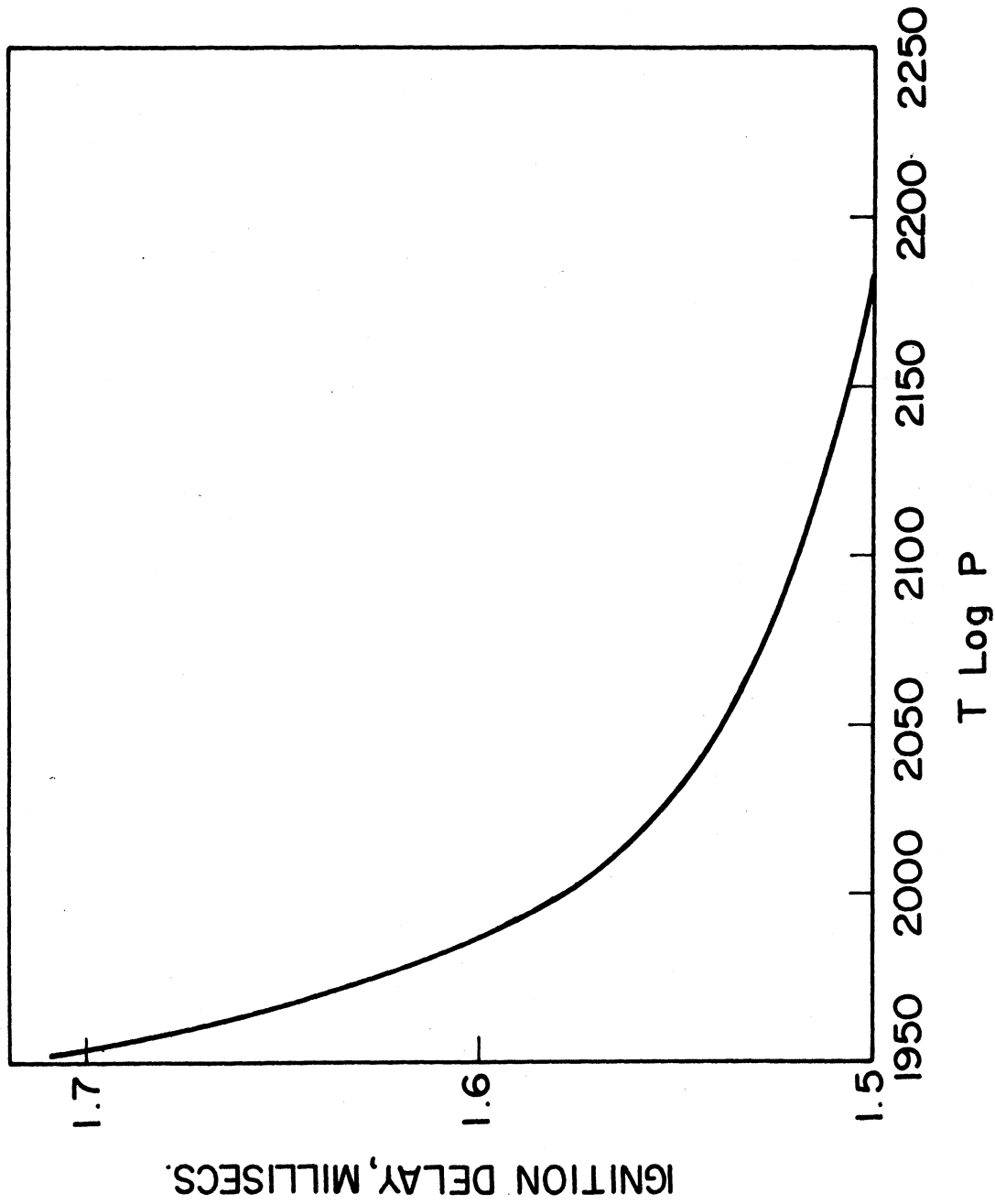


Figure 1. Relation between I.D.p and T log P, by West, et al.

and chemical structure had relatively little influence on the rate of heat transfer to the fuel during the physical delay period. The chemical delay was influenced by the composition of the fuels and by gas-to-fuel heat transfer rates during the pre-reaction period.

Yu, et al.,³² in 1956 measured the small pressure changes occurring during the ignition delay in a single cylinder GM-71 engine. They also studied fuel vaporization with no oxidation reactions present by injecting fuel into nitrogen instead of air in the combustion chamber. These small pressure changes were measured by applying the hot motored technique. This technique includes taking pressure-crank angle traces for the engine fired and misfired in two consecutive cycles. They found the maximum pressure drop to depend upon the properties of the fuel, and mainly, on the cetane number. The fuel volatility had little effect on the rate of heating of the fuel.

El-Wakil, et al.,³³ in 1956 analyzed the events that occur to the fuel from the beginning of injection to the end of the pressure rise delay period. They analyzed the process of jet break up, drop vaporization with and without interaction with other drops. They indicated that spray break up was not an important part of the physical delay period. Their analysis on the spray evaporation showed that the condition of adiabatic saturation was approached very closely in the spray core, while the fuel/air ratio varied with the distance from the spray core in a different manner for fuels of different viscosities and volatilities. They found that under adiabatic saturation conditions a nonvolatile fuel has as good or a better chance as a volatile fuel to achieve the combination of temperature and vapor-air ratio required for self ignition and rapid combustion. They compared pressure rise delays in bombs³¹ and in engines³² and found that they are smaller in the engines than in combustion bombs.

Garner, et al.,³⁴ in 1957 measured the illumination delay in a C.F.R. diesel testing unit which incorporated a precombustion cylinder head. They found that the illumination delay decreased as the compression ratio was increased until some critical point was reached, after which the illumination delay again began to lengthen. They found that this applied at all fuel/air ratios for the following two fuels: DI paraffinic secondary reference fuel of 70 cetane number, and a naphthenic gas oil of 32 cetane number. This critical compression ratio was 23:1 for the low cetane naphthenic fuel and 25:1 for the higher cetane fuel. They noticed a break (zero illumination delay) at a compression ratio = 24.5:1 for both fuels.

Garner, et al.,³⁵ in 1961 continued their work and calculated the energy released during the delay period. They concluded that the preflame energy release is constant for any given fuel and the energy released is directly proportional to the delay period.

Tsao, et al.,³⁶ in 1962 measured the temperature rise delay in a modified C.F.R. engine. They measured the gas temperature inside the cylinder by

the "Null Method," of the infrared technique. The operating variables investigated were the intake air temperatures, the fuel quantity per cycle, the intake air pressure, the engine speed and the fuel cetane number.

The empirical relationship they developed to correlate the temperature, the pressure, the engine speed, and the temperature rise delay is as follows:

$$I.D.T = 1000 e^x - 1000 \quad (9)$$

where:

$$x = \frac{1}{1000} \left(\frac{123}{P} + 0.415 \right) \left\{ \left(\frac{-36.6}{T} + 0.0222 \right) N + \left[\left(\frac{47.45 \times 10^3}{T} \right) - 26.66 \right] \right. \\ \left. + \left(\frac{T}{1000} - 1.45 \right) \left(\frac{1000 - N}{60} \right) \right\} \quad (10)$$

This equation in the simplified form is as follows:

$$I.D. = \left(\frac{123}{P} + 0.415 \right) \left\{ \left(\frac{-36.3}{T} + 0.0222 \right) N + \left(\frac{47.45 \times 10^3}{T} - 26.66 \right) + \right. \\ \left. \left(\frac{T}{1000} - 1.45 \right) \left(\frac{1000 - N}{60} \right) \right\} \quad (11)$$

It is noted that this is the first formula to include the engine speed as a factor affecting the ignition delay period.

Sitkei³⁷ in 1963 measured the illumination delay, in a single cylinder precombustion chamber diesel engine and in an air cell engine. He divided the chemical portion of the illumination delay into three phases, so the illumination delay can be given by:

$$I.D.II = I.D.Ph + I.D.C.F. + I.D.B.F. + I.D.E.F. \quad (12)$$

where:

$$I.D.C.F. = \text{ignition delay of the cold flame}$$

I.D._{B.F.} = ignition delay of the blue flame

I.D._{E.F.} = ignition delay of the explosion flame

He found that the last two terms of Eq. (12) are difficult to separate and suggested that they be combined in one term where:

$$I.D._{(B+E)F} = I.D._{B.F.} + I.D._{E.F.}$$

thus the Eq. (12) becomes:

$$I.D._{I1} = I.D._{Ph} + I.D._{C.F.} + I.D._{(B+E)F} \quad (13)$$

He estimated the physical delay as being equal to 0.5 millisecc and evaluated I.D._{C.F.} and I.D._{(B+E)F} in the above described engines, and gave the following formula for the illumination delay.

$$I.D._{I1} = 0.5 + \frac{0.135 e^{7800/RT}}{P^{0.7}} + \frac{4.8 e^{7800/RT}}{P^{1.8}} \quad (14)$$

where P is in atmospheres and T in degrees Kelvin.

Lyn and Valdmanis³⁸ in 1966 studied the effects of air temperature, air pressure, and injection system parameters on the pressure rise delay, in two engines with modified chambers to accommodate schlieren photography.³⁹ They applied the motored engine technique with single shot injection. They concluded that the cylinder temperature and pressure, and the injection timing are the main factors that affect the pressure rise delay. Air velocity, fuel injection pressure and nozzle configuration have a secondary effect. Injection quantity (or fuel/air ratio) has negligible effect.

From the literature review it can be noticed that different delay periods were measured in a variety of combustion chambers under different operating conditions. The formulae available now for the ignition delay are mainly that by Wolfer for the pressure rise delay in bombs, Bauer and West for the pressure rise delay in an open-chamber engine, Tsao, et al., for the temperature rise delay in a modified open chamber C.F.R. engine, and Sitkei for the illumination delay in a divided combustion chamber engine.

From an engineering point of view the pressure rise delay or the temperature rise delay are the most important but the pressure rise delay is much

easier to measure. In the previous investigations on the pressure rise delay most of the experiments were done in bombs or in open combustion chambers where the turbulence is limited to relatively small values. Among all the formulae available on ignition delay in engines there is only the formulae by Tsao, et al., that took into consideration the effect of engine speed. In the present study the effect of turbulence and other factors that affect the pressure rise delay will be studied in a turbulent combustion chamber.

THERMODYNAMIC CONSIDERATIONS

In this theoretical analysis a study is made of the factors that affect the pressure rise delay in a constant volume bomb and in an engine. A discussion is given of the thermodynamic factors that cause differences in the delay periods of bombs and engine cylinders.

Consider the gas in the combustion chamber as a system. The end of the pressure rise delay for this system is determined from the pressure trace at the point where a change in the slope ($dP/d\theta$) occurs due to combustion. The slope ($dP/d\theta$) can be computed from the balance of the different types of energies involved, from the time of start of injection to the end of the pressure rise delay. The energies involved are as follows:

1. Work done by or on the system. In a bomb this work is equal to zero since the volume is constant, but in an engine the volume is continuously changing during the delay period. If all the delay occurs during the compression stroke, then work will be done by the piston on the system resulting in an increase in its internal energy. However, if a portion of the delay occurs after T.D.C. then during this portion work will be done by the system on the piston, which results in a corresponding drop in the internal energy of the system, and longer pressure rise delays.
2. Heat exchange between the system and the surroundings which depends on the combined effect of convection and conduction.
3. Sensible internal energy changes due to evaporation and heating of the vapor to the self-ignition temperature of the fuel.
4. Chemical internal energy changes due to the exothermic reaction between the fuel and oxygen.

The slope of the pressure trace is derived in Appendix II and is given in Eq. (26):

$$\left(\frac{dP}{d\theta}\right) = \frac{R}{c_v} \cdot \frac{1}{V} \left[\frac{dQ}{d\theta} - P \frac{dV}{d\theta} \left(\frac{c_v}{R} + 1\right) + T c_v \frac{dm}{d\theta} \right] \quad (15)$$

This equation indicates that the rate of pressure rise depends upon the following factors:

1. The volume of the mixture, V . The bigger the volume of the container, with all parameters constant, the smaller will be $dP/d\theta$. From the review of previous experimental work done on ignition delays, it is noticed that the combustion chambers used were of different volumes. It is believed that this is one of the factors that contribute to the differences between the results of different investigators.
2. The rate of heat addition to the mixture $dQ/d\theta$. This represents the net heat added to the mixture as a result of the heat of reaction $dQ_{Ch}/d\theta$ and the heat transfer losses to the walls, $dQ_C/d\theta$. The heat added to the system can be given by,

$$\frac{dQ}{d\theta} = \left[\frac{dQ_{Ch}}{d\theta} - \frac{dQ_C}{d\theta} \right] \quad (16)$$

$dQ_{Ch}/d\theta$ is proportional to the velocity of the chemical reaction, the volume of reactants and their concentration. The velocity of reaction was given by Semenov²⁵ for simple elementary reactions as:

$$W = K_1 a^n e^{-(E/RT)} \quad (17)$$

The reactions included in the autoignition of hydrocarbon fuels are in general very complicated, and the detailed mechanisms are not known. However, there is nearly general agreement that autoignition of hydrocarbons proceeds by a mechanism involving a chain of simple reactions for which Eq. (17) can be applied.

$$\frac{dQ_{Ch}}{d\theta} = \frac{d}{d\theta} \left[K \cdot V' \cdot U_R \cdot a^{n'} \cdot e^{-(E/RT)} \right] \quad (18)$$

where V' is the sum of the elementary volumes containing a combustible mixture. V' is a function of many factors that influence the fuel injection, evaporation and distribution in the combustion chamber. Therefore it depends upon the type of fuel, rate of fuel injection, type of fuel nozzle, mean diameter of droplets, jet velocity, air turbulence, air temperature and density. Almost all these factors can be kept the same in bombs and in engines, except for the air turbulence which is believed to be one of the factors that cause the difference between the two cases.

Equation (18) indicates that the energy released by the chemical reaction is a function of the factors that affect V' together with the average

concentration of fuel and air in the different parts of the combustion chamber, the heat of reaction, the activation energy and the absolute temperature.

The heat loss to the walls, $dQ_C/d\theta$, is a function of the temperature difference between the gas and the walls, the area of heat transfer, and the coefficient of heat transfer. It can be given by

$$\frac{dQ_C}{d\theta} = \frac{d}{d\theta} \left[\alpha \cdot A \cdot (T_g - T_w) \right] \quad (19)$$

The heat losses in an engine are in general greater than in a bomb of the same size and under the same gas and wall conditions because of the higher coefficient of heat transfer.

Equation (15) can take the form:

$$\frac{dP}{d\theta} = \frac{R}{c_v} \cdot \frac{1}{V} \left[\left(\frac{dQ_{Ch}}{d\theta} - \frac{dQ_C}{d\theta} \right) - P \frac{dV}{d\theta} \left(\frac{c_v}{R} + 1 \right) + T c_v \frac{dm}{d\theta} \right] \quad (20)$$

The different types of energy included in Eq. (20) are represented in Figures 2 and 3. The last term in Eq. (20) will be neglected for simplicity since its effect is very small. Figure 2 is for an engine without injection. Figure 3 is for the same engine with fuel injection and combustion. In Figure 2, curve "a" represents the work done by the piston on the system. This work causes an increase in internal energy of the system before T.D.C. and a drop in internal energy after T.D.C. The change in internal energy at T.D.C. due to piston work is zero. Curve "b" shows the heat loss from the gas to the cylinder walls. Its effect is to decrease the internal energy of the system at different rates which mainly depend upon the turbulence in the chamber. Curve "c" is the algebraic sum of curves "a" and "b." It represents the energy to be released by combustion before the end of the pressure rise delay can be detected at any crank angle. The balance between the chemical energy released and the other types of energies is shown in Figure 3. In this figure curve "c" is inverted to simplify the analysis. Three cases of energy release rates are considered. Case 1 is for a high rate of energy release where the delay period ends during the compression stroke. Case 2 is for a lower rate of energy release where the delay period ends during the expansion stroke, resulting in a longer delay period. Under such conditions the energy released $(dQ_{Ch}/d\theta)_2$ should be more than $(dQ_{Ch}/d\theta)_1$, released in the first case. The increase in the rate of energy release in the second case is mainly to account for the work of expansion after T.D.C. Case 3 is for a very low rate of energy release where no pressure rise due to combustion can be detected.

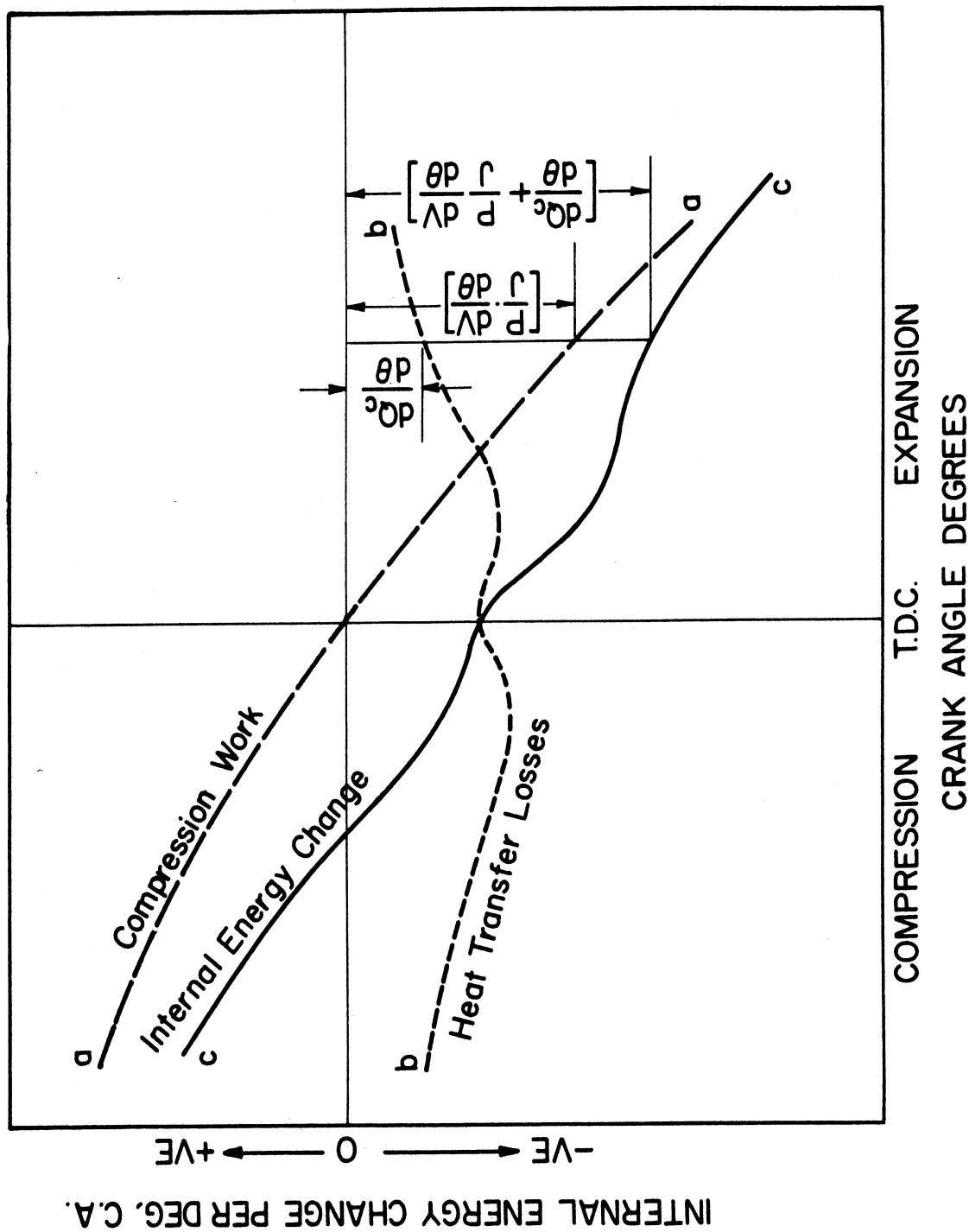
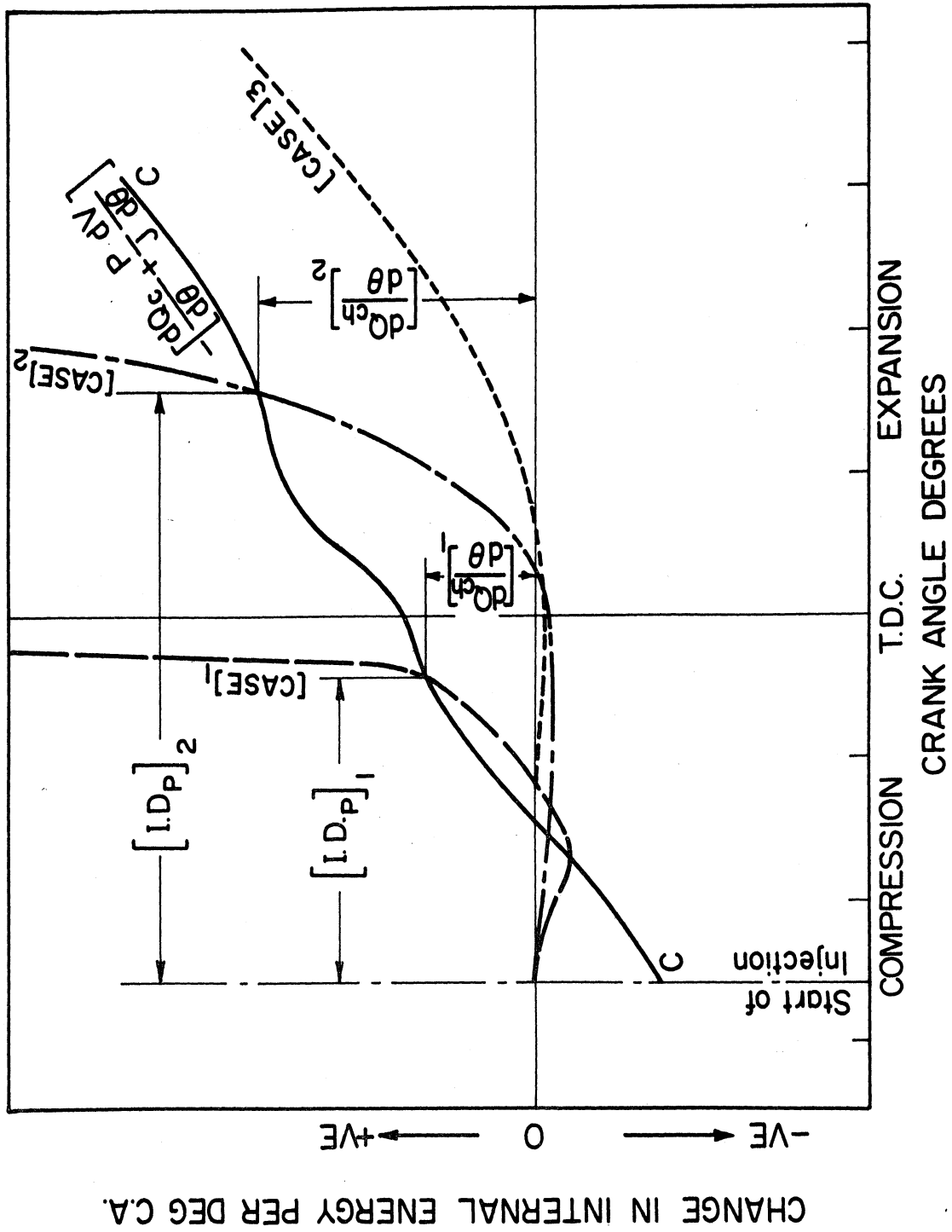


Figure 2. Change of internal energy of the system near T.D.C. without injection.



The conditions in a bomb are different from an engine for the following reasons:

1. No work is done on or by the system since the volume is constant.
2. The turbulence in a bomb is negligible compared to the engine. The main effect of turbulence is on the heat transfer losses and the mixing of the fuel and air. It causes the heat transfer losses in engines to be greater than in bombs of the same size and under the same conditions of pressure and temperature. However, the effect of the increased heat transfer losses due to turbulence is small compared to the increase in the rate of chemical release due to the better mixing. Equation (18) indicates that the rate of chemical energy release depends on, V' , the volume having optimum concentrations for the reaction. It is believed that the chances are better in engines to obtain better concentrations and higher combustion reaction rates.
3. In some of the bomb tests the walls are used to heat the air, so heat is added to the system during the delay period instead of being lost from the system to the walls as in the engines.

This analysis indicates that the pressure rise delay is not only a function of the physical and chemical delays, it is also a function of the thermodynamic factors that affect the balance between the energy generated from the chemical reaction, the heat lost to the surroundings, the work done on or by the system.

EQUIPMENT

A general view of the experimental Lister-Blackstone engine is shown in Figure 4. The engine is a single cylinder, four-stroke cycle, liquid cooled, 4-1/2-inch bore, 4-3/8-inch stroke, and has a rated power of 8 BHP at 1200 rpm. This engine is especially useful for combustion research because of easy access to the swirl chamber, or turbulent chamber. The design, therefore, makes it practical to modify the swirl chamber, and to place pressure pick-ups and other instruments into the wall of the swirl chamber. It was also found to be practical to modify the combustion chamber to permit change of compression ratio. Figure 5 shows a section of the cylinder head with its original auxiliary chamber and the compression ratio changeover valve. Figure 6 shows the cylinder head after modification and shows the variable compression ratio sleeve and the chamber plug. The construction of this plug allows the compression ratio to be varied from 13.92:1 to 22:1. For the experimental part of the paper, all the tests were run at a constant compression ratio of 13.92:1.

Shop air was used to supercharge the engine after being passed through a surge tank fitted just before the engine. The pressure in the tank is measured and considered equal to the supercharging pressure. The temperature is measured in the tank and in the cylinder head before the inlet valve. The air consumption is measured by a critical pressure-type flowmeter.

The gas pressure inside the cylinder is obtained by the use of an oscilloscope, together with a Kistler pressure transducer and a degree-marking unit. The Kistler transducer is mounted on the combustion chamber plug as nearly flush as possible with the inside surface of the combustion chamber. The output of the transducer is fed to a charge amplifier and then to a dual-beam oscilloscope. The trace obtained on the screen is photographed by a Polaroid camera attached to the oscilloscope.

The crank angles are measured every three degrees in a manner similar to that used in previous work.⁴⁰

The fuel injection system consists of a Bosch single hole injector and a Bosch injection pump driven by the engine camshaft. The injector opening pressure was varied from 1000 to 4000 psi. Unfortunately, the injector timing could not be varied on this engine.

The fuel injector is instrumented, Figure 7, so that the start and rate of injection can be calculated from measurements of the needle lift and fuel pressure before the nozzle. The needle lift is measured by a Bentley D-152 distance detector system. The injection is considered to begin at the instant the needle lift begins. The fuel pressure before the nozzle is ob-

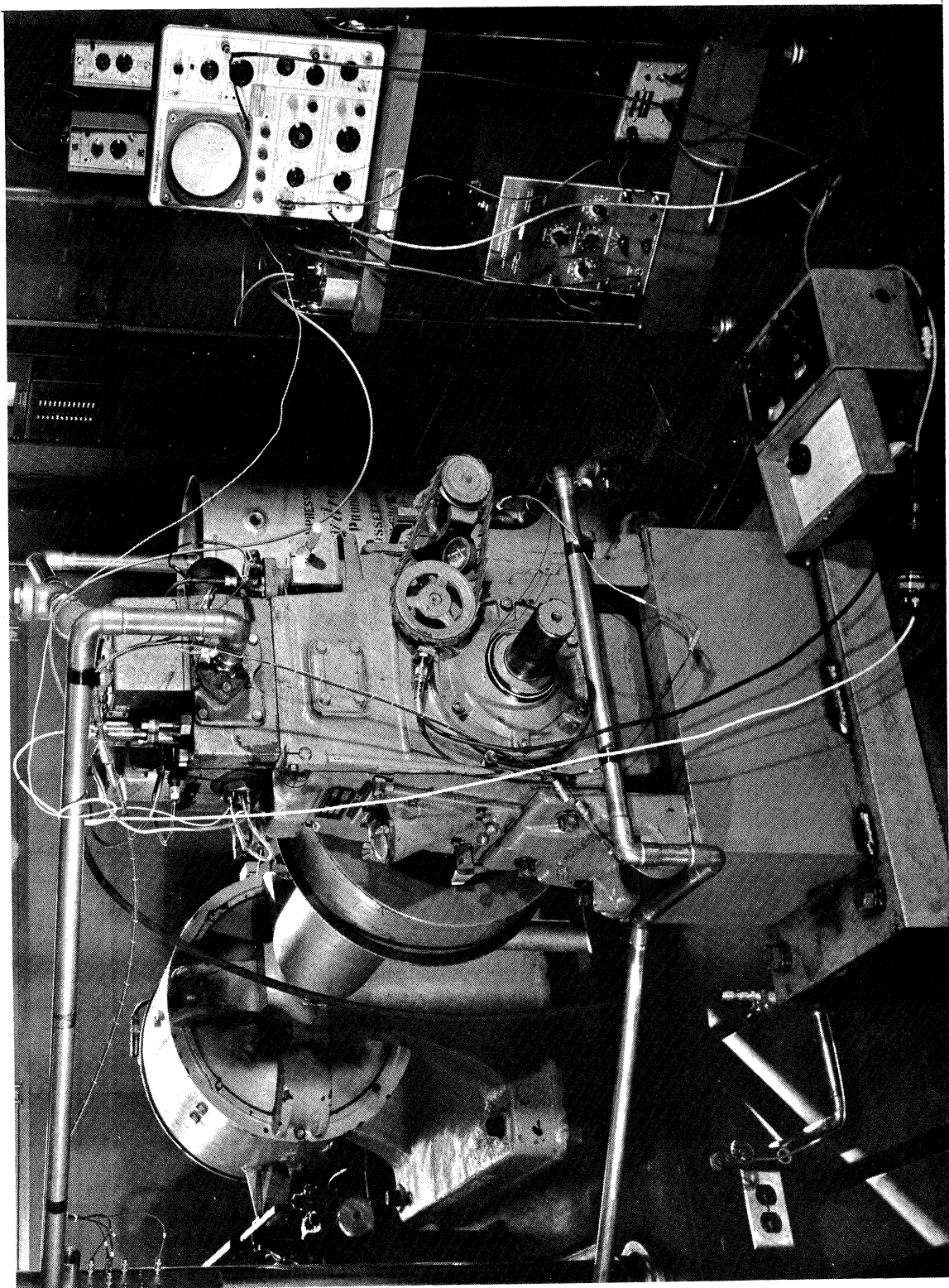


Figure 4. Photograph of Lister-Blackstone engine and equipment.

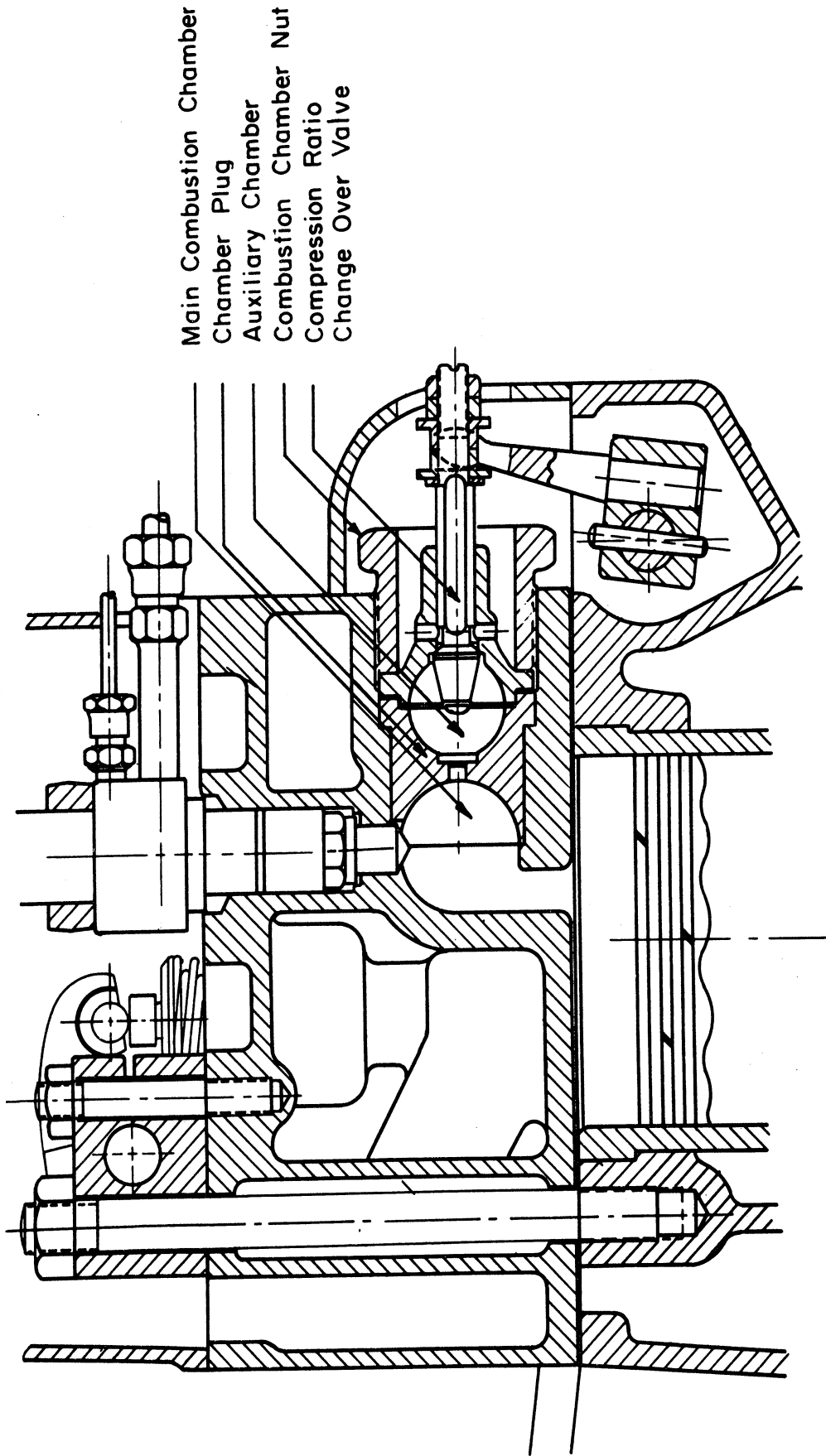
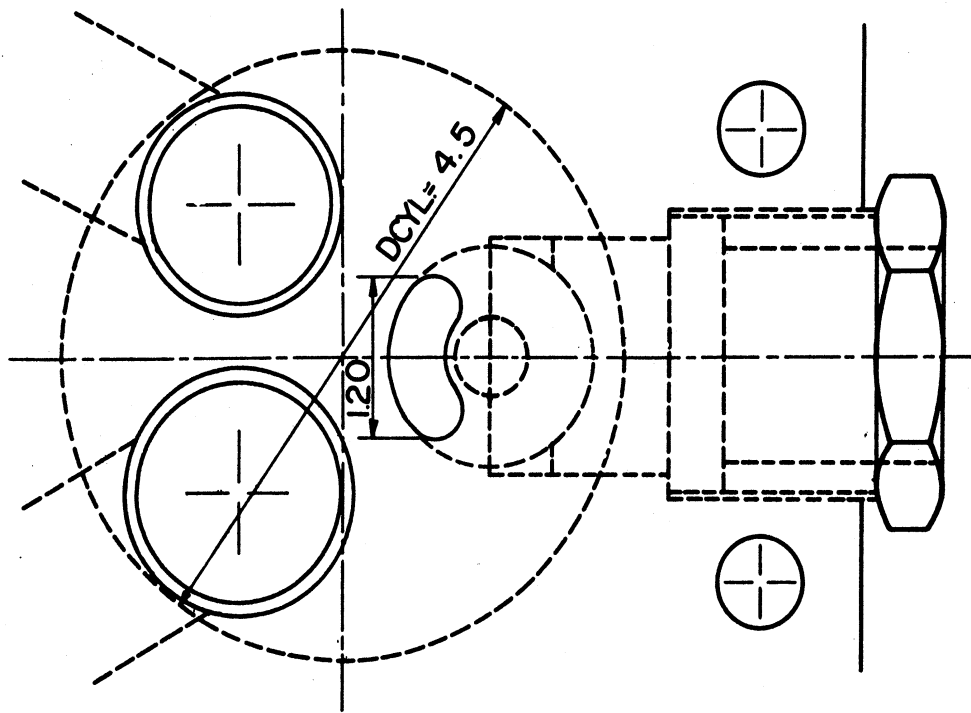
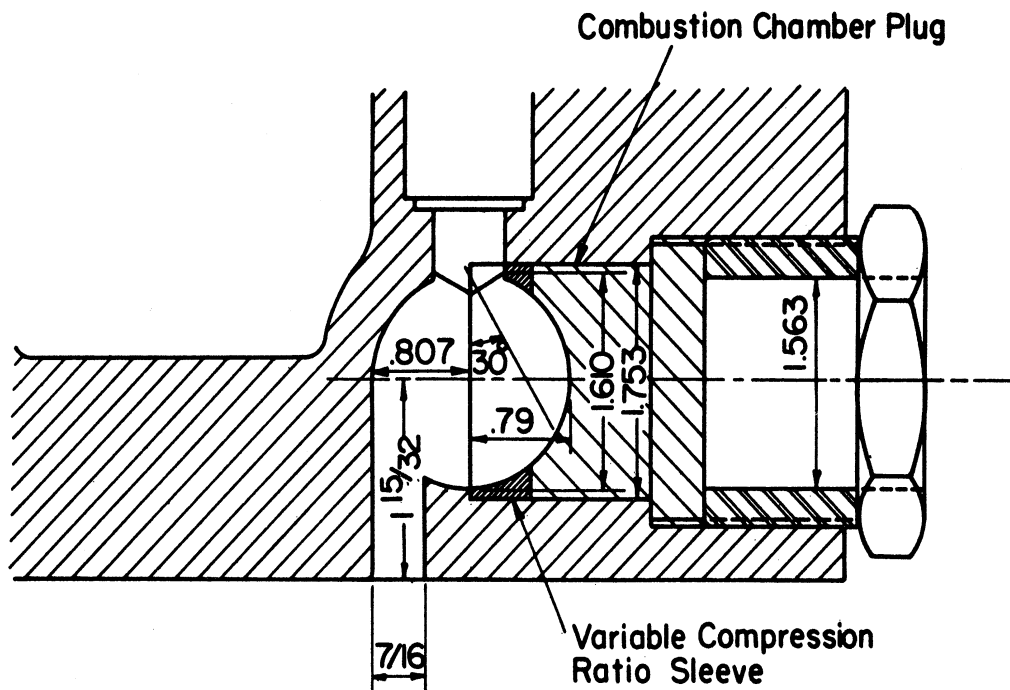


Figure 5. Original combustion chamber of Lister-Blackstone engine.



TOP VIEW



SECTIONAL VIEW

Figure 6. Modified combustion chamber of Lister-Blackstone engine.

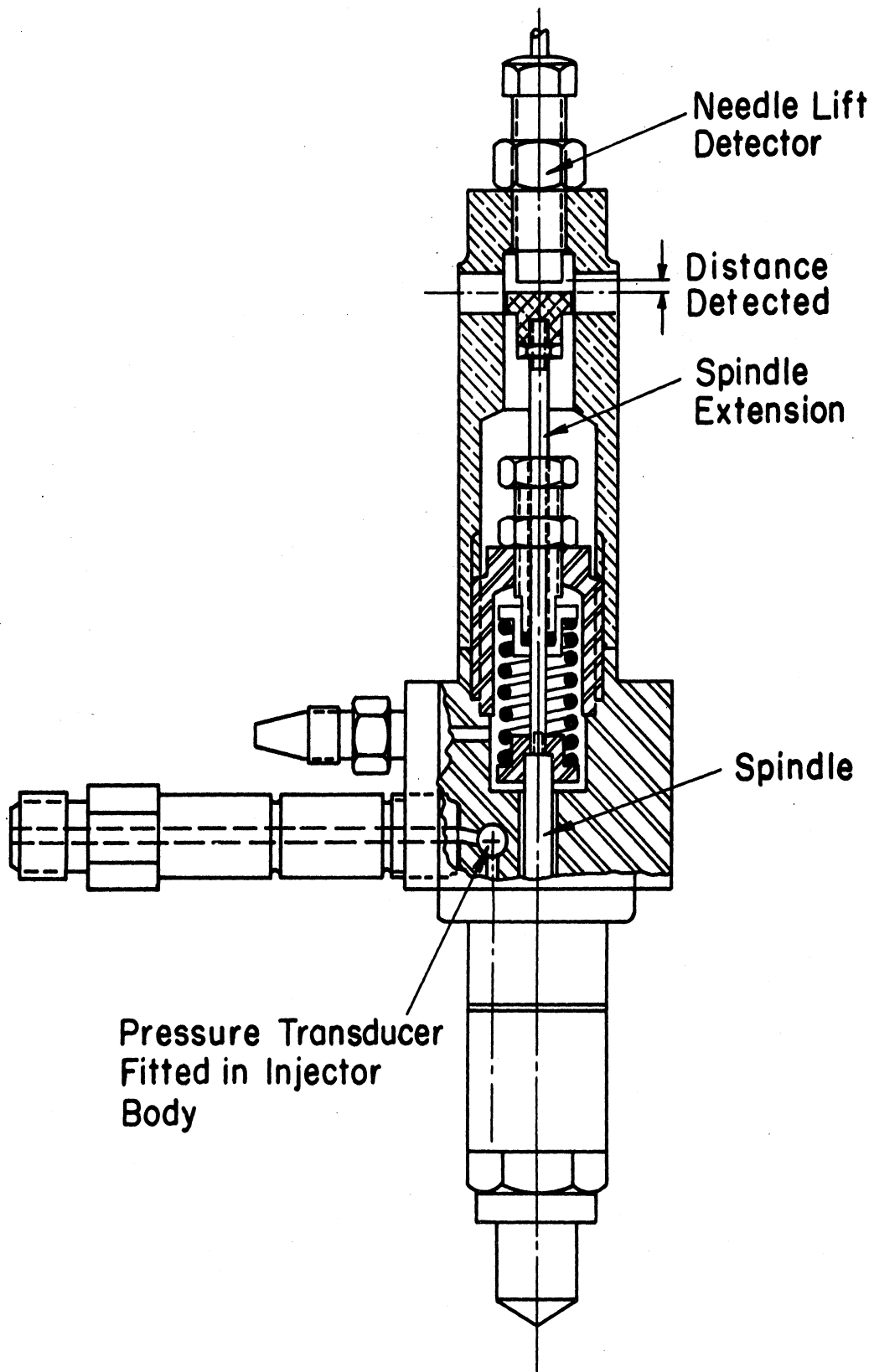


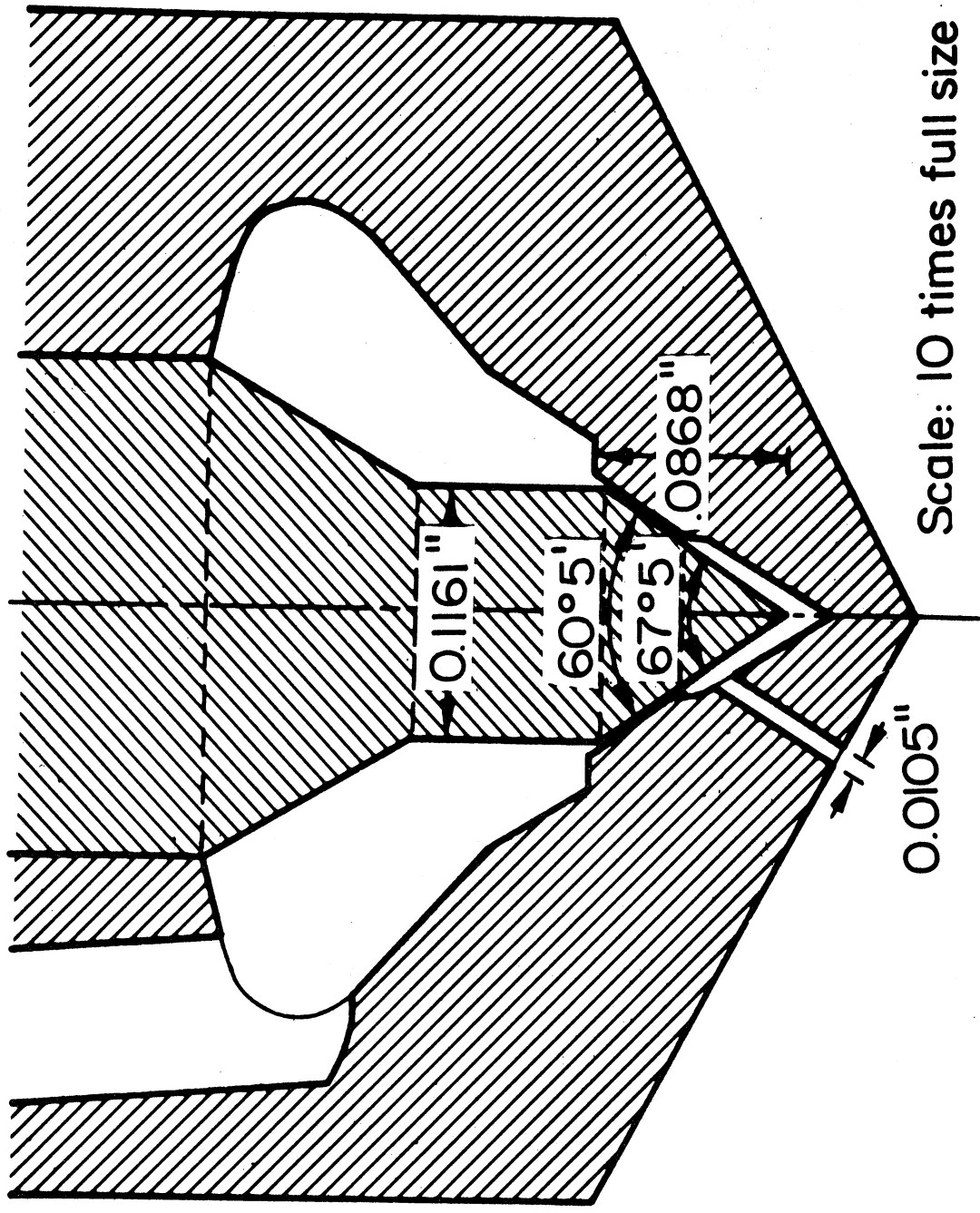
Figure 7. Fuel injector fitted with a needle lift detector and a pressure transducer.

tained by a Kistler transducer fitted on the injector body. The rate of injection (especially during the delay period) is calculated from the pressure difference before and after the nozzle and the areas of flow as computed from needle lift measurements. A cross section of the nozzle is shown in Figure 8.

A sample of the traces obtained for the gas pressure, fuel pressure, needle lift, solar cell output and crank degrees is shown in Figures 9 through 12.

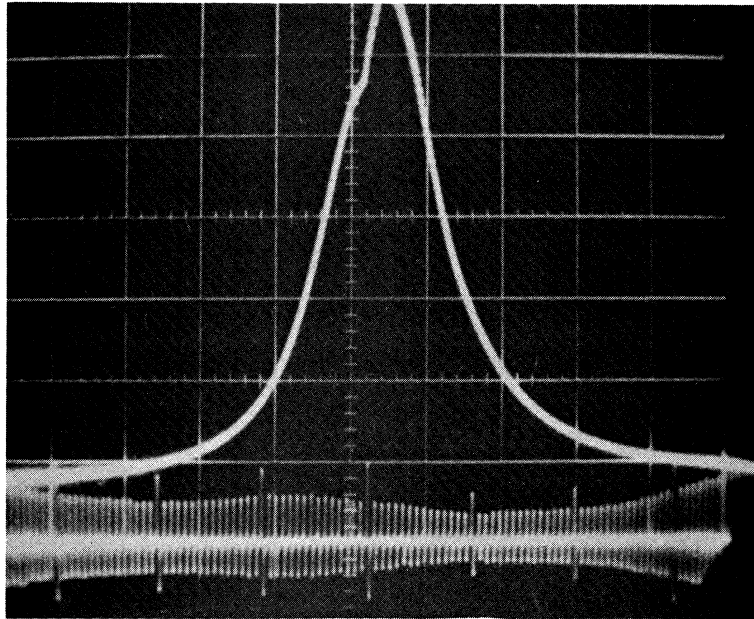
The engine is connected to a 25 hp G. E. dynamometer. The intake air pressure was controlled by a regulating valve and could be varied over a wide range; but the exhaust was kept at atmospheric pressure. The fuel used in these tests was Standard Oil Company No. 2 diesel fuel.

The point of illumination was determined by using a Hoffman silicon solar cell (type 55C).

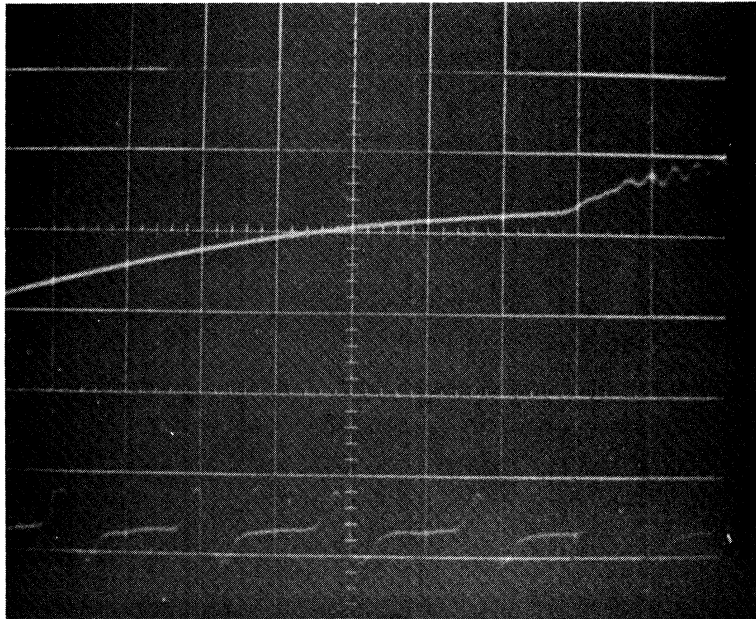


Scale: 10 times full size

Figure 8. Nozzle needle assembly.

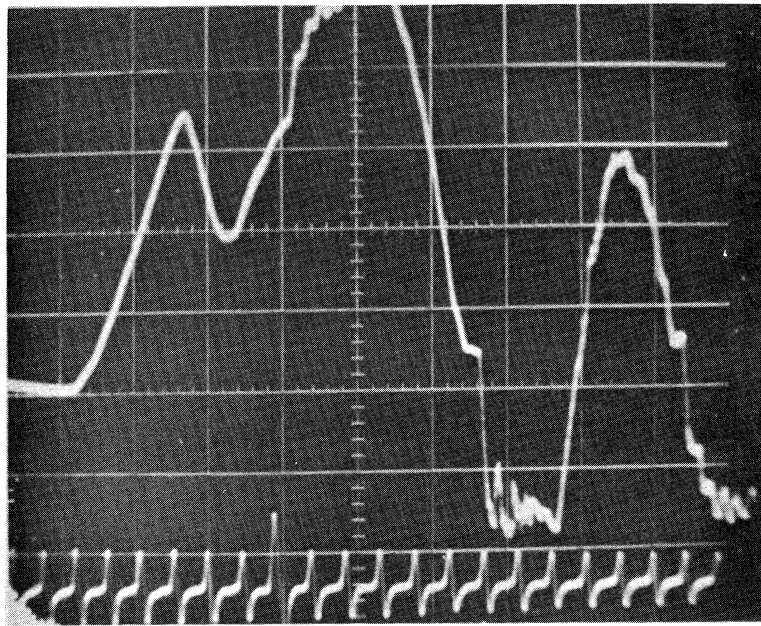


→ 45° ←
T.D.C.

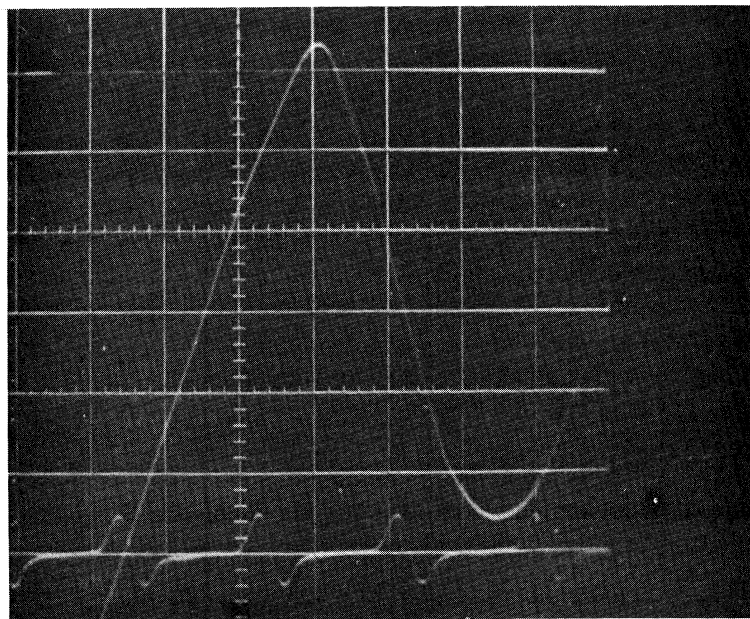


→ 3° ←
T.D.C.

Figure 9. Cylinder pressure-crank angle diagram. Upper: compression and expansion strokes. Lower: during pressure rise delay.

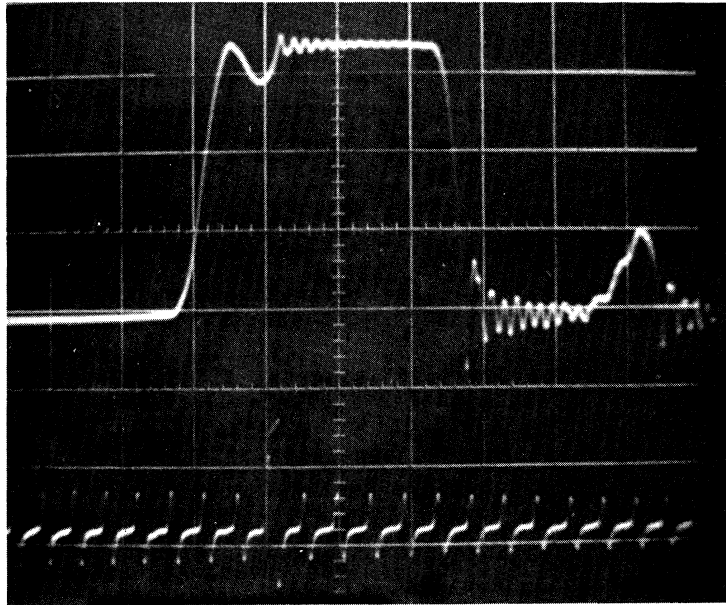


|
T.D.C.

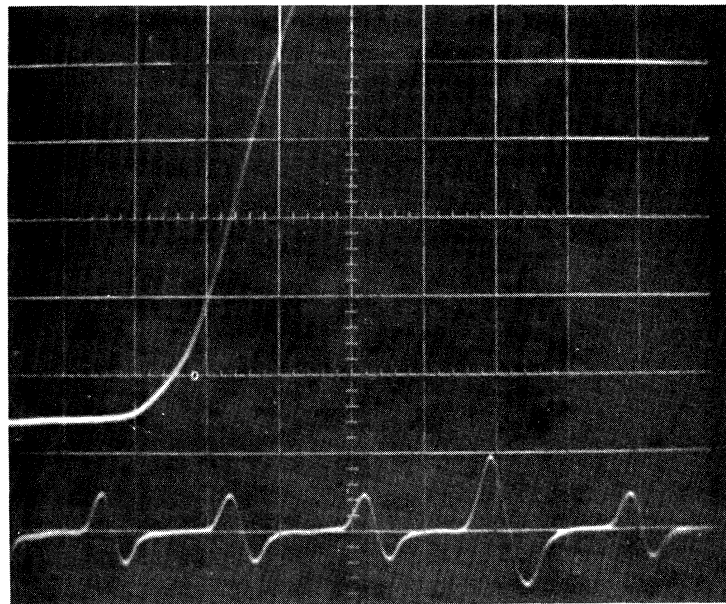


|
T.D.C.

Figure 10. Fuel pressure-crank angle diagram. Upper: for whole period of injection. Lower: at start of injection.

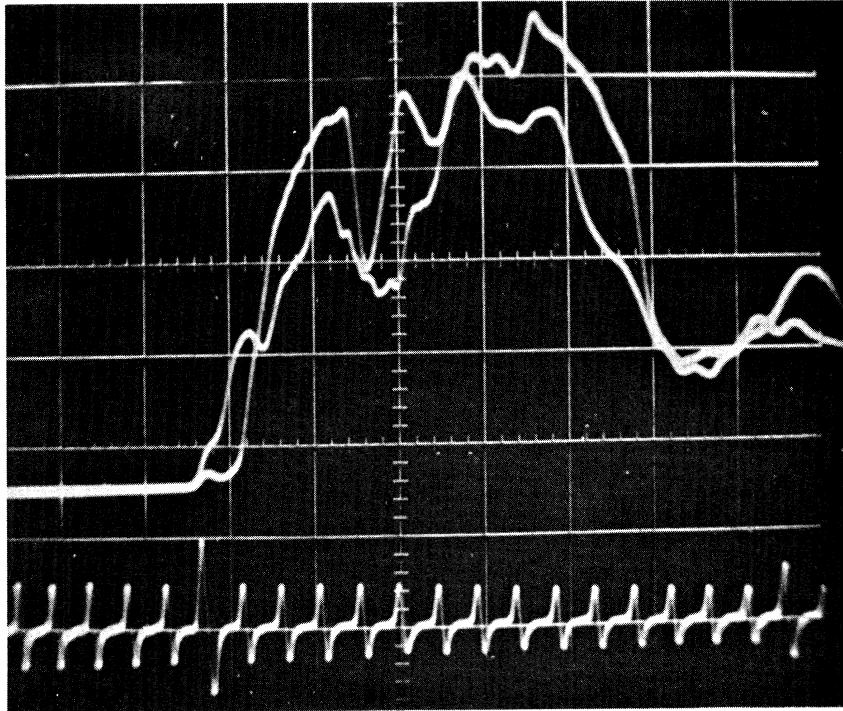


|
T.D.C.



|
T.D.C.

Figure 11. Needle lift-crank angle diagram. Upper: for whole period of injection. Lower: at start of injection.



T.D.C.

Figure 12. Illumination-crank angle diagram.

EXPERIMENTAL RESULTS AND DISCUSSION

The main purpose of the experimental work was to study the effect of pressure on the pressure rise delay. However, it was found necessary, in the early stages of the work to make a preliminary study of the other parameters that affect the delay period. These parameters include the fuel/air ratio, the injection pressure, the coolant temperature, and turbulence. This was done to establish a test procedure for the runs that would be made to investigate the effect of pressure.

In this section, the different series of tests are reported in their chronological order in which they were carried out.

EFFECT OF FUEL/AIR RATIO ON PRESSURE RISE AND ILLUMINATION DELAYS

These tests were run at variable fuel/air ratios with the other parameters kept constant. On the lean side the engine was motored with fuel injection and combustion. The amount of fuel injected was reduced, and fuel/air ratios as low as 0.0022 (0.0325 stoichiometric), were reached. With the engine producing power the fuel/air ratio was increased up to 85% the stoichiometric ratio. With higher fuel/air ratios, erratic operation of the engine occurred due to a very late after-injection. By examining the cylinder pressure under these conditions it was noticed that injection of the left over fuel from the previous cycle occurred before the start of injection.

The results of this series of runs are plotted in Figure 13. The general trend of this figure indicates that both the pressure rise and illumination ignition delays decrease with increase in fuel/air ratio. An increase in fuel/air ratio from .0022 to .0431 caused the illumination delay to decrease by 38.2%. It was noticed that at higher fuel/air ratios, the solar cell did not operate properly. The decrease in pressure rise delay amounted to 37.6% by an increase in fuel/air ratio from 0.0022 to 0.0567. The effect of fuel/air ratio on decreasing the ignition delay is actually more than that indicated in Figure 13, because at higher fuel/air ratios fuel injection starts at an earlier angle before T.D.C., i.e., at lower air pressures and temperatures, and densities. The advance in the start of fuel injection at different fuel/air ratios is shown on the same figure.

An examination of this figure indicates that at very lean fuel/air ratios the ignition delay reaches very high values. The variations in the delay at fuel/air ratios below 0.011 are believed to be due to changes in fuel injection timing. Ignition or combustion were not observed at fuel/air ratios less than 0.0022. The minimum fuel/air ratio probably differs from one engine to another and depends on many factors that influence the balance be-

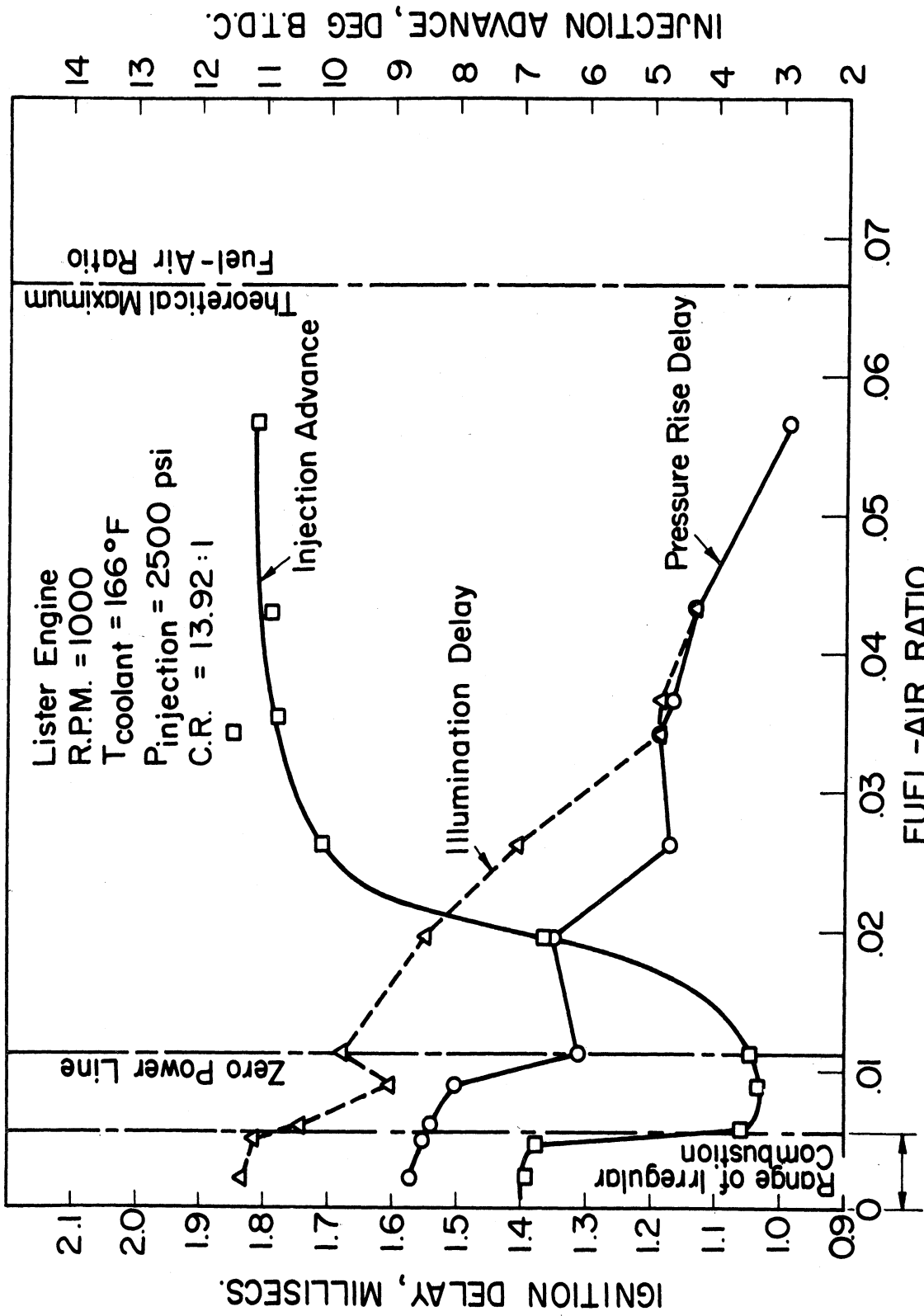


Figure 13. Effect of fuel/air ratio on ignition delay.

tween the energy added to and lost from the system as indicated in Figure 3. In photographic work concerning combustion in a diesel engine, Miller⁴¹ indicated that the minimum fuel/air ratio was 0.01 when illumination was not observed.

By comparing the traces for the illumination and pressure rise delays in Figure 13, it is noticed that for fuel/air ratios up to 0.035, the illumination delay is longer than the pressure rise delay. For higher fuel/air ratios the two types of delay have equal values. For fuel/air ratios less than 0.035 it seems that pre-illumination reactions take place in the combustion chamber and cause a temperature rise with a corresponding pressure rise. For mixtures richer than 0.035 it seems that the pre-illumination reactions are not enough to produce a temperature rise sufficient to produce a measurable pressure rise before illumination occurs.

EFFECT OF INJECTION PRESSURE ON IGNITION DELAY

Many factors influence mixture formation in the diesel engine, including the mean spray velocity at the nozzle, atomization, penetration, evaporation, and mixing with air. The differential pressure across the nozzle orifice substantially affects the mixture formation especially near the beginning of the injection process. The fuel pressure before the nozzle is primarily a function of the setting of the needle opening pressure. In order to investigate the effect of changing the fuel atomization and distribution in the combustion chamber the opening pressure was changed from 1000 psi to 4000 psi. The experimental results for the effect of injector opening pressure on the pressure rise and illumination delays are shown in Figure 14. As the injector opening pressure is increased, from 1000 psi the illumination delay is reduced reaching a minimum at a pressure of 2100 psi. At higher injection pressures the illumination delay is again increased. Sitkei³⁷ also noticed such an increase in illumination delay with an increase in the injection pressure.

The pressure rise delay remains constant for all injector opening pressures. The increase in the injection pressure is expected to increase the initial jet velocity at the tip,⁴² reduce the average drop size,⁴³ and has some effect on penetration.⁴⁴ These changes in the spray pattern seem to have a small effect on the rate of combustion which starts in the spray envelope.¹⁷

EFFECT OF COOLING WATER TEMPERATURE ON IGNITION DELAY

Preliminary engine tests indicated that the pressure near T.D.C. is affected by the heat losses because maximum pressure occurred before T.D.C. in the motored engine. The crank position for maximum pressure and temperature in the motored engine is shown in Appendix III. Since the ignition delay depends on gas pressure and temperature, it is to be expected that cooling

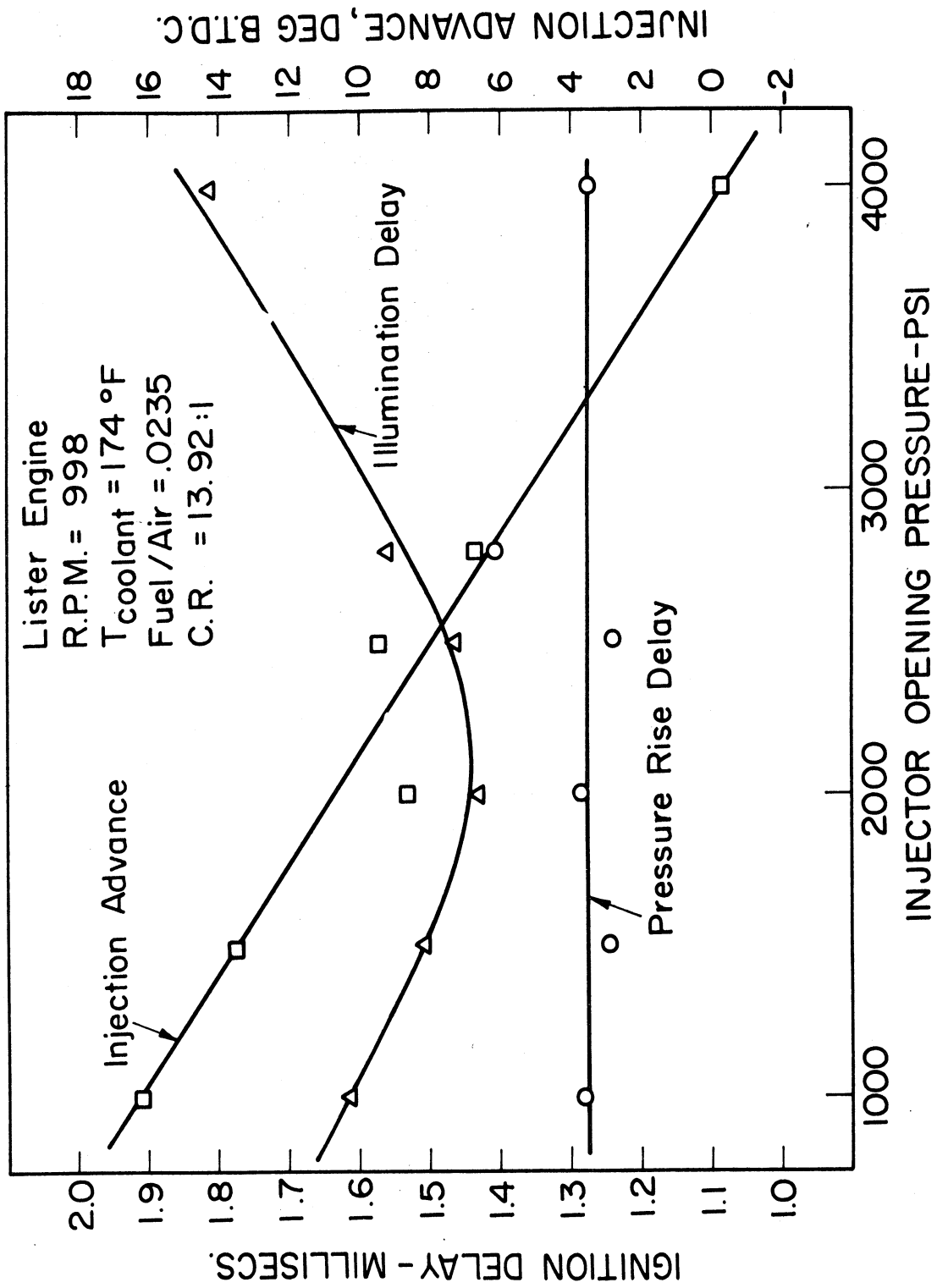


Figure 14. Effect of injector opening pressure on ignition delay.

water temperature would affect ignition delay. To investigate this point a series of tests were carried out on the engine at various cooling water temperatures ranging from 70°F up to 200°F. The results are plotted in Figure 15. This curve was drawn through every plot point rather than attempting to present a faired curve. It can be noted that the shape of the ignition delay curve follows the same pattern as that of the injection advance. However, the curve generally indicates that at higher temperatures, the ignition delay is reduced. The reduction in pressure rise delay amounted to 14.8% by increasing the cooling temperature from 70°F to 200°F.

EFFECT OF PRESSURE ON PRESSURE RISE DELAY

The influence of pressure on the pressure rise delay is shown for a speed of 1000 rpm in Figure 16, which reveals that the pressure rise delay decreases with increase in air pressure at the time of injection. This is believed to be mainly due to the following factors:

1. The drop in the self-ignition temperature of the fuel at higher air pressures, as indicated by Tausz and Schulte.⁹
2. The increase in the availability of oxygen at higher air pressures, which increases the rate of release by oxidation reactions in the early stages of combustion.³⁵
3. The increase in the heat transfer rate from the air to the fuel droplets caused by the increased density of air, resulting in a shorter physical delay period.

The increase of the air pressure also affects other important variables, including the spray pattern, local fuel concentrations, and the local cooling effect due to fuel evaporation.

After trying to correlate ignition delay with air pressure it was found that the best correlation is between $\log I.D._p$ and $\log P$.

Figure 17 is a plot of $\log_e I.D._p$ vs. $\log_e P$, and indicates that, at a constant temperature, the relation between the two variables has a linear relationship, or

$$I.D._p = \frac{C}{P^n} \quad (21)$$

under these conditions $C = 64740$ and $n = 1.774$.

This relationship has the same form as that of Schmidt at a constant tem-

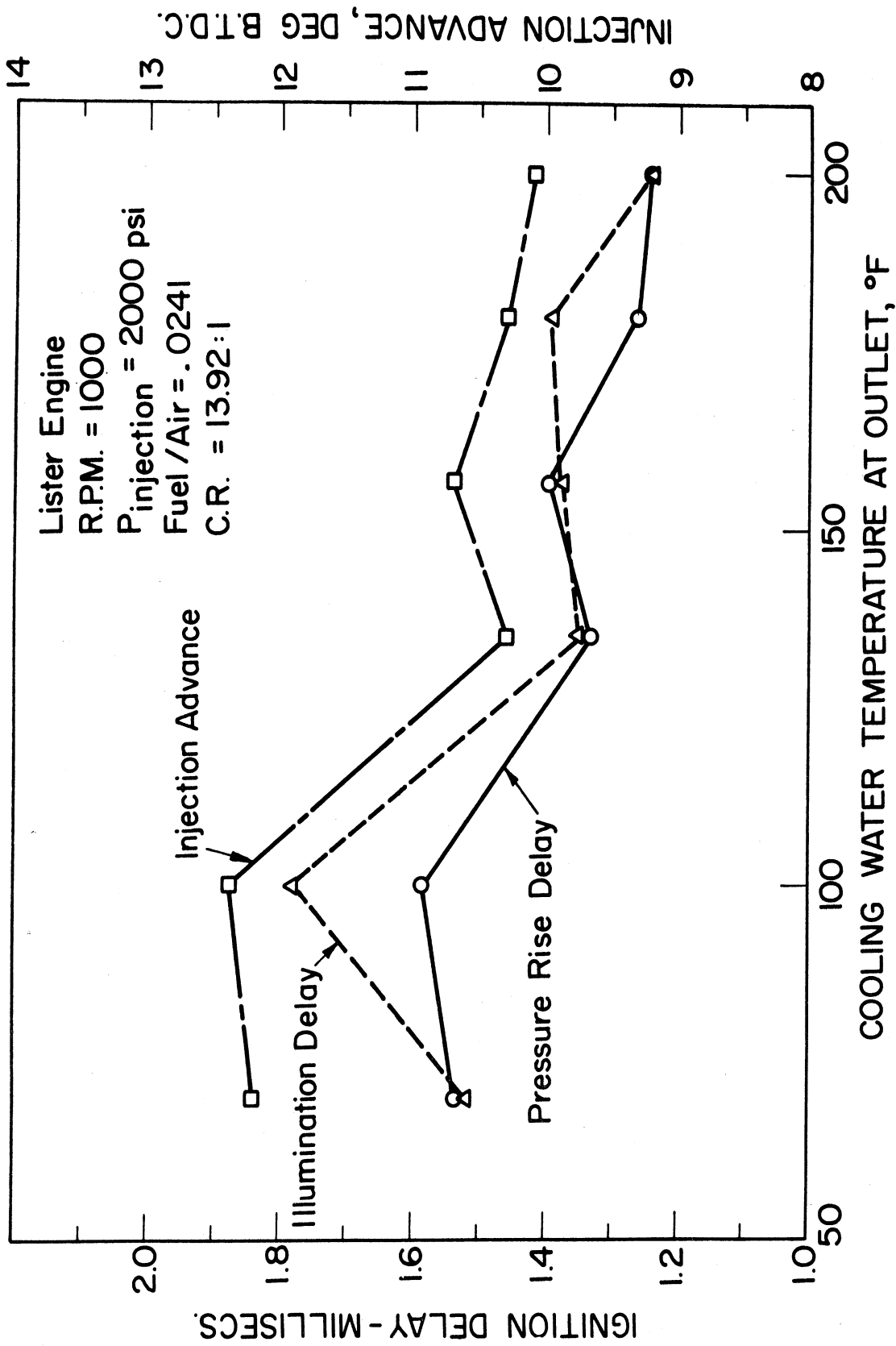


Figure 15. Effect of coolant temperature on ignition delay.

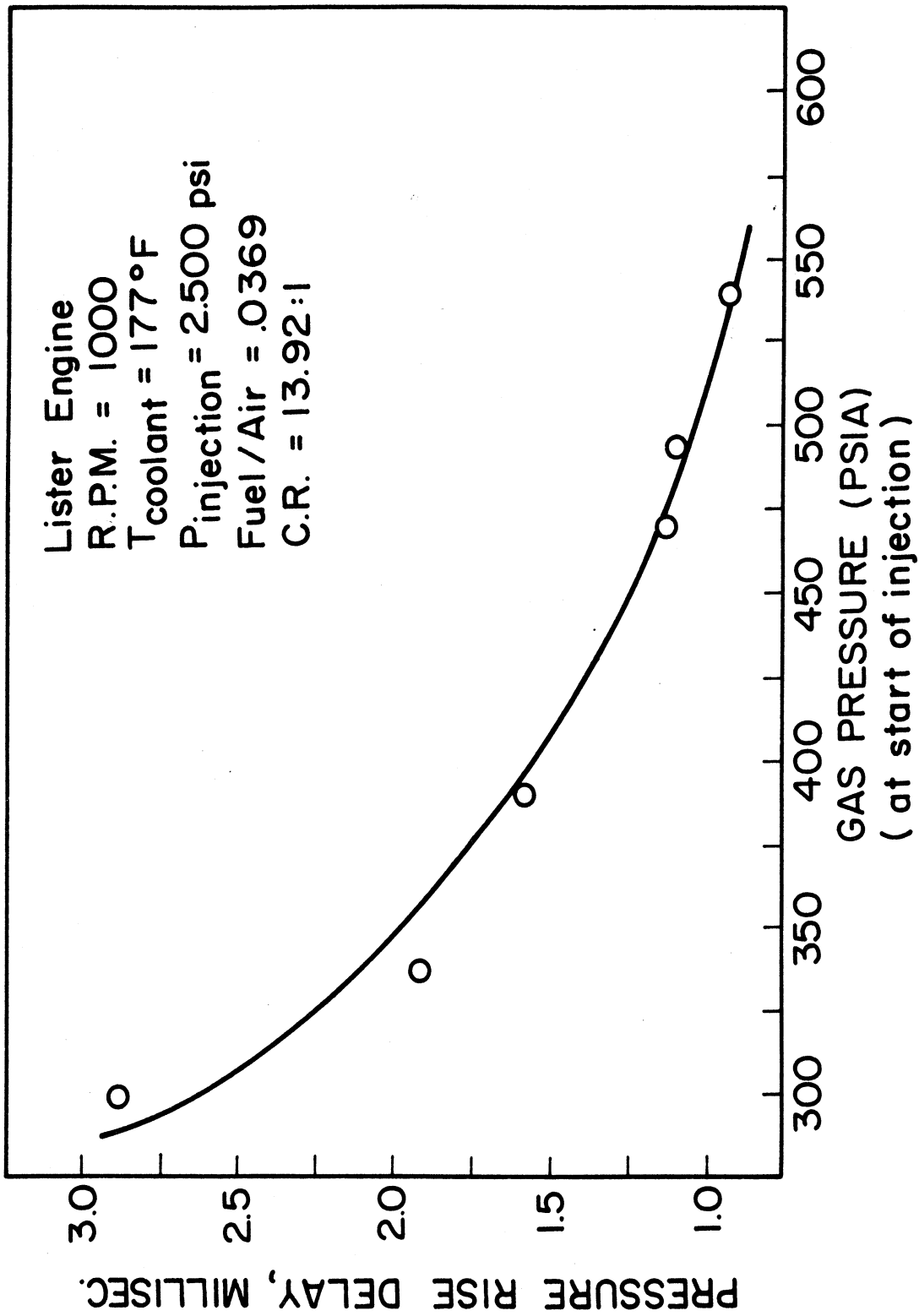


Figure 16. Effect of cylinder pressure on pressure rise delay at 1000 rpm.

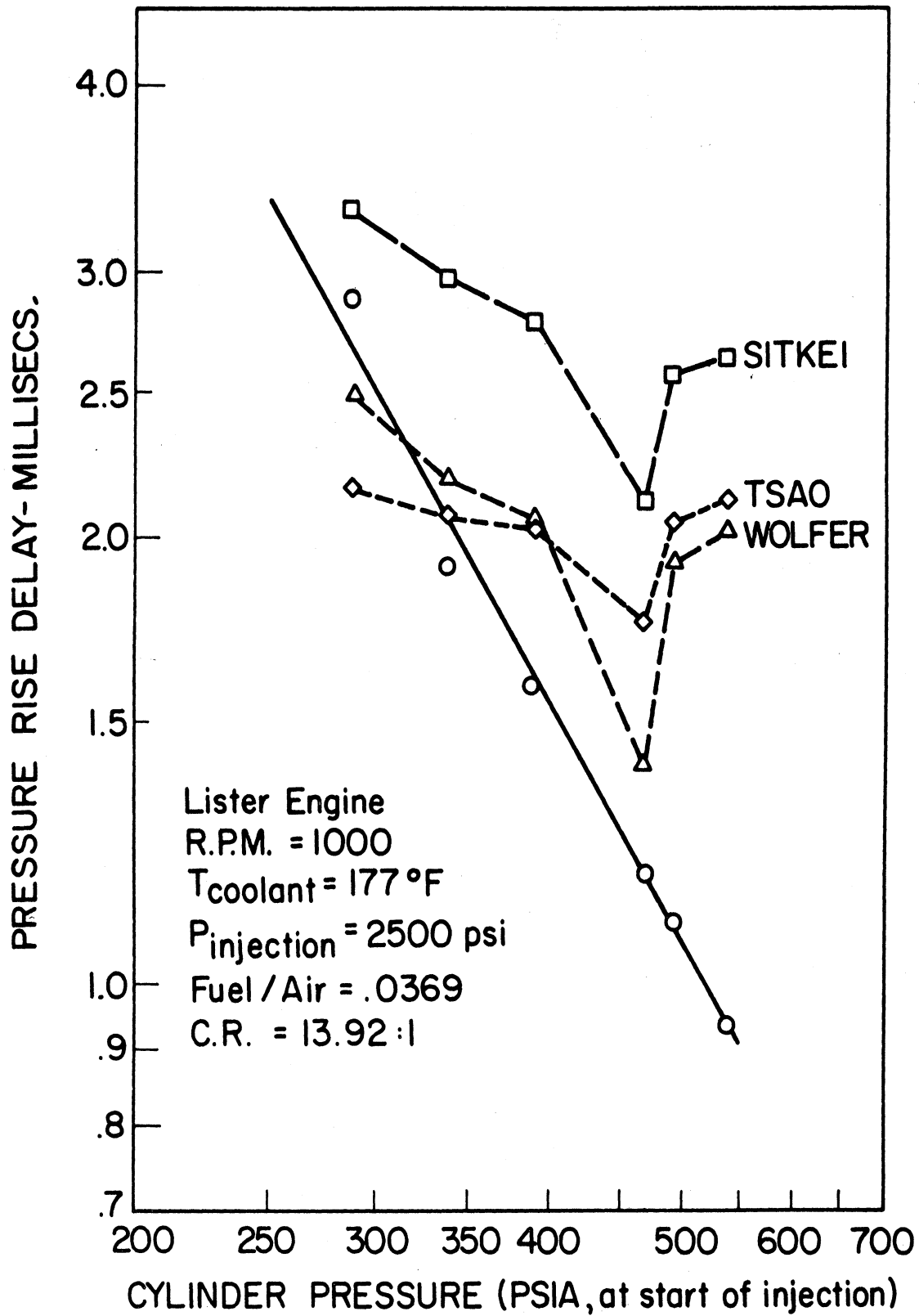


Figure 17. Effect of cylinder pressure on pressure rise delay at 1000 rpm.

perature, Eq. (5). The constant C, and exponent n differ from those reported by Wolfer.¹⁸ The difference between Wolfer's equation, determined from bomb experiments, and Eq. (21) is believed to be principally due to the turbulence, and other factors that will be discussed later.

A comparison is made between the measured ignition delays (solid line) and the values calculated from the available formulae of Wolfer, Tsao, et al., and Sitkei. The results are shown on Figure 17.

EFFECT OF TURBULENCE ON IGNITION DELAY

In the Lister engine the turbulence at the end of the compression stroke is caused by forcing the air through the tangential passage between the main chamber and the spherical prechamber, as shown in Figure 18. At the compression ratio of 13.92:1 used for the runs reported, the volume of the swirl chamber is equivalent to 6.55% of the total swept volume, and the area ratio of the connecting passage to the piston area is 3.22%. With this configuration, the air in the passage is estimated to obtain velocities as high as 164 ft/sec during the compression stroke, at an engine speed of 1000 rpm.⁴⁵ The swirl produced in the swirl chamber is directly proportional to the air velocity in the tangential passage.

In order to find the effect of turbulence on the ignition delay and the index n in Eq. (21), a series of runs was carried out at an engine speed of 600 rpm. This will be compared with the previous series at 1000 rpm. During these runs the air surge tank pressure was changed to allow the measurement of the pressure rise delay at different pressures ranging from 260 psia to 650 psia. The results of these runs are shown in Figure 19 together with the results computed from the equations of Wolfer, Tsao, and Sitkei.

By comparing the ignition delays in Figures 17 and 19 it can be noted that the increase in turbulence at the higher engine speed shortens the delay period. The increase in turbulence results in better mixing of fuel and air, and better chances for the production of optimum concentrations and higher rates of chemical reactions. Turbulence also increases the heat loss to the walls. However, the increase in the rate of chemical energy release is believed to exceed the effect of increased heat loss, resulting in shorter delays at higher speeds. The effect of turbulence on reducing the delay period has also been shown by Boerlage and Broeze,⁴⁶ Gerrish,¹³ Elliott,²⁷ in a discussion by Landen,²⁷ El Wakil,³³ Tsao,³⁶ and Bassi.⁴⁷

Figure 19 indicates also that the linear relationship can express the variation of I.D._p with change in pressure. It is noticed that the index n changes with increase in engine speed. It increases from 1.46 at 600 rpm to 1.775 at 1000 rpm.

One of the factors that contributes to the discrepancy between Wolfer's

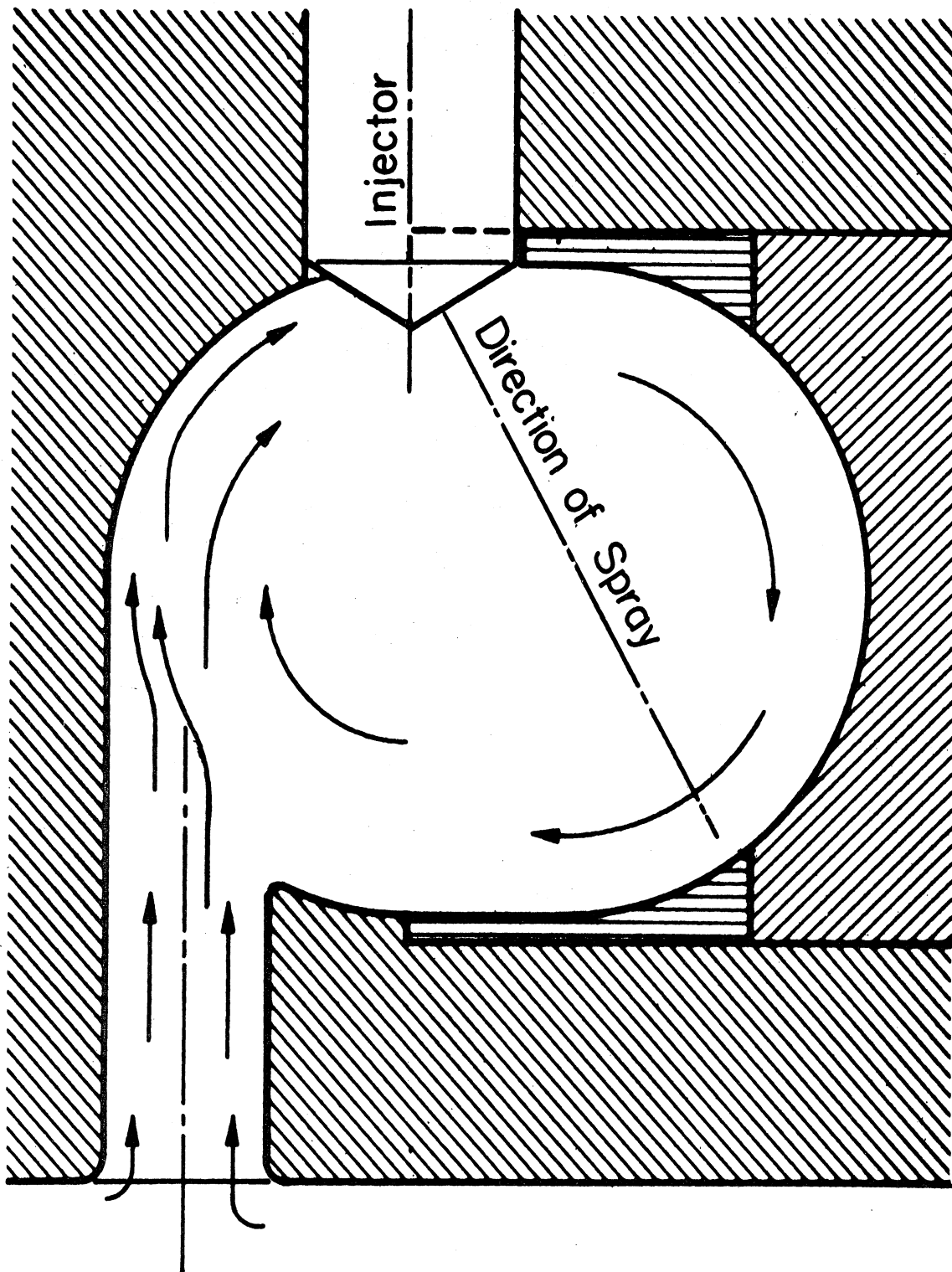


Figure 18. Turbulence in modified combustion chamber of Lister-Blackstone engine.

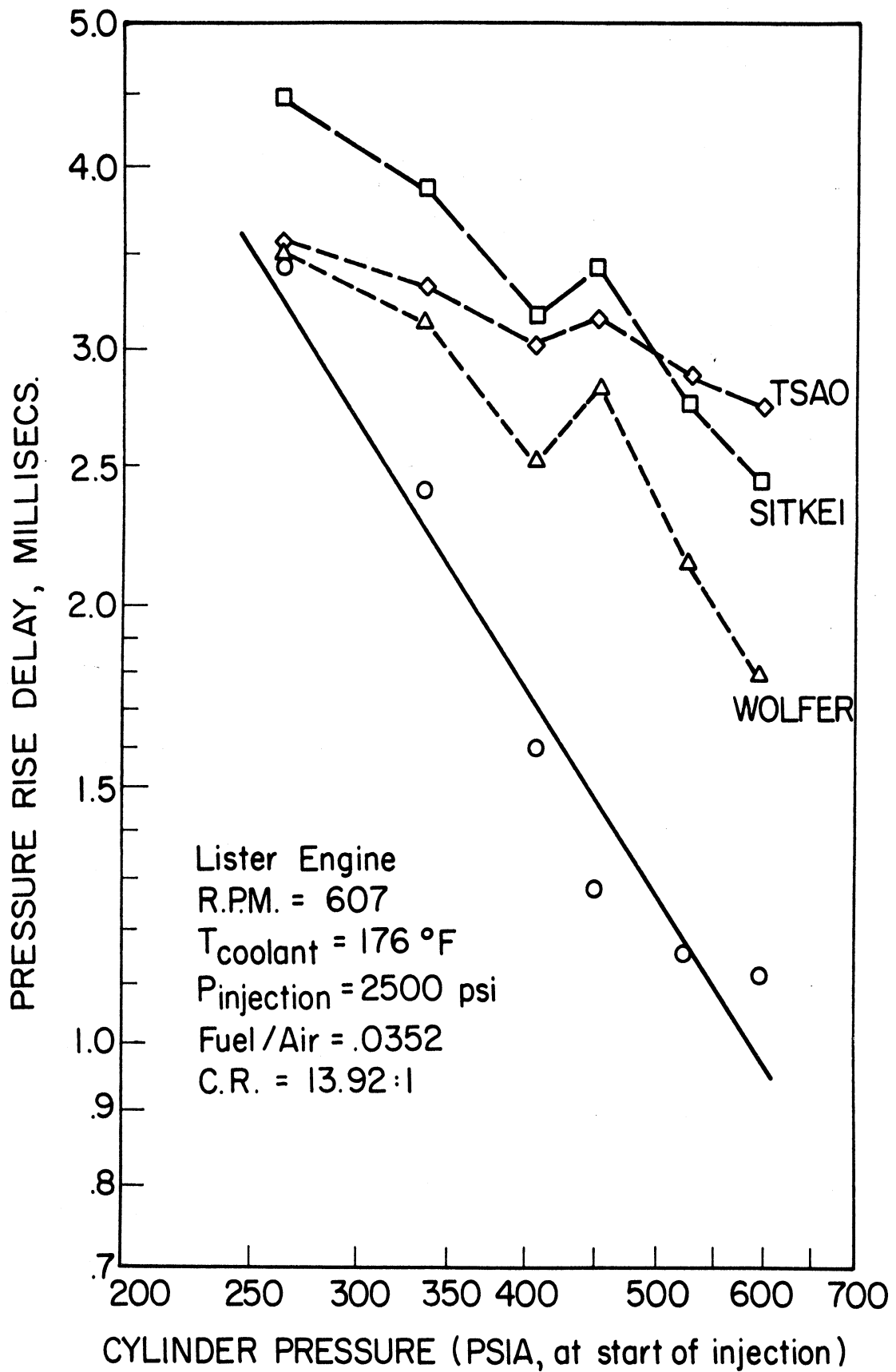


Figure 19. Effect of cylinder pressure on pressure rise delay at 600 rpm.

equation obtained from tests on bombs and the present experiments on an engine is the change of air pressure and temperature during the delay period. In the bomb the pressure is steady and the volume is constant, but in the engine, the volume changes and consequently the pressure changes. In order to account for this effect, the index n and constant C in Eq. (21) were calculated by using the mean pressure during the delay period as found from this relationship:

$$P_{\text{mean}} = \frac{\int_{\theta_1}^{\theta_2} P \, d\theta}{\theta_2 - \theta_1} \quad (22)$$

where θ_1 and θ_2 are the crank angle degrees at the beginning and the end of the pressure rise delay, respectively.

The value of n is found to be lower with the mean pressure than with the pressure at the start of injection. This applies for the two engine speeds. The values of n were also computed for all the runs at 600 rpm and 1000 rpm in terms of the pressure at the start of injection and the mean pressure, and were found to be 1.575 and 1.499, respectively.

Comparison of values of pressure rise delay obtained with the Lister engine with those calculated from the equations of Wolfer,¹⁸ Tsao, et al.,³⁶ and Sitkei,³⁷ reveal that the Lister engine values are in general shorter than the computed values. This is believed to be due to the following:

1. Except for Wolfer's formula, these formulae were obtained by observing different phenomena. Tsao, Myers, et al., used the temperature rise delay, while Sitkei used the illumination delay.
2. Different types of combustion chambers were used. Wolfer used a constant volume bomb; Tsao, et al., used an open combustion chamber, and Sitkei used a precombustion chamber. In the Lister engine, the turbulence is believed to be higher than for all these engines. This results in different rates of heat addition to, and rejection from the chamber.
3. The volume of the different combustion chambers is not the same. For Wolfer the volume is 146.1 cu in., for Hurn it equals 17.2 cu in., for Tsao it equals 2.52 cu in., for Sitkei it equals 4.63 or 6 cu in., and for our engine it equals 5.377 cu in. The effect of using different volumes on the pressure rise delay can be shown by using Eq. (20). In general larger volumes have longer delays, if all the other factors are kept constant.

4. The rates of injection during the delay period are expected to be different.
5. The fuels used in the different investigations are expected to have different combustion qualities.

To examine the validity of the form of Eq. (21) for ignition delay computations, the published experimental data of West,²⁵ Tsao, *et al.*,³⁶ and Hurn and Hughes³⁰ were put in a computer program and the values of n and C evaluated. The results are plotted in Figure 20 and given in Table 1. The standard deviation was found to be within 2.4% for all data except that of Hurn and Hughes at an oxygen concentration of 21% where the standard deviation reached 6.0%.

TABLE 1

	Combustion Chamber	No. of Points	C	n	Standard Deviation
West	Engine	6	8.85	0.271	1.8%
Tsao	Engine	5	32.4	0.411	0.9%
Hurn and Hughes at					
1510°R		6	15.9	0.286	0.4%
1460°R	Bomb	6	29.4	0.339	1.5%
1410°R		6	55.4	0.397	2.4%
21% O ₂		4	196.0	0.635	6.0%

From Table 1 it can be noted that Eq. (21) correlates very well the experimental data on ignition delay in bombs and engines, at a constant temperature. The exponent " n " is different for each set of data and is different from the exponent given by Wolfer. The turbulence seems to be a factor that influences the exponent " n ." The variation in the constant " C " is believed to be mainly due to differences in the gas temperature between the different sets of runs.

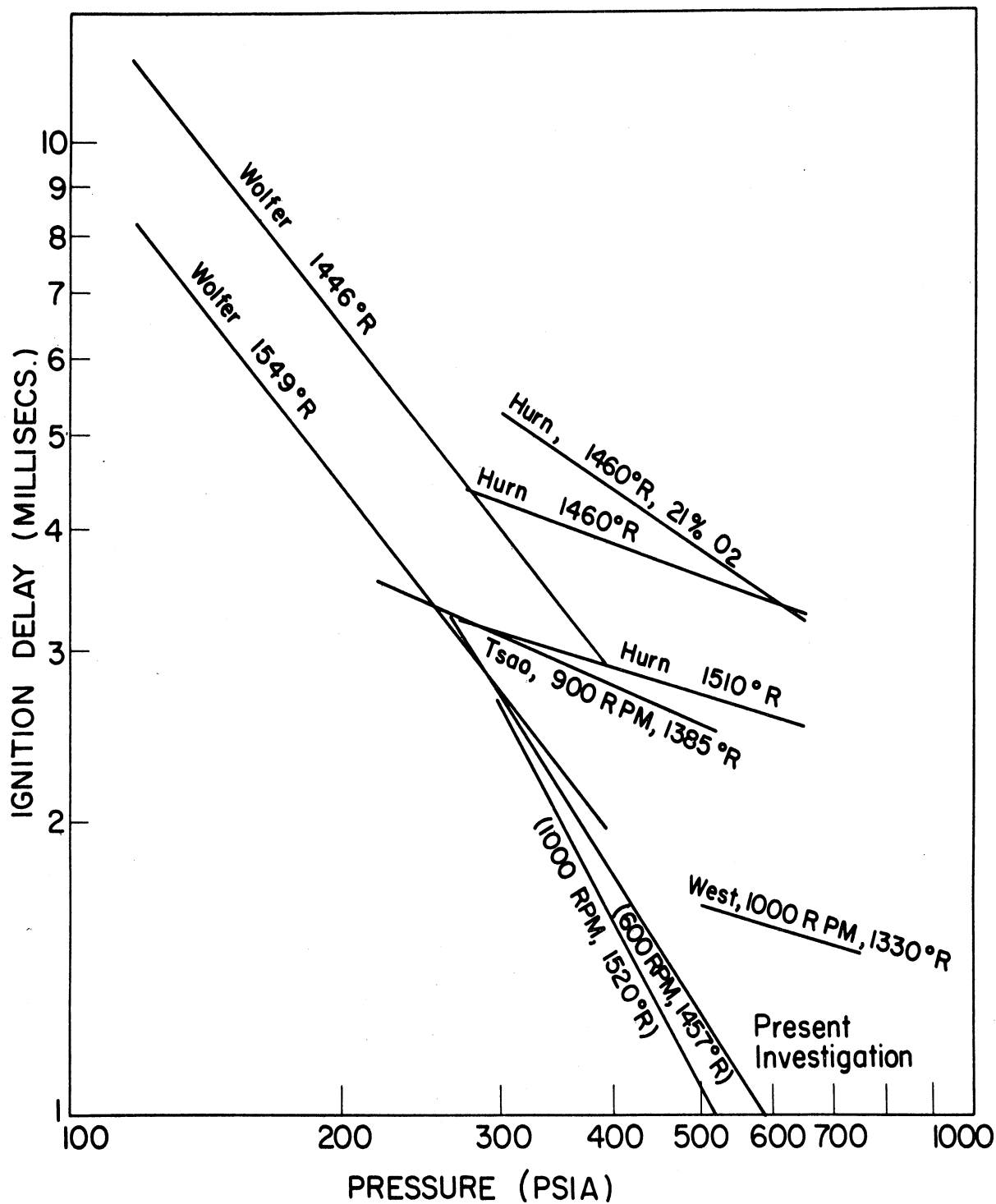


Figure 20. Effect of pressure on ignition delay for different bombs and engines.

CONCLUSIONS

1. The criteria which are most useful to indicate the start of diesel combustion are the pressure rise due to combustion, and the illumination resulting from combustion.

2. Our experimental work showed that in general illumination due to combustion does not occur simultaneously with the pressure rise. Illumination usually occurs after measurable pressure rise, or in other words, the illumination delay period is longer than the pressure rise delay.

3. Measurement of ignition delay in terms of the pressure rise is the most practical, and was found to be the more reproducible. It also has the greater engineering significance.

4. The engine tests demonstrate that increase in cylinder air pressure, fuel/air ratio, cooling water temperature, and engine speed shorten the delay period. Change in fuel injection pressure has a little effect on the pressure rise delay, but greatly affects the illumination delay.

5. The best equation for correlating the pressure rise delay and the cylinder air pressure at the start of injection with constant air temperature, is found to be similar to that of Wolfer,¹⁸ and is

$$\text{I.D.}_p = \frac{C}{p^n}$$

the value of n is found to be a function of speed. At 600 rpm it has a value of 1.46, and at 1000 rpm, $n = 1.77$. This is believed to be due to the increase in turbulence with increase in speed. These values of n are greater than those reported by Wolfer, taken in a bomb with some induced turbulence. It is probable, however, that this turbulence was much less than that of the swirl chamber of the Lister-Blackstone engine.

6. Analysis indicates that the measured pressure rise ignition delay is partially dependent on several thermodynamic characteristics of the chamber including its volume, rates of heat addition and loss, and any work done during the delay period. A portion of the differences in the ignition delays reported for bombs and engines are due to these factors.

APPENDIX I

LIST OF SYMBOLS

- a' = concentration
- A = area
- b, b' = constants
- c, C = constants
- C.A. = crank angle
- C.R. = compression ratio
- c_v = specific heat at constant volume
- d = diameter
- E = energy of activation
- F_n, F_n' = functions
- I.D. = ignition delay, milliseconds
- J = mechanical equivalent of heat
- K, K_1 = constants
- m = mass
- n, n' = exponents
- N = engine speed, rpm
- P = pressure
- Q = heat quantity
- R = gas constant
- T = temperature
- U = internal energy

U_r = energy of reaction

V, V' = volume

w = velocity of chemical reaction

W = work

x = exponent

θ = crank angle, degrees

α = overall coefficient of heat transfer

Subscripts

c = cooling

Ch = chemical

g = gas

Il = illumination

p = pressure

Ph = physical

T = temperature

W = wall

APPENDIX II

CALCULATION OF $dP/d\theta$

According to the first law of thermodynamics for a closed system

$$\frac{dQ}{d\theta} = \frac{dU}{d\theta} + \frac{dW}{d\theta}$$

The internal energy U of the system is equal to the sum of the internal energies of the air and the fuel. For this analysis the system is assumed to follow the ideal gas laws because the fuel is found to be evaporated immediately after injection,⁴⁶ and its amount during the delay period is very small compared to the mass of air. Therefore

$$\frac{dQ}{d\theta} = m c_v \frac{dT}{d\theta} + P \frac{dV}{d\theta} \quad (23)$$

From the equation of state $dT/d\theta$ is given by:

$$\frac{dT}{d\theta} = \frac{1}{mR} \left[P \frac{dV}{d\theta} + V \frac{dP}{d\theta} - TR \frac{dm}{d\theta} \right] \quad (24)$$

Substituting in Eq. (23)

$$\frac{dQ}{d\theta} = P \frac{dV}{d\theta} \left[\frac{c_v}{R} + 1 \right] + V \frac{dP}{d\theta} \cdot \frac{c_v}{R} - T c_v \frac{dm}{d\theta} \quad (25)$$

The slope $dP/d\theta$ is obtained from Eq. (25) as

$$\frac{dP}{d\theta} = \frac{R}{c_v} \cdot \frac{1}{V} \left[\frac{dQ}{d\theta} - P \frac{dV}{d\theta} \left(\frac{c_v}{R} + 1 \right) + T c_v \frac{dm}{d\theta} \right] \quad (26)$$

Equation (26) relates the slope of the pressure trace to the rate of heat addition to the system, pressure, volume, mass, specific heat, and the gas constant.

APPENDIX III

CRANK POSITIONS FOR MAXIMUM PRESSURE AND TEMPERATURE IN A MOTORED ENGINE

It has commonly been assumed that the maximum pressure occurs at T.D.C. in a motored engine and the pressure would rise during compression and fall again symmetrically during expansion. Often the maximum pressure points has been used to determine the phase relationship. In our experimental data on the Lister engine it was noticed that the point of maximum pressure occurs in advance of the T.D.C. as shown in Figure 21. In this report the difference between the crank angle at which maximum pressure occurs, and the T.D.C., will be called the maximum pressure advance in a motored engine. After re-examining the accuracy of the marking unit, which is set to determine the crank degrees on the scope screen, the engine was motored in the reverse direction. The pressure traces obtained indicated that maximum pressure also occurs, at almost the same point, before T.D.C. The difference between the maximum pressure advances in the two opposite directions is 0.2° of a crank angle. This is considered to be due to the change in heat losses caused by the change in valve timing when the engine was cranked in the opposite direction. This test indicated that the settings of the degree marking disc and pickup probe are correct.

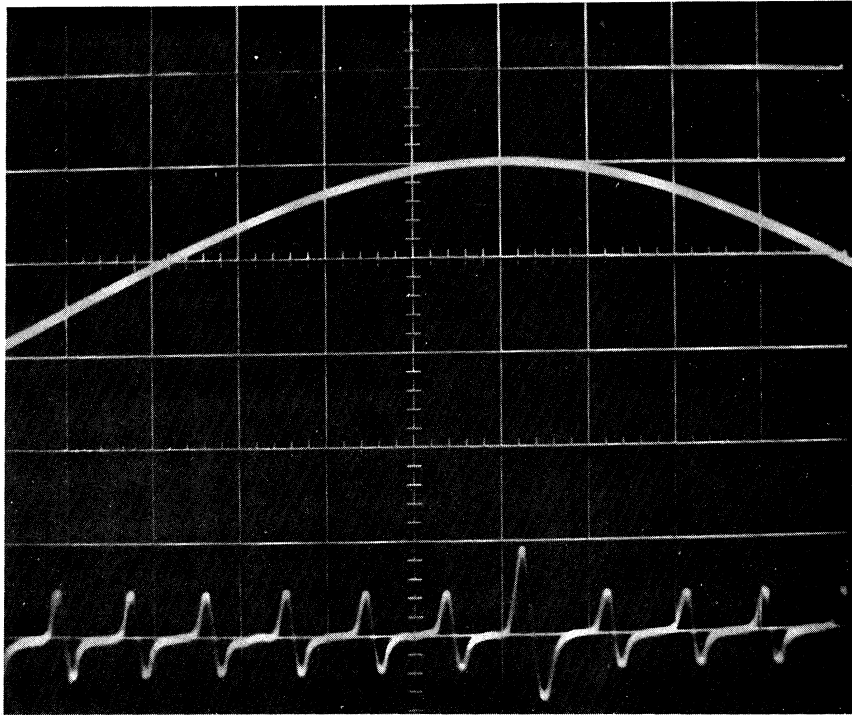
A thermodynamic analysis was then made on the air during the compression stroke and the following formula was obtained for the pressure gradient at T.D.C.

$$\frac{dP}{d\theta} = \frac{R}{c_v} \cdot \frac{1}{V} \cdot \frac{dQ}{d\theta}$$

where $dQ/d\theta$ = rate of heat transfer to the air with respect to crank angle.

At the end of the compression stroke the heat transfer $dQ/d\theta$ has a negative sign because heat is lost from the air to cylinder walls. Therefore $dP/d\theta$ should have a negative sign indicating that the maximum pressure for a motored engine should occur before T.D.C. In Figure 22 the pressure and temperature are plotted vs. crank angles for the motoring run shown in Figure 21. The maximum temperature advance amounts to 4.5 crank angle degrees. The drop in air temperature at T.D.C. is 11.7°F below the maximum temperature.

This conclusion is also supported by published data of Tsao, et al.,³⁶ for the compression temperature in a diesel engine. The compression temperature was measured by applying the infrared null method. Figures 3, 5, and 9, of this reference, indicate that the maximum temperature occurs before T.D.C.



Point of
↓ Max. Press.
|
T.D.C.
1.15° C.A.
↓ Advance

Figure 21. Maximum pressure advance in motored Lister-Blackstone engine.

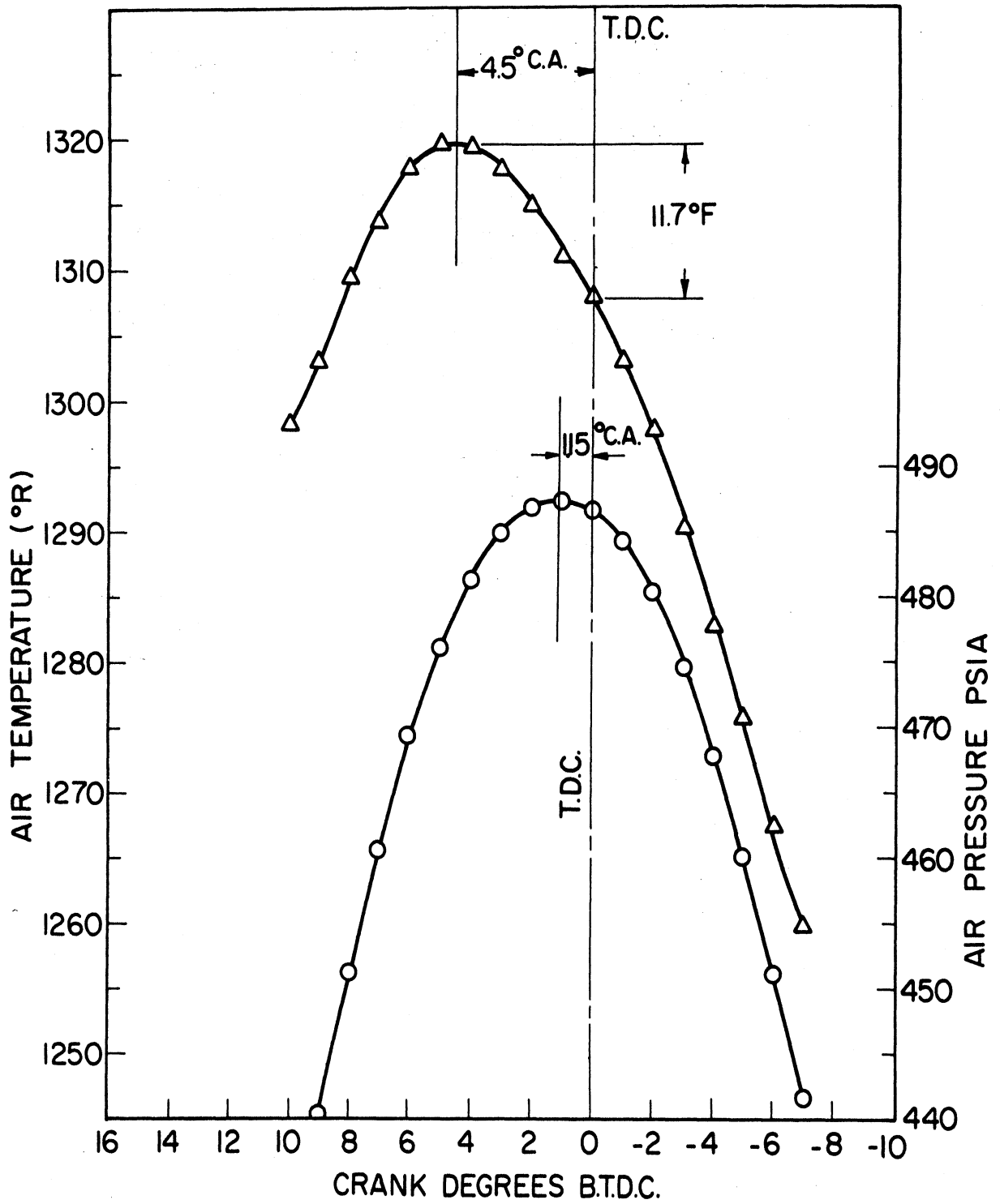


Figure 22. Maximum pressure and temperature advances in motored Lister-Blackstone engine.

during the compression stroke.

This analysis indicates that the maximum pressure and temperature advances at the end of the compression stroke of a motored engine are mainly caused by the cooling losses.

BIBLIOGRAPHY

1. Tizard, H. T., and D. R. Pye, "Experiments on the Ignition of Gases by Sudden Compression," Philosophical Magazine, 44, 79-121 (1922).
2. Tizard, H. T., and D. R. Pye, "Ignition of Gases by Sudden Compression," Philosophical Magazine, 1094-1105 (1926).
3. Alt, Otto, "Combustion of Liquid Fuels in Diesel Engine," NACA T. M. 281, 1924.
4. Neumann, K., "Experiments on Self Ignition of Liquid Fuels," NACA T. M. 391, 1926.
5. Sass, F., "Ignition and Combustion Phenomena in Diesel Engines," NACA T. M. 482, 1928.
6. Tausz, J., and F. Schulte, "Determination of Ignition Points of Liquid Fuels Under Pressure," NACA T. M. 299, 1925.
7. Tausz, J., and F. Schulte, "Ignition Points and Combustion Reactions in Diesel Engines—Part I," NACA T. M. 483, 1928.
8. Tausz, J., and F. Schulte, "Ignition Points and Combustion Reactions in Diesel Engines—Part II," NACA T. M. 484, 1928.
9. Rothrock, A. M., and C. D. Waldron, "Fuel Vaporization and Its Effect on Combustion in a High Speed C.I. Engine," NACA T. R. 435, 1932.
10. Rothrock, A. M., "The NACA Apparatus for Studying the Formation and Combustion of Fuel Sprays and the Results from Preliminary Tests," NACA T. R. 429, 1932.
11. Boerlage, G. D., and J. J. Broeze, "The Ignition Quality of Fuels in Compression Ignition Engines," Engineering, 603-606, 687-689, 755-757, November 13, 1931.
12. Boerlage, G. D., and Broeze, J. J., "Ignition Quality of Diesel Fuels as Expressed in Cetane Numbers," SAE Journal, 31, 283 (1932).
13. Gerrish, H. D., and Voss, F., "Influence of Several Factors on Ignition Lag in a Compression-Ignition Engine," NACA T. N. 434, 1932.
14. Ware, M., "Description of the NACA Universal Test Engine and Some Test Results," NACA T. R. 250, 1927.

15. Wentzel, W., "Ignition Process in Diesel Engines," NACA T. M. 797, 1936.
16. Wentzel, W., "Der Zund-und Verbrennungsvorgang in Kompressorlosen Dieselmotor," VDI - Forschungsheft 366, Berlin, 1934.
17. Holfelder, O., "Ignition and Flame Development in the Case of Diesel Fuel Injection," NACA T. M. 790, 1936.
18. Wolfer, H. H., "Ignition Lag in the Diesel Engine," VDI - Forschungsheft No. 392, 1938, Trans. by Royal Aircraft Establishment, Farnborough Library No. 358, August, 1959, U.D.C. No. 621-436.047.
19. Small, J., "Vagaries of Internal Combustion," Engineer (London), 164, 642, 668 (1937).
20. Selden, R. F., "Auto-Ignition and Combustion of Diesel Fuel in a Constant Volume Bomb," NACA R. 617, 1938.
21. Selden, R. F., "A Comparison of Ignition Characteristics of Diesel Fuels as Determined in Engines and in a Constant-Volume Bomb," NACA T. N. 710, 1939.
22. Schmidt, F.A.F., "Theoretical and Experimental Study of Ignition Lag and Engine Knock," NACA T. M. 891, 1939.
23. Bauer, S. G., "Ignition Lag in Compression Ignition Engines," Engineering, 148, No. 9, 368 (1939).
24. Semenov, N. N., "Thermal Theory of Combustion and Explosion," NACA T. M. 1024.
25. West, A. C., and Denis Taylor, "Ignition Lag in a Supercharged C. I. Engine," Engineering, 281-282 (1941).
26. Starkman, E., "Ignition Delay in Diesel Engines," Trans. AIChE, 42, 107-120 (1946).
27. Elliott, M. A., "Combustion of Diesel Fuel," SAE Quart. Trans., 3, 490-515 (1949).
28. Mueller, R., "Untersuchung des Verbrennungsvorgangs deutscher Schweröle in einer Versuchsbombe," Kraftfahretech, Forschungsarb. No. 3, 1, 1-10 (1936).
29. Jost, W., "Explosion and Combustion Processes in Gases," McGraw-Hill Book Company, New York, 1946.
30. Hurn, R. W., and K. J. Hughes, "Combustion Characteristics of Diesel Fuels as Measured in a Constant-Volume Bomb," SAE Quart. Trans., 6, 24-35 (1952).

31. Hurn, R. W., J. O. Chase, C. F. Ellis, and K. J. Hughes., "Fuel Heat Gain and Release in Bomb Ignition," SAE Trans., 64, 703-711 (1956).
32. Yu, T. C., R. N. Collins, K. Mahadevan, O. A. Uyehara, and P. S. Myers, "Physical and Chemical Ignition Delay in an Operating Diesel Engine Using the Hot-Motored Technique," SAE Trans., 64, 690-702 (1956).
33. El Wakil, M. M., P. S. Myers, and O. A. Uyehara, "Fuel Vaporization and Ignition Lag in Diesel Combustion," SAE Trans., 64, 712-726 (1956).
34. Garner, F. H., F. Morton, J. B. Saunby, and G. H. Grigg, "Preflame Reactions in Diesel Engines," J. Inst. Petrol., 43, 124-130 (1957).
35. Garner, F. H., F. Morton, and J. B. Saunby, "Preflame Reactions in Diesel Engines, Part V," J. Inst. Petrol., 47, 175-193 (1961).
36. Tsao, K. C., P. S. Myers, and O. A. Uyehara, "Gas Temperatures During Compression in Motored and Fired Diesel Engines," Trans. SAE, 70, 136-145 (1962).
37. Sitkei, G., "Uber den dieselmotorischen Zundverzug," M.T.Z., Jahrg 24, Heft 6, Juni 63.
38. Lyn, W. T., and Valdmanis, E., "The effects of Physical Factors on Ignition Delay," paper IME (London), Automobile Division, November, 1966.
39. Lyn, W. T., and E. Valdmanis, "The Application of High Speed Schlieren Photography to Diesel Combustion Research," J. of Photographic Science, 10, 74-82 (1962).
40. Henein, N. A., "Instantaneous Heat Transfer Rates and Coefficients Between the Gas and Combustion Chamber in a Diesel Engine," SAE Int'l. Automotive Engr. Congress, January 11-15, 1965.
41. Miller, C. D., "Slow-Motion Study of Injection and Combustion of Fuel in a Diesel Engine," SAE Trans., 53, 719-735 (1945).
42. Schweitzer, P. H., "Penetration of Oil Sprays," Penn. State College Engr. Exp. Station Bulletin 46, 1937.
43. Sass, F., "Compressorless Diesel Engines," Berlin, Julius Springer, 1929.
44. Parks, M. V., C. Pobnski, and R. Toye, "Penetration of Diesel Fuel Sprays in Gases," SAE Paper No. 660747, October, 1966.
45. Alcock, J. P., "Air Swirl in Oil Engines," Proc. IME (London), 128, 123-193 (1934).
46. Boerlage, G. D., and J. J. Broeze, "Combustion Process in the Diesel Engine," 1st and 2nd Symposium on Combustion, 1928, 1937, pp. 285-300.
47. Bassi, A., "Experimental Investigation into Diesel Engine Injection Systems," Sulzer Research No. 1963.

ACKNOWLEDGMENT

The authors wish to acknowledge the advice and help of Professor E. T. Vincent during the course of this work. The sponsorship and financial support of this work by the U. S. Army Tank-Automotive Command (ATAC) is also greatly appreciated. The help of graduate students and laboratory personnel at the Automotive Laboratory of The University of Michigan is also gratefully acknowledged.

SECTION 7

PROGRESS REPORT NO. 7

- a. Development of Instrumentation to Measure Smoke Intensity
- b. Author's Reply to the Discussions on the SAE paper,
"Ignition Delay in Diesel Engines"

PROGRESS REPORT NO. 7

DIESEL ENGINE IGNITION AND COMBUSTION

JAY A. BOLT
N. A. HENEIN

PERIOD DECEMBER 1, 1966 TO MARCH 31, 1967

APRIL, 1967

This project is under the technical supervision of the:

Propulsion Systems Laboratory
U.S. Army Tank-Automotive Center
Warren, Michigan

and is work performed by the:

Department of Mechanical Engineering
The University of Michigan
Ann Arbor, Michigan

under Contract No. DA-20-018-AMC-1669(T)

TABLE OF CONTENTS

	Page
LIST OF FIGURES	272
I. BACKGROUND	273
II. OBJECTIVES	273
III. CUMULATIVE PROGRESS	273
A. Review and Analysis of Previous Work	274
B. Theoretical Analysis	276
C. Experimental Work on Lister-Blackstone Engine	278
D. Comparison Between the Present and Previous Results	278
E. Progress Work on ATAC Open Combustion Chamber Engine	279
IV. PROGRESS DURING THIS PERIOD ON ATAC ENGINE	280
A. Engine Equipment and Instrumentation	280
B. Calibration of Instruments	284
C. Experimental Work on the Open Combustion Chamber ATAC Engine	284
D. Computer Programs	287
E. Authors' Reply to Discussions on SAE Paper "Ignition Delay in Diesel Engines"	287
V. PROBLEM AREAS AND CORRECTIVE ACTIONS	287
VI. FUTURE PLANS	289
A. Next Period	289
B. Overall	289
C. Change From Original	289
VII. SIGNIFICANT ACCOMPLISHMENTS	289
VIII. PROJECT STATUS	290
IX. BIBLIOGRAPHY	291
ADDENDUM	
A. DISCUSSIONS ON SAE PAPER "IGNITION DELAY IN DIESEL ENGINES," BY N. A. HENEIN AND JAY A. BOLT, SAE ANNUAL MEETING, JANUARY 9-13, 1967	292
B. AUTHORS' REPLY ON DISCUSSIONS	305

LIST OF FIGURES

Figure	Page
1. Different types of delay period in diesel combustion.	275
2. Relation between the energy terms and the different delay periods.	277
3. Fuel injection pump fitted with micrometers to control the rack position and injection timing.	281
4. View of installation of ATAC engine.	282
5. View of installation of ATAC engine.	283
6. Smokemeter connected to the ATAC engine.	285
7. Hartridge Smokemeter connected to the ATAC exhaust pipe.	286
8. Blowby flowmeter mounted on newly installed dip stick type oil level indicator.	288

I. BACKGROUND

A program to study the combustion process in supercharged diesel engines has been developed at The University of Michigan. This program is primarily concerned with the ignition delay and the effect of the different parameters on it. A special concern is given to the effect of pressure, temperature, and density on the ignition delay.

The different types of delay have been studied and an emphasis is made on the pressure rise delay and illumination delay. The instruments needed for the measurement of these two delay periods have been developed and a continuous effort is being made to improve their accuracy.

This research is being made on two experimental engines. One is the ATAC high output open combustion chamber engine, and the other is a Lister-Blackstone swirl combustion chamber engine.

II. OBJECTIVES

A. To study how gas pressure at the time of injection affects ignition delay and combustion. The effects will be studied at pressures ranging from approximately 300 to 1000 psia.

B. To study how gas temperature at the time of injection affects ignition delay. The temperatures will range from approximately 900°F to 1500°F.

C. To study various combinations of pressures and temperatures to determine whether density is an independent variable affecting ignition delay.

D. To conduct all these studies with three fuels: CITE refree grade (Mil-F-45121) fuel, diesel no. 2 fuel, and Mil-G-3056 refree grade gasoline.

III. CUMULATIVE PROGRESS

Cumulative progress has been made in the following areas:

- A. Review and analysis of previous work
- B. Theoretical analysis
- C. Experimental work on Lister-Blackstone engine

- D. Comparison between the present and previous work
- E. Progress work on the ATAC open chamber engine

The above items have been discussed in detail in the previous progress reports. The following is a comprehensive summary of the cumulative progress made, and the results reached.

A. Review and Analysis of Previous Work

The following is the result of the study made to analyze the previous work done on ignition delay in diesel engines:

1. Different types of ignition delay have been measured and referred to as the ignition delay period. Since these periods are unequal we found it necessary to identify each of them according to the criteria used to define its end. Thus we have the following four types of delay periods:

- a. Pressure rise delay; I.D._p
- b. Temperature rise delay; I.D._T
- c. Illumination delay, I.D._{Il}
- d. Hot motored technique delay; ¹I.D._{H.M.T}

These delay periods are represented graphically in Fig. 1, as they can be detected in an actual engine. Note that in this case the pressure rise delay is longer than the temperature rise delay. These two delay periods would be of equal value if both end during the compression stroke.

2. The previous experimental work has been made in bombs and in engines. It is noticed that delays measured in bombs are in general longer than those measured in engines. A comparison between the conditions in bombs and engines is given under the "theoretical analysis"; item B of this part of the report.

3. Different formulae have been given for the ignition delay. These formulae are given by: Wolfer; Bauer and West; Tsoa, Myers and Uyehara; and Sitkei.

All of these formulae are for the ignition delay as a function of the gas pressure and temperature. However, these formulae express different functions. In the present study an attempt has been made to compare between these different functions by taking into consideration both the theoretical and experimental results.

The results of this study is given under item D of this part of the report.

*Numbers refer to bibliography.

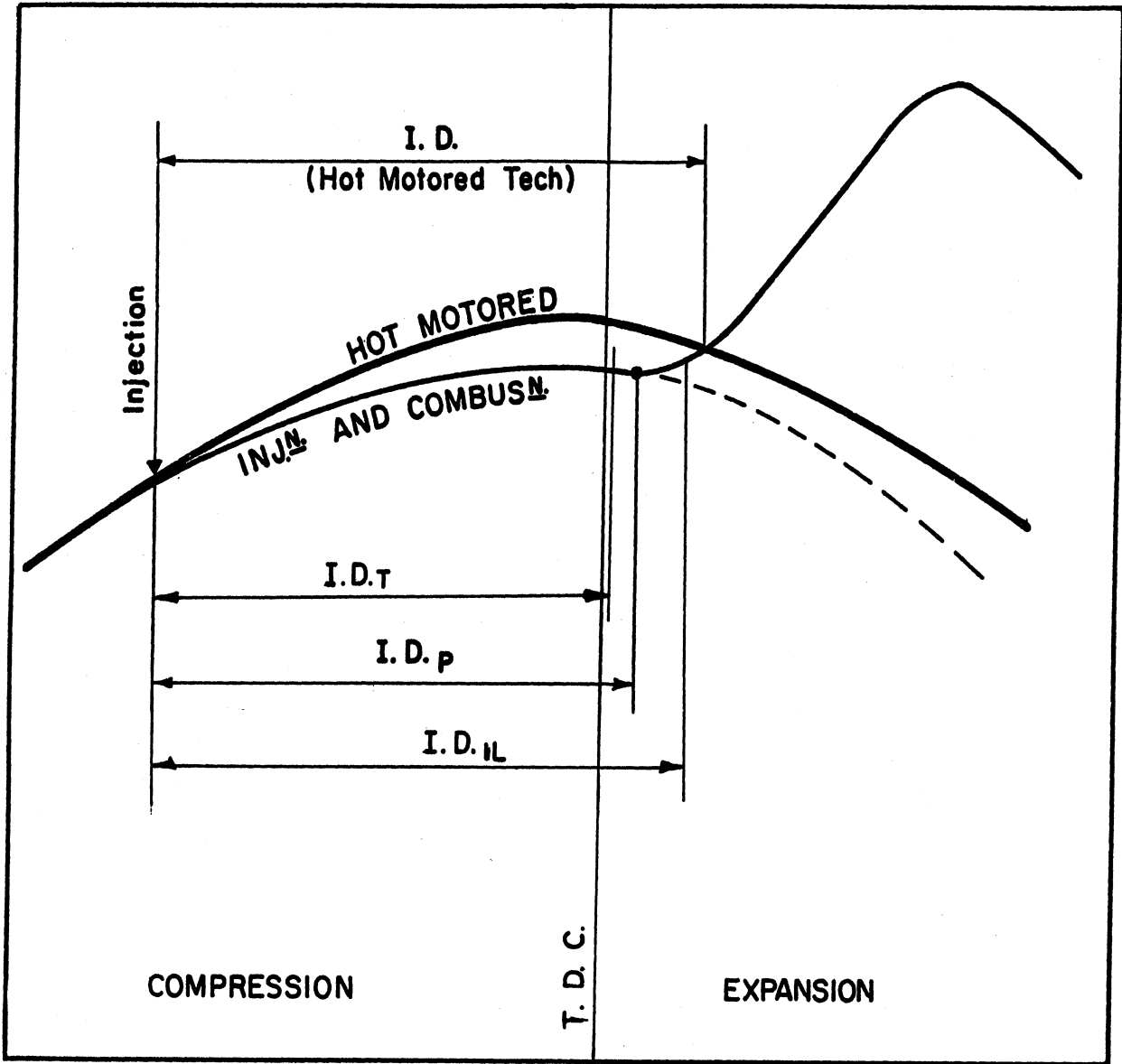


Fig. 1. Different types of delay period in diesel combustion.

4. It has been previously agreed on dividing the delay period into two parts²⁻⁸: the physical delay, I.D._{Ph} and the chemical delay, I.D._{Ch}. This concept has been examined, and we found that, under some conditions in engines, another division of the delay takes place, which is called the "energy delay," I.D._E. This is discussed under the "Theoretical Analysis," item B of this part of the report.

B. Theoretical Analysis

In this part a study is made of the different types of energy that are involved in engines during the delay period. These types of energy are:

1. Compression work, dW .
2. Heat exchange between the gas and the combustion chamber walls, dQ_C .
3. Heat released from the fuel, dQ_{Ch} .

A graphical presentation of these types of energy for the different delay periods in engines is shown in Fig. 2. From this figure, the physical and chemical delays can be considered to have ended at point "e," after which the heat produced from the chemical reaction exceeds that absorbed in the physical changes which take place in the fuel. It is noticed that in this case the pressure rise and temperature rise delays end later. The difference between the total delay period and the sum of the physical and chemical delays is called the "energy delay." Therefore:

$$I.D._p = I.D._{(Ph+Ch)} + I.D._E \quad (1)$$

The value of the energy delay period depends upon the rate of heat release from the chemical reaction, the heat loss to the cooling medium, and the work done by the gas.

The conditions in bombs are different from those in engines from the following points:

1. In engines the turbulence is generally much higher resulting in better mixing and higher rates of energy release by the chemical reaction. This is the main factor that causes the delay period in engines to be shorter than in bombs.

2. In engines the cylinder volume is continuously changing with time while in bombs it remains constant. The corresponding work done in engines causes an increase or a decrease in the internal energy of the gases depending on whether the work is compression or expansion, respectively. In engines most of the delay period occurs during the compression stroke, and energy is added to the gas resulting in delay periods shorter than in bombs.

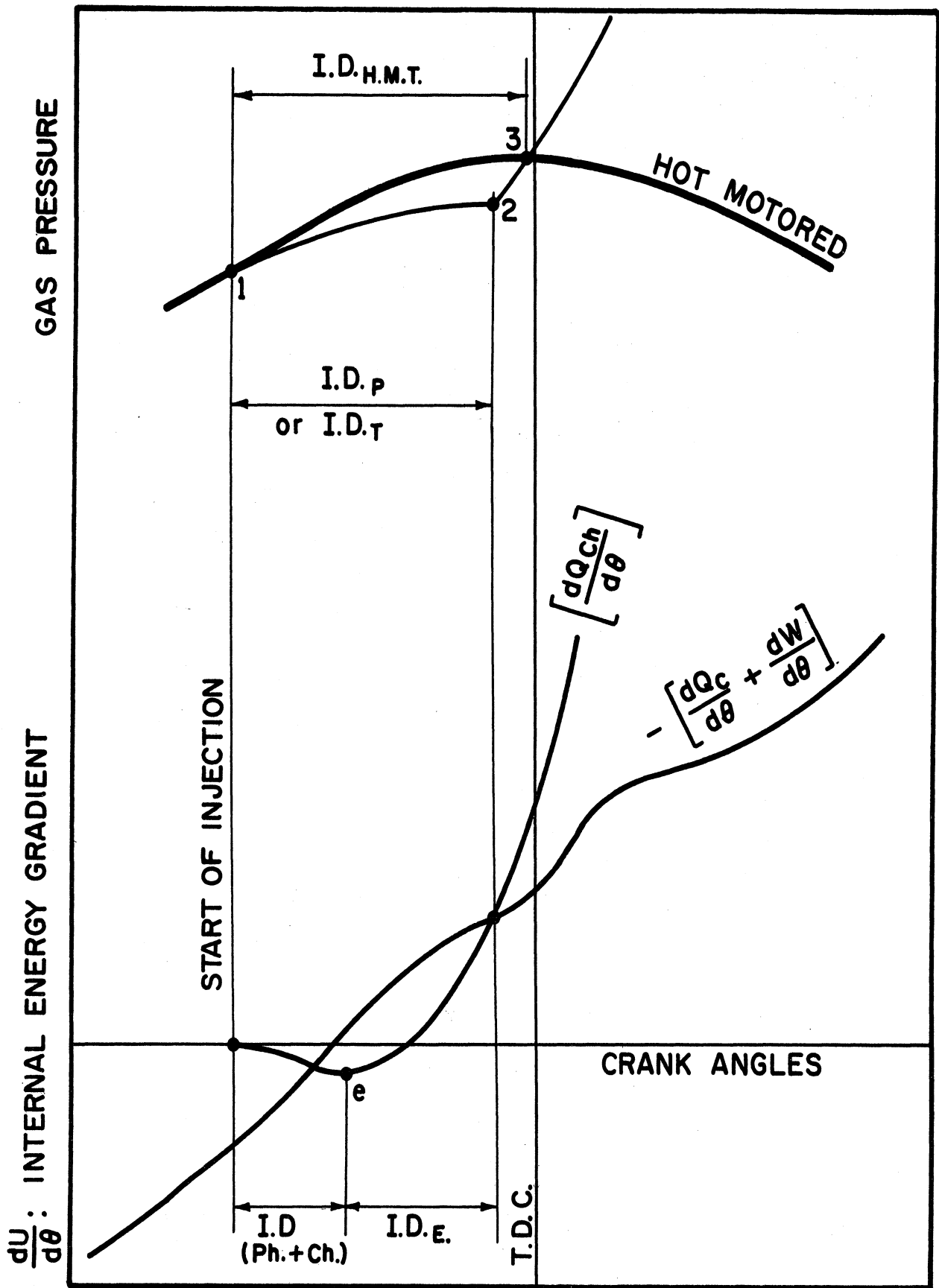


Fig. 2. Relation between the energy terms and the different delay periods.

3. In engines heat is lost from the gases to the walls, while in bombs, where the walls are used for heating, heat is generally added to the gases. The heat loss in engines does not balance the above two factors, and the final result is a shorter delay period in engines.

C. Experimental Work on Lister-Blackstone Engine

Four series of tests were carried out on the Lister engine to find the effect of the following factors on the pressure rise and illumination delay periods: the fuel-air ratio, the injector opening pressure, the cooling water temperature, the cylinder pressure, and engine speed. The results of these runs can be summarized as follows:

1. The pressure rise delay is in general longer than the illumination delay. The difference between these two types of delay periods, as well as their values, depend upon the fuel-air ratio, the injector opening pressure, and the cooling water temperature.

2. The increase in the cylinder pressure at the point of injection reduces the pressure rise delay.

3. The best correlation between the pressure rise delay and the cylinder pressure at the point of injection (at constant temperature) has been found to be:

$$I.D._p = \frac{C}{P^n} \quad (2)$$

where:

C = a constant at a constant temperature
n = the exponent of the pressure

4. The effect of the speed on the pressure rise delay is obtained by comparing the results of two series of tests carried out at two different speeds. It has been found that an increase in speed from (600 rpm to 1000 rpm) shortens the pressure rise delay and increased the exponent "n," in Eq. (2).

D. Comparison Between the Present and Previous Results

By comparing the present results with the previous results published by West,* Tsao,* and Hurn* the following conclusions are reached.

*References are included in Progress Report No. 6.

1. The values of the pressure rise delays measured on the Lister engine are shorter than the previously published data. This is believed to be due to the turbulence in the Lister engine which is much higher than that in previous investigations.

2. The form of Eq. (2) which has been obtained from Lister engine agrees with the theoretical formulae given by Wolfer,* Schmidt,* and Semenov.*

3. The value of the index n is higher than the value given by Wolfer for ignition delay in bombs. This is believed to be due to the higher turbulence in the Lister engine.

4. It is interesting to note that the previously published results on ignition delay in bombs and engines can be very well correlated to the corresponding gas pressures by an equation similar to Eq. (2). Thus the function expressed by Eq. (1) seems to be the most suitable for ignition delay correlations w.r.t. pressure (at a constant temperature). It is to be noted here that the value of the exponent " n " is different for each apparatus. It is greater for the runs made at higher turbulence.

The effect of temperature will be studied on the ATAC engine, in order to find a correlation between the ignition delay, and both pressure and temperature.

E. Progress Work on ATAC Open Combustion Chamber Engine

The engine has been connected to an electric dynamometer. It is supercharged with shop air that has been passed through a surge tank fitted just before the engine. Another surge tank is fitted on the exhaust side. The pressures in the two tanks can be regulated to the required values.

A Kistler pressure transducer is fitted in the hole furnished by the International Harvester Company. Two more holes were drilled in the cylinder head above the piston cavity. One hole is fitted with a quartz window, and the other is to be fitted with a surface thermocouple.

The top dead center of the engine determined by the dial gage method, was found to be $1/2$ crank degree past the top dead center mark engraved on the flywheel.

The degree marks are produced by a steel disk 18 inches in diameter and $1/8$ inch thick, mounted on the coupling between the crankshaft and the dynamometer. Holes $1/16$ inch in diameter are drilled around the periphery at 3° intervals, and larger holes, $1/8$ inch in diameter, at 45° intervals. A magnetic pickup has been used to produce corresponding pips on the oscilloscope screen every 3° , with bigger pips every 45° . One of the bigger holes is aligned at top dead center.

*Reference are included in Progress Report No. 6.

The temperature of the inside surface of the combustion chamber is measured by a surface thermocouple placed between the inlet and exhaust valves.

The fuel-injection system is instrumented so that the start and rate of injection can be calculated from measurements of the needle lift and fuel pressure before the nozzle. The position of the plunger w.r.t. the barrel, and the injection timing are both controlled by micrometers, as shown in Fig. 3.

IV. PROGRESS DURING THIS PERIOD ON ATAC ENGINE

The progress during this period has been mainly done on the ATAC engine, with the open combustion chamber head. The progress covers the following areas:

- A. Engine equipment and instrumentation
- B. Calibration of instruments
- C. Experimental work on the open combustion chamber ATAC engine
- D. Computer programs
- E. Authors' reply to discussions on SAE paper, "Ignition Delay in Diesel Engines."

A. Engine Equipment and Instrumentation

A general view of the ATAC engine equipment is shown in Figs. 4 and 5. The following equipment and instruments have been fitted to the engine.

1. Electric Heater.—An electric heater has been fitted between the critical flow meter and the inlet surge tank. All the piping between the heater, engine, and exhaust tank are insulated by 1.5-inch thick calcium silicate pipe insulation.

2. Water Spray for Exhaust Tank Cooling.—The cooling of the exhaust surge tank has been accomplished by spraying tap water into the tank. The direction of the spray is such as not to interfere with the flow of gases from the engine to the tank or with the exhaust thermocouple or smokemeter probe.

3. Electronic Instruments.—A new oscilloscope (Tektronix type 502A) and a new polaroid camera are now in use to obtain and record the different traces for the combustion process in the engine. A special projected graticule is now in use with the camera, in order to eliminate the parallex which had been noticed before using this attachment.

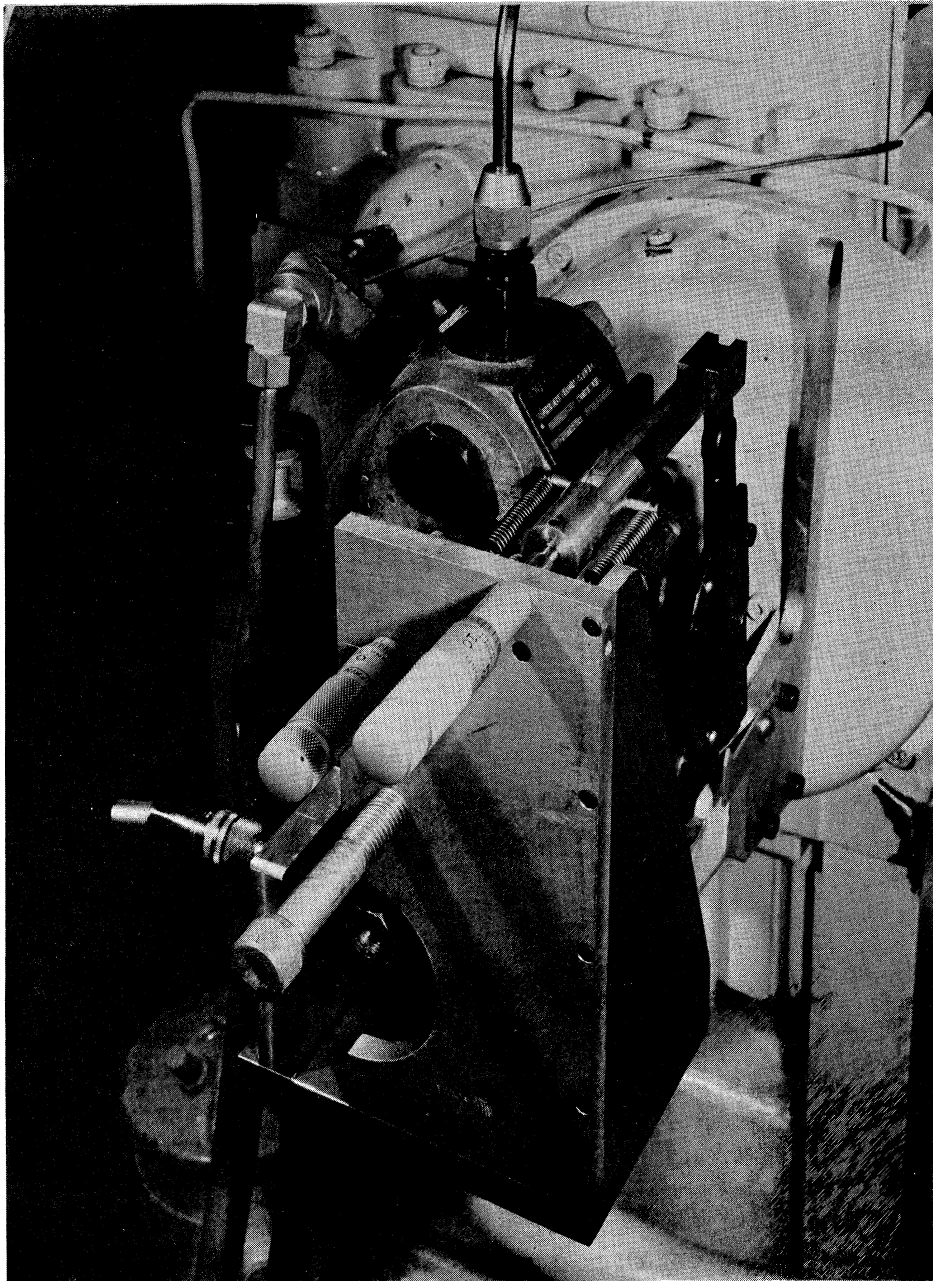


Fig. 3. Fuel injection pump fitted with micrometers to control the rack position and injection timing.

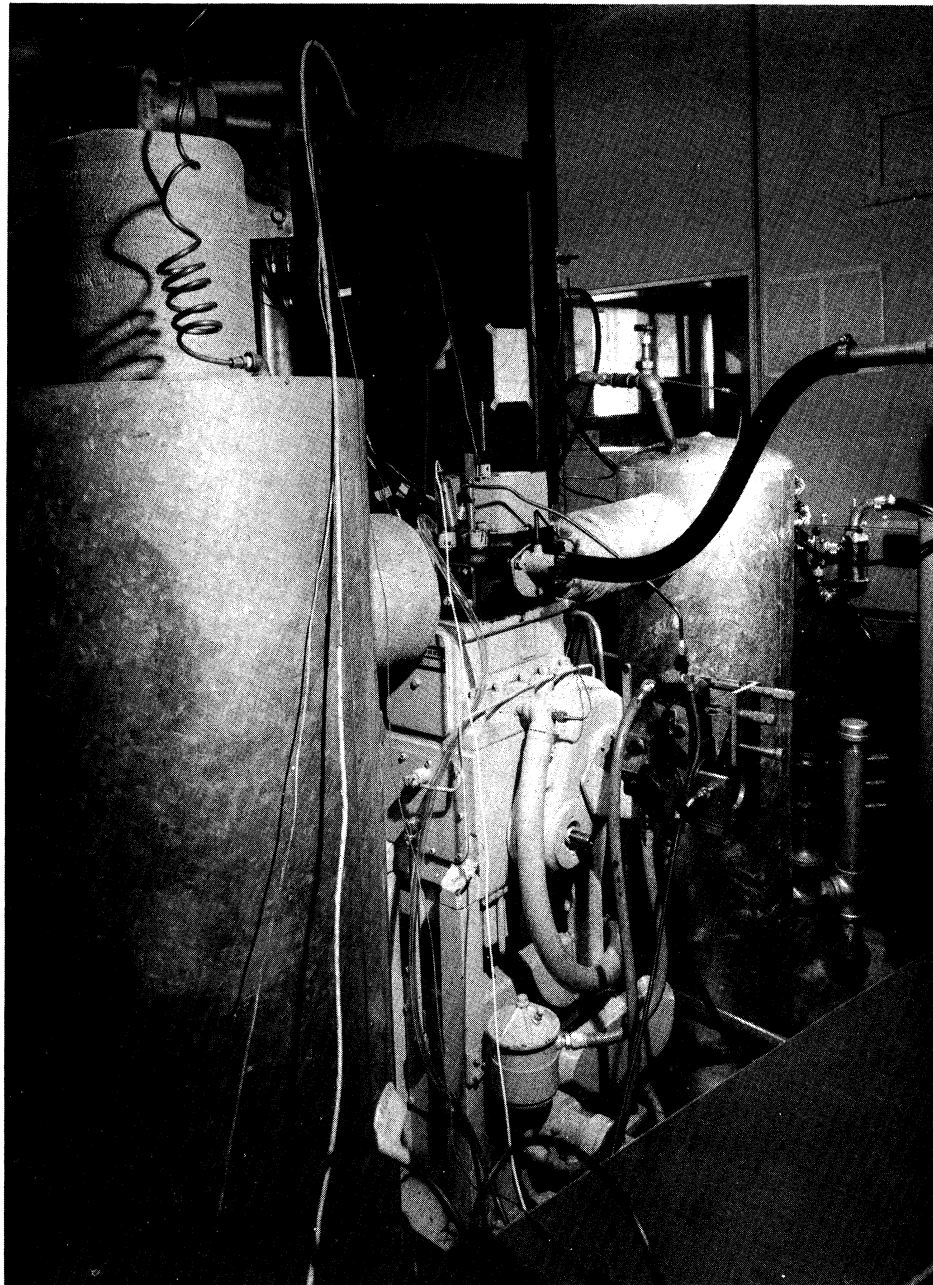


Fig. 4. View of installation of ATAC engine.

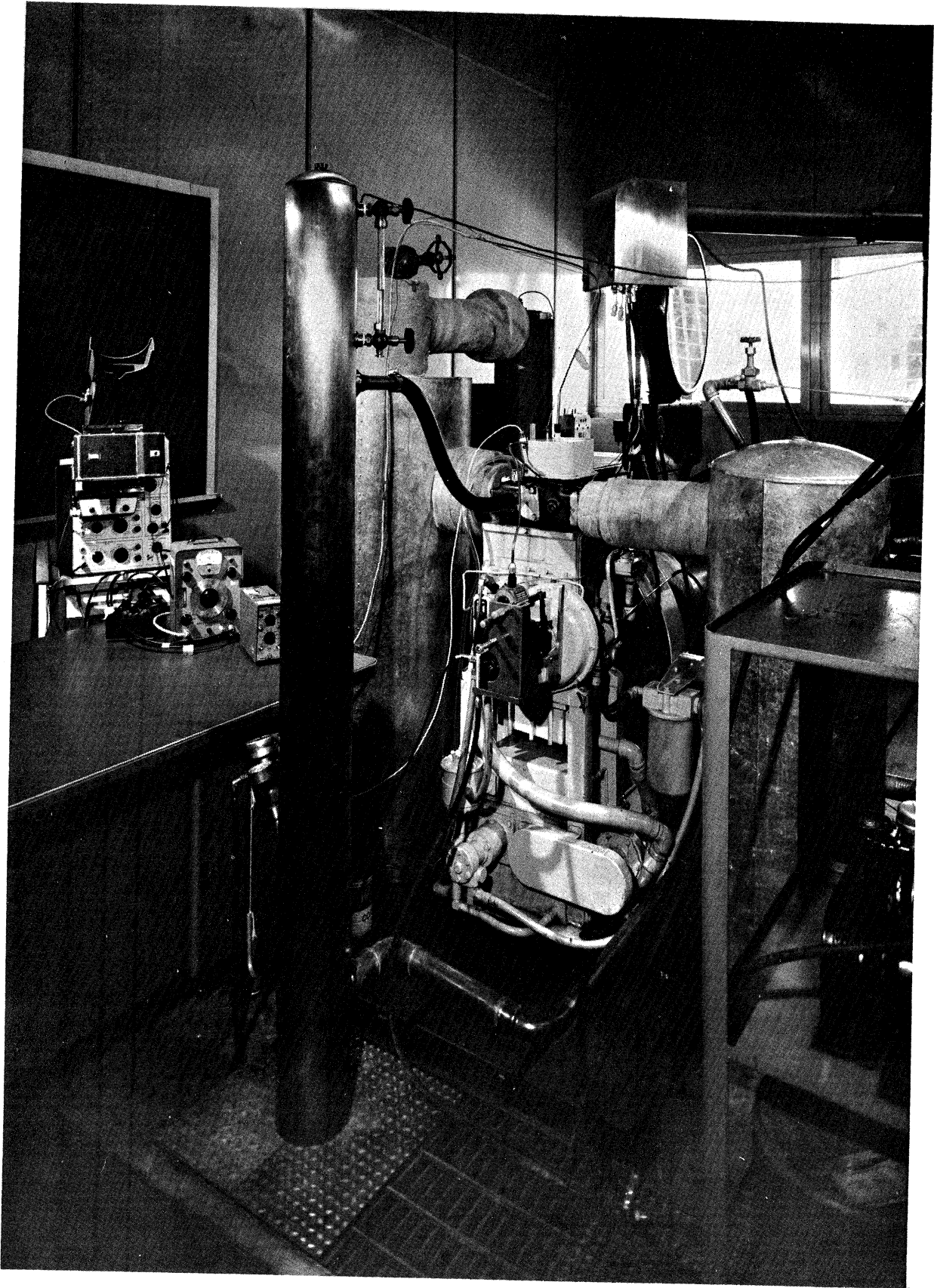


Fig. 5. View of installation of ATAC engine.

4. Blowby Flowmeter (shown in Fig. 8).--A flowmeter has been connected to the crankcase ventilation tube to measure the rate of flow of the blowby gases. An oil separator has been installed between the ventilating tube and the flowmeter to collect the oil droplets discharged with the blowby gases before reaching the flowmeter. The value of the blowby rate will be recorded together with all other data while running the engine.

5. Smoke Measurements.--In order to measure the intensity of the smoke produced in the exhaust of the ATAC engine a "Hartridge Smokeometer" is connected to the exhaust, as shown in Figs. 6 and 7.

B. Calibration of Instruments

During this period a great effort has been made to calibrate and improve the accuracy of the different instruments. These include the following:

1. Calibration of the critical flowmeter used to measure the rate of air flow into the engine. This calibration has been done by using an inverted bell positive displacement unit in the Fluids Laboratory, The University of Michigan. The inverted bell has an inside diameter of 104.0 inches, and a net displacement of 226.1 cubic feet used for the calibration.

2. Calibration of the Kistler pressure transducer (type 401A) together with the charge amplifier (type 655, S/N 1194), by using a dead weight tester. This transducer is used for measuring the gas pressure in the cylinder.

3. Calibration of Kistler pressure transducer (type 601H) together with the charge amplifier (type 503, S/N 359), by using a dead weight tester. This transducer is used for measuring the fuel pressure before the nozzle.

4. Calibration of the distance detector used to measure the needle lift.

5. Calibration of the surface thermocouple used to measure the inside wall surface temperature. The thermocouple output is found to agree with the standard thermocouple tables.

6. Calibration and zero adjustment of the Honeywell thermocouple (rotating disk type) used to measure the air, water, oil, and exhaust gas temperature.

C. Experimental Work on the Open Combustion Chamber ATAC Engine

Tests are now being carried out to study the ignition delay and other combustion phenomena of the following fuels:

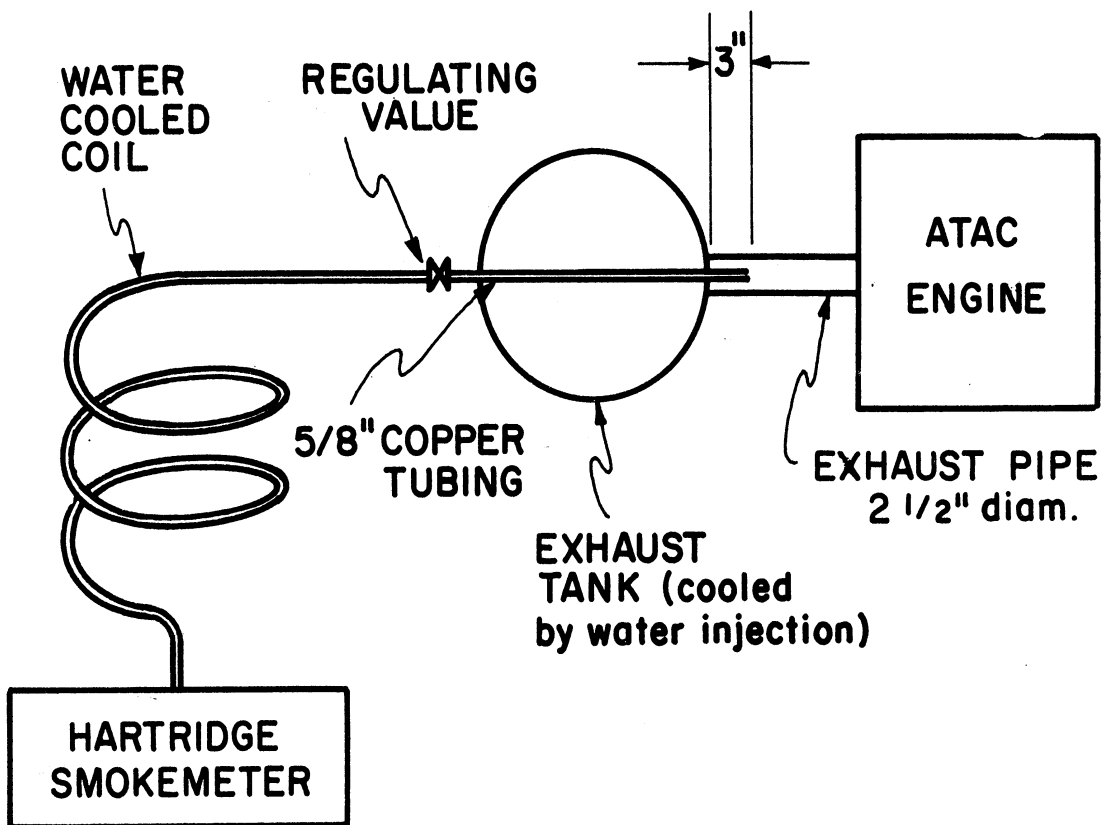


Fig. 6. Smokemeter connected to the ATAC engine.

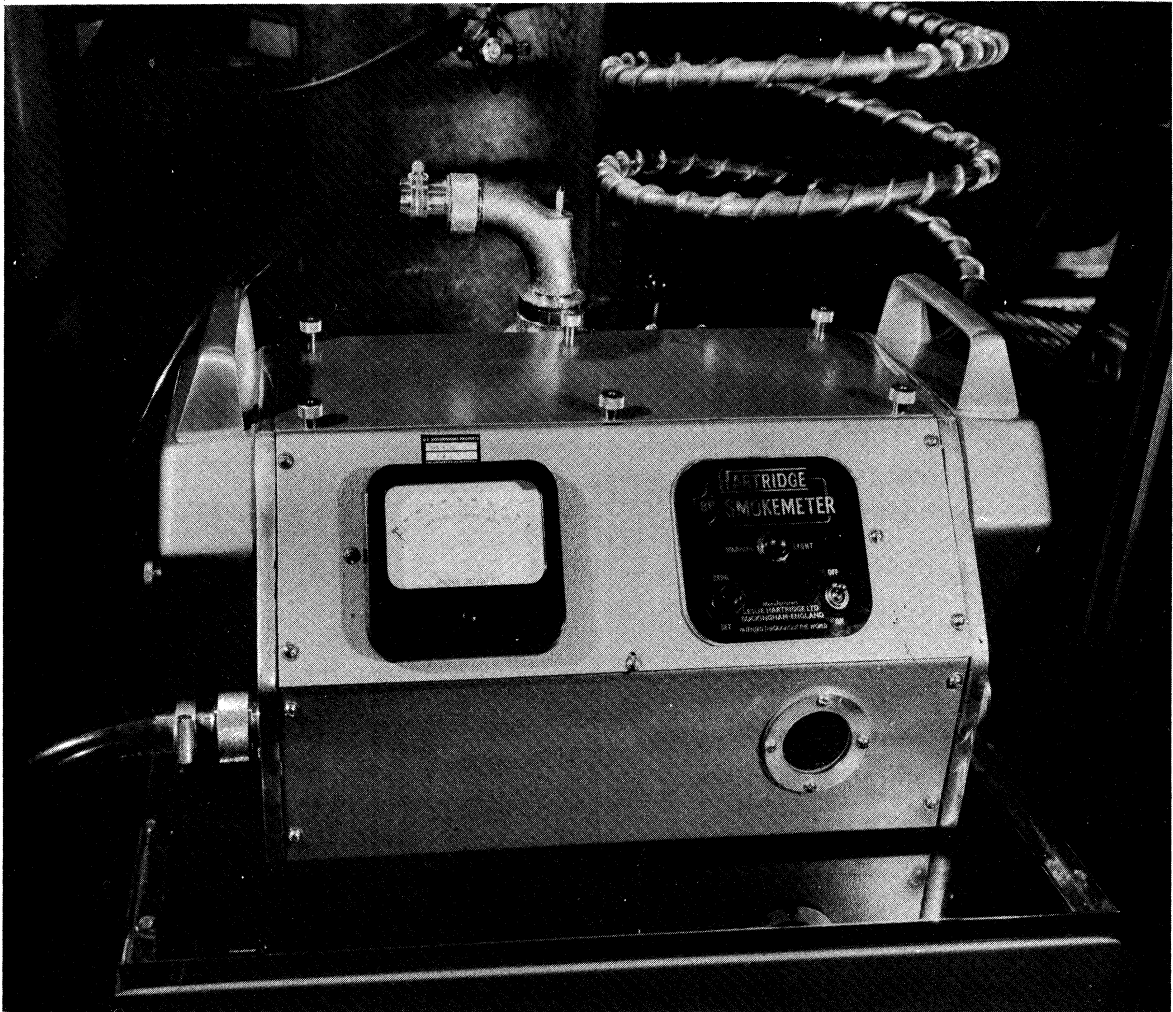


Fig. 7. Hartridge Smokemeter connected to the ATAC exhaust pipe.

1. CITE refree grade (MIL-F-45121) fuel
2. Diesel no. 2 fuel
3. MIL-G-3056 refree grade gasoline fuel

It has been noticed that the engine runs properly on the first two fuels. But with the gasoline it is noticed that the engine runs irregularly with frequent misfirings. The details of this series of tests will be given in the future progress reports.

D. Computer Programs

Most of the computations needed for this project are now carried out on an IBM 7090, in The University of Michigan Computing Center. Statistical and curve fitting procedures are made to assist in the following programs:

1. Data synthesis programs; to combine related data into an orderly sequence.
2. Combustion analysis programs; to calculate the thermodynamic conditions of the gases in the cylinder at any point in the cycle.
3. Delay analysis programs; to process ignition delay data and seek correlations between the experimental results and other operating parameters.

E. Authors' Reply to Discussions on SAE Paper "Ignition Delay in Diesel Engines"

The discussions on the SAE paper indicated the great interest in ignition delay investigations, and the great need for combustion research in super-charged engines.

A copy of these discussions and authors' reply is given in the Addendum.

V. PROBLEM AREAS AND CORRECTIVE ACTIONS

1. The faulty Kistler transducer mentioned in Progress Report No. 6 has been replaced.
2. It was difficult to detect the oil level in the lower sump of the ATAC engine. This was corrected by constructing a sealed dip stick device that can be reached easily. This device is shown together with a blowby flowmeter in Fig. 8.

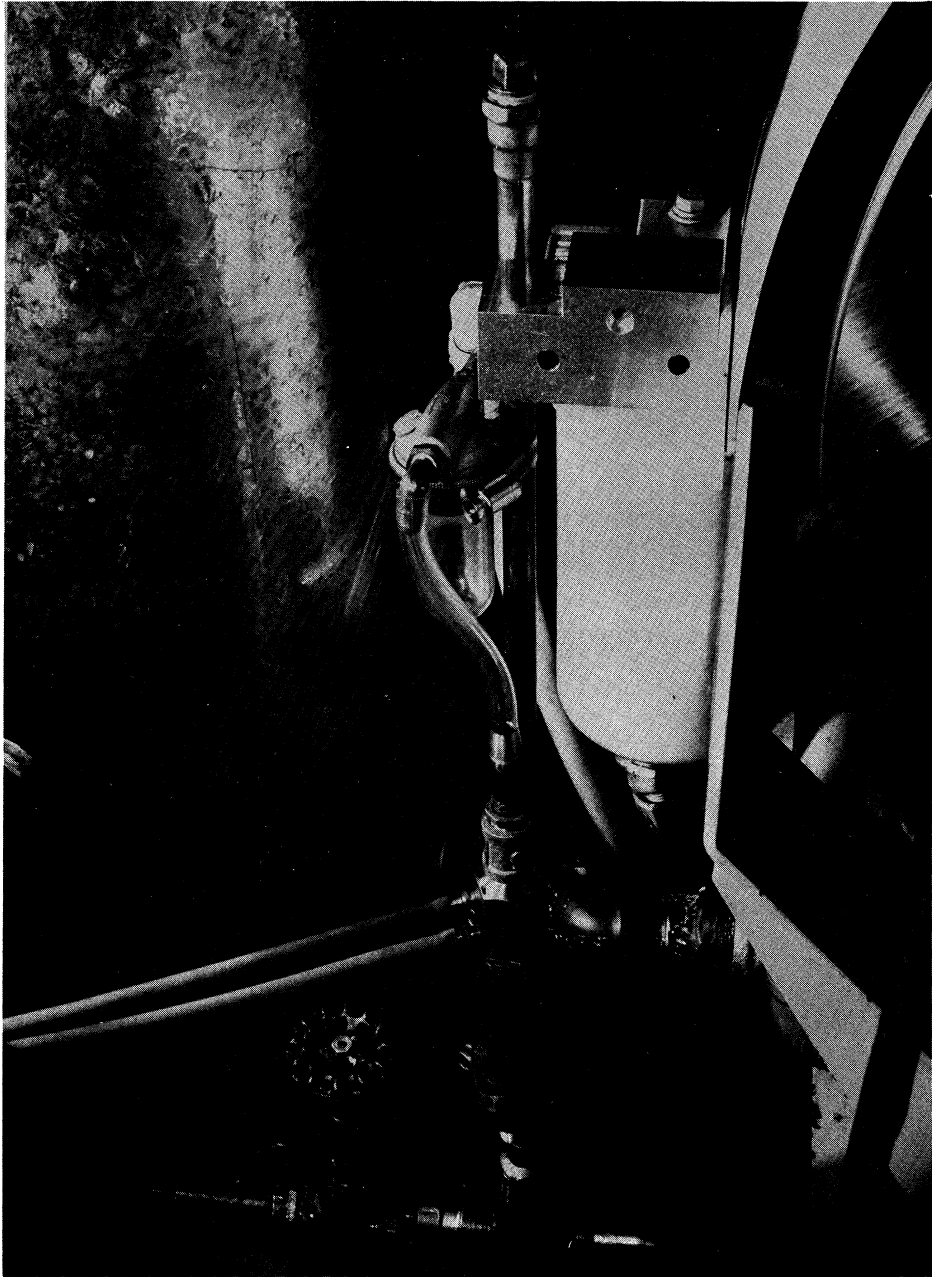


Fig. 8. Blowby flowmeter mounted on newly installed dip stick type oil level indicator.

3. The vacuum in the crankcase was noticed to be less than 4 inches of water, specified by the manufacturer. This caused flow of lubricating oil out with the blowby gases. This was corrected by cleaning and adjusting the relief valve.

4. The engine has been noticed to operate erratically when gasoline is used as fuel. In order to avoid running the engine for long periods of time on gasoline without combustion, an injection test rig will be constructed to make gasoline injection studies away from the engine.

VI. FUTURE PLANS

A. Next Period

To run tests on the ATAC engine to compare between the ignition delays and combustion phenomena of the three fuels mentioned before.

B. Overall

1. To investigate the effect of pressure, temperature, and density on ignition delay with the different fuels.

2. To process the experimental data on a digital computer.

3. Report the results.

C. Change From Original

Since turbulence has been found to affect ignition delay significantly, it will be studied along with temperature, pressure, and density.

VII. SIGNIFICANT ACCOMPLISHMENTS

1. Newly identified definitions of the ignition delay have been made.

2. The theoretical work indicated that the ignition delay in engines can be divided into a physical, a chemical, and an energy delay.

3. Correlations of experimental results of ignition delay, with gas pressure, gave a formula that is found to correlate very well all previous ignition delay results in bombs and engines, with the corresponding gas pressure.
4. Completion of the equipment and instrumentation of the ATAC engine.

VIII. PROJECT STATUS

Funds and Expiration Date of Contract

Original contract

July 1, 1964, to January 1, 1965.....\$ 23,020

Modification No. 7

Extension of contract to February 28, 1966;

addition of \$18,000 to contract funds for a total of.....\$ 41,020

Modification No. 8

Extension of contract to February 27, 1967;

addition of \$37,000 to contract funds for a total of.....\$ 78,020

(funds will be exhausted about January 1, 1967)

Modification No. 10

Extension of contract to December 1, 1967;

addition of \$45,000 to contract funds for a total of.....\$123,020

IX. BIBLIOGRAPHY

1. Chiang, C. W., Myers, P. S., and Uyehara, O. E., "Physical and Chemical Ignition Delay in an Operating Diesel Engine Using the Hot Motored Technique," SAE Trans., Vol. 68, 562-570, 1960.
2. Elliott, M. A., "Diesel Fuel Combustion," American Chemical Society, Advances in Chemistry, Series No. 20, pp. 280-293.
3. Elliott, M. A., "Diesel Fuel Oil-Production Characteristics and Combustion," ASME, New York, 57-120, 1948.
4. Elliott, M. A., "Combustion of Diesel Fuel," SAE Quarterly Trans. 3, 490-515, 1949.
5. Starkman, E., "Ignition Delay in Diesel Engines," Trans. American Institute of Chemical Engr., Vol. 42, 107-120, Feb, 1946.
6. Boerlage, G. D. and Broeze, J. J., "Combustion Qualities of Diesel Fuel," Industrial and Engineering Chemistry, Vol. 28, No. 10, 1229-1234, 1936.
7. El-Wakil, M. M., Myers, P. S., and Uyehara, O. A., "Fuel Vaporization and Ignition Lag in Diesel Combustion," SAE Trans., Vol. 64, 712-726, 1956.
8. Yu, T. C., Collins, R. N., Maladevan, K, Uyehara, O. A., and Myers, P. S., "Physical and Chemical Ignition Delay in an Operating Diesel Engine Using the Hot Motored Technique," SAE Trans., Vol. 64, 1956.

A D D E N D U M

A. DISCUSSIONS ON SAE PAPER "IGNITION DELAY IN DIESEL ENGINES,"
BY N. A. HENEIN AND JAY A. BOLT, SAE ANNUAL MEETING,
JANUARY 9-13, 1967

1. K. C. Tsao

Associate Professor, South Dakota School of Mines and Technology

Professors Henein and Bolt are to be congratulated for their contributions in adding another piece of work to the literature regarding diesel combustion. In particular, the authors have (i) successfully correlated the ignition delay* among the three published data by a simple expression, (ii) explored the effect of air turbulence on ignition delay, and (iii) obtained additional experimental information on the effect of cooling water temperature on ignition delay. The following comments are presented for the sole purpose of strengthening the authors' findings and do not detract, in any form, the merit of their paper.

Authors' Eq. (21) indicates that at a given temperature and probably at given engine speed, the ignition delay is a hyperbolic type function of pressure. The constant C and the exponent n would differ for different sets of operating conditions. For the engine designer, having only the information of the intake air temperature, the intake air pressure and the engine speed, an estimate of ignition delay would require knowledge including the selection of C and n values. Hence, it seems that Eq. (21) may present itself as a limited application, but it does validate that the cylinder pressure at the start of injection process is of primary importance in delay correlations among various engines. It would be useful and rewarding in the engine design if the authors would give some details on selecting the values of the constant C and the exponent n as some functions of engine operating variables.

In the course of their presentation, the authors raise one important, yet unresolved question: the effect of engine turbulence in ignition delay. The engine turbulence, as most of the engine researchers realize, is an extremely difficult and perplexing subject, but with the pressing need of understanding the diesel combustion phenomenon. It was thought that the engine speed is the principal cause of air turbulence, which includes the air flow pattern, inside the combustion chamber. It seems unlikely that the air turbulence would have the same flow pattern inside the cylinder when the engine rpm increases from 607 rpm to 1000 rpm. By comparing the authors' data of Fig. 17 and Fig. 19, the ignition delays are nearly equal at cylinder air pressure of

*The ignition delay is defined here in its most general sense whether it be the temperature rise delay or pressure rise delay.

250 psia, while the rest of the operating variables were held nearly the same. Would it be correct to assume that the engine speed (or air turbulence) has no effect on ignition delay in a Lister engine at the listed operating conditions? Or would it be correct to assume that the engine speed (or air turbulence) does have effect, to some degree, on ignition delay, but this effect has been compensated by an undetermined variable or variables? If so, then what are the other undetermined variables?

The effect of engine cooling water temperature on ignition delay as shown in authors' paper, Fig. 15, is very interesting. In a previous publication,* the peak motored compression temperature was correlated and modeled with the engine operating variables, the intake air temperature, the engine speed, the engine compression ratio and the cooling water temperature. It was also shown that the ignition delay** is affected by the air temperature at the point of injection, the air pressure at the point of injection and the engine speed. Hence, it seems reasonable to assume that the temperature at the point of injection in a fired diesel engine must also be affected by the jacket cooling water temperature, which in turn, will affect, to a certain degree, the ignition delay.

Since there is no semi-empirical relationship available in the literature for computing the air temperature at the point of injection, it was then decided to apply the motored compression temperature model to calculate the air temperature at the point of injection. In the process of computation, the intake air temperature was chosen as 530°R; the engine speed as 1200 rpm, the engine compression ratio as 12.5 and the jacket cooling water temperature varies from 530°F to 660°R. It must be noted that the actual compression ratio at the point of injection (injection at 27° BTDC)** was about 6.5 instead of 12.5. The choice of compression ratio of 12.5 is simply to eliminate the engine compression ratio effect which appears as an exponent in Eq. (2),* and to compensate the difference of air temperature between a motored and a fired diesel engine.

By so doing, the computed peak temperatures change from 1445.3°R to 1493.4°R when the cooling water temperature increases from 530°R to 660°R. These computed temperatures agree fairly well as the temperatures at the start of injection in a fired diesel engine.** In turn, they are employed to calculate the ignition delay.

The pressure at the point of injection and the engine speed were chosen as 300 and 600 psia, and 1200 rpm, respectively. The following figure presents the computed and the experimental ignition delay vs. the cooling water temperature. The authors' experimental data agrees very well with the calculated values. However, it must be noted that the reduction in ignition de-

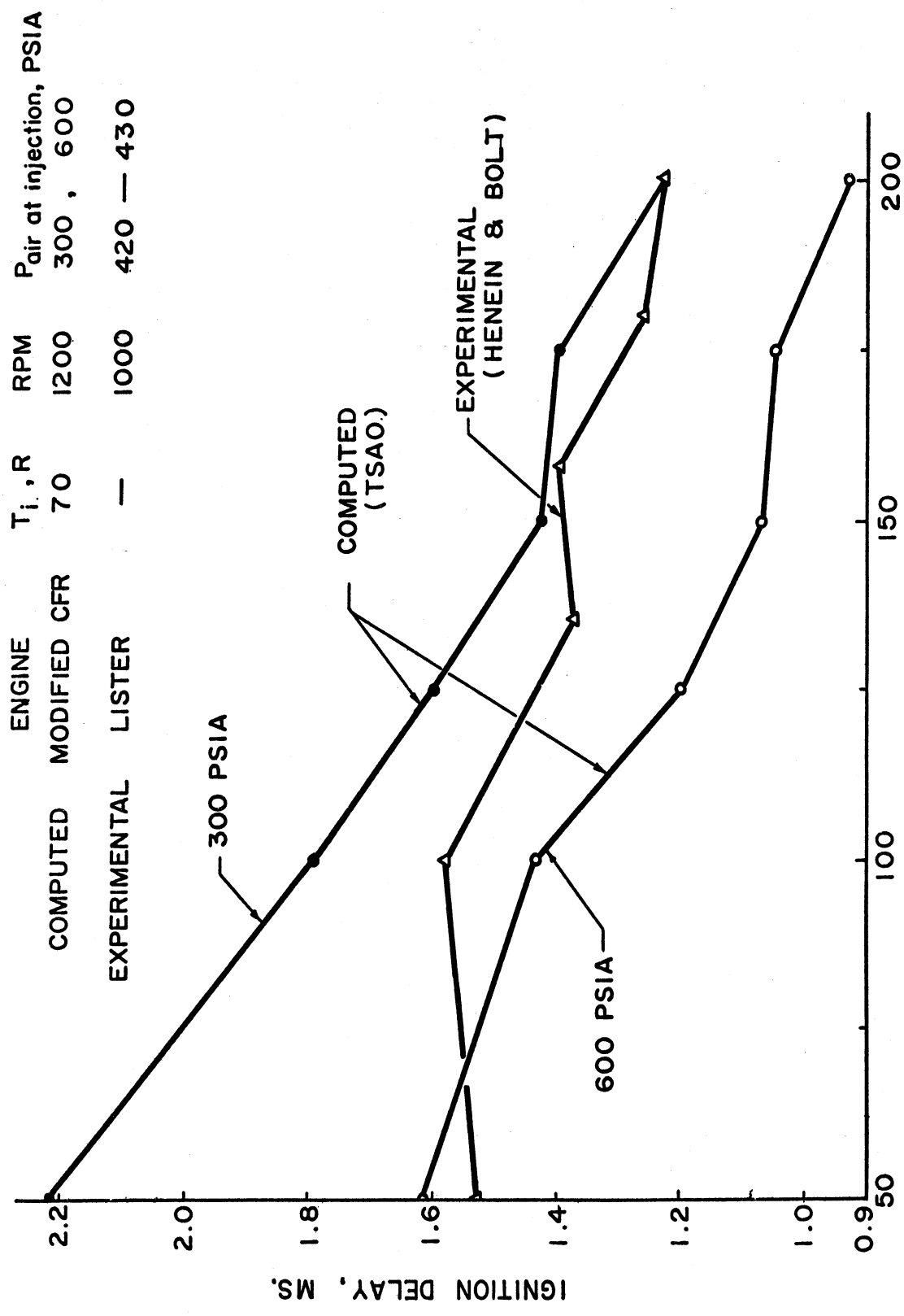
*K. C. Tsao and S. M. Wu, "On the Mathematical Model of Motored Compression Temperature," SAE Paper 650453 or SAE Trans., 1966, p. 594.

**Authors' reference (36).

lays by increasing the cooling water temperature from 70 to 200°F are different. It is 14.8% in a Lister engine and 42.8% in the computed delays.

Finally, I have noted the maximum pressure and temperature advances in a motored Lister engine as given in authors' Fig. 22. These same phenomena were also observed in a modified C.F.R. engine motored cycle.*

*K. C. Tsao, "The Effect of Operating Variables on Compression Temperature in a Compression Ignition Engine," Ph.D. Thesis, University of Wisconsin, 1961, Figs. 13, 15, 19, 21, and 26.



COOLING WATER TEMPERATURE. ° F

Effect of cooling water temperature on ignition delay.

2. C. W. Chiang
Associate Professor, University of Denver

The authors should be complimented on their fine research work on ignition delays which are still not very well known.

A few comments in regard to the thermodynamic considerations of the paper are as follows:

1. Equation (26) of Appendix II does not seem to be for a closed system. dm in Eq. (26), means that there exists a change of mass due to the injection of fuel crossing the boundary of the system and thus implies an open system. It is then obvious, if the system is considered as a closed system, there should not exist any term of dm .

2. During the period of ignition delays, the fuel is injected into the combustion chamber and an amount of fuel dm_f or dm is crossing the boundary of the system. According to the first law of thermodynamics written for an open system

$$\delta Q + dm(u_f + P_f V_f) = \delta W + dU \quad (1)$$

or

$$\frac{\delta Q}{d\theta} + \frac{dm}{d\theta} h_f = \frac{PdV}{d\theta} + mc_v \frac{dT}{d\theta} \quad (2)$$

where h_f is the enthalpy of the injected fuel at injected pressure

$$m = m_f + m_a, \text{ the mass of air, } m_a, \text{ remains constant.}$$

Other notations remain the same as those in the paper.

Now applying the ideal gas law

$$d(PV) = d(mRT) \quad (3)$$

or

$$PdV + VdP = mRdT + RTdm \quad (4)$$

Combining Eqs. (2) and (4) gives

$$\frac{dP}{d\theta} = \frac{R}{c_v} \frac{1}{V} \left[\frac{\delta Q}{d\theta} - P \frac{dV}{d\theta} \left(\frac{c_v}{R} + 1 \right) + (h_f + c_v T) \frac{dm}{d\theta} \right] \quad (5)$$

Basically, Eq. (5) is similar to Eqs. (26) or (15) of the paper except that the sign of the last term of Eqs. (26) or (15) is supposed to be (+). The only difference is the enthalpy of the fuel h_f which may be neglected. However, the last term in Eq. (5) is of considerable importance and may not be neglected.

3. To demonstrate the importance of the last term in Eq. (5) a numerical estimate is given. Although the estimate is crude, it only serves as qualitative analysis. Since the ignition delay is usually in the order of 10 crank angle degrees, the total pressure change after the ignition delay may be obtained by integrating Eq. (5) as follows:

$$\Delta P = \frac{R}{c_v} \frac{1}{V} \Delta Q - P \Delta V \left(\frac{c_v}{R} + 1 \right) + (h_f + c_v T) \Delta m \quad (6)$$

(a) Comparison of the last two terms.

Taking data from the paper listed as follows:

Piston displacement, V	approx. 278 in. ³
Compression ratio	14:1
T (Fig. 22, 9° B.T.D.C.)	1200°R
P (Fig. 22, 9° B.T.D.C.)	440 psia
$m_a \left(\frac{278}{1728} \times .076 \right)$	approx. 1.22×10^{-2} lb
m_f (Take fuel air ratio of .03)	approx. 3.66×10^{-4} lb
c_v (air)	.17 Btu lb ⁻¹ F ⁻¹
R (air)	approx. .07 Btu lb ⁻¹ F ⁻¹
ΔV (for 10 crank angle degree B.T.D.C.)	approx. 4.2 in. ³
neglecting h_f , and heat of vaporization of the fuel	

$$c_v T \Delta m = .17 \times 1200 \times 3.66 \times 10^{-4} = 7.5 \times 10^{-2} \text{ Btu}$$

$$\left(1 + \frac{c_v}{R}\right) P\Delta V = \frac{440 \times 4.2}{778 \times 12} \left(1 + \frac{.17}{.07}\right) = 6.8 \times 10^{-1} \text{ Btu}$$

$$\frac{c_v T \Delta m}{\left(1 + \frac{c_v}{R}\right) P\Delta V} \approx 11\%$$

With higher fuel-air ratio, this percentage is proportionally higher. Thus, the last term amounts to a good percentage of the term before it.

(b) Total pressure drop after 10° ignition delay in the absence of combustion due to the contribution of the last term.

Assuming 1200 rpm and T wall ≈ 300°F or 760°R, the film coefficient of heat transfer due to convection at this speed is estimated at 2 Btu hr⁻¹ ft⁻² F⁻¹. ΔQ is found negligibly small.

$$\begin{aligned} \Delta P &= \frac{R}{c_v V} [c_v T \Delta m] \\ &= \frac{53.4}{278} \times 1200 \times 3.66 \times 10^{-4} \\ &= 1 \text{ psi} \end{aligned}$$

Although, in this case, the contribution to pressure rise is rather small, nevertheless, for higher compression rates or higher T, lower V, the pressure rise may amount to 7 or 8 psi, as experienced in Yu's paper.

In conclusion, the authors had good intentions of having thermodynamic considerations; however, this approach should be pursued further.

4. Although the authors did mention briefly the importance of different fuels, unfortunately they did not consider them in their experiments. In the literature survey the cetane number is known to be a vital influential parameter to ignition delays. A further study is deemed necessary.

3. C. W. Bouchillon
Professor, Mississippi State University

INTRODUCTION

The period of time which lapses between fuel injection and some physical manifestation of auto-ignition has been classically referred to as the ignition delay period. Professors Henein and Bolt have presented an excellent discussion of the concepts and findings of previous investigations of this phenomena as presented in the literature. Their literature review was comprehensive and the basic contributions to gaining an understanding of the ignition delay phenomena were succinctly presented. Both the theoretical and the empirical findings were discussed in sufficient detail that the reader is brought through the historical developments up to the report of the present investigation being conducted by Professors Henein and Bolt.

The equipment is described in sufficient detail to give the reader a very clear picture of the nature of the experimental techniques.

The instrumentation utilized was verified through motoring techniques, etc., in order to establish reliability of the results obtained.

It is interesting to note the following trends in the variation of the pressure rise delay with the several physical variables involved in the experimental investigation. The pressure rise delay is seen to decrease with an increasing fuel to air ratio as presented in Fig. 13. The injector opening pressure did not have a significant effect on the pressure rise delay times for the study presented in Fig. 14. An increase in cooling water temperature at the outlet resulted in a reduction in the pressure rise delay times for the runs reported in Fig. 15. And finally, the variation in pressure rise delay with gas pressure at the start of injection was represented approximately by a constant divided by the pressure raised to some power as reflected in Figs. 17 and 19. The authors present a simplified thermodynamic analysis of the cylinder and combustion chamber, however, it appears that the vaporization of the fuel was assumed to be instantaneous upon injection into the cylinder and no energy exchange was entered into the thermodynamic analysis to account for the latent heat of vaporization of the fuel.

The simplified thermodynamic approach to the analysis of a system can often yield surprisingly good cause-effect relationships and it is at this point that the following analysis is presented as a possible means to extend the theoretical portion of the paper, and as a consequence, some slightly different conclusions might be drawn from the experimental findings than those presented by Professors Henein and Bolt.

THERMODYNAMIC ANALYSIS

In that the fuel injection process represents an unsteady flow phenomena, it may be more appropriate to employ the unsteady energy equation for an open system by

$$\left. \frac{\Delta E}{\Delta t} \right|_{c.v.} = \dot{m}_f h_f - \frac{\delta W}{\Delta t} + \frac{\delta Q}{\Delta t} \quad (1D)$$

where the subscript f refers to the fuel. Equation (1D) may then be divided by the angular velocity $\Delta\theta/\Delta t$ to yield

$$\left. \frac{\Delta E}{\Delta\theta} \right|_{c.v.} = \frac{\delta m_f}{\Delta\theta} h_f - \frac{\delta W}{\Delta\theta} + \frac{\delta Q}{\Delta\theta} \quad (2D)$$

where δm_f is the increment of fuel introduced during the crank angle $\Delta\theta$.

Now solving for the heat transfer and introducing the internal energies in the control volume at crank angles θ and $\theta+\Delta\theta$, there results

$$\frac{\delta Q}{\Delta\theta} = \frac{M_A C_{vA} (T_{\theta+\Delta\theta} - T_{\theta}) + \delta m_f U_{f\theta+\Delta\theta}}{\Delta\theta} - \frac{\delta m_f}{\Delta\theta} h_{f\theta} + \frac{PdV}{\Delta\theta}$$

which reduces to

$$\frac{\delta Q}{\Delta\theta} = M_A C_{vA} \left(\frac{\Delta T}{\Delta\theta} \right) + \frac{\delta m_f}{\Delta\theta} (U_{f\theta+\Delta\theta} - U_{f\theta}) - \frac{\delta m_f}{\Delta\theta} \left(\frac{Pv}{J} \right)_{f\theta} + \frac{PdV}{\Delta\theta} \quad (3D)$$

Assuming that at least some of the fuel vaporizes on injection during the period $\Delta\theta$, then $U_{f\theta+\Delta\theta}$ represents the internal energy of the vaporized fuel with a temperature approximately equal to the chamber air temperature and at a relatively low partial pressure in comparison with the cylinder pressure. This may be assumed because of the small values of fuel/air ratio being used.

Introducing

$$h_{fg} = U_{f\theta+\Delta\theta} - U_{f\theta} + \left(\frac{Pv}{J} \right)_{\theta+\Delta\theta} - \left(\frac{Pv}{J} \right)_{\theta}$$

and assuming that the latter terms may be considered negligible at the relatively low partial pressures of the fuel in the chamber, then

$$U_{f_{\theta+\Delta\theta}} - U_{f_{\theta}} \simeq h_{fg} \delta m_f \quad (4D)$$

Then assuming that during the crank angle position relative to TDC-15° < θ < 15°, the total volume is approximately constant, then Eq. (3D) in combination with Eq. (4D) yields

$$\frac{\delta Q}{\Delta\theta} \simeq M_A C_{vA} \frac{\Delta T}{\Delta\theta} + \frac{\delta m_f}{\Delta\theta} h_{fg} \quad (5D)$$

Then assuming that the temperature may be approximately represented by

$$T = \frac{PV}{mR}$$

and neglecting any volume or mass changes,

$$\frac{\Delta T}{\Delta\theta} = \frac{V}{mR} \frac{\Delta P}{\Delta\theta} \quad (6D)$$

In combining Eqs. (5D) and (6D), there results

$$\frac{\Delta P}{\Delta\theta} \simeq \frac{mR}{M_A C_{vA} V} \left[\frac{\delta Q}{\Delta\theta} - \frac{\delta m_f}{\Delta\theta} h_{fg} \right]$$

Now if the heat transfer is assumed to consist of the chemical energy supplied from the combustion process and of the convection losses to the cylinder walls as did the authors, along with the assumption that $M_A \simeq m = M_A + M_f$ there results

$$\frac{\Delta P}{\Delta\theta} \simeq \frac{R}{C_{vA} V} \left[\frac{\delta Q_{Ch}}{\Delta\theta} - \frac{\delta Q_c}{\Delta\theta} - \frac{\delta m_f}{\Delta\theta} h_{fg} \right] \quad (7D)$$

Consider that the latent heat of vaporization for the fuel at relatively low pressures may be given approximately by

$$h_{fg} \simeq K_1 - K_2 \ln \frac{P_f}{T_f} \quad (8D)$$

as suggested by and presented in for other hydrocarbons. Also, the heat transfer to the walls may be approximated by

$$\frac{\delta Q_c}{\Delta \theta} \approx A \cdot \alpha \cdot \frac{\Delta(T_g - T_w)}{\Delta \theta} \cdot \Delta t \quad (9D)$$

Then a prediction equation may be developed for the ignition delay time by solving for $\Delta \theta$. This yields

$$\Delta \theta \approx \frac{C_{vA} V(\Delta P)}{R \left\{ \frac{\delta Q_{Ch}}{\Delta \theta} - A \cdot \alpha \cdot \frac{\Delta(T_g - T_w)}{\Delta \theta} \cdot \Delta t - \frac{\delta m_f}{\Delta \theta} \left(K_1 - K_2 \ln \frac{P_f}{T_f} \right) \right\}} \quad (10D)$$

Now for a constant fuel/air ratio, with higher initial chamber pressures at the start of injection, there will result higher partial pressures of the fuel in the chamber; because of the reduced volume, and as a consequence, Eq. (10D) may be modified to yield

$$\Delta \theta \approx \frac{C_v V(\Delta P)}{R \left\{ \frac{\delta Q_{Ch}}{\Delta \theta} - A \cdot \alpha \cdot \frac{\Delta(T_g - T_w)}{\Delta \theta} \cdot \Delta t - \frac{\delta m_f}{\Delta \theta} \left(K_4 - K_3 \ln \frac{P_c}{T_f} \right) \right\}} \quad (11D)$$

Let us now consider the results obtained by experiment in relation to the approximate predictions of Eq. (11D).

Case I. Pressure Variations

Increasing chamber pressures result in an increase in the denominator and therefore a decrease in the ignition delay time (see Figs. 17 and 19).

Case II. Fuel/Air Ratio Variations

Because of the very short time involved in the ignition delay period, the heat transfer to the walls should be small in comparison with the chemical and vaporization energies, therefore the ignition delay time should be inversely proportional to the fuel/air ratio (see Fig. 13).

Case III. Cooling Water Temperature

A reduction in the cooling water temperature should result in an increase in the heat transferred to the walls, thereby reducing the denominator of Eq. (11D) and as a consequence, the delay time would be increased (see Fig. 15).

Case IV. Injection Pressure

The injection pressure effects do not appear in Eq. (11D) and as a consequence may not affect the ignition delay time (see Fig. 14).

Case V. Engine Speed

An engine speed increase of the order of 2 would reduce the time for heat transfer to the walls by 1/2 and unless there is a significant increase in the heat transfer coefficient, the net effect would be to reduce the heat transfer to the walls.

In order to draw a comparison with the data presented in Fig. 20, the different chamber temperature effects must also be considered.

$$\frac{\delta Q_c}{\Delta \theta} \simeq A \cdot \alpha \cdot \frac{\Delta(T_g - T_w)}{\Delta \theta} \cdot \Delta t$$

Assuming that the heat transfer coefficient increases as \sqrt{V} , then the net effect will be a reduction in the heat transfer with an increase in speed for this case.

$$\frac{\frac{\delta Q_c}{\Delta \theta} \Big|_{1000}}{\frac{\delta Q_c}{\Delta \theta} \Big|_{500}} \simeq \frac{A \sqrt{1000} \left[\frac{\Delta(1520-500)}{\Delta \theta} \right] \Delta t_{1000}}{A \sqrt{500} \left[\frac{\Delta(1457-500)}{\Delta \theta} \right] \Delta t_{600}} < 1$$

This results in an increase in the denominator and consequently a reduction in the ignition delay time with increase in engine speed.

Case VI. Increase in Chamber Temperature

Increase in chamber temperature appears to be significant as evidenced by the ignition delays reported by West in comparison to the present investigation (Fig. 20).

This may be due to the fact that the heat of vaporization of the fuel term is probably significantly larger than the heat transfer to the walls. As a consequence, this evaporative process could be effected more rapidly in the higher temperature conditions, thereby reducing the ignition delay time for the higher temperature runs.

The above arguments are admittedly qualitative and are presented only to indicate that careful theoretical analysis may yield useful quantitative results if the qualitative trends are correct.

CONCLUSIONS

Professors Henein and Bolt have presented an excellent literature review and have obtained and reported some significant experimental observations of ignition delay.

In order to obtain a clearer understanding of the physical phenomena involved, it is necessary to make theoretical attacks on the problem yielding results which are in agreement with the experimental findings. It appears that the fuel vaporization phenomena may be one of the major controlling influences on the ignition delay as defined by the time lapse from the beginning of injection to the onset of pressure rise in the chamber. Further attention to thermodynamic and heat transfer analyses of the injected fuel stream may prove beneficial and further efforts in this direction are required in order to evaluate this hypothesis.

In order to establish a theoretical approach to predicting the delay time as described by the time from the start of injection to onset of illumination, it appears that the combustion energy release rate is significantly involved. Further analytical attack may reveal that through thermodynamic analysis of the fuel vaporization phenomena and the application of the theory of combustion kinetics, explanations of the illumination delay time may be obtained.

Many facets of this phenomena remain to be explained and the authors are to be commended for their contribution by bringing additional information on the subject of ignition delay in diesel engines.

B. AUTHORS' REPLY ON DISCUSSIONS

(February, 1967)

The authors wish to thank the discussors for their interest in the paper, and for the valuable points brought up in the discussions.

IN REPLY TO PROFESSOR K. C. TSAO

1. For fundamental studies, we believe it is better to correlate the pressure rise delay with the pressure and temperature in the cylinder at the beginning of injection, rather than in the intake manifold of the engine. If the correlations are made in terms of the intake air pressure and temperature, as suggested by Professor Tsao, the resulting formula would have included two additional factors which vary among engines. The first is the compression ratio at start of injection, which depends on the injection timing. The second is the average index of compression which depends mainly on the cooling losses and engine speed. Equation (21) can be used for any engine if the pressure and temperature at the beginning of injection are calculated. It is expected that the engine designer would be familiar with such calculations as applied to his engine.

2. The effect of increased turbulence is to decrease the ignition delay in the range of pressures and temperatures occurring in the actual diesel engine at the start of injection. Below 250 psia, we cannot draw any conclusions based on experimental data. Our tests did not cover these low pressures because they are outside the range of present use.

3. The results of computations made by Professor Tsao indicate that an increase in cooling water temperature from 70°F to 200°F causes an increase in the air temperature at the end of compression from 1445.3°R to 1493.4°R or an increase of 48.1°F. According to his calculations, this increase causes a drop of 42.8% in the pressure rise delay. Our experimental results show a drop of only 14.8%.

At this time we cannot give a conclusive answer, based on experimental work, for the effect of temperature on ignition delay because this work is still in progress at The University of Michigan. However, we believe that the decrease in delay, as computed by Professor Tsao, is very large. This can be shown by comparing the computed change with the results of several formulae available for the ignition delay. Wolfer's formula (Eq. (2)) gives a value of 17.8%, and Elliott's formula (Eq. (8)) gives a value of 4.45%. Sitkei's formula (Eq. (14)), gives a value of 13%. These values are much lower than the 42.8% given by Professor Tsao, and close to our reported experimental results.

4. We agree with Professor Tsao that a correlation is needed between the gas pressure, temperature, and engine speed, and the constant "C" and exponent "n" in Eq. (21). This, and the effect of gas temperature on ignition delay, are among the main goals of the work now in progress under sponsorship of the U.S. Army Tank Automotive Command.

IN REPLY TO PROFESSOR C. W. CHIANG

The authors wish to thank Professor Chiang for calling their attention to a printing error in Eqs. (15), (20), and (26). The sign of the last term in these equations should be positive.

However, we do not agree with Prof. Chiang about the importance of this last term for the graphical presentation made in Figs. 2 and 3 of the text. This term represents the effect of the change in the mass of the system on the slope of the pressure-time trace. In the demonstration made by Professor Chiang he assumed that all the fuel is injected before the end of the delay period. We do not believe this assumption is justified. Under the conditions quoted by Professor Chiang, the amount of fuel actually injected during the ignition delay is about 20% of the total amount injected. The ratio of 11.1% given in his demonstration therefore is 2.2%, which can be neglected in the graphical representation.

This conclusion is also supported by Part b of item 3 of the discussion. This indicates that the error in the pressure caused by neglecting this last term is 1 psi in 440 psi. This corresponds to an error of 0.2% only.

The authors appreciate the effect of the fuel cetane number on ignition delay. This, however, was not the subject of the present paper. For our program now in progress three fuels of different cetane numbers are being tested for ignition delay.

IN REPLY TO PROFESSOR C. W. BOUCHILLON

The discussion of Professor Bouchillon is based on the assumption that the physical delay is the dominating factor in the total ignition delay. This assumption cannot be justified in view of the previous theoretical and experimental work done.

Wentzel (16)* computed the physical delay and found it much shorter than the pressure rise delay.

Boerlage and Broeze (11) proved experimentally that the chemical portion of the delay period is the controlling factor in the total delay. They com-

*Numbers refer to Bibliography of the original paper.

pared cetane ($C_{16}H_{32}$) and Tetraisobutylene ($C_{16}H_{32}$) and found that the latter has a longer ignition delay due to its molecular structure. This occurred in spite of the fact that the two fuels have the same number of carbon and hydrogen atoms.

Another interesting experiment was made by Starkman (26) to prove the small effect of the physical delay on the total delay. He measured the total delay of a mixture of a diesel fuel and Tetra-ethyl lead. He found that the ignition delay increased with addition of T.E.L. Since T.E.L. has no known effect on the physical delay, and since the ignition delay increases with T.E.L., Starkman concluded that the chemical delay is the major part of the ignition delay.

Another experiment that supports our point of view was made by Hurn, R. W., et al. (31). They studied the effects of the physical and chemical properties of the fuels on the ignition delay in bombs. They concluded that the greatest difference between the autoignition behavior of fuels is in those factors that affect chemical reaction, rather than in those that affect the physical processes.

From the above discussion it can be concluded that the assumption made regarding the importance of the physical part of the delay period is not justified.

SECTION 8

PROGRESS REPORT NO. 8

EFFECT OF AIR CHARGE TEMPERATURE ON I.D. AND OTHER COMBUSTION
PHENOMENA OF THREE FUELS

PROGRESS REPORT NO. 8

DIESEL ENGINE IGNITION AND COMBUSTION

JAY A. BOLT
N. A. HENEIN

PERIOD APRIL 1, 1967 TO DECEMBER 30, 1967

DECEMBER 1967

This project is under the technical supervision of the:

Propulsion Systems Laboratory
U. S. Army Tank-Automotive Center
Warren, Michigan

and is work performed by the:

Department of Mechanical Engineering
The University of Michigan
Ann Arbor, Michigan

under Contract No. DA-20-018-AMC-1669(T)

TABLE OF CONTENTS

	Page
LIST OF TABLES	315
LIST OF FIGURES	317
Part I: Summary	
I. BACKGROUND	321
II. OBJECTIVES	322
III. CUMULATIVE PROGRESS	323
IV. PROGRESS DURING THIS PERIOD	326
V. CONCLUSIONS	328
A. Ignition Delay (I.D. _p)	328
B. Activation Energy (E)	328
C. Noise	329
D. Smoke	329
E. Troubles in Engine Performance	329
VI. PROBLEM AREAS AND CORRECTIVE ACTION	330
A. Fuel Leakage	330
B. Drainage of Fuel-Pump Sump	330
C. Surface Thermocouple Failure	330
D. Failure of Pressure Transducers	330
E. Fouling of Injection Nozzle Holes and Needle	331
F. Failure of 502A Oscilloscope	331
VII. FUTURE PLANS	332
A. Next Period	332
B. Overall	332
VIII. SIGNIFICANT ACCOMPLISHMENTS	333
IX. PROJECT STATUS	334

TABLE OF CONTENTS (Concluded)

	Page
Part II: Experimental Data and Results	
X. DATA AND RESULTS OF A SAMPLE RUN	337
A. Recorded Data (Photographs)	337
B. Test Conditions (as they Appear in Computer Sheets)	337
C. Results Obtained From Traces	337
D. Computed Results	338
E. Comparison Between Measured I.D. _p With That Calculated From Various Formulae	338
XI. EXPERIMENTAL WORK AND RESULTS	343
A. Series A2A	343
B. Series A2B	347
C. Series A2C	349
D. Series A2D	354
XII. COMPARISON BETWEEN THE THREE FUELS	357
A. Delay Period and Activation Energy	357
B. Noise Level	362
C. Smoke Intensity in Exhaust	369
D. Specific Fuel Consumption	369
APPENDIX A: FUEL SPECIFICATIONS	372
APPENDIX B: CALCULATION OF THE CLEARANCE VOLUME	377
APPENDIX C: VOLUME-CRANK ANGLES RELATIONSHIP	381
APPENDIX D: DIGITAL COMPUTATIONS	385

LIST OF TABLES

Table	Page
1. Comparison Between Measured I.D. _p with that Calculated from Various Formulae	338
2. Activation Energy for Different Fuels	362
3. ATAC Engine Cylinder Volume and Gradients at Crank Angles from 0 to 180°, Compression Stroke	383
4. ATAC Engine Cylinder Volume and Gradients at Crank Angles from 0 to -180°, Expansion Stroke	384
5. List of Symbols, Headings, and Representations as they Appear on the Computer Sheets of Table 8	387
6. List of Symbols, Headings, and Representations as they Appear on the Computer Sheets of Table 9	389
7. List of Symbols, Headings, and Representations as they Appear on the Computer Sheets of Table 10	391
8. Computer Data Sheet, Recorded Data, Series A2A for CITE Fuel	392
9. Computer Data Sheet, Computation Results, Series A2A for CITE Fuel	393
10. Computer Data Sheet, Comparison with Previous Work, Series A2A for CITE Fuel	394
11. Computer Data Sheet, Recorded Data, Series A2B for CITE Fuel	395
12. Computer Data Sheet, Computation Results, Series A2B for CITE Fuel	396
13. Computer Data Sheet, Comparison with Previous Work, Series A2B for CITE Fuel	397
14. Computer Data Sheet, Recorded Data, Series A2C for Diesel Fuel	398
15. Computer Data Sheet, Computation Results, Series A2C for Diesel Fuel	399
16. Computer Data Sheet, Comparison with Previous Work, Series A2C for Diesel Fuel	400

LIST OF TABLES (Concluded)

Table	Page
17. Computer Data Sheet, Recorded Data, Series A2D for Gasoline Fuel	401
18. Computer Data Sheet, Computstion Results, Series A2D for Gasoline Fuel	402
19. Computer Data Sheet, Comparison with Previous Work, Series A2D for Gasoline Fuel	403

LIST OF FIGURES

Figure	Page
1. Cylinder pressure for one complete engine cycle.	339
2. Cylinder pressure for the exhaust and inlet strokes.	339
3. Needle lift at start of injection.	340
4. Measurement of I.D. _p from cylinder pressure and needle lift traces.	340
5. Fuel line pressure.	341
6. Needle lift diagram.	341
7. Combustion chamber surface temperature.	342
8. Swing in wall-surface temperature.	342
9. Effect of intake air temperature on pressure at the start of injection (surge tank pressure = 15 in. Hg g).	344
10. Effect of intake air temperature on mean pressure during ignition delay (surge tank pressure = 15 in. Hg g).	345
11. Effect of temperature on I.D. _p of CITE fuel.	346
12. Effect of intake air temperature on minimum combustion chamber wall surface temperature.	348
13. Surge tank pressure at various intake temperatures, for a constant mean pressure of 706 psia during I.D. _p .	350
14. Ignition delay, I.D. _p as a function of mean temperature during ignition delay for CITE fuel.	351
15. Effect of intake air temperature on the volumetric efficiency.	352
16. Mass-flow rate at various intake air temperatures.	353
17. Ignition delay I.D. _p as a function of mean temperature during ignition delay for diesel no. 2 fuel.	355

LIST OF FIGURES (Concluded)

Figure	Page
18. Ignition delay, $I.D._p$ as a function of mean temperature during ignition delay for gasoline fuel.	356
19. Comparison between the ignition delay, $I.D._p$, of different fuels.	358
20. Logarithm of ignition delay, $I.D._p$, as a function of the reciprocal of the absolute mean temperature, for CITE fuel.	359
21. Logarithm of ignition delay, $I.D._p$, as a function of the reciprocal of the absolute mean temperature for diesel no. 2 fuel.	360
22. Logarithm of ignition delay, $I.D._p$, as a function of the reciprocal of the absolute mean temperature, for gasoline fuel.	361
23. Maximum cylinder pressure for different fuels.	363
24. Maximum pressure gradient for different fuels.	364
25. Maximum pressure gradient for different fuels as a function of the length of ignition delay.	365
26. Rate of change of pressure gradient for different fuels.	366
27. Rate of change of pressure gradients for different fuels as a function of the mean temperature during ignition delay.	367
28. Rate of change of pressure gradient for different fuels as a function of the length of ignition delay.	368
29. Smoke intensity for different fuels.	370
30. Brake specific fuel consumption as a function of BMEP for different fuels (constant mean pressure during the ignition delay).	371
31. Details of ATAC engine open combustion chamber.	378
32. Details of recesses in ATAC engine piston.	379
33. ATAC engine two-bar mechanism.	382

PART I
SUMMARY

I. BACKGROUND

A program of activity to study the combustion process in supercharged diesel engines has been developed at The University of Michigan. This program is primarily concerned with the ignition delay and the effect of the several parameters on it. A special concern is given to the effect of pressure, temperature, and density of the cylinder air charge on ignition delay.

The different types of delay have been studied in detail and an emphasis is made on the pressure rise delay and illumination delay. The instruments needed for the measurement of these two delay periods have been developed and a continuous effort is being made to improve their accuracy.

This research is being made on two experimental engines. One is the ATAC high output open combustion chamber engine, and the other is a Lister-Blackstone swirl combustion chamber engine. Three fuels have been used in these tests.

II. OBJECTIVES

A. To study how gas pressure at the time of injection affects ignition delay and combustion. The effects are to be studied at pressures ranging from approximately 300 to 1000 psia.

B. To study how gas temperature at the time of injection affects ignition delay. The temperatures range from approximately 900°F to 1500°F.

C. To study various combinations of pressures and temperatures to determine whether density is an independent variable affecting ignition delay.

D. To conduct all these studies with three fuels: CITE refree grade (Mil-F-45121) fuel, diesel no. 2 fuel, and Mil-G-3056 refree grade gasoline.

III. CUMULATIVE PROGRESS

Cumulative progress has been made in the following areas:

- A. Review and analysis of previous work.
- B. Theoretical analysis.
- C. Experimental work on Lister-Blackstone engine.
- D. Comparison between the present work done on the Lister engine and previous work in bombs and engines.
- E. Experimental work done on the ATAC open combustion chamber engine, using three different fuels.

Items A through D have been discussed in detail in previous progress reports. Item E will be discussed in the following paragraphs.

ITEM E: CUMULATIVE PROGRESS ON ATAC OPEN COMBUSTION CHAMBER ENGINE

The engine has been connected to an electric dynamometer. It is supercharged with shop air that has been passed through a surge tank fitted just before the engine. Another surge tank is fitted on the exhaust side. The pressures in the two tanks can be regulated to the required values.

A Kistler pressure transducer is fitted in the hole furnished by the International Harvester Company. Two more holes were drilled in the cylinder head above the piston cavity. One hole is fitted with a quartz window, and the other is fitted with a surface thermocouple.

The top dead center of the engine, as determined by the dial gage method, was found to be $1/2$ crank degree past the top dead center mark engraved on the flywheel.

The degree marks are produced by a steel disk 18 in. in diameter and $1/8$ in. thick, mounted on the coupling between the crankshaft and the dynamometer. Holes $1/16$ in. in diameter are drilled around the periphery at 3° intervals, and larger holes, $1/8$ in. in diameter, at 45° intervals. A magnetic pickup has been used to produce corresponding pips on the oscilloscope screen every 3° , with bigger pips every 45° . One of the bigger holes is aligned at top dead center.

The temperature of the inside surface of the combustion chamber is measured by a surface thermocouple placed between the inlet and exhaust valves.

The fuel-injection system is instrumented so that the start and rate of injection can be calculated from measurements of the needle lift and fuel pressure before the nozzle. The position of the plunger w.r.t., the barrel, and the injection timing are both controlled by micrometers.

An electric heater has been fitted between the critical flowmeter and the inlet surge tank. All the piping between the heater, engine, and exhaust tank are insulated by 1.5 in. thick calcium silicate pipe insulation.

The exhaust surge tank is cooled by spraying tap water into the tank. The direction of the spray is such as not to interfere with the flow of gases from the engine to the tank or with the exhaust thermocouple or smokemeter probe.

A new oscilloscope (Taktronix type 502A) and a new Polaroid camera are now in use to obtain and record the different traces for the combustion process in the engine. A special projected graticule is now in use with the camera, in order to eliminate the parallex which had been noticed before using this attachment.

The flow rate of blowby gases is measured by a flowmeter connected to the crankcase ventilation tube. An oil separator has been installed between the ventilating tube and the flowmeter to collect the oil droplets discharged with the blowby gases before reaching the flowmeter. The value of the blowby rate will be recorded together with all other data while running the engine.

The smoke produced in the exhaust of the ATAC engine is measured by a "Hartridge Smokemeter."

The different instruments used in this research project have been calibrated. These instruments are:

1. The critical flowmeter used to measure the rate of air flow into the engine.
2. Kistler pressure transducer (type 401A) together with the charge amplifier (type 655, S/N 1194). This transducer is used for measuring the gas pressure in the cylinder.
3. Kistler pressure transducer (type 601H) together with the charge amplifier (type 503, S/N 359). This transducer is used for measuring the fuel pressure before the nozzle.
4. The Bently distance detector used to measure the needle lift.
5. The surface thermocouple used to measure the inside wall surface temperature. The thermocouple output is found to agree with the standard thermocouple tables.

6. The Honeywell thermocouple (rotating disk type) used to measure the air, water, oil, and exhaust gas temperature.

Most of the computations needed for this project are now carried out on an IBM 7090 computer, in The University of Michigan Computing Center. Statistical and curve fitting procedures are made to assist in data synthesis programs, combustion analysis programs, and delay analysis programs.

IV. PROGRESS DURING THIS PERIOD

During this period the experimental work for the effect of temperature on I.D. and combustion characteristics of three different fuels have been completed. The air temperature before the inlet valve was changed over a range from 95°F to 750°F, in steps of 50°F.

Five series of runs have been made, with all the parameters held constant except the inlet air temperature and the inlet air pressure. These parameters include: the engine speed, the fuel-air ratio, the cooling water temperature, the injector opening pressure, and the injection timing. The fuels used in these tests are:

1. CITE refree grade (Mil-F-45121) fuel;
2. Diesel no. 2 fuel; and
3. Mil-G-3056 refree grade gasoline fuel.

These fuels have been purchased from the Ashland Oil and Refining Company and a copy of the certificates of analysis is given in Appendix A. Two batches of CITE fuel have been used in the experiments: Batch no. 13 dated December 3, 1965, and batch no. 19 dated March 29, 1967. The difference in their behavior in the engine is within the experimental error.

The five series of runs were made to study the following:

Series A1: Comparison between the three fuels under naturally aspirated conditions. Series A2A: Effect of temperature on I.D. of CITE fuel at constant inlet surge tank pressure of 15 in. Hg g. Series A2B: Effect of temperature on I.D. of CITE fuel at a constant mean pressure during the delay period. Series A2C: Effect of temperature on I.D. of diesel no. 2 fuel at a constant mean pressure during the delay period. Series A2D: Effect of temperature on I.D. of gasoline fuel at a constant mean pressure during the delay period. The mean pressures during the delay period were held constant for the three fuels.

All the data and results obtained from the last four series together with discussions are given in this report. The analysis of the results of Series A1, which is made to study the combustion kinetics of the different fuels under naturally aspirated conditions has not been finished yet as it includes a large amount of analytical and computational work. These results will be given in a future progress report.

In order to determine the thermodynamic state of the gases at any point in the cycle, the volume of these gases is required with the greatest accuracy possible. In order to achieve such accuracy the clearance volume of the engine

was calculated and the results checked by actual measurements. The details of these computations are given in Appendix B. The swept volume is also calculated at different crank angle positions, taking into consideration the eccentricity or offset of the piston pin in the piston. The details of these computations are given in Appendix C.

The present report also includes experimental results of interest, other than the ignition delays. These are:

1. Smoke intensity in the exhaust gases.
2. Wall temperature measured on the inside surface of the combustion chamber on the centerline between the inlet and exhaust valves.
3. Maximum pressures reached in the cycle.
4. Maximum pressure gradient due to combustion.
5. The rate of change of the pressure gradient from the end of ignition delay to the point of maximum pressure gradient.

The results of the present work on the ATAC engine are compared with the previous experimental work done in engines and in bombs. For this comparison the previous data were replotted and analyzed to compute the activation energy, and compare it with the values obtained on the ATAC engine.

The results of the comparison between the present and previous data indicated that the experimental activation energy is a function of some of the physical factors in engine performance. A theoretical study of the factors that affect the activation energy is being done, in an effort to correlate between the results of different investigators under the different running conditions. These studies are still on the way and will be reported as soon as they are finished.

V. CONCLUSIONS

These conclusions are based on the tests made on the three fuels during this reporting period.

A. IGNITION DELAY (I.D. _p)

1. For all the three fuels, the I.D. _p decreased continuously with the increase in temperature. A slight increase in the I.D. _p of CITE fuel has been noticed between 700°F and 745°F. The factors that might cause such a behavior are related to the mechanism of the chemical reactions taking place during the ignition delay.

2. The rate of decrease of the I.D. _p with the increase in temperature is greatest for gasoline. At a temperature of 106°F the ignition delay of gasoline is 2.142 times that of CITE fuel. But, at 700°F the ignition delay of gasoline is almost equal to that of the CITE fuel.

B. ACTIVATION ENERGY (E)

The temperature dependence of the ignition delay can be expressed in terms of an activation energy "E."* The activation energy can be considered equal to the minimum energy that should be achieved by the reactants before the start of combustion.

$$\text{I. D. } p = \frac{Ae^{E/RT}}{p^n}$$

where

A = constant

E = activation energy, Btu/lb mole

R = Universal gas constant, Btu/lb mole · °R

T = absolute temperature, °R

p = absolute pressure

n = index of pressure

*M. E. Elliott, "Combustion of Diesel Fuel," SAE Quart. Trans. 3, 1949.

The experimental results show that the activation energy for the different fuels is as follows:

<u>Fuel</u>	<u>E, Btu/lb mole</u>
Diesel no. 2	5,230
CITE fuel	10,430
Gasoline fuel	14,780

C. NOISE

Two methods have been used to find the noise level: (1) Direct observation. (2) Analysis of the pressure crank angle traces to determine the maximum pressure gradient and its rate of change. At atmospheric temperature the highest noise level is produced with the engine running on gasoline. However, at high inlet temperatures, above 600°F, the noise level with gasoline is the same as CITE and diesel fuels.

D. SMOKE

The smoke is measured with a Hartridge smokemeter. The lowest smoke concentration is obtained with gasoline, followed by diesel no. 2 fuel. CITE fuel produced the highest smoke intensity. The high smoke level of CITE fuel is partly due to the after-injection which has been observed with this fuel.

E. TROUBLES IN ENGINE PERFORMANCE

1. The fuel leakage past the injector needle and the fuel plunger has been noticed to be excessive with CITE and gasoline fuels. This required frequent change of the lubricating oil in the fuel-pump sump, and cleaning of the injector.

2. Gasoline fuel produced a deposit over the injection system parts and required frequent cleaning.

VI. PROBLEM AREAS AND CORRECTIVE ACTION

A. FUEL LEAKAGE

Problem. Gasoline and CITE fuels have high leakage rates past fuel injection nozzle needle. In average, the rates of leakage of the different fuels are as follows:

Diesel = 0.07 litre/hr
CITE = 0.26 litre/hr
Gasoline = 0.38 litre/hr

Corrective Action. A visit was made to American Bosch Company in Springfield, Massachusetts, to discuss this problem with them. We found that they construct a special plunger barrel assembly to avoid this excessive leakage by means of a relief annulus. Buying this assembly is now under consideration.

B. DRAINAGE OF FUEL-PUMP SUMP

Problem. The drainage of lubricating oil from pump-sump was found impossible without taking the pump off the bracket.

Corrective Action. A slot is made opposite to the drainage plug. The original slot made in the bracket was on the wrong side.

C. SURFACE THERMOCOUPLE FAILURE

Problem. The thermocouple output was found faulty due to a break in the silver solder holding the top piece to the adapter.

Corrective Action. The sensing tip of the thermocouple was checked and found in good condition. A new adapter was designed and constructed to hold the top to the adapter by a screw connection thus ensuring proper operation.

D. FAILURE OF PRESSURE TRANSDUCERS

Problem. Failure occurred after 75 working hours in the fuel injection line.

Corrective Action. A spare transducer is ordered. This represented an expenditure of about \$330.00 for the replacement of the faulty transducer. This cost is after a credit of \$50.00 made for the trade-in.

E. FOULING OF INJECTION NOZZLE HOLES AND NEEDLE

Problem. Fouling of injection nozzle holes and needles have been noticed with CITE fuel and gasoline.

Corrective Action. A Robert Bosch nozzle cleaning kit, and a nozzle re-conditioning kit were ordered and are now in use for cleaning purposes.

F. FAILURE OF 502A OSCILLOSCOPE

Problem. Lower beam of this scope was noticed not to operate properly.

Corrective Action. This was fixed in the Mechanical Analysis Laboratory of the Department of Mechanical Engineering. Spare parts and labor costs were charged to Tektronix Company.

VII. FUTURE PLANS

A. NEXT PERIOD

1. Experimental

a. To run tests on the ATAC open chamber engine, to find effect of pressure on ignition delay and combustion phenomena of CITE fuel.

b. To study the effect of speed on I.D.

c. To prepare the cooling system for the use of ethylene glycol instead of water.

2. Analytical

To study the kinetics of the combustion process as far as its effect on the ignition delay and combustion characteristics of the different fuels.

B. OVERALL

1. Experimental

a. To run tests on the ATAC open chamber engine, to find the effect of raising the coolant temperature to 250°F on ignition delay and combustion phenomena of CITE fuel.

b. To study the effect of raising the coolant temperature to 250°F on the injection process and on the engine performance in general.

2. Analytical

To analyze the data published by other investigators, on ignition delays in bombs and engines, in order to compare their results with the results of the ATAC engine.

VIII. SIGNIFICANT ACCOMPLISHMENTS

All the tests on the effect of temperature on the pressure-rise delays are completed for CITE, diesel, and gasoline fuels. The results showed that all the instruments are operating properly and showed a very good degree of reproducibility.

All the computer programs prepared for this project are ready to record, compute, and analyze the data. A comparison between the results obtained with the ATAC engine and from formulae based on previous research has also been made with the aid of the computer. This analytical work will continue. This is being done in an effort to reach general conclusions regarding the cause of the discrepancy between tests in bombs and in engines. A comparison between the results of ignition delay in different engines will also be made.

IX. PROJECT STATUS

FUNDS AND EXPIRATION DATE OF CONTRACT

Original contract	
July 1, 1964 to January 1, 1965	\$ 23,020
Modification No. 7	
Extension of contract to February 28, 1966	
Addition of \$18,000 to contract funds for a total of	41,020
Modification No. 8	
Extension of contract to February 27, 1967	
Addition of \$37,000 to contract funds for a total of	78,020
Modification No. 10	
Extension of contract to December 1, 1967	
Addition of \$45,000 to contract funds for a total of	123,020
Modification No. 12	
Extension of contract to December 1, 1968	
Addition of \$45,000 to contract funds for a total of	168,020

PART II

EXPERIMENTAL DATA AND RESULTS

X. DATA AND RESULTS OF A SAMPLE RUN

A. RECORDED DATA (Photographs)

A sample of the traces recorded during a test on the ATAC engine are shown in Figs. 1 to 8, for run number 13, with CITE fuel.

The following are the test conditions and results for this run.

B. TEST CONDITIONS (as they Appear in Computer Sheets)

Speed = 1999 rpm
Load on dynamometer = 9.0 lb
Mass of fuel consumed, "D"* = 0.5007 lbm
Critical flowmeter orifice, "D"* = 7/32 in. dia
Time for fuel consumption = 5.79 min
Fuel leakage past injector = 0.17 liters/hr
Air pressure before flowmeter orifice = 38.1 psig
Air temperature before flowmeter orifice = 79°F
Air temperature before inlet valve = 464°F
Cooling water temperature at outlet = 167°F
Barometric pressure = 29.2 in. Hg
Surge tank pressure = 15.1 in. Hg
Exhaust temperature = 851°F
Smokemeter reading = 30 H.U.

C. RESULTS OBTAINED FROM TRACES

Minimum inside wall surface temperature = 454°F
Temperature swing on inside surface = 47°F
Pressure at close of I.V. w.r.t. surge tank pressure = 3.0 psi
Pressure in cylinder at the start of injection, w.r.t. pressure at I.V.C. = 415 psi
Pressure at the end of ignition delay w.r.t. to pressure at start of injection = 194 psi
Start of needle lift before T.D.C. = 21.4° C.A.
End of ignition delay before T.D.C. = 13.4° C.A.

*Refer to Appendix D.2 for identification.

D. COMPUTED RESULTS

Brake horsepower = 6.0
 BMEP = 33.2 psi
 BSFC = 0.817 lbm/BHP hr
 Fuel-air ratio = 0.0317
 Air/cycle in (lbm/1000) = 2.58
 Exhaust gases/cycle in (lbm/1000) = 0.11
 Surge tank pressure = 21.8 psia
 Volumetric efficiency = 98.0%
 Temperature at I.V.C. = 477°F
 Pressure of charge at start of injection = 440 psia
 Density of charge at start of injection = 0.609 lbm/cu ft
 Temperature of charge at start of injection = 1926°R
 Average pressure during I.D. = 533 psia
 Average density during I.D. = 0.707 lbm/cu ft
 Average temperature during I.D. = 2010°R
 I.D._p = 0.667 msec

E. COMPARISON BETWEEN MEASURED I.D._p WITH THAT CALCULATED FROM VARIOUS FORMULAE

TABLE 1

COMPARISON BETWEEN MEASURED I.D._p WITH THAT CALCULATED FROM VARIOUS FORMULAE

Formula	Calculated I.D. _p		Measured, msec
	Based on Conditions at Start of Injection	Based on Average Conditions During I.D.	
Wolfer	0.595	0.394	.667
Elliott	1.930	1.851	.667
Sitkei	1.406	1.119	.667
Tsao (at 1000 rpm)	0.924	0.702	.667

Sample of Recorded Data
ATAC - Open Chamber
Run No. 13

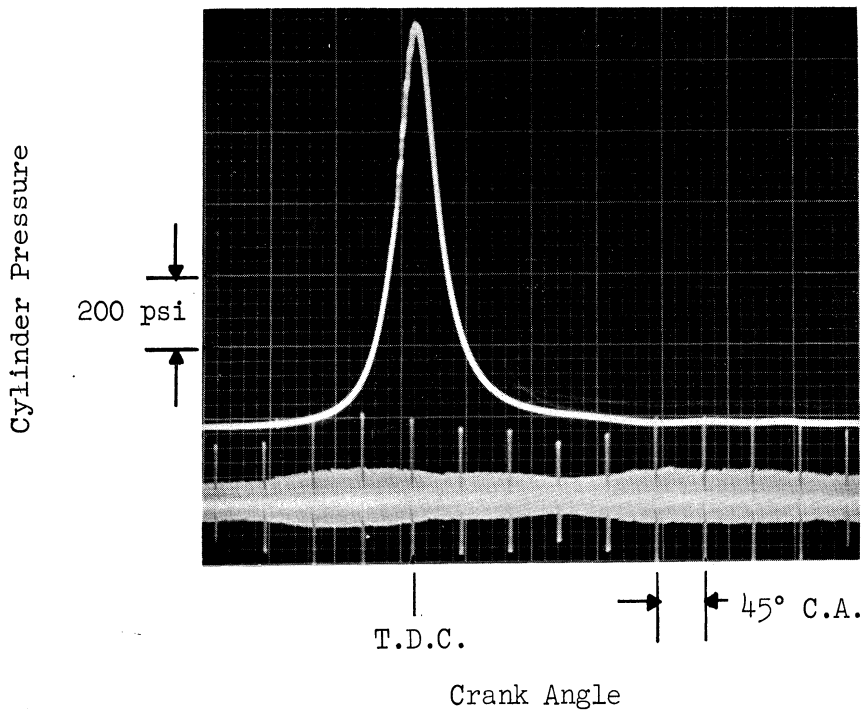


Fig. 1. Cylinder pressure for one complete engine cycle.

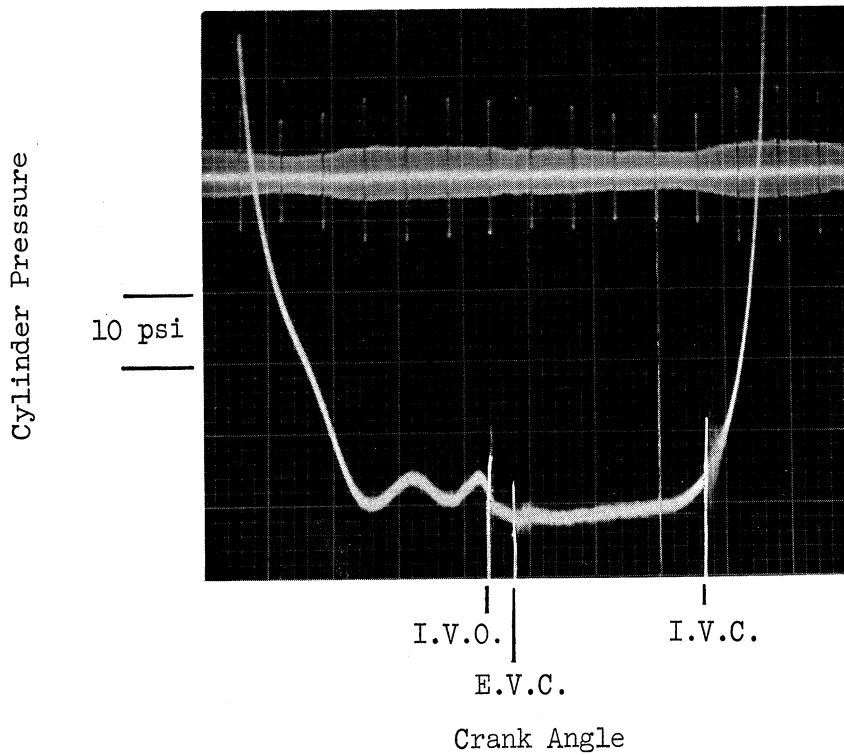


Fig. 2. Cylinder pressure for the exhaust and inlet strokes.

Sample of Recorded Data
ATAC - Open Chamber
Run No. 13

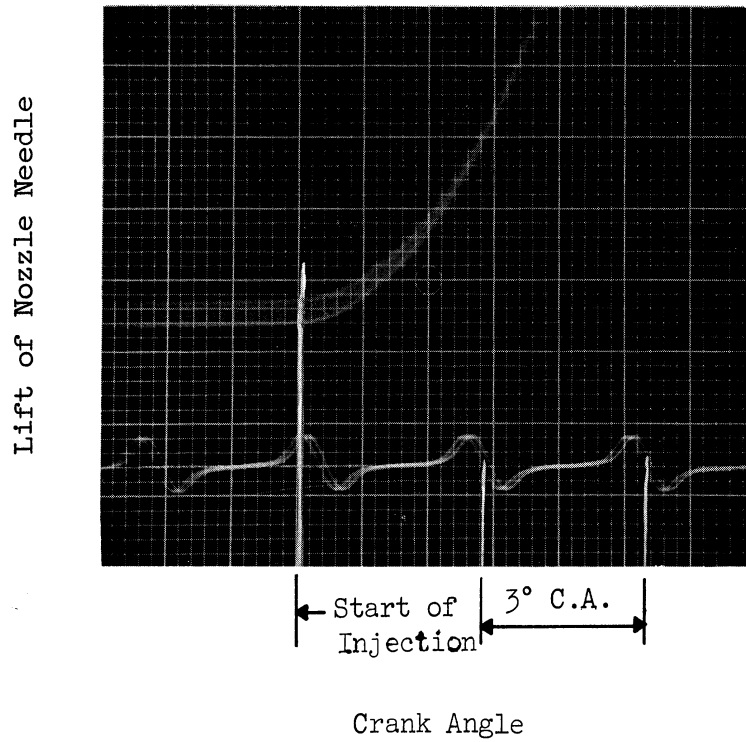


Fig. 3. Needle lift at start of injection.

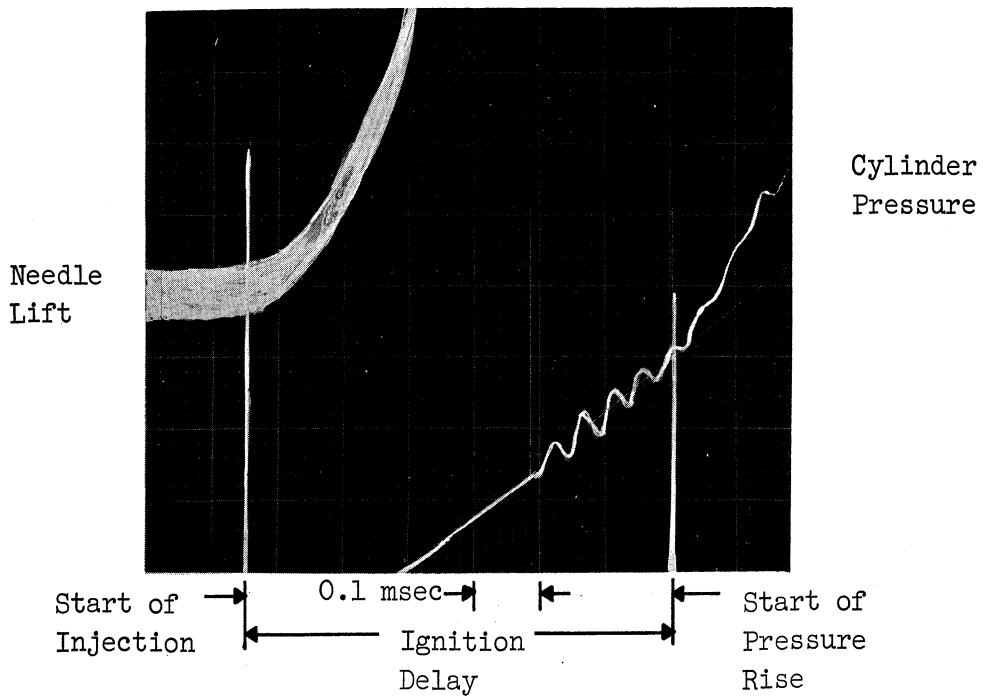


Fig. 4. Measurement of I.D._p from cylinder pressure and needle lift traces.

Sample of Recorded Data
ATAC - Open Chamber
Run No. 13

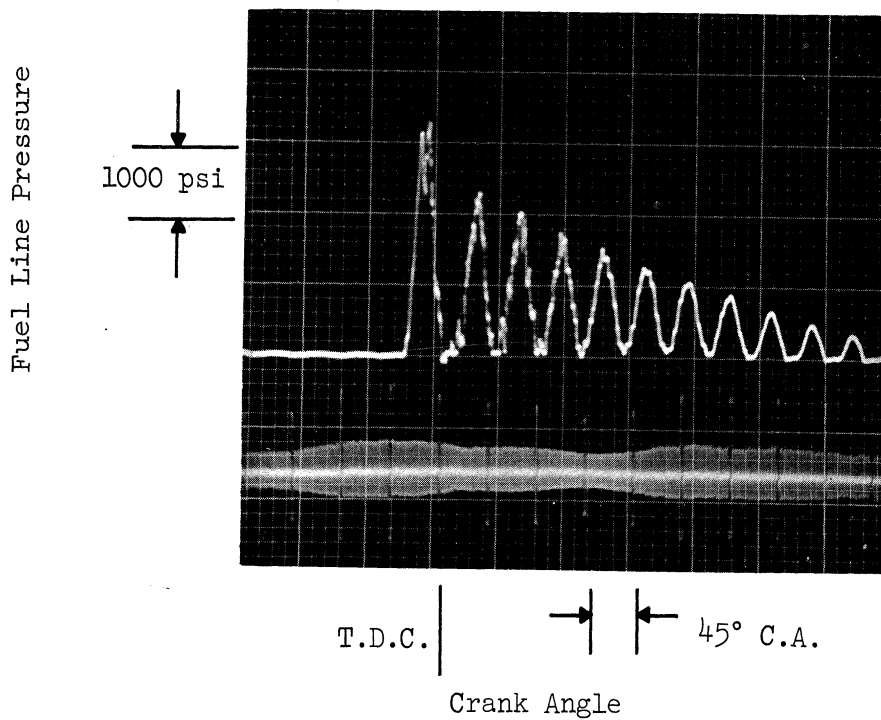


Fig. 5. Fuel line pressure.

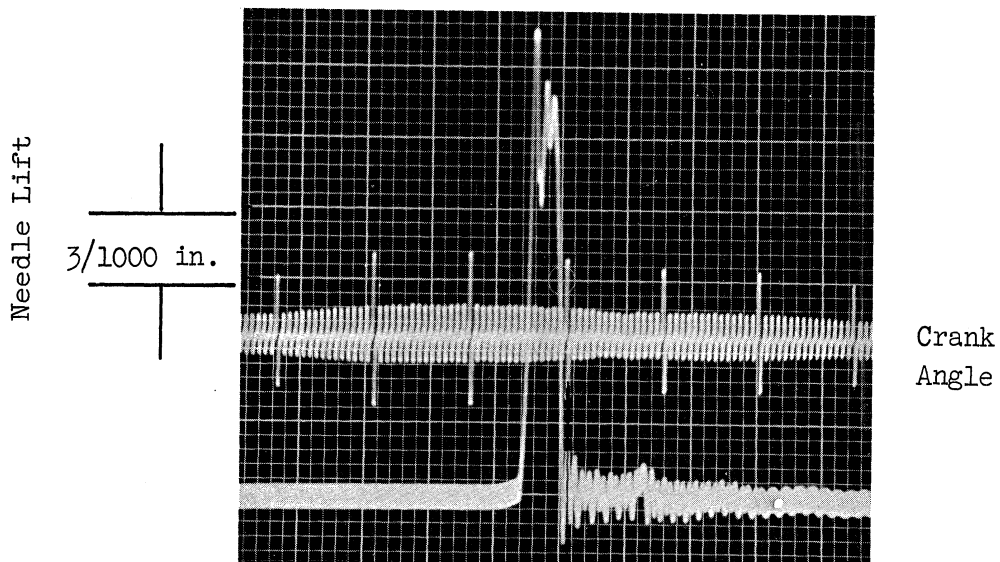


Fig. 6. Needle lift diagram.

Sample of Recorded Data
ATAC - Open Chamber
Run No. 13

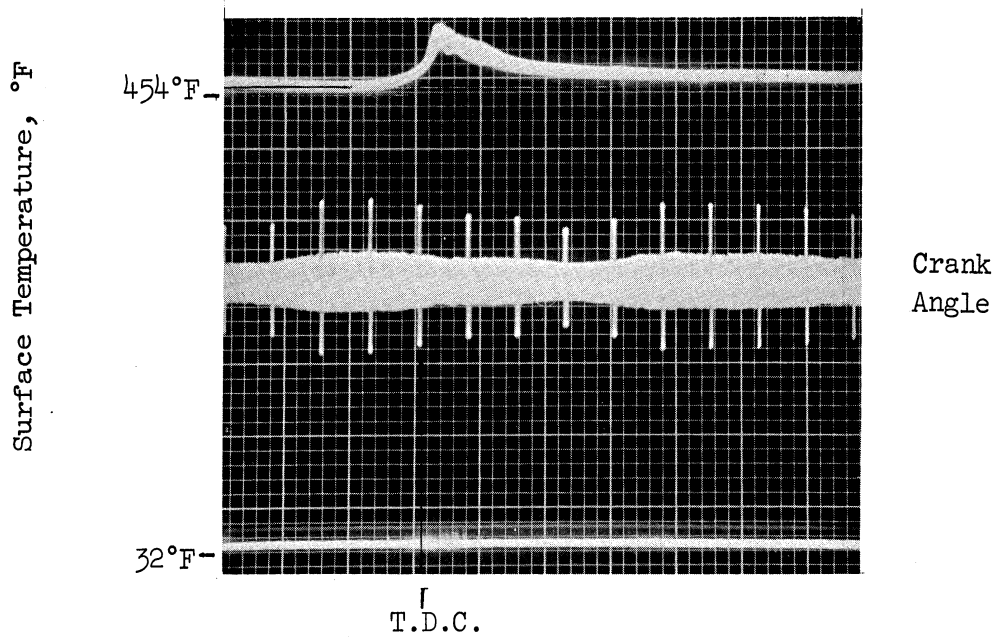


Fig. 7. Combustion chamber surface temperature.

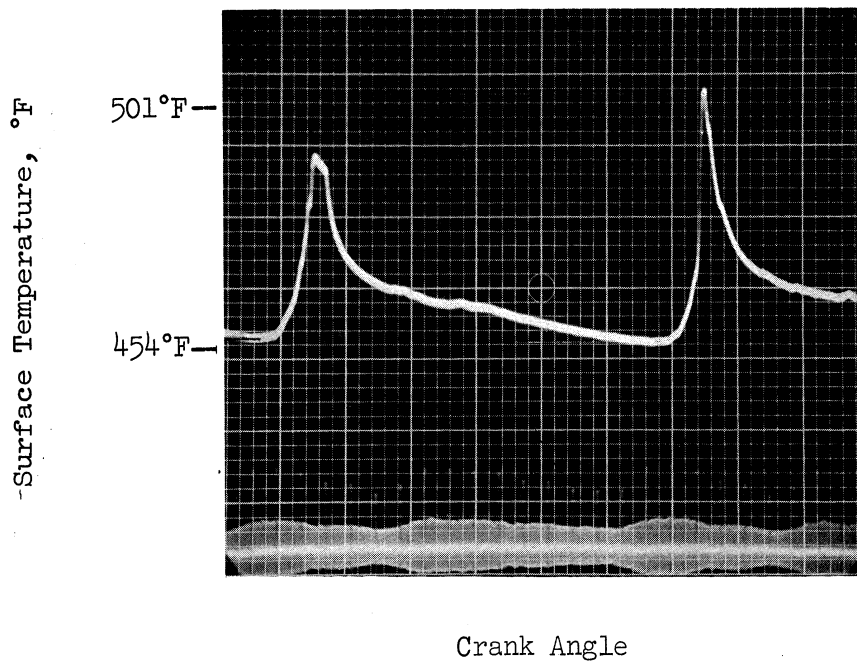


Fig. 8. Swing in wall-surface temperature.

XI. EXPERIMENTAL WORK AND RESULTS

A. SERIES A2A

Effect of Temperature on I.D. p of CITE Fuel, at Constant Inlet Surge Tank Pressure

Conditions:

Fuel = CITE refree grade (Mil-F-45121) fuel
Intake air pressure in surge tank = 15 in. Hg g
Exhaust pressure in surge tank = 15 in. Hg g
Cooling water temperature at outlet = 169°F
rpm = 2000
Fuel-air ratio = 0.0316
Injector opening pressure = 3000 psi
Injection timing (needle lift) = 21.3° BTDC

Variable:

Inlet air temperature from 97°F to 513°F.

The results of this series indicate that the pressure at the start of injection, as well as the average pressure during the ignition delay, vary with change in inlet air temperature.

An increase in the inlet air temperature from 97°F to 513°F caused a drop of 97 psi in the gas pressure at the start of injection, and a drop of 191 psi in the average pressure during the delay period. The pressure at the start of injection at different inlet temperatures is shown in Fig. 9. The corresponding average pressures are shown in Fig. 10.

The drop in pressure at higher temperatures is mainly due to the increased heat losses from the gases to the cylinder walls.

The results of this series concerning I.D. are given in Table 8 and plotted in Fig. 11, curve A. It shows that in the range of temperatures between 100°F to 501°F the ignition delay decreases continuously with increase in temperature.

It should be noted that the net change in I.D. is due to two opposing factors:

1. An increase in gas temperature which causes a decrease in ignition delay.

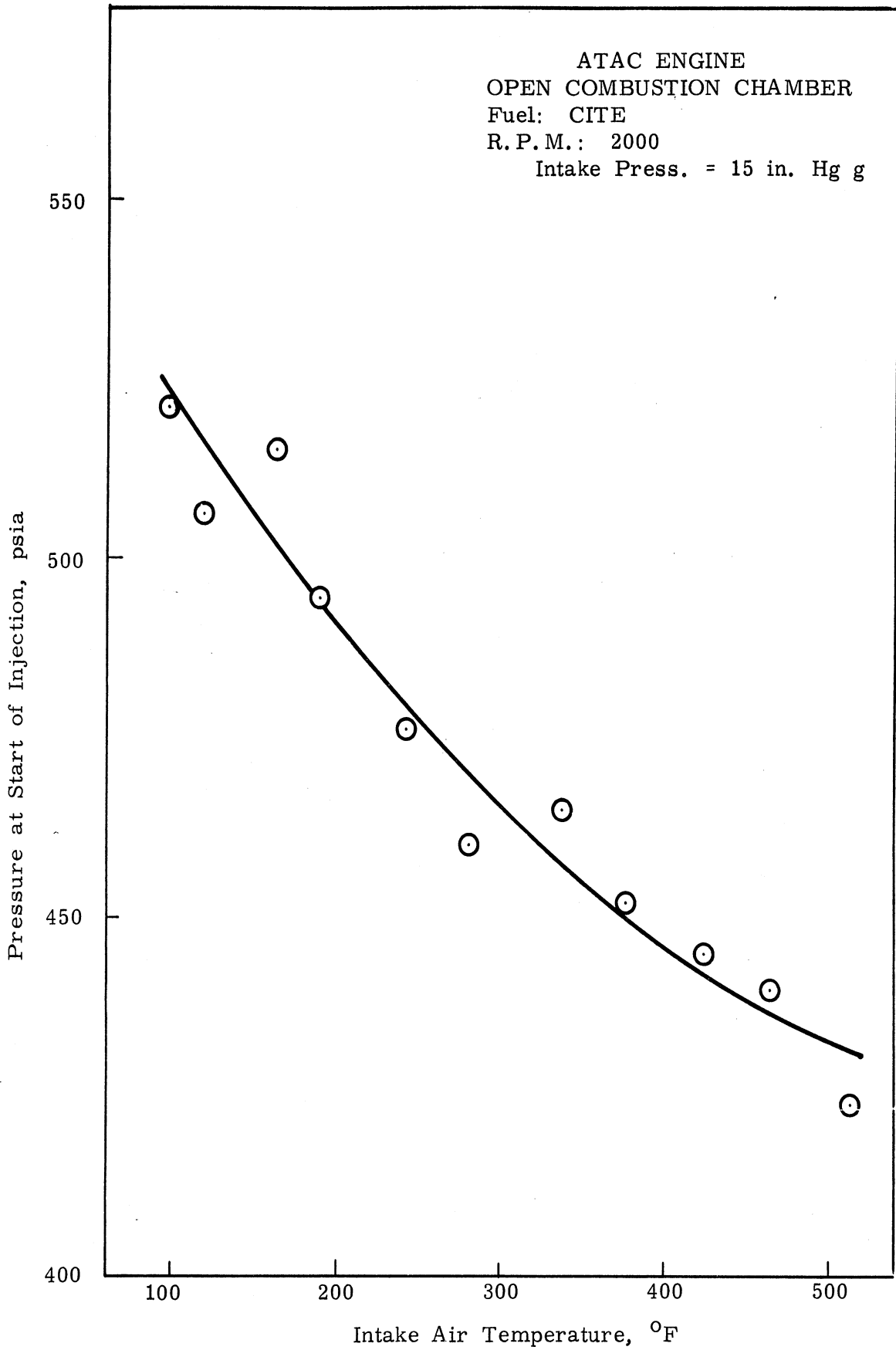


Fig. 9. Effect of intake air temperature on pressure at the start of injection (surge tank pressure = 15 in. Hg g).

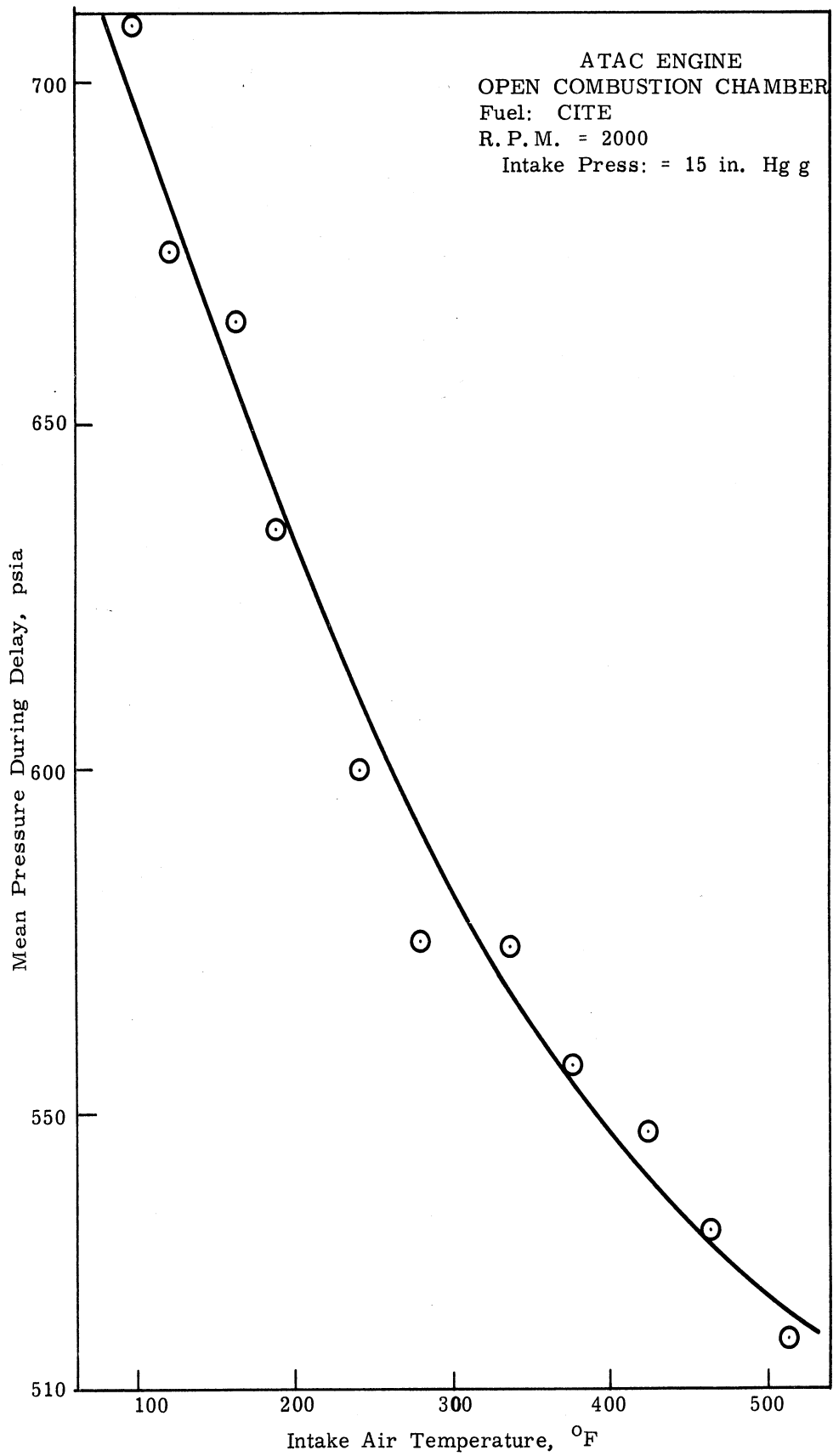


Fig. 10. Effect of intake air temperature on mean pressure during ignition delay (surge tank pressure = 15 in. Hg g).

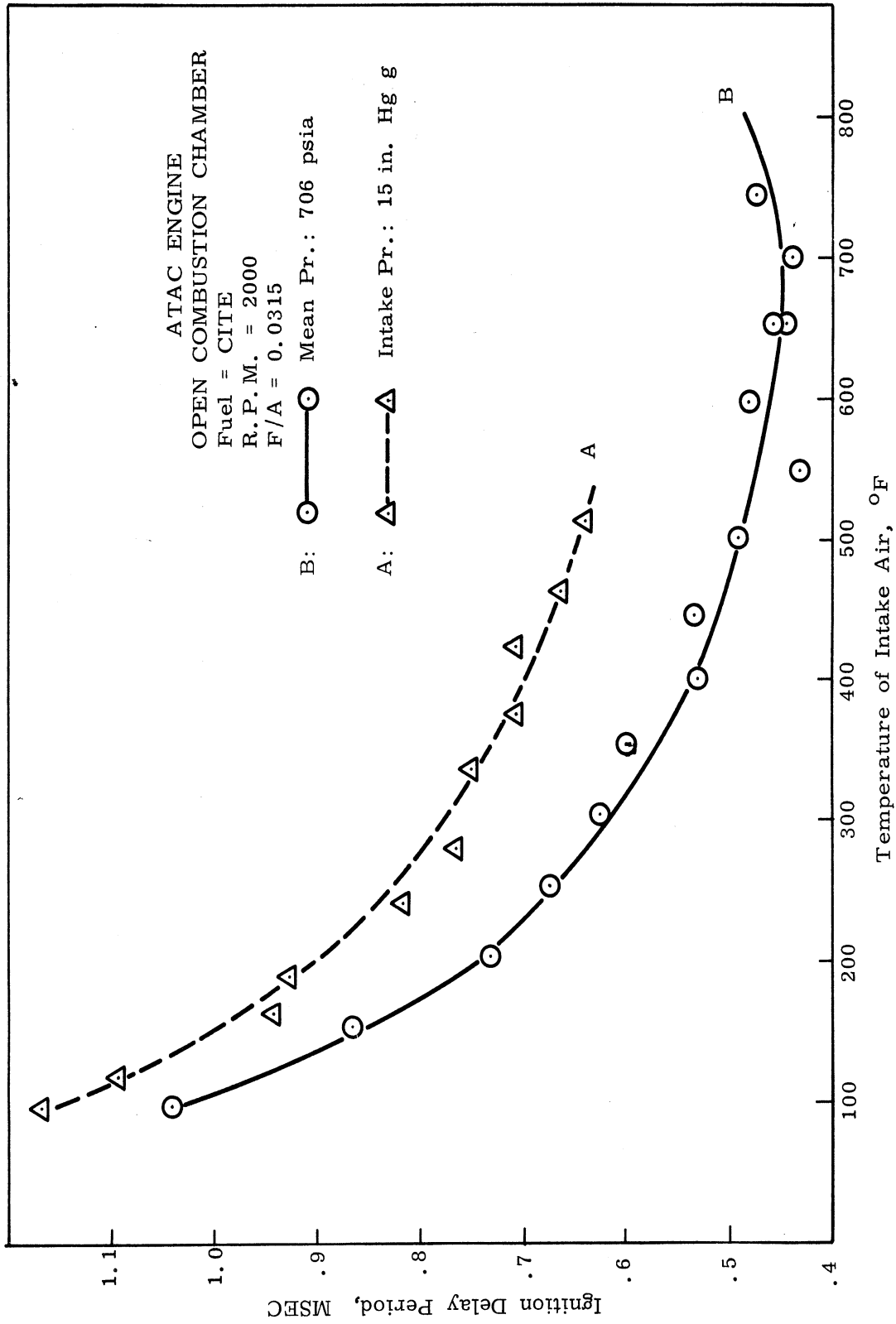


Fig. 11. Effect of temperature on I.D.p of CITE fuel.

2. A drop in gas pressure causing an increase in ignition delay.

In order to eliminate the effect of pressure on I.D., the surge tank pressure was changed in each run, such that the mean pressure during the delay period remains constant. The results of these tests are plotted in Fig. 11, curve B, and are discussed under series A2B.

Wall Surface Temperature

The temperature of the inside surface of the combustion chamber is measured by a special thermocouple placed between the inlet and exhaust valve and on the line between their two centers. A record of the surface temperatures is shown in Figs. 7 and 8, together with the crank angles.

In Fig. 7 the surface temperature is shown together with the reference temperature, which is 32°F. The minimum temperature in this photograph is 454°F. The temperature swing due to combustion as indicated in the photograph of Fig. 8, reached 47°F.

The change of the minimum surface temperature for this series is plotted in Fig. 12. It shows that the minimum temperature has changed from 354°F, at 97°F inlet air temperature, to 483°F at 513°F inlet air temperature.

B. SERIES A2B

Effect of Temperature on I.D. _p of CITE Fuel, at a Constant Mean Pressure During the Ignition Delay

To maintain the average pressure during the ignition delay constant, the surge tank pressure was increased with temperature. The average pressure during the delay period was kept at a constant mean value of 706 psia for all the runs of this series.

Conditions:

Fuel = CITE refree grade (Mil-F-45121) fuel
Mean pressure during delay period = 706 psia
rpm = 2000
Fuel-air ratio = 0.0315
Injector opening pressure = 3000 psi
Injection timing (needle lift) = 20.9 BTDC
Cooling water temperature at outlet = 171°F

Variables:

Inlet air temperature from 97°F to 745°F
Inlet air pressure from 15 in. Hg to 41.9 in. Hg g

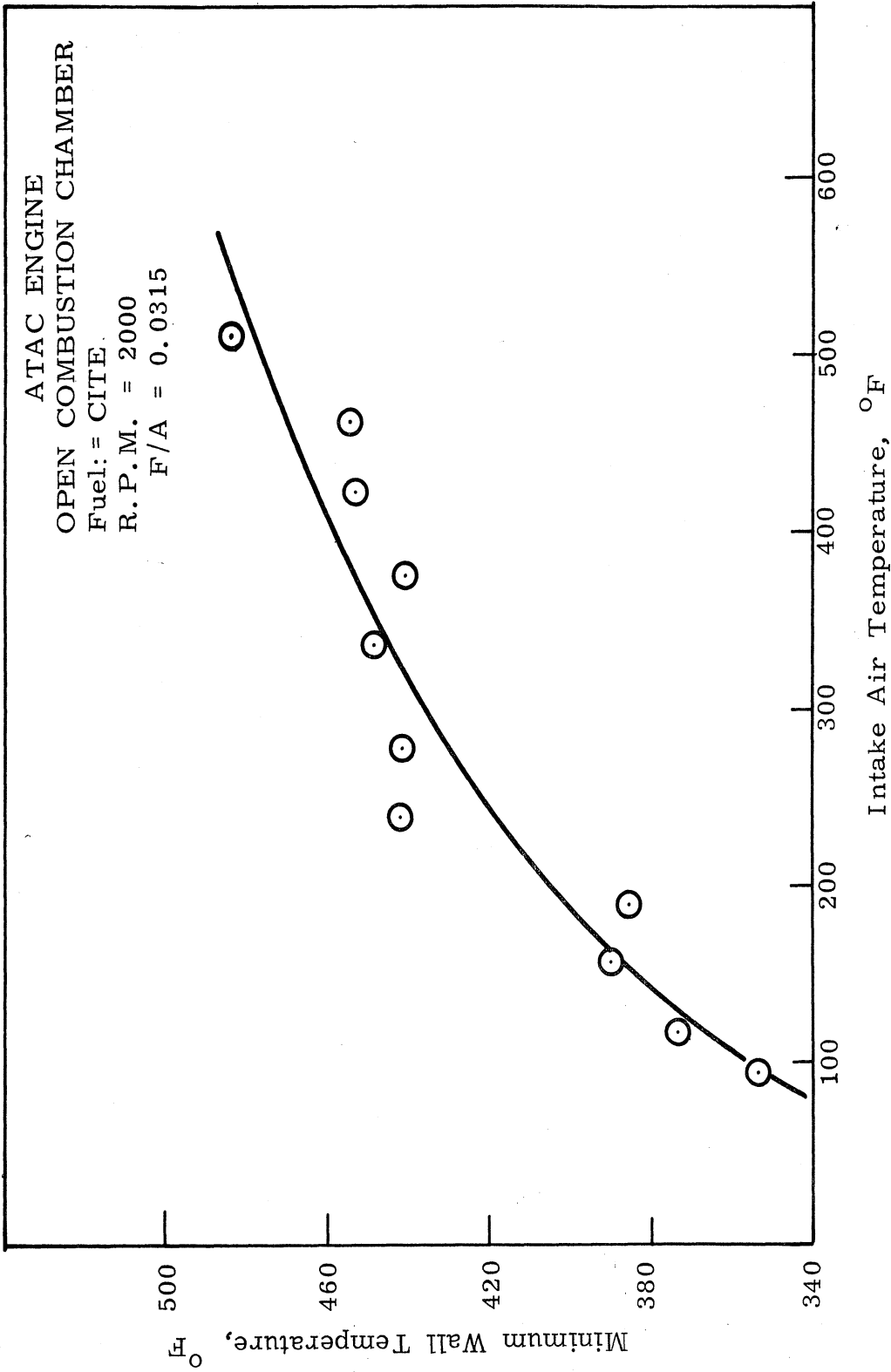


Fig. 12. Effect of intake air temperature on minimum combustion chamber wall surface temperature.

In order to keep the mean pressure at a constant value of 706 psia, the pressure in the inlet surge tank was 15 in. Hg boost at 97°F and reached 41.9 in. Hg boost at 745°F. The values of the air surge tank pressure are plotted as a function of the inlet air temperature in Fig. 13.

The results of this series of runs are plotted in Figs. 11, curve B, and Fig. 14. Figure 11, curve B, shows the results at constant average pressure together with the results at constant surge tank pressure (curve A).

The increase in ignition delays shown by curve A, above the values of curve B, are due to the lower pressures occurring during the delay period.

The results for the I.D. _p for CITE fuel are plotted in Fig. 14. The ignition delay decreases with increase in temperature up to about 2150°R after which it appears to increase.

Effect of Intake Air Temperature on the Volumetric Efficiency

In this report the volumetric efficiency is defined as:

$$\text{Volumetric efficiency} = \frac{\text{Actual mass flow rate}}{\text{Theoretical mass flow rate based on intake manifold conditions}}$$

The change in the volumetric efficiency at the different air temperatures, for test series A2A and A2B is shown in Fig. 15. It shows a slight drop in efficiency between 556°R and 600°R and a continuous increase with any further increase in temperature. This change is caused by the heat transfer phenomena between the air and the manifold and cylinder walls.

The change in the flow rate of air at the different temperatures is given in Fig. 16. It shows that for series A2A the air mass is reduced by 37.4% with the increase in inlet air temperature from 97°F to 513°F. This reduction is not so great in series A2B because the inlet surge tank pressure was changed to give a constant average pressure of 706 psia during the delay period.

C. SERIES A2C

Effect of Temperature on I.D. _p of Diesel Fuel, at a Constant Mean Pressure During the Ignition Delay

Conditions and Variables:

These are the same as in series A2B except that the fuel used is diesel no. 2.

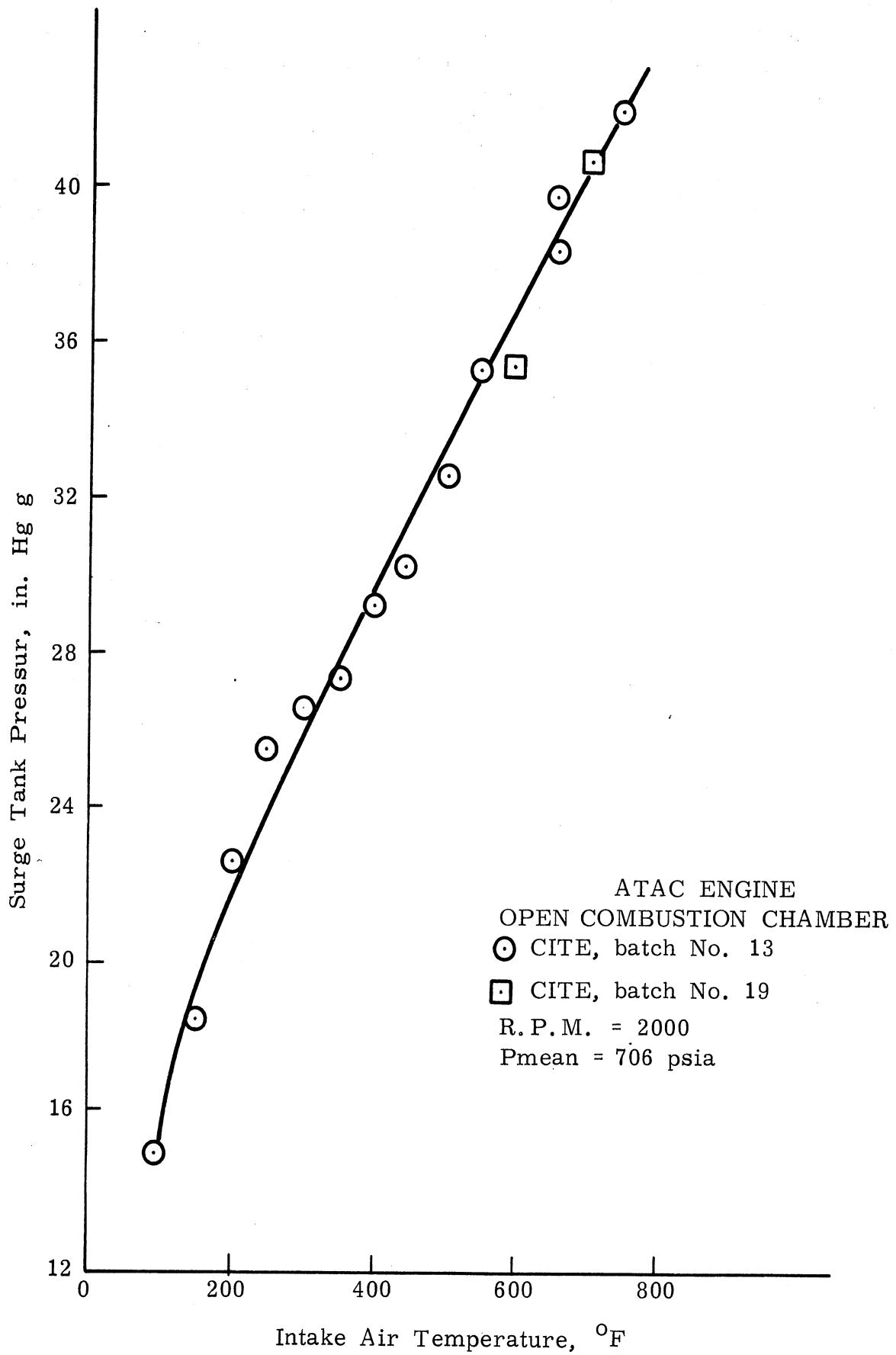


Fig. 13. Surge tank pressure at various intake temperatures, for a constant mean pressure of 706 psia during I.D.p.

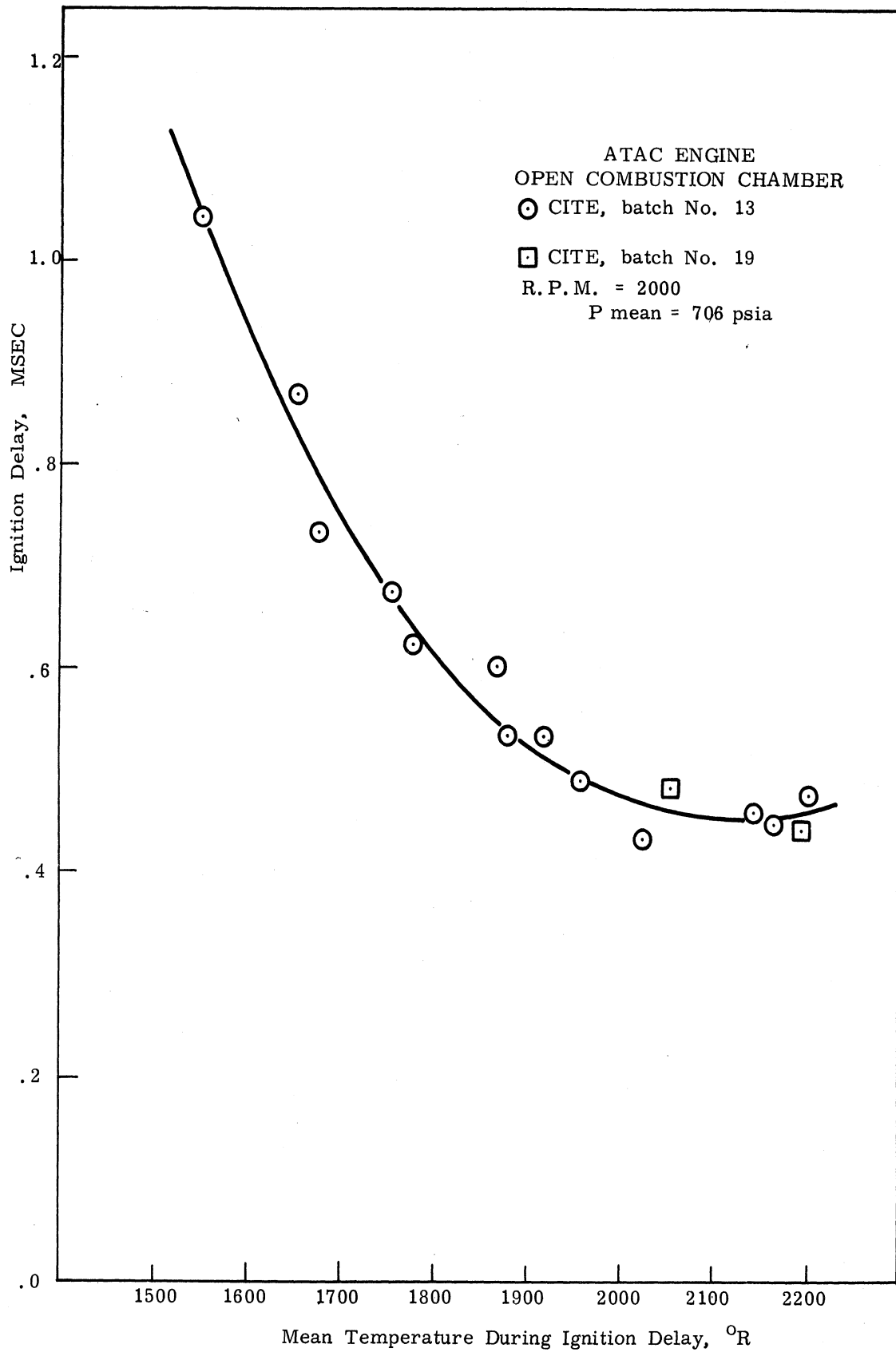


Fig. 14. Ignition delay, $I.D._p$ as a function of mean temperature during ignition delay for CITE fuel.

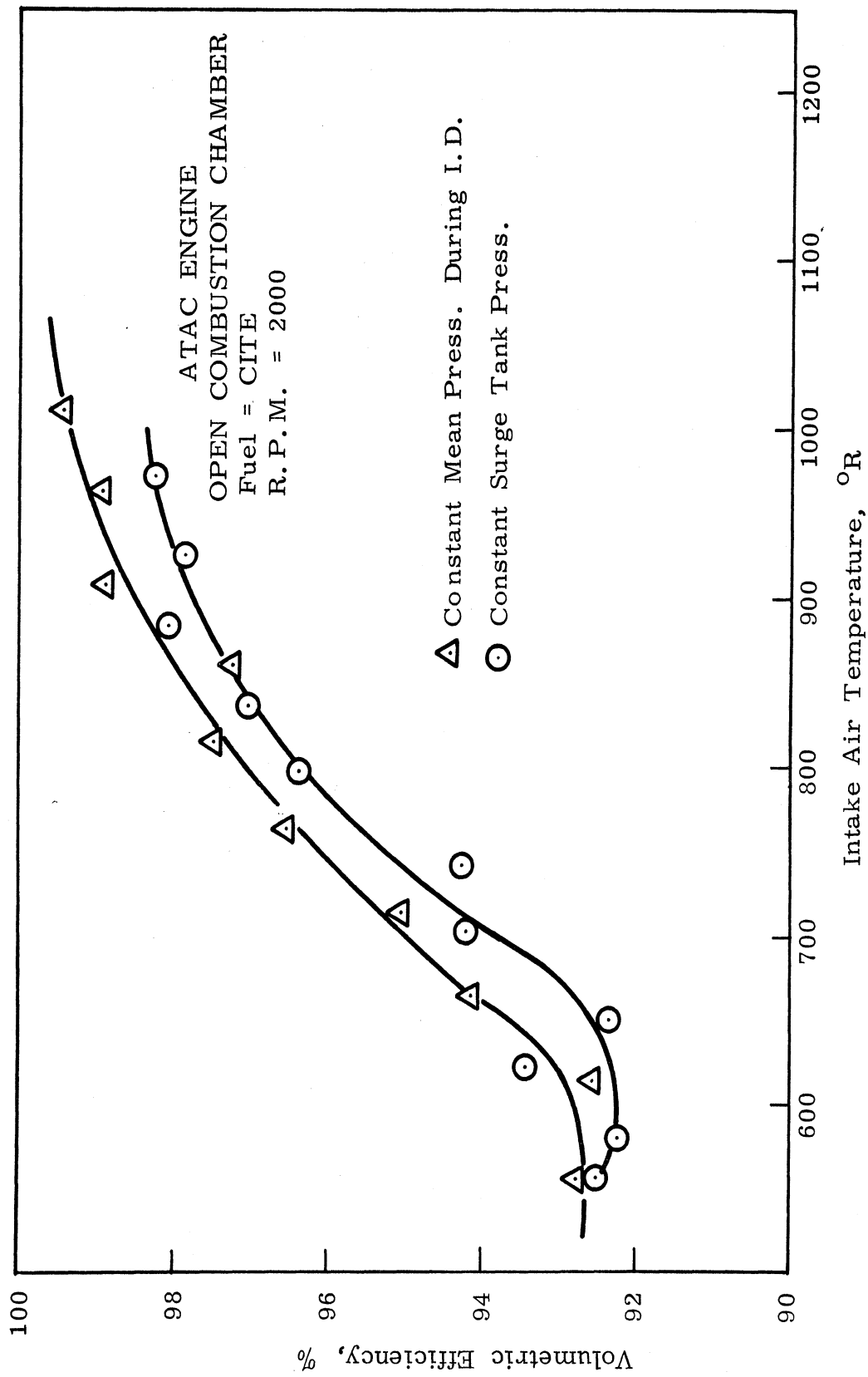


Fig. 15. Effect of intake air temperature on the volumetric efficiency.

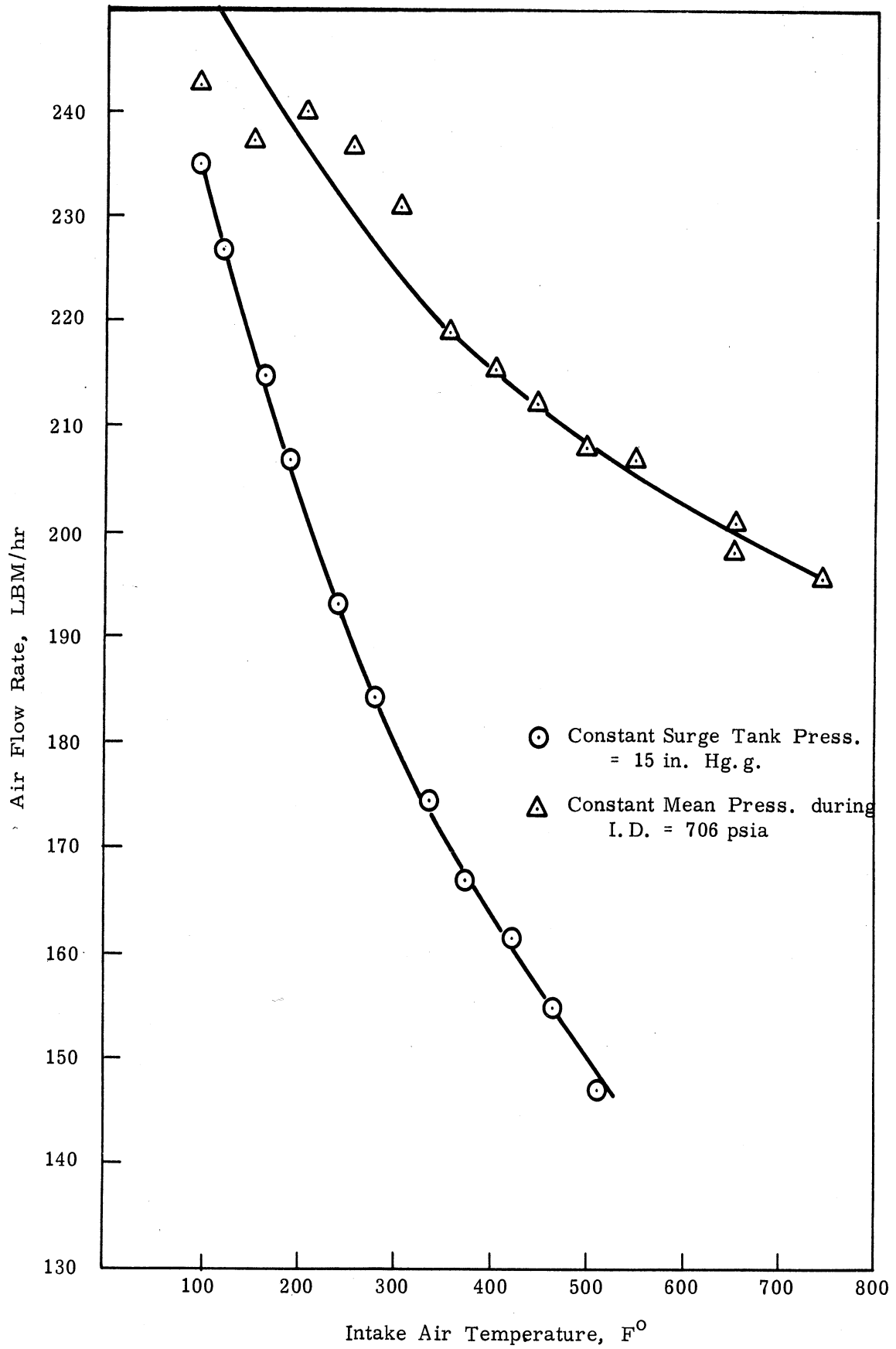


Fig. 16. Mass-flow rate at various intake air temperatures.

The results of this series of tests are shown in Fig. 17. It shows a drop of 40.3% in I.D. by an increase in the mean air temperature during I.D. from 1565°R to 2292°R.

D. SERIES A2D

Effect of Temperature on I.D. _p of Gasoline Fuel at a Constant Mean Pressure During the Ignition Delay

Conditions and Variables:

These are the same as in series A2B except that the fuel used is Mil-G-3056 ree-free grade gasoline fuel.

The results of this series of tests is shown in Fig. 18. It shows a drop of 76.2% in I.D. by an increase in the mean air temperature during I.D. from 1665°R to 2500°R.

Summary of Observations made on Gasoline Combustion

Many attempts have been made during this reporting period to examine the factors that affect the combustion of gasoline in the ATAC engine. First, in Series A1 of these tests, the engine has been run on gasoline with simulated naturally aspirated conditions. No combustion was observed. In order to obtain burning the speed was reduced to about 900 rpm, and irregular combustion was observed.

It has been interesting to note that, with atmospheric inlet air temperature, an increase of 15 in. Hg in the air pressure in the surge tank made the combustion much more regular, although the I.D. was very long.

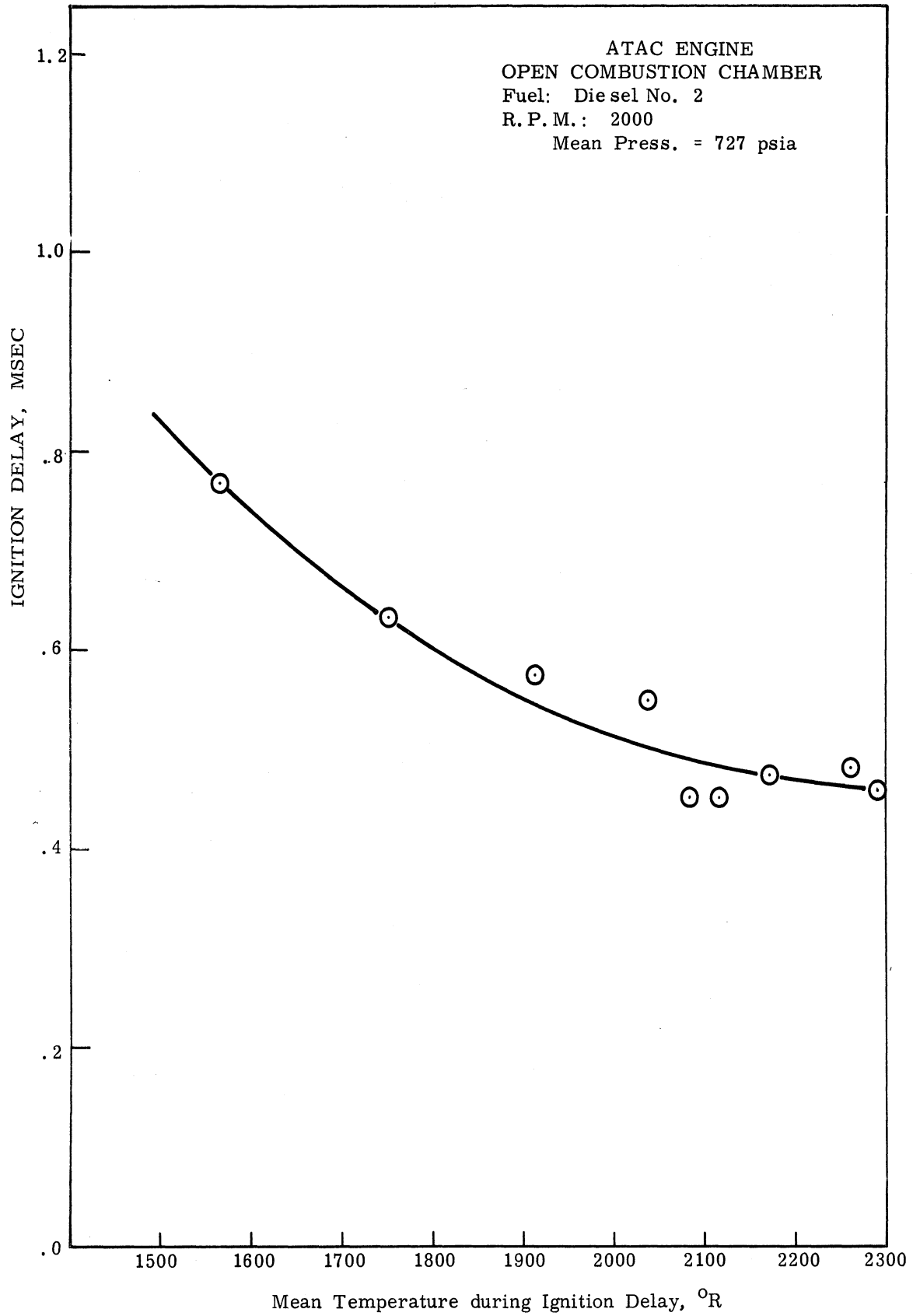


Fig. 17. Ignition delay $I.D._p$ as a function of mean temperature during ignition delay for diesel no. 2 fuel.

ATAC ENGINE
OPEN COMBUSTION CHAMBER
Fuel: Gasoline
R. P. M. = 2000
Mean Press. = 705 psia

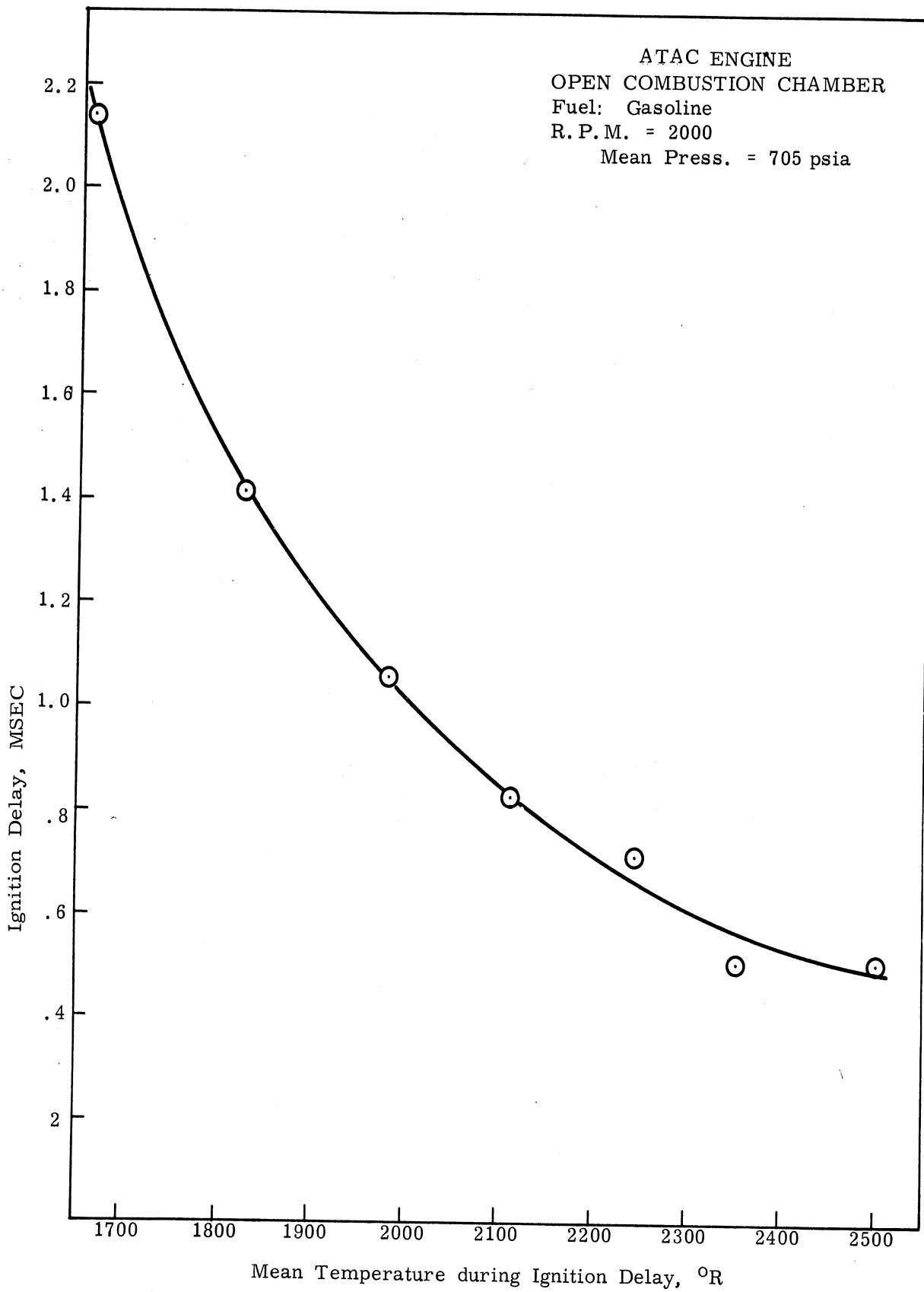


Fig. 18. Ignition delay, I.D._p, as a function of mean temperature during ignition delay for gasoline fuel.

XII. COMPARISON BETWEEN THE THREE FUELS

A comparison will be made between the CITE, diesel, and gasoline fuels, regarding their combustion characteristics. This comparison covers the following:

- A. Delay period and activation energy
- B. Noise level
 - 1. Maximum pressure
 - 2. Maximum pressure gradient
 - 3. The rate of change of pressure gradient
- C. Smoke intensity in exhaust
- D. Specific fuel consumption.

A. DELAY PERIOD AND ACTIVATION ENERGY

To compare between three fuels, all the results of I.D. are plotted on the same diagram in Fig. 19. It shows that diesel no. 2 has the lowest ignition delay, while gasoline has the highest values.

At a temperature of 106°F the gasoline has an ignition delay of 2.142 msec, while the values for CITE and diesel are 1.0 msec and 0.752 msec, respectively. However, at an air inlet temperature of 700°F the three fuels have almost equal ignition delays of 0.45 msec.

The difference between the CITE fuel and diesel no. 2 fuel is probably not significant for inlet air temperatures above 200°F.

The values for I.D. are plotted in Figs. 20, 21, and 22 for the different fuels on a log scale versus the reciprocal of the absolute temperature. The slope of these lines gives the value of (E/R) , where E is the activation energy and R is the universal gas constant. The value of the activation energy for the different fuels, as calculated from the corresponding graphs is given in Table 2.

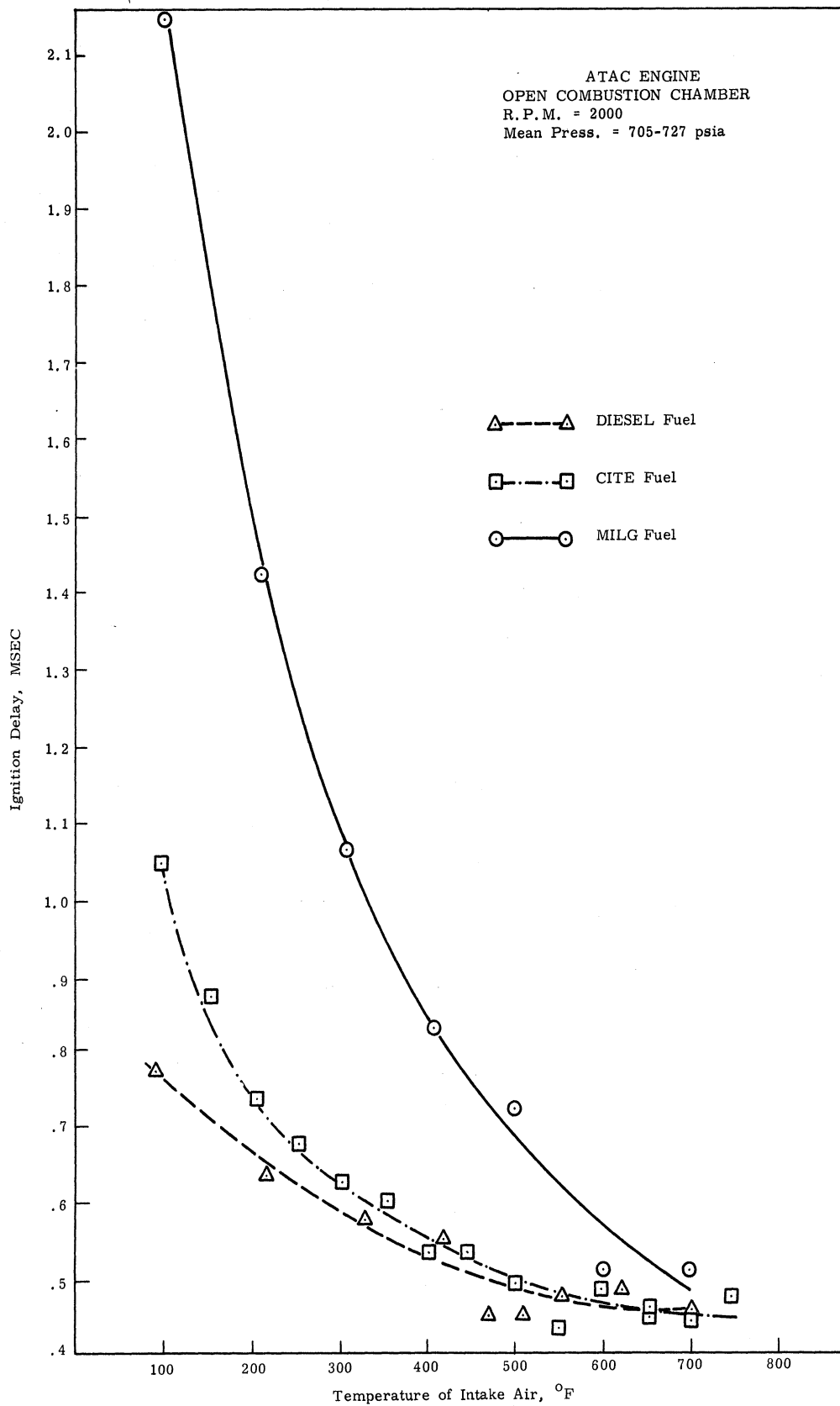


Fig. 19. Comparison between the ignition delay, I.D._p, of different fuels.

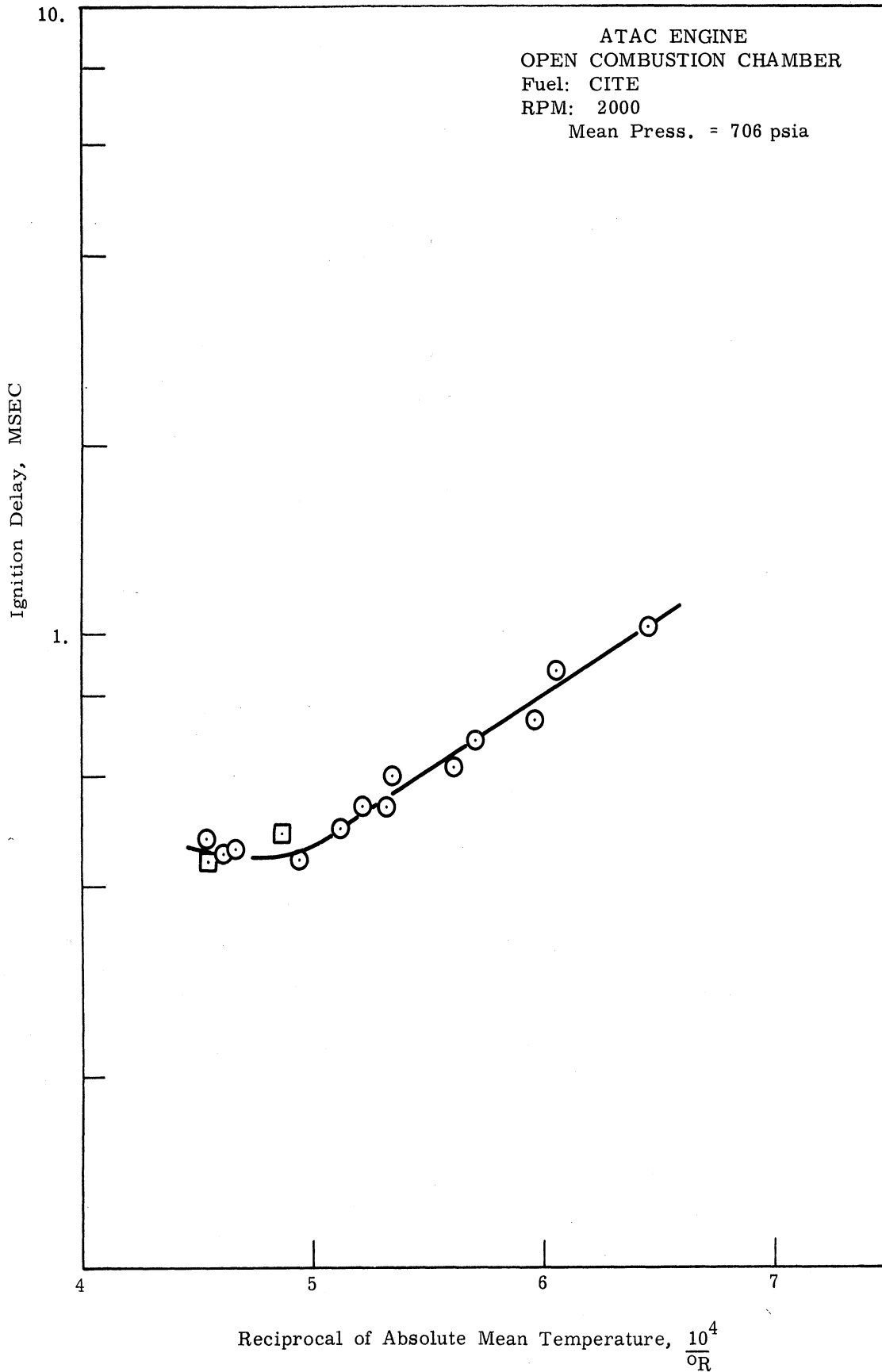


Fig. 20. Logarithm of ignition delay, I.D._p, as a function of the reciprocal of the absolute mean temperature, for CITE fuel.

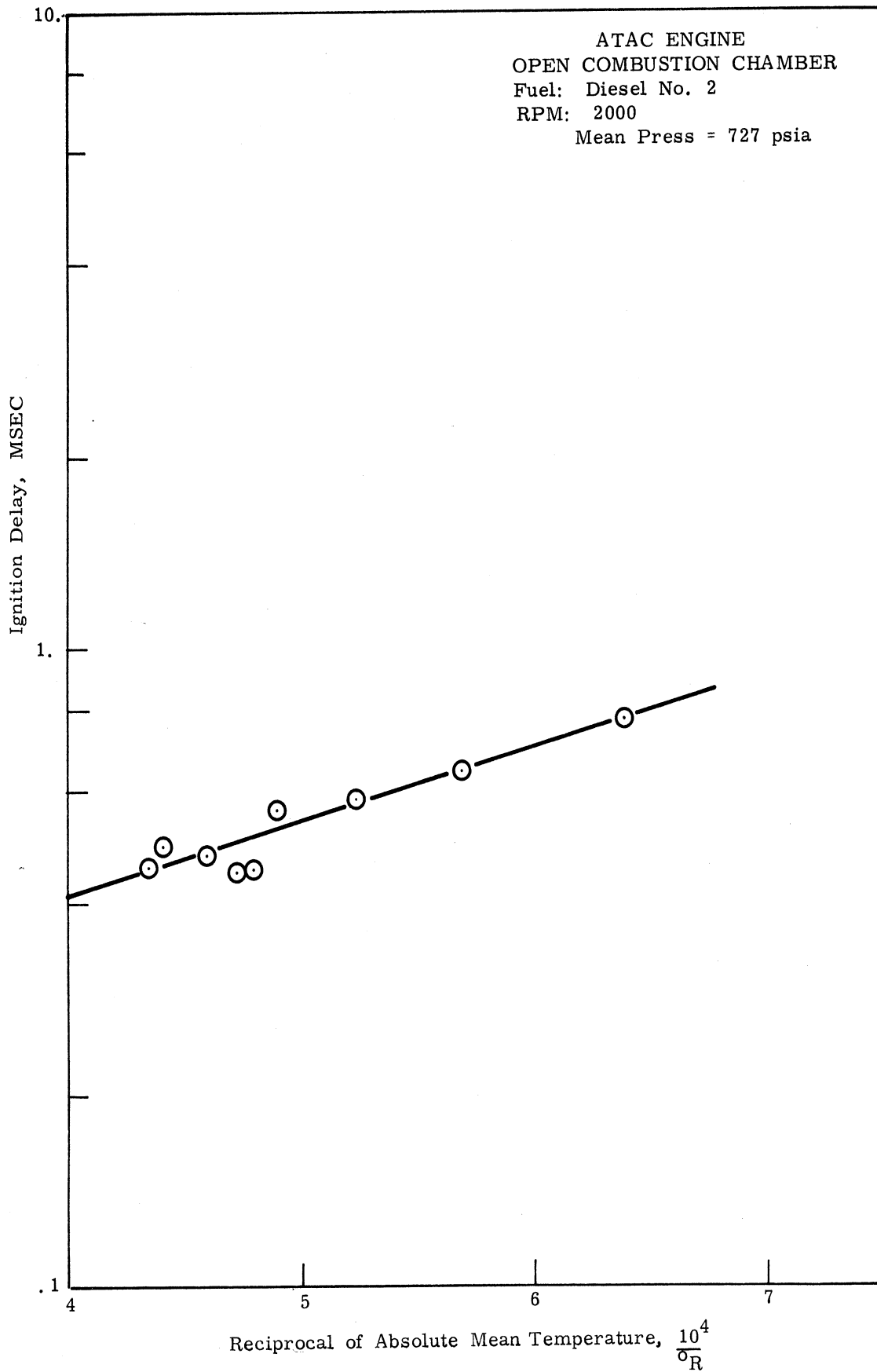


Fig. 21. Logarithm of ignition delay, I.D._p, as a function of the reciprocal of the absolute mean temperature for diesel no. 2 fuel.

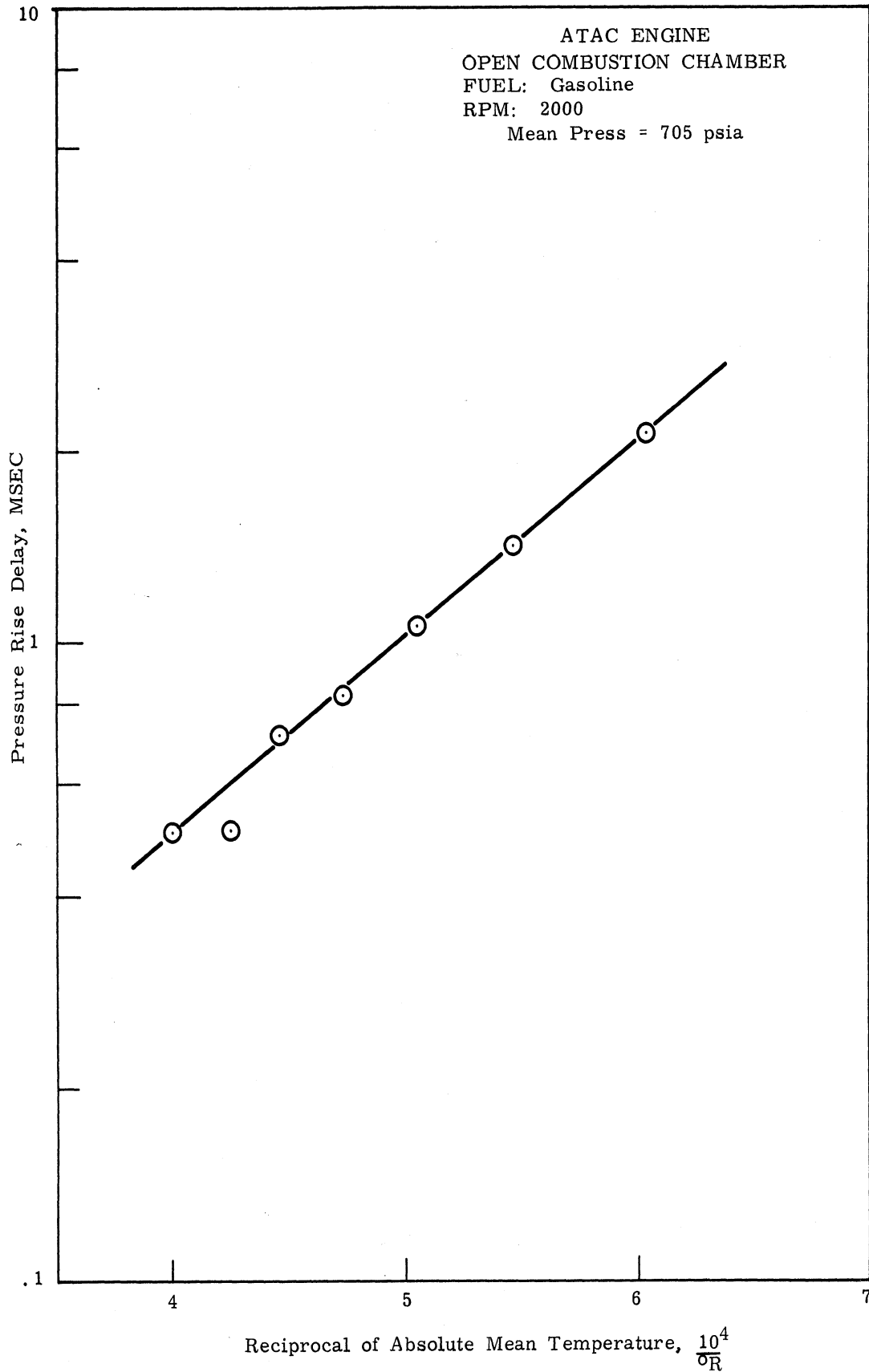


Fig. 22. Logarithm of ignition delay, I.D.p, as a function of the reciprocal of the absolute mean temperature, for gasoline fuel.

TABLE 2

ACTIVATION ENERGY FOR DIFFERENT FUELS

Fuel	Activation Energy, Btu/lb mole
CITE	10,430
Diesel no. 2	5,230
Gasoline	14,780

B. NOISE LEVEL

1. Maximum Pressure

The maximum pressure reached in the cylinder near the end of the combustion process is one of the factors that affects the noise level in the diesel engine. The maximum pressures reached with the different fuels are plotted in Fig. 23 against the intake air temperature. Over the whole temperature range, the order of magnitude of the maximum pressures reached with CITE and diesel fuels is almost the same. The maximum pressure with gasoline is much higher than the other two fuels at intake temperatures below about 250°F. It is to be noticed that the maximum pressure with gasoline at 100°F is low because of the very late combustion.

2. Maximum Pressure Gradient

The maximum rate of pressure rise is among the factors that affects the noise level of the engine. The values obtained for the maximum $(dP/d\theta)$ are plotted in Fig. 24. It shows that gasoline has the highest values, which can be attributed to its long ignition delay and the large amounts of fuels accumulated in the combustion chamber at the end of the delay period. This is shown in Fig. 25 in which $(dP/d\theta)_{\max}$ is plotted versus the length of ignition delay in crank angles.

3. The Rate of Change of Pressure Gradient

The rate of change of the pressure gradient with crank angles from the end of the delay period to the point of maximum $(dP/d\theta)$ is among the factors that affect the noise level and engine vibrations. Values of $(d^2P/d\theta^2)$ for the three fuels is plotted versus the intake air temperature in Fig. 26, and versus the mean temperature during the delay period in Fig. 27. The highest values of $(d^2P/d\theta^2)$ is for gasoline. The effect of the length of the I.D. on $(d^2P/d\theta^2)$ is shown in Fig. 28. From this figure it seems that the absolute length of I.D. is the main factor controlling $(d^2P/d\theta^2)$, for gasoline and CITE fuels.

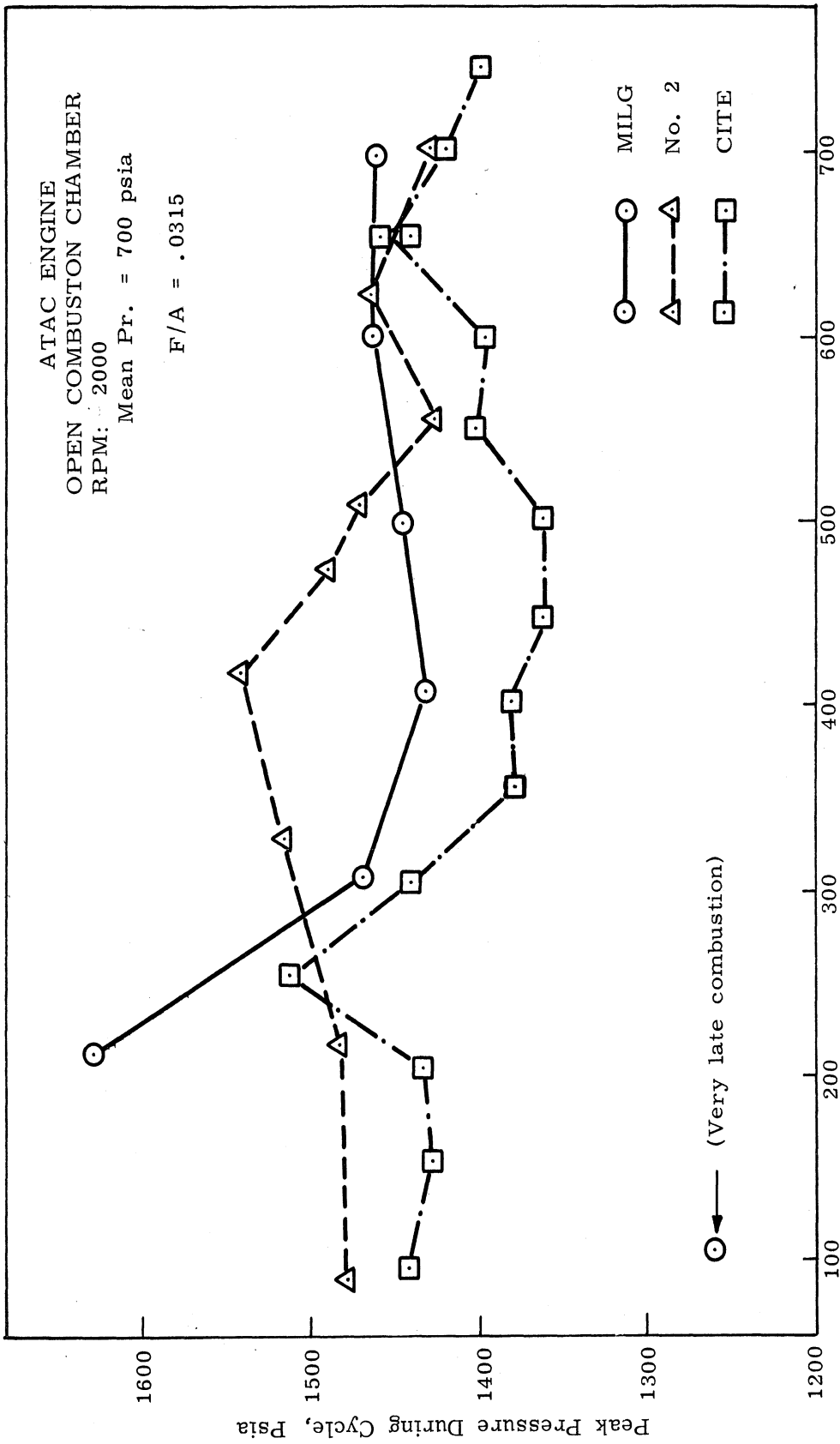


Fig. 23. Maximum cylinder pressure for different fuel

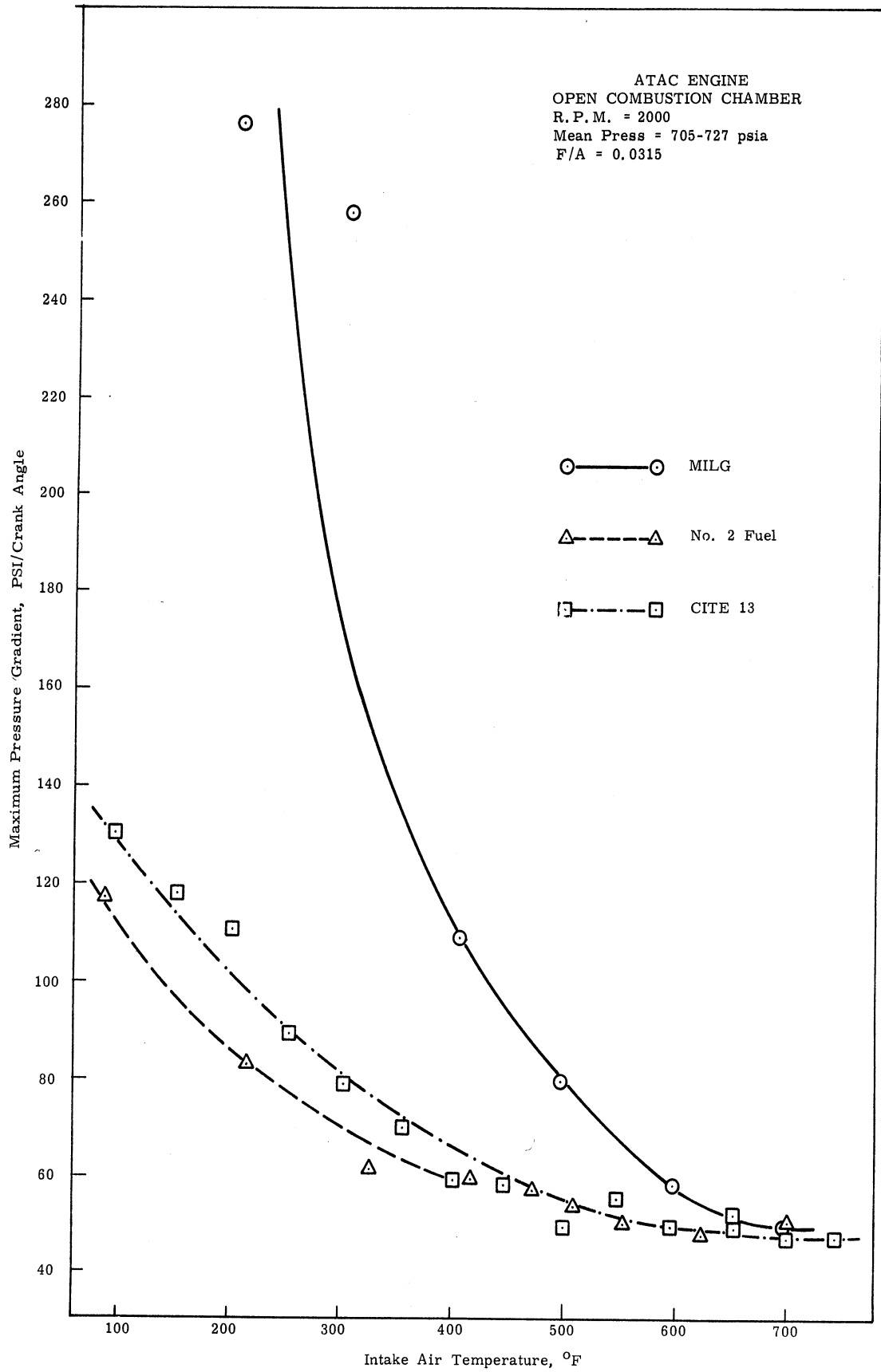


Fig. 24. Maximum pressure gradient for different fuels.

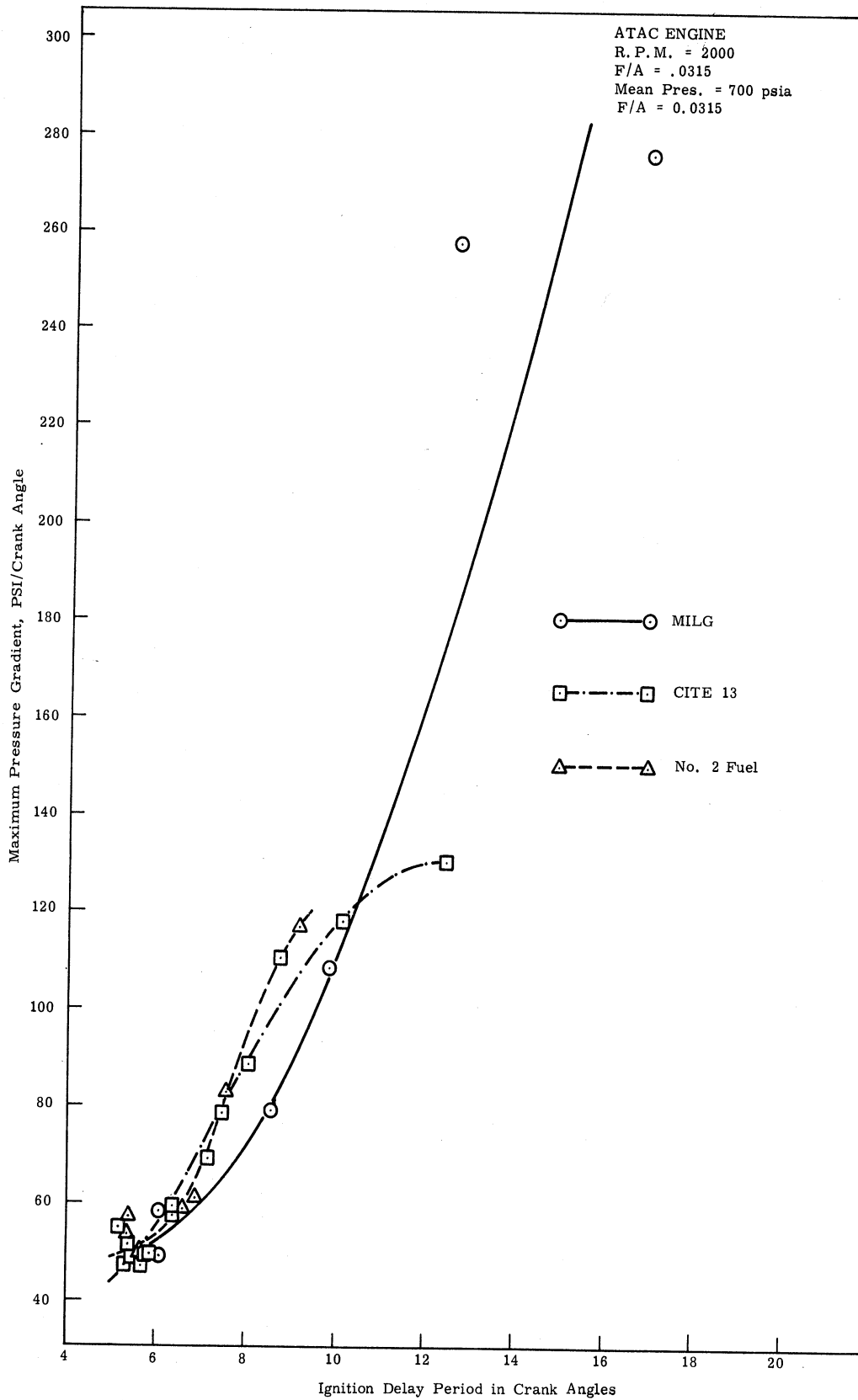


Fig. 25. Maximum pressure gradient for different fuels as a function of the length of ignition delay.

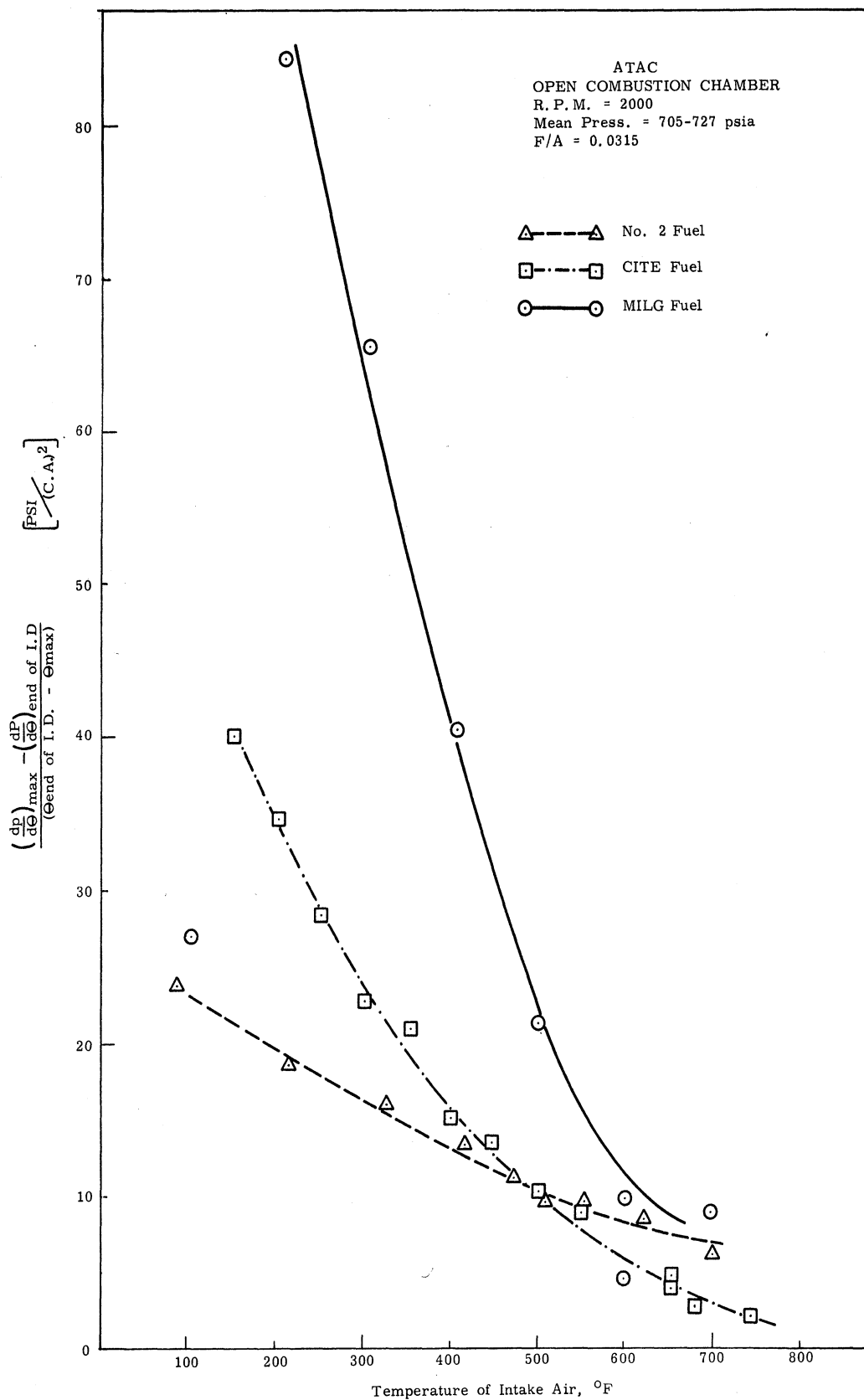


Fig. 26. Rate of change of pressure gradient for different fuels.

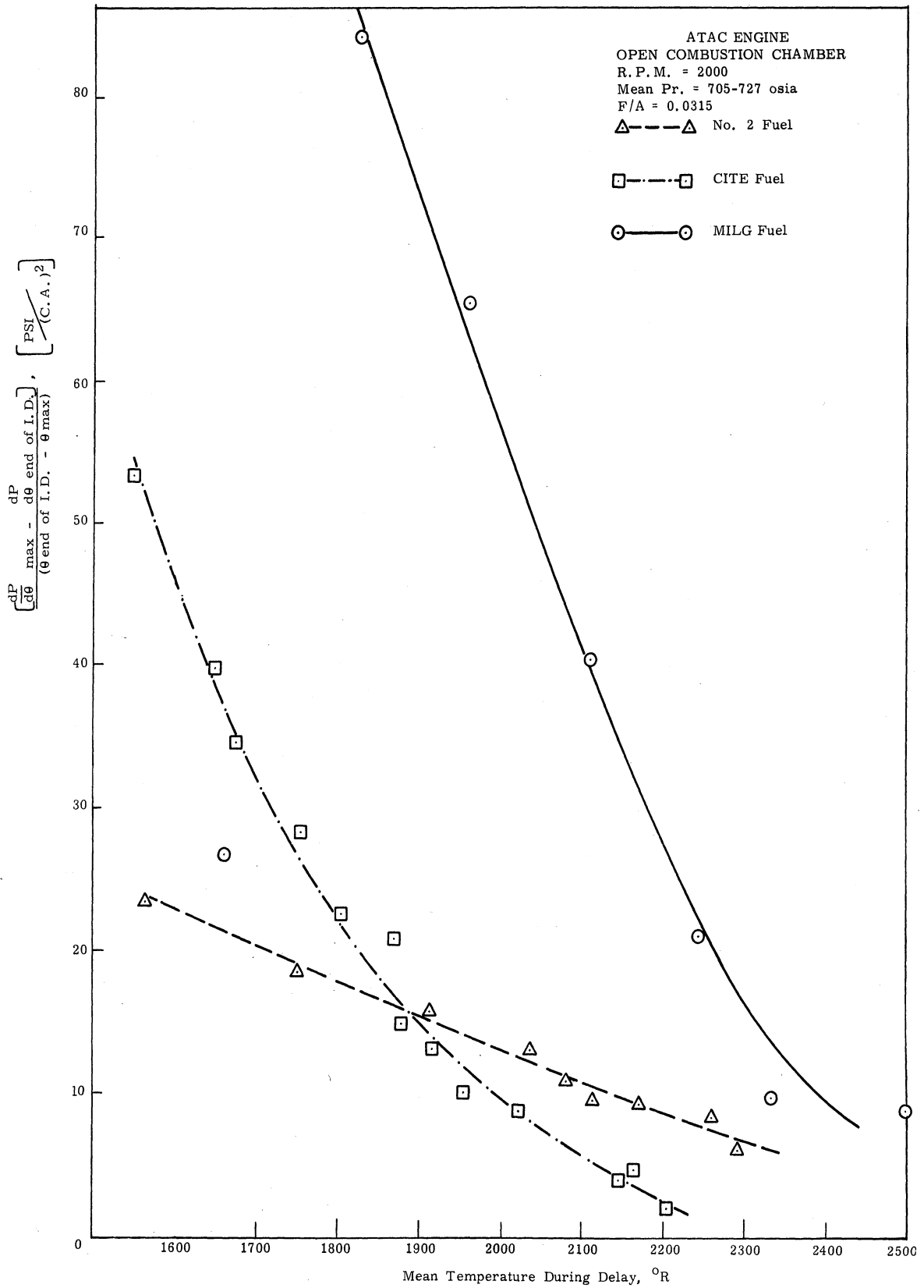


Fig. 27. Rate of change of pressure gradients for different fuels as a function of the mean temperature during ignition delay.

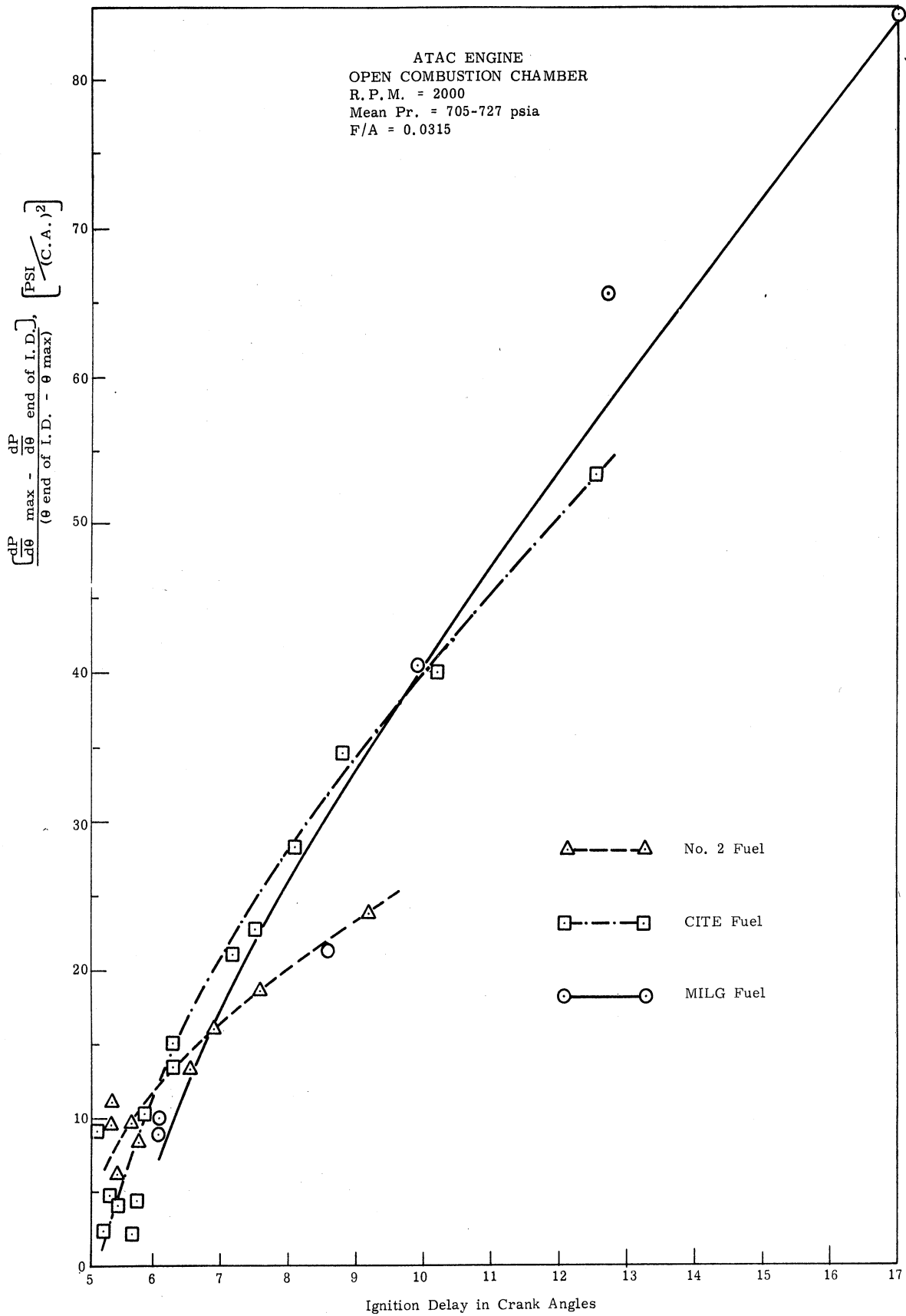


Fig. 28. Rate of change of pressure gradient for different fuels as a function of the length of ignition delay.

From this analysis it can be concluded that the phenomena of I.D. is useful in rating the different fuels in diesel engines.

C. SMOKE INTENSITY IN EXHAUST

The intensity of smoke in the exhaust gases was measured by using a "Hart-ridge Smokemeter," as described in Progress Report No. 7. The smokemeter readings were taken under an effective pressure of 5 in. Hg acting on the flow-meter. The results of the smokemeter readings are plotted for the three fuels in Fig. 29. It can be noticed that the CITE fuel has the highest average smoke intensity. It ranged from 40 to 71 Hartridge units. The gasoline has the lowest smoke intensity, and ranged from 6 to 19 Hartridge units. The high smoke level of CITE fuel is partly due to the after injection which has been observed with this fuel.

D. SPECIFIC FUEL CONSUMPTION

The brake specific fuel consumption for the ATAC engine is plotted in Fig. 30 against the brake mean effective pressure for different fuels. The conditions at which these data were obtained were as follows:

1. A constant fuel-air ratio of 0.0315.
2. A constant mean pressure during the ignition delay of about 700 psia. This required a change in the intake air pressure at each temperature to keep the mean pressure constant. The charge temperature and pressure before the inlet valve are shown opposite to the end points on each curve.
3. A constant speed of 2000 rpm.
4. A constant cooling water temperature at 175°F at outlet from the cylinder head.
5. A constant injection timing at 21 crank angle degrees before top dead center.
6. A constant injector opening pressure of 3000 psia.

Under the above conditions Fig. 30 shows that in the range of BMEP from 35 to 80 psi, the lowest specific consumption is obtained when the engine is run with gasoline. The highest specific fuel consumption is obtained with CITE fuel.

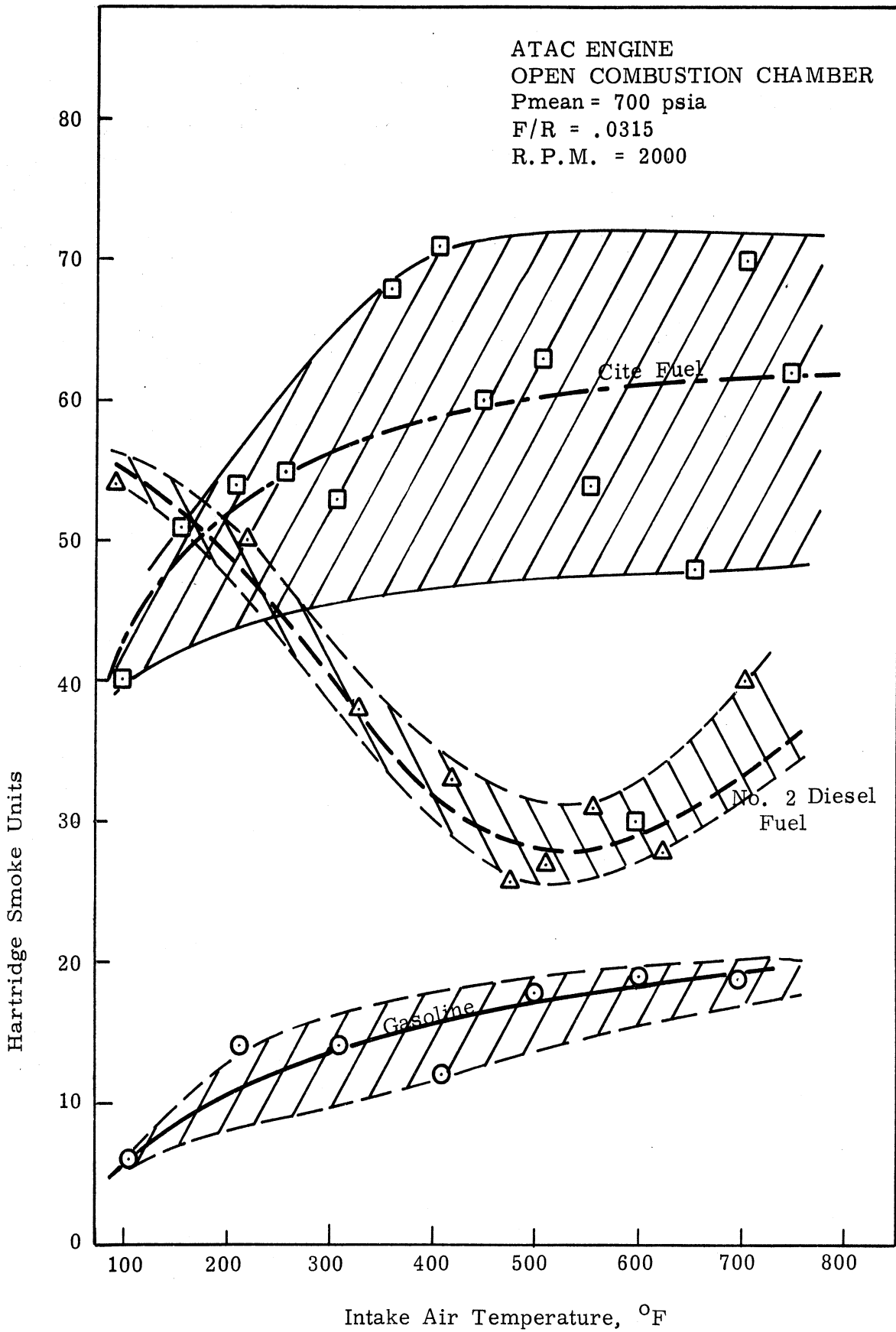


Fig. 29. Smoke intensity for different fuels.

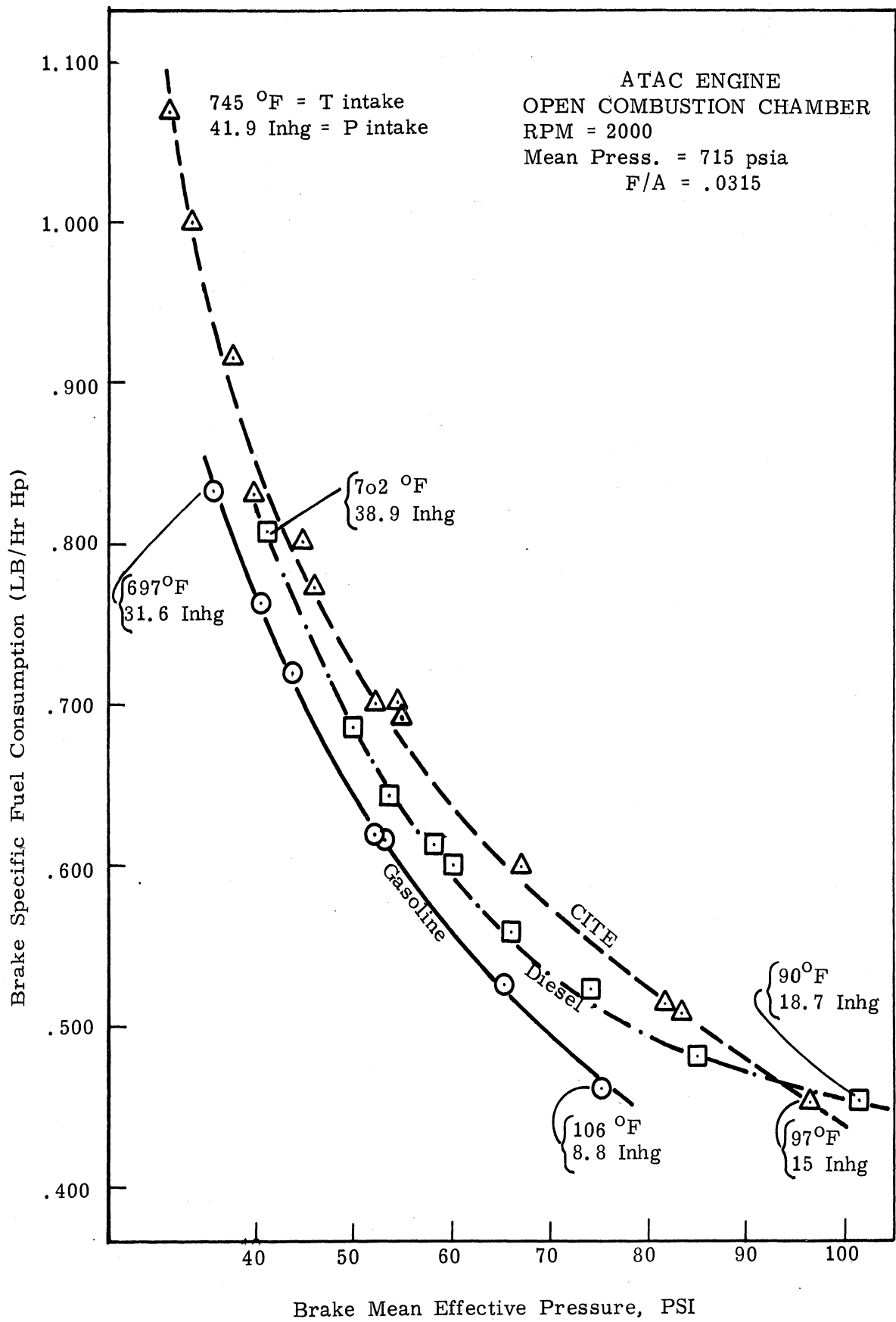


Fig. 30. Brake specific fuel consumption as a function of BMEP for different fuels (constant mean pressure during the ignition delay).

APPENDIX A

FUEL SPECIFICATIONS

The following certificates have been received from Ashland Oil and Refining Company. These are for the following fuels:

- (a) Diesel fuel VV-F-800 Grade II. Dated December 29, 1965.
- (b) Automotive Combat, Refree grade Mil-G-3056B. Dated September 17, 1965.
- (c) CITE fuel, Mil-F-45121B Batch No. 13. Dated December 3, 1965.
- (d) CITE fuel, Mil-F-45121B Batch No. 19. Dated March 29, 1967.

CERTIFICATE OF ANALYSIS

December 29, 1965

I, Eldon Sloan, certify that I am employed by Ashland Oil and Refining Company as Coordinator of Laboratories, and did supervise the following tests on Diesel Fuel VV-F-800 Grade II.

	Specification VV-F-800 <u>Grade DF-2</u>	<u>Drum</u>
Flash Point, °F, min	125	165
Cloud Point, °F, max	15	4
Pour Point, °F, max	5	-5
Kinematic Vis. at 100°F, cs, min	1.8 - 6.0	2.5
Water and Sediment, % by vol., max	0.05	nil
Sulfur, %	1.00	0.11
Ash, % max	0.02	0.001
Corrosion, cu strip 3 hr at 122 ASTM No., max	3	1
Distillation, °F		
50%	Record	516
90%	675	590
End Point	725	604
Ignition Quality, Cetane No.	40	57.5
Gravity, °API	Record	39.1

ASHLAND OIL AND REFINING CO.

Eldon Sloan
Coordinator of Laboratories

CERTIFICATE OF ANALYSIS

September 17, 1965

I, Eldon Sloan, certify that I am employed by Ashland Oil and Refining Company as Coordinator of Laboratories and did personally supervise the following tests on Automotive Combat, Refree Grade Mil-G-3056B dated 4 June 1958 with following exceptions and/or limits, manufactured in 737 Tank as Batch No. 4 on Sept. 17, 1965.

	Specifications		737 Tank Batch No. 4
	Min	Max	
Distillation			
10% evap. °F	131	158	132
20% evap. °F	To be recorded		152
50% evap. °F	194	239	220
90% evap. °F	275	356	320
Residue		2%	1.0
RVP, psi	7.5	9.5	8.7
CRC Calculated Temperature			
V/L Ratio of 10	125°F	135°F	133
V/L Ratio of 30	140°F	150°F	148
Gravity			61.0
Octane Number - Motor	82	86	85.9
- Research	90	93	92.8
Gum, mg/100 ml (before wash)		4	1.2
(after wash)	To be recorded		0.8
Sulfur, % by weight		0.15	0.003
Aromatics, %	25	40	26.5
Olefins	Record		9.0
Corrosion		ASTM No. 1	1A
Metallic Lead Content			
grams/US gal	2.11	3.17	2.2
Oxidation Stability, min	480	Record	600/
Color	Equal to Standard		OK
Oxidation Inhibitor,			
1b/1000 bbl	10	10	10
Type and Amount			2,6 Ditertiary butylphenol
Metal Deactivator			
1b/1000 bbl	3	3	3
			N,N'disalicylidene 1,2 Propanediamine

ASHLAND OIL AND REFINING COMPANY

Eldon Sloan
Coordinator of Laboratories

CERTIFICATE OF ANALYSIS

December 3, 1965

I, Eldon Sloan, certify that I am employed by Ashland Oil and Refining Company as Coordinator of Laboratories, and did personally supervise the following tests on CITE Fuel, Mil-F-45121B manufactured in 708 Tank as Batch No. 13 on December 2, 1965.

	Mil-F-45121B Specifications		708 Tank
	Min	Max	Batch No. 13
Gravity, °API			49.5
Distillation, °F			
Initial	130	160	156
10%	200	260	226
50%	300	375	370
90%	450	500	456
End Point		575	476
Residue, %		2	1
Loss, %		2	1
Reid Vapor Pressure	1	3	2.0
Total Sulfur, % weight	0.25	0.4	0.30
Copper Strip Corr. at 212°		1	1A
Olefin Content, vol %	2.0	5.0	2.3
Aromatic Content, vol. % (D1319)	15.0	25.0	16.2
Gum, Ext. Steam Evap. mgs/100 ml		7.0	0.6
Potential Gum, mg/100 ml		14.0	2.2
Freezing Point, °F		-67	-68
Kinematic Viscosity			
CS at 100°F	0.9		0.98
CS at -30°F		16.5	3.74
Cetane Number	35	40	38.0
Additives, lb/1000 bbl			
(a) Oxidation Inhibitor	5	9	8
(b) Metal Deactivator	1	2	2
Smoke Point, MM	17		21
Thermal Stability			
Change in pressure in 5 hr in Hg		15	0
Preheater/filter deposit			
300/400°F		3	1
Water Separation Index Mod. WSIM	75		88

ASHLAND OIL AND REFINING CO.

Eldon Sloan
Coordinator of Laboratories

CERTIFICATE OF ANALYSIS

March 29, 1967

I, Eldon Sloan, certify that I am employed by Ashland Oil and Refining Company as Coordinator of Laboratories, and did personally supervise the following tests on CITE Fuel, Mil-F-45121B manufactured in 708 Tank as Batch No. 19 on March 21, 1967.

	Mil-F-45121B		708 Tank Batch No. 19
	Specifications Min	Max	
Gravity, °API			49.2
Distillation, °F			
Initial	130	160	134
10%	200	260	204
50%	300	375	342
90%	450	500	454
End Point		575	484
Residue, %		2	1
Loss, %		2	1
Reid Vapor Pressure	1	3	2.8
Total Sulfur, % weight	0.25	0.4	0.27
Copper Strip Corr. at 212°		1	1A
Olefin Content, vol. %	2.0	5.0	1.7
Aromatic Content, vol. % (D1319)	15.0	25.0	17.6
Gum, Ext. Steam Evap. mgs/100 ml		7.0	0.4
Potential Gum, mg/100 ml		14.0	2.2
Freezing Point, °F		-67	-73
Kinematic Viscosity			
CS at 100°F	0.9		0.95
CS at -30°F		16.5	3.5
Cetane Number	35	40	37.5
Additives, lb/1000 bbl			
(a) Oxidation Inhibitor	5	9	8
(b) Metal Deactivator	1	2	2
Smoke Point, MM	17		20
Thermal Stability			
Change in pressure in 5 hr in Hg.		15	0.3
Preheater filter deposit			
300/400°F		3	1
Water Separation Index Mod. WSIM	75		90

ASHLAND OIL AND REFINING CO.

Eldon Sloan
Coordinator of Laboratories

APPENDIX B

CALCULATION OF THE CLEARANCE VOLUME

The clearance volume is computed from the dimensions of the original combustion chamber and the recesses made for the instruments. The dimensions used for these computations are shown in Figs. 31 and 32. These are obtained from engine drawings or from direct measurements made on the engine. The clearance volume constitutes of the following:

A. In piston top

1. Volume of dish = 3.6339 cu in.
2. Volume of intake valve recess = 0.4101 cu in.
3. Volume of exhaust valve recess = 0.1983 cu in.
4. Volume gained due to rounding of piston edge = .0048 cu in.
Total volume of piston recesses = 4.2471 cu in.
5. Volume between piston top and cylinder head = 0.7189 cu in.
6. Volume of quartz window hole (with the quartz in place)
= 0.0067 cu in.
7. Volume of pressure pickup hole = 0.0063 cu in.
8. Net volume of injector and hole = 0.0014 cu in.
9. Volume of intake valve protrusion = -0.2966.
10. Volume of exhaust valve protrusion = -0.1228.

NOTE: The following volumes are excluded because they are usually full of carbon deposits:

- a. Volume between piston and sleeve till the first ring = 0.1568 cu in.
- b. Volume between sleeve top and cylinder head = 0.0788 cu in.
- c. Volume between gasket and sleeve = 0.0459.

Total clearance volume (clean surfaces) = 4.5610 cu in.

Compression ratio (clean surfaces) = 16.692:1.

EFFECT OF CARBON DEPOSIT ON C. R.

The effect of a carbon deposit $\frac{3}{1000}$ in. thick on the combustion chamber walls is found to increase the compression ratio from 16.692:1 to 17.116:1, or 2.54%.

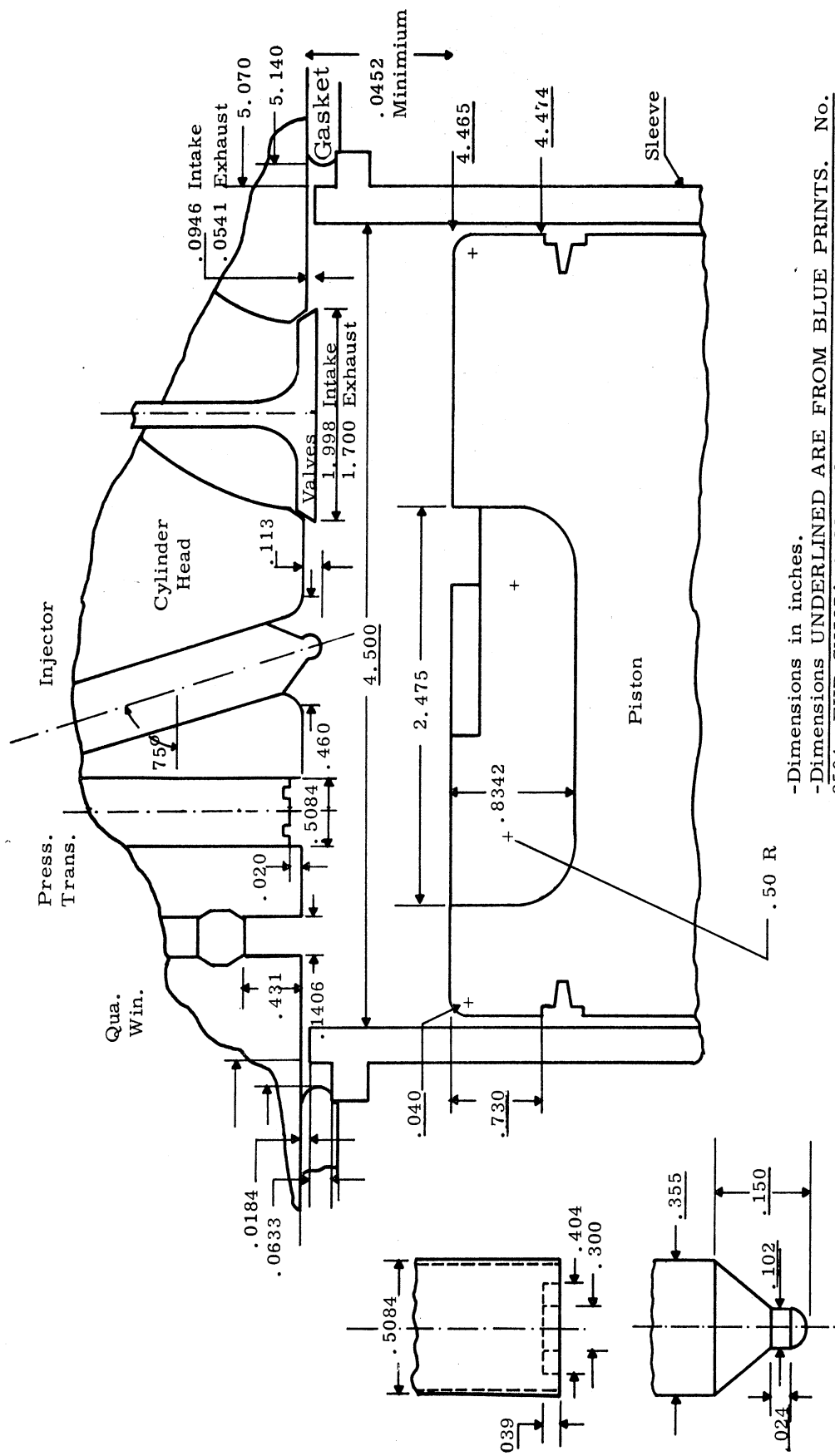


Fig. 31. Details of ATAC engine open combustion chamber.
 (Drawing is not to scale)

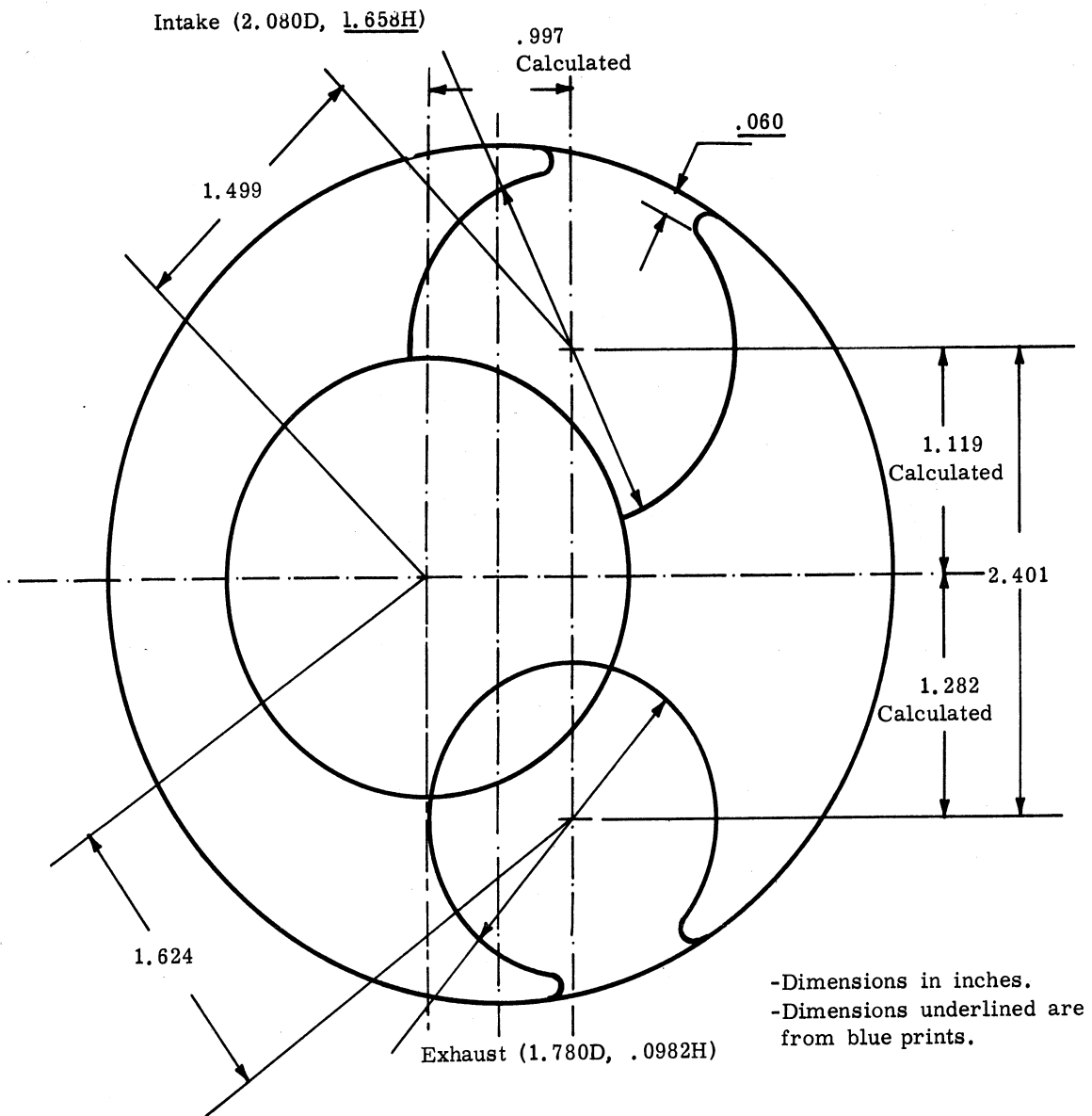


Fig. 32. Details of recesses in ATAC engine piston.

COMPRESSION RATIO USED IN COMPUTATIONS

Upon checking the surface of the combustion chamber walls, after running for periods of 100 working hours, they were found to be fairly clean. For the data analysis a compression ratio of 16.692:1 is therefore used.

APPENDIX C

VOLUME-CRANK ANGLES RELATIONSHIP

The volume of gas enclosed in the ATAC engine cylinder is calculated for the different crank angle positions as follows:

$$V = V_c + V_s$$

where

V_c = clearance volume calculated in Appendix B

V_s = swept volume obtained from the piston displacement from T.D.C. position.

The formula used for computing the cylinder volume took into consideration the offset of the piston pin with respect to piston center. This offset shown in Fig. 33 is obtained from the engine drawings and amounts to 60/1000 in.

The cylinder volume is calculated for all crank angles from -180° to $+180^\circ$. To facilitate any further programming on the computer, the cylinder volume and the rate of change of volume w.r.t. crank angles are calculated and tabulated for intervals of $1/10^\circ$ crank angle. A summary of these are shown in Tables 3 and 4.

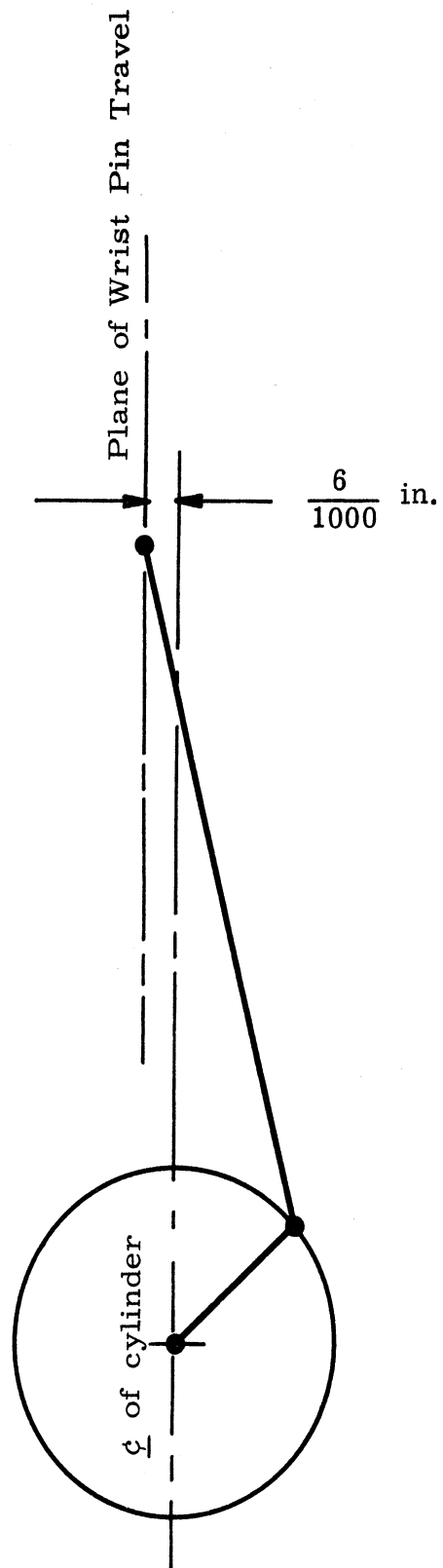


Fig. 33. ATAC engine two-bar mechanism.

TABLE 3

ATAC ENGINE CYLINDER VOLUME AND GRADIENTS AT CRANK ANGLES
FROM 0 TO 180°, COMPRESSION STROKE

C. R. = 16.692:1

Angle θ Measured from T. D. C.

Angle θ , deg	Volume, cu in.	Volume Gradient	Angle θ , deg	Volume, cu in.	Volume Gradient	Angle θ , deg	Volume, cu in.	Volume Gradient
0	4.5610	.0000						
2	4.5882	-.0272	62	27.1041	-.6188	122	62.6310	-.4576
4	4.6699	-.0544	64	28.3487	-.6255	124	63.5322	-.4435
6	4.8060	-.0815	66	29.6056	-.6312	126	64.4048	-.4291
8	4.9960	-.1085	68	30.8729	-.6359	128	65.2484	-.4144
10	5.2398	-.1352	70	32.1485	-.6396	130	66.0624	-.3996
12	5.5368	-.1617	72	33.4306	-.6423	132	66.8465	-.3845
14	5.8864	-.1879	74	34.7171	-.6441	134	67.6002	-.3693
16	6.2882	-.2137	76	36.0062	-.6449	136	68.3234	-.3539
18	6.7411	-.2392	78	37.2959	-.6447	138	69.0156	-.3383
20	7.2446	-.2642	80	38.5845	-.6437	140	69.6765	-.3226
22	7.7975	-.2887	82	39.8700	-.6417	142	70.3061	-.3069
24	8.3998	-.3126	84	41.1507	-.6389	144	70.9039	-.2910
26	9.0475	-.3360	86	42.4250	-.6352	146	71.4700	-.2750
28	9.7423	-.3587	88	43.6910	-.6308	148	72.0040	-.2590
30	10.4820	-.3808	90	44.9473	-.6254	150	72.5059	-.2429
32	11.2651	-.4022	92	46.1923	-.6194	152	72.9756	-.2268
34	12.0902	-.4228	94	47.4244	-.6126	154	73.4129	-.2106
36	12.9559	-.4427	96	48.6422	-.6051	156	73.8178	-.1943
38	13.8605	-.4618	98	49.8443	-.5969	158	74.1902	-.1781
40	14.8023	-.4800	100	51.0295	-.5881	160	74.5300	-.1618
42	15.7798	-.4973	102	52.1964	-.5787	162	74.8373	-.1455
44	16.7910	-.5138	104	53.3440	-.5687	164	75.1119	-.1291
46	17.8343	-.5293	106	54.4709	-.5581	166	75.3539	-.1128
48	18.9078	-.5440	108	55.5762	-.5471	168	75.5631	-.0965
50	20.0095	-.5576	110	56.6589	-.5355	170	75.7397	-.0801
52	21.1376	-.5703	112	57.7180	-.5235	172	75.8836	-.0638
54	22.2900	-.5820	114	58.7526	-.5111	174	75.9947	-.0474
56	23.4649	-.5927	116	59.7620	-.4982	176	76.0732	-.0310
58	24.6602	-.6024	118	60.7453	-.4850	178	76.1189	-.0147
60	25.8740	-.6111	120	61.7019	-.4715	180	76.1319	.0017

TABLE 4

ATAC ENGINE CYLINDER VOLUME AND GRADIENTS AT CRANK ANGLES
FROM 0 TO -180°, EXPANSION STROKE

C.R. = 16.692:1

Angle θ Measured From T.D.C.

Angle θ , deg	Volume, cu in.	Volume Gradient	Angle θ , deg	Volume, cu in.	Volume Gradient	Angle θ , deg	Volume, cu in.	Volume Gradient
0	4.5610	.0000						
- 2	4.5882	.0272	- 62	27.0498	.6168	-122	62.4968	.4581
- 4	4.6699	.0544	- 64	28.2902	.6235	-124	63.3991	.4441
- 6	4.8059	.0815	- 66	29.5430	.6291	-126	64.2731	.4299
- 8	4.9958	.1084	- 68	30.8061	.6338	-128	65.1184	.4154
-10	5.2394	.1351	- 70	32.0775	.6375	-130	65.9345	.4007
-12	5.5362	.1616	- 72	33.3553	.6402	-132	66.7210	.3858
-14	5.8856	.1877	- 74	34.6376	.6419	-134	67.4774	.3707
-16	6.2869	.2135	- 76	35.9225	.6426	-136	68.2035	.3554
-18	6.7393	.2389	- 78	37.2080	.6426	-138	68.8990	.3400
-20	7.2421	.2638	- 80	38.4924	.6416	-140	69.5635	.3245
-22	7.7942	.2882	- 82	39.7739	.6397	-142	70.1969	.3089
-24	8.3946	.3121	- 84	41.0507	.6369	-144	70.7989	.2931
-26	9.0422	.3354	- 86	42.3211	.6333	-146	71.6426	.2693
-28	9.7358	.3581	- 88	43.5835	.6289	-148	71.9079	.2614
-30	10.4740	.3801	- 90	44.8362	.6237	-150	72.4147	.2454
-32	11.2555	.4013	- 92	46.0778	.6178	-152	72.8894	.2293
-34	12.0789	.4219	- 94	47.3068	.6111	-154	73.3320	.2132
-36	12.9426	.4417	- 96	48.5217	.6037	-156	73.7423	.1971
-38	13.8450	.4606	- 98	49.7211	.5956	-158	74.1204	.1809
-40	14.7846	.4788	-100	50.9038	.5869	-160	74.4660	.1647
-42	15.7595	.4960	-102	52.0685	.5777	-162	74.7792	.1485
-44	16.7681	.5124	-104	53.2140	.5678	-164	75.0599	.1322
-46	17.8085	.5279	-106	54.3393	.5574	-166	75.3081	.1159
-48	18.8789	.5424	-108	55.4432	.5464	-168	75.5237	.0997
-50	19.9774	.5560	-110	56.5247	.5350	-170	75.7067	.0833
-52	21.1021	.5686	-112	57.5830	.5232	-172	75.8571	.0670
-54	22.2510	.5802	-114	58.6172	.5109	-174	75.9748	.0507
-56	23.4223	.5909	-116	59.6264	.4982	-176	76.0599	.0344
-58	24.6138	.6005	-118	60.6098	.4852	-178	76.1122	.0180
-60	25.8236	.6092	-120	61.5669	.4718	-180	76.1319	.0017

APPENDIX D

DIGITAL COMPUTATIONS

A computer program has been developed for the present project, for the analysis of the data. The recorded information include:

(a) The experimental data obtained from the tests, (b) the results of computations based on the experimental data, and (c) a comparison between the present results and previously published data.

1. DATA RECORDING

The data recorded includes the following items, arranged according to their order, in the attached computer records:

Data Set A2A: A, stands for ATAC

2, stands for Group 2 of runs (Group 1 will be included in a future report)

A, stands for the first series in this group, in which fuel used is CITE fuel, Batch 13 or 19. Runs at constant intake surge tank pressure of 15 in. Hg g.

Data Set A2B: as set A2A, except that the mean pressure during the ignition delay is kept constant.

Data Set A2C: as set A2B, with diesel no. 2 fuel.

Data Set A2D: as set A2B, with gasoline fuel.

2. IDENTIFICATION

a. Mass of Fuel

<u>Symbol</u>	<u>Mass, lbm</u>
B	0.12667
C	0.25247
D	0.5007
E	0.9985

b. Critical Flowmeter Orifice

<u>Symbol</u>	<u>Diameter of Orifice</u>
A	3/32 in.
B	1/8
C	3/16
D	7/32
E	D and A
F	D and B
G	D and C
H	D, C, and A
I	D, C, and B
J	D, C, B, and A

TABLE 5

LIST OF SYMBOLS, HEADINGS, AND REPRESENTATIONS AS THEY
APPEAR ON THE COMPUTER SHEETS OF TABLE 8

Column	Heading	Representation
1	For Run	Identification of run, serial number
2	Use W	Identification of mass used for fuel consumption measurements.
3	Use O	Identification of the orifice combination, used for air flow rate measurements (critical flowmeter).
4	Speed RPM	Engine speed, rpm.
5	Load lbs	Load, lb.
6	Fuel min	Fuel consumption time, min.
7	Fuel L/hr	Fuel leakage rate, liters/hr.
8	Air PSIG	Pressure before orifice, psig.
9	Air F	Temperature before orifice, °F.
10	Blow CFPM	Blowby rate in cu ft/min.
11	Temperatures (F) Air	Temperature of air before the inlet valve, °F.
12	Temperatures (F) Out	Temperature of cooling water at outlet from the engine, °F.
13	Temperatures (F) Min	Minimum temperature of the inside surface of the combustion chamber, °F.
14	Temperatures (F) Inc	Swing in temperature of the inside surface of the combustion chamber, °F.
15	Room In HG	Barometric pressure in room, in. Hg.
16	Surge In HG	Pressure in surge tanks, inlet and exhaust above barometric pressure, in. Hg.
17	At I VC PSI	Cylinder pressure at the point of I.V.C., above surge tank pressure, psi.
18	At INJ PSI	Cylinder pressure at the point of start of fuel injection.
19	RISE PSI	Cylinder pressure at the end of the pressure-rise delay w.r.t. pressure at start of injection.

TABLE 5 (Concluded)

Column	Heading	Representation
20	DBTDC LIFT	Point of needle lift, in crank angle degrees before T.D.C.
21	At Start of Rise	Point of start of pressure rise due to combustion, in crank angle degrees.
22	At Start of Illum	Point of start of illumination due to combustion, in crank angle degrees.
23	Exhaust F	Exhaust temperature, °F.
24	Exhaust HU	Smokemeter reading in Hartridge units.

TABLE 6

LIST OF SYMBOLS, HEADINGS, AND REPRESENTATIONS AS THEY
APPEAR ON THE COMPUTER SHEETS OF TABLE 9

Column	Heading	Representation
1	Ror Run	Identification of run, serial number.
2	Brake HP	Brake horsepower.
3	BMEP PSI	Brake mean effective pressure, psi.
4	BSFC #/HR HP	Brake specific fuel consumption in lb/hr/ brake horsepower.
5	FUEL/ AIR	Fuel-air ratio.
6	Cycle (LBM/1000) AIR	Mass of air used per cycle in lbm/1000
7	Cycle (LBM/1000) BLOW	Mass of blowby gases per cycle in lbm/1000
8	Cycle (LBM/1000) EXH	Mass of exhaust gases in clearance volume/ cycle in lbm/1000.
9	SURGE PSIA	Absolute pressure in surge tank, psia.
10	EFF PCT	Volumetric efficiency, percentage.
11	At I VC F	Gas temperature at the closing of inlet valve, °F.
12	At Start of Injection Index	Index of compression from the point of in- let valve closing to start of injection.
13	At Start of Injection PSIA	Gas pressure at start of injection, psia.
14	At Start of Injection #/CU FT	Gas density at start of injection in lbm/ ft ³ .
15	At Start of Injection R	Gas temperature at start of injection, °R.
16	Averaged during delay Index	Average index of compression during the ignition delay period.

TABLE 6 (Concluded)

Column	Heading	Representation
17	Averaged during delay PSIA	Average gas pressure during the ignition delay period.
18	Averaged during delay #/CU FT	Average gas density during the ignition delay period, in lbm/ft ³ .
19	Averaged during delay R	Average gas temperature during the igni- tion delay period, °R.
20	Delay (MSEC) PRISE	Pressure-rise delay, msec.
21	Delay (MSEC) ILLUM.	Illumination delay, msec.

TABLE 7

LIST OF SYMBOLS, HEADINGS, AND REPRESENTATIONS, AS THEY
APPEAR ON THE COMPUTER SHEETS OF TABLE 10

Column	Heading	Representation
1	For Run	Identification of run, serial number.
2	Experimental PRD	Experimental value of the pressure rise delay, msec.
3	Experimental Ild	Experimental value of the illumination delay, msec.
4	WOLFER START	Calculated values of ignition delay, by using Wolfer's Equation, based on pressure and temperature at start of injection.
5	WOLFER MEAN	Calculated values of ignition delay, using Wolfer's Equation, based on the mean pressure and temperature during the delay period.
6	ELLIOTT START	Calculated values of ignition delay, by using Elliott's Equation, based on the pressure and temperature at start of injection.
7	ELLIOTT MEAN	Calculated values of ignition delay, by using Elliott's Equation, based on the mean pressure and temperature during the delay period.
8	SITKEI START	Calculated values of ignition delay, by using Sitkei's Equation, based on the pressure and temperature at start of injection.
9	SITKEI MEAN	Calculated values of ignition delay, by using Sitkei's Equation, based on the mean pressure and temperature during the delay period.
10	TSAO	Calculated values of ignition delay, by using Tsao's Equation, based on the pressure and temperature at start of injection and the actual engine speed.
11	TSAO MEAN	Calculated values of ignition delay, by using Tsao's Equation, based on the mean pressure and temperature during the ignition delay and the actual engine speed.
12	TSAO at 1000 START	Same as (10), except that the speed used is 1000 rpm, instead of the actual engine speed.
13	TSAO at 1000 MEAN	Same as (11), except that the speed used is 1000 rpm, instead of the actual engine speed.

TABLE 8

COMPUTER DATA SHEET, RECORDED DATA, SERIES A2A FOR CIITE FUEL

EFFECT OF INLET TEMPERATURE ON IGNITION DELAY
 RUNS TAKEN AT CONSTANT INLET PRESSURE

DATA SET A2A HAVING 11 RUN(S) FOLLOWS. THE ATAC ENGINE WAS TESTED (INJECTOR OPENING PRESSURE SET AT 3000 PSIG) USING CI13 FUEL.

FOR USE	SPEED	LOAD	FUEL	AIR	BLCW	TEMPERATURES(F)	ROOM<SURGE<a>IVC<@INJ<RIS	DBTDC	AT START OF	EXHAUST											
RUN W O	RPM	LBS	MIN L/HR	PSIG	F CFFM	AIR OUT MIN INC	INHG INHG PSI PSI	LIFT	RISE ILLUM	F HU											
4 E D	2000	17.8	7.49	.27	66.0	78	-0.0	97	165	354	12	28.1	15.1	4.0	496	373	21.3	7.3	-0.0	804	61
5 E D	2002	17.4	7.57	.28	63.0	80	-0.0	115	172	373	11	28.7	15.0	3.4	481	341	21.2	8.1	-0.0	838	63
6 E D	1999	13.6	8.33	.25	58.5	80	-0.0	163	169	390	5	28.8	15.1	3.8	490	305	20.7	9.4	-0.0	842	55
7 E D	2001	11.9	8.73	.24	56.2	80	-0.0	190	165	386	-0.0	28.8	14.9	1.6	471	287	21.0	5.5	-0.0	832	-0
8 E D	2000	17.1	9.28	.20	51.2	77	-0.0	242	170	422	53	28.9	15.0	2.6	452	255	21.4	11.6	-0.0	784	31
9 E D	2000	15.7	9.74	.20	48.2	78	-0.0	281	170	422	47	29.0	14.9	3.7	435	238	21.9	12.7	-0.0	793	35
10 C D	2000	12.9	9.18	.18	44.8	78	-0.0	337	168	448	48	28.9	15.0	3.2	440	225	21.3	12.3	-0.0	805	52
11 C D	2001	10.6	9.46	.24	42.5	75	-0.0	376	169	441	47	28.9	15.0	3.0	427	219	21.5	13.0	-0.0	788	28
12 C D	1999	9.9	9.58	.20	40.2	77	-0.0	424	169	454	48	29.3	15.0	3.7	420	210	21.2	12.7	-0.0	842	40
13 C D	1999	9.0	9.79	.17	38.1	75	-0.0	464	167	454	47	29.2	15.1	3.0	415	194	21.4	13.4	-0.0	851	30
14 C D	2001	8.2	6.11	.17	35.6	75	-0.0	513	171	483	46	25.3	15.0	3.4	359	194	21.7	14.0	-0.0	866	40
AVERAGES	2000	13.1	7.21	.22	45.5	75	-0.0	291	165	421	37	28.9	15.0	3.2	448	258	21.3	11.3	-0.0	822	44
RMS ERRS	1	3.3	1.58	.04	5.9	1	-0.0	136	1	38	17	.3	.1	.6	31	58	.3	2.2	-0.0	27	13

TABLE 9

COMPUTER DATA SHEET, COMPUTATION RESULTS, SERIES A2A FOR CITE FUEL

H/C RATIO = 1.592/1, DENSITY AT 6C = 48.75 #/CUFT, CLEARANCE VOLUME = 4.5610 CUIN, COMPRESSION RATIO = 16.69/1, IVC = 128 D81DC

FOR RUN	HP	BRAKE PSI	BMEP PSI	HRHP	AIR	FUEL	AIR	CYCLE (LBM/1000)	AIR	BLGW	EXH	PSIA	SURGE	EFF PCT	AT START OF INJECTION	INDEX PSIA	#/CUFT	R	AVERAGED DURING DELAY	INDEX PSIA	#/CUFT	R	DELAY (MSEC)	PRISE ILLUM
4	11.9	65.7	63.5	.0320	3.92	-0.0	.11	21.2	92.1	176	1.408	521	.517	1510	1.221	708	1.176	1592	1.167	-0.000			1.167	-0.000
5	11.6	64.2	64.0	.0328	3.78	-0.0	.11	21.5	91.2	161	1.399	506	.887	1516	1.224	675	1.122	1594	1.091	-0.000			1.091	-0.000
6	9.1	59.2	74.7	.0315	3.58	-0.0	.11	21.6	92.7	239	1.386	515	.859	1595	1.253	665	1.053	1676	.942	-0.000			.942	-0.000
7	7.9	43.9	813	.0312	3.45	-0.0	.11	21.5	93.5	200	1.418	494	.818	1676	1.240	635	1.001	1682	.925	-0.000			.925	-0.000
8	11.4	63.1	536	.0316	3.22	-0.0	.12	21.6	93.5	277	1.389	476	.756	1677	1.273	600	.506	1758	.817	-0.000			.817	-0.000
9	17.5	57.9	555	.0316	3.07	-0.0	.12	21.0	94.4	347	1.364	460	.708	1732	1.292	575	.841	1817	.767	-0.000			.767	-0.000
10	9.6	47.6	539	.0316	2.90	-0.0	.11	21.6	96.0	376	1.364	465	.685	1807	1.264	574	.810	1885	.750	-0.000			.750	-0.000
11	7.1	38.1	720	.0305	2.78	-0.0	.12	21.6	96.6	402	1.359	452	.654	1840	1.327	557	.767	1934	.708	-0.000			.708	-0.000
12	6.6	36.5	764	.0313	2.65	-0.0	.11	21.8	97.8	465	1.329	445	.639	1859	1.304	547	.748	1947	.709	-0.000			.709	-0.000
13	6.0	33.2	817	.0317	2.58	-0.0	.11	21.8	98.6	477	1.340	440	.609	1926	1.297	533	.707	2010	.667	-0.000			.667	-0.000
14	5.5	30.2	846	.0314	2.45	-0.0	.11	21.8	98.3	538	1.323	424	.574	1970	1.377	517	.664	2077	.641	-0.000			.641	-0.000
MEAN	8.7	48.3	701	.0316	3.13	-0.0	.11	21.6	95.0	335	1.371	473	.737	1731	1.279	559	.890	1816	.835	-0.000			.835	-0.000
ERRS	2.2	12.3	.102	.0005	.48	-0.00	.00	.02	2.4	121	.030	31	.113	154	.045	60	.166	160	.166	-0.000			.166	-0.000

TABLE 10

COMPUTER DATA SHEET, COMPARISON WITH PREVIOUS WORK, SERIES A2A FOR CITE FUEL

FOR RUN	EXPERIMENTAL PRD	ILC	WCLFER START	WCLFER MEAN	ELIUCI START	ELIUCI MEAN	SITKEI START	SITKEI MEAN	TSAG START	TSAG MEAN	TSAG @ 1000 START	TSAG @ 1000 MEAN
4	1.167	-.000	1.607	.841	2.542	2.381	2.536	1.641	.054	-.249	1.904	1.499
5	1.091	-.000	1.633	.884	2.530	2.377	2.573	1.654	.031	-.264	1.908	1.516
6	.942	-.000	1.213	.696	2.375	2.241	2.108	1.476	-.289	-.615	1.655	1.317
7	.925	-.000	1.231	.722	2.356	2.231	2.139	1.511	-.347	-.659	1.650	1.321
8	.817	-.000	1.033	.623	2.240	2.124	1.922	1.398	-.698	-1.053	1.476	1.168
9	.767	-.000	.918	.561	2.159	2.049	1.795	1.326	-1.007	-1.395	1.351	1.055
10	.750	-.000	.741	.476	2.061	1.972	1.579	1.219	-1.446	-1.795	1.163	.916
11	.708	-.000	.706	.441	2.022	1.922	1.542	1.177	-1.671	-2.119	1.100	.830
12	.709	-.000	.685	.438	2.001	1.909	1.518	1.174	-1.797	-2.209	1.063	.811
13	.667	-.000	.595	.394	1.930	1.851	1.406	1.119	-2.254	-2.645	.924	.702
14	.641	-.000	.563	.358	1.887	1.795	1.371	1.073	-2.606	-3.142	.846	.594
MEAN	.835	-.000	.993	.585	2.191	2.077	1.863	1.346	-1.094	-1.468	1.367	1.066
ERRS	.166	-.000	.367	.173	.222	.198	.411	.203	.881	.942	.361	.306

TABLE 11

COMPUTER DATA SHEET, RECORDED DATA, SERIES A2B FOR CITE FUEL

EFFECT OF GAS TEMPERATURE ON IGNITION DELAY WITH CITE FUEL (BATCH 13)
 RUNS TAKEN AT CONSTANT MEAN PRESSURE DURING DELAY

DATA SET A2B HAVING 13 RUN(S) FOLLOWS. THE ATAC ENGINE WAS TESTED (INJECTOR OPENING PRESSURE SET AT 3000 PSIG) USING CT13 FUEL.

FOR USE	SPEED	LOAD	FUEL	AIR	BLW	TEMPERATURES(F)	ROOM<SURGE<@IVC<@INJ<CRIS	DBTDC AT START OF	EXHAUST	
RUN W O	RPM	LBS	MIN L/HR	PSIG	F	CFPM	INHG	LIFT	F	
								RISE ILLUM	HU	
15 E D	2000	26.1	7.32	67.5	75	-C	29.4	21.1	8.6	729 40
16 E D	2000	22.2	7.51	66.0	78	-C	29.3	20.8	10.4	768 51
17 E D	2000	22.2	7.46	66.5	78	-C	29.2	20.8	12.0	795 54
18 E D	2000	22.6	7.44	65.8	76	-C	29.2	20.9	12.8	838 55
19 E D	2000	18.2	7.71	64.0	77	-C	29.2	20.8	13.3	900 53
20 E D	2000	14.8	8.05	60.0	78	-C	29.2	20.5	13.3	928 68
21 E D	2001	14.5	8.22	55.1	82	-C	29.2	20.9	14.5	968 71
22 E D	2000	14.2	8.44	58.0	82	-C	29.2	20.9	14.5	967 60
23 E D	2001	12.2	8.66	56.7	83	-C	29.1	20.8	14.9	976 63
24 E D	2000	12.5	8.68	56.3	83	-C	29.1	20.8	15.6	1012 54
26 E D	1959	10.8	9.22	54.5	85	-C	29.1	21.4	15.6	1027 -0
28 E D	2000	10.5	8.78	53.6	90	-C	29.2	21.4	15.5	1024 48
27 E D	2000	8.6	9.08	53.0	93	-C	29.0	21.5	15.8	1105 62
AVERAGES	2000	16.2	8.20	60.1	82	-C	29.2	20.9	13.6	926 57
RMS ERRS	1	5.3	.64	.04	5	.C	.1	.3	2.1	109 8

EFFECT OF GAS TEMPERATURE ON IGNITION DELAY WITH CITE FUEL (BATCH 15)
 RUNS TAKEN AT CONSTANT MEAN PRESSURE DURING DELAY

DATA SET A2B HAVING 2 RUN(S) FOLLOWS. THE ATAC ENGINE WAS TESTED (INJECTOR OPENING PRESSURE SET AT 3000 PSIG) USING CT19 FUEL.

FOR USE	SPEED	LOAD	FUEL	AIR	BLW	TEMPERATURES(F)	ROOM<SURGE<@IVC<@INJ<CRIS	DBTDC AT START OF	EXHAUST	
RUN W O	RPM	LBS	MIN L/HR	PSIG	F	CFPM	INHG	LIFT	F	
								RISE ILLUM	HU	
29 E D	2000	11.3	8.58	54.1	98	-C	29.1	20.3	14.5	978 30
30 E D	1959	9.1	8.84	52.6	82	-C	29.2	21.1	15.8	1042 70
AVERAGES	2000	10.2	8.71	53.3	90	-C	29.1	20.7	15.1	1010 50
RMS ERRS	0	1.1	.13	.01	.7	.0	.0	.4	.6	32 20

TABLE 12

COMPUTER DATA SHEET, COMPUTATION RESULTS, SERIES A2B FOR CITE FUEL

H/C RATIO = 1.592/1, DENSITY AT C = 48.75 #/CUFT, CLEARANCE VOLUME = 4.5610 CUIN, COMPRESSION RATIO = 16.69/1, IVC = 128 DBTDC

FOR RUN	BRAKE HP	BMEP PSI	#/HRFP	BSFC AIR	FUEL/HRFP	CYCLE(LBM/1000) AIR	BLOW	EXH	PSIA	SURGE	EFF PCT	@IVC F	AT START OF INJECTION INDEX PSIA	#/CUFT R	AVERAGED DURING DELAY INDEX PSIA	#/CUFT R	DELAY(MSEC) PRISE ILLUM					
15	17.4	56.3	.453	.0325	4.04	-.00	.12	21.8	92.4	183	92.4	183	1.391	529	.953	1475	1.23C	699	1.193	1550	1.041	-.000
16	14.8	81.9	.513	.0320	3.95	-.00	.13	23.4	92.7	245	92.7	245	1.381	564	.944	1586	1.220	711	1.141	1651	.867	-.000
17	14.8	81.9	.516	.0319	3.99	-.00	.14	25.4	93.6	260	93.6	260	1.380	582	.956	1617	1.234	711	1.124	1677	.733	-.000
18	15.1	83.4	.508	.0324	3.94	-.00	.14	26.8	94.2	258	94.2	258	1.379	602	.942	1696	1.237	725	1.095	1755	.675	-.000
19	12.1	67.1	.598	.0314	3.85	-.00	.14	27.4	96.4	353	96.4	353	1.357	604	.924	1735	1.218	715	1.062	1786	.625	-.000
20	9.9	54.6	.702	.0316	3.65	-.00	.13	27.6	96.8	400	96.8	400	1.349	605	.887	1811	1.242	714	1.014	1868	.600	-.000
21	9.9	55.0	.692	.0319	3.55	-.00	.14	26.6	96.9	441	96.9	441	1.331	589	.860	1818	1.290	687	.971	1880	.533	-.000
22	9.5	52.4	.699	.0312	3.54	-.00	.14	29.2	98.7	476	98.7	476	1.322	593	.849	1855	1.289	691	.958	1917	.533	-.000
23	8.1	45.0	.800	.0312	3.47	-.00	.14	30.3	98.8	521	98.8	521	1.312	600	.837	1904	1.259	689	.935	1957	.491	-.000
24	8.3	46.1	.771	.0310	3.45	-.00	.14	31.6	95.0	574	95.0	574	1.304	619	.833	1972	1.272	700	.920	2023	.433	-.000
26	7.2	39.8	.829	.0297	3.35	-.00	.15	33.8	98.9	638	98.9	638	1.310	641	.805	2114	1.243	726	.892	2165	.450	-.000
28	7.3	40.2	.871	.0320	3.30	.05	.15	33.2	95.5	669	95.5	669	1.294	617	.782	2097	1.229	701	.869	2146	.458	-.000
27	5.7	31.7	1.068	.0313	3.26	-.00	.15	34.8	101.1	671	101.1	671	1.304	620	.770	2141	1.286	712	.858	2205	.475	-.000
MEAN	10.8	59.6	.694	.0315	3.65	.05	.14	28.8	96.8	441	96.8	441	1.340	597	.873	1832	1.250	706	1.002	1891	.609	-.000
ERRS	3.5	19.6	.169	.0007	.27	.00	.01	3.8	2.7	161	2.7	161	.033	27	.064	202	.025	12	.107	198	.174	-.000

H/C RATIO = 1.999/1, DENSITY AT 60 = 48.84 #/CUFT, CLEARANCE VOLUME = 4.5610 CUIN, COMPRESSION RATIO = 16.69/1, IVC = 128 DBTDC

FOR RUN	BRAKE HP	BMEP PSI	#/HRFP	BSFC AIR	FUEL/HRFP	CYCLE(LBM/1000) AIR	BLOW	EXH	PSIA	SURGE	EFF PCT	@IVC F	AT START OF INJECTION INDEX PSIA	#/CUFT R	AVERAGED DURING DELAY INDEX PSIA	#/CUFT R	DELAY(MSEC) PRISE ILLUM					
29	7.5	41.7	.827	.0315	3.30	.05	.15	31.7	98.8	580	98.8	580	1.307	615	.813	2009	1.214	701	.907	2054	.483	-.000
30	6.1	33.6	1.002	.0309	3.28	.05	.15	34.3	99.5	748	99.5	748	1.273	636	.786	2148	1.227	718	.870	2195	.442	-.000
MEAN	6.8	37.6	.915	.0312	3.29	.05	.15	33.0	99.2	664	99.2	664	1.290	626	.800	2078	1.220	709	.888	2125	.463	-.000
ERRS	.7	4.1	.088	.0003	.01	.00	.00	1.3	.4	84	.4	84	.017	10	.014	69	.006	9	.018	70	.021	-.000

TABLE 13

COMPUTER DATA SHEET, COMPARISON WITH PREVIOUS WORK, SERIES A2B FOR CITE FUEL

FOR RUN	EXPERIMENTAL PRD	ILD	WCLFFR START	WCLFFR MEAN	ELLCI START	ELLCI MEAN	SITKEI START	SITKEI MEAN	TSAO START	TSAO MEAN	TSAO @ START	TSAO @ MEAN
15	1.041	-.000	1.802	.585	2.621	2.460	2.738	1.805	.175	-.091	2.009	1.618
16	.867	-.000	1.121	.692	2.391	2.280	1.986	1.468	-.245	-.456	1.627	1.349
17	.733	-.000	.979	.641	2.337	2.240	1.820	1.407	-.372	-.610	1.528	1.289
18	.675	-.000	.736	.500	2.210	2.127	1.534	1.235	-.738	-.980	1.309	1.106
19	.625	-.000	.658	.468	2.154	2.087	1.440	1.195	-.931	-1.141	1.217	1.046
20	.600	-.000	.536	.382	2.056	1.990	1.290	1.086	-1.339	-1.581	1.049	.886
21	.533	-.000	.544	.389	2.048	1.978	1.302	1.096	-1.392	-1.667	1.044	.874
22	.533	-.000	.493	.354	2.006	1.939	1.238	1.050	-1.596	-1.876	.966	.804
23	.491	-.000	.432	.325	1.952	1.899	1.159	1.012	-1.885	-2.116	.866	.734
24	.433	-.000	.358	.278	1.886	1.840	1.061	.948	-2.274	-2.501	.734	.622
26	.450	-.000	.258	.203	1.766	1.728	.924	.843	-3.162	-3.374	.494	.404
28	.458	-.000	.279	.219	1.779	1.742	.954	.866	-3.089	-3.287	.526	.435
27	.475	-.000	.256	.194	1.746	1.701	.922	.830	-3.379	-3.666	.460	.351
MEAN	.605	-.000	.650	.433	2.073	2.001	1.413	1.142	-1.556	-1.799	1.064	.886
ERRS	.174	-.000	.420	.219	.254	.222	.456	.271	1.114	1.109	.451	.373

FOR RUN	EXPERIMENTAL PRD	ILD	WCLFER START	WCLFER MEAN	ELLCI START	ELLCI MEAN	SITKEI START	SITKEI MEAN	TSAO START	TSAO MEAN	TSAO @ START	TSAO @ MEAN
29	.483	-.000	.333	.260	1.852	1.813	1.028	.924	-2.516	-2.697	.670	.572
30	.442	-.000	.245	.195	1.741	1.707	.906	.832	-3.397	-3.586	.445	.363
MEAN	.463	-.000	.289	.228	1.796	1.760	.967	.878	-2.957	-3.141	.558	.468
ERRS	.021	-.000	.044	.033	.056	.053	.061	.046	.440	.445	.112	.104

TABLE 14

COMPUTER DATA SHEET, RECORDED DATA, SERIES A2C FOR DIESEL FUEL

EFFECT OF GAS TEMPERATURE ON IGNITION DELAY WITH NO. 2 DIESEL FUEL
 RUNS TAKEN AT CONSTANT MEAN PRESSURE DURING DELAY

DATA SET A2C		HAVING		9 RUN(S) FOLLOWS.		THE ATAC ENGINE WAS TESTED (INJECTOR OPENING PRESSURE SET AT 3000 PSIG) USING NO.2 FUEL.														
FOR USE	SPEED	LOAD	FUEL	AIR	BLCW	TEMPERATURES(F)		ROOM<SURGE<@INJ<CRIS	DBTDC AT START OF		EXHAUST									
RUN W O	RPM	LBS	MIN L/HR	PSIG	F	CFPM	AIR OUT MIN INC	INHG	INHG	PSI	PSI	LIFT	RISE ILLUM	F	HU					
41 E D	2000	27.5	7.13	74.1	73	.8	90	173	-0	-0	29.4	18.7	4.6	560	276	21.1	11.9	8.7	740	54
36 E D	2000	23.0	7.96	66.5	87	.9	217	168	-0	-0	28.2	23.2	4.5	568	237	21.0	13.4	11.0	803	50
33 E D	2000	20.1	8.46	61.5	81	.8	328	170	-0	-0	29.3	26.7	6.3	583	230	21.0	14.1	11.4	850	38
34 E D	2000	17.9	8.89	64	86	.9	418	170	-0	-0	25.3	25.8	6.8	596	221	21.0	14.4	14.6	888	33
37 E D	2000	16.3	9.02	66.5	77	.8	474	171	-0	-0	29.0	31.9	4.8	606	171	21.0	15.6	14.7	909	26
43 E D	2000	15.8	9.11	67	83	.8	505	171	-0	-0	29.0	33.4	5.2	607	173	21.1	15.7	14.0	917	27
35 E D	2000	14.5	9.40	65	80	.7	555	171	-0	-0	29.0	33.4	4.8	602	182	21.0	15.3	14.9	944	31
40 E D	2000	13.5	9.43	62.5	87	.8	623	165	-0	-0	29.0	36.9	4.1	612	192	21.2	15.4	15.7	985	28
44 D C	2001	11.2	4.88	67	87	.8	702	170	-0	-0	29.0	38.9	5.5	597	180	21.4	15.9	16.1	997	40
AVERAGES	2000	17.8	8.25	61.4	82	.8	435	170	-0	-0	29.1	30.3	5.2	592	207	21.1	14.6	13.5	893	36
RMS ERRS	0	4.8	1.38	7.6	5	.1	184	1	-0	-0	.2	6.1	.8	17	34	.1	1.2	2.4	79	10

TABLE 15

COMPUTER DATA SHEET, COMPUTATION RESULTS, SERIES A2C FOR DIESEL FUEL

H/C RATIO = 1.837/1, DENSITY AT 60 = 51.6C #/CUFT, CLEARANCE VOLUME = 4.5610 CUIN, COMPRESSION RATIO = 16.69/1, IVC = 128 DBTDC

FOR RUN	HP	BRAKE PSI	BMEP PSI	BSFC #/HRHP	FUEL/ AIR	CYCLE (LBM/1000)	AIR BLOW	EXH	PSIA	SURGE	EFF PCT	@ IVC	INDEX	AT START OF INJECTION	INDEX	PSIA	#/CUFT	R	AVERAGED DURING DELAY	INDEX	PSIA	#/CUFT	R	PRISE	ILLUM	DELAY (MSEC)
41	18.3	101.4	84.8	.452	.0316	4.37	.05	.13	23.6	91.1	178	1.408	588	1.031	1513	1.208	722	1.223	1565	.767	1.033					
36	15.3	84.8	74.1	.481	.0312	3.94	.06	.14	25.7	92.8	255	1.381	558	.937	1694	1.244	713	1.080	1751	.633	.833					
33	13.4	74.1	66.0	.523	.0314	3.72	.05	.14	27.5	95.4	431	1.344	617	.887	1845	1.291	728	1.010	1913	.575	.800					
34	11.9	66.0	60.1	.559	.0313	3.55	.06	.15	29.0	96.4	525	1.328	632	.851	1972	1.273	739	.963	2037	.550	.533					
37	10.9	60.1	58.3	.601	.0313	3.48	.05	.15	29.9	97.4	513	1.345	641	.834	2040	1.210	724	.524	2083	.450	.525					
43	10.5	58.3	53.5	.612	.0312	3.45	.05	.15	30.6	97.8	553	1.338	643	.825	2070	1.218	727	.914	2114	.450	.592					
39	9.7	53.5	49.8	.643	.0312	3.32	.05	.15	30.6	98.6	575	1.337	637	.798	2123	1.222	726	.889	2172	.475	.508					
40	9.0	49.8	41.3	.686	.0314	3.27	.05	.15	32.4	98.1	623	1.336	648	.781	2205	1.238	742	.872	2261	.483	.458					
44	7.5	41.3	35.5	.807	.0316	3.18	.05	.15	33.3	99.4	724	1.302	636	.756	2236	1.247	723	.839	2292	.458	.441					
MEAN	11.8	65.5	59.6	.596	.0314	3.55	.05	.15	25.2	96.3	451	1.347	627	.856	1966	1.239	727	.968	2021	.538	.636					
ERRS	3.2	17.6	.103	.0002		.35	.00	.01	2.9	2.6	158	.029	20	.081	227	.027	8	.114	226	.101	.193					

TABLE 16

COMPUTER DATA SHEET, COMPARISON WITH PREVIOUS WORK, SERIES A2C FOR DIESEL FUEL

FOR RUN	EXPERIMENTAL		WOLFER		ELLIOT		SIITKEI		TSAC		TSAO @ 1000	
	PRD	ILD	START	MEAN	START	MEAN	START	MEAN	START	MEAN	START	MEAN
41	.767	1.033	1.377	.897	2.535	2.430	2.259	1.703	.041	-.146	1.817	1.560
36	.633	.833	.747	.516	2.213	2.132	1.547	1.255	-.729	-.965	1.317	1.120
33	.575	.800	.481	.336	2.016	1.943	1.220	1.025	-1.520	-1.821	.973	.800
34	.550	.533	.349	.253	1.886	1.828	1.048	.513	-2.261	-2.548	.729	.590
37	.450	.525	.298	.237	1.825	1.750	.979	.891	-2.683	-2.851	.610	.523
43	.450	.552	.280	.222	1.800	1.765	.954	.870	-2.871	-3.049	.562	.475
39	.475	.508	.256	.200	1.759	1.724	.921	.839	-3.228	-3.423	.482	.394
40	.483	.458	.216	.168	1.701	1.664	.865	.792	-3.771	-3.997	.361	.274
44	.458	.441	.210	.164	1.680	1.645	.856	.787	-4.016	-4.245	.321	.237
MEAN	.538	.636	.468	.333	1.935	1.880	1.183	1.008	-2.337	-2.561	.797	.664
ERRS	.101	.193	.359	.224	.264	.240	.432	.281	1.291	1.286	.466	.408

TABLE 17

COMPUTER DATA SHEET, RECORDED DATA, SERIES A2D FOR GASOLINE FUEL

EFFECT OF GAS TEMPERATURE ON IGNITION DELAY WITH MILG FUEL
 RUNS TAKEN AT CONSTANT MEAN PRESSURE DURING DELAY

DATA SET A2D HAVING 7 RUN(S) FOLLOWS. THE ATAC ENGINE WAS TESTED (INJECTOR OPENING PRESSURE SET AT 3000 PSIG) USING MILG FUEL.

FOR USE	SPEED	LOAD	FUEL	AIR	ELCW	TEMPERATURES(F)	ROOM<	SURGE<	INHG	INHG	PSI	PSI	PSI	DBTDC	AT START	OF	EXHAUST				
RUN W U	RPM	LBS	MIN	L/HR	F	CFPM	AIR	OUT	MIN	INC	INHG	INHG	PSI	PSI	PSI	LIFT	RISE	ILLUM	F	HU	
52 E D	2001	20.4	8.80	.33	54.0	85	.8	106	165	-0	-0	28.9	8.8	4.1	446	336	21.0	-4.7	-5.0	724	6
53 E D	2001	17.7	8.82	.36	53.0	87	.9	212	172	-0	-0	28.9	14.8	6.2	483	390	21.0	4.0	3.5	760	14
54 D D	2000	14.3	4.58	.42	45.5	93	.7	308	170	-0	-0	29.0	17.0	5.6	505	326	20.8	8.1	6.4	797	14
55 D D	2000	14.2	4.62	.40	48.5	86	.6	408	172	-0	-0	29.0	21.9	5.0	529	281	21.1	11.2	10.7	875	12
56 D D	1999	11.9	4.75	.35	46.6	90	.5	499	172	-0	-0	29.0	25.0	5.0	549	252	21.0	12.4	13.4	907	18
57 D D	1959	11.0	4.84	.35	46.0	86	1.0	600	169	-0	-0	29.0	29.6	5.4	576	189	21.0	14.9	15.1	946	19
58 C C	2001	9.7	4.99	.40	62.5	90	.5	697	172	-0	-0	29.0	31.6	5.9	581	188	21.0	14.9	16.0	1008	19
AVERAGES	2000	14.2	5.51	.38	51.4	85	.5	404	171	-0	-0	29.0	21.2	5.3	524	280	21.0	8.7	8.6	860	15
RMS ERRS	1	3.5	1.84	.03	5.2	2	.1	196	1	-0	-0	.0	7.6	.6	46	71	.1	6.5	7.0	96	4

TABLE 18

COMPUTER DATA SHEET, COMPUTATION RESULTS, SERIES A2D FOR GASOLINE FUEL

H/C RATIO = 2.141/1, DENSITY AT 60 = 45.87 #/CUFT, CLEARANCE VOLUME = 4.5610 CUIN, COMPRESSION RATIO = 16.69/1, IVC = 128 DBTDC

FOR RUN	BRAKE HP	BMEP PSI	BSFC #/HRHP	FUEL/AIR	CYCLE (LBM/1000) AIR	EXH PSIA	SURGE PCT	EFF @IVC	INDEX PSIA	AT START OF INJECTION	AVERAGED DURING DELAY	DELAY (MSEC)
					BLOW	EXH		F		#/CUFT R	INDEX PSIA #/CUFT R	RISE ILLUM
52	13.6	75.3	.461	.0316	3.31	.05	18.5	90.7	1.402	.786	1.138	2.141
53	11.8	65.3	.526	.0316	3.27	.06	21.5	91.8	1.349	.779	1.172	2.166
54	9.5	52.8	.617	.0318	3.05	.05	22.6	94.1	1.356	.743	1.177	1.458
55	9.5	52.4	.619	.0319	3.06	.05	25.0	95.2	1.356	.730	1.207	1.200
56	7.9	43.9	.719	.0321	2.96	.06	26.5	95.9	1.348	.710	1.208	.867
57	7.3	40.6	.762	.0317	2.94	.07	28.8	97.0	1.333	.708	1.234	.717
58	6.5	35.8	.831	.0322	2.75	.06	25.8	97.1	1.319	.672	1.217	.509
MEAN	9.4	52.3	.648	.0318	3.06	.06	24.7	94.5	1.352	.733	1.193	.508
ERRS	2.3	13.0	.121	.0002	.17	.01	3.8	2.3	.024	.038	.030	1.025
								176	50	281	273	.580

TABLE 19

COMPUTER DATA SHEET, COMPARISON WITH PREVIOUS WORK, SERIES A2D FOR GASOLINE FUEL

FOR RUN	EXPERIMENTAL		WOLFER		ELLICIT		SITKEI		TSAD		TSAD @	
	PRD	ILC	START	MEAN	START	MEAN	START	MEAN	START	MEAN	START	MEAN
52	2.141	2.166	1.398	.665	2.390	2.258	2.341	1.435	-0.265	-0.559	1.741	1.317
53	1.416	1.458	.786	.420	2.144	2.037	1.616	1.135	-1.032	-1.358	1.272	.963
54	1.058	1.200	.493	.304	1.948	1.876	1.248	.984	-1.984	-2.258	.894	.689
55	.825	.867	.353	.235	1.827	1.767	1.060	.889	-2.786	-3.073	.643	.485
56	.717	.634	.260	.184	1.722	1.675	.931	.816	-3.688	-3.944	.419	.300
57	.509	.492	.201	.155	1.644	1.610	.845	.774	-4.474	-4.704	.248	.165
58	.508	.416	.159	.124	1.563	1.534	.783	.727	-5.568	-5.769	.066	.000
MEAN	1.025	1.033	.521	.298	1.891	1.822	1.261	.566	-2.828	-3.095	.755	.560
ERRS	.543	.580	.409	.176	.272	.237	.513	.230	1.751	1.716	.550	.430

SECTION 9

PROGRESS REPORT NO. 9

EFFECT OF THE FOLLOWING VARIABLES ON I.D. AND OTHER COMBUSTION
PHENOMENA:

1. Air Charge Temperature
2. Type of Fuel
3. Engine Speed
4. Coolant Temperature

PROGRESS REPORT NO. 9

DIESEL ENGINE IGNITION AND COMBUSTION

Effect of Type of Fuel, Engine Speed, and Coolant Temperature
on Ignition Delay and Other Combustion Phenomena

JAY A. BOLT

N. A. HENEIN

PERIOD JANUARY 1, 1968 TO JUNE 30, 1968

OCTOBER 1968

This project is under the technical supervision of the:

Propulsion Systems Laboratory
U.S. Army Tank-Automotive Center
Warren, Michigan

and is work performed by the:

Department of Mechanical Engineering
The University of Michigan
Ann Arbor, Michigan

under Contract No. DA-20-018-AMC-1669(T)

TABLE OF CONTENTS

	Page
LIST OF ILLUSTRATIONS	411
Part I: Summary	
I. BACKGROUND	415
II. OBJECTIVES	416
III. CUMULATIVE PROGRESS	417
A. Lister-Blackstone Engine	417
B. ATAC-1 Open Combustion Chamber Engine	417
1. Engine instrumentation	417
2. Experimental work on ATAC	417
3. Theoretical analysis	418
IV. PROGRESS DURING THIS PERIOD	419
V. CONCLUSIONS	420
A. Effect of Type of Fuel on I.D. and Heat Release Rate	420
B. Effect of Speed on Ignition Delay, Smoke, Wall Temperature, and Thermal Loading	421
1. Effect of engine speed on ignition delay	421
2. Effect of speed on smoky intensity	421
3. Effect of speed on wall temperatures	421
4. Effect of speed on thermal loading	421
C. Effect of Coolant Temperature on Combustion Phenomena	422
1. Effect of coolant temperature on ignition delay	422
2. Effect of coolant temperature on thermal loading	422
3. Effect of coolant temperature on after injection	422
VI. PROBLEM AREAS AND CORRECTIVE ACTIONS	423
A. Fuel Leakage Past Pump-Plunger	423
B. Failure of Pressure Transducer	423
C. Surface Thermocouple Failures	423
D. Engine Vibration	423
VII. FUTURE PLANS	424

TABLE OF CONTENTS (Concluded)

	Page
A. Next Period	424
B. Overall	424
VIII. SIGNIFICANT ACCOMPLISHMENTS	425
Part II: Instrumentation, Experimental, and Analytical Results	
I. INSTRUMENTATION	429
A. Fire Deck Wall Temperature	429
B. Coolant Flow Rate	429
C. Temperature Rise of Coolant Across the Engine	429
D. Lubricating Oil Flow Rate	429
E. Temperature Drop Across the Oil Cooler	429
II. HEAT RELEASE COMPUTATIONS AND RESULTS	435
III. EFFECT OF SPEED ON IGNITION DELAY AND OTHER COMBUSTION PHENOMENA	444
A1. Effect of Speed on I.D.p at Mean Pressure = 500 psia	444
A2. Effect of Speed on I.D.p, Mean Pressure - 700 psia	445
B. Effect of Speed on Smoke Intensity	451
C. Effect of Speed on Combustion Chamber Wall Temperatures	451
D. Effect of Speed on Thermal Loading	454
IV. EFFECT OF COOLANT TEMPERATURE ON IGNITION DELAY AND OTHER COMBUSTION PHENOMENA	456
A. Effect of Coolant Temperature on Combustion Phenomena	457
B. Effect of Coolant Temperature on Thermal Load	457
C. Effect of Coolant Temperature on Injection Process	457
V. PISTON AND LINER INSPECTION AFTER THE HIGH COOLANT TEMPERATURE TESTS	462
APPENDIX A: COMPUTER PROGRAMS	463
APPENDIX B: TABLES	531
APPENDIX C: REFERENCES	537

LIST OF ILLUSTRATIONS

Table	Page
1. Effect of Engine Speed on Ignition Delay Using CITE Fuel at a Mean Pressure of 500 psia During the Ignition Delay	532
2. Effect of Engine Speed on Ignition Delay Using CITE Fuel at a Mean Pressure of 700 psia During the Ignition Delay	533
3. Effect of Coolant Temperature on Ignition Delay	534
4. Equivalent Area for Fuel Flow in Injector Nozzle Versus Needle Lift	535

Figure

1. Position of thermocouples in the fire deck near the intake and exhaust valve seats.	430
2. Closed cooling system for the use of ethylene-glycol at high temperatures.	431
3. Photograph of the closed cooling system for ATAC-1 engine.	432
4. Photograph of the coolant flow meter.	433
5. Lubricating oil cooling system.	434
6. Pressure trace for ATAC-1 engine plotted by the computer.	437
7. Fuel pressure and needle lift traces for ATAC-1 engine plotted by the computer.	438
8. Rate and accumulated fuel injection for ATAC-1 engine plotted by the computer.	439
9. Detailed pressure trace for ATAC-1 engine during combustion.	440
10. Heat release diagram for ATAC engine with CITE Fuel plotted by the computer.	441
11. Heat release diagram for ATAC engine with diesel no. 2 fuel plotted by the computer.	443
12. Effect of engine speed on ignition delay at a mean pressure of 500 psia.	446

LIST OF ILLUSTRATIONS (Concluded)

Figure	Page
13. Corrected ignition delay versus engine speed (reference temperature = 1619°R).	447
14. Effect of engine speed on ignition delay at a mean pressure of 700 psia.	449
15. Effect of speed on the mean gas temperature during the ignition delay.	450
16. Effect of speed on smoke intensity.	452
17. Effect of engine speed on wall temperature.	453
18. Effect of engine speed on thermal loading.	455
19. Effect of coolant temperature on thermal loading.	458
20. Effect of coolant temperature on % heat lost to coolant and lubricating oil.	459
21. Effect of coolant temperature on needle lift during after injection.	460
22. Needle lift diagrams with coolant temperatures of 217°F and 304.3°F.	461
23. Equivalent area for fuel flow in injector nozzle versus needle lift.	536

PART I

SUMMARY

I. BACKGROUND

A program of activity to study the combustion process in supercharged diesel engines has been developed at The University of Michigan. This program is primarily concerned with the ignition delay and the effect of the several parameters on it. A special concern is given to the effect of the pressure and temperature of the cylinder air charge and engine speed on ignition delay. The program also includes the study of the effect of these variables on the other combustion phenomena such as smoke, rate of pressure rise, and maximum pressure reached in the cylinder.

The different types of delay have been studied in detail and an emphasis is made on the pressure rise delay and illumination delay. The instruments needed for the measurement of these two delay periods have been developed and a continuous effort is being made to improve their accuracy.

This research is being made on two experimental diesel engines. One is the ATAC high output open combustion chamber engine, and the other is a Lister-Blackstone swirl combustion chamber engine. Three fuels have been used in these tests.

II. OBJECTIVES

- A. To study how gas pressure at the time of injection affects ignition delay and combustion. The effects are to be studied at pressures ranging from approximately 300 to 1000 psia.
- B. To study how gas temperature at the time of injection affects ignition delay. The temperature ranges from approximately 900°F to 1500°F.
- C. To study various combinations of pressures and temperatures to determine whether density is an independent variable affecting ignition delay.
- D. To conduct all these studies with three fuels: CITE refree grade (Mil-F-45121) fuel, diesel no. 2 fuel, and Mil-G-3056 refree grade gasoline.
- E. To study the effect of engine speed on the ignition delay and the other combustion phenomena. The engine speed covered a range from 1000 rpm to 3000 rpm.
- F. To study the effect of the coolant temperature on the combustion process and the wall temperatures. Coolant temperatures range from 150°F to 300°F.
- G. To study the effect of anti-smoke additives on the combustion process and the smoke. The anti-smoke additive is Lubrizol barium compound.

on ignition delay and combustion characteristics of the following fuels:

- a. CITE refree grade (Mil-F-45121) fuel
- b. Diesel no. 2 fuel
- c. Mil-G-3056 refree grade gasoline fuel

The experimental results of this part were given in Progress Report No. 8, under A2A, A2B, A2C, and A2D series.

3. Theoretical Analysis

A thermodynamic analysis was made to study the different types of energy and processes taking place during the ignition delay, and to compare between the different definitions used in the literature for the ignition delay. This study will be published in an SAE paper which will be presented in the International Meeting in Detroit, on January 17, 1969.

IV. PROGRESS DURING THIS PERIOD

During this period the experimental and analytical work on the ATAC engine has been completed, as follows:

- a. A comparison between the combustion phenomena and the rate of heat release for the following fuels, under naturally aspirated conditions. The series of tests conducted for this comparison is referred to as series AI.
 1. CITE refree grade (Mil-F-45121) fuel
 2. Diesel no. 2 fuel, and
 3. Mil-G-3056 refree grade gasoline fuel

The experimental work demonstrated that it was difficult to burn gasoline in the ATAC engine with its present compression ratio of 16.7:1, under naturally aspirated conditions. The heat release computations were therefore only made for CITE and diesel no. 2 fuels. The several computer programs made for these elaborate computations proved to be very successful, and can be used in future heat release computations under any set of running conditions.

- b. Effect of engine speed on the ignition delay and other combustion phenomena. Engine speeds covered a range from 1000 rpm to 3000 rpm.
- c. Effect of coolant temperature on the combustion process of CITE fuel. The coolant used for these tests was ethylene glycol at temperatures up to 305°F.

V. CONCLUSIONS

The conclusions are stated under the following headings:

- A. Effect of type of fuel on I.D. and heat release rate
- B. Effect of engine speed on I.D. and other combustion phenomena
- C. Effect of coolant temperature on the different combustion phenomena

A. EFFECT OF TYPE OF FUEL ON I.D. AND HEAT RELEASE RATE

The results of the heat release computations, for the diesel no. 2 and CITE fuels, showed that the following processes occur during the ignition delay before the pressure rise due to combustion is detected:

1. A negative heat release at the beginning of the ignition delay, due to fuel evaporation and the endothermic reactions that take place shortly after fuel injection. The negative heat release is observed for the two fuels during a major part of the ignition delay.

2. The negative heat release is followed by very slow reactions causing a slight increase in the rate of heat release. The end of the pressure rise delay measured from the pressure trace, coincides with the end of these slow reactions, before the start of the very high speed reactions.

The negative heat release period as well as the total ignition delay period are shorter for diesel no. 2 fuel than for CITE fuel. These results support the previous conclusions reached,^{1*} that the activation energy for diesel no. 2 fuel is smaller than that for CITE fuel, causing the preignition reactions for the diesel fuel to be faster and the delay period shorter than for the CITE fuel.

The ignition delay is followed by a period of very rapid or explosive type reactions during which the energy of reaction of the fuel is released. These reactions occupied a relatively short period compared with the total ignition delay.

The maximum rate of heat release for the diesel fuel was found to be about 75% of that for CITE fuel.

*Numbers refer to list of references.

B. EFFECT OF SPEED ON IGNITION DELAY, SMOKE, WALL TEMPERATURE, AND THERMAL LOADING

1. Effect of Engine Speed on Ignition Delay

The apparent effect of the increase in engine speed is to decrease the ignition delay. However, if a correction is made for the effect of increase in the charge temperature with speed, the ignition delay was found to increase with speed. The conditions of the tests carried out to study the effect of speed on ignition delay were carefully adjusted to eliminate the change in any parameter other than the engine speed.

2. Effect of Speed on Smoky Intensity

An increase in speed from 1500 rpm and 3000 rpm caused an increase in the smoke intensity from 40 to 60 Hartridge units.

3. Effect of Speed on Wall Temperatures

The increase in speed produced the following effects in the wall temperature at the different locations in the cylinder head.

- a. The wall surface temperature in the valve bridge of the fire deck increased at a high rate with the increase in speed from 1000 rpm to 2000 rpm, after which the temperature leveled off. At 1000 rpm the surface temperature was 435°F and reached 509°F at 2900 rpm.
- b. The swing in the surface temperature decreased from 37°F at 1000 rpm to 13°F at 2900 rpm.
- c. The wall temperature at the midpoint between the gas side and coolant side in the fire deck showed a different trend.
 - (1). near the exhaust valve the temperature increased from 326°F at 1000 rpm to 360°F at 2900 rpm.
 - (2). near the inlet valve the temperature remained constant at about 267°F.

4. Effect of Speed on Thermal Loading

The thermal loading which is equal to the sum of the heat lost to the water jackets and lubricating oil increased with speed. However, the thermal loading as a percentage of the heat input in the fuel decreased from 20% at

1000 rpm to 14% at 2900 rpm.

C. EFFECT OF COOLANT TEMPERATURE ON COMBUSTION PHENOMENA

1. Effect of Coolant Temperature on Ignition Delay

The increase in the coolant temperature from 156°F to 305°F did not affect the ignition delay. The value of I.D.p over the whole temperature range at a mean pressure of 700 psia was 0.680 millisecond.

2. Effect of Coolant Temperature on Thermal Loading

The increase in coolant temperature reduced the percentage heat loss to the coolant and lubricating oil from 17.7% at 156°F to 13.8% at 305°F. The total heat loss decreased from 1660 Btu/hp. hr. at 156°F to 1230 Btu/hp. hr. at 305°F.

3. Effect of Coolant Temperature on After Injection

The increase in coolant temperature caused the after injection to decrease till a temperature of about 230°F, after which it increased again.

VI. PROBLEM AREAS AND CORRECTIVE ACTIONS

A. FUEL LEAKAGE PAST PUMP-PLUNGER

Problem: Excessive leakage of CITE fuel past the pump plunger and dilution of the lubricating oil in the sump.

Corrective Action: A new pump was installed.

B. FAILURE OF PRESSURE TRANSDUCER

Problem: Failure of fuel line pressure transducer type 601H.

Corrective Action: To avoid any delay in the progress of the experimental work a dummy transducer was made and installed.

C. SURFACE THERMOCOUPLE FAILURES

Problem: Failure of surface thermocouple.

Corrective Action: Design and manufacture of a new adaptor to relieve the tightening stress in the thermocouple body. The assembled body of a new thermocouple and adaptor were installed in the cylinder head with the thermocouple surface flush with the inside wall surface.

D. ENGINE VIBRATION

Problem: Excessive vibration of the engine was noted at high speeds (above 2800 rpm).

Corrective Action: The balancing weights were checked and the left balancing shaft found 90° ahead of the position indicated in the drawings. The front plate of the auxiliary drive was taken off and the shaft position adjusted to conform with the engine specifications.

VII. FUTURE PLANS

A. NEXT PERIOD

1. Experimental. Run tests on ATAC open chamber engine to find the effect of anti-smoke additives on the ignition delay and the rate of heat release.

2. Publication of part of the results in national meetings. To prepare a paper to be presented to the SAE on "Correlation of the Air Charge Temperature and Ignition Delay for Several Fuels in a Diesel Engine." Permission for this publication has been requested from ATAC.

B. OVERALL

1. Experimental. To complete the runs on the effect of gas pressure on the ignition delay and other combustion phenomena.

2. Analytical. To study the effect of pressure on the ignition delay, and to compare the results obtained on the ATAC engine and the results of previous work done in bombs and engines.

VIII SIGNIFICANT ACCOMPLISHMENTS

The paper presented before the Society of Automotive Engineers in January, 1967, covering the experimental results on the Lister-Blackstone engine will be published in the SAE Transactions of 1968. The title of this paper is "Ignition Delay in Diesel Engines," by the authors of this report.

The computer programs made for the calculation of the rates of heat release proved to be successful. The results reached reflect the accuracy with which the experimental and analytical data have been taken.

These computer programs are now ready to study the effect of fuel additives on the combustion process and rates of heat release.

PART II

INSTRUMENTATION, EXPERIMENTAL, AND ANALYTICAL RESULTS

Additional instrumentation made during this reporting period has included means to measure the wall temperatures, thermal loads on the cooling and lubricating systems, including the high coolant temperature running conditions.

The experimental and analytical results covered the following areas:

- A. Heat release computations and results.
- B. Effect of speed on ignition delay and other combustion phenomena.
- C. Effect of coolant temperature on ignition delay and other combustion phenomena.

I. INSTRUMENTATION

During this period the engine was instrumented to measure the following:

A FIRE DECK WALL TEMPERATURE

The temperature of the metal midway between the gas and coolant sides of the fire deck was measured by an iron-constantan thermocouple. Two thermocouples were used, to measure the temperature at a radial distance of $1/8$ in. from the exhaust the inlet valve inserts. The position of these thermocouples is shown in Fig. 1.

B. COOLANT FLOW RATE

The cooling system piping was changed to allow the use of a closed system with a heat exchanger, as shown in Figs. 2 and 3. The coolant flow rate was measured by a standard ASME sharp edge orifice as shown in Fig. 4. The coolant used was ethylene-glycol.

C. TEMPERATURE RISE OF COOLANT ACROSS THE ENGINE

The rise in the coolant temperature from its entrance to the exit from the engine was measured by two iron-constantan thermocouples. This temperature rise and the coolant flow rate were used to calculate the thermal load on the cooling system.

D. LUBRICATING OIL FLOW RATE

The rate of flow of the lubricating oil was measured by a turbine type meter. The oil was cooled in a heat exchanger to a constant temperature of 200°F . The oil cooling system is shown diagrammatically in Fig. 5.

E. TEMPERATURE DROP ACROSS THE OIL COOLER

The increase in oil temperature across the engine was measured by two iron-constantan thermocouples. This was used to calculate the thermal load on the lubricating system.

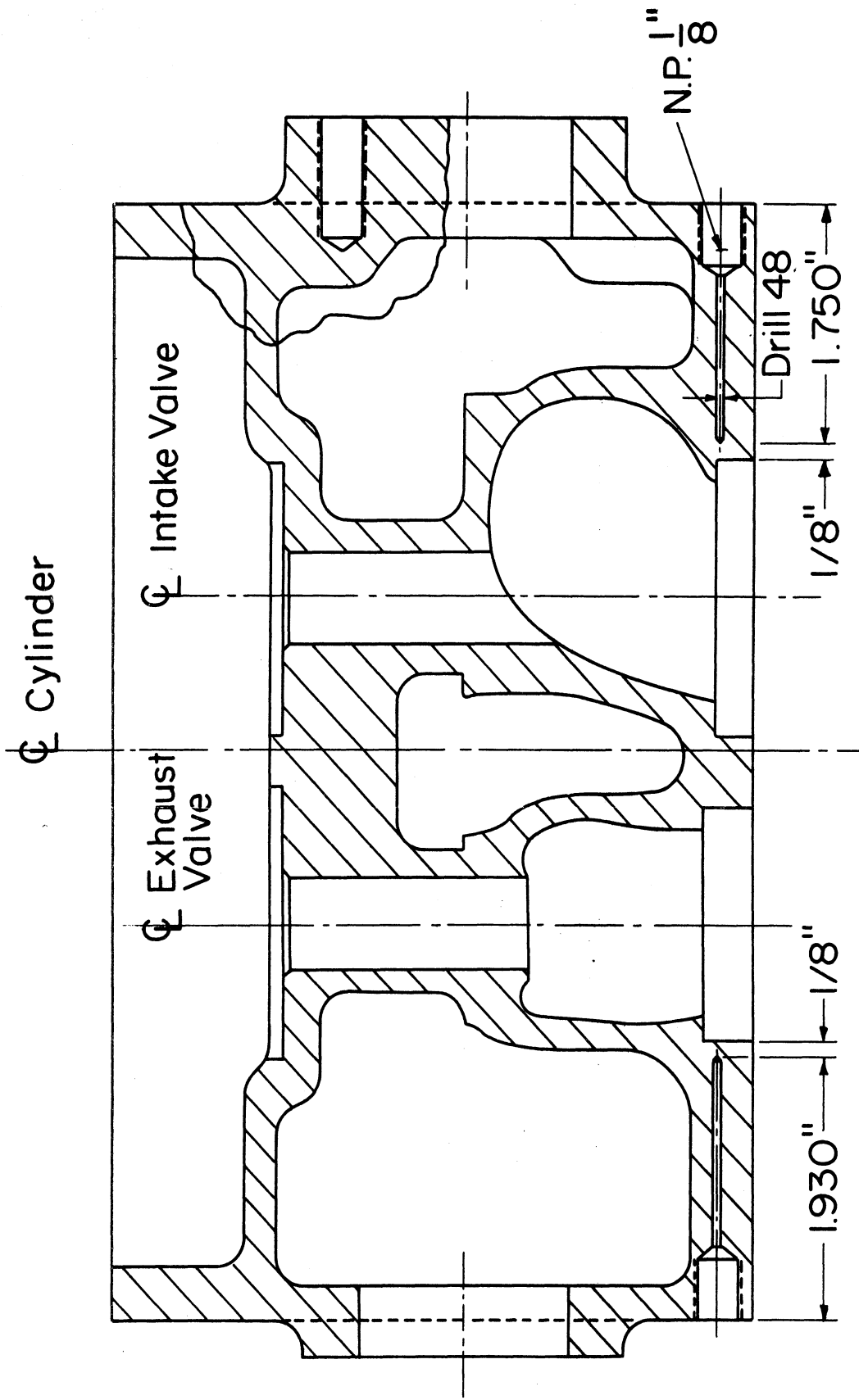


Fig. 1. Position of thermocouples in the fire deck near the intake and exhaust valve seats.

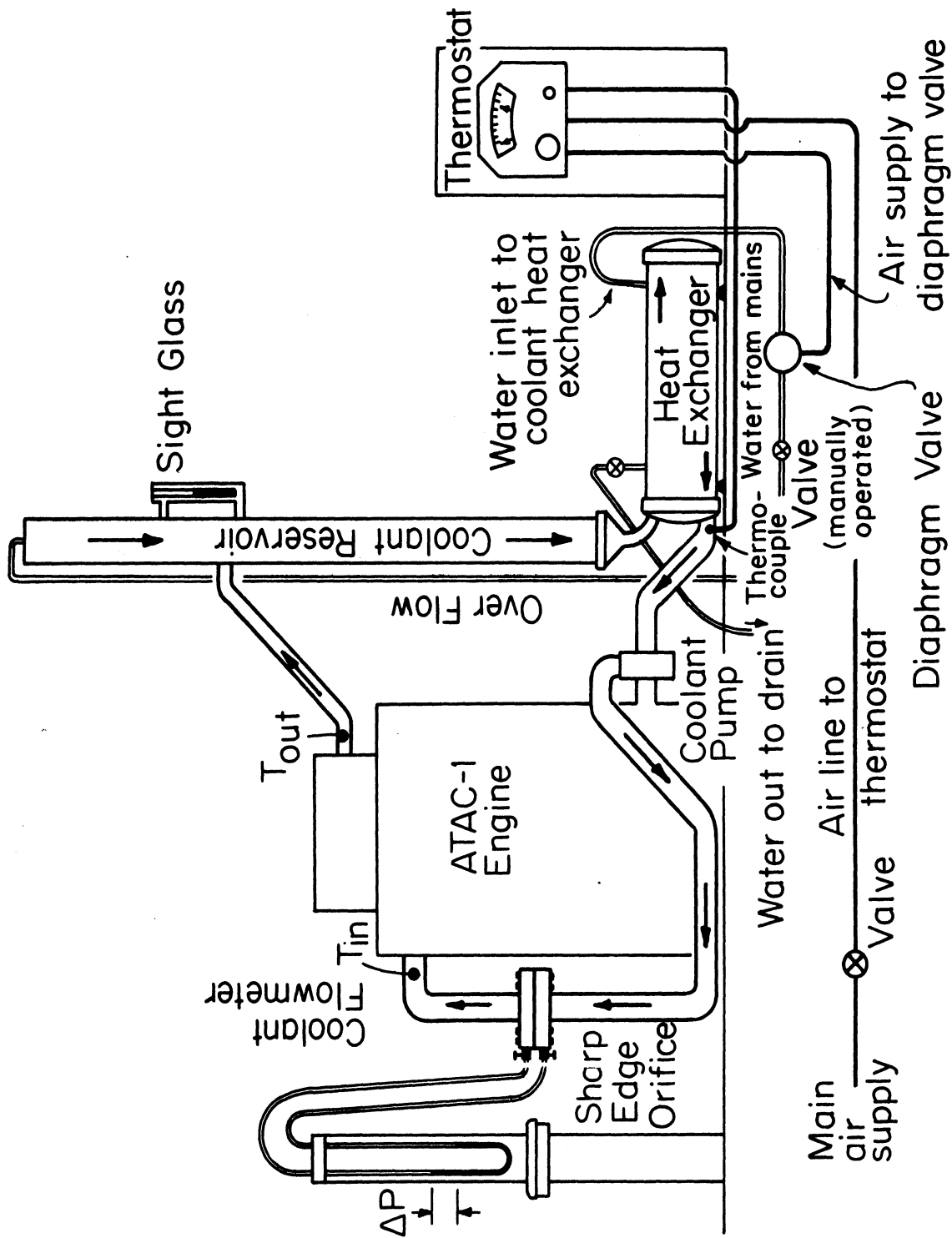


Fig. 2. Closed cooling system for the use of ethylene-glycol at high temperatures.

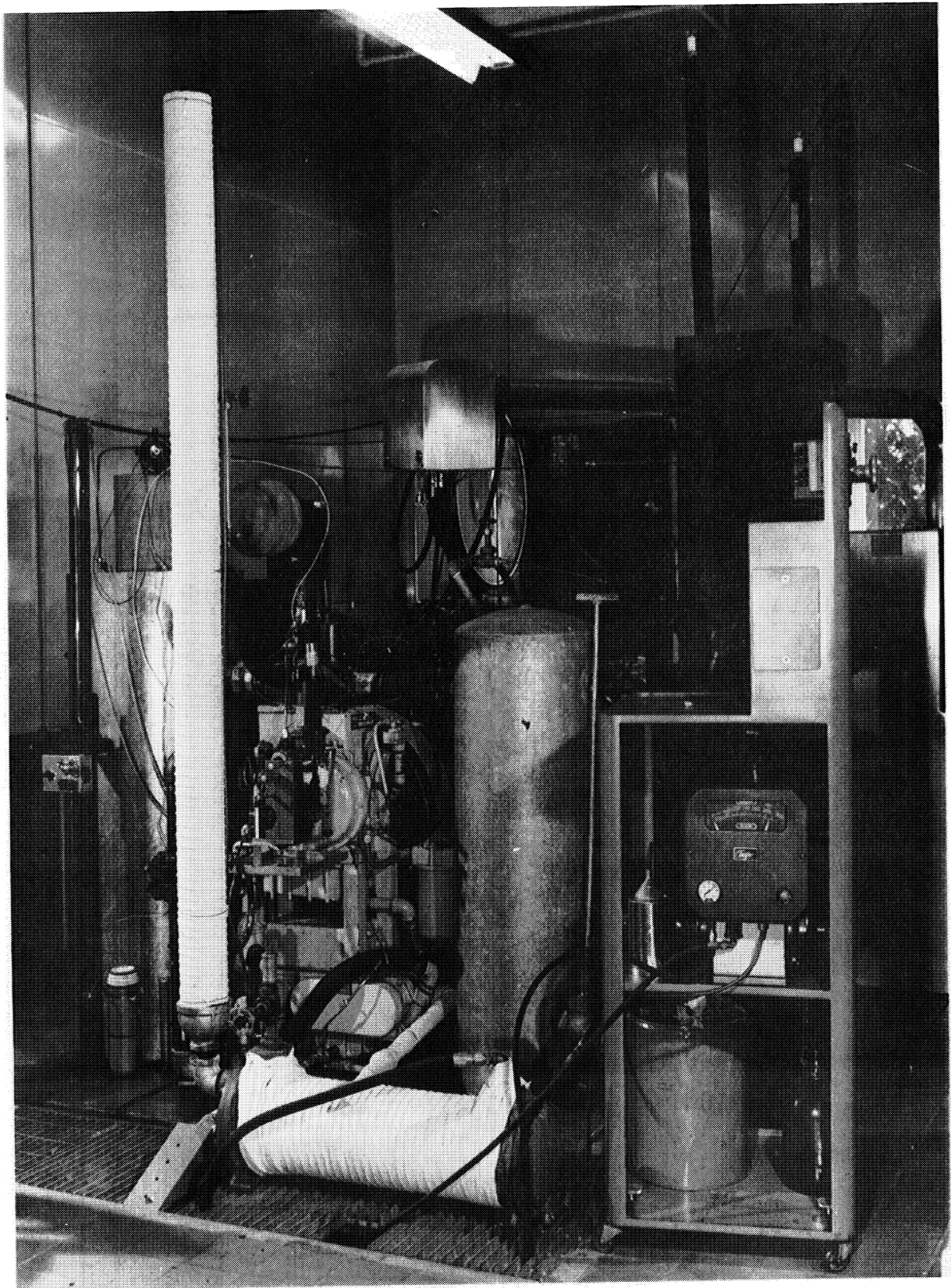


Fig. 3. Photograph of the closed cooling system for ATAC-1 engine.

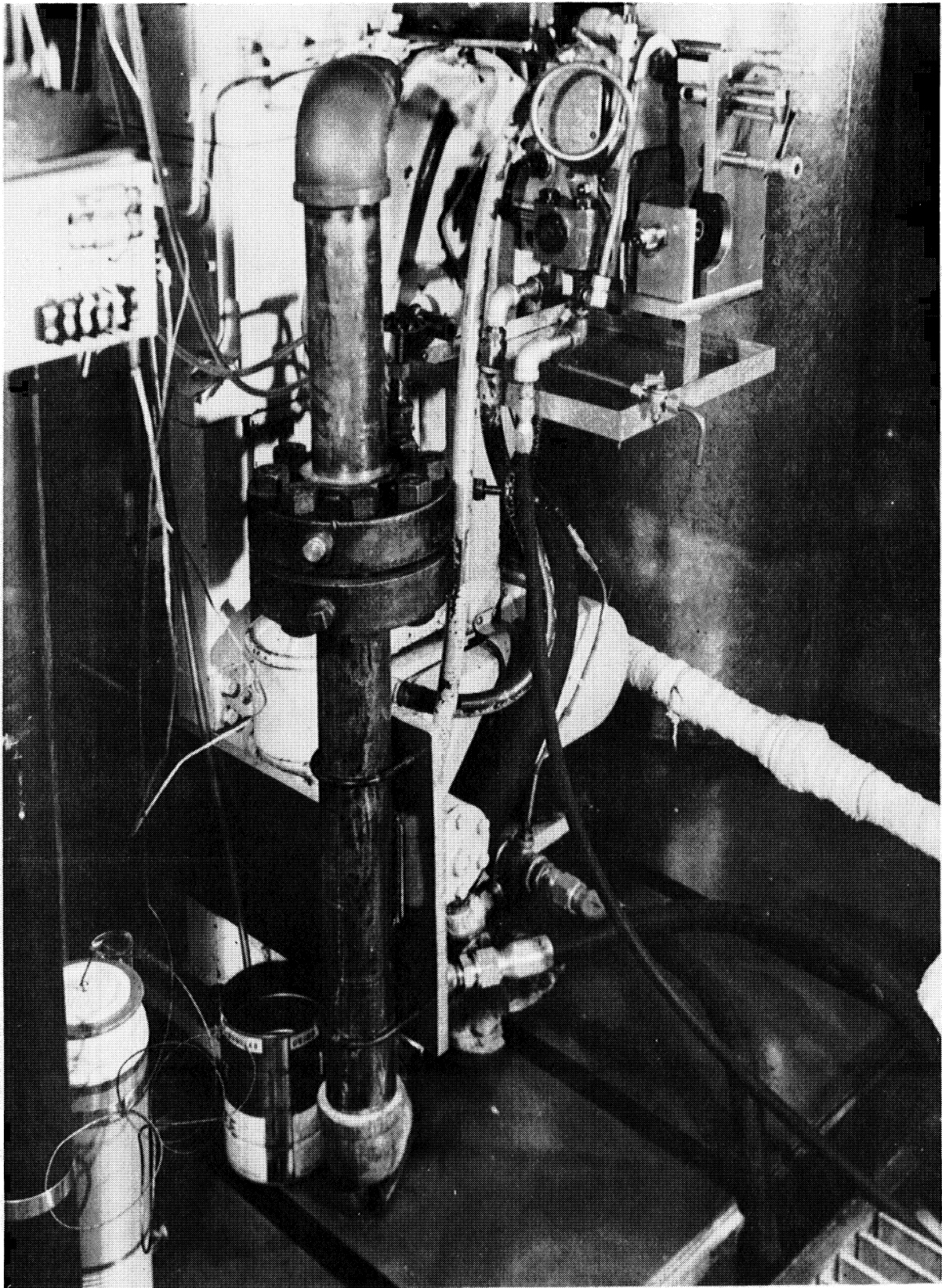


Fig. 4. Photograph of the coolant flow meter.

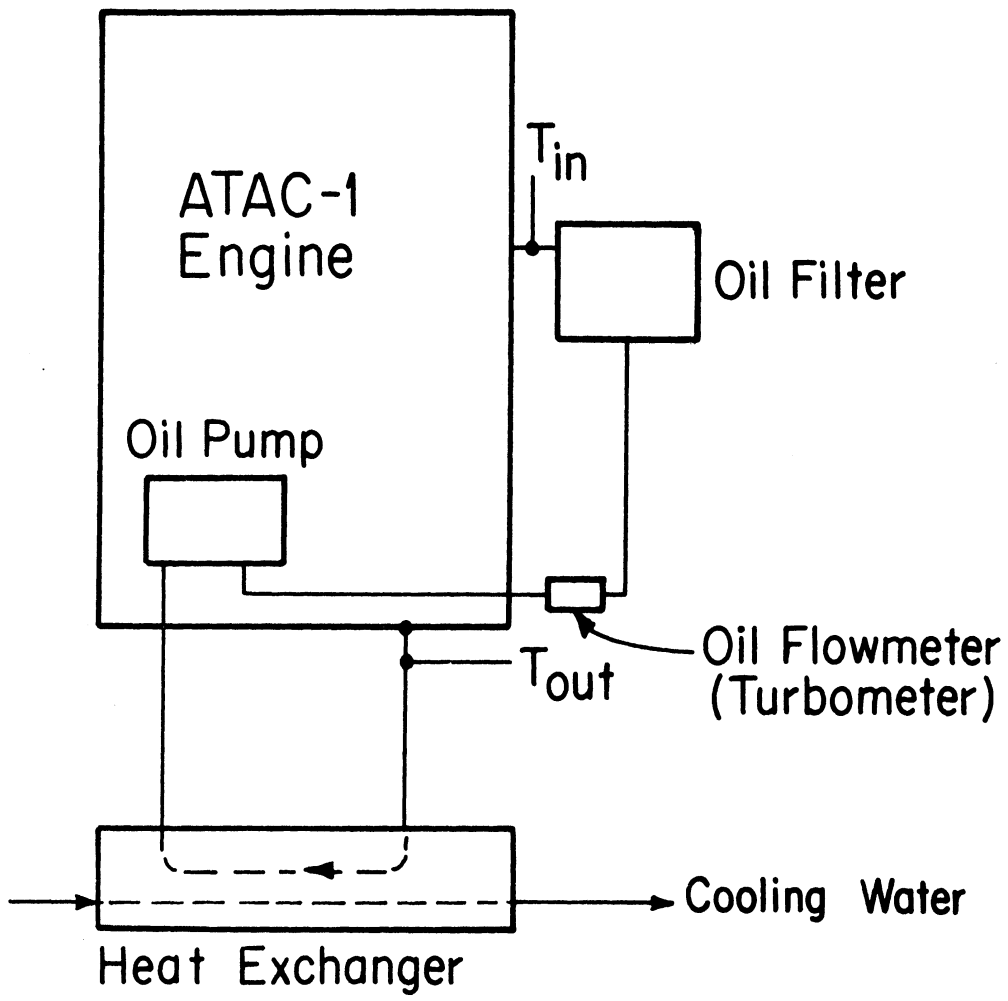


Fig. 5. Lubricating oil cooling system.

II. HEAT RELEASE COMPUTATIONS AND RESULTS

The rate of heat release in the ATAC engine, during the combustion process was calculated for diesel no. 2, and CITE fuels, under the following running conditions:

<u>Fuel</u>	<u>Diesel No. 2</u>	<u>CITE (Mil-F-45121)</u>
Pressure in surge tanks, in. Hg absolute	29.3	29.4
Inlet air temperature, °F	96.0	94.0
Fuel-air ratio	0.0301	0.0299
Injector opening pressure, psia (static)	3000.0	3000.0
Injector timing, (dynamic) degrees before T.D.C.	20.2	20.3
Engine speed, rpm	2001.0	2000.0
Coolant temperature at outlet, °F	174.0	170.0

The following traces were observed on the oscilloscope screen and photographed by the polaroid camera.

- a. Gas pressure—crank angles
- b. Fuel pressure—crank angles
- c. Needle lift—crank angles
- d. Surface wall temperature—crank angles

The gas pressure—crank angles trace was taken for the whole cycle and for successive divisions of the cycle. The duration of each division depend on the events taking place in the cycle during this division. In some cases a photograph was taken for the details of the pressure trace over a period of six or nine crank angles only during the ignition delay and the rapid pressure rise periods. The gas pressure at any crank angle was calculated from these traces by a statistical adjustment of the values obtained from the sequence of pressure

traces and that from the trace for the whole cycle.

The statistically adjusted values were used to plot the pressure trace for the whole cycle or any part of it by the computer. A sample trace for the pressure trace plotted by the computer for the engine running on CITE fuel is shown in Fig. 6. The points shown on this trace correspond to the reference points on the pressure trace taken for the whole cycle.

The corresponding traces plotted by the computer for the needle lift and fuel pressure are shown in Fig. 7. It shows that the needle lift started at 20.3° before T.D.C., when the fuel pressure was 3650 psia. The fuel pressure reached a maximum value of 4200 psia at 18.3° crank angles before T.D.C., while the needle lift was 2/1000 in. After this point the fuel pressure dropped due to the discharge of the fuel into the cylinder. The maximum needle lift was 15.3/1000 in., at an angle of 13.5° before T.D.C. The needle was completely closed, at zero lift, at an angle of 7.4° before T.D.C. At this crank angle the fuel pressure was about 1550 psia. The fluctuations in the needle lift trace after its closure are due to the bouncing of the needle on its seat.

The theoretical rate of fuel injection was calculated from the equivalent area for fuel flow, the difference between the fuel and gas pressures. The coefficient of discharge was assumed constant during the injection period and was computed from the ratio of the actual fuel consumption and the theoretical accumulated fuel. The equivalent area for fuel flow was calculated from the needle seat area and the holes area, as shown plotted in Fig. 23 and tabulated in Table 4.

The rate of fuel injection, the accumulated fuel injection, and the percentage of injected fuel are shown plotted by the computer in Fig. 8. The maximum rate of fuel injection was 370 lb per hour at an angle of 15.5° before T.D.C. At this location only 32% of the total fuel injection was accumulated in the cylinder. When the needle was first closed, 95% of the fuel was injected into the cylinder. This means that the after injection amounted to 4% of the total fuel. In this test the end of the pressure rise delay was at 4.5° before T.D.C. after almost all the fuel has been injected into the cylinder. The total amount of fuel injected per cycle is 79.5×10^{-6} lbm.

The detailed pressure trace during the ignition delay and the rest of the combustion process is shown in Fig. 9. The pressure fluctuations in this trace, near the maximum pressure, were smoothed by taking their averages, and used for the heat release computations. The heat release diagram calculated for this cycle is shown in Fig. 10. This figure shows that the preignition reactions occur in two distinct stages:

1. The first stage from the start of injection at 20.3° before T.D.C. to 6° before T.D.C. During this stage negative heat release occurs and is believed to be due to the fuel evaporation and the endothermic reactions.

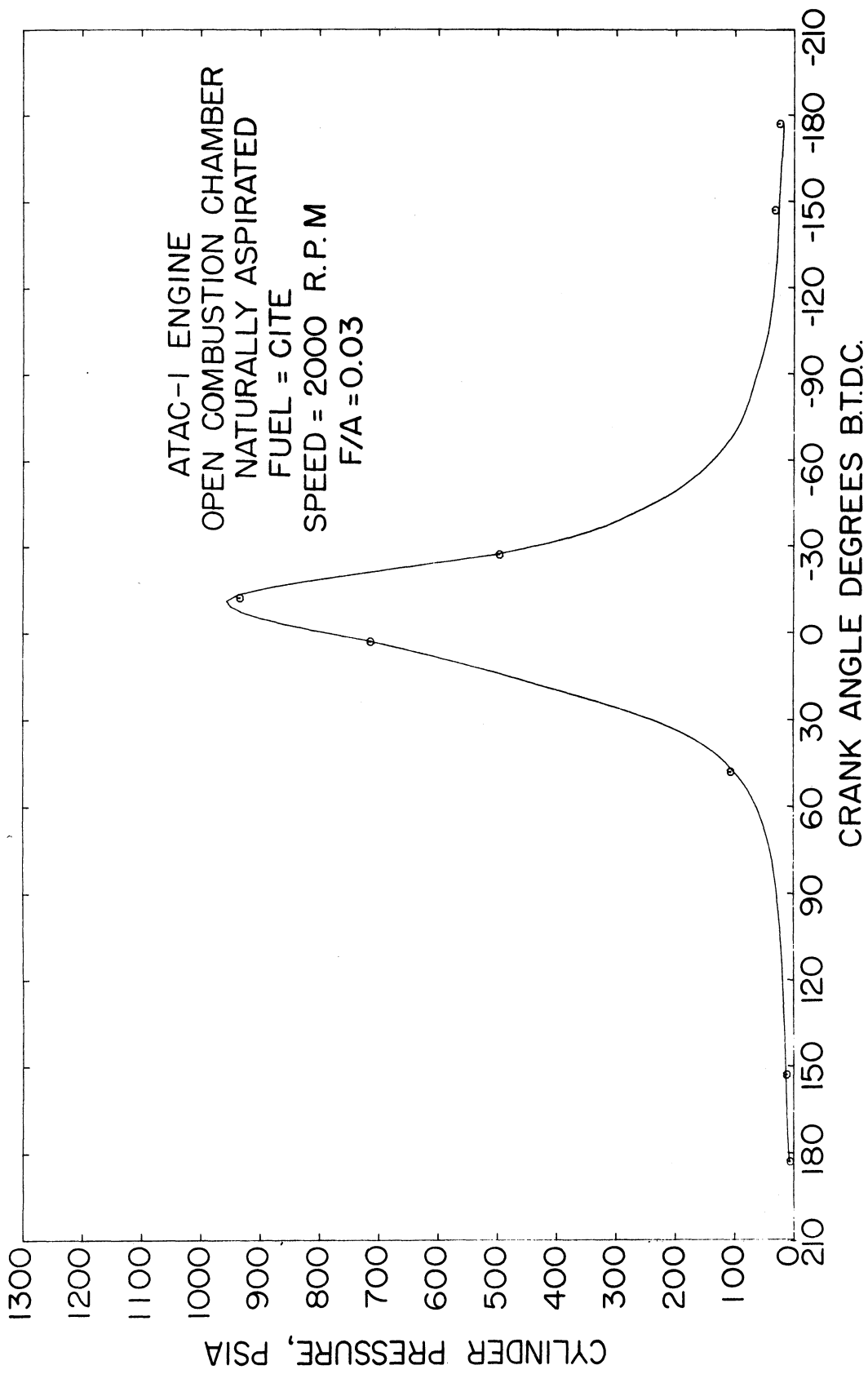


Fig. 6. Pressure trace for ATAC-1 engine plotted by the computer.

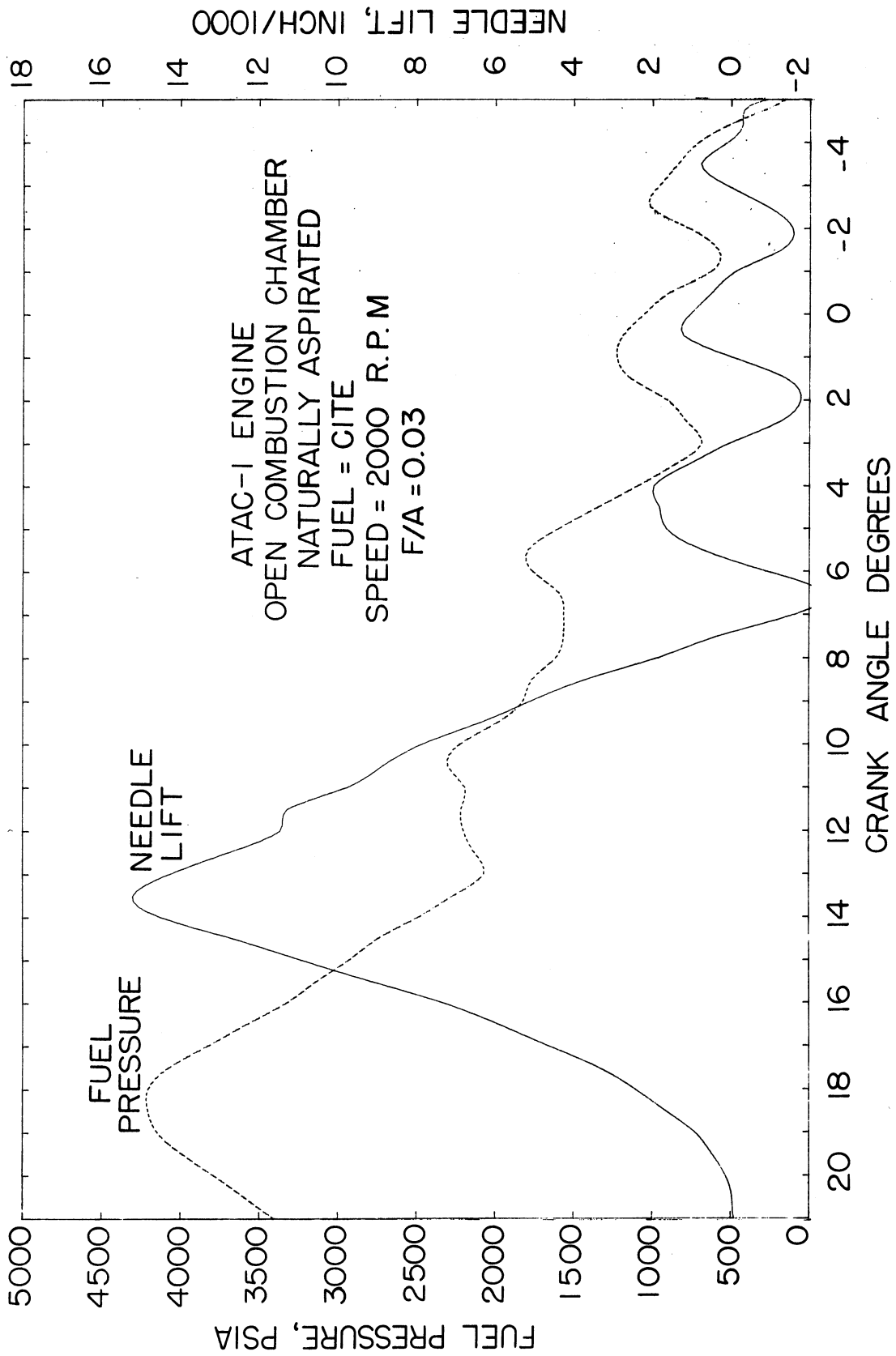


Fig. 7. Fuel pressure and needle lift traces for ATAC-1 engine plotted by the computer.

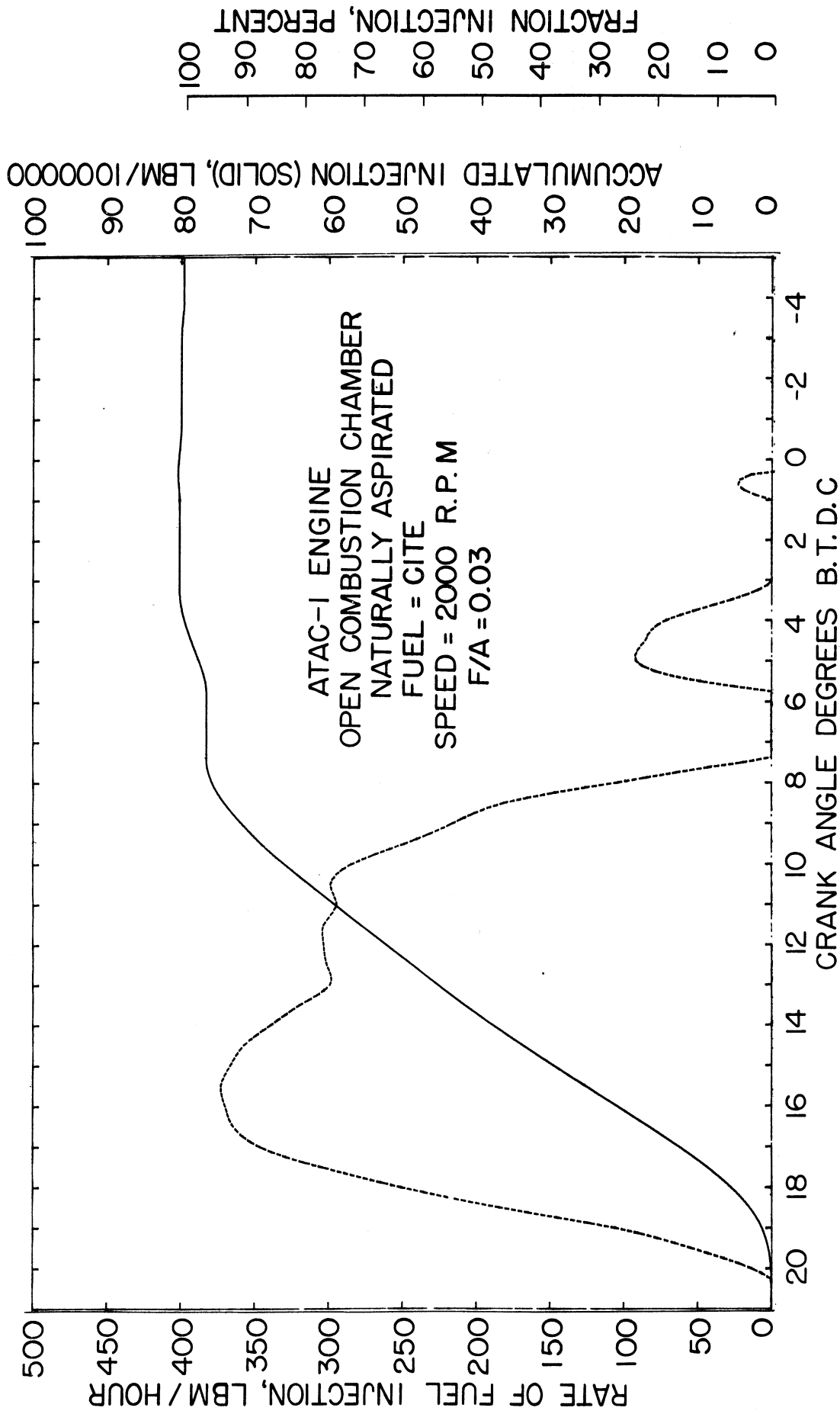


Fig. 8. Rate and accumulated fuel injection for ATAC-1 engine plotted by the computer.

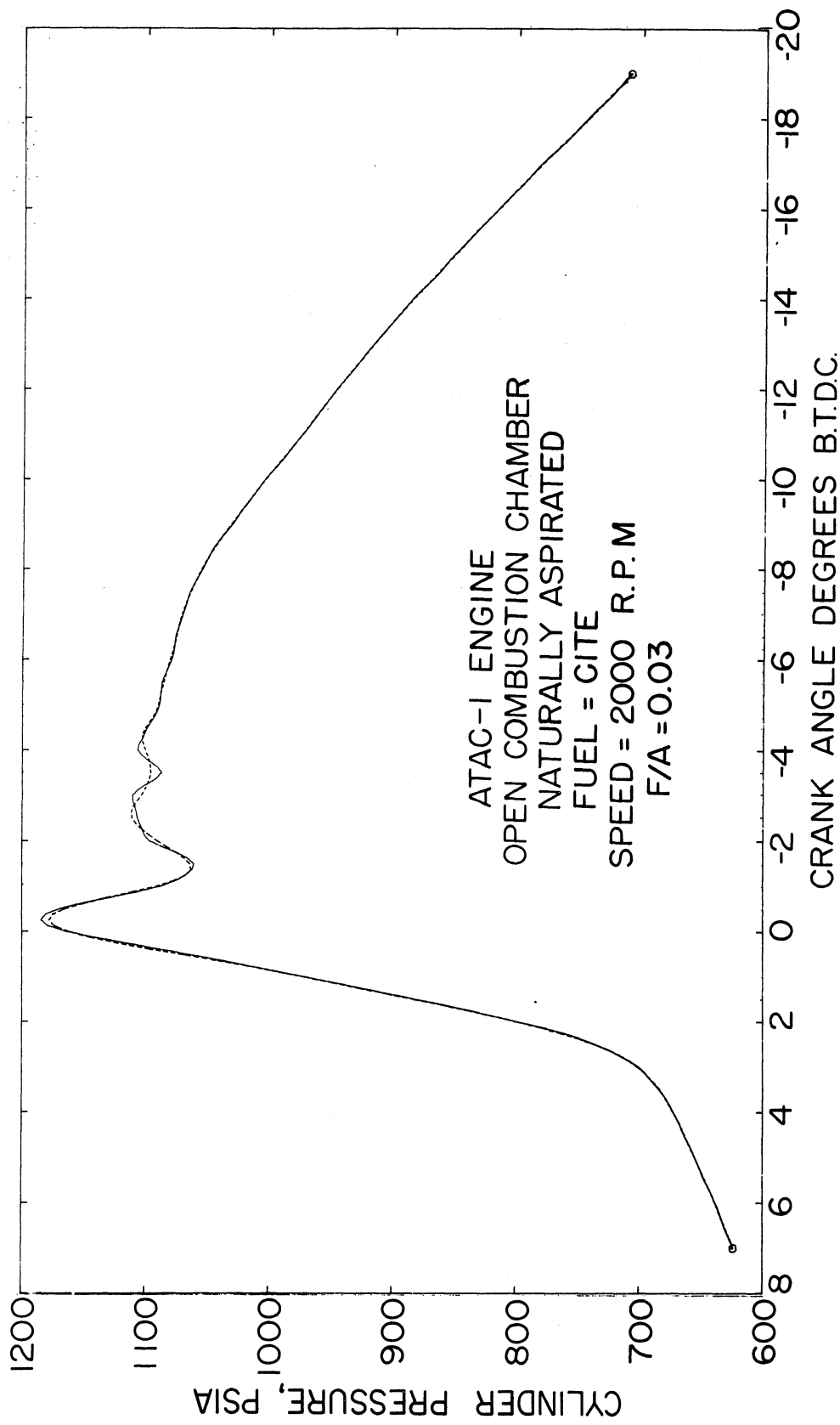


Fig. 9. Detailed pressure trace for ATAC-1 engine during combustion.

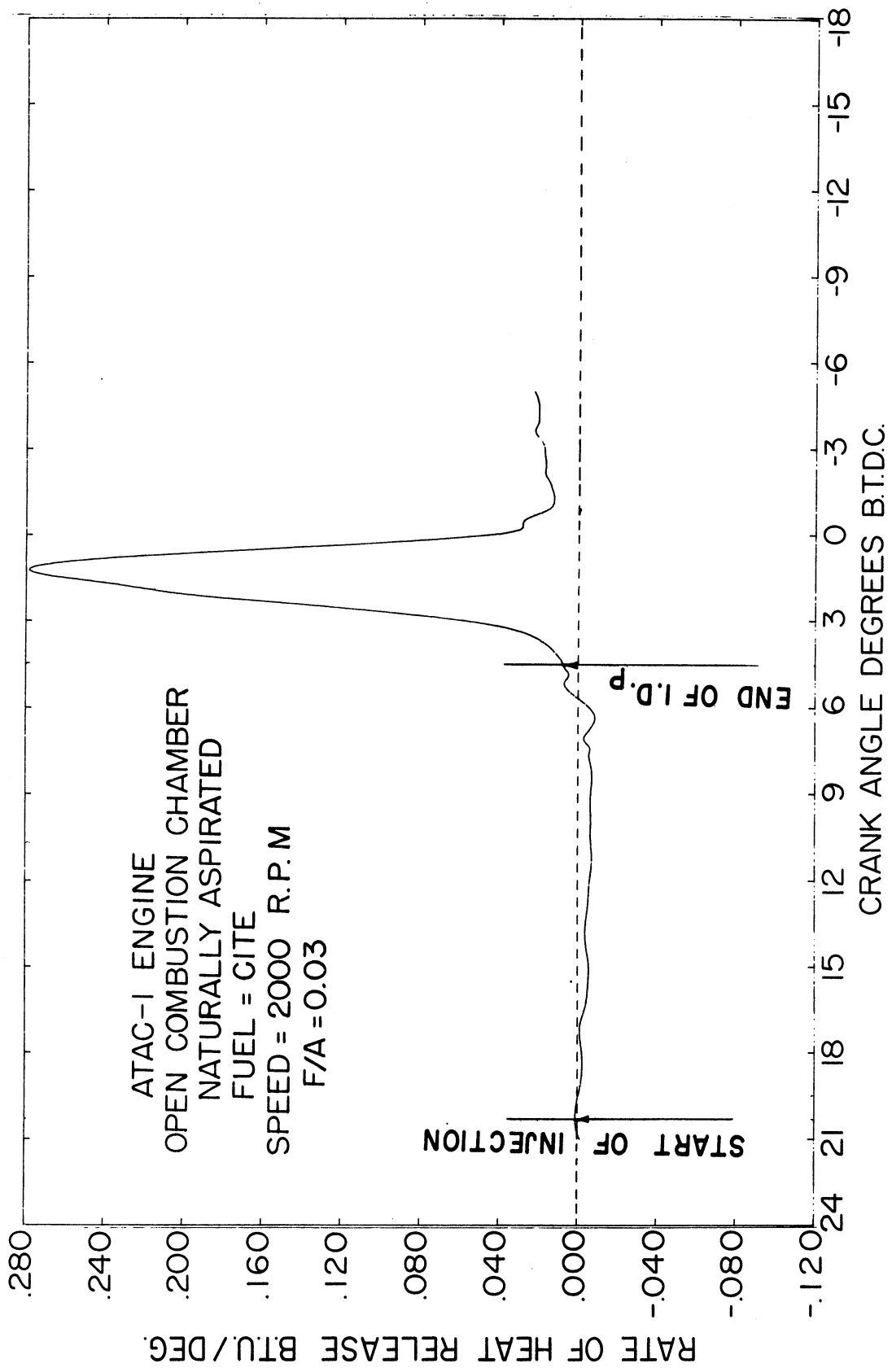


Fig. 10. Heat release diagram for ATAC engine with CITE fuel plotted by the computer.

2. The second stage is from 6° B.T.D.C. to 4.5° B.T.D.C., during which very slow reactions occur resulting in a small rate of heat release. These slow reactions are followed by explosive type reactions, resulting in a maximum rate of heat release of 0.28 Btu per crank degree. It is interesting to note that the ignition delay period was 15.8° , while the following rapid combustion process lasted only for about 4.5° .

The two stage preignition reactions were also observed in the heat release diagram for diesel no. 2 fuel shown in Fig. 11. In this case the ignition delay was shorter and the maximum rate of heat release was 0.21 Btu per crank degree, or 75% that of CITE fuel. The two stage preignition reactions in the combustion of hydrocarbon fuels were observed by other investigators as Jost,² Andreev,³ and Aivagov and Neumann.⁴

COMPUTER PROGRAMS MADE FOR THE HEAT RELEASE CALCULATIONS

The following computer programs were used for the cycle analysis and heat release computations made for the ATAC engine.

Program No. 1: Heat release calculations

Program No. 2: Sequential cycle data analysis

Program No. 3: Curve fitting

Program No. 4: Cylinder volume and gradient

Program No. 5: Cylinder gas properties

Program No. 6: Engine data reading and printing

Program No. 7: Engine data calculations

The detail of each of these programs is given in Appendix A.

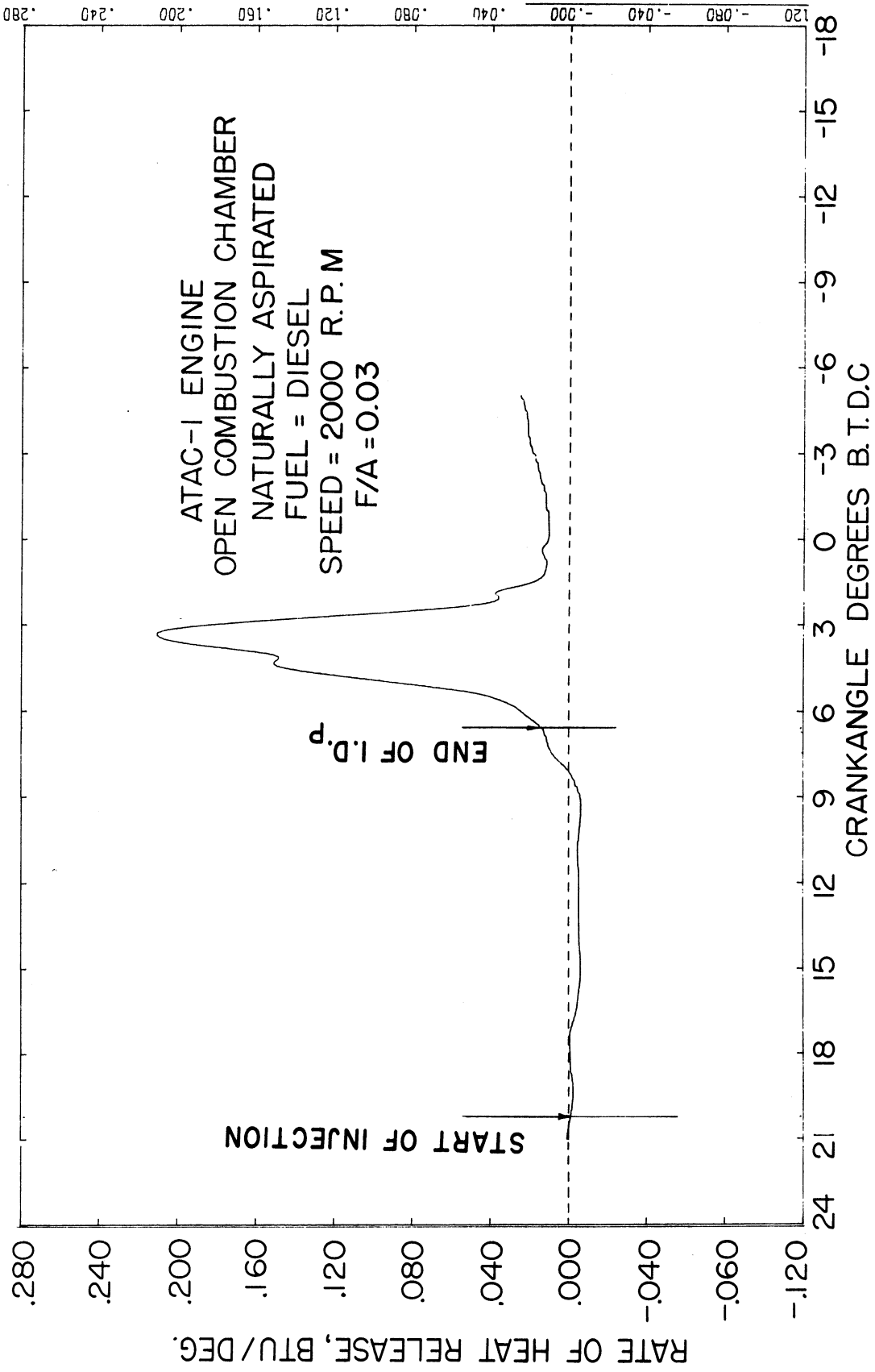


Fig. 11. Heat release diagram for ATAC engine with diesel no. 2 fuel plotted by the computer.

III. EFFECT OF SPEED ON IGNITION DELAY AND OTHER COMBUSTION PHENOMENA

To study the effect of speed on ignition delay and the other combustion phenomena, two series of runs were made, covering a speed range from 1000 rpm to 2900 rpm. One of these series was at a mean pressure of 500 psia and the other at 700 psia.

The change in engine speed was found to cause changes in other parameters that affect the combustion process, like cylinder pressure and temperature, and injection timing. To study the effect of speed alone on the combustion phenomena, experimental adjustments were made to eliminate the effect of these parameters or to correct for their effect on ignition delay. The injection timing was manually adjusted so that the needle lift would start at a constant crank angle before the T.D.C., at all engine speeds. The mean cylinder pressure during the ignition delay was kept at a constant value of 500 psia or 700 psia, by changing the pressure in the surge tank. The effect of the change in the mean temperature during the ignition delay was corrected for by using a correction formula based on the previous experimental results on the ATAC engine, with the same fuel under the same mean pressure during the ignition delay.

A1. EFFECT OF SPEED ON I.D._p AT MEAN PRESSURE = 500 psia

Conditions of Test

Fuel: CITE refree grade (Mil-F-45121 fuel)

Mean pressure during I.D._p = 500 psia

Inlet air temperature = 80°F

Fuel-air ratio = 0.0315

Injector opening pressure = 3000 psia

Injection timing (start of needle lift) = 20.9° B.T.D.C.

Cooling water at outlet = 176°F

Variables

Engine speed: from 1000 to 2800 rpm

Inlet air surge tank pressure: from barometric to 10.7 in. Hg boost

Results

The effect of speed on ignition delay is shown in Fig. 12. The measured pressure rise delay I.D._p decreased from 1.567 millisecc at 1000 rpm to 1.149 millisecc at 2800 rpm. The illumination delay I.D._{IL} was always longer than the pressure rise delay, and decreased from 1.883 millisecc at 1000 rpm, to 1.525 millisecc at 2800 rpm. Under the test conditions the observed change in ignition delay with engine speed is due to variations in air velocity and air temperature. To eliminate the effect of the change in the air temperature on ignition delay, a correction formula based on Arrhenius equation was used.

$$\frac{\text{I.D.}_{\text{corrected}}}{\text{I.D.}_{\text{measured}}} = e^{\left[\frac{E}{R_u} \left(\frac{1}{T_{\text{ref.}}} - \frac{1}{T_m} \right) \right]} \quad (1)$$

where

E = activation energy

R_u = universal gas constant

T_{ref.} = a reference temperature to which the ignition delay is corrected
= 1619°

T_M = the mean temperature during ignition delay.

The value of the activation energy E was determined for CITE fuel under a mean pressure of 700 psia, and found equal to 10430 Btu/lb mole. The details of this work is given in Ref. 1. Upon using this value of E in Eq. (1), it was noticed that the corrected ignition delay increased with speed as shown in Fig. 13. Since this result seemed to be contrary to previously published data for the effect of speed on ignition delay, it was decided to repeat this series of runs with a mean pressure during the ignition delay at 700 psia, the pressure at which the activation energy was determined.

A2. EFFECT OF SPEED ON I.D._p, MEAN PRESSURE - 700 psia

Conditions as in A1, except that the mean pressure during I.D._p = 700 psia.

Variables

Engine speed: from 1000 rpm to 2900 rpm

Inlet surge tank pressure: from 22.9 in. Hgg to 10.6 Hgg.

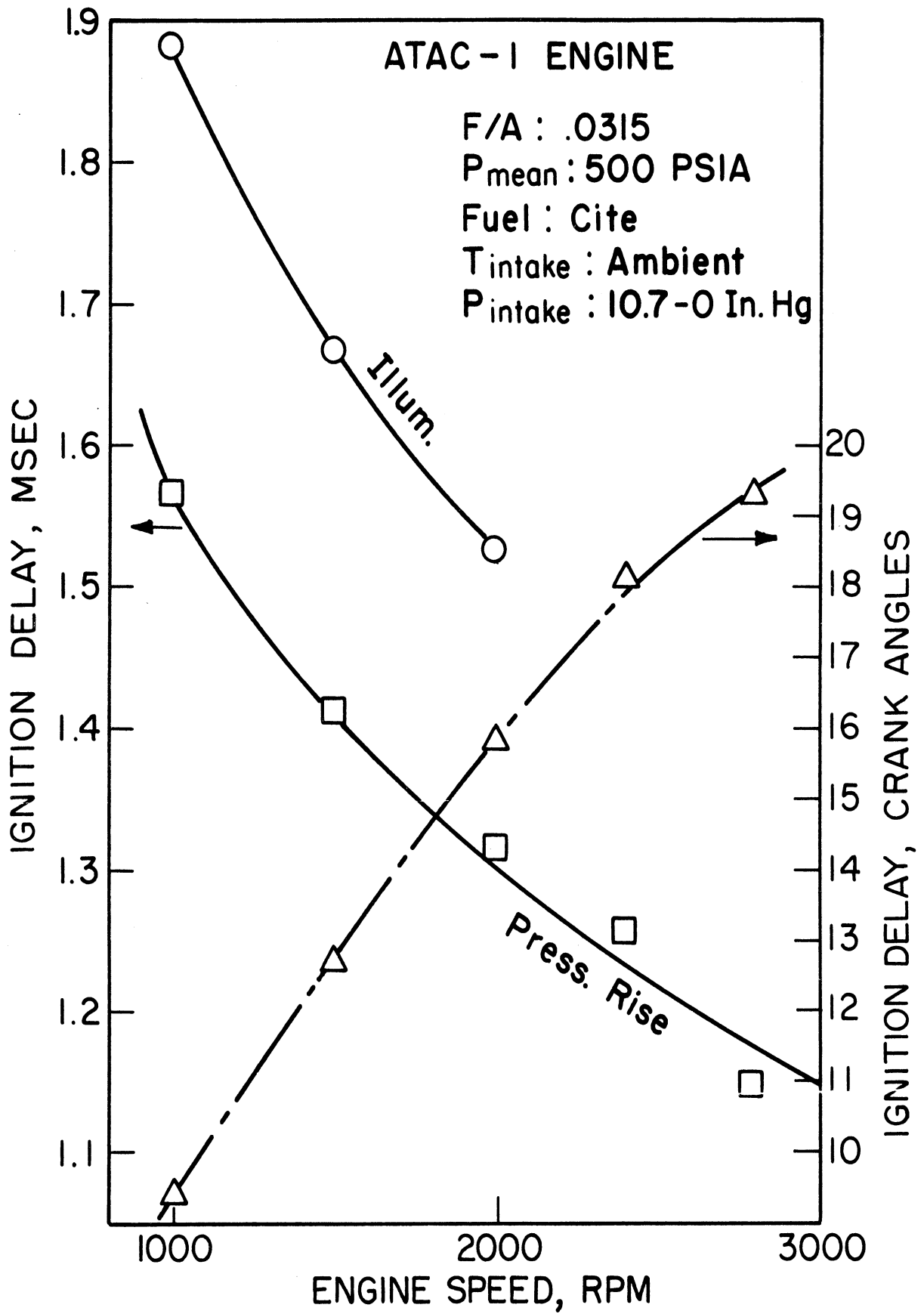


Fig. 12. Effect of engine speed on ignition delay at a mean pressure of 500 psia.

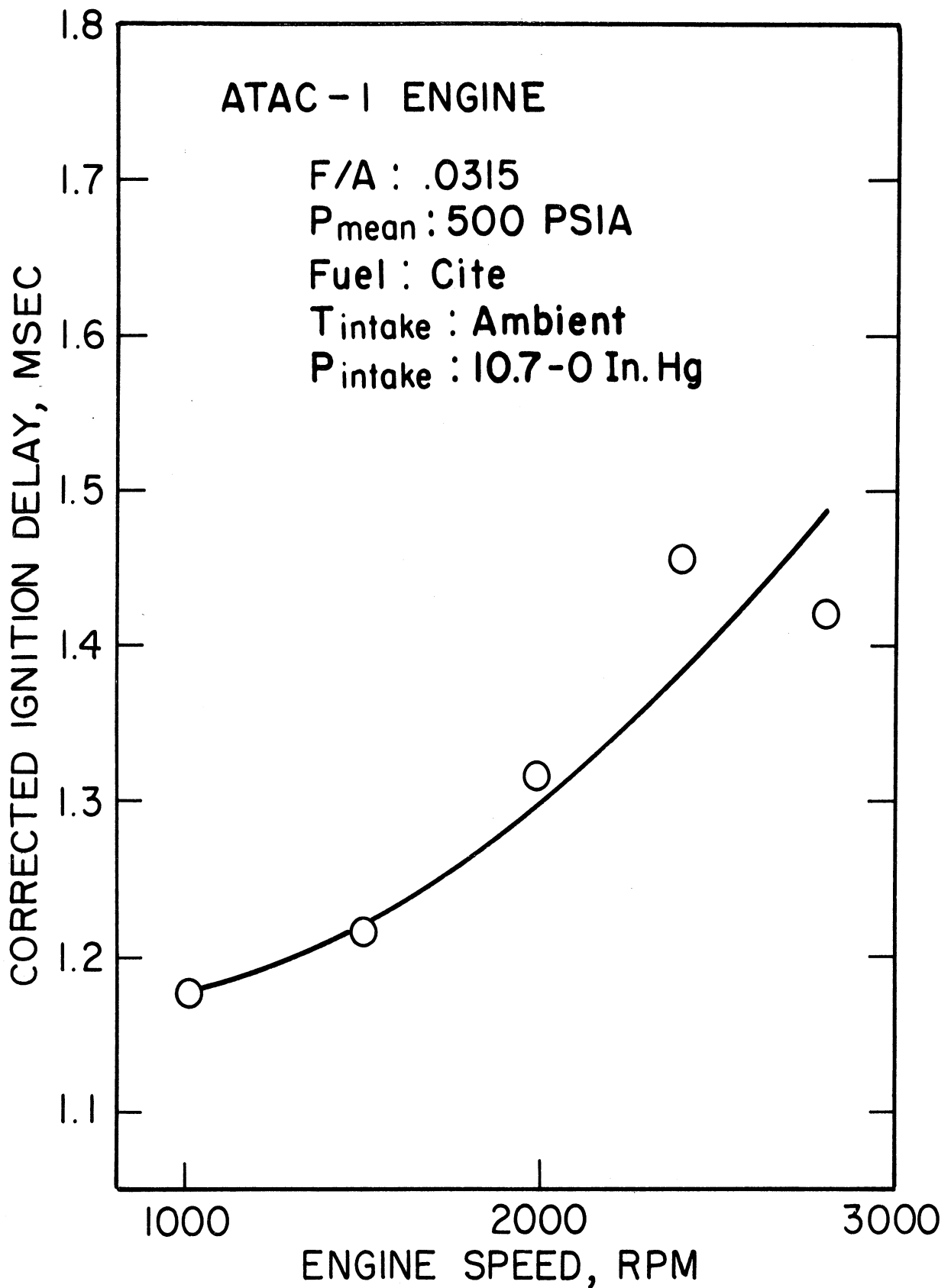


Fig. 13. Corrected ignition delay versus engine speed (reference temperature = 1619°R).

Under the above conditions the mean temperature during the ignition delay changed from 1436°R at 1000 rpm to 1707°R at 2900 rpm. The ignition delay was corrected for the change in temperature by using Eq. (1). The reference temperature, T_{ref} , was chosen to be the mean temperature during the ignition delay at 2000 rpm which is equal to 1557°R.

Results

Effect of speed on I.D.p. The results of the ignition delay in crank angle degrees and in milliseconds are plotted versus engine speed in Fig. 14. The ignition delay is 7.2° at 1000 rpm, and has increased to 15.9° at 2900 rpm. However, in terms of milliseconds, the ignition delay has dropped from 1.2 millisecc at 1000 rpm, to 0.914 millisecc at 2900 rpm.

The drop in the ignition delay with the increase in speed can be attributed to either the increase in turbulence with speed, or to the increase in the mean temperature during the ignition delay with speed.

The mean gas temperature, is shown in Fig. 15, increased from 1436°R at 1000 rpm, to 1707°R at 2900 rpm. This is an increase of 271°F. To correct for the effect of temperature on the ignition delay, Eq. (1) was used, and the results are plotted in Fig. 14. These values of ignition delay can be considered to be at the same mean temperature and pressure, and the only variable is the engine speed. From Fig. 14, it can be concluded that the increase in speed from 1000 rpm to 2900 rpm caused an increase in the ignition delay from 0.9 millisecc to 1.23 millisecc.

Similar observations concerning the increase in ignition delay with speed were reported by Small.⁵

The reason for the increase in the ignition delay with speed may be attributed to the increased leanness of the fuel-air mixture, in the region where combustion starts in the combustion chamber. Photographic studies on diesel combustion^{6,7,8} showed that ignition starts in the periphery of the fuel spray, where the fuel droplets have access to the oxygen. The change in the mixture strength in this region is expected to affect the rate of reaction between the oxygen and fuel.

An increase in engine speed is expected to reduce the physical delay, which is the time required for the fuel to evaporate and form a combustible mixture. So if the physical parameters are the main controlling factors in the length of the ignition delay, it would be expected that an increase in engine speed would reduce the length of the ignition delay. However, the present experimental results show that the ignition delay increases with the speed. This might be an indication that the chemical processes, rather than the physical processes, are the main controlling factors on the ignition delay.

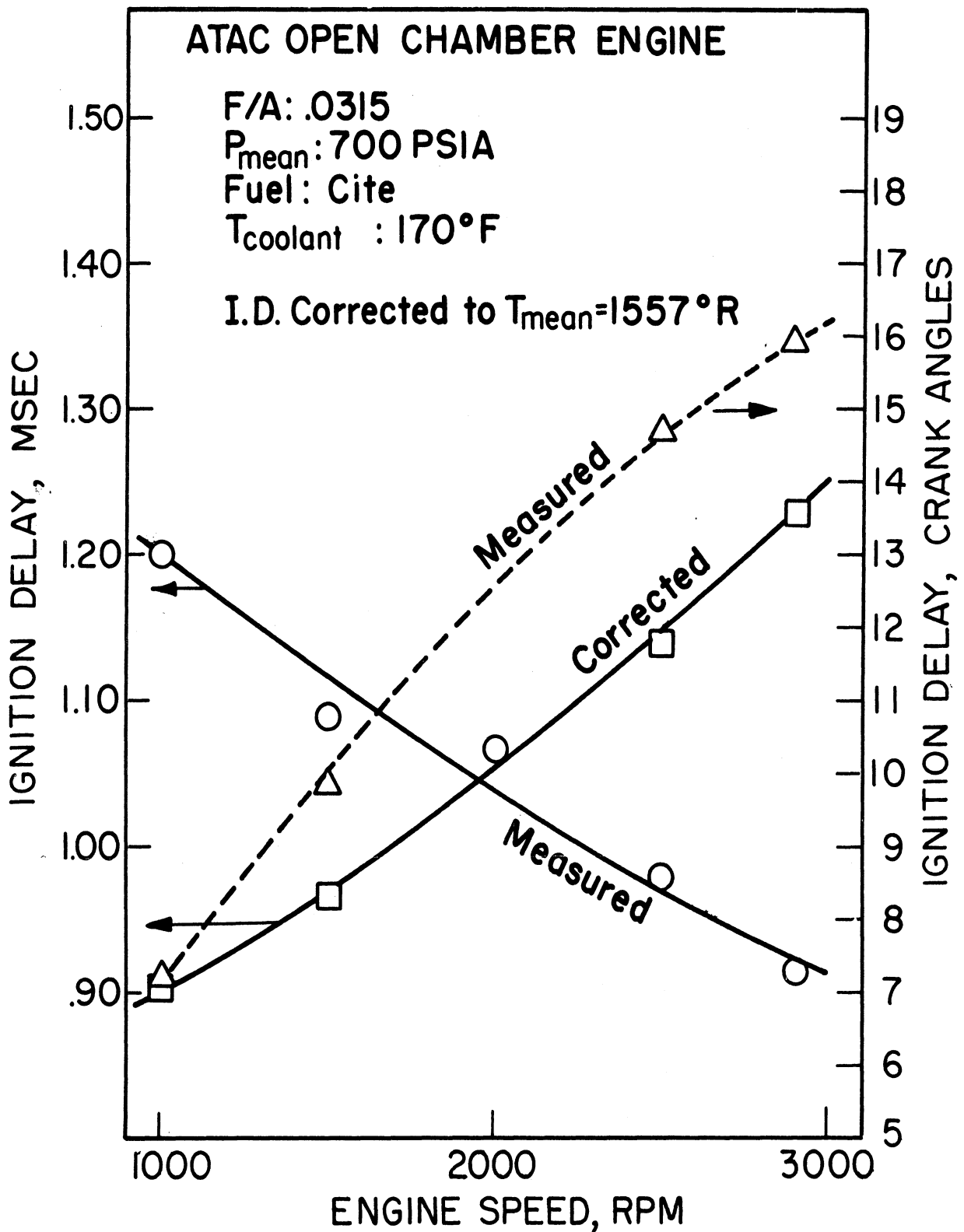


Fig. 14. Effect of engine speed on ignition delay at a mean pressure of 700 psia.

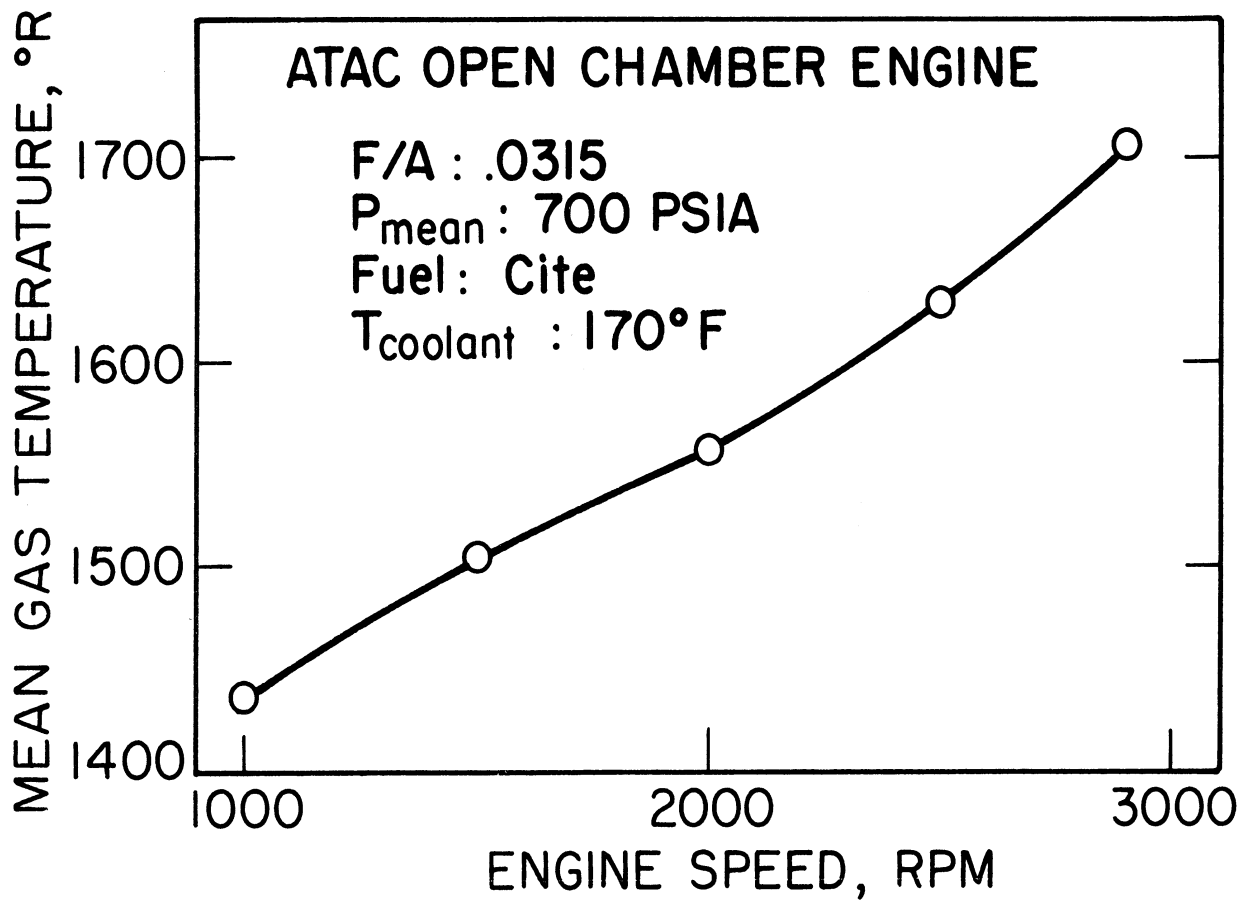


Fig. 15. Effect of speed on the mean gas temperature during the ignition delay.

B. EFFECT OF SPEED ON SMOKE INTENSITY

The results of smoke intensity in Hartridge Units are plotted versus engine speed in Fig. 16. Below 1500 rpm, there is one data point at 1000 rpm, which shows a heavy smoke intensity reading. The trend of change in smoke intensity between 1000 rpm to 1500 rpm cannot be concluded from the data point at 1000 rpm. But between 1500 rpm and 2900 rpm, the smoke intensity is shown to increase with speed. The increase in speed is expected to improve the mixing between the fuel and air, and increase the combustion efficiency. However, at higher speeds the time available for the chemical reactions to take place, at a certain temperature level, is reduced. Thus the carbon particles formed during the combustion process will have a shorter residence time, at the temperature below which they cannot combine with the oxygen.

From these experimental results it seems that the process of mixing is not the controlling process for carbon formation, but rather the temperature level and time available for the chemical reactions to take place are the main factors that affect carbon formation and removal, and thus the smoke intensity in the exhaust.

C. EFFECT OF SPEED ON COMBUSTION CHAMBER WALL TEMPERATURES

The wall temperatures are measured in the fire deck at three different locations:

1. The surface of the combustion chamber in the midpoint between the inlet and exhaust valves.
2. The wall temperature at a radial distance of $1/8$ in. from the inlet valve insert, and $1/4$ in. from the gas side.
3. The wall temperature at a radial distance of $1/8$ in. from the exhaust valve insert, and $1/4$ in. from the gas side.

The temperature of the fire-deck wall, at the three different locations, is plotted versus engine speed in Fig. 17.

The surface temperature in the valves bridge increased from 435°F at 1000 rpm to 509°F at 2900 rpm. The increase in surface temperature occurred between 1000 rpm and 2000 rpm, and was very little between 2000 rpm and 2900 rpm.

The wall temperature near the exhaust valve increased from 326°F at 1000 rpm to 360°F at 2900 rpm.

The wall temperature near the inlet valve was almost constant all over the whole speed range, at about 267°F .

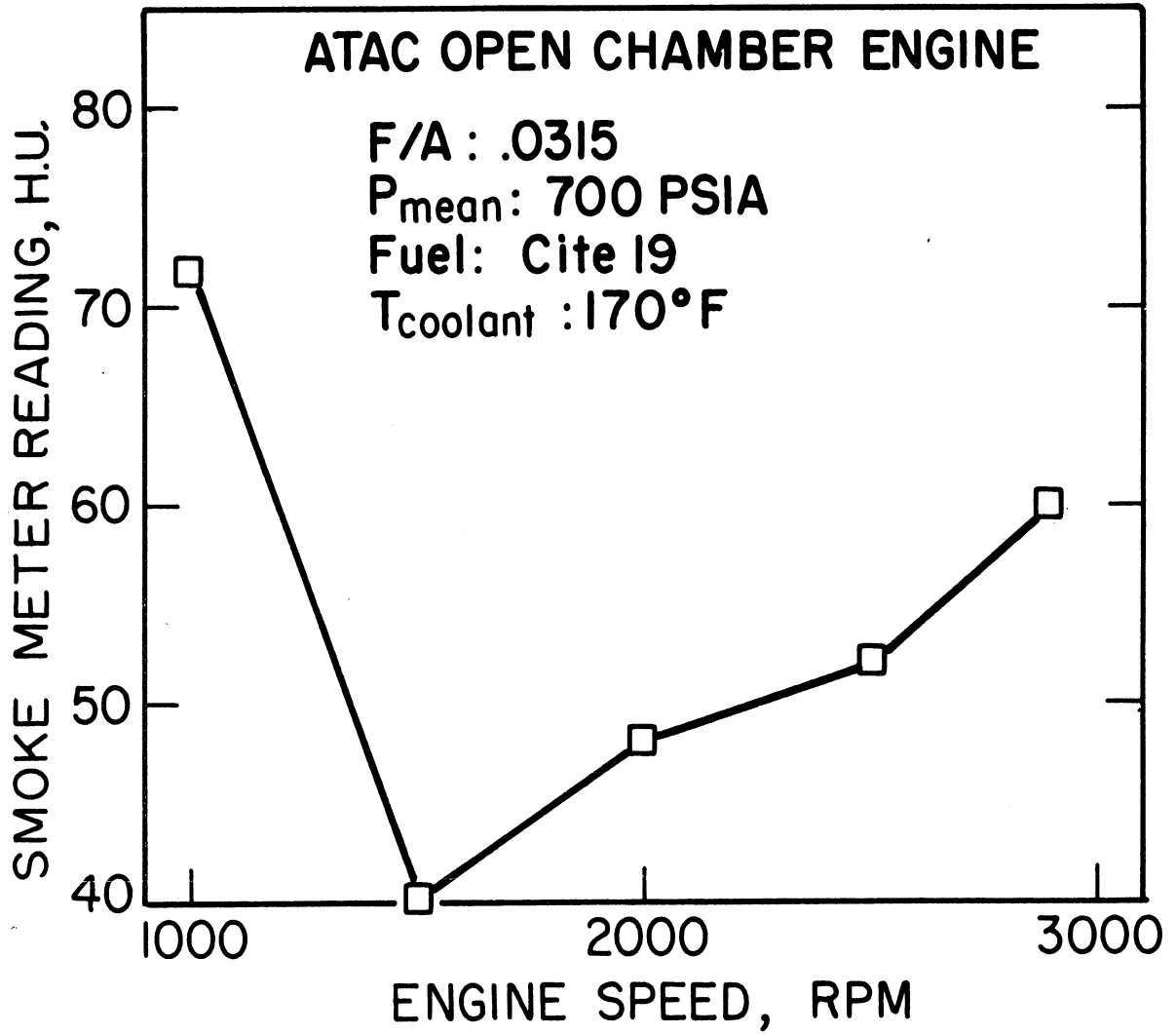


Fig. 16. Effect of speed on smoke intensity.

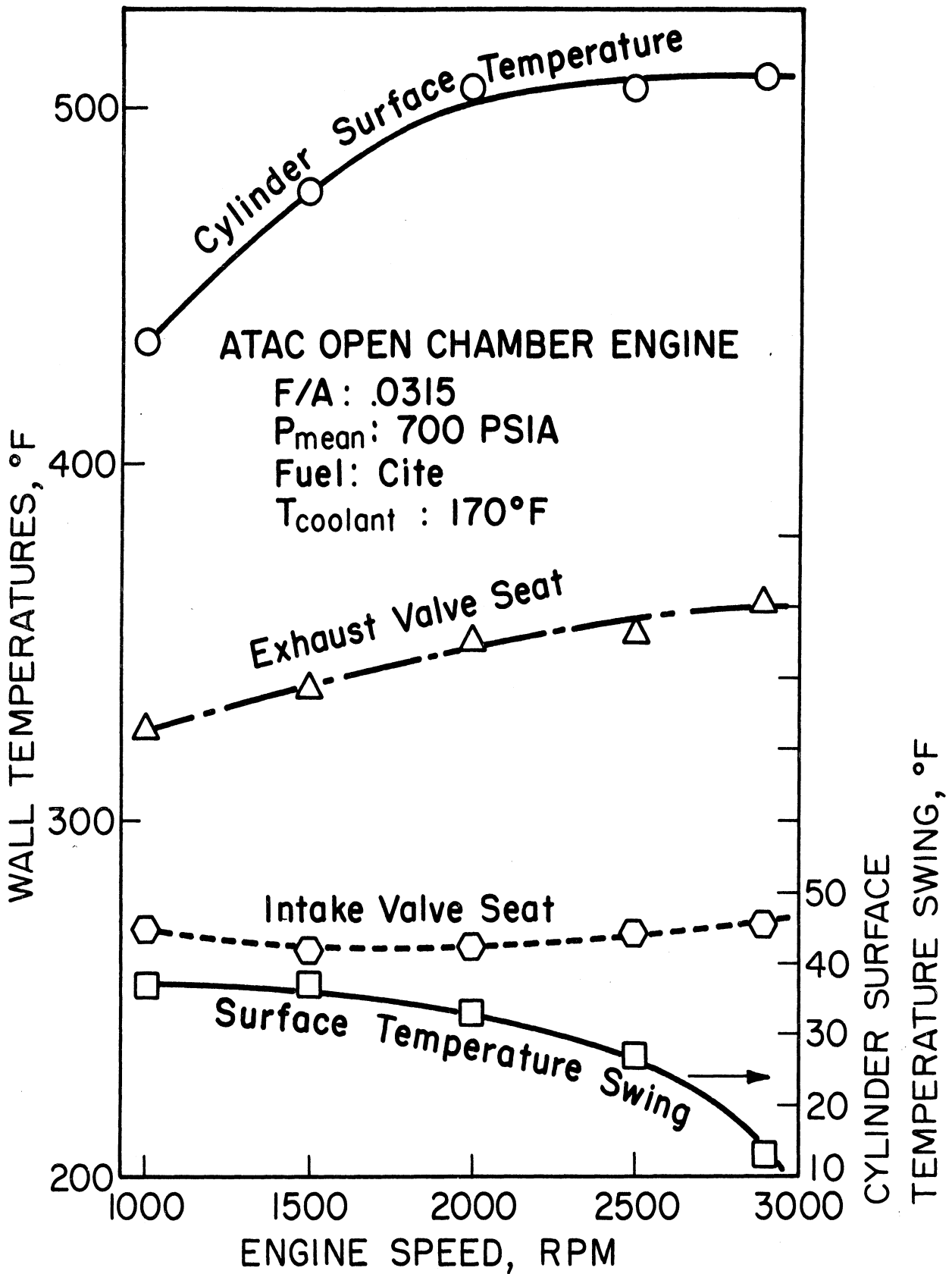


Fig. 17. Effect of engine speed on wall temperature.

The swing in the surface temperature decreased from 37°F at 1000 rpm to 13°F at 2900 rpm.

It is to be noted that all the above variations in temperature occurred with the following parameters kept at a constant value: fuel-air ratio, coolant temperature, injection opening pressure and timing, mean pressure during delay, and inlet air temperature. Thus the changes in the wall temperatures can be attributed only to changes in the heat transfer phenomena associated with engine speed.

D. EFFECT OF SPEED ON THERMAL LOADING

The heat lost from the gases to the combustion chamber walls, is transferred to the jackets cooling water or to the lubricating oil heat exchanger. Figure 18 shows that the heat lost to the water jackets increased slightly from 4.0 Btu/sec at 1000 rpm to 4.1 Btu/sec at 2900 rpm, and reached a maximum of 5.8 Btu/sec at 2500 rpm. The heat lost to the lubricating oil was 0.5 Btu/sec over a speed range from 1000 rpm to 2000 rpm, after which it increased gradually till it reached 2.8 Btu/sec, at 2900 rpm. The sum of the heat lost to the coolant and lubricating oil showed a continuous increase with speed.

The thermal loading as a percentage of the heat added in the fuel is plotted in Fig. 18. It shows an increasing trend in the percentage heat lost to the lubricating oil with speed. The percentage heat lost to the coolant and the total losses showed a continuous decrease with speed. About 20% of the heating value of the fuel is lost at 1000 rpm and it decreases to 14% at 2900 rpm.

The results of this series of runs are shown tabulated by computer in Appendix B, Tables 1 and 2.

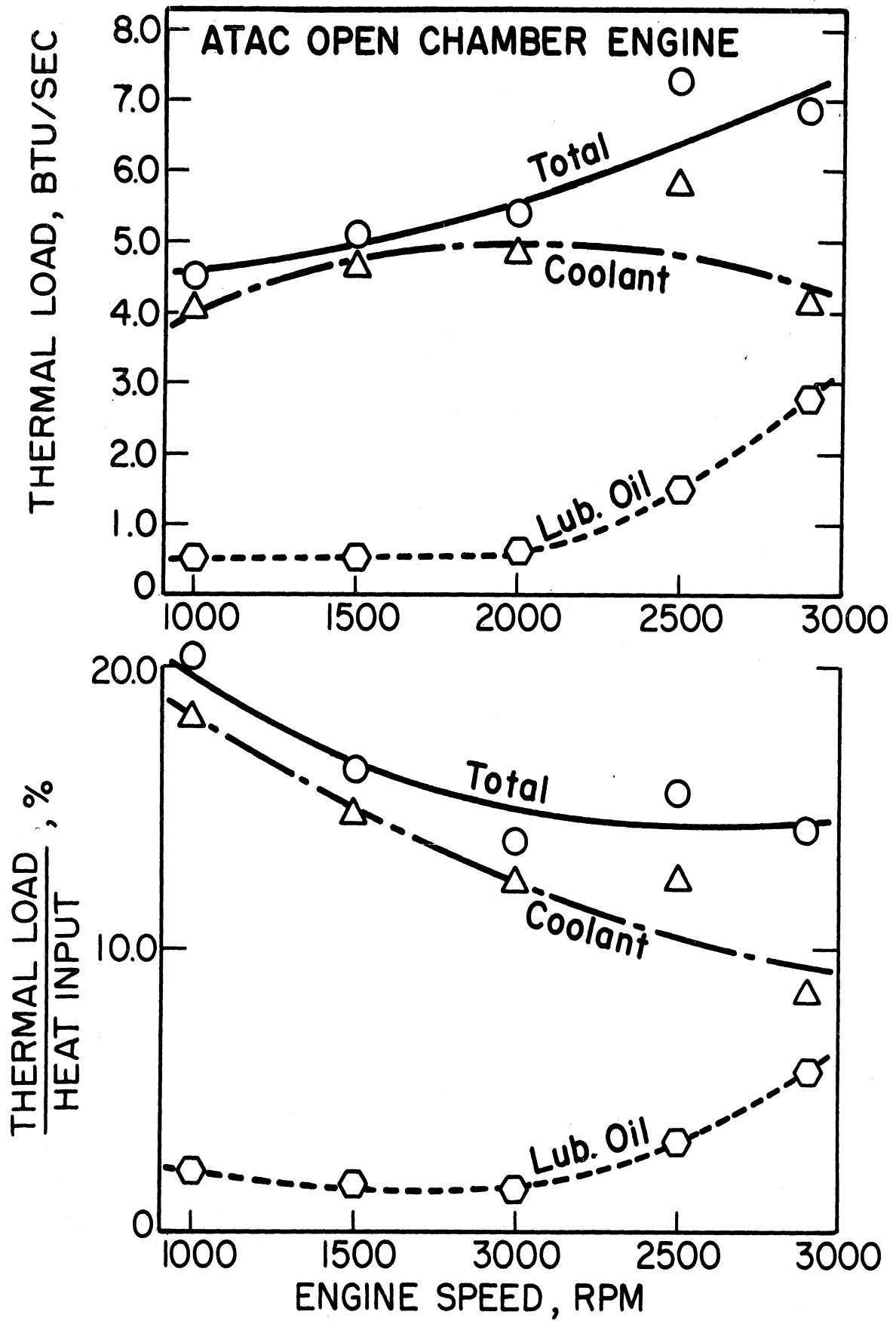


Fig. 18. Effect of engine speed on thermal loading.

IV. EFFECT OF COOLANT TEMPERATURE ON IGNITION DELAY AND OTHER COMBUSTION PHENOMENA

This series of tests was run to study the effect of coolant temperature on the combustion process in the ATAC engine, in an effort to evaluate the possibility of running coolant systems at temperatures higher than the present temperature levels of about 200°F. The increase in the coolant temperature results in an increase in the temperature differential between the coolant and air, and reduce the size of the radiator for a certain cooling load. At the present time, it seems that the radiator size might limit the increase in power output of diesel engines, specially in some military applications. In the present experimental study the thermal loading was measured, and the coolant used was "ethylene glycol."

The tests covered a range of coolant temperatures from 150°F to 300°F. The temperature of the lubricating oil in the crankcase was kept at a constant level of 200°F. This limitation was made to avoid any trouble that might occur due to the increase in the lubricating oil temperature.

Conditions of the Test

Fuel - CITE refree grade (Mil-F-45121)

Pressure in surge tanks = barometric

Inlet air temperature = 81°F

Fuel-air ratio = 0.0313

Injector opening pressure = 3000 psia

Injector timing (start of needle lift) = 21° B.T.D.C.

Lubricating oil temperature = 200°F

Engine speed = 2000 rpm

Variables

Outlet coolant temperature: 156°F-305°F

Results

The results for the effect of coolant temperature on the different combustion phenomena are given in Table 3 in Appendix B.

A. EFFECT OF COOLANT TEMPERATURE ON COMBUSTION PHENOMENA

The pressure rise delay did not change with the increase in coolant temperature. The average value for the ignition delay for seven runs was 0.681 s sec, the maximum ignition delay was 0.709; or 4% above the average. The minimum ignition delay was 0.667; or 2% below the average. These changes in ignition delays can be considered as random changes.

The experimental results showed no effect for the coolant temperature upon the compression pressure, maximum cycle pressure and rate of pressure rise. The exhaust gas temperature increased with the coolant temperature. At a coolant temperature of 156°F the exhaust temperature was 846°F, and increased to 950°F at coolant temperature of 305°F.

B. EFFECT OF COOLANT TEMPERATURE ON THERMAL LOAD

The thermal load can be considered to be composed of heat losses to the coolant, and heat losses to the lubricating oil. The variation in these heat losses with coolant temperatures is shown in Fig. 19. The increase in temperature from 156.6°F to 305°F reduced the total thermal loading from 30,600 Btu/hr to about 20,500 Btu/hr. This is mainly due to the reduction in the temperature difference between the gases and the walls. The corresponding thermal loading as a percentage of the power output is 1660 Btu/B.H.P. hr and 1240 Btu/H.P. hr respectively.

The percentage heat loss to the coolant, shown in Fig. 20, decreased from 15.3% at 156°F, to 8.4% at 305°F. For the lubricating oil the percentage heat losses increased from 2.4% at 156°F to 5.4% at 305°F. The percentage total heat losses to the coolant and the lubricating oil decreased from 17.7% at 156°F to 13.8% at 305°F.

C. EFFECT OF COOLANT TEMPERATURE ON INJECTION PROCESS

No effect was observed for the coolant temperature on injection timing, the period of main injection or the period of after injection. The only effect on the injection system was observed in the amount of after injection. The needle lift during after injection shown in Fig. 21 was observed to decrease with the increase in coolant temperature up to 230°F, after which it increased again. Figure 22 shows the needle lift diagrams at coolant temperatures of 217°F and 304.3°F. It is noticed that at the higher temperature the needle lift, was approximately twice as much as that at the lower temperature.

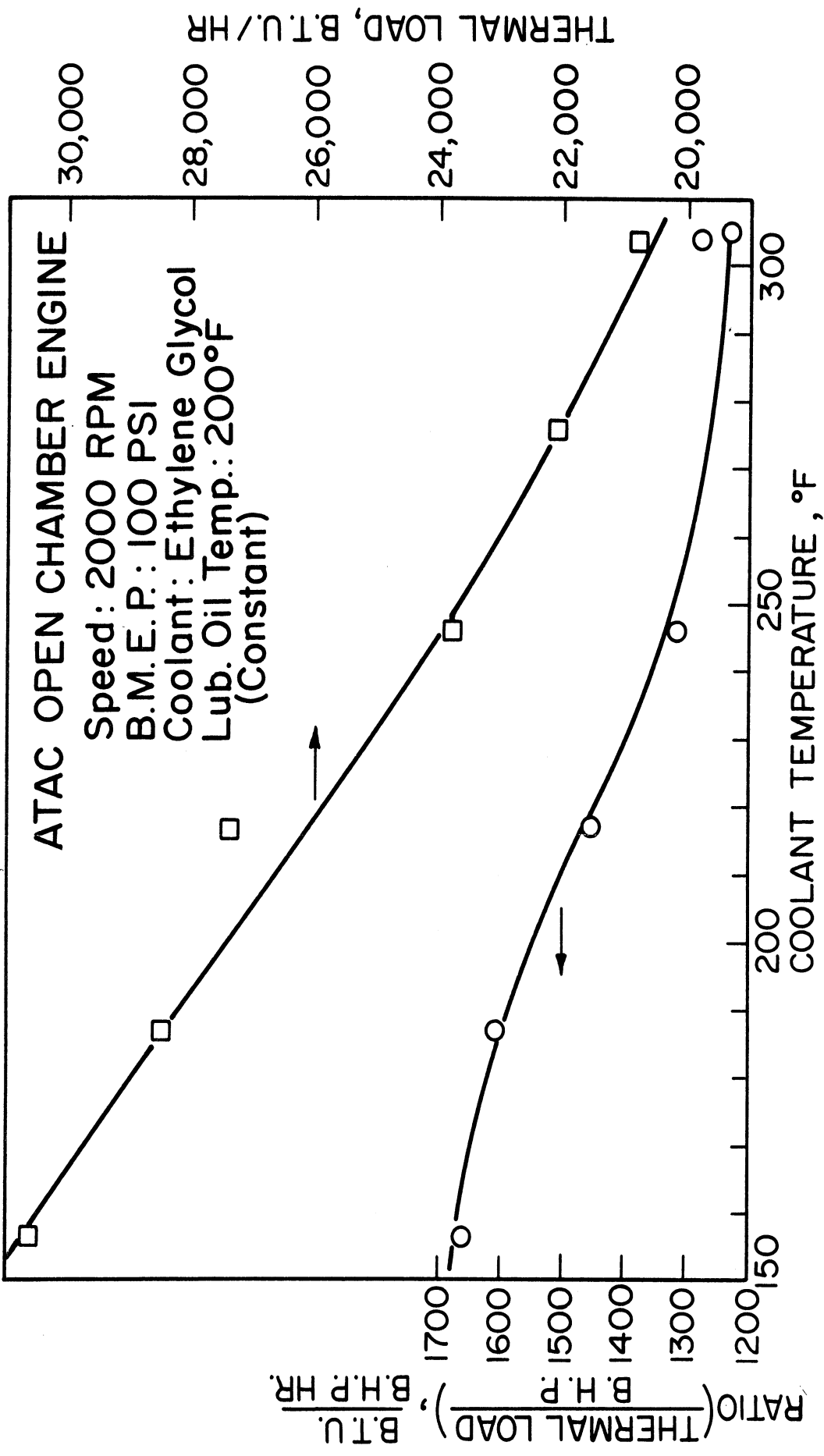


Fig. 19. Effect of coolant temperature on thermal loading.

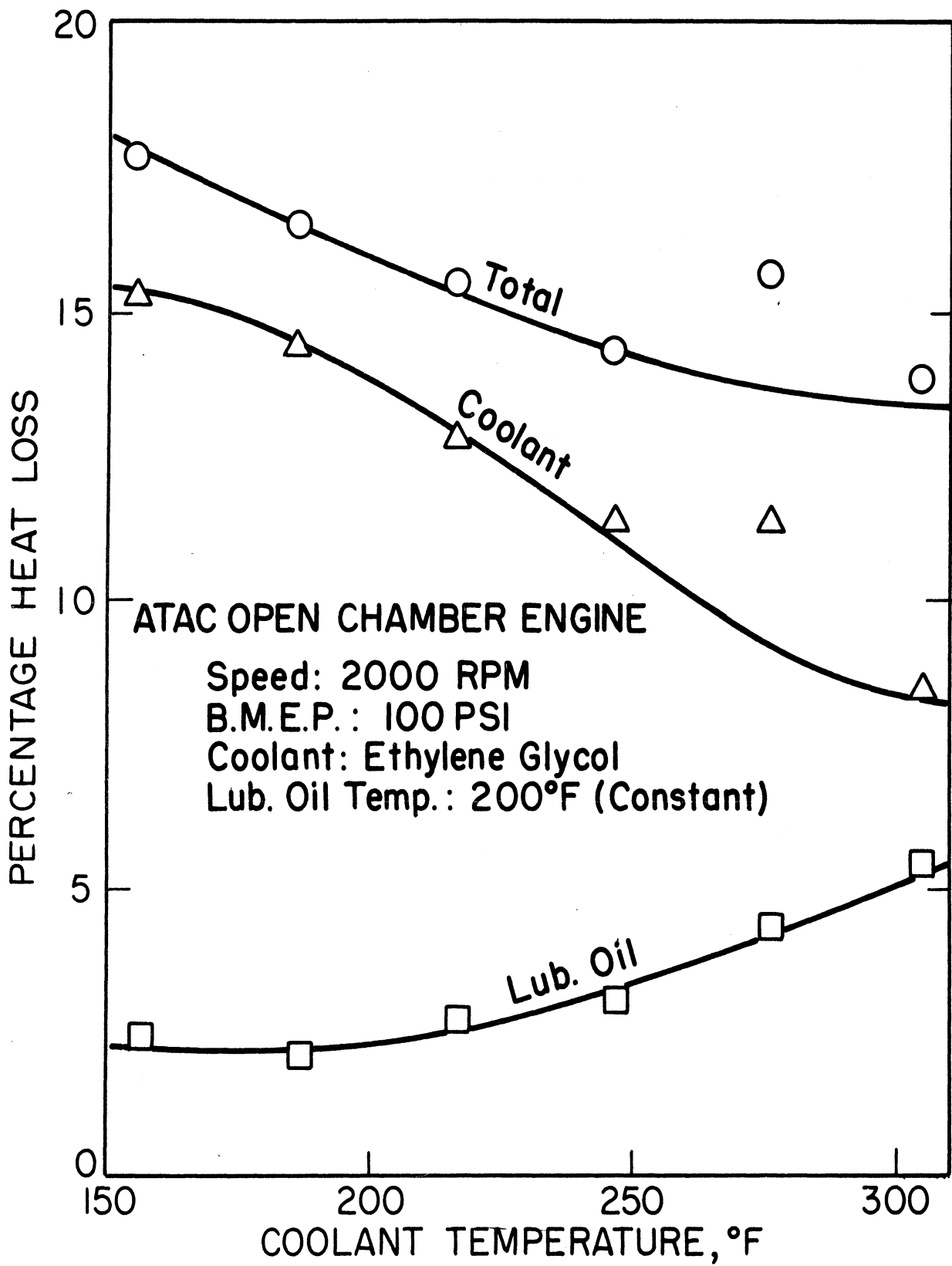


Fig. 20. Effect of coolant temperature on % heat lost to coolant and lubricating oil.

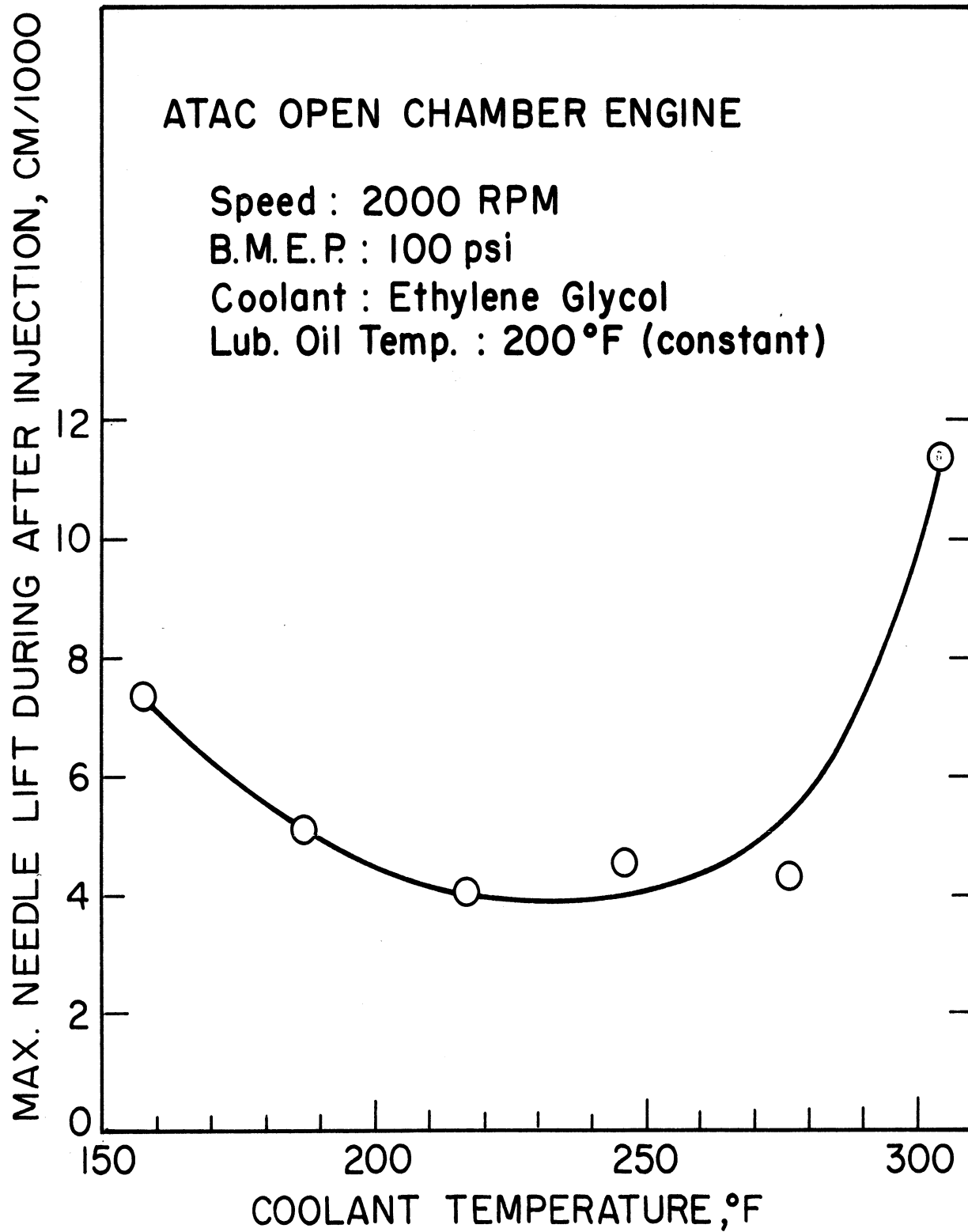
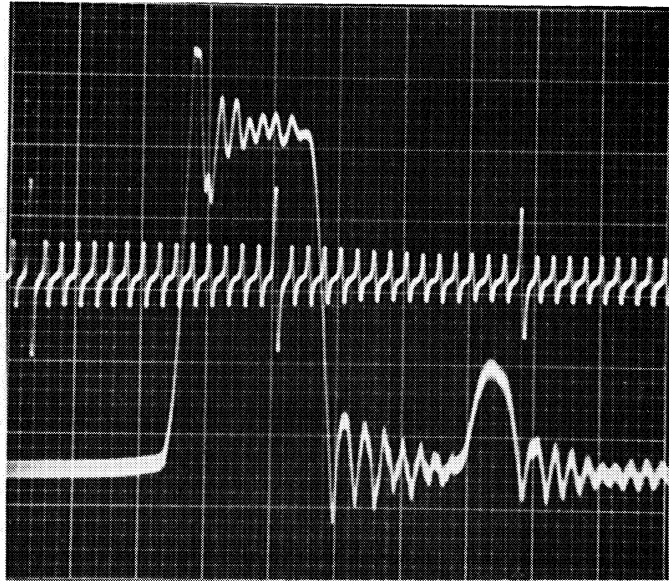
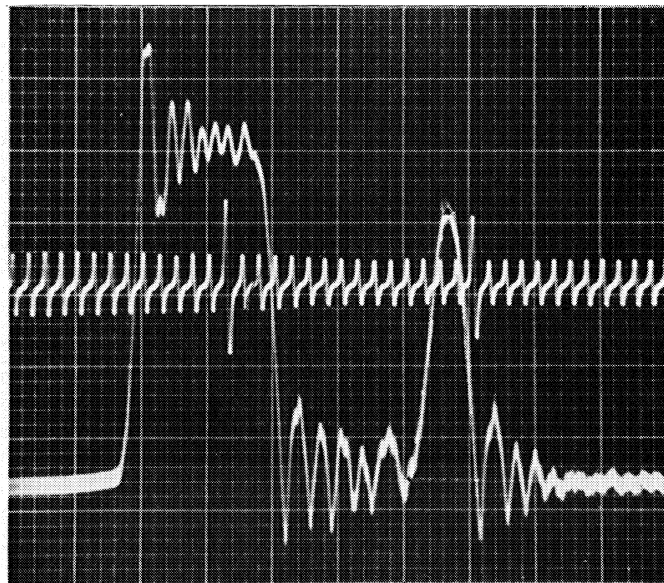


Fig. 21. Effect of coolant temperature on needle lift during after injection.



(a) Coolant temperature = 217°F



(b) Coolant temperature = 304.3°F

Fig. 22. Needle lift diagrams with coolant temperatures of 217°F and 304.3°F.

V. PISTON AND LINER INSPECTION AFTER THE HIGH COOLANT TEMPERATURE TESTS

To check the condition of piston, liner and valve seats after the completion of the high coolant temperature tests, the cylinder head was removed. The liner, piston and valves were examined and found in a fair condition without any sign of overheating. The piston rings and valves were replaced with new ones. The new valves were lapped on the seats.

APPENDIX A

COMPUTER PROGRAMS

1. MAIN COMPUTER PROGRAMS

These computer programs are written in the Michigan Algorithm Decoder (MAD) language which is the language used at The University of Michigan Computing Center.

Program

1. Heat Release Calculations
2. Sequential Cycle Data Analysis
3. Engine Data Reading and Printing (ENGDAT)
4. Engine Data Calculations (ENGCAL)
5. Fuel Injection System Analysis
6. Equivalent Area of Injection as a Function of Injector-Needle Lift (AREAS)
7. Integration of Given Data (INTDER)
8. Best Straight Line to Fit a Group of Points (BLINE)
9. Curve Fitting (DB4T11)
10. Cylinder Volume and Gradient (CYLVOL, CYLGRA)
11. Cylinder Gas Properties (BBCFAC, BBRAN, BBFAR, BBLFT3)
12. Title Printing (TITLE)
13. Fuel Properties (FULHCR, FULDEN, FULFLO)
14. Coolant and Oil Properties (COLID, OILID, COLDEN, OILDEN, COLCP, OILCP, COLNU)
15. Calculation of the Integral Mean Value of Given Data (MEAN)
16. Interpolation (INTERP)

17. Air Flow Rate (AIRFLO)
18. Average Values and Errors (AVEERR)
19. Cylinder Wall Temperature from Millivolt Readings (THERMO)
20. Check on Missing Data (LACK)
21. Rounding of Numbers (IROUND)

2. DATA PLOTTING ROUTINES

Program

22. Axes Plotting (AXIS)
23. Curve Plotting (GRAPH)
24. Results Punching (PUNCH)

Computer Program 1

Title: Heat Release Calculations

Purpose: To calculate the net heat release from the combustion reactions over a range of crank angles starting from the point of injection to near the end of the combustion process.

Input:

1. Cylinder pressure obtained and punched from the program, "Sequential Cycle Data Analysis"
2. Engine test data

Procedure:

1. Read cylinder pressure, from the program, "Sequential Cycle Data Analysis", program 2.
2. Interpolate and determine the pressure every one-eighth of a crank-angle degree.
3. Calculate the mass of the charge in the cylinder by using the program "ENGCAL", program 4.
4. Calculate the average temperature of the gases from their pressure, volume, and mass, by using the "Beattie-Bridgeman" equation of state. The subroutine used for these calculations is given in program no. 11.
5. Calculate the rate of change of temperature ($dT/d\theta$), w.r.t. the crank angles, by using the program 9.
6. Calculate the volume gradient ($dV/d\theta$) by using the program 10.
7. Calculate the rate of doing work at any crank angle θ ,

$$\frac{\delta w}{\delta \theta} = 1.07116 \times 10^{-4} \times \frac{dV}{d\theta}$$

where $dV/d\theta$ is the change in cylinder volume w.r.t. the crank angles.

8. Calculate the change of the internal energy, dU , by using the following equation:

$$\frac{dU}{d\theta} = M \times c_v \times \frac{dT}{d\theta}$$

where c_v is the specific heat at constant volume,

$$c_v = \left(7.864 - \frac{36.1}{\sqrt{T}} - \frac{2387}{T} + \frac{905000}{T^2} \right)$$

9. Calculate the rate of heat release from

$$\frac{\delta Q}{\delta \theta} = \frac{dU}{d\theta} + \frac{\delta w}{\delta \theta}$$

where Q is heat transfer

List of Assisting Subroutines:

1. Program to calculate the mass of the charge and the fuel-air ratio (name: ENGCAL) program 4.
2. Program to calculate the hydrogen to carbon ratio of the fuel (name: FULHCR) program 13.
3. Program to round out numbers (name: I ROUND) program 21.
4. Program for interpolation (name: INTERP) program 16.
5. Program to calculate the temperature in degrees Rankine (name: BBRAN) program 11.
6. Program to calculate the temperature gradient (name: DB4T11) program 9.
7. Program to calculate the cylinder volume gradient (CYLGRA) program 10.
8. Program to punch the results (PUNCH) program 24.
9. Library plotting subroutines (PLTPAP., PLTMAX, PLTOFS., PLINE., PLTEND).

Computer Program 1

Heat Release Calculations

```

D'N SPEC(18), ID(3), DATA(21), CALC(20),
I (DBTDC, CP, T, DW, DU, DT, STORE, DQ)(1024)
I'R IROUND., NUMDAT, ENDDAT, NUMSEQ, ENDSEQ, I
AGAIN ENGCAL.(1,SPEC,ID(1),DATA(1),CALC(1))
GAS = CALC(5) + CALC(7)
RGAS = (CALC(5)*.371110 + CALC(7)*(.371110 + CALC(4)/
1 (.3757 + 4.4769/FULHCR.(SPEC(4))))/(1 + CALC(4)))/GAS
DU = GAS/28.966
GAS = GAS*1728.
R'T $S15,F16.10,S5,F16.10,S7,F16.10*$, BEGIN, EVERY, END
NUMDAT = 1 + IROUND.((END-BEGIN)/EVERY)
ENDDAT = 1 + 8*NUMDAT
NUMSEQ = ENDDAT - 8
ENDSEQ = NUMSEQ + 1
DELSEQ = EVERY/8.
DBTDC = BEGIN - DELSEQ
(I = 1, 1, I .E. ENDSEQ,
I DBTDC(I) = DBTDC + I*DELSEQ,
2 DBTDC(I) = 0. + DBTDC(I))
R'T $S10,I0F7.3*$, (I = 1, 8, I .E. ENDDAT, CP(I))
INTERP.(NUMDAT,DBTDC(1),8,CP(1))
DW = 1.7.3676/14.696/1728.
T'H LOOP1, FOR I = 1, 1, I .E. ENDSEQ
DBTDC = DBTDC(I)
CP = CP(I)
T = BBRAN.(CP,GAS/CYLVOL.(DBTDC),RGAS)
T(I) = T
DW(I) = 1.07116E-4*CP*CYLGRA.(DBTDC)
LOOP1 DU(I) = DU*(7.864 - 36.1/SQRT.(T) - 2387./T + 905000./T/T)
DB4T11.(NUMSEQ,-DELSEQ,I,T(I),STORE(I),DT(I),
1 STORE(1),STORE(1),STORE(1))
T'H LOOP2, FOR I = 1, 1, I .E. ENDSEQ
LOOP2 DU(I) = DU(I)*DT(I)
DQ(I) = DW(I) + DU(I)
READ DATA
P'T $(IH1/IH054(7F10.4,2F10.1,3P4F10.2))*$,
1 (I = 1, 1, I .E. ENDSEQ,
2 DBTDC(I), CP(I), T(I), DW(I), DU(I), DQ(I),
3 DQ(I)*EXP.(SLOPE/T(I)))
PUNCH.(ID(1),$DQ $,I,NUMSEQ,I,DQ(I))
PLTPAP.($400$)
PLTXMX.(14.90)
PLTOFS.(21.,-2.,-.2,.06666666667,.65,.41)
PLINE.(DBTDC(I),DQ(I),NUMSEQ,I,0,0,I.)
PLTEND.
T'O AGAIN
E'M

```

Computer Program 2

Title: Sequential Cycle Data Analysis

Purpose: To determine the cylinder pressure during the cycle from the time of inlet valve closing to the exhaust valve opening.

Input: Data points measured from a group of traces taken for different intervals during the cycle from the inlet valve closing to exhaust valve opening.

Procedure:

1. Read a sequence of data points as indicated under "Input".
2. Statistically adjust the data giving adjusted values, errors, deviations, and probabilities.
3. Curve fit the adjusted values by applying a fourth degree polynomial curve through eleven consecutive points. The program for this step is known as DB4T11 program.
4. Print, punch or plot the results.

List of Assisting Subroutines:

1. Program to print the title (name: TITLE) program 12.
2. Program to curve fit the adjusted values (name: DB4T11) program 9.
3. Program to use the program in (2), for the required number of times and for interpolation (USEDDB4, INTERP) program 16.
4. Program to calculate cylinder well temperature from millivolt readings of traces (THERMO) program 19.
5. Punching, plotting and graphing programs (PLOT, GRAPH, PUNCH) program 23 and 24.

NOTE: This program was used to calculate cylinder gas pressure as shown in Fig. 6.

Computer Program 2

Sequential Cycle Data Analysis

```

D'N CM(1689), (DBTDC, DATA, BEST)(1441), (COMMON, ERRCOM)
1 (498), (MVCM, CMREF, ERRREF, UNITCM, BTDC, REF, REFERR,
2 BLO, BLOERR, ADJ, ADJERR)(250), SPEC(19), YTITLE(17),
3 HEAD(16), VALUES(7), SCALES(5), NUMBER(3)
EQUIVALENCE (DBTDC, UNITCM), (BEST, REFERR),
1 (BEST(251), BLO), (BEST(502), BLOERR), (BEST(753), ADJ),
2 (BEST(1004), ADJERR)
I'R TITLE., LINE, NUMBER, P, COMMON, BGN, END, LAST, OBS, FV,
1 I, J, LINES, SPEC, NUMDAT, YTITLE, HEAD, IROUND., DEL,
2 BCDRN.
R'N EXACT, DOPLOT, DOGRPH, DUREAD, DOPRNT, DOPNCH, DOTELL,
1 DIDDB4, WT
F'IE FV
NXTSET LINE = TITLE.(1,SPEC)
READ DATA
SPACE.(LINE,6,24)
P'T $10H-DATA SET C4,9H; RUN # C4,15H; RESULTS SET C4,4H HA
1SI4,23H PHOTOS (SCALE FACTOR =F11.6,30H UNITS/MV); DATA TAKE
2N @ EACHFR.2,6H DBTDC*$,
3 SPEC...SPEC(2), NUMBER, VALUES, VALUES(2)
UNITCM(1) = VALUES*MVCM(1)
ZERO.(COMMON,END,REF(1),BLO(1))
BTDC(1) = VALUES(1)
REFERR = UNITCM(1)*ERRREF(1)
REFERR(1) = REFERR*REFERR
BLOERR(1) = REFERR(1)
T'H PHOTOS, FOR P = 2, 1, P .G. NUMBER
UNITCM = VALUES*MVCM(P)
UNITCM(P) = UNITCM
COMMON = COMMON + 1
BGN = COMMON(COMMON)
W'R BGN .NE. END + 1, ERROR.
BGNERR = UNITCM*ERRCOM(COMMON)
COMMON = COMMON + 1
END = COMMON(COMMON)
ENDERR = UNITCM*ERRCOM(COMMON)
LAST = P - 1
BTDC(P) = BTDC(LAST) + (END - BGN)*VALUES(2)
REF(P) = UNITCM(1)*(CMREF(P) - CMREF(1))
REFERR = UNITCM(1)*ERRREF(P)
REFERR(P) = REFERR*REFERR
BLO(P) = BLO(LAST) + UNITCM*(CM(END) - CM(BGN))
BLOERR(P) = BLOERR(LAST) + ENDERR*ENDERR + BGNERR*BGNERR
T'H ADJUST, FOR P = 1, 1, P .G. NUMBER
EXACT = 0R
ADJ = 0.
ADJERR = 0.
T'H OBSERV, FOR OBS = 1, 1, OBS .G. NUMBER
NUMER = REF(OBS) + BLO(P) - BLO(OBS)
DENOM = REFERR(OBS) + .ABS. (BLOERR(P) - BLOERR(OBS))
W'R DENOM .E. 0.
W'R EXACT
W'R .ABS. ((ADJ - NUMER)/UNITCM(P)) .G. .005, ERROR.
O'IE
EXACT = 1R
ADJ = NUMER
ADJ(P) = NUMER
ADJERR(P) = 0.
F'IL
    
```

NXTSET

PHOTOS

Computer Program 2 (Continued)

```

O'R .NOT. EXACT
ADJ = ADJ + NUMER/DENOM
ADJERR = ADJERR + 1./DENOM
E'L
C'E
-----
W'R .NOT. EXACT
ADJ(P) = ADJ/ADJERR
ADJERR(P) = 1./ADJERR
E'L
ADJUST C'E
P'T TOP
V'S TOP = $132H01--SEQUENTIAL PHOTO ANALYSIS DATA (#1 = REFER
1 ENCE FOR SEQUENTIAL BLOWUPS)--1 PERCENT REFERENCE
2 BLOWUPS ADJUSTMENTS/104H PHO MV/CM DBTDC ON 1 ERR SEQ
3 UENTIAL CENTIMETER MEASUREMENTS ON THE BLOWUPS, PROBAB FACTOR
4 UNITS ERR2(14H UNITS ERR)*$
P'T 4H 1F9.3*$, MVCM(1)
P = 1
FV = 5 - NUMBER(1)
POINT.
LINE = LINE + 8
COMMON = 0
I = 1
J = 1
DATA(1) = ADJ(1)
T'H PRINT, FOR P = 2, 1, P .G. NUMBER
COMMON = COMMON + 1
BGN = COMMON(COMMON)
BGNERR = ERRCOM(COMMON)
COMMON = COMMON + 1
END = COMMON(COMMON)
LINES = 4 + (END - BGN)/10
LINE = LINE + LINES
W'R LINE .G. 60
P'T $1H1/1H-/1H0*$
P'T TOP
LINE = 12 + LINES
E'L
LAST = P - 1
ADJ = ADJ(P) - ADJ(LAST)
BLO = BLO(P) - BLO(LAST)
FACTOR = ADJ/BLO
UNITCM = FACTOR*UNITCM(P)
DATA = ADJ(LAST) - UNITCM*CM(BGN)
(I = I + 1, 1, I .G. END,
1 J = J + NUMBER(3),
2 DATA(J) = DATA + UNITCM*CM(I))
P'T $F27.2/I4,F9.3,S65,F6.2,F8.3*$,
1 BGNERR, P, MVCM(P),
2 100.*(1. - ERF.(.ABS.(BLO - ADJ)/SORT.(2.*(
3 BLOERR(P) - BLOERR(LAST) + ADJERR(P) + ADJERR(LAST))))),
4 100.*(FACTOR - 1.)
W'R LINES .E. 4
P'T $1H+S26,10F5.2*$, CM(BGN)...CM(END)
O'E
P'T $1H+S26,10F5.2/(S27,10F5.2)*$, CM(BGN)...CM(END)
E'L
P'T $F27.2*$, ERRCOM(COMMON)
PRINT POINT.
DOPLOT = SPEC(3) .E. $PLOTS$

```

Computer Program 2 (Continued)

```

DOGRPH = SPEC(4) .E. $GRPH$
DORFAD = DOGRPH .OR. DOPLNT
DOPRNT = SPEC(5) .E. $PRNT$
DOPNCH = SPEC(6) .F. $PNCH$
DOTELL = DOPNCH ;OR. DOPRNT
W'R DOTELL .OR. DOREAD
DELINT = VALUES(2)/NUMBER(3)
P'T $26H-DATA WILL BE CURVE FITTED 12,23H TIMES, SHIFTED SO TH
1ATER 8.2,10H DBTDC HAS 10.4,20H UNITS, INTERPOLATED 13,11H TO 1
2(EACH 12.6,7H DBTDC)*$,
3 NUMBER(2), VALUES(3), VALUES(4), NUMBER(3), DELINT
NUMDAT = 1 + (J - 1)/NUMBER(3)
DBTDC(1) = RTDC(1)
DBTDC = RTDC(1) - DELINT
(I = 1, 1, I .G. J,
1 DBTDC(I) = DBTDC + I*DELINT)
USED4.(NUMDAT,VALUES(2),NUMBER(3),DATA(1),BEST(1),
1 NUMBER(2),NODR4)
DIDDR4 = 1R
TERM = VALUES(4) - TAB.(VALUES(3),DBTDC(1),BEST(1),NUMBER(3),
1 NUMBER(3),5,NUMDAT,1.)
NODR4 T'D SKIP
DIDDR4 = 0R
TERM = VALUES(4) - TAB.(VALUES(3),DBTDC(1),DATA(1),NUMBER(3),
1 NUMBER(3),5,NUMDAT,1.)
SKIP WT = SPEC(2) .RS. 24 .E. $0000WT$
W'R TERM .NE. 0.
W'R DOGRPH
T'H SHIFTR, FOR P = 1, 1, P .G. NUMBER
REF(P) = REF(P) + TERM
SHIFTR W'R WT, REF(P) = THERMO.(REF(P))
F'L
T'H SHIFTD, FOR I = 1, NUMBER(3), I .G. J
DATA(I) = DATA(I) + TERM
W'R DIDDR4, BEST(I) = BEST(I) + TERM
W'R WT
DATA(I) = THERMO.(DATA(I))
SHIFTD W'R DIDDR4, BEST(I) = THERMO.(BEST(I))
F'L
E'L
INTERP.(NUMDAT,DBTDC(1),NUMBER(3),DATA(1))
W'R DIDDR4, INTERP.(NUMDAT,DBTDC(1),NUMBER(3),BEST(1))
W'R DOREAD
XTITLE = $F4$
XTITLE(1) = 23
V'S XTITLE(2) = $CRANKANGLE DEGREES BTDC$
READ DATA
W'R DOPLNT
W'R DIDDR4
PLOT.(SCALES,XTITLE,YTITLE,HEAD,J,DBTDC(1),BEST(1))
O'E
PLOT.(SCALES,XTITLE,YTITLE,HEAD,J,DBTDC(1),DATA(1))
E'L
E'L
W'R DOGRPH
GRAPH.(SCALES,XTITLE,YTITLE,HEAD)
PLINE.(BTDC(1),REF(1),NUMBER,1,-1,1,1.)
I = 1. + .06*.ABS.(SCALES(1)/SCALES(2)/DELINT)
J = 1 + (J - 1)/I
PLINE.(DBTDC(1),DATA(1),J,I,0,0,1.)

```

Computer Program 2 (Concluded)

```

W'R D1DDR4, PDSHLN.(DBTDC(1),BEST(1),J,I,.05,1.)
PLTFND.
E'L
E'L
W'R D0TELL
W'R D1DDR4
TELL.(BEST)
D'E
TELL.(DATA)
E'L
E'L
E'L
T'0 NXTSET
I'M POINT.
P'T $F18.2,F5.2,F4.2,S51,F6.2,S6,3(F8.'FV',F6.'FV')*$,
1 RTDC(P), CMREF(P), FRRREF(P), 100.*(1. - ERF.(.ABS.
2 (REF(P) - ADJ(P))/SORT.(2.*(RFFERR(P) + ADJERR(P)))),
3 REF(P), SORT.(REFERR(P)), BLO(P), SORT.(BLOERR(P)),
4 ADJ(P), SORT.(ADJERR(P))
F'N
F'N
I'M TELL.(DAT)
BGN = 1 + IROUND.((VALUES(5) - VALUES(1))/DELINT)
DEL = IROUND.(VALUES(6)/DELINT)
NUMDAT = 1 + IROUND.((VALUES(7) - VALUES(5))/DELINT)/DEL
END = BGN + NUMDAT*DEL
FV = FV + 2
W'R WT, FV = FV - 1
W'R D0PRNT, P'T $1H1/1H-5(F13.'FV',2H @F10.4,1H,)/(S1,5(F13.'
1FV',2H @F10.4,1H,))*$,
2 (I = BGN, DEL, I .E. END, DAT(I), DBTDC(I))
W'R D0PNCH
SPEC(1) = ACDBN.(SPEC(1))
PUNCH FORMAT $I4,S2,C4,5HBGN @F16.10,5H, FORF16.10,7H, END @F
116.10,5H RTDC*$, SPEC(1), SPEC(2), DBTDC(BGN),
2 DBTDC(DEL) - DBTDC, DBTDC(END - DEL)
PUNCH.(SPEC(1),SPEC(2),7-FV,NUMDAT,DEL,DAT(BGN))
E'L
F'N
F'N
F'N

```

Computer Program 3

Title: Engine Data Reading and Printing

Purpose: To read engine data and specifications, calculate the mean values and root mean square errors, and tabulate the experimental observations.

Input:

A. Engine Specifications and Conditions of Test

1. Runs identification
2. Fuel used
3. Injector opening pressure
4. Oil used
5. Coolant used
6. Fuel consumption weight
7. Air flowmeter orifice

B. Engine Data

1. Engine speed in rpm
2. Load in lbs
3. Fuel consumption time in minutes
4. Fuel leakage past injector needle in liters per hour
5. Air pressure before air flowmeter orifice, in psia
6. Air temperature before air flowmeter orifice, in °F
7. Blowby rate, in ft^3/min
8. Barometric pressure, in in. Hg
9. Air surge tank gauge pressure, in. Hg

10. Cylinder pressure at the time of I.V. closing above the air surge tank pressure, in psi
11. Cylinder pressure at the point of injection above the cylinder pressure at I.V. closing, in psi
12. Cylinder pressure at the end of ignition delay, I.D.p above the pressure at start of injection, in psi
13. Crank angle at the start of needle lift, in degrees
14. Crank angle at the end of ignition delay, in degrees
15. Crank angle at the start of illumination, in degrees
16. Inlet air temperature, degrees Fahrenheit
17. Minimum surface temperature of the combustion chamber wall, in millivolts
18. Surface temperature swing due to combustion, in millivolts
19. Exhaust gas temperature, in degrees Fahrenheit
20. Smoke meter reading, in Hartridge units
21. Oil temperatures at inlet and outlet of the oil cooler, in degrees Fahrenheit
22. Oil flowmeter reading, in cycles per sec
23. Coolant temperature at inlet and outlet from engine, in degree Fahrenheit
24. Pressure drop across the sharp edge orifice of the coolant flowmeter, in in. Hg

Procedure:

1. Read and print the engine specifications, conditions of runs, and data, in tabulated form.

List of Assisting Programs:

1. Program to print a title (TITLE) program 12.
2. Program to calculate the averages and errors (AVERMS) program 18.

NOTE: Items 10, 11, 12, 13, 14, 15, 17, 18 are obtained from the different oscilloscope traces photographed for the cycle.

Computer Program 3

Engine Data Reading and Printing (ENGDAT)

```

EXTERNAL FUNCTION ENGDAT.(USING,SPEC,ID,DATA)
  I'R TITLE., LINE, BCDBN., N, SPEC, MAX, USING, USE, USE2,
  1 USE3, USE20, END20, END26, R, S, ID, END, BGN
  W'N MORE, LACK.
  LINE = TITLE.(1,SPEC)
  N = BCDBN.(SPEC(1))
  SPEC(1) = N
  MORE = N .G. 1
  W'R MORE
  MAX = N + 2
  O'E
  MAX = 1
  E'L
  USE = USING
  W'R N .L. 1 .OR. MAX .G. USE
  ERROR RETURN
  E'L
  USE2 = USE + USE
  USE3 = USE2 + USE
  USE20 = 20*USE
  END20 = USE20 - 1
  END26 = 26*USE - 1
  R'I' $I4,2C1,F5,F4.1,F3.2,F2.2,F3.1,F2,2F2.1,F4.1,F3.1,F4,F3,3
  IF4.1,F3,F3.1,F3.2,F4,F2/I4,F4.1,F3.1,F3,F4.1,2F3.1*$,
  2 (R = 0, 1, R .E. N, ID(R), ID(USE+R), ID(USE2+R),
  3 (S = R, USE, S .G. END20, DATA(S)),
  4 ID(USE3+R), (S = S, USE, S .G. END26, DATA(S)))
  T'H CHANGE, FOR R = 0, 1, R .E. N
  S = USE3 + R
  W'R ID(S) .NE. ID(R), T'O NOGOOD
  S = S + USE2
  TORF = DATA(S)
  W'R .NOT. LACK.(TORF) .AND. TORF .L. 40.,
  1 DATA(S) = 100. + TORF
  S = S + USE2
  PBAR = DATA(S)
  W'R .NOT. LACK.(PBAR)
  W'R PBAR .G. 2.
  PBAR = 20. + PBAR
  O'E
  PBAR = 30. + PBAR
  E'L
  DATA(S) = PBAR
  CHANGE
  E'L
  W'R MORE
  T'H COLMNS, FOR S = 0, USE, S .G. END26
  COLMNS
  AVEERR.(N,DATA(S))
  E'L
  MORE1
  BGNEND.(LINE,6,MAX,BGN,END,DONE1)
  W'R END .G. N, END = N
  P'I' $10H-DATA SET C4,4H HASI5,12H RUNS. THE C4,9H ENGINE (C4
  1,14H SLEEVE, IVC @C4,13H DBTDC) USED C4,7H FUEL (C4,7H PSI),
  2C4,10H OIL, AND C4,9H COOLANT.*$, SPEC...SPEC(8)
  P'I' $114H0 FOR USE SPEED LOAD FUEL AIR BLOW ROOM
  1-SURGE-@IVC-@INJ-RIS DBTDC AT START OF AIR MILLVOLTS EXHAUS
  2T/114H RUN W D RPM LBS MIN L/HR PSIG F CFPM INHG I
  3NHG PSI PSI PSI LIFT RISE ILLUM F MIN INC F HU/(
  4I5,2(S1,C1),F8,F6.1,F5.2,F4.2,F6.1,F4,F4.1,2F6.1,F5.1,F5,F4,F
  57.1,2F6.1,F5,F5.1,F5.2,F5,F3)*$,
  6 (R = BGN, 1, R .E. END, ID(R), ID(USE+R), ID(USE2+R),

```


Computer Program 3 (Concluded)

```

7 (S = R, USE, S .G. END20, DATA(S))
T'D MORE1
DONE1 W'R MORE, P'T $5H MEANF12,F6.1,F5.2,F4.2,F6.1,F4,F4.1,2F6.1,F
15.1,F5,F4,F7.1,2F6.1,F5,F5.1,F5.2,F5,F3/5H ERRSF12,F6.1,F5.2,
2F4.2,F6.1,F4,F4.1,2F6.1,F5.1,F5,F4,F7.1,2F6.1,F5,F5.1,F5.2,F5
3,F3*$, (R = N, I, R .E. MAX,
4 (S = R, USE, S .G. END20, DATA(S))
MORE2 BGNEND.(LINE,4,MAX,BGN,END,DONE2)
W'R END .G. N, END = N
P'T $37H- FOR CRANKCASE OILS COOLANT SYSTEM/38H RUN OUT(F
1)INC CPS OUT(F)INC INHG/(I5,F7.1,F5.1,F4,F7.1,2F5.1)*$,
2 (R = BGN, I, R .E. END, ID(R),
3 (S = USE20+R, USE, S .G. END26, DATA(S))
T'D MORE2
DONE2 W'R MORE, P'T $5H MEANF7.1,F5.1,F4,F7.1,2F5.1/5H ERRSF7.1,F5.
11,F4,F7.1,2F5.1*$, (R = N, I, R .E. MAX,
2 (S = USE20+R, USE, S .G. END26, DATA(S))
F'N LINE
E'N

```

Computer Program 4

Title: Engine Data Calculations

Purpose: To calculate the different parameters of interest in the study of the combustion process.

Input: Same as ENGDAT (engine testing data and specifications) see ENGDAT input.

Procedure:

The following calculations, together with their mean values and root mean square curves are calculated.

1. Brake horsepower
2. Brake mean effective pressure, in psi
3. Brake specific fuel consumption in lb/hp/hr
4. Fuel-air ratio
5. Inlet air/cycle in lbm/cycle
6. Air blowby per cycle in lbm/cycle
7. Residual exhaust gas in lbm/cycle
8. Surge tank pressure in psia
9. Volumetric efficiency in %
10. Temperature at inlet valve close in degrees Fahrenheit
11. Average index of compression from inlet valve close to beginning of injection
12. Pressure at start of injection, psia
13. Density at start of injection, lbrsm/ft³
14. Temperature at start of injection, degrees Rankine
15. Average index of compression during delay

16. Average pressure during delay, psia
17. Average density during delay, lbm/ft^3
18. Average temperature during delay, degrees Rankine
19. Pressure rise delay in Msecs
20. Illumination delay in Msecs
21. Minimum cylinder wall temperature in degrees Fahrenheit
22. Maximum temperature swing during combustion in degrees Fahrenheit
23. Lubricating oil flow rate in gallons/min
24. Rate of heat loss to oil in Btu/sec
25. Percent of heat loss to oil
26. Coolant flow rate in gallons/min
27. Rate of heat loss to coolant in Btu/sec
28. Percent of heat loss to coolant

List of Assisting Programs:

1. Program DB4T11 (9)
2. Program CYLVOL, CYLGRA (10)
3. Program BBRAN, BBLFT3, BBFAR (11)
4. Program ENGDAT (3)
5. Program INTDER (7)
6. Program TITLE (12)
7. Program FULHCR, FULDEN, FULFLO (13)
8. Program 14 (coolant and oil properties)
9. Program MEAN (15)
10. Program AIRFLO (17)

11. Program AVEERR (18)
12. Program THERMO (19)
13. Program LACK (20)

Computer Program 4

Engine Data Calculations (ENGCAL)

```

EXTERNAL FUNCTION ENGCAL.(USING,SPEC,ID,DATA,CALC)
D'N STORE(54), (DAT, CAL)(28), (P, D, T)(10)
I'R ENGDAT., LINE, SPEC, N, MAX, USING, USE, USE22, END22,
1  END28, E, BCDBN., R, S, I, ID, RUN, END, BGN
B'N MORE, LACK., LACK2., LACK3., LACK4.
LINE = ENGDAT.(USING,SPEC,ID,DATA)
N = SPEC(1)
MORE = N .G. 1
W'R MORE
MAX = N + 2
D'E
MAX = 1
E'L
USE = USING
USE22 = 22*USE
END22 = USE22 - 1
END28 = 28*USE - 1
V'S DYNAM = 3000., 3571.
V'S BMEP = 3.689, 3.187
V'S EFF = 2414.38, 2483.42
W'R SPEC(2) .E. $ATAC$
E = 0
D'E
E = 1
E'L
RATIO = COMRAT.(VCLEAR,SPEC(2),SPEC(3))
CLEAR = VCLEAR/1728.
IVC = BCDBN.(SPEC(4))
IVC = - 0. + IVC
VIVC = CYLVOL.(IVC)
DEN60 = FULPRO.(SPEC(5),HTOC,HETVAL)
RVAPOR = 1./(17.908 + 1.503*HTOC)
KEXH = .3757 + 4.4769/HTOC
OILID.(HAVORIL,SPEC(7))
COLID.(0,SPEC(8))
DEN80 = COLDEN.(80.)
FUELO = HETVAL/360000.
HEAD = 70.3863/DEN80 - .08333333333
T'H COMPUT, FOR R = 0, 1, R .E. N
S = R
(I = 1, 1, I .E. 29, DAT(I) = DATA(S),
1  CAL(I) = - 0., S = S + USE)
W'R .NOT. LACK.(VCLEAR)
W'R .NOT. LACK.(DAT(1)), CAL(1) = DAT(1)*DAT(2)/DYNAM(E)
CAL(2) = BMEP(E)*DAT(2)
E'L
S = USE + R
FUEL = FULFLO.(ID(S),DAT(3),DAT(4))
AIR = AIRFLO.(ID(S+USE),DAT(6),DAT(5),DAT(8),DAT(9))
W'R .NOT. LACK.(FUEL)
CAL(3) = FUEL/CAL(1)
CAL(4) = FUEL/AIR
E'L
PBAR = .4911570*DAT(8)
VINJ = CYLVOL.(DAT(13))
W'R .NOT. LACK2.(PBAR,DAT(9))
CAL(8) = PBAR + .4911570*DAT(9)
W'R .NOT. LACK.(DAT(10))
CAL = CAL(8) + DAT(10)

```

Computer Program 4 (Continued)

```

W'R .NOT. LACK.(DAT(11))
CAL(12) = CAL + DAT(11)
W'R .NOT. LACK2.(VIVC,VINJ),
1 CAL(11) = ELOG.(CAL(12)/CAL)/ELOG.(VIVC/VINJ)
E'L
E'L
E'L
W'R .NOT. LACK.(DAT(1))
CYCLES = 30.*DAT(1)
CAL(5) = AIR/CYCLES
RUN = ID(R)
W'R RUN .GE. 1 .AND. RUN .LE. 74 .AND. LACK.(DAT(21))
TBLO = DAT(24)
O'E
TBLO = DAT(21)
E'L
W'R .NOT. LACK.(DAT(7)), CAL(6) = 16.408644*
1 SORT.(BBLFT3.(TBLO,PBAR,.371110))*DAT(7)/CYCLES
E'L
W'R .NOT. LACK2.(VCLEAR,CAL(8))
W'R .NOT. LACK.(CAL(5)),
1 CAL(9) = EFF(E)*CAL(5)/BBLFT3.(DAT(16),CAL(8),.371110)
W'R .NOT. LACK2.(CAL(4),DAT(19))
REXH = (.371110 + CAL(4)/KEXH)/(1. + CAL(4))
CAL(7) = BBLFT3.(DAT(19)+75.,CAL(8),REXH)*CLEAR
W'R .NOT. LACK.(CAL(5))
GAS = CAL(5) + CAL(7)
RGAS = (CAL(5)*.371110 + CAL(7)*REXH)/GAS
GAS = 1728.*GAS
CAL(10) = BBFAR.(CAL,GAS/VIVC,RGAS)
CAL(13) = GAS/VINJ
CAL(14) = BBRAN.(CAL(12),CAL(13),RGAS)
W'R .NOT. LACK3.(DAT(12),DAT(14),CAL(14))
P = CAL(12)
D = CAL(13)
T = CAL(14)
DEL = (DAT(14) - DAT(13))/10.
FUELIN = 1728.*FUEL/CYCLES
GASR = GAS*RGAS
T'H DELAY, FOR I = 10, -1, I .E. 0
VAPOR = PART(I)*FUELIN
V'S PART(1) = .025, .050, .075, .100, .125, .150, .175, .200,
1 .225, .250
MIX = GAS + VAPOR
RMIX = (GASR + VAPOR*RVAPOR)/MIX
V = CYLVOL.(DAT(13) + I*DEL)
D(I) = MIX/V
W'R I .E. 10
P(10) = CAL(12) + DAT(12)
T(10) = BBRAN.(P(10),D(10),RMIX)
INDEX = ELOG.(T(10)/T)/ELOG.(VINJ/V)
CAL(15) = 1. + INDEX
K = T*VINJ.P.INDEX
O'E
T(I) = K/V.P.INDEX
P(I) = D(I)*RMIX*T(I)*BBCFAC.(D(I),T(I),RMIX)
E'L
CAL(16) = MEAN.(11,P,STORE)
CAL(17) = MEAN.(11,D,STORE)
CAL(18) = MEAN.(11,T,STORE)

```

DELAY

Computer Program 4 (Continued)

```

E'L
E'L
E'L
E'L
W'R .NOT. LACK.(DAT(13))
CA = 166.6666667/DAT(1)
W'R .NOT. LACK.(DAT(14)), CAL(19) = CA*(DAT(13) - DAT(14))
W'R .NOT. LACK.(DAT(15)), CAL(20) = CA*(DAT(13) - DAT(15))
E'L
CAL(21) = THERMO.(DAT(17))
W'R .NOT. LACK2.(CAL(21),DAT(18)),
1 CAL(22) = THERMO.(DAT(17)+DAT(18)) - CAL(21)
CAL(23) = .071165*DAT(23)
W'R .NOT. LACK3.(DAT(21),DAT(22),HAVOIL), CAL(24) = .002228*
1 OPLDEN.(DAT(21)-DAT(22))*CAL(23)*
2 OILCP.(DAT(21)-DAT(22)/2.)*DAT(22)
W'R .NOT. LACK4.(DEN80,DAT(24),DAT(25),DAT(26))
TCOLIN = DAT(24) - DAT(25)
ROOTH = SQRT.(.166666667 + DAT(26)*HEAD)
NUCOL = COLNU.(TCOLIN)
CAL(26) = 6.15836*ROOTH*(.5 +
1 SQRT.(.25 + .010205*NUCOL/ROOTH))
RN = 4391.75*CAL(26)/NUCOL
W'R RN .G. 2000.
CAL(27) = .002228*COLDEN.(TCOLIN)*CAL(26)*
1 COLCP.(DAT(24)-DAT(25)/2.)*DAT(25)
O'E
CAL(26) = -0.
E'L
E'L
W'R .NOT. LACK.(FUEL)
QFUEL = FUELQ*FUEL
CAL(25) = CAL(24)/QFUEL
CAL(28) = CAL(27)/QFUEL
E'L
S = R
COMPUT (I = 1, 1, I .E. 29, CALC(S) = CAL(I), S = S + USE)
W'R MORE
T'H COLMNS, FOR S = 0, USE, S .G. END28
COLMNS AVEERR.(N,CALC(S))
E'L
MORE1 BGNEND.(LINE,6,MAX,BGN,END,DONE1)
W'R END .G. N, END = N
P'T $12H-ENGINE WITHF6.2,12H/1 RATIO HASF7.4,27H CUIN CLEARAN
1CE. FUEL WITHF6.3,12H/1 RATIO HASF6.2,29H LBM/CUFT (@60) AND
2 LIBERATESF6,9H BTU/LBM.*$,
3 RATIO, VCLEAR, HTOC, DEN60, HETVAL
P'T $129H0 FOR BRAKE BMEP BSFC FUEL/ CYCLE(LBM/1000) SURGE
1 EFF @IVC AT START OF INJECTION AVERAGED DURING DELAY DELA
2Y(MSEC) WALL(F)/129H RUN HP PSI #/HRHP AIR AIR BLO
3W EXH PSIA PCT F INDEX PSIA #/CUFT R INDEX PSIA #/CU
4FT R PRISE ILLUM MIN INC/(I5,2F6.1,F6.3,F6.4,3PF7.2,3P2F5
5.2,F5.1,F6.1,F4,2(F7.3,F5,F6.3,F5),F7.3,F6.3,F5,F4)*$,
6 (R = BGN, 1, R .E. END, ID(R),
7 (S = R, USE, S .G. END22, CALC(S)))
T'D MORE1
DONE1 W'R MORE, P'T $5H MEAN2F6.1,F6.3,F6.4,3PF7.2,3P2F5.2,F5.1,F6.
11,F4,2(F7.3,F5,F6.3,F5),F7.3,F6.3,F5,F4/5H ERRS2F6.1,F6.3,F6.
24,3PF7.2,3P2F5.2,F5.1,F6.1,F4,2(F7.3,F5,F6.3,F5),F7.3,F6.3,F5
3,F4*$, (R = N, 1, R .E. MAX,

```

Computer Program 4 (Concluded)

```

4 (S = R, USE, S .G. END22, CALC(S))
MORE? BGNEND.(LINE,4,MAX,BGN,END,DONE2)
      W'R END .G. N, END = N
      V'S OUT2 = $37H- FOR CRANKCASE OILS COOLANT SYSTEM/5H RUN2
      1(16H GPM BTU/SEC$, 601260346174K, $15,F6.2,2F5.1,F6.1,2F5.1*
      2$
      P'T OUT2, (R = BGN, 1, R .E. END, ID(R),
      1 (S = USE22+R, USE, S .G. END28, CALC(S))
      T'0 MORE2
DONE? W'R MORE, P'T $5H MEANF6.2,2F5.1,F6.1,2F5.1/5H ERRSF6.2,2F5.1
      1,F6.1,2F5.1*$, (R = N, 1, R .E. MAX,
      2 (S = USE22+R, USE, S .G. END28, CALC(S))
      F'N LINE
      E'N

```


Computer Program 5

Title: Fuel Injection System Analysis

Purpose: To calculate the fuel mass flow rate, the accumulated injection and the average coefficient of discharge over the injection period.

Input: A sequence of needle lift, cylinder pressure, and fuel pressure, over the period of injection (are fed from oscilloscope traces).

Procedures:

1. Use ENGDAT to calculate the engine parameters
2. Use program AREAS to calculate the effective area of fuel flow
3. Calculate theoretical mass flow rate of fuel

$$Q = A \sqrt{2g(P_{\text{fuel}} - P_{\text{cyl.}}) / \rho_{\text{fuel}}}$$

4. Calculate the theoretically accumulated injection over the injection period
5. Knowing the actual accumulated fuel/cycle from ENGCAL and the theoretical accumulated fuel/cycle, therefore an average coefficient of discharge is calculated.
6. Calculate the actual mass flow rate over the period of injection
7. Gives a printed, punched or plotted values of mass flow and accumulated injection over the injection period

Computer Program 5

Fuel Injection System Analysis

AGAIN

```

D'N SPEC(19), ID(3), DATA(21), CALC(20), (DBTDC, NL, FP, CP,
1  SAVE, AREA, LBMHR, DO, D1, D2, D3, D4, LBM)(1000),
2  STORE(5000)
EQUIVALENCE (SAVE, AREA), (STORE, DO, LBM), (STORE(1000), D1)
1  ,(STORE(2000), D2), (STORE(3000), D3), (STORE(4000), D4)
I'R IROUND., NUMDIV, BCDBN., NUMINT, NUMDAT, ENDDAT, NUMSEQ,
1  ENDSEQ, I, FV, FVF, J, LINE, START, STOP, SPEC
F'E FVF
ENGCAL.(I,SPEC,ID(1),DATA(1),CALC(1))
P'T $1H-/1H0*$
AREAS1.
DENFUL = FULDEN.(SPEC(4),DATA(9))
FUEL = FULFLO.(ID(2),DATA(3),DATA(4))/DATA(1)/30.
R'T $S15,F16.10,S5,F16.10,S7,F16.10*$, BEGIN, EVERY, END
NUMINT = BCDBN.(SPEC(7))
NUMDAT = 1 + IROUND.((END - BEGIN)/EVERY)
ENDDAT = 1 + NUMINT*NUMDAT
NUMSEQ = ENDDAT - NUMINT
W'R NUMSEQ .G. 1000, T'O FIN
ENDSEQ = NUMSEQ + 1
DELSEQ = EVERY/NUMINT
DBTDC = BEGIN - DELSEQ
(I = 1, 1, I .E. ENDSEQ,
1  DBTDC(I) = DBTDC + I*DELSEQ)
READ.(NL,2)
READ.(FP,4)
READ.(CP,4)
LBMHR = SQRT.(DENFUL)/415.53855
LBM = LBMHR/-21600./DATA(1)
(I = 1, 1, I .E. ENDSEQ,
1  P = FP(I) - CP(I),
2  SAVE(I) = P/SQRT.(.ABS.P),
3  LBMHR(I) = AREAS3.(NL(I))*SAVE(I))
AREAS2.(FUEL/MEAN.(NUMSEQ,LBMHR(1),STORE(1))
1  /(DBTDC(NUMSEQ)-DBTDC(1))/LBM)
(I = 1, 1, I .E. ENDSEQ,
1  AREA = AREAS3.(NL(I)),
2  LBMHR(I) = AREA*SAVE(I),
3  AREA(I) = AREA)
DB4T11.(NUMSEQ,DELSEQ,1,LBMHR(1),DO(1),D1(1),D2(1),D3(1),
1  D4(1))
LBM(1) = -0.
(I = 2, 1, I .E. ENDSEQ,
1  J = I - 1,
2  LBM(I) = LBM(J) + INTDER.(DBTDC(J),DBTDC(I),DBTDC(1),
3  NUMSEQ,DELSEQ,1,LBMHR(1),D1(1),
4  D2(1),D3(1),D4(1)))
COEFF = FUEL/LBM(NUMSEQ)/LBM
P'T $1H-/42HOFUEL DENSITY (@ TEMPERATURE OF COOLANT) =F6.2,43
1H LBM/CUFT, TOTAL FUEL INJECTED PER CYCLE =6PF7.2,12H LBM/10.
200000/1H-/50H-INTEGRATION OF DATA GIVES DISCHARGE COEFFICIENT
3 =F7.4*$, DENFUL, FUEL, COEFF
LBMHR = COEFF*LBMHR
LBM = COEFF*LBM
FUEL = FUEL/100.
(I = 1, 1, I .E. ENDSEQ,
1  LBMHR(I) = LBMHR*LBMHR(I),
2  LBM(I) = LBM*LBM(I))
LINE = 60

```

Computer Program 5 (Concluded)

```

MORE      RGNEND.(LINE,6,NUMDAT,START,STOP,DONE)
          ENDDAT = 1 + NUMINT*STOP
          P'T $1H-S8,48H|----DATA FROM SEQUENTIAL PHOTO ANALYSIS----|
          1|13(1H-)30H|INCLUDES DISCHARGE COEFFICIENT12(1H-)1H|/132H0  A
          2T  NEEDLE LIFT FUEL PRESSURE CYLINDER PRESSURE EQUIVALENT
          3 AREA RATE OF INJECTION ACCUMULATED INJECTION FRACTION INJ
          4ECTED/7H DBTDC6,4HMILSS10,4HPSIAS12,4HPSIAS10,13HSQ IN/1000
          5000S7,8HLBM/HOURS12,11HLBM/1000000S14,3HPCT/(F7.1,F10.2,F14,F
          617.1,2F18.1,6PF21.2,F21.2)*$,
          7 (I = 1 + NUMINT*START, NUMINT, I .E. ENDDAT,
          8 DBTDC(I), NL(I), FP(I), CP(I), AREA(I), LBMHR(I), LBM(I),
          9 LBM(I)/FUEL)
          T'D MORE
DONE      W'R SPEC(8) .E. $PNC$
          PUNCH FORMAT $I4,6HINJECT,5HRGN @F16.10,5H, FORF16.10,7H, END
          1 @F16.10,5H BTDC*$, ID(1), DBTDC(1), DELSEQ, DBTDC(NUMSEQ)
          PUNCH.(ID(1),$/HR$,3,NUMSEQ,1,LBMHR(1))
          PUNCH.(ID(1),$/ACC$,3,NUMSEQ,1,LBM(1))
          F'IL
          T'D AGAIN
          I'N READ.(DAT,FV)
          FVF = 7 - FV
          R'IT $S10,10F7.'FVF'*$, (I = 1, NUMINT, I .E. ENDDAT, DAT(I))
          INTERP.(NUMDAT,DBTDC(1),NUMINT,DAT(1))
          F'IN
          E'IN
FIN      E'IN

```

Computer Program 6

Title: Calculation of Equivalent Area of Injection

Purpose: To calculate the effective area of injection at any needle lift, where effective area is the area to which we can write

$$Q = C_{d \text{ eff.}} A \sqrt{2g \frac{\Delta P}{\rho}}$$

Input:

1. Needle lift
2. An assumed value of coefficient of discharge

Procedure:

The pressure difference between fuel at inlet to injector and fuel out of the injector is measured. Due to the change in area between inlet and outlet an effective area was derived using the energy equation.

Computer Program 6

Equivalent Area of Injection as a Function of Injector-Needle Lift (AREAS)

```

LIF
EXTERNAL FUNCTION (ARG)
DIM DIM(4)
PIR PI(3.141592654)
EIO AREAS1.
RIT $4F10.5,F10.2,F10.4*$, DIM...DIM(4), COEFF
AHOLES = PI*DIM*DIM*1.E6
ABODY = PI*DIM(1)*DIM(1)*.25E6
TAN = (DIM(2) - DIM(1))/2./DIM(3)
ALPHA = ATAN.(TAN)
COSINE = COS.(ALPHA)
BETA = DIM(4)*PI/360.
DIF = BETA - ALPHA
RATIO = SIN.(BETA)/SIN.(DIF)
K1 = PI*DIM(1)*DIF*RATIO*1000.
K2 = 2.*PI*(DIF*COSINE*TAN + COS.(BETA) - COSINE)*RATIO*R TIO
P T $132H-RATE OF INJECTION = DISCHARGE COEFFICIENT * EQUI VAL
1ENT AREA * SORT.(FUEL DENSITY * |FUEL PRESSURE - CYLINDER PRE
2SSURE|) / 415.53855/14H (LBM/HOUR)S32,13HSQ IN/1000000S11,
310H(LBM/CUFT)S8,6H(PSIA)S12,6H(PSIA)/18H0INJECTOR HAS FOURF7.
45,43H INCH HOLES, CONTACT SURFACE HAS DIAMETERS F7.5,2H &F7.
55,11H AND HEIGHTF7.5,15H, TIP ANGLE ISF7.2,8H DEGREES/132HOE
6EQUIVALENT AREA = 1/SORT.(1/(OUTLET AREA FOR NEEDLE & SEAT).P.
72 + 1/(AREA OF HOLES).P.2 - (DISCHARGE COEFFICIENT/AREA OF BO
8DY).P.2)/S31,6HMILS*(F6.1,2H -F7.4,6H*MILS)F21.1,F44.1*$,
9 DIM...DIM(4), K1, -K2, AHOLES, ABODY
TIO SKIP
EIO AREAS2.
COEFF = ARG
SQUARE = COEFF/ABODY
SQUARE = 1./AHOLES/AHOLES - SQUARE*SQUARE
FIN
EIO AREAS3.
MILS = ARG
WIR MILS .LE. 0.
FIN 0.
OIE
ADUT = MILS*(K1 + K2*MILS)
FIN 1./SORT.(1./ADUT/ADUT + SQUARE)
EIL
EIN
    
```

SKIP

Computer Program 7

Title: Integration of a Given Data $Y_{(x)}$, Taken at Equal Intervals of x

Purpose: To apply numerical integration

Input:

1. Data to be integrated
2. Adjusted values of data and derivatives from applying DB4T11 (curve fitting program)

Procedure:

The given data are curve fitted with the best 5th degree polynomial for each point, the derivatives are found and used in expressing the function according to a Taylor series expansion that help in performing the integration.

Computer Program 7

Integration of Given Data (INTDER)

```

L'F
EXTERNAL FUNCTION INTDER.(FROM,TO,BGN,N,DEL,ADD,
1 DO,D1,D2,D3,D4)
I'R LOWERI, UPPERI, N, ADD, ADDS, ENDI, I, AT
DELX = DEL
LOWERZ = (FROM - BGN)/DELX
UPPERZ = (TO - BGN)/DELX
W'R LOWERZ .G. UPPERZ
ANSWER = LOWERZ
LOWERZ = UPPERZ
UPPERZ = ANSWER
ANSWER = -1.
O'E
ANSWER = +1.
E'L
LOWERI = LOWERZ + .5
UPPERI = UPPERZ + .5
W'R LOWERI .L. 0 .OR. UPPERI .G. N - 1, ERROR RETURN
LOWERZ = LOWERZ - LOWERI
UPPERZ = UPPERZ - UPPERI
ADDS = ADD
LOWERI = LOWERI*ADDS
UPPERI = UPPERI*ADDS
ENDI = UPPERI - ADDS
ZERO.(SUM0,SUM2,SUM4)
(I = LOWERI + ADDS, ADDS, I .G. ENDI, SUM0 = SUM0 + D0(I),
1 SUM2 = SUM2 + D2(I), SUM4 = SUM4 + D4(I))
F'N ANSWER*(ENDS.(.5,LOWERI) - ENDS.(LOWERZ,LOWERI) + DELX*
1 (SUM0 + DELX*DELX*(SUM2 + DELX*DELX*SUM4/80.)/24.) +
2 ENDS.(UPPERZ,UPPERI) - ENDS.(-.5,UPPERI))
I'N ENDS.(Z,AT)
X = Z*DELX
I = AT
F'N X*(D0(I) + X*(D1(I) + X*(D2(I) + X*(D3(I) + X*D4(I)
1 /5.)/4.)/3.)/2.)
E'N
E'N

```

Computer Program 8

Title: Best Straight Line to Fit a Group of Points

Purpose: To curve fit the given data Y according to the relation $Y = A+Bx$ and to give A , B , standard error in A , standard error in B , an estimate of standard error in data, standard errors in calculated values, adjusted values of Y , deviations of data from adjusted values and probability of occurrence of deviations.

Input: A sequence of Y data points at equally spaced intervals of x .

Procedure:

A least square best fitting straight line technique is applied to the given data.

Computer Program 8

Best Straight Line to Fit a Group of Points (BLINE)

MAD (06 JAN 1967 VERSION) PROGRAM LISTING

BLINE., CLINE., ELINE., DLINE., OLINE., WLINE.

```

EXTERNAL FUNCTION (N,RESULT,X,Y)
INTEGER N, GOOD, LAST, I, TYPE, BAD
BOOLEAN NOPTS, SAMEX, NOERRS, LACK.
DIMENSION ANSWER(5)
ENTRY TO BLINE.
GOOD = N
LAST = GOOD - 1
ZERO.(SUMX,SUMY,SUMXX,SUMXY,SUMYY)
NOPTS = 1B
SAMEX = 1B
THROUGH SUMS, FOR I = 0, 1, I .G. LAST
XI = X(I)
YI = Y(I)
WHENEVER LACK.(XI) .OR. LACK.(YI)
GOOD = GOOD - 1
OTHERWISE
SUMX = SUMX + XI
SUMY = SUMY + YI
SUMXX = SUMXX + XI*XI
SUMXY = SUMXY + XI*YI
SUMYY = SUMYY + YI*YI
WHENEVER SAMEX
WHENEVER NOPTS
NOPTS = 0B
XFIRST = XI
OTHERWISE
SAMEX = XI .E. XFIRST
END OF CONDITIONAL
END OF CONDITIONAL
END OF CONDITIONAL
NUM = GOOD
DEL = NUM*SUMXX - SUMX*SUMX
WHENEVER DEL .E. 0. .OR. SAMEX, ERROR RETURN
ANSWER(1) = (SUMY*SUMXX - SUMX*SUMXY)/DEL
ANSWER(1) = 0. + ANSWER(1)
ANSWER(3) = (NUM*SUMXY - SUMX*SUMY)/DEL
ANSWER(3) = 0. + ANSWER(3)
NOERRS = GOOD .E. 2
WHENEVER NOERRS
OBS = -0.
OTHERWISE
OBS = (SUMY - (SUMY*SUMY + ANSWER(3)*ANSWER(3)*DEL)
1 /NUM)/(NUM - 2.)
OBS = 0. + OBS
END OF CONDITIONAL
CAL = OBS/NUM
AVE = SUMX/NUM
MU = DEL/(NUM*NUM)
ANSWER(0) = SQRT.(2.*CAL)
ANSWER(2) = SQRT.(CAL*(1. + AVE*AVE/MU))
ANSWER(4) = SQRT.(CAL/MU)
ANSWER(5) = SQRT.(OBS)
MOVER.(ANSWER...ANSWER(5),RESULT...RESULT(5))

```

SUMS

Computer Program 8 (Continued)

```

FUNCTION RETURN
VECTOR VALUES, FUNCT(1) = 08, 08, 08, 08, 08
ENTRY TO CLINE.
TYPE = 1
TRANSFER TO BEGIN
ENTRY TO ELINE.
TYPE = 2
TRANSFER TO BEGIN
ENTRY TO DLINE.
TYPE = 3
TRANSFER TO BEGIN
ENTRY TO OLINE.
TYPE = 4
TRANSFER TO BEGIN
ENTRY TO WLINE.
TYPE = 5
NOPTS = 18
FUNCT(TYPE) = 18
LAST = N - 1
WHENEVER .NOT. (FUNCT(1) .OR. FUNCT(3)) .AND. NOERRS
WHENEVER FUNCT(5)
YDEV = -0.
CALC = -0.
BAD = -0
TRANSFER TO ENDS
OTHERWISE
SPRAY.(-0.,RESULT...RESULT(LAST))
TRANSFER TO END
END OF CONDITIONAL
END OF CONDITIONAL
THROUGH ALLPTS, FOR I = 0, 1, I .G. LAST
XI = X(I)
WHENEVER LACK.(XI)
CALC = -0.
OTHERWISE
YCAL = ANSWER(1) + ANSWER(3)*XI
YCAL = 0. + YCAL
WHENEVER FUNCT(1)
CALC = YCAL
OTHERWISE
WHENEVER .NOT. FUNCT(3)
ERR = XI - AVE
ERR = CAL*(1. + ERR*ERR/MU)
END OF CONDITIONAL
WHENEVER FUNCT(2)
CALC = SQRT.(ERR)
CALC = 0. + CALC
OTHERWISE
YI = Y(I)
WHENEVER LACK.(YI)
CALC = -0.
OTHERWISE
YDEV = YI - YCAL
YDEV = 0. + YDEV
WHENEVER FUNCT(3)
CALC = YDEV
OTHERWISE
DEV = YDEV*YDEV/(OBS + ERR)
WHENEVER FUNCT(4)
CALC = 100.*(1. - ERF.(SQRT.(DEV/2.)))

```

BEGIN

NOMAX

Computer Program 8 (Concluded)

```
OTHERWISE
WHENEVER NOPTS
NOPTS = 08
OTHERWISE
WHENEVER DEV .L. MAXDEV, TRANSFER TO ALLPTS
END OF CONDITIONAL
MAXDEV = DEV
BAD = I
TRANSFER TO ALLPTS
END OF CONDITIONAL
END OF CONDITIONAL
END OF CONDITIONAL
END OF CONDITIONAL
END OF CONDITIONAL
END OF CONDITIONAL
RESULT(I) = CALC
ALLPTS CONTINUE
WHENEVER FUNCT(5)
WHENEVER NOPTS, TRANSFER TO NOMAX
YDEV = Y(BAD) - ANSWER(1) - ANSWER(3) * Y(BAD)
YDEV = 0. + YDEV
CALC = 100. * (1. - ERF.(SQRT.(MAXDEV/2.)))
Y(BAD) = -0.
END5 FUNCT(5) = 08
RESULT(0) = YDEV
RESULT(1) = CALC
FUNCTION RETURN BAD
OTHERWISE
END FUNCT(TYPE) = 08
FUNCTION RETURN
END OF CONDITIONAL
END OF FUNCTION
```

Computer Program 9

Title: Curve Fitting (DB4T11)

Purpose: To reduce the effect of random errors in data.

Input: Data points at equal intervals

Procedure:

1. Read data
2. Statistically adjust the data to fit a 4th degree polynomial through 11 consecutive points by the use of Taylor's expansion up to the 5th term.
3. Give adjusted values of the middle point and the derivatives up to the 4th derivative. These derivatives are used for another program for integration.

Computer Program 9

Curve Fitting (DB4T11)

```

L'F
EXTERNAL FUNCTION DB4T11.(N,DEL,ADD,DATA,D0,D1,D2,D3,D4)
I'R N, NUM, ADD, ADDS(5), I, J, STOP, P
D'N (DELX,FACTOR,C)(4), (SUM,DIF)(5), K(6)
R'N BEGIN
NUM = N
W'R NUM .L. 11, ERROR RETURN
BEGIN = 18
V'S DELX = 1.
V'S FACTOR = 1.
ADDS(1) = ADD
I = 1
J = 0
CONSTS
DELX(I) = DEL*DELX(J)
FACTOR(I) = I*FACTOR(J)/DELX(1)
J = I
I = I + 1
ADDS(I) = ADDS(J) + ADDS(1)
W'R I .L. 5, T'0 CONSTS
STOP = (NUM - 6)*ADDS(1)
T'H INPTS, FOR P = ADDS(5), ADDS(1), P .G. STOP
OBS = DATA(P)
(I = 1, 1, I .G. 5, SUM = DATA(P + ADDS(I)), DIF =
1 DATA(P - ADDS(I)), SUM(I) = SUM + DIF, DIF(I) = SUM - DIF)
C(4) = (6.*(SUM(5) - SUM(4) - SUM(3) + OBS) - SUM(2) +
1 4.*SUM(1))/3432.
D4(P) = FACTOR(4)*C(4)
C(3) = (30.*DIF(5) - 6.*DIF(4) - 22.*DIF(3) - 23.*DIF(2) -
1 14.*DIF(1))/5148.
D3(P) = FACTOR(3)*C(3)
C(2) = (15.*SUM(5) + 6.*(SUM(4) - SUM(2)) - SUM(3) -
1 9.*SUM(1) - 10.*OBS)/858. - 25.*C(4)
D2(P) = FACTOR(2)*C(2)
C(1) = (5.*DIF(5) + 4.*DIF(4) + 3.*DIF(3) + 2.*DIF(2) +
1 DIF(1))/110. - 17.8*C(3)
D1(P) = FACTOR(1)*C(1)
C(0) = (SUM(5) + SUM(4) + SUM(3) + SUM(2) + SUM(1) +
1 OBS)/11. - 10.*C(2) - 178.*C(4)
D0(P) = C(0)
W'R BEGIN, T'0 ENDPTS
INPTS
C'F
P = STOP
ENDPTS
K(0) = FACTOR(4)*C(4)
K(1) = 2.*C(2)
K(2) = 3.*C(3)
K(3) = 4.*C(4)
K(4) = 6.*C(3)
K(5) = 12.*C(4)
K(6) = 24.*C(4)
T'H SERIES, FOR I = 1, 1, I .G. 5
W'R BEGIN
Z = - I
J = P - ADDS(I)
O'F
Z = I
J = P + ADDS(I)
E'L
D4(J) = K(0)
D3(J) = (K(4) + Z*K(6))/DELX(3)
D2(J) = (K(1) + Z*(K(4) + Z*K(5)))/DELX(2)
D1(J) = (C(1) + Z*(K(1) + Z*(K(2) + Z*(K(3))))/DELX(1)
SERIES
D0(J) = C(0) + Z*(C(1) + Z*(C(2) + Z*(C(3) + Z*(C(4))))
W'R BEGIN
BEGIN = 08
T'0 INPTS
E'L
F'N
E'N

```

Computer Program 10

Title: Cylinder Volume and Gradient

Purpose: To calculate the cylinder volume and cylinder volume gradient at any crank angle.

Input: Crank angle to give corresponding cylinder volume and cylinder gradient.

Procedure:

A mathematical formula was derived including the effect of a slight wrist pin offset (center line of the wrist pin is offset from center line of the cylinder).

List of Assisting Program

1. Program to check for missing data (LACK)

Computer Program 10

Cylinder Volume and Gradient (CYLVOL, CYLGRA)

```

L'F
EXTERNAL FUNCTION (ARG1,ENGINE,SLEEVE)
I'R ENGINE, S, SLEEVE
B'N HAVEID, VOLUME, LACK.
V'S VCLEAR = 4.5610, 5.377, -0.
V'S RATIO = 16.69197512, 13.94055545, -0.
V'S DEL = .00533335856, 0.
V'S A = .25, .257292401
V'S B = .006666666667, 0.
V'S K1 = 183.4819679, 175.3861518
V'S K2 = 35.78470367, 34.79068412
V'S K3 = 143.1388147, 135.2184669
V'S K4 = .624560900, .607211986
E'O COMRAT.
W'R ENGINE .E. $ATAC$
S = 0
O'R ENGINE .E. $LIST$ .AND. SLEEVE .E. $NO.I$
S = 1
O'E
S = 2
E'L
HAVEID = S .NE. 2
ARG1 = VCLEAR(S)
F'N RATIO(S)
E'O CYLGRA.
VOLUME = 0B
E'O CYLVOL.
ALPHA = ARG1
W'R HAVEID .AND. .NOT. LACK.(ALPHA)
ALPHA = .01745329252*ALPHA - DEL(S)
SALPHA = SIN.(ALPHA)
CALPHA = COS.(ALPHA)
SBETA = A(S)*SALPHA + B(S)
CBETA = SORT.(1. - SBETA*SBETA)
W'R VOLUME
ANSWER = K1(S) - K2(S)*CALPHA - K3(S)*CBETA
O'E
ANSWER = - K4(S)*(SALPHA + CALPHA*SBETA/CBETA)
E'L
O'E
ANSWER = - 0.
E'L
VOLUME = 1B
F'N ANSWER
E'N

```

Computer Program 11

Title: Cylinder Gas Properties

Purpose: To calculate the compressibility factor, temperature, and density of the gas, using the Beatti-Bridgeman equation of state.

Input:

1. Cylinder gas pressure and density, in order to calculate the average gas temperature.
2. Cylinder gas pressure and temperature, in order to calculate the gas density.

Procedure:

1. To estimate the gas temperature at any crank angle, from the measured pressure, mass and cylinder volume, by using the perfect gas law.
2. To use the above estimated temperature to calculate the compressibility factor as obtained from the "Beatti-Bridgeman Equation"

$$P = \rho RT(1-\epsilon)(1+B\rho) - A\rho^2$$

where:

P = absolute cylinder pressure in psia

ρ = mass density in lbm/ft^3

R = gas constant

T = gas temperature in degrees Rankine

$$\epsilon = C\rho/T^3$$

$$B = B_0(1-b\rho)$$

$$A = A_0(1-a\rho)$$

The constants for dry air are obtained from "Fundamentals of Classical Thermodynamics" by G. J. Van Wylen, and Richard E. Sonntag, John Wiley and Sons, Inc. New York, 1964, and converted to the British system as follows:

$$C = 14.0 \times 10^4$$

$$B_o = 0.02550$$

$$b = -0.0006089$$

$$A_o = 5.8483$$

$$a = 0.01068$$

$$R^* \text{ for shop air} = 0.371110 \text{ psi}/(\text{lbm}/\text{ft}^3)^\circ\text{R}$$

The value of Z from the above equation is as follows:

$$Z = \left(1 - \frac{C\rho}{T^3}\right) \left(1 + (B_o - B_o b\rho)\rho\right) - (A_o - A_o a\rho) \frac{\rho}{RT}$$

3. To use the above calculated compressibility factor to check temperature calculated in step 1.
4. To iterate the above steps until the final gas temperature calculated fulfills the Beatti-Bridgeman equation

List of Assisting Programs:

1. Program to check for missing data (LACK)

*The shop air is supplied at 98 psig and 80°F and assumed saturated with water pressure of 0.5 psi, i.e. water mole fraction of 0.004454. The correction due to water vapor is 0.2%

Computer Program 11

Cylinder Gas Properties (BBCFAC, BBRAN, BBFAR, BBLFT3)

```

L'F
EXTERNAL FUNCTION (ARG1,ARG2,RGAS)
R'N LACK3., FAREN
E'0 BBCFAC.
D = ARG1
T = ARG2
R = RGAS
W'R LACK3.(D,T,R), T'0 NOGOOD
COMFAC.
ANSWER = Z
T'0 RETURN
E'0 BBLFT3.
T = ARG1
P = ARG2
R = RGAS
W'R LACK3.(T,P,R), T'0 NOGOOD
T = T + 459.69
DIDEAL = P/R/T
D = DIDEAL
COMFAC.
DNEXT ZLAST = Z
D = DIDEAL/ZLAST
COMFAC.
W'R .ABS.(Z - ZLAST) .G. 2E-8, T'0 DNEXT
ANSWER = D
T'0 RETURN
E'0 BBRAN.
FAREN = 0B
T'0 SKIP
E'0 BBFAR.
FAREN = 1B
SKIP P = ARG1
D = ARG2
R = RGAS
W'R LACK3.(P,D,R), T'0 NOGOOD
TIDEAL = P/D/R
T = TIDEAL
COMFAC.
TNEXT ZLAST = Z
T = TIDEAL/ZLAST
COMFAC.
W'R .ABS.(Z - ZLAST) .G. 2E-8, T'0 TNEXT
W'R FAREN, T = T - 459.69
ANSWER = T
T'0 RETURN
NOGOOD ANSWER = - 0.
RETURN F'N ANSWER
I'N COMFAC.
Z = (1. - 14.0E4*D/T/T/T)*(1. + (.02550 + .00001553*D)*D) -
1 (5.8483 - .06245*D)*D/R/T
F'N
E'N
E'N

```

Computer Program 12

Title: Title Printing (TITLE)

Purpose: To print a title and read specifications to be used by other programs.

Input:

1. Required title
2. Specifications

Procedure:

The title and specifications are read according to a certain format and the title is printed according to another format.

Computer Program 12

Title Printing (TITLE)

MAU (17 MAY 1967 VERSION) PROGRAM LISTING

TITLE.

```
EXTERNAL FUNCTION TITLE.(JOB, SPEC)
DIMENSION ID(3), REMARK(19)
BOOLEAN START, JOB, SPEC
NORMAL MODE IS INTEGER
WHENEVER START
START = 08
VECTOR VALUES ID = 1
ID(1) = S8.(0)
TODAY.(ID(2), ID(3))
ID(2) = ID(2) .LS. 18 .V. ID(2) .RS. 24 .V. $000 00$
OR WHENEVER JOB
ID = ID + 1
END OF CONDITIONAL
PRINT FORMAT $1H/1H-S16,98HDIESEL ENGINE IGNITION AND COMBUSTION: JA
1 Y A. BOLT, N. A. HENEIN: COMPUTER PROGRAM BY A. SNIVELY/88H
2 ARMY CONTRACT NO. DA-20-018-AMC-1669T: ORA PROJECT 06720: C
3 OMPUTER PROJECT NO. S986F:13,8H OF JOB C6,15H: COMPUTED ON C
4 6,1H,C5*$, ID...ID(3)
LINE = 8
WHENEVER SPEC
READ FORMAT $19C4,C3,I1*$, SPEC...SPEC(19), MORE
WHENEVER MORE .G. 0
READ FORMAT $11,19C4,C3*$, SPACE, REMARK...REMARK(19)
HEAD = CARCON(SPACE)
VECTOR VALUES CARCON = $1H+$/, $1H $, $1H0$, $1H-$, $1H-/1H$
VECTOR VALUES HEAD(1) = $ $26,19C4,C3*$
PRINT FORMAT HEAD, REMARK...REMARK(19)
LINE = LINE + SPACE
MORE = MORE - 1
TRANSFER TO AGAIN
END OF CONDITIONAL
END OF CONDITIONAL
FUNCTION RETURN LINE
END OF FUNCTION
```

AGAIN

Computer Program 13

Title: Fuel Properties

FULPRO (FUEL, HTOC, HETVAL)
FULDEN (FUEL, FAREN)
FULFLO (WEIGHT, MINUTS, LEAK)

Purpose:

FULPRO, to compute fuel properties
FULDEN, to compute fuel density
FULFLO, to compute rate of fuel flow

Usage:

A call on FULPRO, or FULDEN, must come first

Arguments:

FUEL = fuel identification (4 letter BCD)
HTDC = H/C atom ratio
HETVAL = heating value in Btu/lbm
FULPRO = fuel density at 60° F in lbm/ft³
FAREN = fuel temperature in °F
FULDEN = fuel density in lbm/ft³
WEIGHT = timer weight identification (1 letter BCD)
MINUTS = fuel consumption time in min
LEAK = fuel leakage in liters/hr
FULFLO = rate of fuel flow in lbm/hr

Formulas:

$\rho_{60^\circ} = 8824.90 / (\text{API} + 131.5)$, $\rho = \rho_{60^\circ \text{F}} - \Delta x (t - 60)$
flow = LBM x 60/MINUTS - .03531542 x LEAK x $\rho_{80^\circ \text{F}}$

Constants:

<u>FUEL</u>	<u>HTOC</u>	<u>HETVAL</u>	<u>API</u>	<u>Δ</u>	<u>WEIGHT</u>	<u>LBM</u>
\$SHOP\$	1.837	18370	34.79	.0235	\$A\$.06262
\$NO.2\$	1.827	18500	39.51	.0239	\$B\$.12667
\$MILG\$	2.141	18905	60.89	.0247	\$C\$.25247
\$CT13\$	1.992	18705	49.37	.0252	\$D\$.5007
\$CT19\$	1.999	18700	49.2	.0252	\$E\$.9985
					\$F\$.006262

Fuel Properties (FULHCR, FULDEN, FULFLO)

MAD (17 MAY 1967 VERSION) PROGRAM LISTING

FULHCR, FULDEN, FULFLO.

EXTERNAL FUNCTION(ID,VALUE1,VALUE2)

INTEGER S, ID

BOOLEAN LACK., LACK2., NOFUEL

VECTOR VALUES FUEL = \$SHOP\$, \$NO.2\$, \$MILG\$, \$CT13\$, \$CT19\$

VECTOR VALUES API = 34.79, 39.51, 60.89, 49.37, 49.2

VECTOR VALUES T50 = 374., 516., 220., 370., 342.

VECTOR VALUES DEL = .0235, .0239, .0247, .0252, .0252

VECTOR VALUES LBM = 3.7572, 7.6002, 15.1482, 30.042, 59.910, .37572

ENTRY TO FULHCR.

FINDS.

FUNCTION RETURN (1.5*API(S) - T50(S)/20. + 47.)P..3333333333/2.3498

ENTRY TO FULDEN.

FINDS.

WHENEVER LACK.(VALUE1), TRANSFER TO ERRORS

FUNCTION RETURN DEN60 - DEL(S)*(VALUE1 - 60.)

ENTRY TO FULFLO.

WHENEVER LACK2.(VALUE1,VALUE2) .OR. NOFUEL, TRANSFER TO ERRORS

S = ID .RS. 30 - 17

WHENEVER S .G. - 1 .AND. S .L. 6

ANSWER = LBM(S)/VALUE1 - VALUE2*DEN80

OTHERWISE

ERRORS

ANSWER = - 0.

END OF CONDITIONAL

FUNCTION RETURN ANSWER

INTERNAL FUNCTION FINDS.

NOFUEL = 0B

FUELS

THROUGH FUELS, FOR S = 0, 1, NOFUEL .OR. ID .E. FUEL(S)

NOFUEL = S .G. 4

WHENEVER NOFUEL, TRANSFER TO ERRORS

DEN60 = 8824.90/(API(S) + 131.5)

DEN80 = .03531542*(DEN60 - 20.*DEL(S))

FUNCTION RETURN

END OF FUNCTION

END OF FUNCTION

Computer Program 14

Title: Coolant and Oil Properties

COLID (FAREN, ID)
COLNU (FAREN)
COLCP (FAREN)
COLDEN (FAREN)
OILID (FAREN, ID)
OILCP (FAREN)
OILDEN (FAREN)

Purpose:

COLID, OILID to find identification of coolant and oil respectively
COLNU, to find coolant kinematic viscosity
COLCP, OILCP to find specific heat for coolant and oil respectively
COLDEN, OILDEN to find density of coolant and oil respectively.

Usage:

A call on COLID must come before a call on COLNU or COLCP or COLDEN.
A call on OILID must come before a call on OILCP or OILDEN

Arguments:

FAREN = temperature in °F
ID = identification of coolant or oil. \$EGLY\$ for ethelene glycol
 \$MDV3\$ for present oil DELVAC 1330
COLNU = coolant kinematic viscosity in centistokes
COLCP = coolant specific heat in Btu/lbm
COLDEN = coolant density in lbm/ft³
OILCP = oil specific heat in Btu/lbm
OILDEN = oil density in lbm/ft³
ARG1 = 1 if proper identification was used, = -0, if wrong identification,
 to be used by LACK.

Formulas:

For kinematic viscosity ν , $\ln(\nu+0.6) = A \ln(FAREN+459.69) + B$
For specific heat CP, $CP = C + D * FAREN$
For density ρ , $\rho = E + F * FAREN$

Constants:

ID	A	B	C	D	E	F
\$EGLY\$	-4.782178	31.144543	.518953	.0006237276	72.546342	-.0253698
\$MDV3\$	---	---	.540	.000	56.694196	-.0200661

Computer Program 14

Coolant and Oil Properties (COLID, OILID, COLDEN, OILDEN, COLCP, OILCP, COLNU)

MAD (17 MAY 1967 VERSION) PROGRAM LISTING

COOLANT AND OIL PROPERTIES

```

EXTERNAL FUNCTION(ARG1, ID)
INTEGER ID, COL, OIL, S
BOOLEAN HAVCOL, HAVOIL, COOLER, NU, CP, LACK.
VFCOR VALUES A = -4.782178, 31.144543, .518933, .54, .0006237276, .0,
1 72.546342, 56.694196, -.0253698, -.0200661
VECTOR VALUES HAVCOL = 0B
VECTOR VALUES HAVOIL = 0B
ENTRY TO COLID.
WHENEVER ID .E. $EGLY$
COL = 0
OTHERWISE
COL = 1
END OF CONDITIONAL
HAVCOL = COL .NE. 1
FUNCTION RETURN
ENTRY TO OILID.
WHENEVER ID .E. $MDV3$
OIL = 1
ARG1 = 1.
OTHERWISE
OIL = 2
ARG1 = -0.
END OF CONDITIONAL
HAVOIL = OIL .NE. 2
FUNCTION RETURN
ENTRY TO COLNU.
COOLER = 1B
NU = 1B
TRANSFER TO BEGIN2
ENTRY TO COLCP.
COOLER = 1B
TRANSFER TO SPHEAT
ENTRY TO OILCP.
COOLER = 0B
SPHEAT
CP = 1B
TRANSFER TO BEGIN1
ENTRY TO COLDEN.
COOLER = 1B
TRANSFER TO DENSTY
ENTRY TO OILDEN.
COOLER = 0B
DENSTY
CP = 0B
BEGIN1
NU = 0B
BEGIN2
T = ARG1
WHENEVER (COOLER .AND. HAVCOL .OR. .NOT. COOLER .AND. HAVOIL)
1 .AND. .NOT. LACK.(T)
WHENEVER COOLER
S = COL
OTHERWISE
S = OIL
END OF CONDITIONAL
WHENEVER NU
ANSWER = EXP.(EXP.(A(S)*ELDG.(T + 459.69) + A(S+1))) - .6
TRANSFER TO END
OR WHENEVER CP
S = S + 2
OTHERWISE
S = S + 6
END OF CONDITIONAL
ANSWER = A(S) + A(S+2)*T
OTHERWISE
ANSWER = -0.
END OF CONDITIONAL
FUNCTION RETURN ANSWER
END OF FUNCTION
END
    
```

Computer Program 15

Title: Integral Mean Value of Given Data

MEAN (N, VALUES, STORE)

Purpose: To calculate the integral mean of a sequence

Arguments:

N = no of values (integer)

VALUES = sequence of values

STORE = region to store D0, D1, D2, D3, D4

MEAN = integral mean

Computer Program 15

Calculation of the Integral Mean Value of Given Data (MEAN)

HAD (17 MAY 1967 VERSION) PROGRAM LISTING

MEAN.

```
EXTERNAL FUNCTION MEAN.(N,VALUES,STORE)
NORMAL MODE IS INTEGER
FLOATING POINT INTDER., TO
NUMBER = N
BGN2 = NUMBER + NUMBER
BGN3 = BGN2 + NUMBER
BGN4 = BGN3 + NUMBER
DB4T11.(NUMBER,1.,1,VALUES,STORE,STORE(NUMBER),STORE(BGN2),
1 STORE(BGN3),STORE(BGN4))
TO = NUMBER - 1
FUNCTION RETURN INTDER.(0.,TO,0.,NUMBER,1.,1,VALUES,STORE(NUMBER),
1 STORE(BGN2),STORE(BGN3),STORE(BGN4))/TO
END OF FUNCTION
```

Computer Program 16

Title: Interpolating Program and Successive use of DB4T11 for Curve Fitting
(INTERP), (USEDDB4)

Purpose:

1. INTERP to give an interpolated value between data points
2. USEDDB4 to use DB4T11 as many times as needed

Procedure:

A library subroutine is used for interpolating and an iterative use of DB4T11 is used for USEDDB4.

Computer Program 16

Interpolation (INTERP)

MAD (06 JAN 1967 VERSION) PROGRAM LISTING

USED84, , INTERP,

EXTERNAL FUNCTION (N,X,ADD,DATA,BEST,NUMDB4)
 INTEGER NUMDB4, N, NUMDAT, ADD, NUMINT, I, NUMBER, STOPAT

ENTRY TO USED84.

WHENEVER NUMDB4 .G. 0

NUMDAT = N

DEL = X

NUMINT = ADD

DB4T11.(NUMDAT,DEL,NUMINT,DATA,BEST,BEST,BEST,BEST,BEST)

THROUGH MORDB4, FOR I = 2, 1, I .G. NUMDB4

MORDB4 DB4T11.(NUMDAT,DEL,NUMINT,BEST,BEST,BEST,BEST,BEST,BEST)

FUNCTION RETURN

OTHERWISE

ERROR RETURN

END OF CONDITIONAL

ENTRY TO INTERP.

NUMINT = ADD

WHENEVER NUMINT .G. 1

NUMDAT = N

NUMBER = (NUMDAT - 1)*NUMINT

THROUGH USETAB, FOR I = 1, 1, I .G. NUMBER

STOPAT = I + NUMINT - 2

THROUGH USETAB, FOR I = 1, 1, I .G. STOPAT

USETAB DATA(I) = TAB.(X(I),X,DATA,NUMINT,NUMINT,5,NUMDAT,1.)

END OF CONDITIONAL

FUNCTION RETURN

END OF FUNCTION

Computer Program 17

Title: Air Flow Rate

AIRFLO (ORF, TORF, PORF, PBAR, PINLET)

Purpose: To calculate rate of air flow

Arguments:

ORF = identification of orifice combination (1 letter BCD)
 TORF = upstream temperature (before orifice) in °F
 PROF = upstream pressure (before orifice) in psig
 PBAR = barometric pressure in in. Hg
 PINLET = pressure after orifice in in. Hg gauge
 AIRFLO = air flow in lbm/hr

Formula:

$$\text{air flow} = B \frac{(\text{upstream pressure in psia} - \text{DEL})}{\sqrt{\text{upstream temperature in } ^\circ\text{R}}}$$

Constants:

<u>ORF</u>	<u>B</u>	<u>DEL</u>
\$1\$ ≡ #1	4.214	1.20
\$2\$ ≡ #2	8.255	0
\$3\$ ≡ #3	17.063	0
\$4\$ ≡ #4	32.642	0
\$5\$ ≡ #5	67.45	0
\$6\$ ≡ #5 and #1	71.67	.070
\$7\$ ≡ #5 and #2	75.71	0
\$8\$ ≡ #5 and #3	84.52	0
\$9\$ ≡ #5 and #4	100.10	0
\$A\$ ≡ 3/32	12.766	1.72
\$B\$ ≡ 1/8	23.229	1.61
\$C\$ ≡ 3/16	51.74	.96
\$D\$ ≡ 7/32	68.35	0
\$E\$ ≡ D and A	81.11	.270
\$F\$ ≡ D and B	91.58	.409
\$G\$ ≡ D and C	120.08	.413
\$H\$ ≡ D and C and A	132.85	.54
\$I\$ ≡ D and C and B	143.31	.61
\$J\$ ≡ D and C and B and A	156.08	.70

Computer Program 17

Air Flow Rate (AIRFLO)

MAD (17 MAY 1967 VERSION) PROGRAM LISTING

AIRFLO.

EXTERNAL FUNCTION AIRFLC.(GRF,TORF,PORF,PBAR,PINLET).

INTEGER ORF, S

BOOLEAN LACK4., LAST, ATAC

VECTOR VALUES B = 4.214, 8.255, 17.063, 32.642, 67.45, 71.67,

1 75.71, 84.52, 100.10, 12.766, 23.229, 51.74,

2 68.35, 81.11, 91.58, 120.08, 132.85, 143.31,

3 156.08

VECTOR VALUES DEL = 1.20, 0., 0., 0., 0., .070, 0., 0., 0.,

1 1.72, 1.61, .96, 0., .270, .409, .413, .54,

2 .61, .70

P = PORF

BAR = PBAR

WHENEVER LACK4.(TORF,P,BAR,PINLET), TRANSFER TO ERRORS

P = P + .4911570*BAR

WHENEVER P .L. .930*(PINLET + BAR), TRANSFER TO ERRORS

S = ORF .RS. 30 - 1

LAST = S .E. 32

ATAC = LAST .OR. S .G. 15 .AND. S .L. 25

WHENEVER ATAC

WHENEVER LAST

S = 18

OTHERWISE

S = S - 7

END OF CONDITIONAL

END OF CONDITIONAL

WHENEVER S .G. - 1 .AND. S .L. 9 .OR. ATAC

FLOW = B(S)*(P - DEL(S))/SQRT.(TORF + 459.69)

OTHERWISE

FLOW = -0.

END OF CONDITIONAL

FUNCTION RETURN FLOW

END OF FUNCTION

ERRORS

Computer Program 18

Title: Average Values and Errors

AVE (N, VALUES)
RMS (N, VALUES)
AVEERR (N, VALUES)

Purpose:

AVE, to find the arithmetic average of a sequence
RMS, to find the RMS average of a sequence
AVEERR, to find the standard deviation of a sequence

Arguments:

N = number of values (INTEGER)
VALUES = sequence of values
AVE = arithmetic average of the nonlacking
RMS = square root of the mean of squares of the nonlacking
standard deviation of the nonlacking
AVEERR = VALUES (N) = AVE
VALUES (N+1) = AVEERR

Computer Program 18

Average Values and Errors (AVEERR)

MAD (17 MAY 1967 VERSION) PROGRAM LISTING

AVE., RMS., AVEERR.

```

EXTERNAL FUNCTION (N,VALUES)
INTEGER N, LAST, GOOD, S
BOOLEAN RMSERR, SQUARE, LACK., OKAY
VECTOR VALUES RMSERR = 0B
ENTRY TO AVEERR.
RMSERR = 1B
TRANSFER TO SKIP1
ENTRY TO RMS.
SQUARE = 1B
TRANSFER TO SKIP2
ENTRY TO AVE.
SKIP1 SQUARE = 0B
SKIP2 LAST = N
BEGIN GOOD = LAST
ANS = - 0.
THROUGH SUM, FOR S = 0, 1, S .E. LAST
VAL = VALUES(S)
WHENEVER LACK.(VAL)
GOOD = GOOD - 1
OTHERWISE
WHENEVER SQUARE, VAL = VAL*VAL
ANS = ANS + VAL
SUM END OF CONDITIONAL
OKAY = GOOD .G. 0
WHENEVER OKAY
ANS = ANS/GOOD
WHENEVER SQUARE, ANS = SQRT.(ANS)
ANS = 0. + ANS
END OF CONDITIONAL
WHENEVER RMSERR
WHENEVER .NOT. SQUARE
VALUES(LAST) = ANS
WHENEVER .NOT. OKAY, TRANSFER TO ERRORS
MEAN = ANS
SQUARE = 1B
TRANSFER TO BEGIN
OTHERWISE
ERRORS ANS = SQRT.(.ABS. ((ANS - MEAN)*(ANS + MEAN)))
VALUES(LAST+1) = ANS
RMSERR = 0B
END OF CONDITIONAL
END OF CONDITIONAL
FUNCTION RETURN ANS
END OF FUNCTION

```

Computer Program 19

Title: Cylinder Wall Temperature from Millivolt Readings

THERMO (MVOLTS)

Purpose: To find the Farenheit temperature corresponding to a millivolt reading of an iron-constantan thermocouple with reference at 32°F.

Arguments:

MVOLTS = millivolt difference from reference

THERMO = temperature in °F

Formula:

DB4T11, was used on data from the West Instrument Corporation to find the following formula (good within $\pm .1^\circ\text{F}$ in the range from 32°F to 1015°F)

$$^\circ\text{F} = 528.7948 + 324.3723 \times (\Delta v) + 2.1981 \times (\Delta v)^2 + 1.4488 \times (\Delta v)^3 - 2.0224 \times (\Delta v)^4$$

where $\Delta v = (\text{millivolt} - 15)/10$.

Computer Program 19

Cylinder Wall Temperature from Millivolt Readings (THERMO)

MAD (11 MAY 1967 VERSION) PROGRAM LISTING

THERMO.

EXTERNAL FUNCTION THERMO.(MVOLTS)

BOOLEAN LACK.

MV = MVOLTS

WHENEVER LACK.(MV)

FAREN = - 0.

OTHERWISE

MV = (MV - 15.)/10.

FAREN = 528.7948 + MV*(324.3723 + MV*(2.1981 + MV*
1 (1.4488 - MV*2.0224)))

END OF CONDITIONAL

FUNCTION RETURN FAREN

END OF FUNCTION

Computer Program 20

Title: Check on Missing Data

LACK (VALUE1)
LACK2(VALUE1, VALUE2)
LACK3 (VALUE1, VALUE2, VALUE3)
LACK4 (VALUE1, VALUE2, VALUE3, VALUE4)
LACK5 (VALUE1, VALUE2, VALUE3, VALUE4, VALUE5)

Purpose: To test for lacking values (i.e., a value of -0).

Action:

Value of function = 1B if any arguments are lacking
= 0B otherwise (none lacking)

Computer Program 20

Check on Missing Data (LACK)

MAD (17 MAY 1967 VERSION) PROGRAM LISTING

```

LACK. , LACK2. , LACK3. , LACK4. , LACK5.
EXTERNAL FUNCTION (VALUE1,VALUE2,VALUE3,VALUE4,VALUE5)
DEFINE UNARY OPERATOR .LACKS., PRECEDENCE SAME AS .E.
MODE STRUCTURE 2 = .LACKS. 0
JMP      **18,AC,**1
JMP      **12,MQ,**1
JMP      **1,LA,**18
JMP      **1,BT,**8
LAS      =4K11
TRA      LOC+2
TRA      LOC+3
PXD      0,0
TRA      LOC+2
CLA      =1
OUT      AC
SLW      T
JMP      **8
JMP      **1,BT,**3
XCA
JMP      **6
STQ      T
JMP      **3
JMP      **2,BT,**1
STO      T
CLA      B
CAS      =4K11
TRA      LOC+2
TRA      LOC+3
PXD      0,0
TRA      LOC+2
CLA      =1
OUT      AC
END

ENTRY TO LACK5.
WHENEVER .NOT. .LACKS. VALUE5
ENTRY TO LACK4.
WHENEVER .NOT. .LACKS. VALUE4
ENTRY TO LACK3.
WHENEVER .NOT. .LACKS. VALUE3
ENTRY TO LACK2.
WHENEVER .NOT. .LACKS. VALUE2
ENTRY TO LACK.
FUNCTION RETURN .LACKS. VALUE1
END OF CONDITIONAL
END OF CONDITIONAL
END OF CONDITIONAL
END OF CONDITIONAL
FUNCTION RETURN IB
END OF FUNCTION

```

(THE NUMERIC FORM OF THE OPERATOR-MODE ARGUMENT IS 11400) M'E 2 = .LACKS. 0 003

Computer Program 21

Title: Rounding of Numbers

RNDOFF (VALUE, TD)
IROUND (VALUE)

Purpose:

RNDOFF, to find a round off of a value
IROUND, to find the nearest integer of a value

Arguments:

VALUE = value to be rounded
TD = precision of the round off (e.g. 1.0, .5, .1)
RNDOFF = rounded value
IROUND = nearest integer

Computer Program 21

Rounding of Numbers (IROUND)

NAD (17 MAY 1967 VERSION) PROGRAM LISTING

RNDOFF, IROUND.

EXTERNAL FUNCTION (VALUE,TO)

INTEGER WHOLE

BOCLEAN FLOAT

ENTRY TO RNDOFF.

FLCAT = 1B

RNDTO = .ABS. TO

TRANSFER TO SKIP

ENTRY TO IROUND.

FLCAT = 0B

RNDTO = 1.

ANSWER = VALUE

WHENEVER ANSWER .NE. 0.

WHOLE = ANSWER/RNDTO + .ABS. ANSWER/(ANSWER + ANSWER)

WHOLE = 0 + WHOLE

WHENEVER .NOT. FLOAT, FUNCTION RETURN WHOLE

ANSWER = WHOLE*RNDTO

END OF CONDITIONAL

FUNCTION RETURN ANSWER

END OF FUNCTION

SKIP

Computer Program 22

Title: Axes Plotting

AXIS (XO, YO, AXLTH, THETA, AXSCAL, HGTH, TITLE)

Purpose: To either plot an axis (with tic marks) (with or without numbering) or to plot a centered title or both/neither.

Arguments:

XO, YO = coordinates in in. of the beginning of the axis

AXLTH = magnitude is the length of the axis in in., if positive, it is plotted from beginning to end, if negative, it is plotted from end to beginning.

THETA = counterclockwise degrees inclination from horizontal

(0) = value of axis variable at beginning of axis

AXSCAL (1) = increase of axis variable per tic mark

(2) = in. per tic mark on axis

HGHT = magnitude is height of numbers and letters in in. if positive, they are above the axis, if negative, they are below the axis

(0) = 0 to delet axis

TITLE (D) = format for axis numbering (2-5 character BCD)

(1) = no. of characters in title (INTEGER)

(2)... = title to be plotted (BCD string)

Graphics:

Tic marks will be .075 in. on the side opposite title. Centerline of numbering will be HGHT from axis. Centerline of title will be 2.5*HGHT from axis. The numbering is centered about the 3rd position from left.

MAD (17 MAY 1967 VERSION) PROGRAM LISTING

AXIS.

```

EXTERNAL FUNCTION AXIS.(X0,Y0,AXLTH,THETA,AXSCAL,HGHT,TITLE)
INTEGER NUMDIV, TITLE, FMT, NCHAR, CENTER, I
BOOLEAN PLTAXI, PLTNMR, PLTBCD, BGNEND, LACK.
FMT = TITLE
PLTAXI = FMT .NE. 0
HEIGHT = HGHT
PLTNMR = HEIGHT .NE. 0.
WHENEVER PLTNMR
NCHAR = .ABS. TITLE(1)
PLTBCD = NCHAR .G. 0
OTHERWISE
PLTBCD = 0B
END OF CONDITIONAL
WHENEVER PLTAXI .GR. PLTBCD
LENGTH = AXLTH
DELREL = AXSCAL(1)
DELTIC = AXSCAL(2)
BGNEND = LENGTH .L. 0.
WHENEVER BGNEND
LENGTH = - LENGTH
DELREL = - DELREL
DELTIC = - DELTIC
END OF CONDITIONAL
DEGREE = THETA
RADIAN = DEGREE/57.29577951
SINE = SIN.(RADIAN)
COSINE = COS.(RADIAN)
XABS = X0
YABS = Y0
XEND = XABS + LENGTH*COSINE
YEND = YABS + LENGTH*SINE
NUMDIV = (LENGTH + .0001)/ .ABS. DELTIC
ABSHGT = .ABS. HEIGHT
WHENEVER PLTBCD
CENTER = (NUMDIV + 1)/2
XDEL = - (NCHAR/2)*.8571428571*ABSHGT
YDEL = 2.5*HEIGHT - .5*ABSHGT
XBCD = .5*(XABS + XEND) + XDEL*COSINE - YDEL*SINE
YBCD = .5*(YABS + YEND) + XDEL*SINE + YDEL*COSINE
END OF CONDITIONAL
WHENEVER PLTAXI
WHENEVER PLTNMR
XDEL = - 2.*ABSHGT
YDEL = HEIGHT - .5*ABSHGT
XNMR = XDEL*COSINE - YDEL*SINE
YNMR = XDEL*SINE + YDEL*COSINE
XREL = AXSCAL
FMT = FMT .RS. 6 .LS. 6 .V. $00000*$
END OF CONDITIONAL
XTIC = .075*SINE
YTIC = - .075*COSINE
WHENEVER LACK.(HEIGHT - HEIGHT)
XTIC = - XTIC

```

Computer Program 22 (Concluded)

```
YTIC = - YTIC
END OF CONDITIONAL
XDEL = DELTIC*COSINE
YDEL = DELTIC*SINE
I = 0
WHENEVER .NOT. BGNEND
PENUP.(XABS,YABS)
OTHERWISE
PENUP.(XEND,YEND)
NUMBER = NUMDIV
WHENEVER PLTNMR, XREL = XREL - NUMBER*DELREL
XABS = XABS - NUMBER*XDEL
YABS = YABS - NUMBER*YDEL
PENDN.(XABS,YABS)
END OF CONDITIONAL
PENDN.(XABS+XTIC,YABS+YTIC)
WHENEVER PLTNMR
PNUMBR.(XABS+XNMR,YABS+YNMR,ABSHGT,XREL,DEGREE,FMT)
XREL = XREL + DELREL
WHENEVER I .E. CENTER .AND. PLTBCD
PSYMB.(XBCD,YBCD,ABSHGT,TITLE(2),DEGREE,NCHAR)
PLTBCD = 08
END OF CONDITIONAL
END OF CONDITIONAL
PENUP.(XABS,YABS)
WHENEVER I .L. NUMDIV
I = I + 1
XABS = XABS + XDEL
YABS = YABS + YDEL
TRANSFER TO NXTDIV
END OF CONDITIONAL
WHENEVER .NOT. BGNEND, PENDN.(XEND,YEND)
OTHERWISE
PSYMB.(XBCD,YBCD,ABSHGT,TITLE(2),DEGREE,NCHAR)
END OF CONDITIONAL
END OF CONDITIONAL
FUNCTION RETURN
END OF FUNCTION
```

NXTDIV

Computer Program 23

Title: Curve Plotting

GRAPH (SCALES, XTITLE, YTITLE, TITLE)

Purpose: To prepare a graph for data plotting, including output media specifications, coordinate system quantification axes with respective titles and numbering at tic marks, and an overall title.

Arguments:

SCALES (0), (1), (2) = AXSCAL for X axis
(3), (4), (5) = AXSCAL for Y axis see
XTITLE = TITLE for X axis AXIS
YTITLE = TITLE for Y axis
TITLE (0) = no. of characters in overall title (INTEGER)
(1)...(N) = overall title (BCD string)

Graphics:

The axes are chosen to begin at (.65, .41) in. No. of X divisions are such as to use most of 14.000 in. No. of Y divisions are such as to use most of 10.333 in. The border with tic marks is completed on the other 2 sides. Numbering and lettering are done with a height of .13 in. TITLE is treated as a 2nd YTITLE. The above restrict XTITLE to 125 characters (23 words), YTITLE to 92 characters (18 words), TITLE to 92 characters (17 words).

Computer Program 23

Curve Plotting (GRAPH)

MAD (17 MAY 1967 VERSION) PROGRAM LISTING

GRAPH.

```
EXTERNAL FUNCTION GRAPH.(SCALES,XTITLE,YTITLE,TITLE)
VECTOR VALUES YFMT(1) = 0
INTEGER NUMDIV, NCHAR, YTITLE, TITLE
PLTPAP.($400$)
PLTXMX.(14.90)
XTIC = SCALES(2)
YTIC = SCALES(5)
PLTOFS.(SCALES,SCALES(1)/XTIC,SCALES(3),SCALES(4)/YTIC,.65,
.41)
NUMDIV = 14.0001/XTIC
XLTH = NUMDIV*XTIC
NUMDIV = 10.3334/YTIC
YLTH = NUMDIV*YTIC
YFMT = YTITLE
AXIS(.65,.41,XLTH,0.,SCALES,-.13,XTITLE)
AXIS.(XLTH+.65,.41,YLTH,90.,SCALES(3),-.13,YFMT)
AXIS(.65,YLTH+.41,-XLTH,0.,SCALES,0.,XTITLE)
AXIS(.65,.41,-YLTH,90.,SCALES(3),.13,YTITLE)
NCHAR = TITLE
WHENEVER NCHAR .G. 0, PSYMB.(.195,.41+YLTH/2.-(NCHAR/2)*
.1114285714,.13,TITLE(1),90.,NCHAR)

FUNCTION RETURN
END OF FUNCTION
```

Computer Program 24

Title: Results Punching (PUNCH)

Purpose: To punch a given sequence of points according to a given format.

Input: Sequence of values that are required to be punched.

Computer Program 24

Results Punching (PUNCH)

MAD (17 MAY 1967 VERSION) PROGRAM LISTING

PUNCH.

```
EXTERNAL FUNCTION PUNCH.(RUN, ID, BEFORE, N, ADD, VALUES)
NORMAL MODE IS INTEGER
FORMAT VARIABLE FV
ADDS = ADD
ADDTEN = 10*ADDS
IEND = N*ADDS
FV = 7 - BEFORE
PUNCH FORMAT $I4, I2, C4, 'FV'P10F7*$,
1  (I = 0, ADDTEN, I .GE. IEND, RUN, CARD.(I), ID,
2  (J = I, ADDS, J .E. JEND, VALUES(J)))
FUNCTION RETURN
INTERNAL FUNCTION CARD.
JEND = I + ADDTEN
WHENEVER JEND .G. IEND, JEND = IEND
FUNCTION RETURN 1 + I/ADDTEN
END OF FUNCTION
END OF FUNCTION
```

APPENDIX B

TABLES

TABLE 1

EFFECT OF ENGINE SPEED ON IGNITION DELAY USING CITE FUEL AT A MEAN PRESSURE OF 500 PSIA DURING THE IGNITION DELAY

DATA SET A4A HAS		5 RUNS. THE ATAC ENGINE (SLEEVE, IVC @ 128 DBTDC) USEC CITE FUEL (200C PSI), MDV3 OIL, AND H2C COOLANT.																			
FCR USE	SPEED	LOAD	FUEL	AIR	BLOW	ROOM-SURGE-@	INJ-RIS	DBTDC	AT START OF	AIR	MILLVCLTS	EXHAUST									
W O	RPM	LBS	MIN/L/HR	PSIG	F	CFPM	INHG	INHG	PSI	PSI	LIFT	RISE	ILLUM	F	MIN	INC	F	PU			
71	C	1700	21.8	8.17	.18	34.0	75	.6	28.9	10.7	3.1	436	213	20.7	11.3	9.4	96	-.C	-.00	622	14
72	C	1500	17.8	5.96	.30	51.2	73	.6	29.1	6.8	3.3	401	276	21.0	8.3	6.0	51	-.0	-.00	657	49
73	C	2000	13.1	5.01	.27	66.6	76	.8	29.2	3.6	4.0	386	312	20.5	5.1	2.6	54	-.0	-.00	691	51
74	E	2400	11.0	9.12	.29	51.5	76	.8	29.1	1.5	2.9	360	316	21.4	2.3	-.C	52	-.0	-.00	699	52
70	D	2800	9.5	3.73	.25	57.6	78	-.C	29.3	.0	2.7	360	288	20.5	1.2	-.C	51	-.0	-.00	746	-.0
MEAN		1940	14.6	6.40	.26	52.2	76	.7	29.1	4.5	3.2	389	281	20.5	5.9	6.0	52	-.0	-.00	683	42
ERRS		637	4.5	1.95	.04	10.7	2	.1	3.8	.4	28	37	.3	3.6	2.8		2	-.C	-.00	42	16

FCR	CRANKCASE	OILS	COOLANT	SYSTEM	CYL	HD	WALL	TEMP		
RUN	CUI(F)	INC	CPS	OUT(F)	INC	INHG	INT.	(F)	EXH.	(F)
71	-.C	-.C	-.C	168.0	-.C	-.C	-.C	-.C	-.C	-.C
72	-.C	-.C	-.C	171.0	-.C	-.C	-.C	-.C	-.C	-.C
73	-.C	-.C	-.C	172.0	-.C	-.C	-.C	-.C	-.C	-.C
74	-.C	-.C	-.C	171.0	-.C	-.C	-.C	-.C	-.C	-.C
70	-.C	-.C	-.C	170.0	-.C	-.C	-.C	-.C	-.C	-.C
MEAN	-.C	-.C	-.C	170.4	-.C	-.C	-.C	-.C	-.C	-.C
ERRS	-.C	-.C	-.C	1.4	-.C	-.C	-.C	-.C	-.C	-.C

ENGINE WITH 16.69/1 RATIO HAS 4.5610 CUIIN CLEARANCE. FUEL WITH 1.999/1 RATIO HAS 48.84 LBM/CUFT (@6C) AND LIBEFATES 18700 BTU/LBM.																						
FCR	ERAKE	BMEP	RSEC	FUEL/	CYCLE(LBM/1000)	SURGE	EFF	ATVC	AT START OF	INJECTION	AVERAGE	DURING	DELAY	DELAY(MSEC)	WALL(F)							
RUN	HP	PSI	#/HRHP	AIR	BLOW	EXH	PSIA	PCI	F	INDEX	PSIA	#/CUFT	R	INDEX	PSIA	#/CUFT	R	RISE	ILLUM	MIN	INC	
71	7.3	80.4	.454	.0319	3.52	.08	12	19.4	90.2	170	1.387	455	.847	1441	1.192	563	1.006	1488	1.567	1.883	-.C	-.0
72	8.9	65.7	.509	.0313	3.21	.05	11	17.6	89.5	182	1.350	422	.763	1473	1.234	555	.958	1549	1.411	1.667	-.0	-.0
73	8.7	48.3	.634	.0310	2.98	.05	05	16.1	91.7	206	1.388	406	.709	1526	1.227	567	.930	1619	1.317	1.525	-.C	-.0
74	8.8	40.6	.650	.0313	2.70	.05	05	15.0	88.5	195	1.420	378	.631	1598	1.204	547	.856	1696	1.257	-.000	-.C	-.0
70	8.9	35.0	.860	.0359	2.53	-.00	08	14.4	86.6	208	1.419	377	.610	1649	1.169	541	.820	1733	1.145	-.000	-.C	-.0
MEAN	8.5	54.0	.621	.0323	2.99	.06	10	16.5	89.5	192	1.401	408	.712	1537	1.205	555	.916	1617	1.340	1.692	-.C	-.0
ERRS	.6	16.8	.141	.0019	.36	.01	.01	1.8	1.7	14	.015	30	.087	77	.024	10	.065	50	.142	.147	-.C	-.0

TABLE 2

EFFECT OF ENGINE SPEED ON IGNITION DELAY USING CITE FUEL AT A MEAN PRESSURE OF 700 PSIA DURING THE IGNITION DELAY

DATA SET A4B HAS		5 RUNS. THE ATAC ENGINE (SLEEVE, IVC @ 128 DBTDC) USEC C115 FUEL (300C PSI), MDV3 OIL, AND EGLY COOLANT.																			
FOR USE	SPEED LOAD	FUEL	AIR	BLOW	ROOM-SURGE-@IVC-@INJ-RIS	DBTDC AT START OF	AIR MILLVCLTS	EXHAUST													
RUN W O	RPM	LBS MIN L/HR	PSIG	F CFPM	INHG	INHG	PSI	PSI	LIFT	RISE	ILLUM	F	MIN	INC	F	HU					
86	C	1000	27.6	5.74	25	48.5	76	7	29.3	22.9	1.1	552	212	20.8	13.6	-0.0	56	12.1	1.13	769	72
87	E	1500	26.6	8.54	57	73.0	81	7	29.3	15.7	1.0	532	276	20.8	11.0	-0.0	56	13.4	1.15	813	40
88	E	2000	22.9	6.95	60	67.5	75	7	29.2	15.1	1.0	513	340	20.8	8.0	-0.0	55	14.3	1.01	843	48
89	E	2500	18.8	5.82	79	67.1	80	7	29.3	12.7	1.0	513	363	20.5	5.8	-0.0	52	14.3	.82	873	52
90	E	2899	13.9	5.52	80	72.2	82	5	29.1	10.6	3.0	477	370	21.0	5.1	-0.0	101	14.4	.40	931	60
MEAN		1980	22.0	6.51	86	65.7	80	7	29.2	16.0	1.4	517	312	20.8	8.7	-0.0	56	13.7	.90	850	54
ERRS		679	5.1	1.13	11	8.9	2	1	4.4	.8	25	60	.2	3.2	-0.0			.28	.49	11	

FOR CRANKCASE OILS		COOLANT SYSTEM		CYL HD WALL TEMP				
RUN	OUT(F) INC CPS	OUT(F) INC	INHG	INT.(F)	EXH.(F)			
86	178.3	2.2	49	178.8	7.0	.8	269.2	325.9
87	195.3	2.2	55	176.7	5.4	2.0	264.0	336.3
88	205.2	2.2	60	176.2	4.3	3.7	264.9	350.1
89	207.1	4.9	67	175.9	4.1	5.5	268.5	351.8
90	211.1	7.8	80	171.5	2.5	8.3	270.7	360.8
MEAN	199.4	3.9	62	175.8	4.7	4.1	267.5	345.0
ERRS	11.6	2.2	11	2.4	1.5	2.7	2.6	12.3

ENGINE WITH 16.69/1 RATIO HAS 4.5610 CUIV CLEARANCE. FUEL WITH 1.999/1 RATIO HAS 48.84 LBM/CUFT (@60) AND LIBEFATES 18700 BTU/LBM.																						
FOR BRAKE	BMEP	PSFC	FUEL/	CYCLE(LBM/1000)	SURGE	EFF	3IVC	AT START OF	INJECTION	AVERAGE	CURING	DELAY	DELAY(MSEC)	WALL(F)								
RUN	HP	PSI	#/HRHP	AIR	AIR	BLOW	EXH	PSIA	PCT	F	INDEX	PSIA	#/CUFT	R	RISE	ILLUM	MIN	INC				
86	9.2	101.8	4.67	.0310	4.61	.09	14	25.6	89.6	113	1.418	575	1.101	1395	1.225	682	1.255	1436	1.200	-0.000	435	37
87	13.3	98.1	4.54	.0314	4.27	.06	12	23.6	50.2	109	1.439	557	1.019	1450	1.209	651	1.219	1503	1.085	-0.000	477	37
88	15.3	84.5	4.58	.0315	4.02	.05	11	21.8	51.7	101	1.457	536	.956	1488	1.203	705	1.200	1555	1.067	-0.000	506	33
89	15.7	69.4	4.71	.0315	3.78	.04	10	20.6	50.7	107	1.472	535	.910	1561	1.177	721	1.171	1630	.980	-0.000	506	27
90	13.4	51.3	4.70	.0316	3.46	.04	05	19.5	89.0	185	1.434	499	.816	1628	1.181	651	1.072	1707	.914	-0.000	505	13
MEAN	13.4	81.0	4.53	.0314	4.03	.06	11	22.2	90.2	123	1.444	541	.960	1504	1.159	658	1.184	1566	1.050	-0.000	487	29
ERRS	2.3	18.8	0.93	0.002	.40	.02	.32	2.2	.9	31	.019	26	.056	82	.018	14	.063	.95	.698	-0.000	28	9

FOR CRANKCASE OILS		COOLANT SYSTEM				
RUN	GPM	BTU/SEC	%	GPM	BTU/SEC	%
86	3.45	.5	2.2	6.0	4.0	18.1
87	3.91	.5	1.7	8.9	4.6	14.6
88	4.27	.6	1.5	11.8	4.8	12.3
89	4.77	1.5	3.2	14.7	5.8	12.4
90	5.69	2.8	5.7	17.4	4.1	8.4
MEAN	4.43	1.2	2.9	11.8	4.7	13.1
ERRS	.76	.9	1.5	4.0	.6	3.2

TABLE 3

EFFECT OF COOLANT TEMPERATURE ON IGNITION DELAY

DATA SET A5A HAS		8 RUNS. THE ATAC ENGINE (SLEEVE, IVC @ 128 DBTOC) USED C115 FUEL (3000 PSI), MDV3 OIL, AND EGLY COOLANT.																				
FOR USE	SPEC L	LOAD	FUEL	AIR	BLOW	ROOM-	ROOM-	ROOM-	DBTCC	AT	START	CF	AIR	MILLVCLTS	EXHAUST							
RUN W/O	RPM	LBS	MIN/L/HR	PSIG	F	CFPM	INHG	INHG	PSI	PSI	PSI	LIFT	RISE	ILLUM	F	MIN	INC	F	HU			
75	E	2002	27.6	5.65	76	71.0	75	28.9	40.2	7.5	778	338	21.0	12.8	-0	253	-C	-00	846	60		
76	E	2002	26.5	5.66	81	76.8	76	1.0	28.9	40.2	5.9	774	342	21.0	12.8	-0	255	-C	-00	840	55	
80	E	2006	28.3	5.53	84	71.4	85	1.0	29.3	40.1	6.8	780	338	21.0	13.0	-0	253	-C	-00	905	56	
78	E	2100	27.2	5.50	88	71.4	84	1.0	29.3	39.9	6.8	774	341	21.1	13.0	-0	252	-C	-00	902	54	
78	E	2000	27.1	5.52	90	71.1	84	1.0	29.2	40.2	8.7	774	333	20.9	12.9	-0	255	-C	-00	913	58	
77	E	2000	24.4	5.34	91	70.5	84	1.0	29.2	40.2	8.2	782	333	20.9	12.7	-0	257	-C	-00	921	74	
81	E	1999	28.9	5.51	92	71.1	79	1.0	29.4	40.0	8.4	780	350	21.0	12.5	-0	253	-C	-00	950	48	
82		-0	22.8	-00	95	-0	-0	0.5	-0	-0	-0	-0	-0	-0	-0	-0	-0	-0	-0	-0	66	
MEAN		2000	26.6	5.56	87	71.1	81	1.0	29.2	40.1	7.5	775	340	21.0	12.8	-0	254	-C	-00	857	55	
ERRS		1	1.9	0.6	0.6	0.2	4	0.1	0.2	0.1	0.9	7	5	0.1	0.2	-0	0	0	0	0	37	7

FOR CRANKCASE C115		COOLANT SYSTEM				CYL		FD		WALL		TEMP	
RUN	QU(1F)	INC	CP5	QU(1F)	INC	INHG	INI.(F)	EXH.(F)	EXH.(F)	EXH.(F)	EXH.(F)	EXH.(F)	EXH.(F)
75	192.5	3.5	72	156.6	6.6	3.7	-0	-0	-0	-0	-0	-0	-0
76	189.3	3.1	73	187.0	6.0	3.8	-0	-0	-0	-0	-0	-0	-0
80	205.6	4.0	73	217.0	5.6	3.5	-0	-0	-0	-0	-0	-0	-0
78	208.5	4.4	73	246.0	4.8	3.6	-0	-0	-0	-0	-0	-0	-0
78	209.0	6.0	77	276.1	4.7	3.6	-0	-0	-0	-0	-0	-0	-0
77	210.5	7.1	76	304.3	2.9	3.5	-0	-0	-0	-0	-0	-0	-0
81	211.8	7.7	75	305.0	3.3	3.5	-0	-0	-0	-0	-0	-0	-0
82	-0	-0	-0	-0	-0	-0	-0	-0	-0	-0	-0	-0	-0
MEAN	205.1	5.1	74	241.7	4.8	3.7	-0	-0	-0	-0	-0	-0	-0
ERRS	6.4	1.7	2	53.4	1.3	0.1	-0	-0	-0	-0	-0	-0	-0

ENGINE WITH 1.999/1 RATIO HAS 4.5610 CUIN CLEARANCE. FUEL WITH 1.999/1 RATIO HAS 48.84 LBM/CUFT (.860) AND LIBERATES 18700 BTU/LBM.

FOR	FRAC	RNEP	PSFC	FUEL/	CYCLE(LBM/1000)	SRGE	EFF	AVVC	AT	START	OF	INJECTION	AVERAGE	DURING	DELAY	WALL(F)				
RUN	HP	PSI	#/HRHP	AIR	EXH	BLW	EXH	PSIA	#/CUFT	R	INDEX	PSIA	#/CUFT	R	INDEX	ILLUM				
75	18.4	161.8	506	0.312	4.96	0.95	0.17	33.9	53.5	36.0	1.361	819	1.162	1832	1.157	584	1.376	1885	0	
76	17.7	87.8	520	0.317	4.96	0.97	0.18	33.9	53.3	33.2	1.396	814	1.177	1827	1.216	584	1.371	1885	0	
80	18.9	104.4	456	0.316	4.95	0.97	0.17	34.1	52.8	35.2	1.388	821	1.178	1841	1.222	585	1.367	1900	0	
79	18.1	100.2	516	0.316	4.96	0.97	0.17	34.0	53.1	34.9	1.388	815	1.174	1833	1.222	585	1.366	1893	0	
78	18.1	100.0	515	0.314	4.94	0.97	0.17	33.9	53.2	38.9	1.364	817	1.178	1831	1.215	575	1.367	1888	0	
77	18.3	90.0	569	0.313	4.93	0.97	0.17	34.1	52.8	38.5	1.371	824	1.176	1852	1.157	585	1.365	1505	0	
81	19.3	106.6	483	0.312	4.57	0.97	0.16	34.1	53.1	38.2	1.360	802	1.180	1757	1.216	572	1.382	1856	0	
82	-0	84.1	-000	-000	-00	-00	-00	-00	-00	-00	-000	-0	-000	-0	-000	-0	-000	-000	-00	
MEAN	18.1	96.1	516	0.313	4.95	0.97	0.17	34.0	53.1	36.4	1.378	816	1.178	1830	1.212	581	1.371	1888	0	
ERRS	0.9	7.0	0.25	0.002	0.01	0.01	0.00	0.1	0.2	0.0	0.013	6	0.002	0.16	0.010	5	0.005	0.15	0.013	0.000

FOR	CRANKCASE	C115	COOLANT	SYSTEM
RUN	GPM	BTU/SEC	BTU/SEC	BTU/SEC
75	5.12	1.1	2.4	11.9
76	5.20	1.0	2.1	11.6
80	5.20	1.3	2.7	11.4
78	5.34	1.5	3.0	11.6
77	5.41	2.4	5.1	11.5
81	5.34	2.6	5.4	12.0
82	-00	-0	-0	-0
MEAN	5.30	1.7	3.6	11.7
ERRS	0.12	0.6	1.2	0.2

TABLE 4

EQUIVALENT AREA FOR FUEL FLOW IN INJECTOR NOZZLE VERSUS NEEDLE LIFT

(Results of Computations) (See Fig. 23)

RATE OF INJECTION = DISCHARGE COEFFICIENT * EQUIVALENT AREA * SQRT.(FUEL DENSITY * FUEL PRESSURE - CYLINDER PRESSURE) / 415.53855 (LBM/HOUR)

INJECTOR HAS FOUR .01181 INCH HOLES, CONTACT SURFACE HAS DIAMETERS .07320 & .13750 AND HEIGHT .05385, TIP ANGLE IS 66.50 DEGREES

EQUIVALENT AREA = 1/SQRT.(1/(OUTLET AREA FCF NEEDLE & SEAT).P.2 + 1/(AREA CF HOLES).P.2 - (DISCHARGE COEFFICIENT/AREA OF BODY).P.2) MILS*(126.1 - .8046*MILS) 438.2 4208.4

ASSUME DISCHARGE COEFFICIENT = .7000

EQUIVALENT AREA (SQUARE INCHES/1000000) FOR EVERY .05 MIL LIFT (MIL = INCH/1000) FROM .00 TO 30.00 MILS

MILS	.00	.05	.10	.15	.20	.25	.30	.35	.40	.45	.50	.55	.60	.65	.70	.75	.80	.85	.90	.95	1.00	
0.00	6.3	12.6	18.9	25.2	31.5	37.8	44.1	50.4	56.7	63.0	69.3	75.6	81.9	88.2	94.5	100.8	107.1	113.4	119.7	126.0	132.3	
1.00	126.0	126.0	131.5	136.8	142.1	147.3	152.5	157.6	162.6	167.5	172.4	177.1	181.8	186.5	191.0	195.5	200.2	204.2	208.4	212.6	216.6	220.5
2.00	216.6	220.7	224.6	228.5	232.2	235.9	239.6	243.2	246.7	250.1	253.5	256.7	260.0	263.1	266.2	269.3	272.2	275.1	278.0	280.8	283.5	286.2
3.00	283.5	286.2	288.8	291.4	293.9	296.3	298.8	301.1	303.4	305.7	307.9	310.0	312.2	314.2	316.3	318.3	320.2	322.1	324.0	325.8	327.6	329.3
4.00	327.6	329.3	331.1	332.7	334.4	336.0	337.6	339.1	340.6	342.1	343.6	345.0	346.4	347.8	349.1	350.4	351.7	353.0	354.2	355.4	356.6	357.8
5.00	356.6	357.8	358.9	360.0	361.1	362.2	363.3	364.3	365.3	366.3	367.3	368.3	369.2	370.1	371.0	371.9	372.8	373.6	374.5	375.3	376.1	376.9
6.00	376.1	376.9	377.7	378.5	379.2	380.0	380.7	381.4	382.1	382.8	383.5	384.1	384.8	385.4	386.1	386.7	387.3	387.9	388.5	389.1	389.7	390.3
7.00	389.7	390.3	390.8	391.3	391.8	392.4	392.9	393.4	393.9	394.4	394.9	395.4	395.8	396.3	396.7	397.2	397.6	398.1	398.5	398.9	399.3	399.7
8.00	399.7	399.7	400.1	400.5	400.9	401.3	401.7	402.0	402.4	402.8	403.1	403.5	403.8	404.2	404.5	404.8	405.2	405.5	405.8	406.1	406.4	406.6
9.00	406.6	406.7	407.0	407.3	407.6	407.9	408.2	408.5	408.7	409.0	409.3	409.5	409.8	410.1	410.3	410.6	410.8	411.1	411.3	411.5	411.8	412.0
10.00	411.8	412.0	412.2	412.5	412.7	412.9	413.1	413.3	413.5	413.7	413.9	414.1	414.2	414.4	414.6	414.8	415.0	415.1	415.3	415.5	415.7	415.9
11.00	415.9	416.1	416.2	416.4	416.6	416.8	416.9	417.1	417.3	417.4	417.6	417.8	417.9	418.1	418.2	418.4	418.5	418.7	418.8	419.0	419.1	419.2
12.00	419.1	419.3	419.4	419.6	419.7	419.8	419.9	420.0	420.1	420.2	420.3	420.4	420.5	420.6	420.7	420.8	420.9	421.0	421.1	421.2	421.3	421.4
13.00	421.7	421.8	421.9	422.1	422.2	422.3	422.4	422.5	422.6	422.7	422.8	422.9	423.0	423.1	423.2	423.3	423.4	423.5	423.6	423.7	423.8	423.9
14.00	423.8	423.9	424.0	424.1	424.2	424.3	424.4	424.5	424.6	424.7	424.8	424.9	425.0	425.1	425.2	425.3	425.4	425.5	425.6	425.7	425.8	425.9
15.00	425.9	426.0	426.1	426.2	426.3	426.4	426.5	426.6	426.7	426.8	426.9	427.0	427.1	427.2	427.3	427.4	427.5	427.6	427.7	427.8	427.9	428.0
16.00	427.9	428.0	428.1	428.2	428.3	428.4	428.5	428.6	428.7	428.8	428.9	429.0	429.1	429.2	429.3	429.4	429.5	429.6	429.7	429.8	429.9	430.0
17.00	429.9	430.0	430.1	430.2	430.3	430.4	430.5	430.6	430.7	430.8	430.9	431.0	431.1	431.2	431.3	431.4	431.5	431.6	431.7	431.8	431.9	432.0
18.00	432.0	432.1	432.2	432.3	432.4	432.5	432.6	432.7	432.8	432.9	433.0	433.1	433.2	433.3	433.4	433.5	433.6	433.7	433.8	433.9	434.0	434.1
19.00	434.1	434.2	434.3	434.4	434.5	434.6	434.7	434.8	434.9	435.0	435.1	435.2	435.3	435.4	435.5	435.6	435.7	435.8	435.9	436.0	436.1	436.2
20.00	436.2	436.3	436.4	436.5	436.6	436.7	436.8	436.9	437.0	437.1	437.2	437.3	437.4	437.5	437.6	437.7	437.8	437.9	438.0	438.1	438.2	438.3
21.00	438.3	438.4	438.5	438.6	438.7	438.8	438.9	439.0	439.1	439.2	439.3	439.4	439.5	439.6	439.7	439.8	439.9	440.0	440.1	440.2	440.3	440.4
22.00	440.4	440.5	440.6	440.7	440.8	440.9	441.0	441.1	441.2	441.3	441.4	441.5	441.6	441.7	441.8	441.9	442.0	442.1	442.2	442.3	442.4	442.5
23.00	442.5	442.6	442.7	442.8	442.9	443.0	443.1	443.2	443.3	443.4	443.5	443.6	443.7	443.8	443.9	444.0	444.1	444.2	444.3	444.4	444.5	444.6
24.00	444.6	444.7	444.8	444.9	445.0	445.1	445.2	445.3	445.4	445.5	445.6	445.7	445.8	445.9	446.0	446.1	446.2	446.3	446.4	446.5	446.6	446.7
25.00	446.7	446.8	446.9	447.0	447.1	447.2	447.3	447.4	447.5	447.6	447.7	447.8	447.9	448.0	448.1	448.2	448.3	448.4	448.5	448.6	448.7	448.8
26.00	448.8	448.9	449.0	449.1	449.2	449.3	449.4	449.5	449.6	449.7	449.8	449.9	450.0	450.1	450.2	450.3	450.4	450.5	450.6	450.7	450.8	450.9
27.00	450.9	451.0	451.1	451.2	451.3	451.4	451.5	451.6	451.7	451.8	451.9	452.0	452.1	452.2	452.3	452.4	452.5	452.6	452.7	452.8	452.9	453.0
28.00	453.0	453.1	453.2	453.3	453.4	453.5	453.6	453.7	453.8	453.9	454.0	454.1	454.2	454.3	454.4	454.5	454.6	454.7	454.8	454.9	455.0	455.1
29.00	455.1	455.2	455.3	455.4	455.5	455.6	455.7	455.8	455.9	456.0	456.1	456.2	456.3	456.4	456.5	456.6	456.7	456.8	456.9	457.0	457.1	457.2

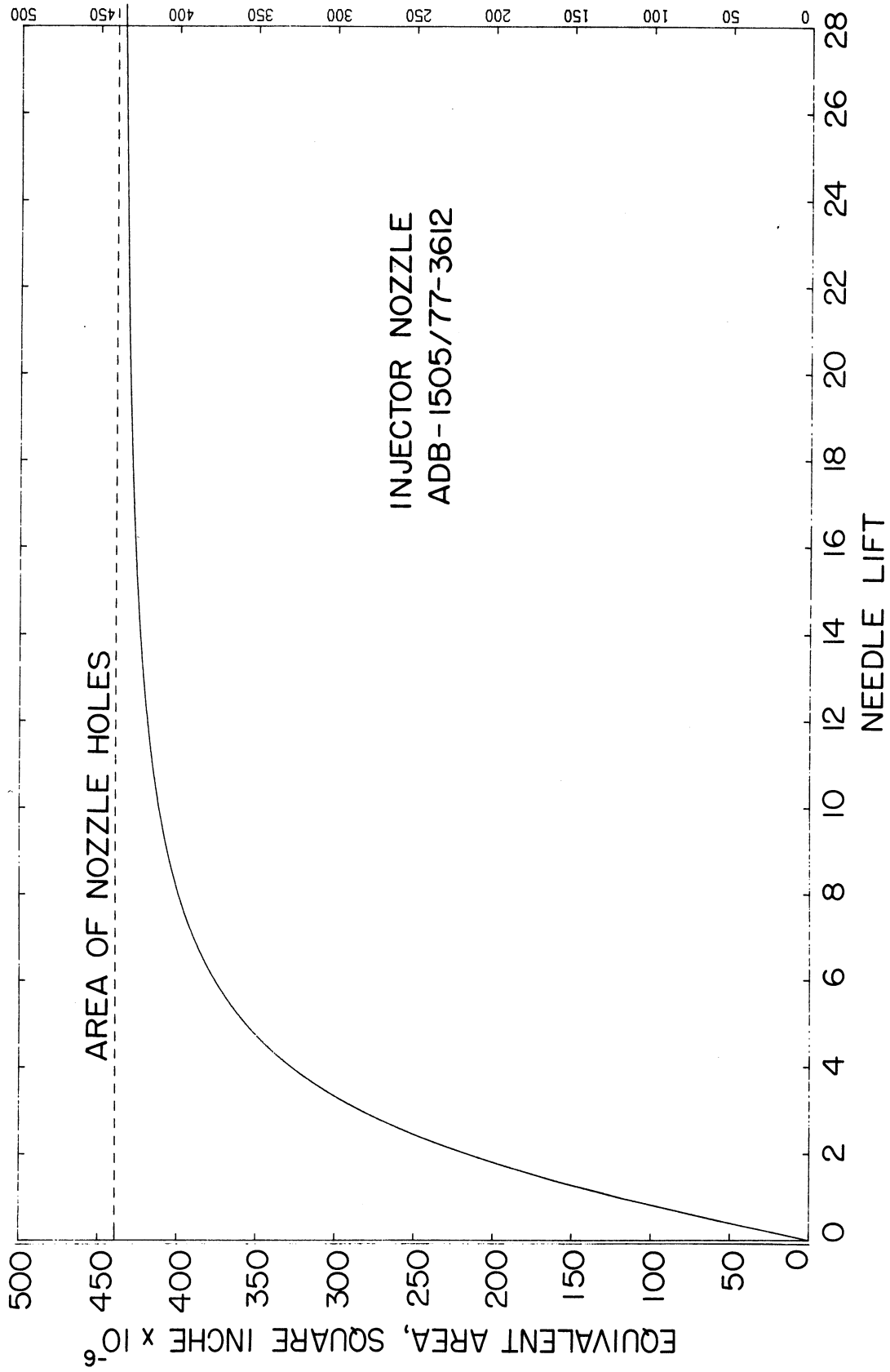


Fig. 23. Equivalent area for fuel flow in injector nozzle versus needle lift.

APPENDIX C

REFERENCES

1. Bolt, Jay A. and N. A. Henein, "Diesel Engine Ignition and Combustion," University of Michigan, ORA 06720-8-P.
2. Jost, W., Explosion and Combustion Processes in Gases, McGraw Hill Book Co., N. Y., 1946, p. 239.
3. Andreev, E. A., Acta Physiocochim (*USSR), 6, p. 57 (1937), c.f., B. Lewis and G. Von Elbe, "Combustion, Flames and Explosions of Gases," Academic Press, N Y , 1961, p. 145.
4. Aivagov, B., and Neumann, M. B., Physik Chem., 1936, B 33, p. 349.
5. Small, J., "Vagaries of Internal Combustion," Engineer (London), 164, 1937, 642.668.
6. Lee, D. W. and Spencer, R. C., "Photomicrographic Studies of Fuel Sprays," NACA TR. 454, 1933.
7. Rothrock, A. M. and Waldron, C. D., NACA report 561, 1936.
8. Miller, C. D., "Slow Motion Study of Injection and Combustion of Fuel in a Diesel Engine," SAE Trans. 53, p. 719-735, 1945.

SECTION 10

EFFECT OF FUEL-AIR RATIO ON IGNITION DELAY AND OTHER COMBUSTION PHENOMENA

Experimental studies were made on the effect of fuel-air ratio on the ignition delay and other combustion phenomena. The fuel-air ratio was varied over a range from .0141 to 0.0566.

This series of tests was run at two different levels of cooling water temperatures, 170°F and 250°F. The following conclusions are reached on the effect of fuel-air ratios:

With water as a coolant at a temperature of 170°F the thermal loading on the cooling and lubricating systems increased with the increase in the fuel-air ratio as shown in Fig. 1. The total thermal loading as a percentage of the heating value of the fuel used decreased as shown in Fig. 2 from 19.8% at a fuel-air ratio of 0.0162 to 13.1% at a fuel-air ratio of 0.0561.

With ethylene glycol, where the coolant temperature was kept at 250°F, the percentage total thermal load increased slightly with the fuel-air ratio. However, if we compare ethylene glycol with water we find that the percentage total thermal loading with ethylene glycol at 250°F was lower than that with water at 170°F. At the highest fuel-air ratio, 0.0566 the percentage total thermal loading was 13.1% at 170°F and 9.8% at 250°F. This reduction in the thermal loading is due to two factors:

1. The lower thermal conductivity of the ethylene glycol as compared with that of water.
2. The higher the wall temperatures when the glycol was used—this reduces the rate of heat transfer from the gases to the walls.

The heat losses to the coolant, and to the lubricating oil increased with the fuel-air ratio. At a coolant temperature of 170°F the total thermal loading on the coolant and lubricating oil increased from 3.3 Btu/sec at .0141 fuel-air ratio, to 8.9 Btu/sec at 0.0561 fuel-air ratio. When the coolant temperature was raised to 250°F, the total heat losses decreased about 40% at the lower fuel-air ratio and 25% at the higher fuel-air ratio.

EFFECT OF F/A RATIO ON THE FIRE-DECK TEMPERATURE

The wall temperature in the fire deck was measured in two locations, near the inlet valve and near the exhaust valve. The wall temperatures near the exhaust valve, as shown in Fig. 3, were always higher than those near the

inlet valve. With the coolant, at 170°F the wall temperature near the exhaust valve increased from 242°F at a fuel-air ratio of 0.0141 to 422°F at a fuel-air ratio of 0.0561.

When the coolant temperature was raised to 250°F, the wall temperature in the two locations were increased. The average increase in wall temperature was 60°F near the inlet valve and 55°F near the exhaust valve. This indicates that the increase in the wall temperature was about 70% the increase in the coolant temperature.

EFFECT OF FUEL-AIR RATIO ON THE WALL SURFACE TEMPERATURE

The results for wall surface temperature in the valve bridge of the fire deck are shown in Fig. 4, plotted versus the fuel-air ratio. These results show that the minimum surface temperature increased almost linearly with the fuel-air ratio. With the coolant at 170°F, the surface temperature was 383°F at a fuel-air ratio of 0.0141 and increased to 665°F at a fuel-air ratio of 0.0561.

The increase in the coolant temperature from 170°F to 250°F caused an average increase of 60°F in the wall-surface temperature.

The temperature swing on the wall surface was almost constant over the whole range of the fuel-air ratio. The increase in the coolant temperature from 170°F to 250°F caused a slight drop in the temperature swing.

EFFECT OF FUEL-AIR RATIO ON THE SMOKE INTENSITY

The smoke intensity as shown in Fig. 5, increased with the fuel-air ratio, and reached very high values at the fuel-air ratio of 0.056. The change in the coolant temperature did not affect the smoke intensity.

EFFECT OF FUEL-AIR RATIO ON THE EXHAUST GAS TEMPERATURE

The exhaust gas temperature, shown in Fig. 6, increased with the fuel-air ratio. At a coolant temperature of 170°F, the exhaust temperature increased from 400°F at a F/A of 0.0142 to 1150°F at a F/A of 0.0561. The increase in the coolant temperature from 170°F to 250°F caused a slight change in the exhaust gas temperature.

EFFECT OF FUEL-AIR RATIO ON THE PRESSURE RISE AND ILLUMINATION DELAYS

The apparent effect of the increase in the fuel-air ratio is to decrease both the pressure rise and illumination delays. But when the ignition delay

was corrected for the change in the mean gas temperature during the ignition delay, both the ignition delays were found to have a constant value over the entire range of the fuel-air-ratio. The observed and corrected pressure rise delays are shown in Fig. 7. The corrected pressure rise and illumination delays are plotted in Fig. 8. The length of the pressure rise delay is about 1.04 msec, and the length of the illumination delay is about 1.2 msec.

The apparent drop in the ignition delay is probably due to the increase in the gas temperature with the fuel-air ratio. The higher fuel-air ratios result in higher wall temperatures and higher gas temperatures during the early stages of the combustion process.

EFFECT OF FUEL-AIR RATIO ON PEAK PRESSURE

The gas peak pressure increased with the fuel-air ratio at the two coolant temperatures of 170° and 250°F, as shown in Fig. 9. The peak pressures with the coolant temperature of 250°F, at any fuel-air ratio, were lower than those at 170°F and the same fuel-air ratio. The peak pressure reached 1520 psia with a coolant temperature of 170°F, and 1400 psia with a coolant temperature of 250°F.

The peak gas pressure is plotted versus the fuel consumption in pounds per hour, in Fig. 10.

EFFECT OF FUEL-AIR RATIO ON BMEP

The BMEP increased with the fuel-air ratio, for the two coolant temperatures as shown in Fig. 11. The BMEP with 250°F were lower than those at 170°F at the same fuel-air ratio. This is due to increased heat losses to the cylinder walls at the higher temperature.

EFFECT OF FUEL-AIR RATIO ON BSFC

The results in Fig. 11 show that the BSFC was minimum at fuel-air ratios around 0.045 for the two coolant temperatures. The fuel economy was better with the lower coolant temperature.

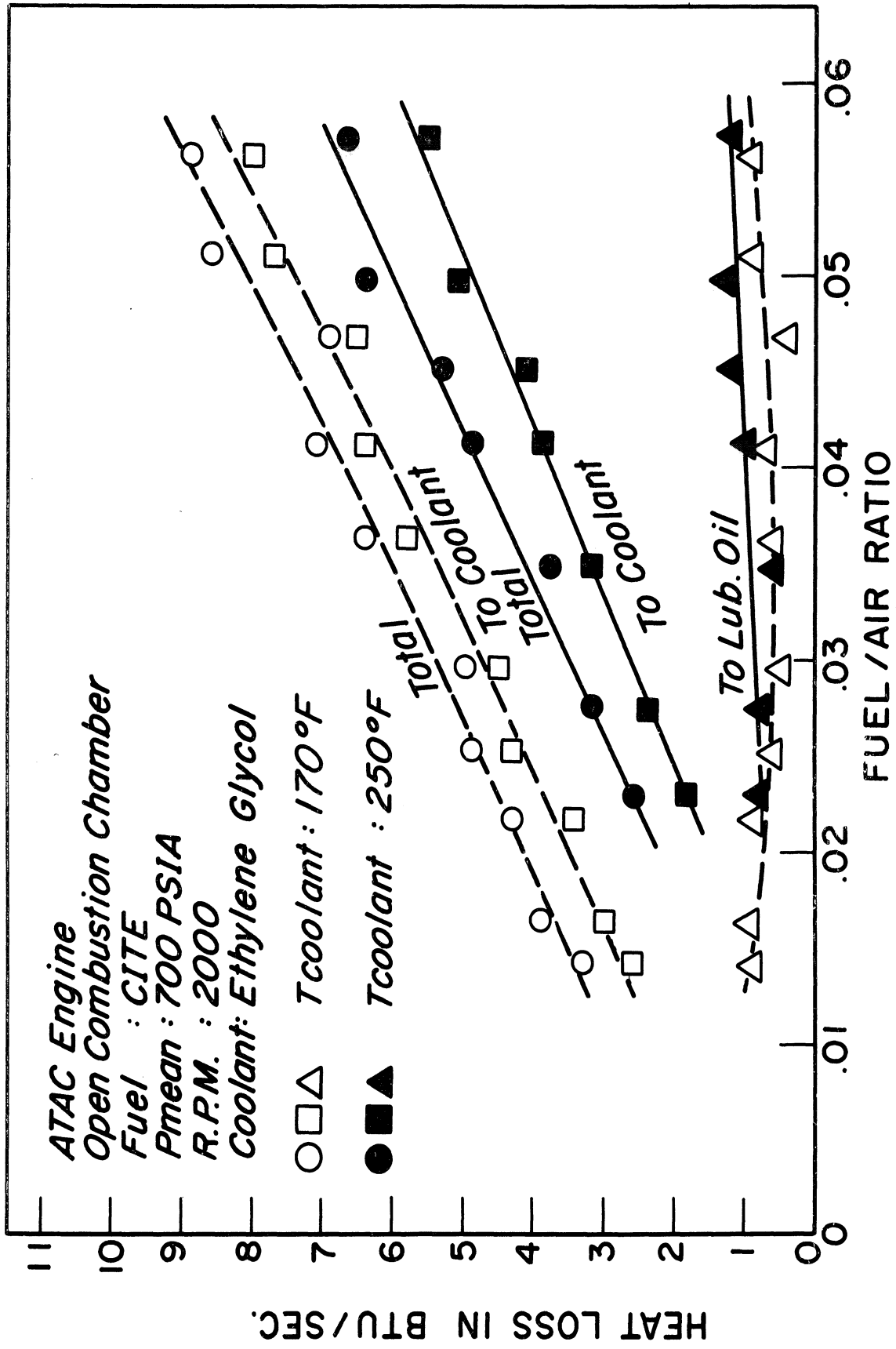


Fig. 1. Effect of fuel-air ratio of thermal loading on cooling and lubricating systems.

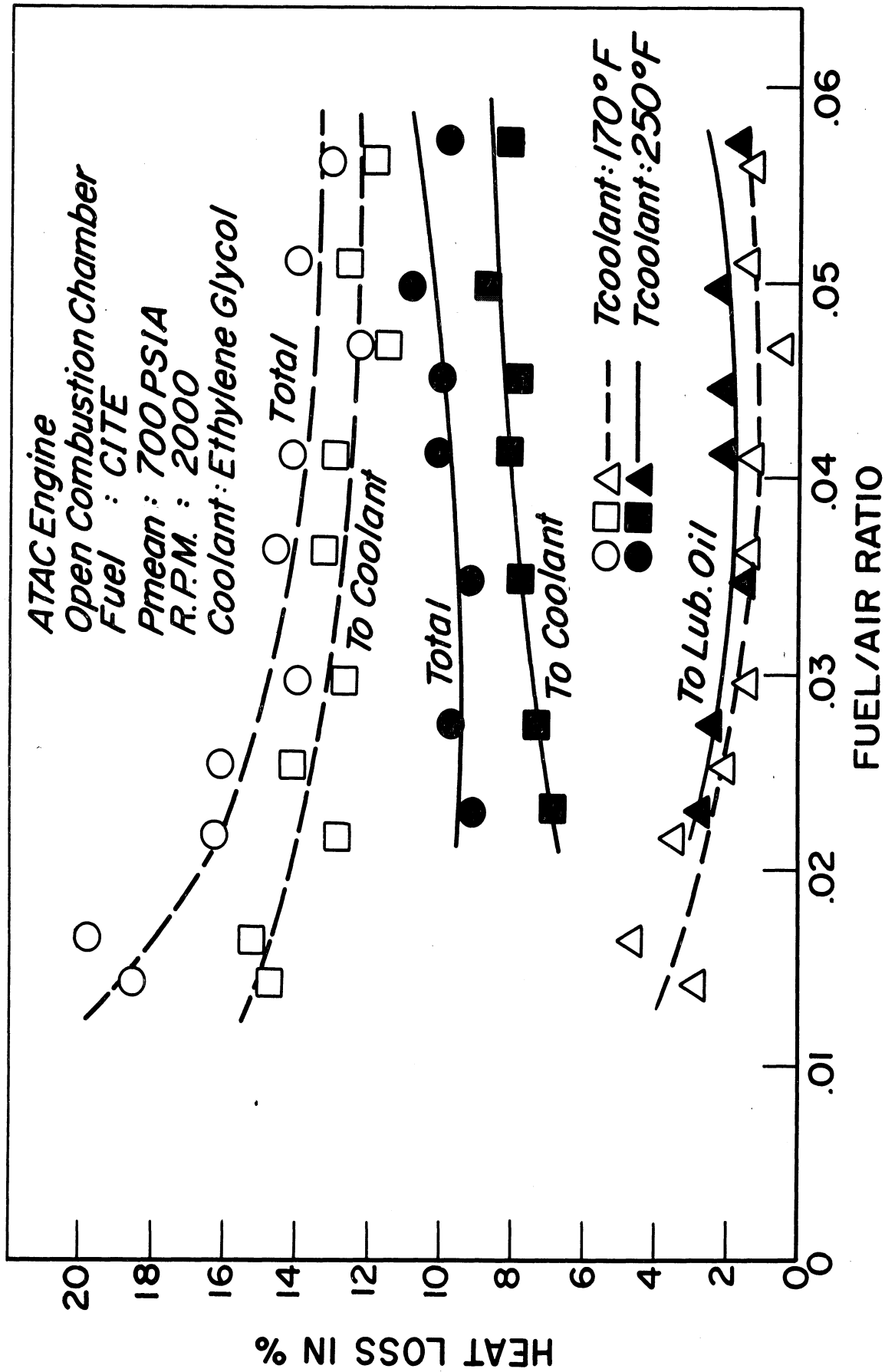


Fig. 2. Effect of fuel-air ratio on percentage heat losses to the cooling and lubricating systems.

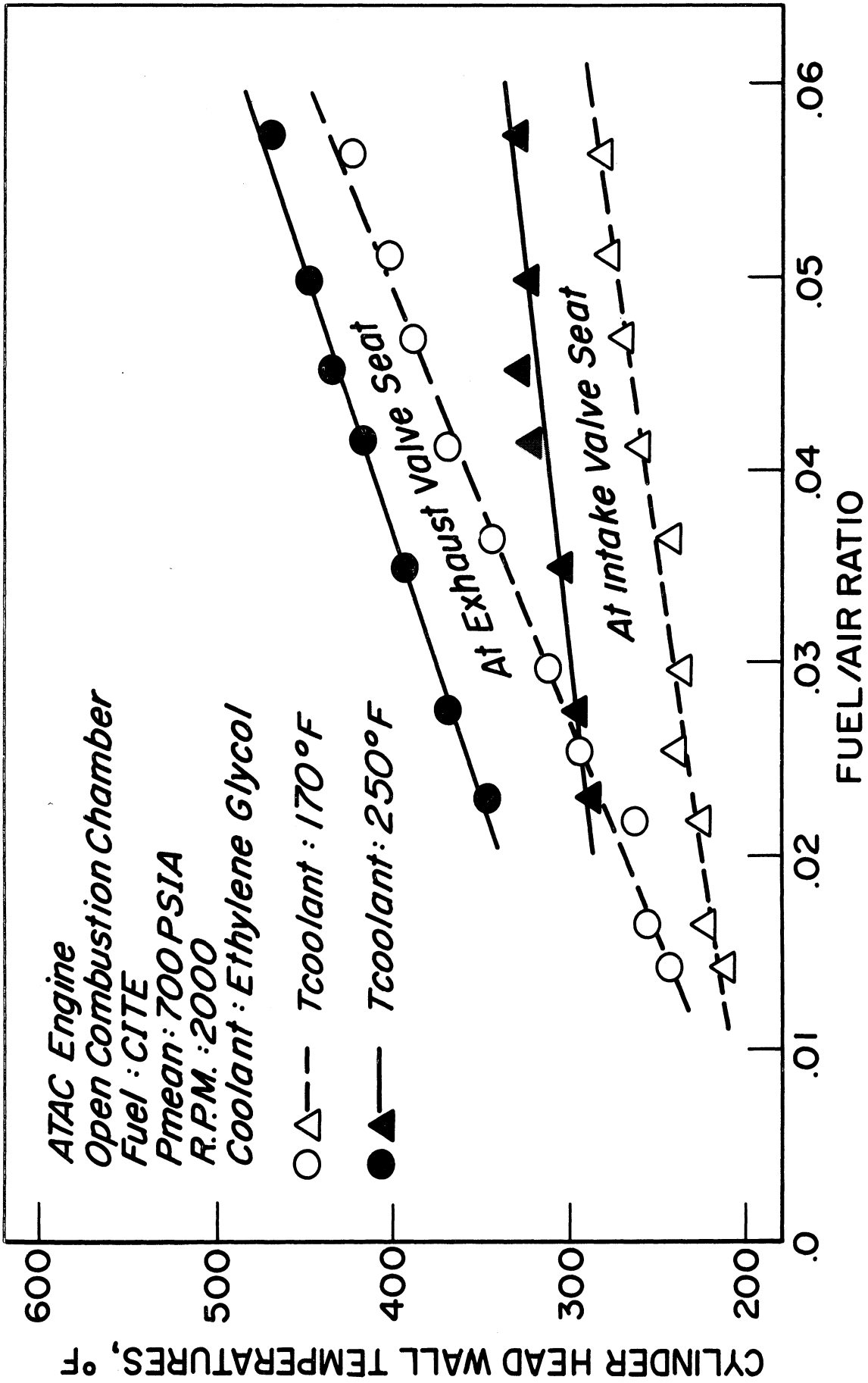


Fig. 3. Effect of fuel-air ratio on cylinder head wall temperature.

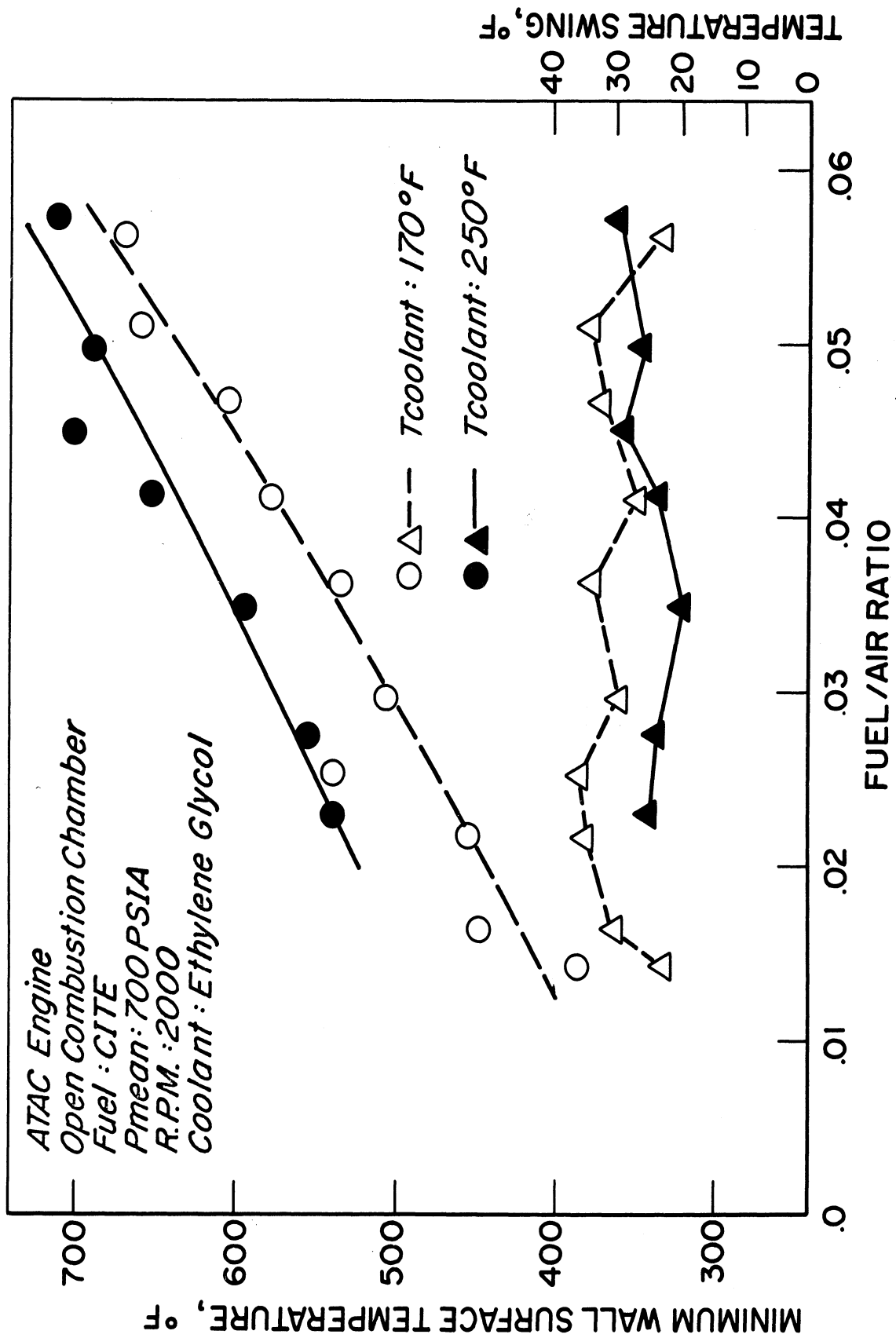


Fig. 4. Effect of fuel-air ratio on minimum wall surface temperature.

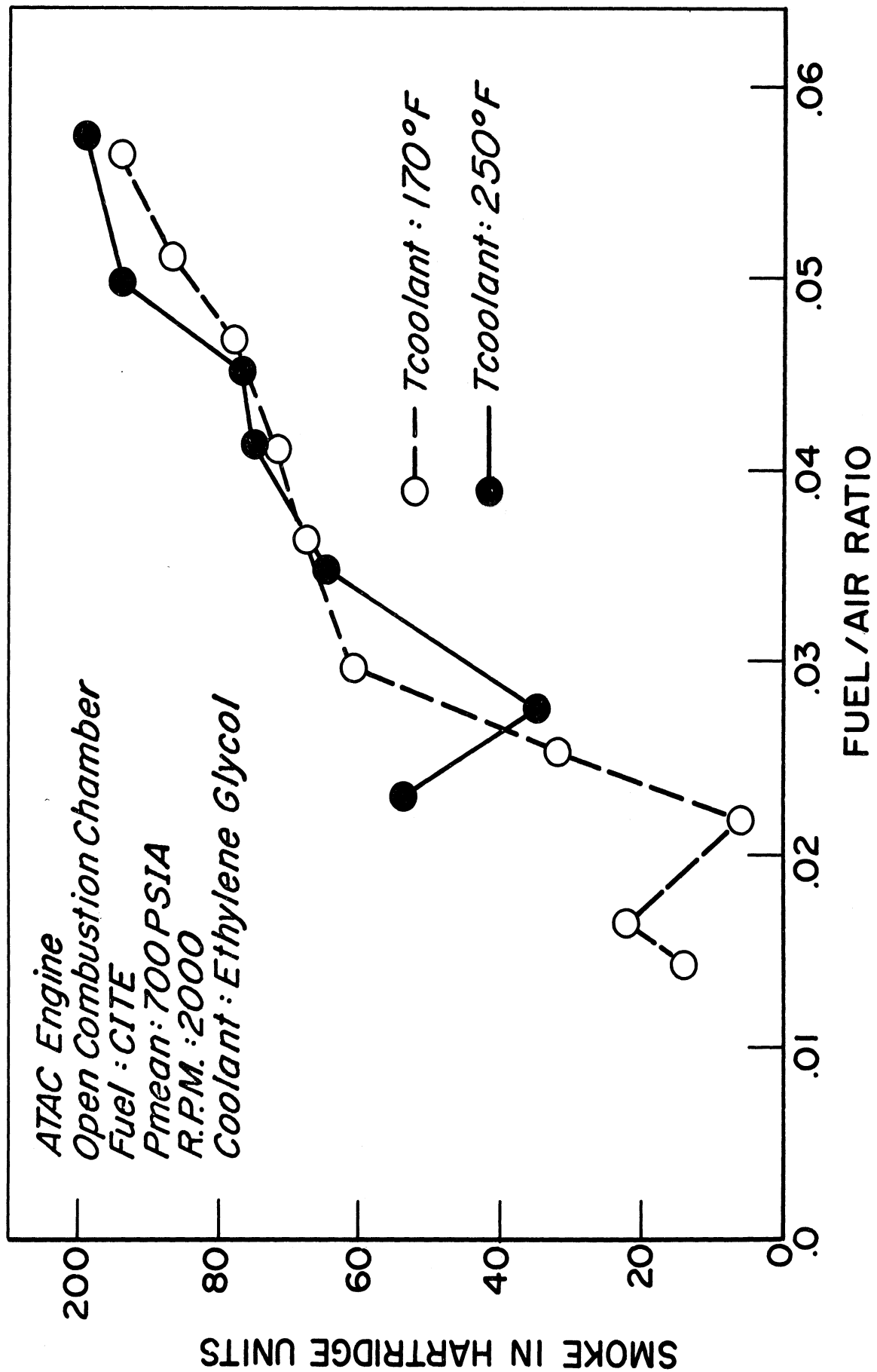


Fig. 5. Effect of fuel-air ratio on the smoke intensity.

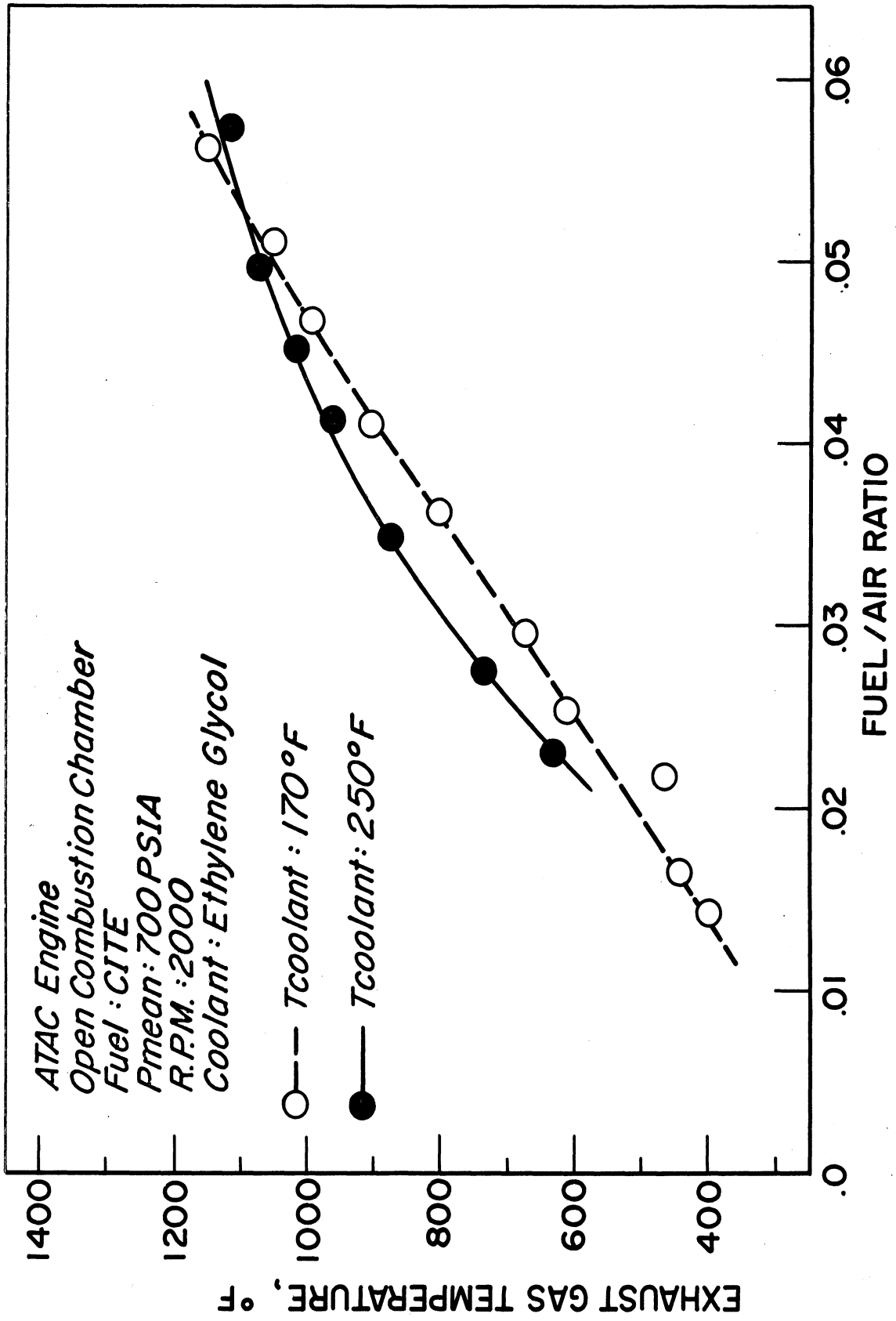


Fig. 6. Effect of fuel-air ratio on exhaust gas temperature.

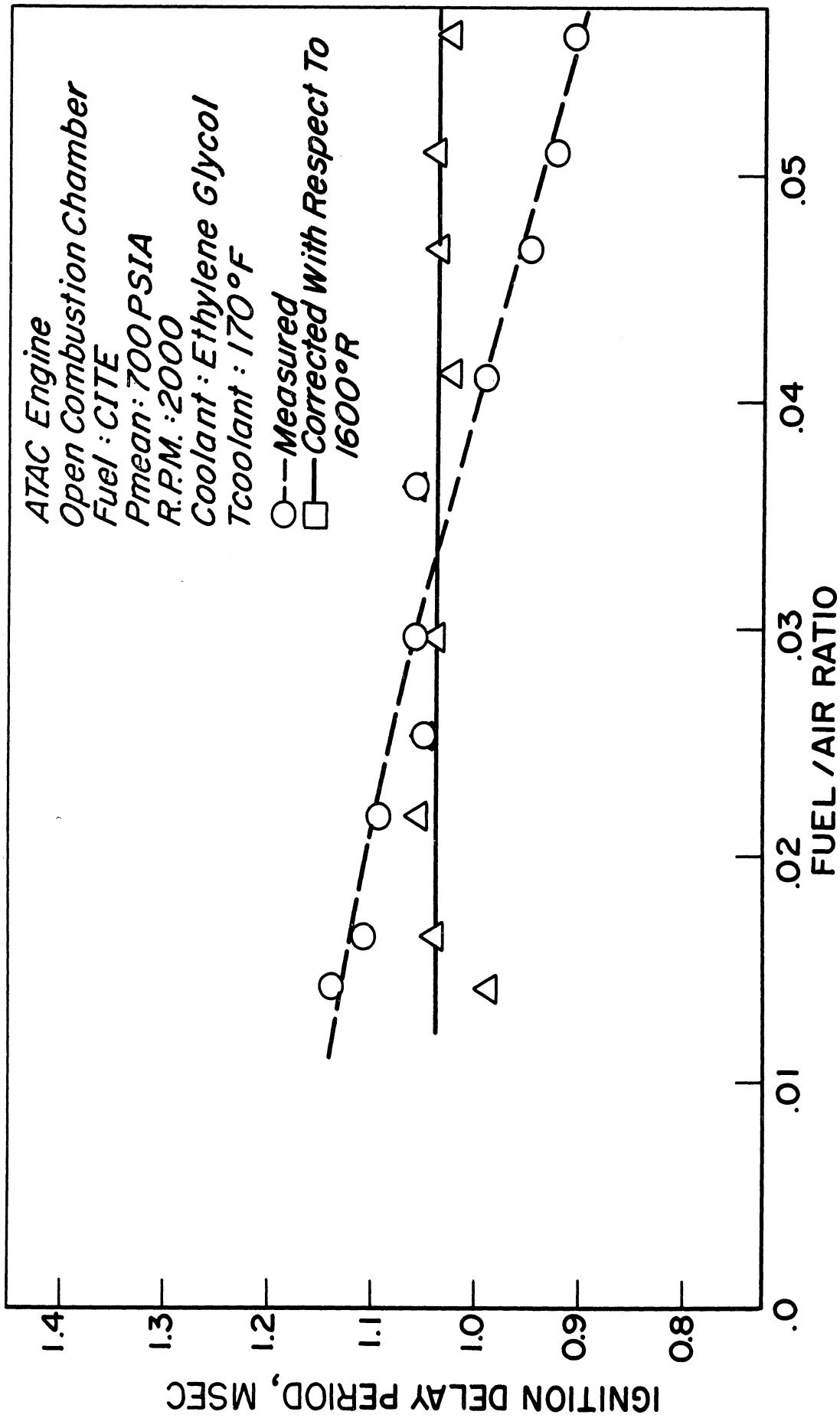


Fig. 7. Effect of fuel-air ratio on ignition delays.

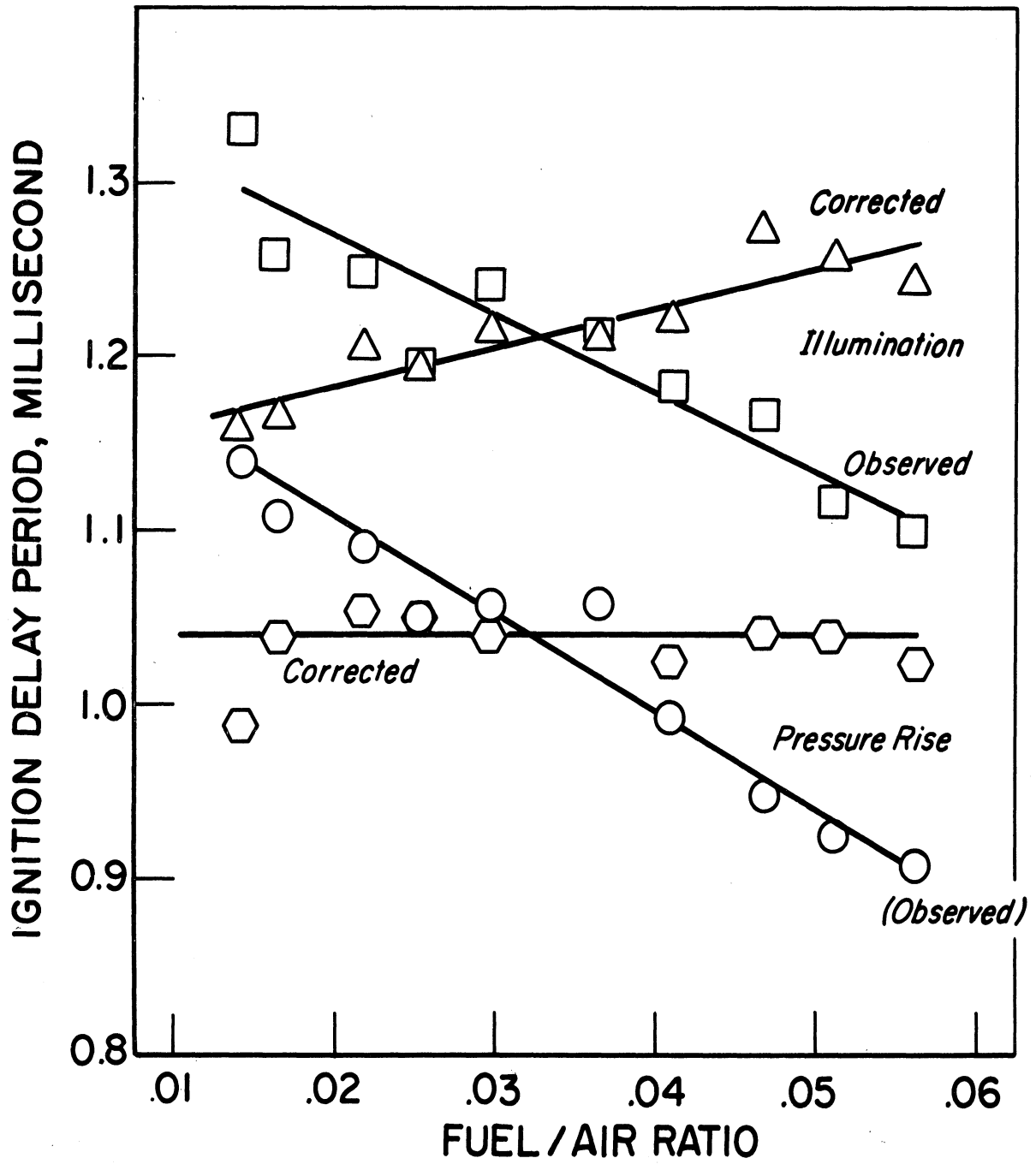


Fig. 8. Ignition delays: Observed and corrected to 1600°R.

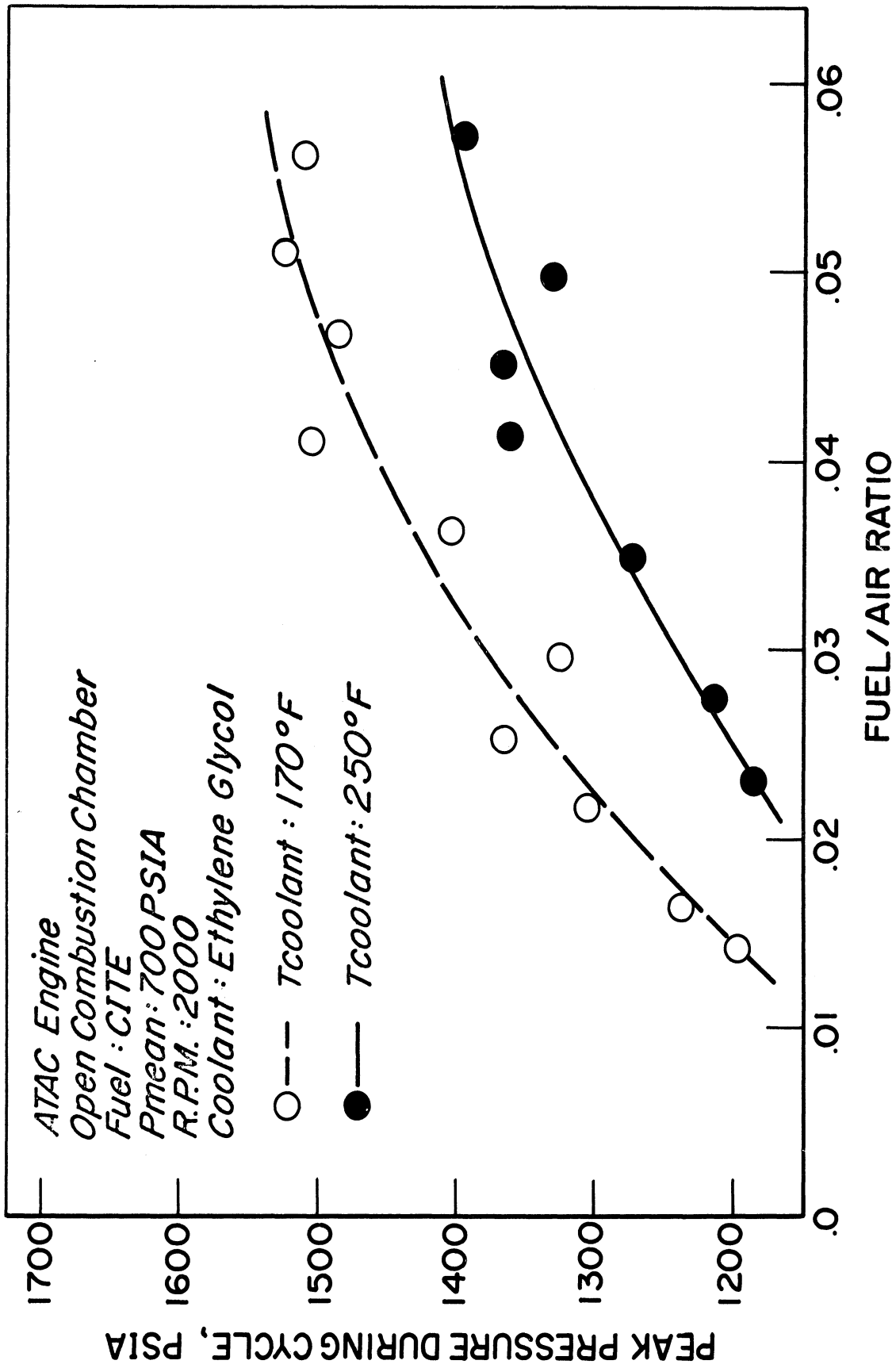


Fig. 9. Effect of fuel-air ratio on peak gas pressure.

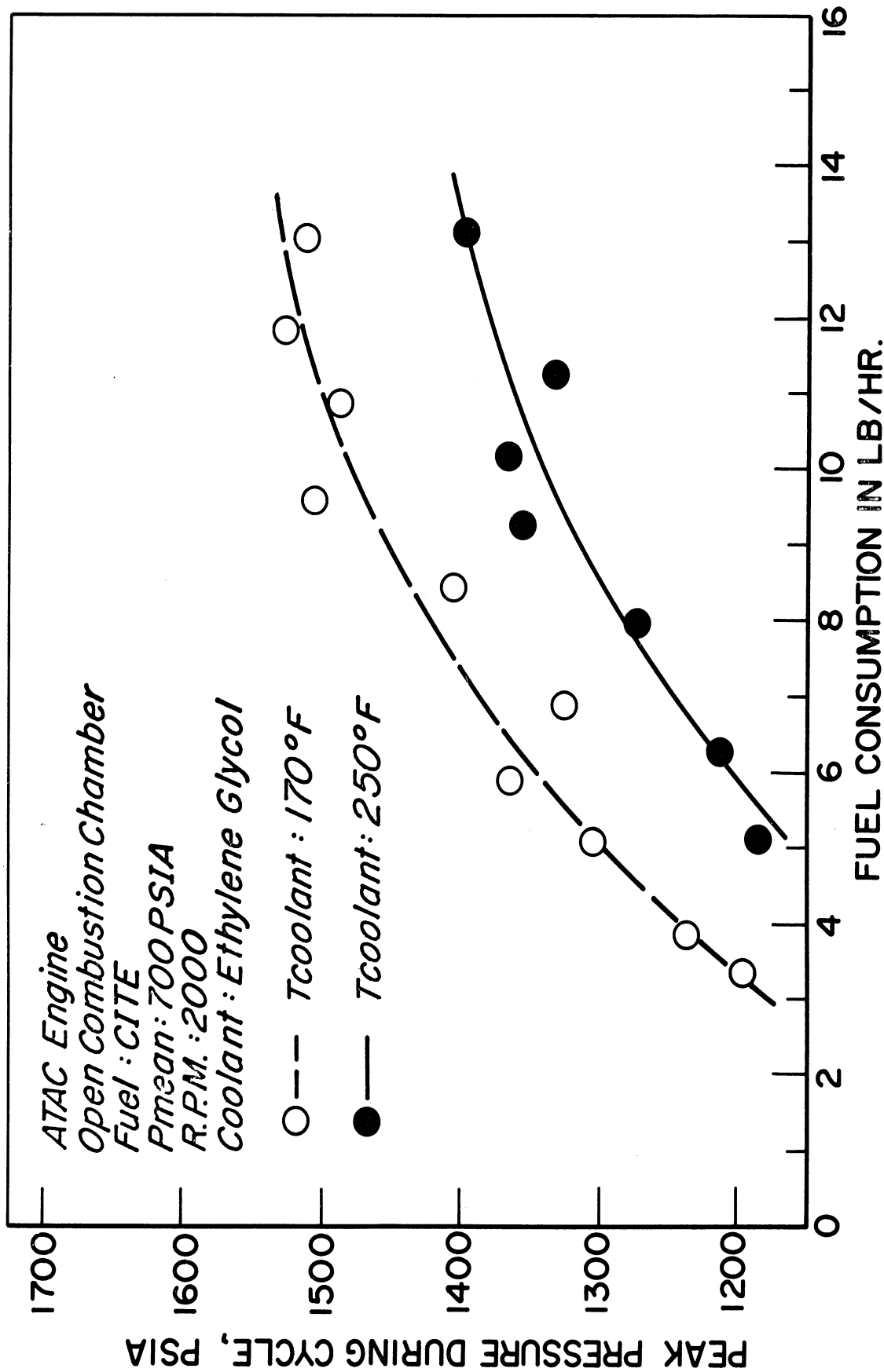


Fig. 10. Effect of fuel consumption per cycle on peak gas pressure.

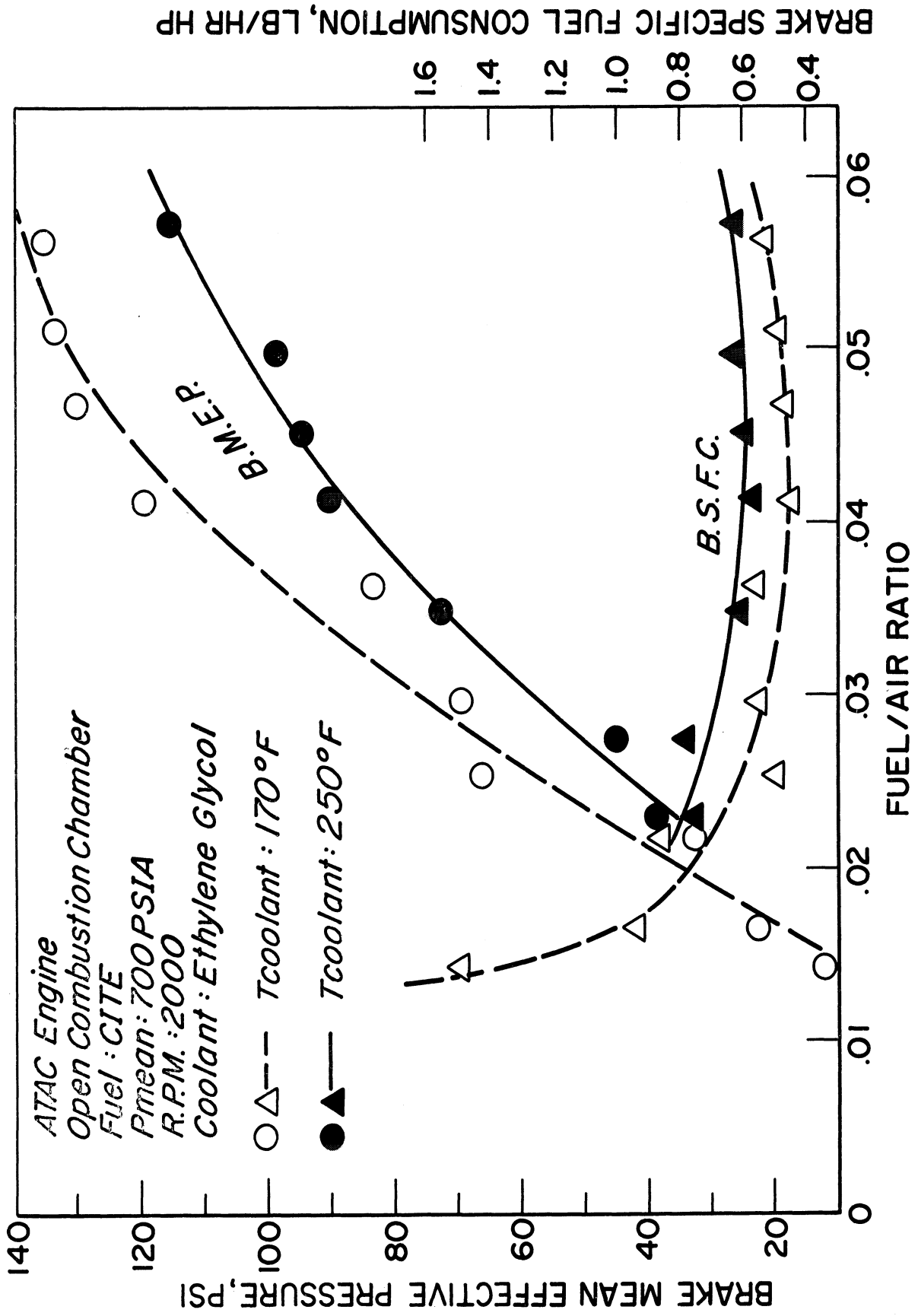


Fig. 11. Effect of fuel-air ratio on BMEP and BSFC.

SECTION 11

EFFECT OF ANTI-SMOKE ADDITIVE ON SMOKE INTENSITY AND OTHER COMBUSTION PHENOMENA

EFFECT OF ANTI-SMOKE ADDITIVE ON SMOKE INTENSITY

The smoke intensity was measured by a Hartridge Smokemeter, over a wide range of supercharging pressures and temperatures. The surge tank pressure ranged from 17.2 in. Hg boost to 31.6 in. Hg boost. The inlet air temperatures ranged from 106°F to 814°F.

The results for the effect of the anti-smoke additive on reducing the smoke intensity are plotted versus the intake air temperature in Fig. 1. It shows that the anti-smoke additive is effective at intake temperatures between 100°F and about 300°F. At higher temperatures its effect is not pronounced.

EFFECT OF ANTI-SMOKE ADDITIVE ON THE MAXIMUM PRESSURE GRADIENT

The maximum pressure gradient due to combustion is plotted in Fig. 2 versus the intake air temperature for diesel no. 2 fuel with and without anti-smoke additive. In general, the maximum pressure gradients increased when the additive was used, especially in the temperature range between 150°F and 400°F. This is the temperature range of practical interest for actual supercharged diesel engines.

The increase in the maximum pressure gradient with the additive indicates a higher rate of heat release during the combustion process. This is illustrated in Fig. 3 which shows that between temperatures of 150°F to 400°F, the rates of change of the pressure gradient are also higher for the diesel fuel with the additive.

The above conclusions agree with the results of the photographic studies made by Scott,* which showed that the duration of the combustion process was shortened with the anti-smoke additive.

*W. M. Scott, "Looking in on Diesel Combustion," SAE Publication SP-345, December 1968.

EFFECT OF THE ANTI-SMOKE ADDITIVE ON THE IGNITION DELAY

Figure 4 is a plot of the ignition delay (I.D._p) against the intake air temperature. This figure shows a small effect of the anti-smoke additive on the ignition delay of the diesel no. 2 fuel.

EFFECT OF ANTI-SMOKE ADDITIVE ON THE APPARENT ACTIVATION ENERGY

A plot of the logarithm of the ignition delay, I.D._p, and the reciprocal of the absolute mean temperature is shown in Figs. 5a and 5b for diesel no. 2 fuel with and without the fuel additive. Ethylene glycol was used as a coolant and its temperature was kept constant at 170°F.

Figures 5a and 5b show that the two lines have almost the same slope.

From the two figures it can be concluded that the anti-smoke additive has an insignificant effect on the apparent activation energy.

EFFECT OF THE ANTI-SMOKE ADDITIVE ON THE EXHAUST GAS TEMPERATURE

The results for the effect of the anti-smoke additive on the exhaust gas temperature at different intake air temperatures is shown in Fig. 6. This figure shows no effect for the anti-smoke additive on the exhaust gas temperature.

EFFECT OF ANTI-SMOKE ADDITIVE ON THE PEAK CYCLE PRESSURE

The peak gas pressure in the cylinder is plotted versus the intake temperature for diesel no. 2 fuel with and without the anti-smoke additive in Fig. 7.

This figure shows that there is no effect of the additive on the maximum gas pressure.

EFFECT OF ANTI-SMOKE ADDITIVE ON BSFC

The results of the BSFC plotted versus BMEP in Fig. 8 show that there is a slight increase in the specific fuel consumption with SMOGO.

EFFECT OF ANTI-SMOKE ADDITIVE ON THE MINIMUM WALL SURFACE TEMPERATURE

Figure 9 shows that there is a slight reduction in the wall surface temperature with the anti-smoke additive.

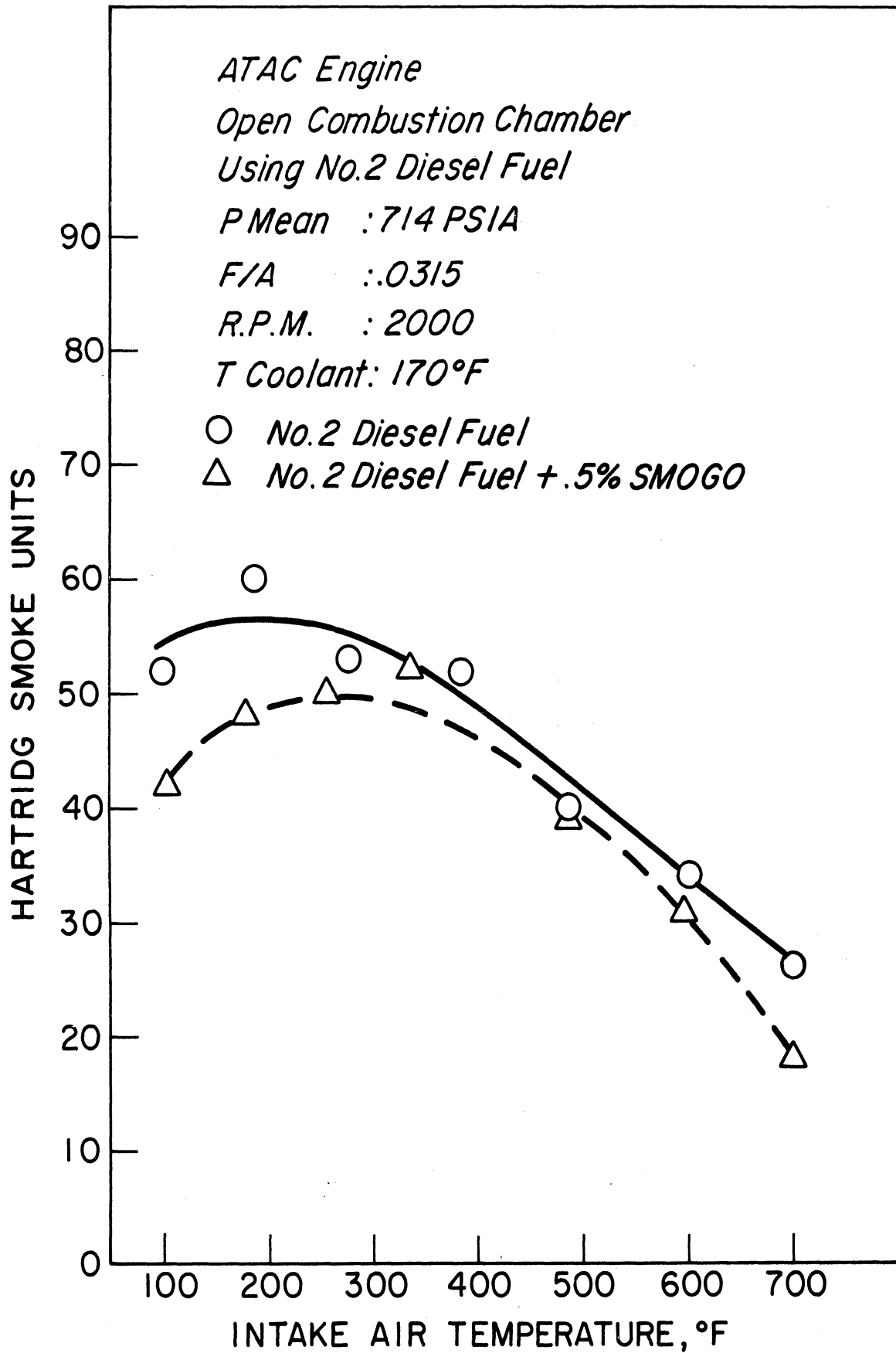


Fig. 1. Smoke intensity for diesel fuel with and without anti-smoke additive.

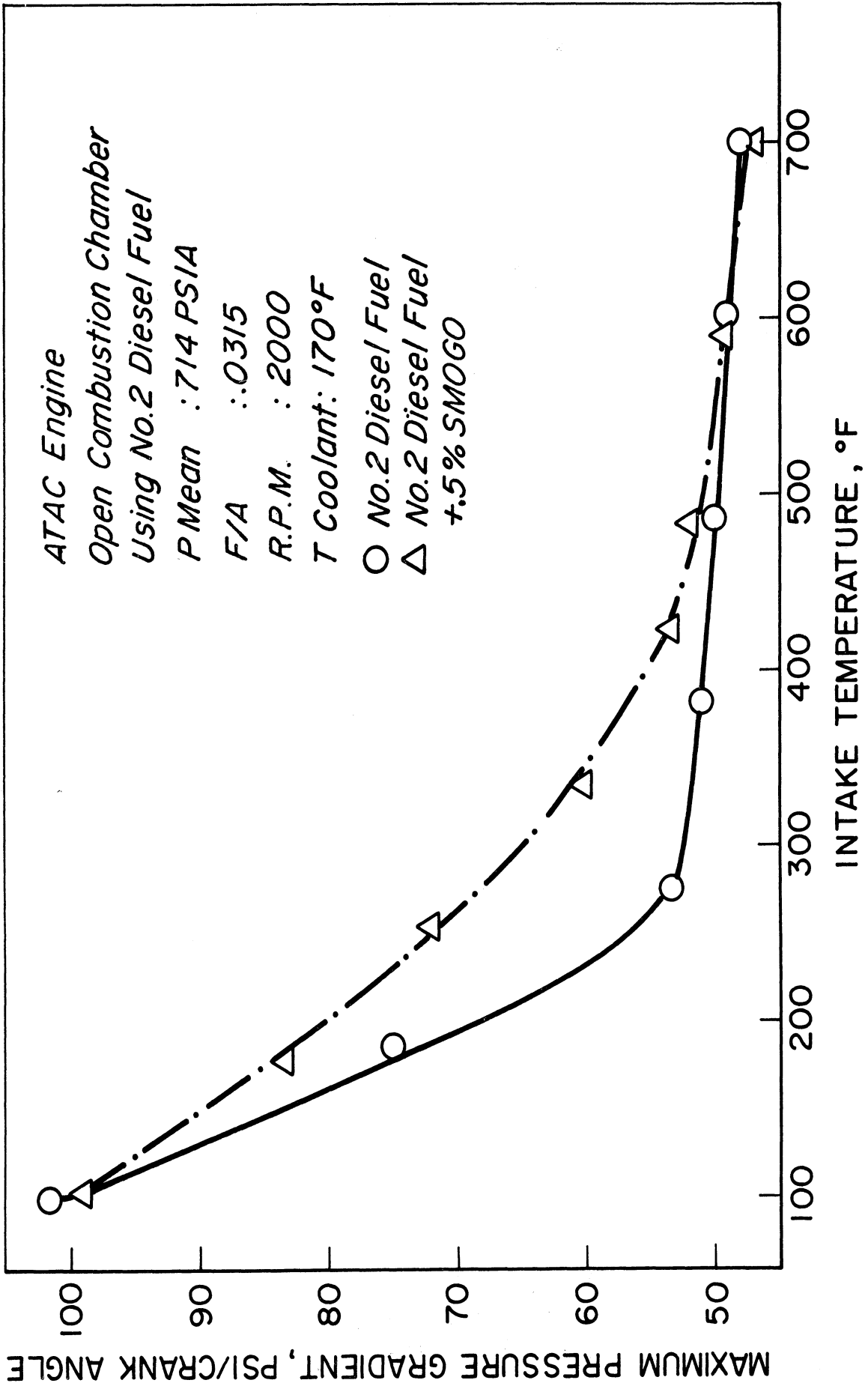


Fig. 2. Maximum pressure gradient for diesel fuel with and without anti-smoke additive.

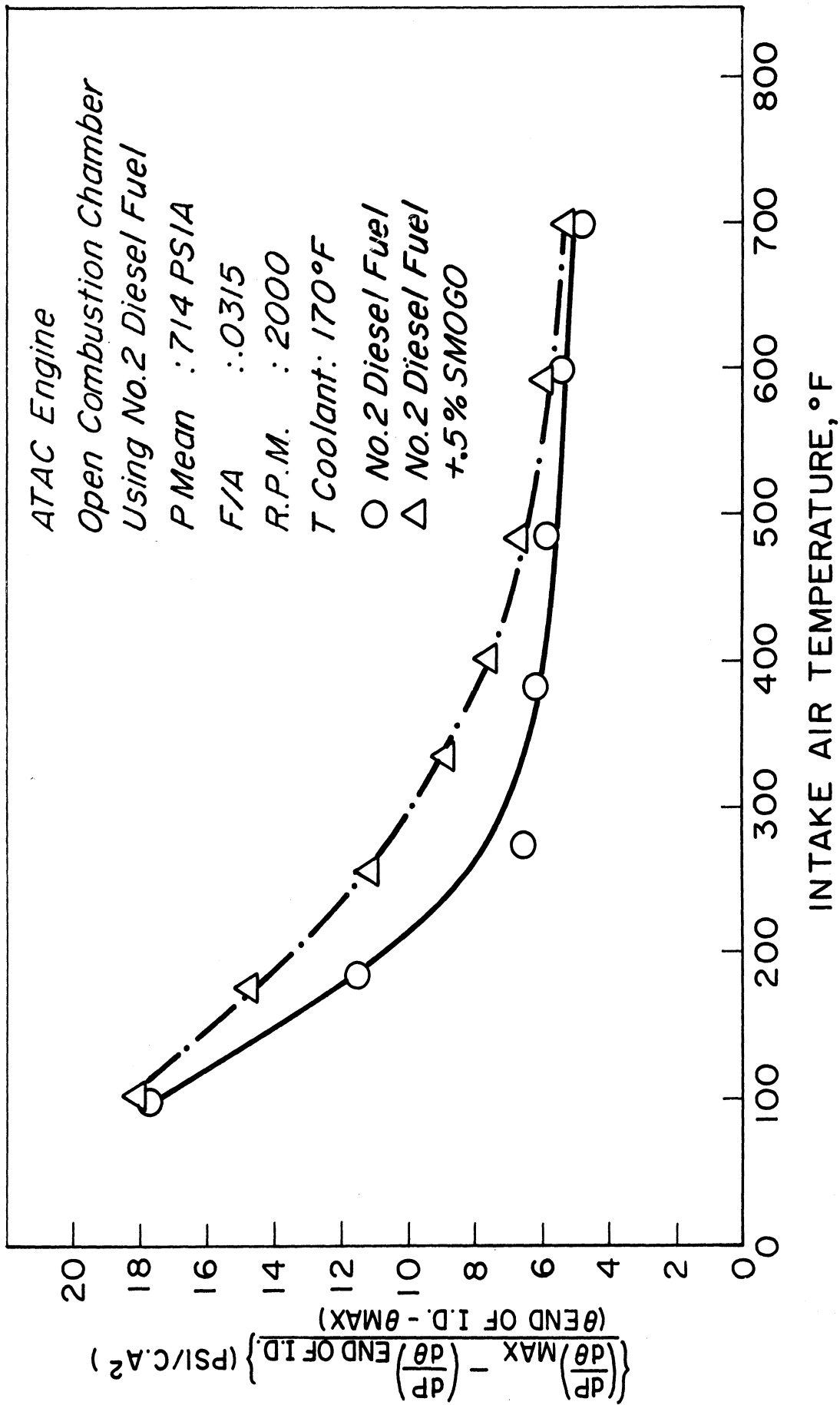


Fig. 3. Rate of change of pressure gradient for diesel fuel with and without anti-smoke additive.

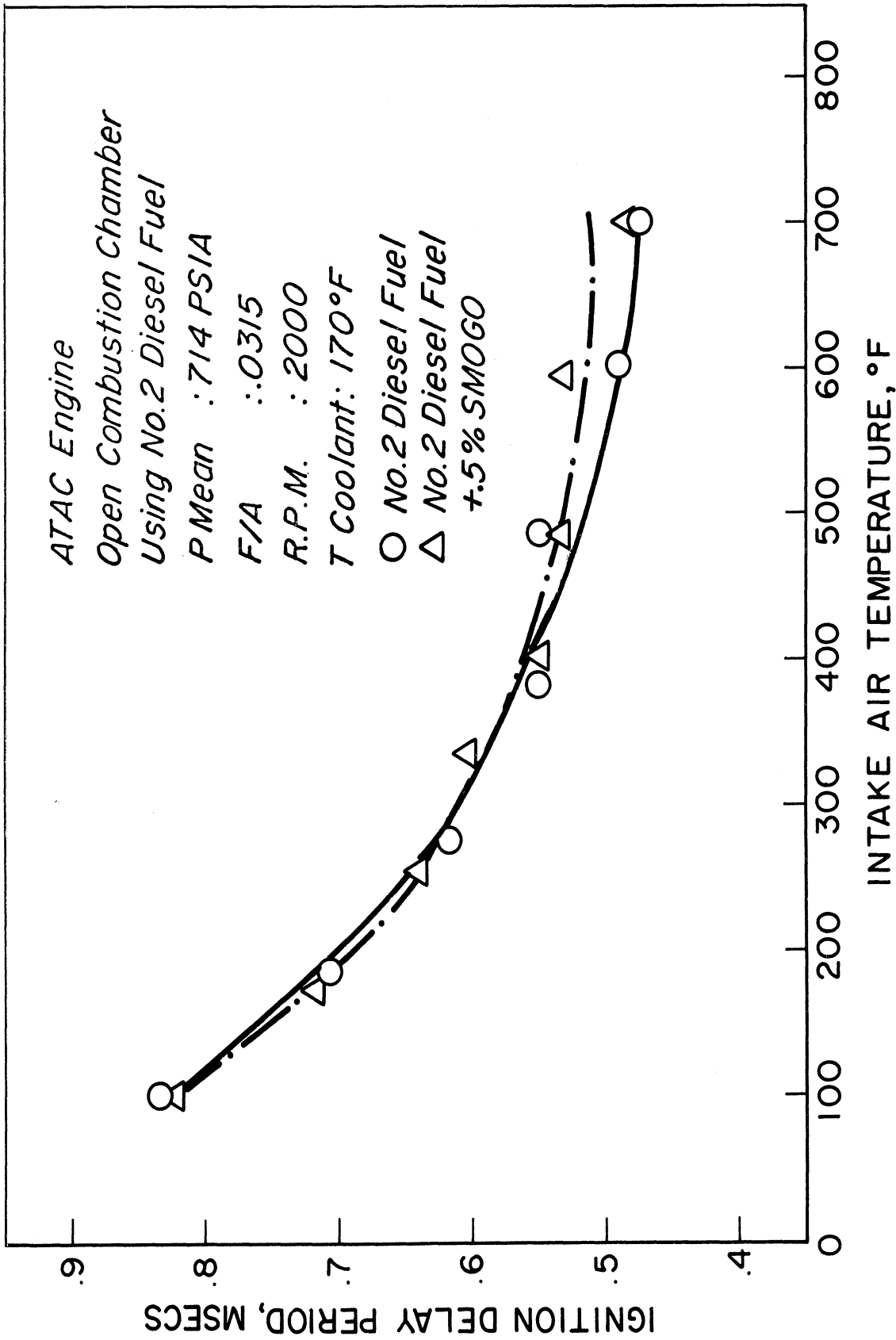


Fig. 4. Effect of anti-smoke additive on the ignition delay.

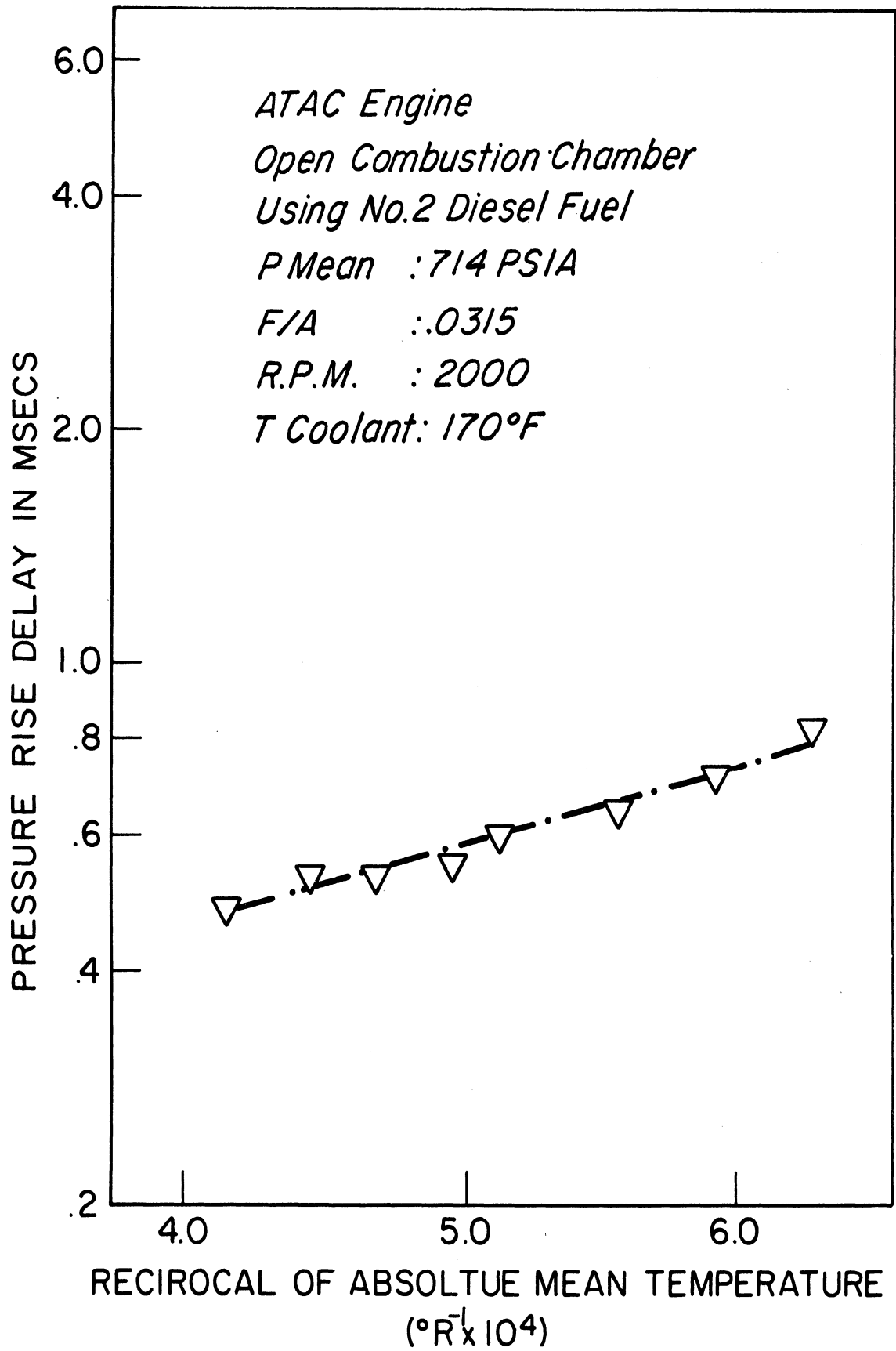


Fig. 5a. Pressure rise delay versus the reciprocal of the absolute mean temperature for diesel fuel with additive.

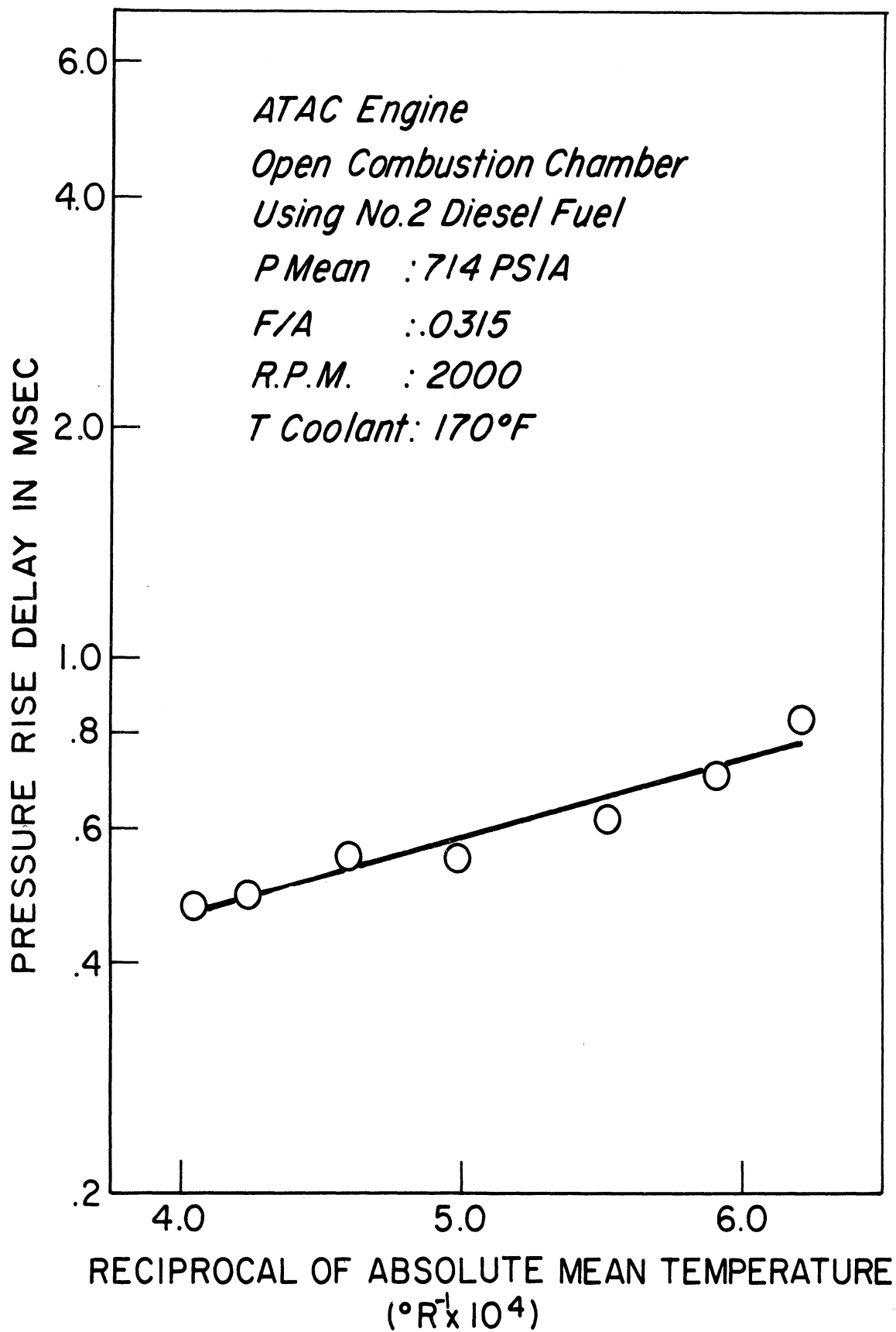


Fig. 5b. Pressure rise delay versus the reciprocal of the absolute mean temperature for diesel fuel without additive.

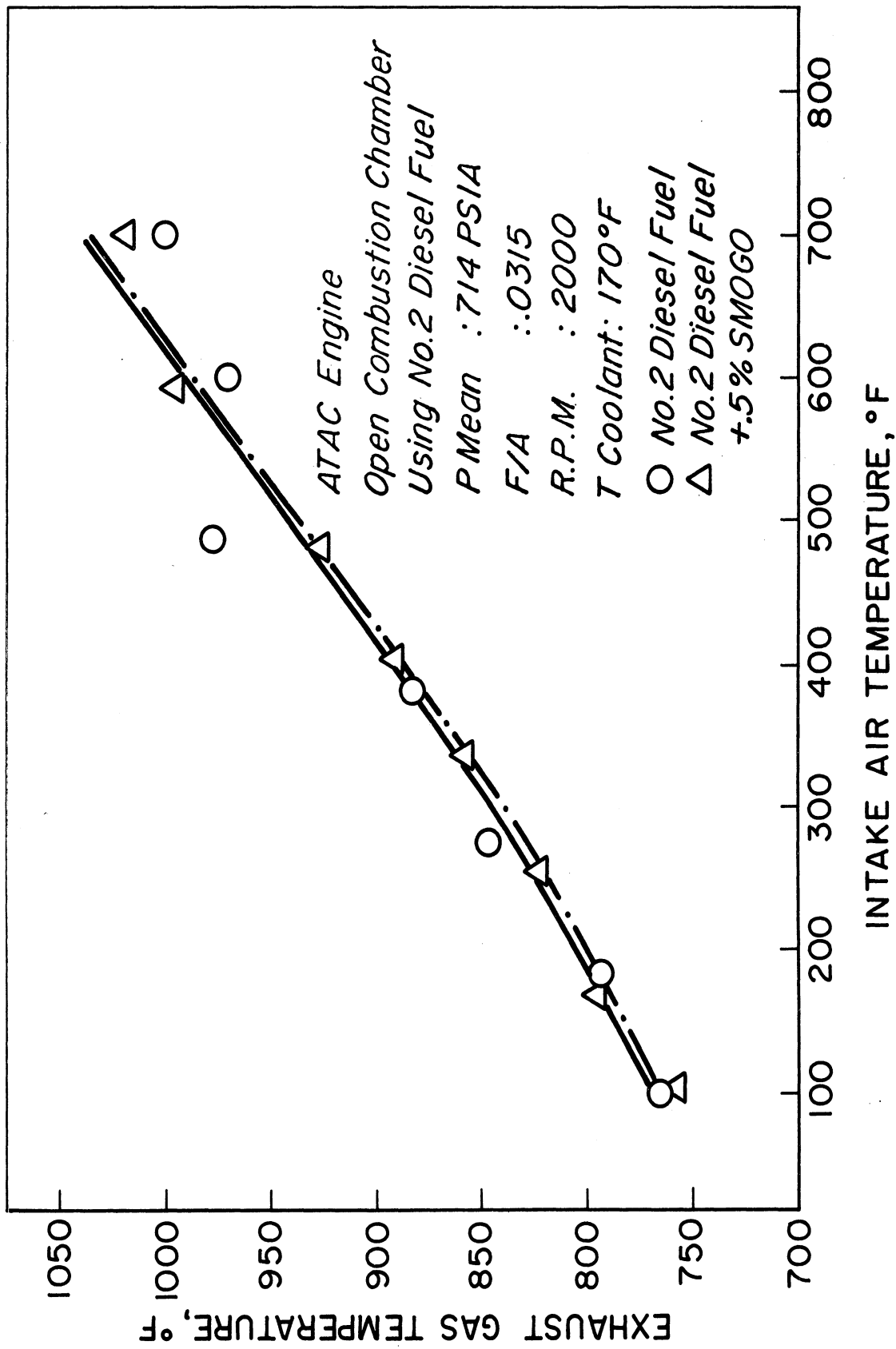


Fig. 6. Effect of anti-smoke additive on exhaust gas temperature.

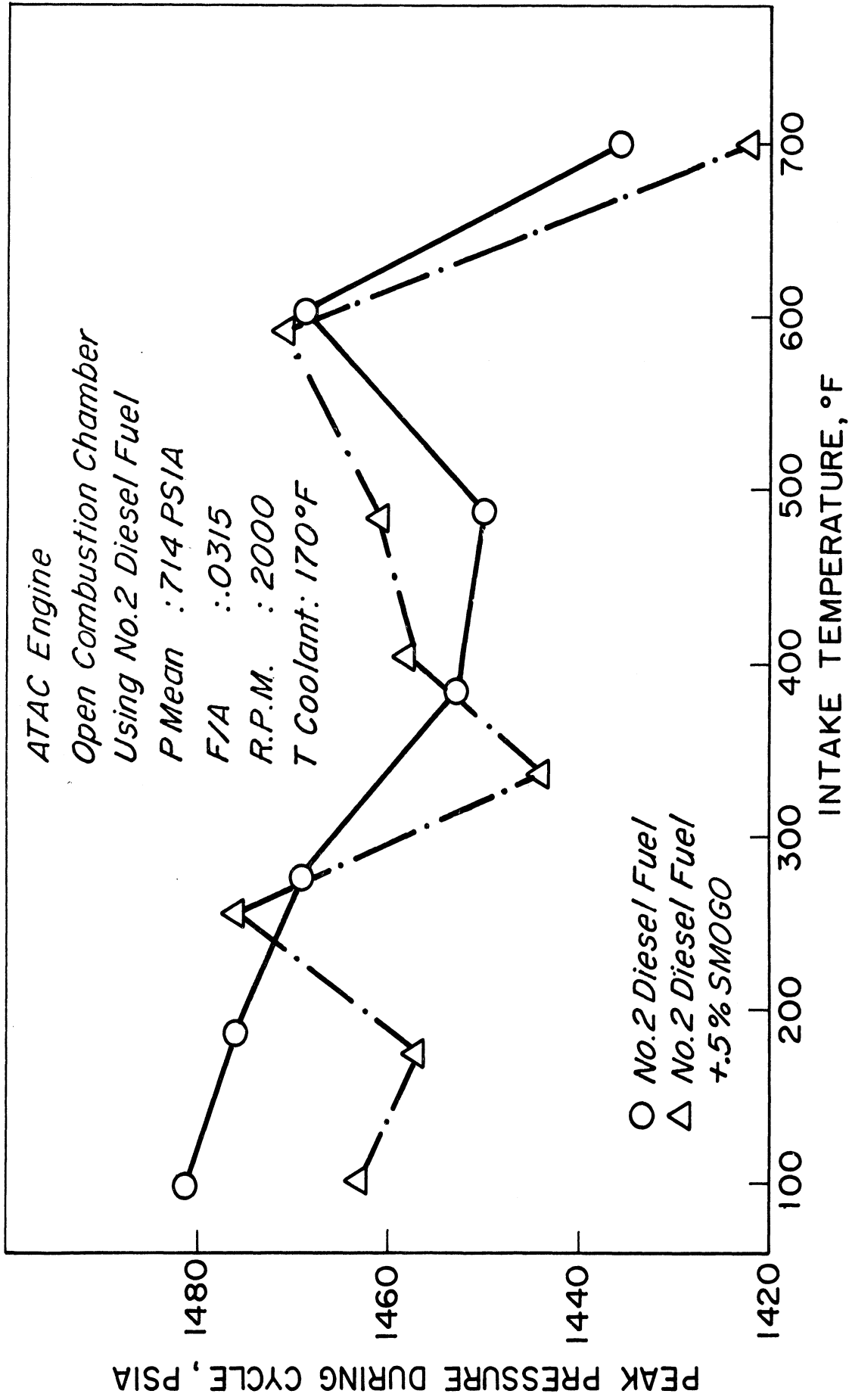


Fig. 7. Effect of anti-smoke additive on the peak gas pressure.

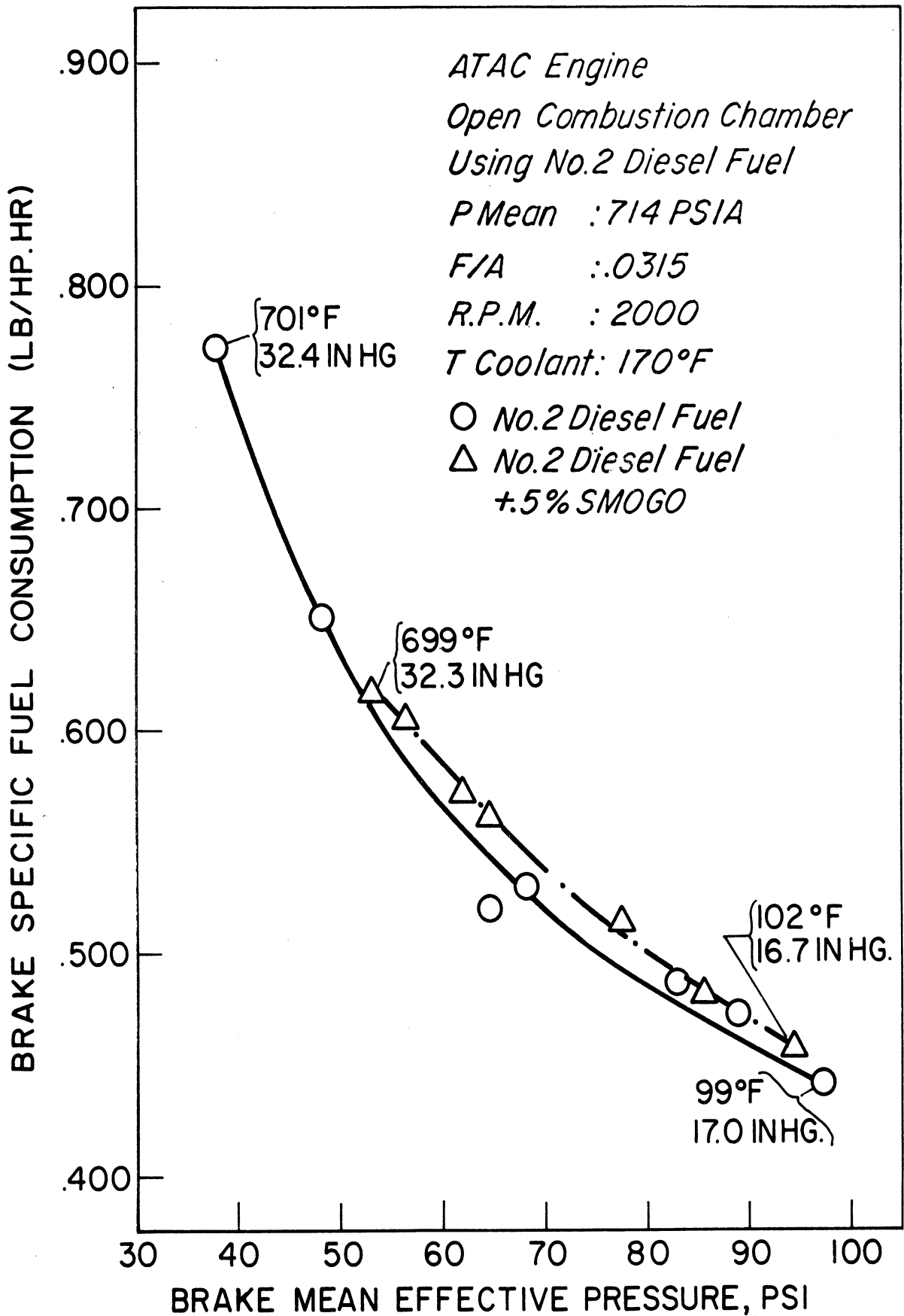


Fig. 8. The specific fuel consumption for diesel fuel with and without additive.

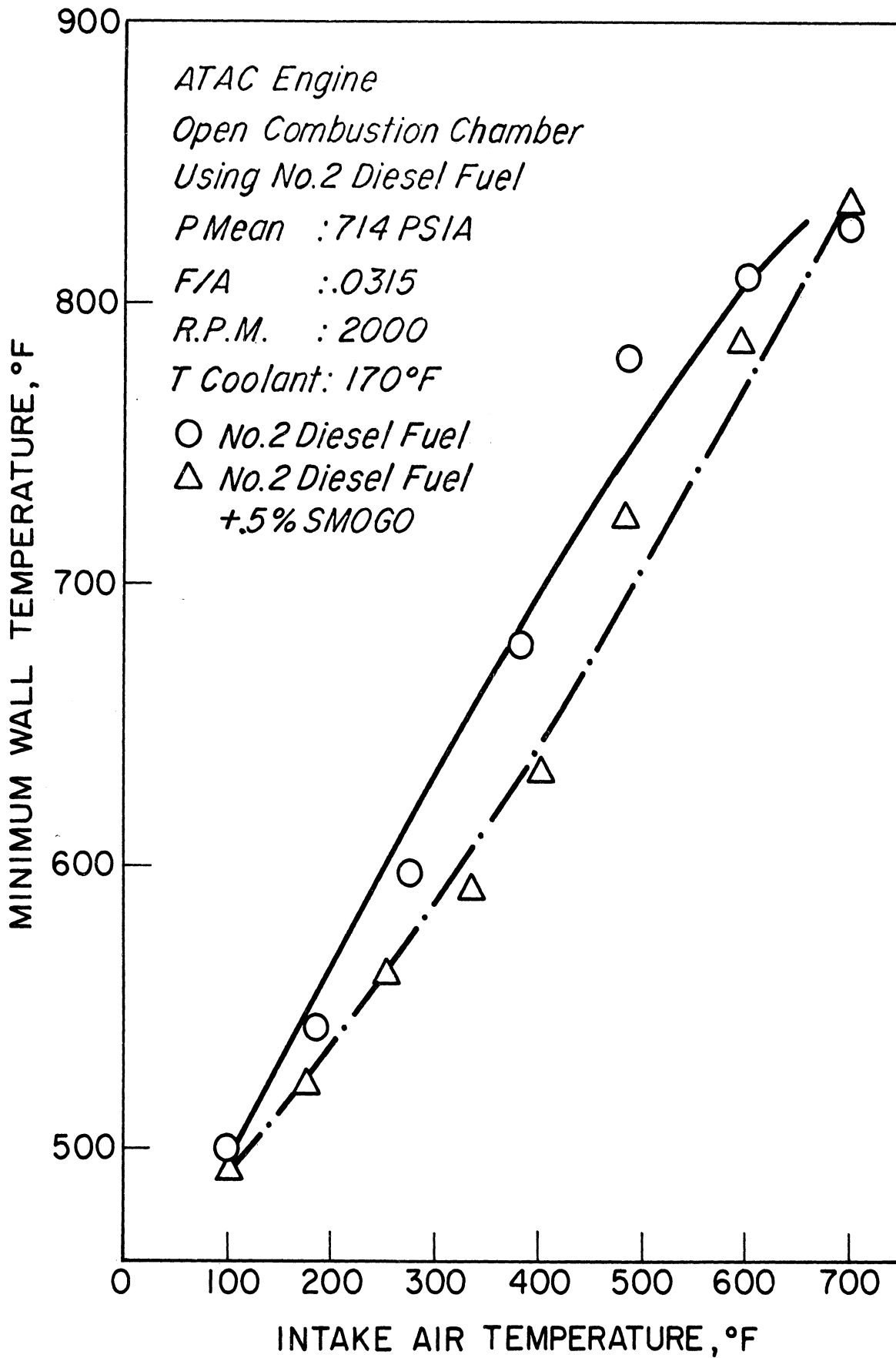


Fig. 9. Effect of the intake air temperature on the wall surface temperature for diesel fuel with and without additive.

SECTION 12

EFFECT OF AIR CHARGE PRESSURE ON IGNITION DELAY AND OTHER COMBUSTION PHENOMENA

EFFECT OF AIR CHARGE PRESSURE ON I.D.

For this study, the air pressure in the surge tank was changed from atmospheric to 60.6 in. Hg. The corresponding pressure at start of injection ranged from 350 psia to 1185 psia, respectively. The air temperature before the inlet valve was almost constant at about 93°F, and the average temperature at start of injection was 1540°R.

The results of these tests for the pressure rise and illumination delays are plotted against the pressure at start of injection in Fig. 1. This figure shows that the ignition delay decreases at a high rate with the increase in pressure and at a lower rate in the high pressure range. The difference between the illumination delay and the pressure rise delay decreases with the increase in pressure. At pressures above 900 psia, both the ignition delays are equal.

The logarithm of the pressure rise delay is plotted against the logarithm of the mean pressure during the delay as shown in Fig. 2. This figure shows that the best fitting curve is composed of two straight lines, the first for mean pressures between 500 psia and 990 psia, the second is a less steep line between mean pressures of 990 psia and 1470 psia. Two similar lines with different slopes were obtained when the logarithm of the ignition delay was plotted against the logarithm of the pressure at start of injection or the pressure in the surge tank. The slopes of the lines obtained with the mean pressure during the ignition delay were used to find a correlation between the ignition delay and the air charge pressure. The slopes of these lines can be considered as the overall order of the preignition reactions. The experimental results in Fig. 2, show that the order of the reactions, in the two pressure ranges is of a fractional nature. For the low pressure range the slope is 0.81. For the high pressure range the slope is 0.292.

The relationship between the pressure rise delay, $I.D._p$, and the mean pressure during the ignition delay can be given by:

$$I.D._p = \frac{A}{p^n}$$

The factor A is mainly a function of the gas temperature. This function was

found to be an exponential nature.*

The values of the factors A and n, based on the mean pressure and the pressure at start of injection, are shown in Table I.

TABLE I

Range		Based on Pressure at Start of Injection	Based on Mean Pressure During I.D.
Low Pressure	A	82.59	229.61
	n	0.684	0.81
	Max. Deviation	2.16%	2.5%
High Pressure	A	5.44	6.79
	n	0.269	0.2918
	Max. Deviation	1.28%	1.55%

EFFECT OF SURGE TANK PRESSURE ON IGNITION DELAY

The ignition delay (I.D._p) is plotted versus the surge tank pressure in Fig. 3. This figure shows that the I.D._p is 1.445 msec at a surge tank pressure of 14.3 psia. It decreases continuously with the increase in the surge tank pressure, and reaches 0.81 msec at 44.3 psia. The rate of decrease is high at the low pressures and decreases with the increase in pressure.

EFFECT OF AIR CHARGE PRESSURE ON THE PEAK GAS PRESSURE AND PRESSURE GRADIENT

Figure 4 shows that under the conditions of the tests, the peak pressure increased continuously with the surge tank pressure. At a surge tank pressure of 14.5 psia the peak pressure was 900 psia. At a surge tank pressure of 44.2 psia the peak gas pressure reached about 2550 psia. The maximum pressure gradient increased from 95 psi per crank angle degree, at atmospheric pressure, to a maximum value of 292 psi per crank angle degree at a surge tank pressure of 28 psia. Any further increase in the surge tank pressure causes a reduction in the maximum pressure gradient.

*N. A. Henein and Jay A. Bolt, "Correlation of Air Charge Temperature and Ignition Delay for Several Fuels in a Diesel Engine," SAE Int'l Automotive Engr. Congress, Detroit, Mich., Jan. 13-17, 1969, paper no. 690252.

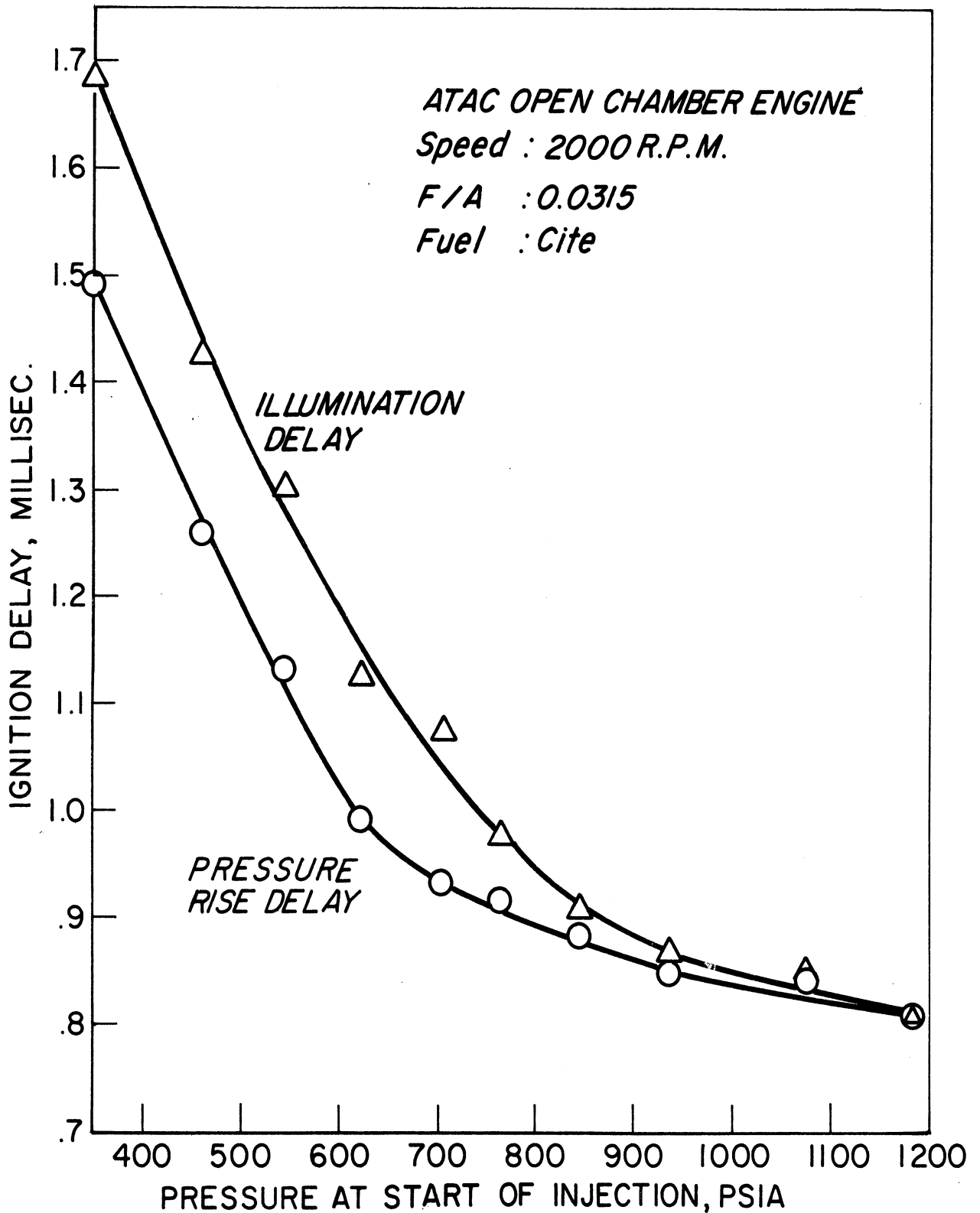


Fig. 1. Effect of pressure at the start of injection on ignition delay.

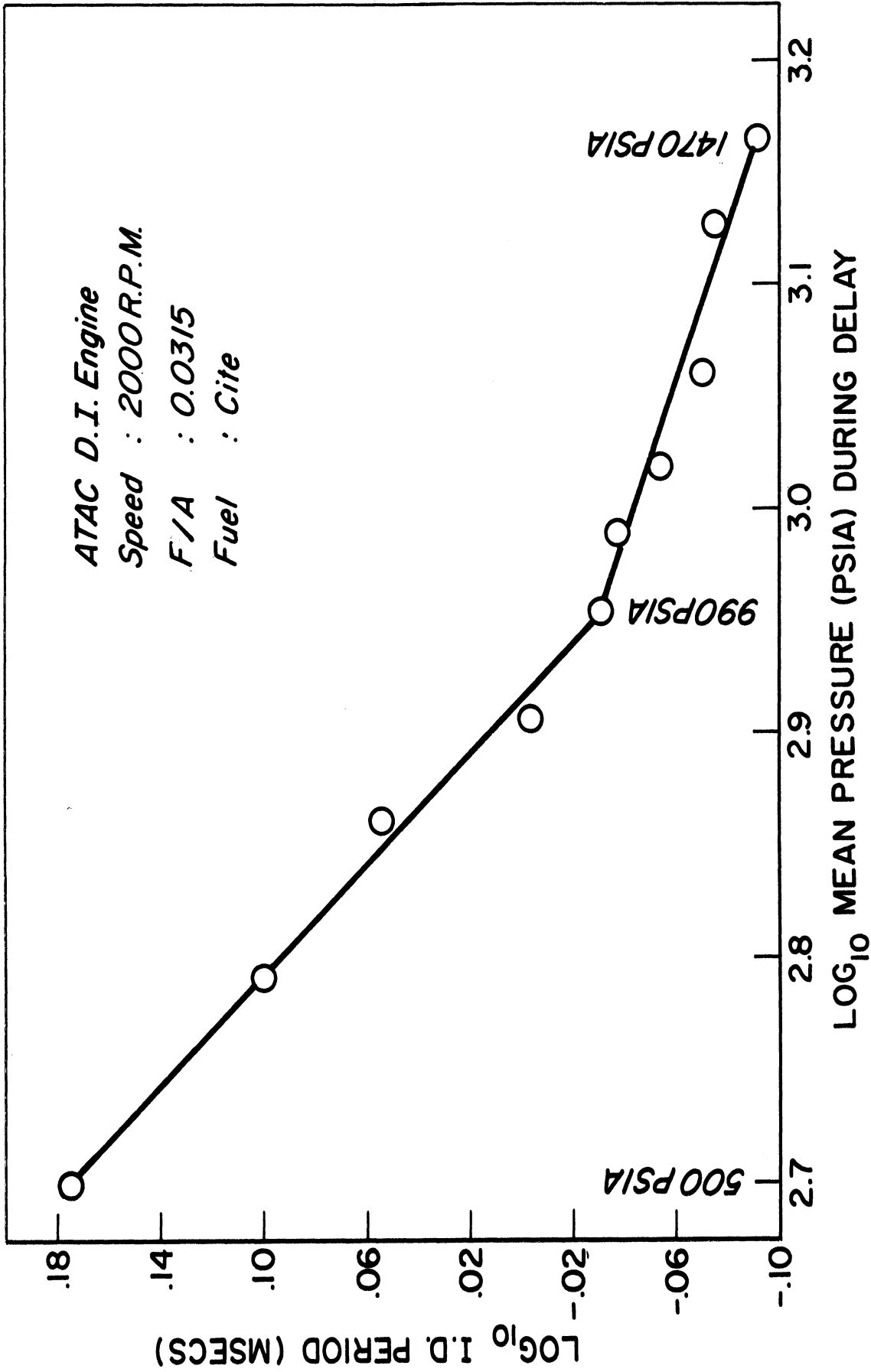


Fig. 2. Log I.D. vs log mean pressure during delay.

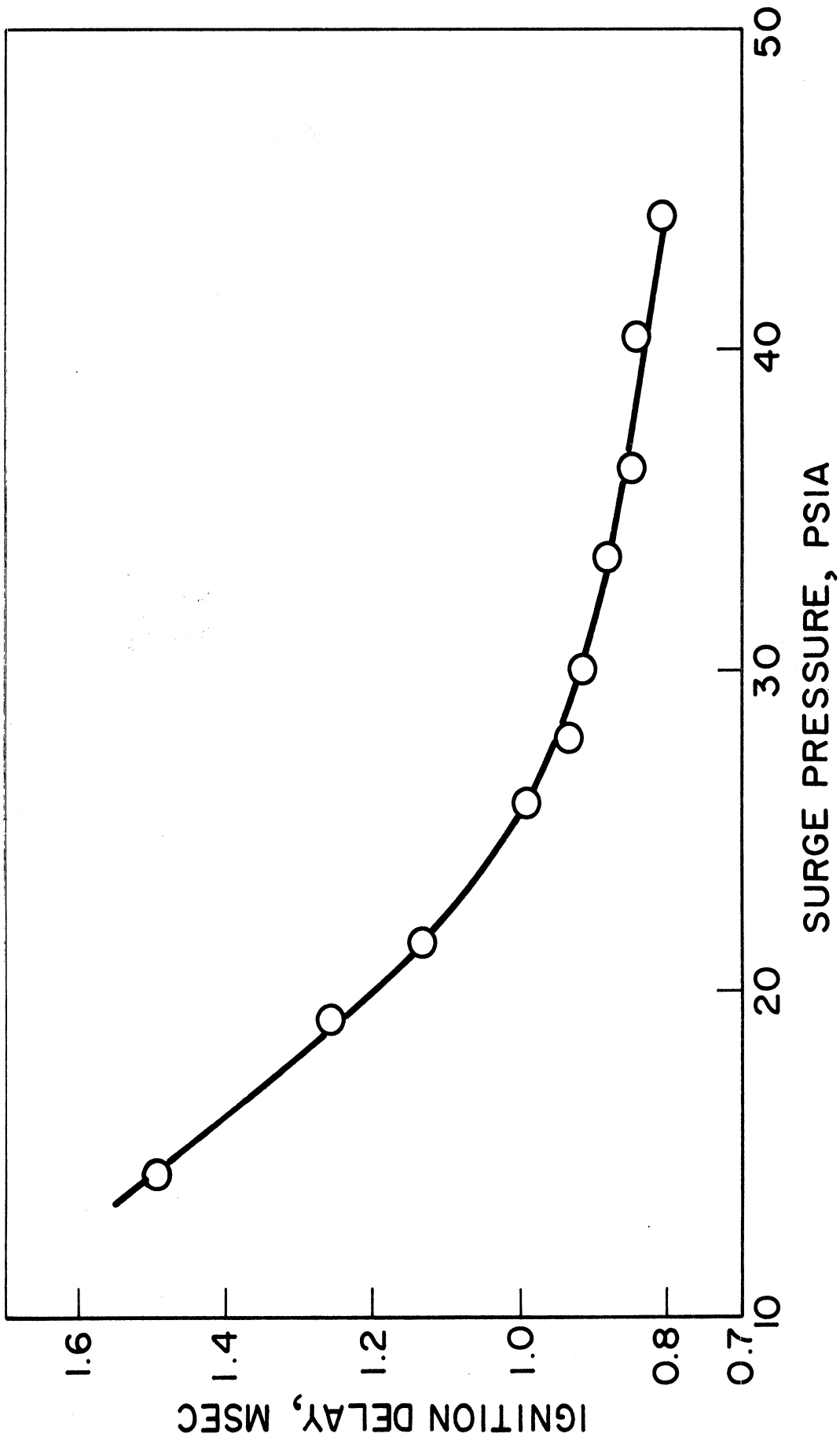


Fig. 3. Effect of inlet surge tank pressure on ignition delay.

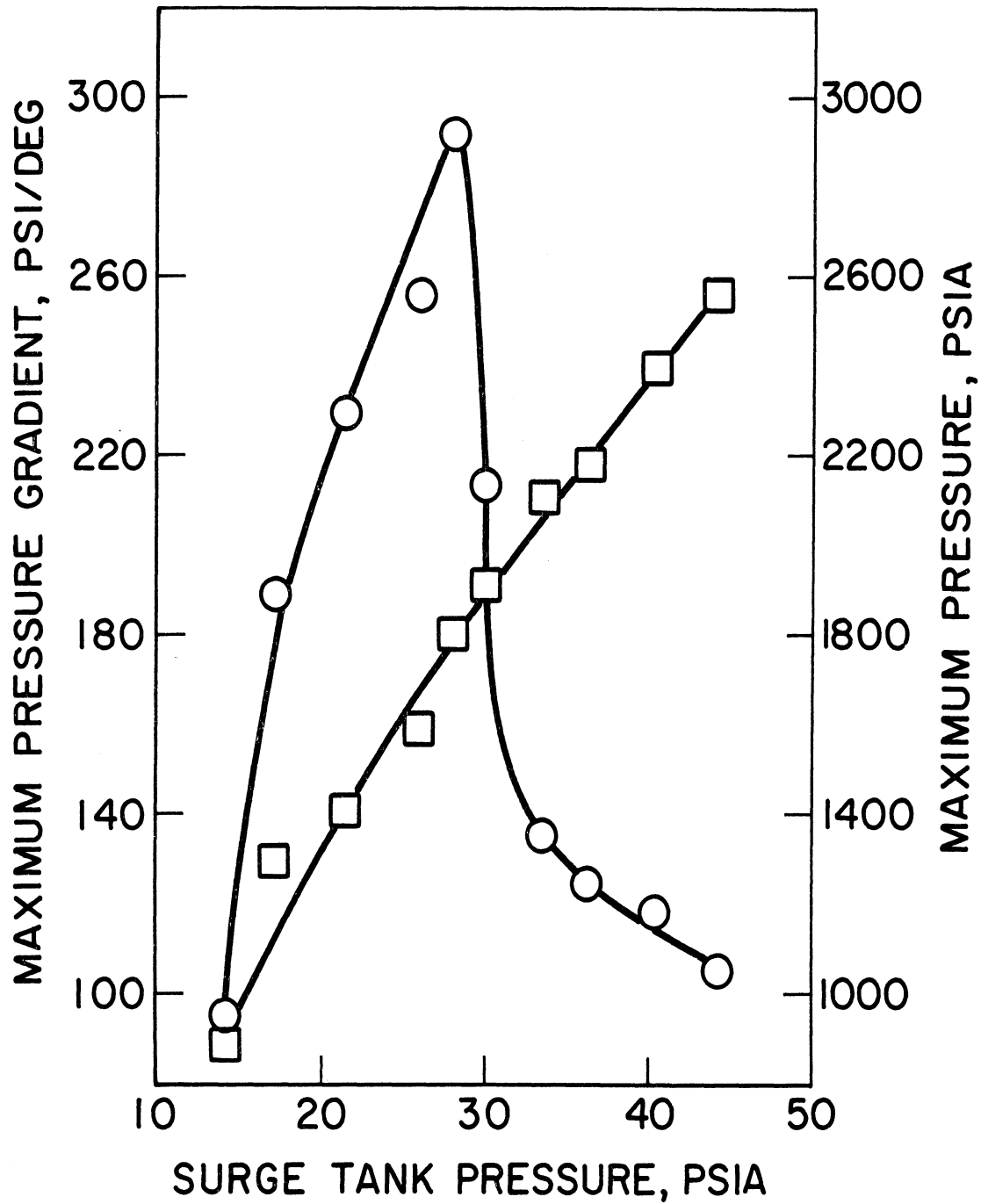


Fig. 4. Effect of surge tank pressure on the peak gas pressure and maximum pressure gradient.

SECTION 13

EFFECT OF DENSITY ON THE IGNITION DELAY

To study if the density is an independent variable affecting the ignition delay, many combinations of air temperature and pressure were used. The results of this study are given below.

EFFECT OF AIR DENSITY ON THE IGNITION DELAY OF DIFFERENT FUELS (Constant Pressure)

The fuels for which this study was made are:

1. CITE referee grade (Mil-F-45121) fuel
2. Diesel no. 2 fuel, and
3. Mil-G-3056 referee grade gasoline fuel

The results of ignition delay (I.D.) are plotted versus the average density during the delay period in Fig. 1. This^p figure shows that increasing the density causes an increase ignition delay. However, it should be noted that the change in air density can be due to changes in two main variables

1. gas temperature
2. gas pressure

In Fig. 1 the mean pressure during the I.D. was kept at a constant value of 700 psia, while the mean temperature was changed from 1550°R to 2500°R. Figure 1 shows that the effect of increasing the air temperature on reducing the I.D. is much more than the effect of air density.

The change in the air density is expected to affect the following processes.

1. Atomization

Increasing the air charge density increases the tendency toward the spray disintegration and atomization.

2. Penetration

Increasing the density will result in a drop in the penetration of the

fuel spray. The maximum velocity of the fuel jet occurs at the tip of the nozzle. Due to jet turbulence, part of the momentum of the fuel will be imparted to the air entrained in the jet. The increase in the air density will cause a corresponding drop in the momentum of the jet and decrease the penetration.

3. Rate of Evaporation

Increasing the density increases the coefficient of heat transfer from the air to the fuel droplets. This can be shown from the following dimensionless relationship.

$$\text{Nu} = f_n(\text{Re})^n (\text{Pr})^m$$

or

$$\frac{hd}{k} = f_n\left(\frac{vd\rho}{u}\right)^n \left(\frac{c_p\mu}{k}\right)^m$$

where Nu = Nusselt number

Re = Reynolds number

Pr = Prandtl number

h = heat transfer coefficient

d = diameter of fuel droplet

k = thermal conductivity of the air-vapor film

v = relative velocity of the droplet with respect to the air

ρ = air density

μ = viscosity

c_p = specific heat at constant pressure

n, m = constants

The above equation shows that the increase in the air density results in an increase in the heat transfer coefficient, and a corresponding increase in the rate of temperature rise of the fuel droplets, and the rate of evaporation. The rate of evaporation will also increase by the increase in the liquid surface area caused by atomization.

4. Rate of Diffusion of the Fuel Vapor into the Air and the Formation of a Combustible Mixture

In this series of tests the change in the air density was achieved by changing the air temperature, while keeping the air pressure at a constant value. This combination of pressure and temperature results in an increase in the coefficient of binary diffusivity. This can be shown from the following relationship, derived from equation (16.3-1), "Transport Phenomena" by

R. B. Bird, W. E. Stewart, and E. N. Lightfoot, John Wiley and Sons, Inc., New York, 1966, page 505.

$$pD_{AB} = CT^b$$

where p = pressure
 D_{AB} = binary diffusivity
 C = constant
 T = temperature
 b = constant

If the pressure is kept constant, as in this present series of tests, an increase in the gas temperature will increase the binary diffusivity.

The above analysis shows that the increase in the air charge density, by keeping the pressure constant and decreasing the temperature, will result in the following:

1. Increased atomization
2. Reduced penetration
3. Increased heat transfer coefficient and surface area of fuel droplets
4. Reduced diffusivity
5. Reduced temperature difference between the air and the fuel

All these changes occur in the physical part of the ignition delay. As far as the changes in the chemical delay period, it is expected that the decrease in temperature will greatly reduce the rate of the chemical reactions leading to preignition.

EFFECT OF AIR DENSITY ON THE IGNITION DELAY OF CITE FUEL (Constant Temperature)

This analysis shows the effect of the air charge density on the ignition delay of CITE fuel. The density was changed by changing the pressure and keeping the temperature at a nearly constant value.

The average density during the ignition delay was changed from 0.84 lbm/cu ft to 2.38 lbm/cu ft, while the mean air temperature during the ignition delay was kept at $1604 \pm 55^\circ\text{F}$.

The results of this analysis are plotted in Fig. 2. This figure shows that the ignition delay decreases with the increase in the air density. The increase in the air density at constant temperature is expected to cause an increase in atomization, reduction in penetration, increase in the heat transfer coefficient, and surface area of the liquid.

Also, the increase in air pressure will cause a drop in the coefficient of binary diffusivity. Besides these changes in the physical factors the increase in density (at constant temperature) is expected to increase the rate of the preignition reactions.

CONCLUSION ON THE EFFECT OF DENSITY ON IGNITION DELAY

From the above analysis it can be concluded that the density is not an independent variable affecting the ignition delay. Any change in the I.D. is due to the changes in pressure or temperature accompanying the change in density.

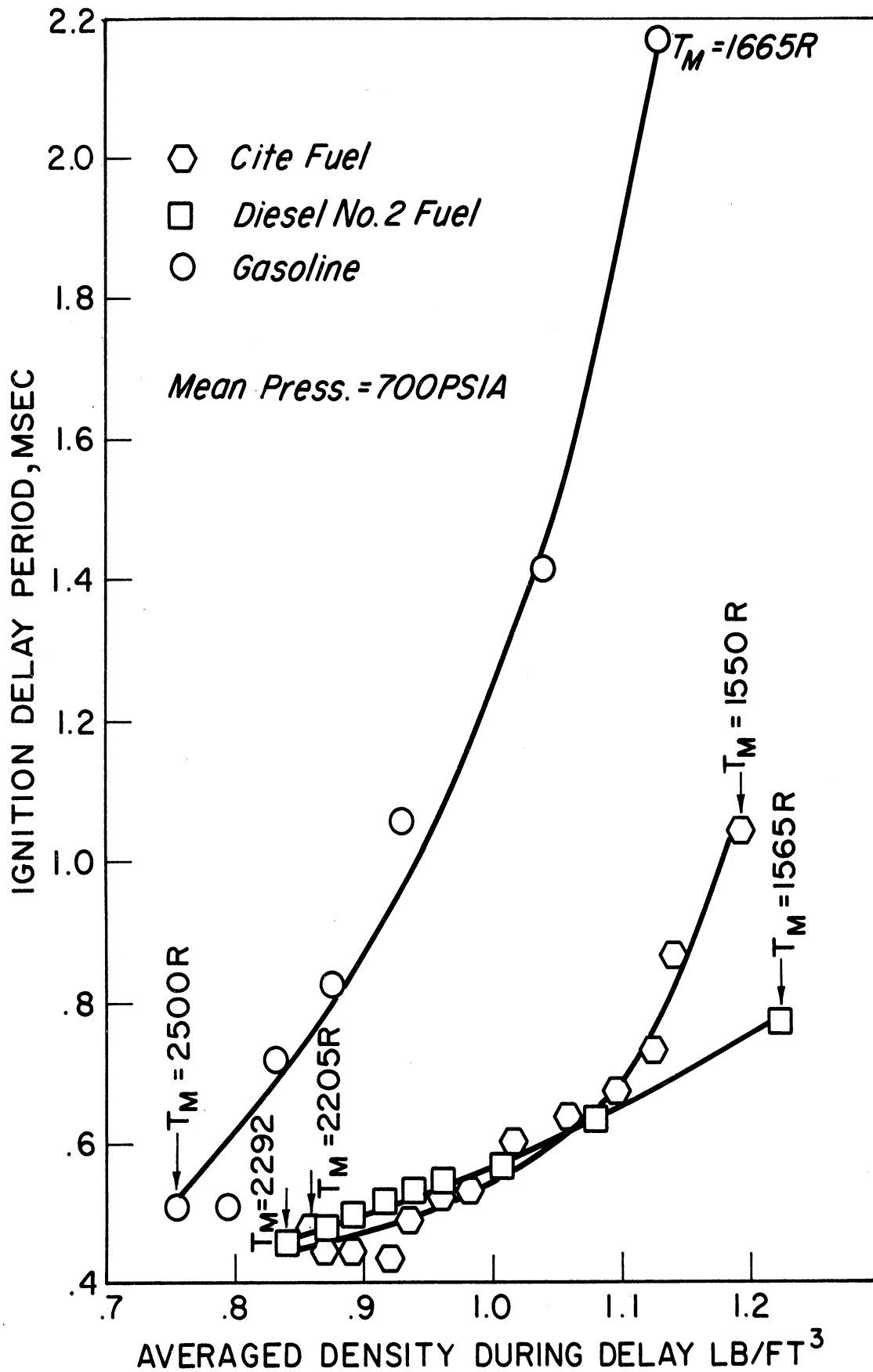


Fig. 1. Effect of density on ignition delay at a constant mean pressure density during I.D.

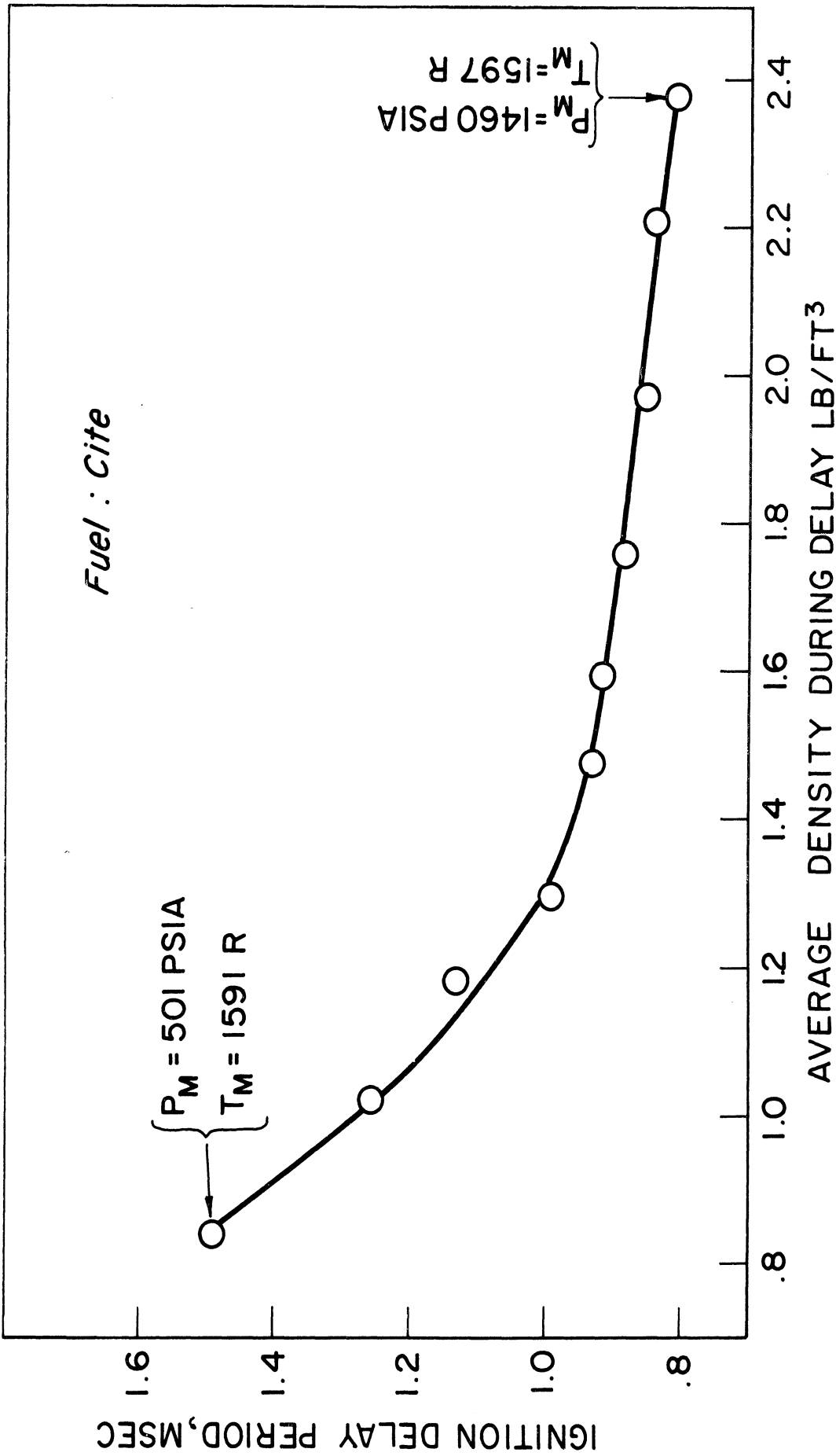


Fig. 2. Effect of density on ignition delay at a constant mean temperature during I.D.